LEABHARLANN CHOLÁISTE NA TRÍONÓIDE, BAILE ÁTHA CLIATH
Ollscoil Átha Cliath
TRINITY COLLEGE LIBRARY DUBLIN
The University of Dublin

Terms and Conditions of Use of Digitised Theses from Trinity College Library Dublin

Copyright statement

All material supplied by Trinity College Library is protected by copyright (under the Copyright and Related Rights Act, 2000 as amended) and other relevant Intellectual Property Rights. By accessing and using a Digitised Thesis from Trinity College Library you acknowledge that all Intellectual Property Rights in any Works supplied are the sole and exclusive property of the copyright and/or other IPR holder. Specific copyright holders may not be explicitly identified. Use of materials from other sources within a thesis should not be construed as a claim over them.

A non-exclusive, non-transferable licence is hereby granted to those using or reproducing, in whole or in part, the material for valid purposes, providing the copyright owners are acknowledged using the normal conventions. Where specific permission to use material is required, this is identified and such permission must be sought from the copyright holder or agency cited.

Liability statement

By using a Digitised Thesis, I accept that Trinity College Dublin bears no legal responsibility for the accuracy, legality or comprehensiveness of materials contained within the thesis, and that Trinity College Dublin accepts no liability for indirect, consequential, or incidental, damages or losses arising from use of the thesis for whatever reason. Information located in a thesis may be subject to specific use constraints, details of which may not be explicitly described. It is the responsibility of potential and actual users to be aware of such constraints and to abide by them. By making use of material from a digitised thesis, you accept these copyright and disclaimer provisions. Where it is brought to the attention of Trinity College Library that there may be a breach of copyright or other restraint, it is the policy to withdraw or take down access to a thesis while the issue is being resolved.

Access Agreement

By using a Digitised Thesis from Trinity College Library you are bound by the following Terms & Conditions. Please read them carefully.

I have read and I understand the following statement: All material supplied via a Digitised Thesis from Trinity College Library is protected by copyright and other intellectual property rights, and duplication or sale of all or part of any of a thesis is not permitted, except that material may be duplicated by you for your research use or for educational purposes in electronic or print form providing the copyright owners are acknowledged using the normal conventions. You must obtain permission for any other use. Electronic or print copies may not be offered, whether for sale or otherwise to anyone. This copy has been supplied on the understanding that it is copyright material and that no quotation from the thesis may be published without proper acknowledgement.

MODELLING OF SITE-SPECIFIC TRAFFIC LOADING ON SHORT TO MEDIUM SPAN BRIDGES

Trinity College Library Dublin



University of Dublin

THIS THESIS MAY BE READ ONLY

IN THE LIBRARY

Trinity College Library College Street Dublin 2 Ireland

Modelling of Site-Specific Traffic Loading on Short to Medium Span Bridges

Modelling of Site-Specific Traffic Loading on Short to Medium Span Bridges

by

Samuel Grave

Thesis Submitted to the University of Dublin, Trinity College,

for the Degree of Doctor of Philosophy

October 2001

TRINITY COLLEGE
11 JUN 2002
LIBRARY DUBLIN
Thesis
6821

DEDICATION

Je dédie cette thèse à mes parents, Jean-Pierre et Maryvonne, et à Victoria

DECLARATION

The author hereby declares that this thesis, in whole or in part, has not been submitted to any other university as an exercise for a degree. Except where reference has been given in the text, it is entirely the author's own work.

The author confirms that the library may lend or copy this thesis upon request, for academic purposes.

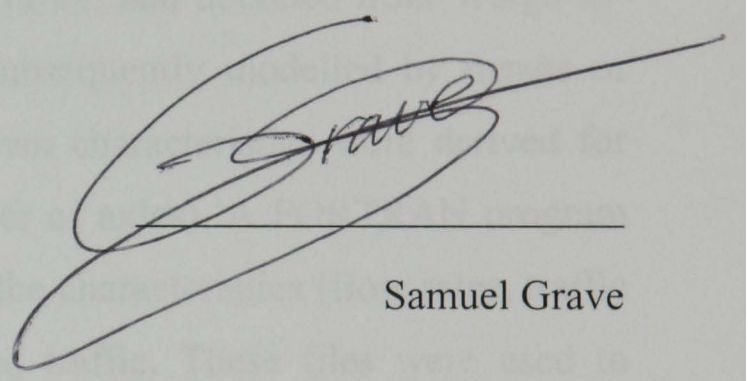

Samuel Grave

October 2001

ABSTRACT

The management of existing bridges is an important task for road authorities; this task involves the assessment of the structural safety of these bridges. Bridge design codes are over conservative when applied to bridge assessment since they allow for uncertainty about the future loading and resistance of a structure. Once a bridge is in service, evaluation can be based upon the actual loads and resistance, thus enabling a more accurate assessment of the structural safety. One of the most important sources of uncertainty when assessing road bridges is that associated with traffic loading. There is therefore a need for methods that consider site-specific traffic data. It is the aim in this thesis to model imposed traffic loading on short to medium span bridges, 20 m - 40 m, which represent the majority of existing bridges.

A number of traffic files representative of European traffic, and obtained from Weigh-In-Motion measurements, were studied in detail and subsequently modelled by means of statistical distributions. Representative trucks of known characteristics were derived for each truck class (i.e., corresponding to a fixed number of axles). A FORTRAN program was developed to generate traffic data files based on the characteristics (flow rates, traffic composition, gross vehicle weights) of the measured traffic. These files were used to simulate the passage of traffic over a series of bridges (simply supported & two-span continuous, length from 20 m to 40 m). Another FORTRAN program was used to calculate the effects induced in the structure as the trucks move along the bridge; six load effects were considered for each bridge analysed. After a detailed analysis of the results, typical critical loading situations were derived for each bridge configuration.

Simplified models were then developed to reproduce these critical loading situations without having to perform the full simulations: one to deal with two lanes of opposing traffic and another for two lanes of unidirectional traffic. In essence, for both models, pairs of heavily loaded trucks are positioned at a critical location (for the bridge and load effect considered), thus inducing the critical load effect in the structure. The models were purposely kept simple, and can be employed by practicing engineers (for the assessment of existing bridges, for example), but are also accurate since they are site-specific. For both approaches, full simulations and simplified models, characteristic values were calculated

for the load effects and bridges considered. Good agreement was found between the full simulations and the simplified models.

The effect of the main traffic characteristics (i.e., truck weights, traffic intensity and truck geometry) was assessed with respect to the critical loading situations and the extrapolated values. The truck weights were shown to be most significant; as was the truck geometry for the shorter bridges. The two factors, weight and geometry, can counteract each other; it was shown that both factors should be accounted for jointly. Also, traffic intensity and bridge length were shown to act jointly: the former having a substantial influence for certain load effects but only for longer bridges (i.e., those making 3- or 4-truck events possible).

ACKNOWLEDGEMENTS

To Victoria; her total support and constant encouragement made my motivation grew stronger by the day, her infinite patience and caring love turned challenging times into pleasing prospects. Thank you so much for everything; by dedicating this thesis to you I hope to show you my sincere gratitude.

A mes parents, qui ont toujours cru en moi et qui m'ont soutenu continuellement durant toutes ces années; en leur dédiant ma thèse j'espère leur témoigner ma gratitude; à Jérôme, Virginie et toute ma famille, sans oublier Loustic, pour leurs encouragements et leur soutien depuis la France, ainsi que leur chaleureux accueil lors de mes visites.

To Professor Eugene O'Brien, my supervisor and mentor, for his proficient guidance, his constant professionalism and his habitual sociability; to Alan, for his expert advice, inspiring suggestions and constant help over the years.

To Arturo, an old friend, with who I shared my office, my pints and so many great memories in so many kingdoms; to Con and Eddie, for their help and for their enjoyable company; it has been a real pleasure to work beside them.

A Alfonso, Marivi, y Alfonso Junior por su apoyo, aliento y especialmente por todas sus atenciones durante mi estancia en su casa en Villajoyosa.

To Bernard Jacob and the Laboratoire Central des Ponts et Chaussees for providing me with traffic data and allowing me to use the application software CASTOR.

To the staff of the Department of Civil, Structural and Environmental Engineering of Trinity College for their kind help and especially to Prof. S. Perry for his financial support.

To all the friends who made these years of research an enjoyable experience: Jesus Chus Berry, Mr President Brian, Piero, Cathy "Green Fingers Plant Care Nursery", Suzanilla and EddyBoy The Dancing Queens, Fergal, and Cristiano.

TABLE OF CONTENTS

	Dedication	ii
	Declaration	iii
	Abstract	iv
	Acknowledgements	vi
	Table of contents	vii
CHAPTER 1	INTRODUCTION	2
1.1	**Background**	2
1.2	**Motivation**	3
1.3	**Related work**	4
1.4	**Aims of this research**	5
1.5	**Outline of the thesis**	6
CHAPTER 2	PROBABILITY CONCEPTS AND STATISTICAL INFERENCE	9
2.1	**Introduction**	9
2.2	Elements of probability theory	9
2.2.1	Sample space and events	9
2.2.2	Terminology	10
2.2.3	Combination of events	10
2.2.4	Mathematics of probability	11
2.3	**Analytical models of random phenomena**	12
2.3.1	Random variables and distributions	12
2.3.2	Main description of a random variable	14
2.3.3	Bivariate distribution	16
2.4	**Useful probability distributions**	18
2.4.1	The normal distribution	19
2.4.2	The logarithmic normal (lognormal) distribution	21
2.4.3	The Poisson process and the Poisson distribution	22
2.4.4	The exponential distribution	24
2.4.5	The Gamma distribution	25
2.4.6	The Beta distribution	27
2.4.7	The Extreme Value distributions	27
2.5	**Statistical Inference**	29
2.5.1	Estimating parameters from observational data	29
2.5.2	Classical approach to estimation of parameters	31

2.5.3	Empirical determination of distribution models and their validity	33
2.5.4	Regression and correlation analysis	36
2.6	**Conclusions**	**38**

CHAPTER 3	**LITERATURE REVIEW**	**41**
3.1	**Introduction**	**41**
3.2	**Live load modelling**	**41**
3.2.1	Use of Poisson processes to model traffic flow	42
3.2.2	Live load models using renewal processes: case studies	48
3.2.3	Simulation of traffic flow	54
3.3	**Use of field measurements and Weigh-In-Motion data**	**61**
3.3.1	The use of WIM data in bridge engineering	61
3.3.2	Dynamic load	65
3.3.3	Truck weight distributions	65
3.4	**Prediction of extreme values**	**70**
3.4.1	Tail equivalence	70
3.4.2	Selection of an appropriate distribution	71
3.4.3	Prediction of extreme loads and load effects	76
3.5	**Summary and conclusions**	**79**

CHAPTER 4	**TRAFFIC DATA AND LOAD EFFECTS**	**82**
4.1	**Introduction**	**82**
4.2	**Description of measured traffic files**	**82**
4.2.1	Introduction	82
4.2.2	Traffic intensity	83
4.2.3	Traffic composition	85
4.2.4	Truck weights	88
4.2.5	Axle weights	91
4.2.6	Axle spacings	94
4.2.7	Speed distribution	95
4.2.8	Headway distribution	97
4.2.9	Conclusions	99
4.3	**Static Effects of Traffic Actions**	**100**
4.3.1	Introduction	100
4.3.2	Influence lines	100
4.3.3	Influence response	103
4.3.4	Conclusions	108
4.4	**Modelling the traffic characteristics**	**109**

4.4.1	Introduction	109
4.4.2	Assumptions	109
4.4.3	Modelling the probability density function of traffic characteristics	110
4.4.4	Modelling of typical trucks	113
4.5	**Conclusions**	**116**

CHAPTER 5	**TRAFFIC GENERATION AND SIMULATION**	**118**
5.1	**Introduction**	**118**
5.2	**Traffic generation**	**118**
5.2.1	Input data	118
5.2.2	Generation of the traffic file	120
5.2.3	Modification of existing traffic files	123
5.3	**Traffic simulation using CASTOR**	**124**
5.3.1	Introduction	124
5.3.2	Running CASTOR	124
5.3.3	Limitations of CASTOR	126
5.4	**Traffic simulation using SIMULTRAFFIC**	**128**
5.4.1	Testing for crossing event	129
5.4.2	Calculate the load effects	131
5.4.3	Filter the duplicated crossing events	131
5.4.4	Output files	133
5.5	**Comparison between CASTOR and SIMULTRAFFIC**	**133**
5.5.1	Introduction	133
5.5.2	Results	134
5.6	**Conclusions**	**135**

CHAPTER 6	**BI-DIRECTIONAL TRAFFIC ANALYSIS AND MODELLING**	**137**
6.1	**Introduction**	**137**
6.2	**Traffic generation**	**137**
6.3	**Traffic simulation**	**140**
6.3.1	Calculation of the load effects	140
6.3.2	Results of the full simulations	142
6.3.3	Extrapolated values: results and comparative study	145
6.3.4	Frequency of crossing events	148
6.4	**Analysis of the critical loading events**	**149**
6.5	**Development of a simplified model**	**153**
6.5.5	Input data for the simplified model	154
6.5.6	Simplified model calibration	157

6.5.7	Simplified model results	160
6.6	**Overview and conclusions**	**163**
CHAPTER 7	**UNIDIRECTIONAL TRAFFIC ANALYSIS AND MODELLING**	**165**
7.1	**Introduction and Terminology**	**165**
7.2	**Traffic description and modelling**	**166**
7.2.1	Traffic intensity	166
7.2.2	Traffic weights	167
7.2.3	Frequency of overtaking events	168
7.3	**Traffic simulations**	**170**
7.3.1	Introduction	170
7.3.2	Traffic simulations	170
7.3.3	Extrapolated values: results and comparative study	172
7.3.4	Critical loading events	173
7.4	**Development of a simplified model**	**175**
7.4.1	Representative trucks	175
7.4.2	Modelling truck weights	177
7.4.3	Speed and headway distributions	181
7.4.4	Estimation of number of overtaking events	182
7.4.5	Simplified model to simulate critical overtaking events	183
7.5	**Results of the simplified model**	**185**
7.6	**Simplified model 2 and 3**	**188**
7.6.1	Simplified Model 2	188
7.6.2	Simplified Model 3	191
7.6.3	Summary	192
7.7	**Conclusions**	**193**
CHAPTER 8	**CONCLUSIONS**	**196**
8.1	**Introduction**	**196**
8.2	**Weigh-In-Motion data description and modelling**	**197**
8.3	**Generation and simulation of traffic files**	**198**
8.4	**Bi-Directional traffic analysis and modelling**	**198**
8.5	**Unidirectional traffic analysis and modelling**	**200**
8.6	**Overview and suggestions for future work**	**202**
	REFERENCES	**204**
Appendix A	**Dynamic load**	**212**

Appendix B	Description of the traffic data	217
Appendix C	Static effects of traffic actions	237
Appendix D	Modelling of the traffic data	246
Appendix E	SIMULTRAFFIC and visualisation programs	256
Appendix F	Prediction of extreme values	265
Appendix G	Plots of the measured effects for the bi-directional traffic	273
Appendix H	Extrapolated values for bi-directional traffic	284
Appendix I	Frequency of crossing events for bi-directional traffic	288
Appendix J	Plots of the critical loading events for bi-directional traffic	297
Appendix K	Plots of the modelled effects for bi-directional traffic	326
Appendix L	Plots of the critical loading events for unidirectional traffic	343
Appendix M	Typical critical loading events for unidirectional traffic	363
Appendix N	Plots of the modelled effects for unidirectional traffic	366
Appendix O	Extrapolated values for SM2 and SM 3 for unidirectional traffic	377

Chapter 1

INTRODUCTION

Chapter 1 INTRODUCTION

1.1 BACKGROUND

Bridge design codes are applied in order to ensure a minimum safety in all structures. The stock of road bridges in service today is perceived as acceptably safe but some bridges may be safer than others. The actual structural safety of a bridge may in fact be different from that implied by current design codes for a number of reasons, among which are: evolution of the design codes over time, uncertainty at the design stage, reduction in the bridge resistance and evolution of imposed loads during its lifetime. These four possible sources of variation in the structural safety of a bridge deserve particular attention.

The older bridge design codes were based on: (i) the selection of reasonable upper bound estimates of normal working loads, (ii) the use of elastic methods of structural analysis and (iii) the provision of some margin in strength by the selection of allowable working stresses separated by a factor of safety from some critical stresses (such as the yield or ultimate stress of the material) (O'Connor & Shaw 2000). This approach did not account for the respective uncertainties associated with the various types of load. The concept of limit states was then developed in order to enable partial safety factors to be assigned to a given design variable (according to the uncertainty associated with it). More uniform levels of safety were achieved using the approach of limit states (in comparison with the working stress approach). Yet, both approaches have been used to build a stock of bridges that are acceptably safe, but to varying extents depending on the design concept originally applied (Bailey 1998). In addition, as traffic loads have increased over the years, loading codes have evolved accordingly. Essentially, the safety of a bridge can vary as a function of the design code that was in force at the time of its construction.

Next, the actual strength of materials and intensity of applied loads to which a structure is subjected are likely to be different from those assumed during design because of the inherent variability of material properties and applied loads. In order to ensure a minimum level of safety while accounting for this inherent variability, conservative design values are adopted. For example, the uncertainty associated with traffic loading at the design stage is

very high; to predict the traffic that will use a bridge is a very difficult task. For this reason, the traffic load models used for design are inherently conservative.

Finally, the loads may change during the lifetime of a bridge (e.g., the traffic loads may increase significantly over time) and the structural resistance may be reduced through deterioration (e.g., apparition of cracks in the structure or corrosion of steel elements). Clearly, for the various reasons explained above and possibly others, the structural safety of an existing bridge is different to that assumed when it was built. In the constantly evolving conditions of traffic and with respect to the always-increasing demand of safety from road and bridge users, the assessment of the actual safety of the bridge stock has become a priority. It is the aim of bridge assessment to determine whether a structure can safely be kept in service by using all available data and taking into account the uncertainty associated with that data.

1.2 MOTIVATION

An important task today is the management of existing bridges in an economically efficient manner. This task involves the identification and prioritisation of needs for intervention within a bridge stock through the evaluation of structural safety, which until recently has been assessed using bridge design codes. Design codes are over conservative when applied to bridge assessment (since they allow for uncertainty about the future loading and resistance of a structure); there is therefore a need for methods that allow for consideration of site-specific data. Once a bridge is in service, evaluation can be based upon the actual loads and resistance, thus enabling a more accurate assessment of the structural safety than during design.

One of the most important sources of uncertainty when assessing road bridges is the one associated with traffic loading. Although the use of conservative design traffic load models leads to a small increase in the cost of construction, the cost of an over-conservative evaluation could be much greater once a structure is in service, if it makes the difference between accepting or rejecting the bridge this justifies the use of an approach which considers actual traffic and the effects it produces in a given structure. Therefore, the key to the assessment of existing structures is the use of updated models of loads and resistance derived from site-specific data (Bailey *et al.* 2000). Indeed, the consideration of site data

reduces uncertainty and facilitates a more accurate assessment. In the case of road bridges, the updating of traffic load models presents perhaps the greatest scope for reducing uncertainty. During recent decades, the majority of research has been aimed at determining load models for bridge design and very little work has addressed the site dependence of traffic load effects. There is therefore a need for new methods that consider site-specific traffic loads as a function of parameters describing the bridge and traffic.

1.3 RELATED WORK

The objectives of the BRIME (BRidge Management in Europe) project are to develop a management system framework applicable to bridges on the European road network and to examine the inputs required for such a system. The European road network is called on to carry steadily increasing heavy goods traffic, and, from time to time, increases in legal vehicle or axle loads (Kaschner *et al.* 2000). This network contains many bridges built before modern design standards were established. Furthermore, as bridges grow older, deterioration caused by heavy traffic and an aggressive environment becomes increasingly significant resulting in a higher frequency of repairs and a reduction in load carrying capacity. For that reason, it is important that assessment standards are safe but not over-conservative, because this will cause network operating costs to rise excessively as bridges as strengthened or replaced unnecessarily and traffic restrictions are imposed. Among the various tasks falling within the scope of the BRIME project figures the development of models for taking into account the bridge specific traffic conditions and material properties.

In England, the Highways Agency is responsible for making the most of the existing trunk road network, which implies maintenance and improvement of the existing network. Bridges form an important part of that network; their importance comes not only from their visual impact on the surrounding environment but also from the substantial resources required for their maintenance (Hays 2000). A 15-year bridge rehabilitation programme for trunk road bridges was started in 1988 and aimed at improving the bridge stock so that it continues to perform adequately under the traffic conditions of today. Local authorities and other bridge owners also carried out similar exercises involving their own bridges (Das 2000). From the results coming out from these exercises so far, it is becoming clear that the current assessment requirements, which are based on the worst possible traffic and other

conditions that may occur in any part of the country, are not flexible enough to deal with bridges in less demanding situations. This is a very important limitation, considering the enormous costs of dealing with the so-called *substandard* bridges, some of which may, in reality, be at extremely low risk. As the rehabilitation programme progressed, it became increasingly apparent that there were some fundamental limitations in the current assessment rules, which clearly were too onerous for some bridge situations (Rochester 2000). For instance, the same assessment rules are applicable equally to bridges carrying dense traffic of heavily loaded trucks and those carrying sparse traffic of lighter trucks, and to bridges of different types irrespective of their deterioration rates. Essentially, the main endeavour of this bridge rehabilitation programme has been to eliminate, as far as possible, any unnecessary strengthening or repairs of bridges.

In his thesis, Bailey (1998) focused on the evaluation of structural safety of road bridges with emphasis on the consideration of the actual traffic at a bridge site. Bridges of medium span (30 to 150 m) are considered as well as types of traffic. In the author's view, of all basic variables, traffic actions are probably the most difficult to predict and are potentially the source of the greatest uncertainty during bridge design and assessment. Design traffic load models are therefore very conservative in certain cases, and there is a need for methods that enable actual traffic to be considered during bridge assessment. In his work, Bailey brings attention to the fact that, with the exception of the Eurocode models, simulations are typically based on the bending moment at mid-span and therefore models may not be appropriate for other action effects, in particular shear effects. Also, Bailey *et al.* (2000) state that the most appropriate approach to gathering site specific traffic data is certainly the use of Weigh-In-Motion techniques, based either on the instrumentation of a bridge or the installation of pavement sensors.

1.4 AIMS OF THIS RESEARCH

Having introduced the background and the motivation of this research, the objectives of this research are now presented:

- To show how Weigh-In-Motion data can be utilised in an appropriate modelling of the traffic characteristics required for the study of traffic loading on bridges.

- To analyse the critical loading situations due to imposed traffic on existing bridges under various traffic conditions.

- To perform this analysis for a number of effects (moment and shear), bridge configurations (i.e. different bridge type and length) and traffic configurations (i.e. unidirectional and bi-directional)

- To develop site-specific simplified models able to reproduce the critical loading situations previously observed; these models should be accurate, easily applied and robust.

- To assess the respective influence of two of the main parameters characterising a type of traffic (traffic intensity and traffic weight) on the severity of traffic loading on bridges.

- To obtain the characteristic values for a number of load effects, bridge lengths and traffic types.

1.5 OUTLINE OF THE THESIS

Finally, having defined the aims of this research, the organisation of the thesis is now outlined. In **Chapter 2**, probability concepts and statistical inference are presented; these are fundamental notions that will be used throughout this thesis and need to be addressed with respect to the subject of bridge loading. **Chapter 3** is concerned with a thorough examination of the literature covering three subjects directly related to this research: the historical development of models for live loads on road and bridges, the use of Weigh-In-Motion (WIM) data and the prediction of extreme effects. In **Chapter 4**, the WIM data used throughout this thesis is described in detail, in terms of traffic intensity, gross vehicle weights (GVW) and truck geometry. Then the static effects of traffic actions are illustrated and the new concept of influence response is introduced. Finally, the traffic characteristics necessary for the development of a live load model (e.g. weight distribution, truck geometry) are modelled. These modelled characteristics are used in the two main programs introduced in **Chapter 5**: one generates traffic files based upon the knowledge of site-specific traffic characteristics, while the other simulates the passage of all the vehicles

contained in a traffic file over a bridge and simultaneously calculates the effects induced in the structure. **Chapter 6** deals with the case of bi-directional traffic on relatively short bridges (20 to 40 m). Using the program presented earlier, full simulations are performed for a number of traffic types; from the results of these simulations typical critical loading situations are derived. A site-specific simplified model aiming at reproducing these critical loading events is then developed; the model requires a knowledge of site characteristics such as the traffic intensity and weight distribution. A comparative study of the extrapolated values is also presented; the influence of a number of parameters (e.g. traffic intensity and weight) is assessed for various bridge configurations. **Chapter 7** is concerned with unidirectional traffic. The process followed is identical: full simulations, then derivation of typical critical loading situations and finally modelling of these through three simplified models. The findings and achievements of this research are finally summarised in **Chapter 8** and future developments are suggested.

Chapter 2

PROBABILITY CONCEPTS

AND

STATISTICAL INFERENCE

Chapter 2 PROBABILITY CONCEPTS AND STATISTICAL INFERENCE

2.1 INTRODUCTION

Probability and statistics are related fields. In problems in probability, statements are made about chances that various events will take place, based on an assumed model, whereas in problems in statistics some observed data is available and one wishes to determine a model that can be used to describe the data (Hahn & Shapiro 1967). Both situations arise frequently in engineering. For example, one may wish to predict the performance of a system of known design, before building it, by assuming various models for the components that make up the system. This requires application of the techniques of probability theory. On other occasions test data on the performance of a system are given. Statistical techniques are then used to construct an appropriate model and to estimate its parameters. Once a model is obtained, it may, of course, be used to predict future performance.

2.2 ELEMENTS OF PROBABILITY THEORY

2.2.1 Sample space and events

Probability refers to the likelihood of occurrence of an event relative to other events; in other words, each event has more than one possibility of occurrence (implicitly at least), otherwise the problem would be deterministic. For quantitative purposes, the probability of an event can be considered as a numerical measure of the likelihood of occurrence of that event relative to the set of all alternative events. Accordingly, the first requirement in the formulation of a probabilistic problem is the determination of the set of all possibilities (i.e., the *possibility space* or *sample space*) and the *event* of interest. Therefore, every problem is defined with reference to a specific probability space (containing more than one possibility), and events are composed of one or more possible outcomes within this

possibility space. Furthermore the probability of an event depends on the probabilities of the individual outcomes within a given possibility space. In order to calculate the probability of an event, a basis for assigning probability measures to the various possible outcomes is necessary. The assignment may be based on prior conditions, deduced on the basis of prescribed assumptions or based on the results of empirical observations.

2.2.2 Terminology

As mentioned above, the set of all possibilities in a probabilistic problem is collectively a *sample space*, and each of the individual possibilities is a *sample point*. An *event* then is defined as a subset of the sample space. Sample spaces may be *discrete* or *continuous*. In the discrete case, the sample points are individually discrete entities and countable; in the continuous case, the sample space is composed of a continuum of sample points. A discrete sample space may be *finite* (that is, composed of a finite number of sample points) or *infinite* (that is, with a countably infinite number of sample points). In a continuous sample space, the number of sample points is infinite. Whether a sample space is discrete or continuous, however, an event is always a subset of the appropriate space; therefore an event always contains one or more sample points (unless it is an impossible event), and the realisation of any of these sample points constitutes the occurrence of the corresponding event.

2.2.3 Combination of events

In many practical problems, the event of interest may be some combination of other events. There are two basic ways that events may be combined or derived from other events: by union or intersection. Consider two events E_1 and E_2: the union of E_1 and E_2, denoted $E_1 \cup E_2$, is another event that means the occurrence of E_1 or E_2, or both. In other words, $E_1 \cup E_2$ is the subset of sample points that belong to E_1 or E_2 (in set theory, "or" is used in an inclusive sense, which means "and/or"). The intersection of E_1 and E_2, denoted $E_1 \cap E_2$, (or simply E_1E_2), is an event that means the joint occurrence of E_1 and E_2; in other words, E_1E_2 is the subset of sample points belonging to both E_1 and E_2. If the occurrence of one event precludes the occurrence of another event, then the two events are

mutually exclusive. The intersection of two mutually exclusive events E_1 and E_2, therefore, is an impossible event; that is, $E_1 E_2 = \varnothing$. Three or more events are mutually exclusive if the occurrence of one precludes the occurrence of all others. Finally, two or more events are collectively exhaustive if the union of all these events constitute the underlying sample space.

2.2.4 Mathematics of probability

The notation $P(E)$ is used to denote the probability of an event E. The three following axioms are the basic assumptions of the mathematical theory of probability (e.g. Benjamin & Cornell 1970, Ang & Tang 1975).

Axiom 1 - For every event E in a sample S, there is a probability *P(E)*:

$$0 \le P(E) \le 1$$ **Equation 2-1**

Axiom 2 - The probability of the certain event S is unity:

$$P(S) = 1.0$$ **Equation 2-2**

Axiom 3 - For two events E1 and E2 that are mutually exclusive,

$$P(E_1 \cup E_2) = P(E_1) + P(E_2)$$ **Equation 2-3**

From the aforementioned axioms, it can shown that

$$P(\overline{E}) = 1 - P(E)$$ **Equation 2-4**

where $\overline{E}$ is the complement of E. More generally, if E_1 and E_2 are not mutually exclusive, then

$$P(E_1 \cup E_2) = P(E_1) + P(E_2) - P(E_1 E_2)$$ **Equation 2-5**

The probability of an event may depend on the occurrence (or non-occurrence) of another event. If this dependence exists, the associated probability is a conditional probability. The *conditional probability of E1 given E2* is given as

$$P(E_1 \mid E_2) = \frac{P(E_1 E_2)}{P(E_2)}$$ **Equation 2-6**

If the occurrence (or non-occurrence) of one event does not affect the probability of another event, the two events are statistically independent. Therefore, if E_1 and E_2 are statistically independent, $P(E_1 \mid E_2) = P(E_1)$ and $P(E_2 \mid E_1) = P(E_2)$. The probability of the joint event $E_1 E_2$ is $P(E_1 E_2) = P(E_1 \mid E_2)\, P(E_2)$ or $P(E_1 E_2) = P(E_2 \mid E_1)\, P(E_1)$. If E1 and E2 are *statistically independent events*, then this multiplication rule becomes

$$P(E_1 E_2) = P(E_1)\, P(E_2)$$ **Equation 2-7**

Although straightforward, the above equations and axioms have been included, as they will be used later in the derivation of the formula to predict the number of meeting events on a bridge as a function of the flow rates (for two opposing lanes of traffic).

2.3 ANALYTICAL MODELS OF RANDOM PHENOMENA

2.3.1 Random variables and distributions

Most civil-engineering problems deal with quantitative measures. Thus in the familiar deterministic formulations of engineering problems, the concepts of mathematical variables and functions of variables have proved to be useful substitutes for quantitative characterizations. Such is also the case in the probabilistic models, where the variable is referred to as *random variable*. It is a numerical variable whose specific value cannot be predicted with certainty before an experiment. The behaviour of a random variable is described by its *probability distribution* (or *probability law*).

If X is a random variable, its probability distribution can always be described by its *cumulative distribution function* (CDF), which is

$$F_X(x) \equiv P(X \leq x) \quad \textit{for all } x$$ **Equation 2-8**

A standard notation is to denote a random variable with a capital letter, and its value with the corresponding lowercase letter. For a discrete random variable X, its probability distribution may also be described in terms of *probability mass function* (PMF), which is simply a function expressing $P(X = x)$ for all x. However, if X is continuous, probabilities are associated with intervals on the real line (since events are defined as intervals on the real line); consequently, at a specific value of X, such as $X = x$, only the *density of probability* is defined. Thus, for a continuous random variable, the probability law may also be described in terms of *probability density function* (PDF), so that if $f_X(x)$ is the PDF of X, the probability of X in the interval $(a,b]$ is

$$P(a < X \leq b) = \int_a^b f_X(x)\, dx \qquad \textbf{Equation 2-9}$$

It follows then that the corresponding distribution function is

$$F_X(x) = P(X \leq x) = \int_{-\infty}^{x} f_X(\xi)\, d\xi \qquad \textbf{Equation 2-10}$$

Accordingly, if $F_X(x)$ has a first derivative, then, from Equation 2-10,

$$f_X(x) = \frac{dF_X(x)}{dx} \qquad \textbf{Equation 2-11}$$

It is important to remember that $f_X(x)$ is not a probability; however, $f_X(x)\, dx = P(x < X \leq x + dx)$ is the probability that values of X will be in the interval $(x, x + dx]$.

It should also be emphasized that any function used to represent the probability distribution of a random variable must necessarily satisfy the axioms of probability (see 2.2.4 Mathematics of probability). For this reason, the function must be non-negative and the probabilities associated with all possible values of the random variable must add up to 1.0. In other words, if $F_X(x)$ is the distribution function of X, then it must have the following properties:

- $F_X(-\infty) = 0$; $F_X(+\infty) = 1.0$
- $F_X(x) \geq 0$, and is non-decreasing with x

- it is continuous with x.

2.3.2 Main description of a random variable

Because of the very nature of a random variable it is not possible to predict the exact value that it will assume in any particular experiment, but a complete description of its behaviour is contained in its probability law, as presented in the CDF (or PDF) of the variable. This complete information can be communicated only by stipulating an entire function, e.g., the PDF. In many situations this much information may not be necessary or available. More concise descriptors, summarizing only the dominant features of the behaviour of a random variable, are often sufficient. One or more simple numbers are used in place of a whole probability density function. These numbers usually take the form of weighted averages of certain functions of the random variable. The weights used are the PMF or the PDF, and the average is called the *mathematical expectation* of the function.

Mathematical expectation – The notion of a weighted average or expected value can be generalized for a function X. The expectation of a continuous function $g(X)$ of a real variable X, with respect to the probability function $P[.]$, is denoted $E[g(X)]$. Given a function $g(X)$, and when the probability function $P[.]$ is specified by a probability density function $f(.)$, its expected value is given by:

$$E[g(X)] = \int_{-\infty}^{+\infty} g(x) f_X(x) dx \qquad \textbf{Equation 2-12}$$

Mean or expected value (a central value) – The mean describes the central tendency of a random variable. For a continuous random variable X with PDF $f_X(x)$, the mean value is

$$E[X] = \mu_X = \int_{-\infty}^{+\infty} x\, f_X(x) dx \qquad \textbf{Equation 2-13}$$

Variance and standard deviation (measures of dispersion) – The most common and most useful measure of the dispersion of a random variable is the *variance* σ_X^2, that is, the

quantity that gives a measure of how closely the values of the variate are clustered (or conversely, how widely they are spread) around the central value. For a continuous random variable X with PDF $f_X(x)$, the variance is

$$Var(X) = \sigma^2 = \int_{-\infty}^{+\infty} (x - \mu_X)^2 \, f_X(x) dx \qquad \textbf{Equation 2-14}$$

It can be observed that this is simply the weighted average of squared deviations, or in accordance with Equation 2-12, it is the mathematical expectation of $g(x) = (X - \mu_X)^2$. Dimensionally, a more convenient measure of dispersion is the positive square root of the variance, or the *standard deviation* σ_X; that is

$$\sigma_X = \sqrt{\sigma_X{}^2} = (+)\left[\int_{-\infty}^{+\infty} (x - \mu_X)^2 \, f_X(x) dx\right]^{\frac{1}{2}} \qquad \textbf{Equation 2-15}$$

Moments – For any integer $n = 1,2,...,$ the expectation of $g(X) = X^n$ with respect to a probability law, $E[X^n]$, is called the nth *moment of the probability law*. It should be noted that the first moment and the mean of a probability law are the same. For any real number c, and for any integer $n = 1,2,...,$ $E[(X - c)^n]$ is called the nth *moment of the probability law about the point* c. Of especial interest is the case in which c is equal to the mean $E[X]$, in which case it is referred to as the nth *moment of the probability law about its mean* or, more briefly, the nth *central moment of the probability law*. The second central moment is simply the variance of the probability law (Parzen 1960).

It is hard to say, solely on the basis of the variance or standard deviation, whether the dispersion is large or small; for this purpose, the measure of dispersion relative to the central value is more useful. In other words, whether the dispersion is large or small is meaningful only relative to the central value. For this reason, the *coefficient of variation (COV)* δ_X,

$$\delta_X = \frac{\sigma_X}{\mu_X} \qquad \textbf{Equation 2-16}$$

is often preferred and is a convenient non-dimensional measure of dispersion or variability.

Fractile - A further way of summarizing information about a distribution is by its *fractiles*. The εth fractile is that value of the random variable that has a proportion ε of the cumulative distribution below it. Thus, for a continuous random variable with probability density $f_X(x)$, the εth fractile is that point $z(\varepsilon)$ such that

$$\int_{-\infty}^{z(\varepsilon)} f_X(x)dx = \varepsilon \qquad \textbf{Equation 2-17}$$

The term *quantile* is on occasion used instead of fractile. Also the term *percentile* is used frequently to refer to the fractiles when expressed in per cent form.

2.3.3 Bivariate distribution

A sample point may be defined in more than one dimension. Multivariate situations that simultaneously involve two or more functions defined on the same sample space are frequently of interest. For example, in the case of parallel lanes of traffic, it is extremely useful to express the gross vehicle weight of both passing truck and truck being overtaken together. The principal case involves two random variables, namely the *bivariate distribution*. Two continuous random variables, x and y, are said to have the *bivariate (or joint) probability density function* $f_{XY}(x,y)$ if, for two pairs of values (x_1, y_1) and (x_2, y_2),

$$P(x_1 < x \le x_2 \text{ and } y_1 < y \le y_2) = \int_{y_1}^{y_2}\int_{x_1}^{x_2} f_{XY}(x,y)dxdy \qquad \textbf{Equation 2-18}$$

The requirements on $f_{XY}(x,y)$ are

$$f_{XY}(x,y) \ge 0 \quad \text{for all } x \text{ and } y \qquad \textbf{Equation 2-19}$$

and

$$\int_{-\infty}^{+\infty}\int_{-\infty}^{+\infty} f_{XY}(x,y)dxdy = 1.0 \qquad \textbf{Equation 2-20}$$

The *bivariate (or joint) cumulative distribution function* for continuous random variables x and y is defined as

$$F_{XY}(x,y) = P(u \le x \text{ and } v \le y) = \int_{-\infty}^{y}\int_{-\infty}^{x} f_{XY}(u,v)dudv \qquad \textbf{Equation 2-21}$$

It should be noted that the density function is a derivative of the cumulative function, now a partial derivative. Thus, if the partial derivatives exist,

$$f_{XY}(x,y) = \frac{\partial^2 F_{XY}(x,y)}{\partial x \partial y} \qquad \textbf{Equation 2-22}$$

The behaviour of a particular variable irrespective of the other is described by the *marginal probability density function*.

$$f_X(x) = \int_{-\infty}^{\infty} f_{XY}(x,y)dy \qquad \textbf{Equation 2-23}$$

and similarly,

$$f_Y(y) = \int_{-\infty}^{\infty} f_{XY}(x,y)dx \qquad \textbf{Equation 2-24}$$

Finally, if one is given the value of one variable, $Y = b$, say, the relative likelihood of X taking a value in the interval $(x, x+dx]$ is $f_{XY}(x,b)dx$. To yield a proper density function (i.e., one whose integral over all values of x is unity) these values must be renormalised by dividing them by their sum, which is

$$\int_{-\infty}^{\infty} f_{XY}(x,b)dx = f_Y(b) \qquad \textbf{Equation 2-25}$$

Therefore, the *conditional probability density function* of X given Y is given as

$$f_{X|Y}(x \mid y) = \frac{f_{XY}(x,y)}{f_Y(y)} \qquad \textbf{Equation 2-26}$$

The *conditional cumulative distribution* is then defined as

$$F_{X|Y}(x \mid y) = P(X \le x \mid Y = b) = \int_{-\infty}^{x} f_{X|Y}(u,b)du \qquad \textbf{Equation 2-27}$$

The characteristics of a joint density function for two continuous random variables X and Y, and the associated marginal densities, are illustrated in Figure 2-1.

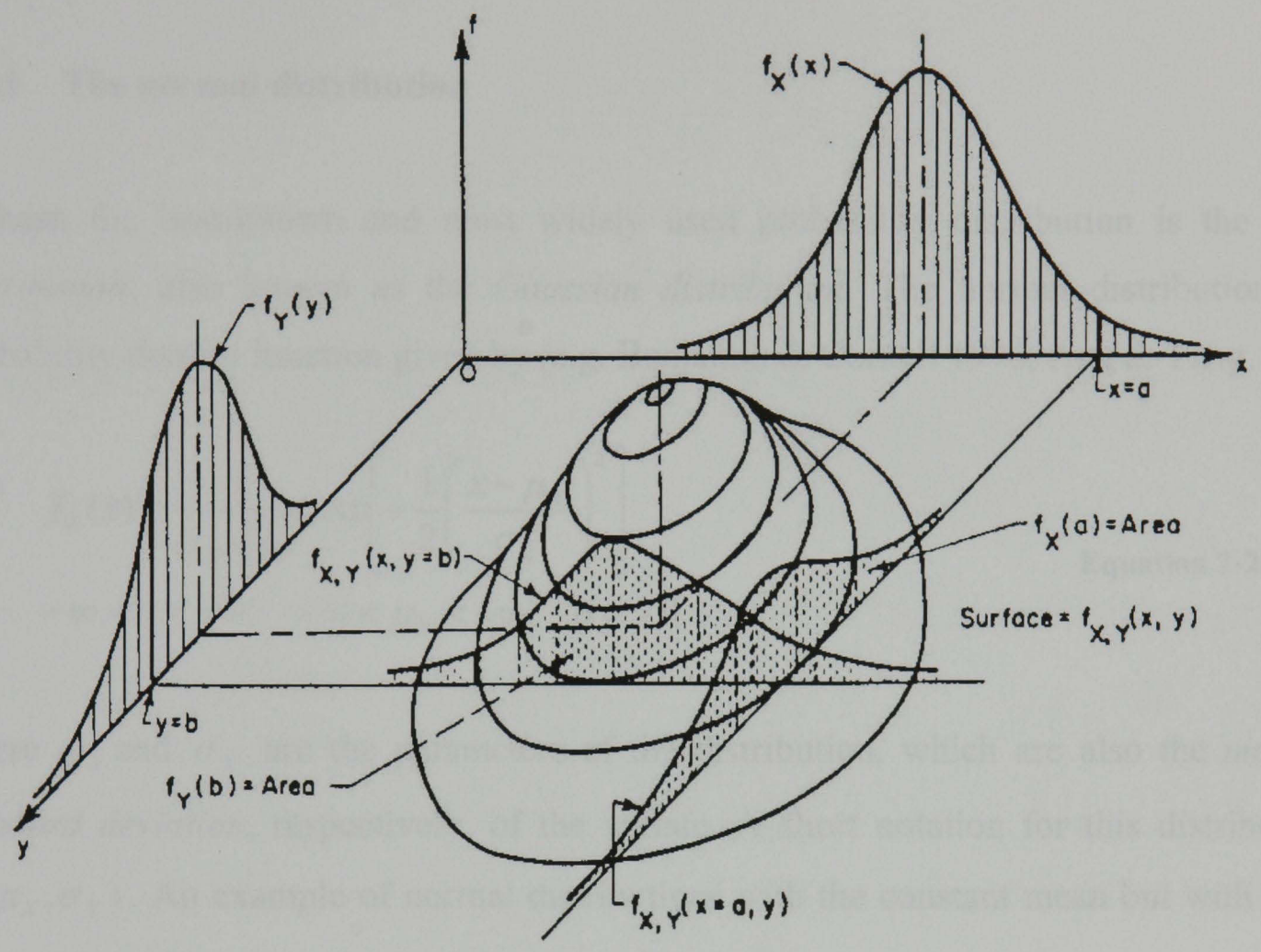

Figure 2-1: Joint and marginal PDF of continuous random variables *X* and *Y* (from Ang & Tang 1975)

2.4 USEFUL PROBABILITY DISTRIBUTIONS

There are a number of discrete and continuous functions that are particularly useful for one or more of the following reasons:

- the function is the result of an underlying physical process and is derived on the basis of certain physically reasonable assumptions;
- the function is the result of some limiting process;
- it is widely known and the necessary statistical information (including probability tables) is available widely.

Several of these probability distribution functions are presented, and their special properties described, in this section. All these distributions have been widely used in traffic modelling and traffic load modelling (e.g. gross vehicle weight distribution, distribution for arrivals of vehicle, extrapolation of extreme effects, etc.) by the author and/or by others. The use of the various distributions presented herein is discussed in details in later chapters.

2.4.1 The normal distribution

Perhaps the best-known and most widely used probability distribution is the *normal distribution*, also known as the *Gaussian distribution*. The normal distribution has a probability density function given by (e.g. Benjamin & Cornell 1970, Ang & Tang 1975):

$$f_X(x) = \frac{1}{\sigma_X \sqrt{2\pi}} \exp\left[-\frac{1}{2}\left(\frac{x-\mu_X}{\sigma_X} \right)^2 \right] \qquad \textbf{Equation 2-28}$$

$$-\infty < x < +\infty; \quad -\infty < \mu_X < +\infty; \quad \sigma_X > 0$$

where μ_X and σ_X are the parameters of the distribution, which are also the *mean* and *standard deviation*, respectively, of the variate. A short notation for this distribution is $N(\mu_X, \sigma_X)$. An example of normal distributions with the constant mean but with various values of standard deviation is illustrated in Figure 2-2.

The standard normal deviation – A normal distribution with parameters $\mu = 0$ and $\sigma = 1.0$ is known as the *standard normal* distribution and is denoted appropriately as $N(0,1)$. The density function, accordingly, is:

$$f_S(s) = \frac{1}{\sqrt{2\pi}} \exp\left[-(1/2)s^2 \right] \quad -\infty < s < +\infty \qquad \textbf{Equation 2-29}$$

Because of its wide usage, a special notation $\phi(s)$ is commonly used to designate the distribution function of the *standard normal variate* S; that is, $\phi(s) = F_S(s)$, where S has $N(0,1)$ distribution.

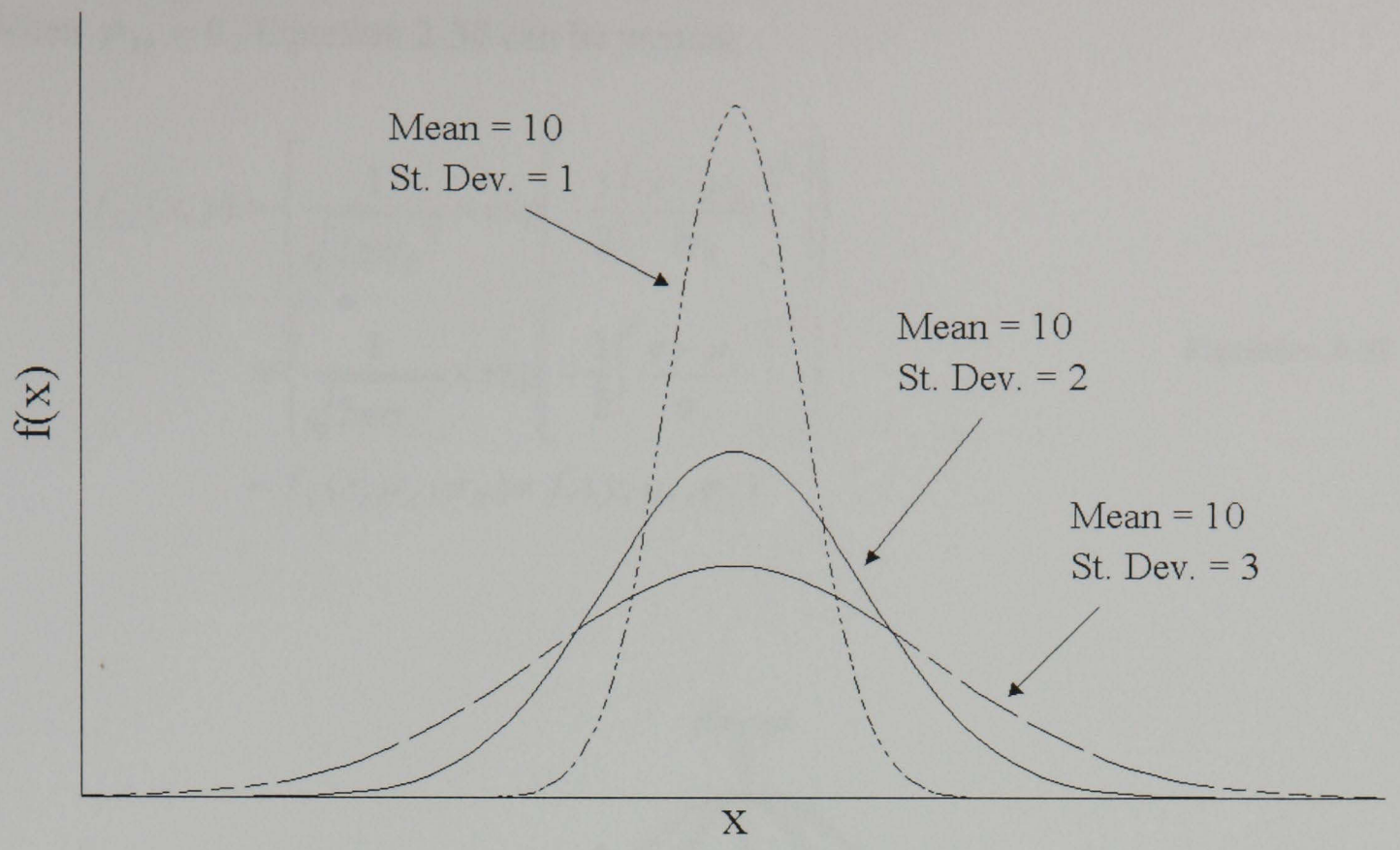

Figure 2-2: PDF of the normal distribution for different values of standard deviation and constant value for the mean

Bivariate normal distribution - The *bivariate normal density function* of two continuous random variables X and Y is given by:

$$f_{XY}(x,y) = \frac{1}{2\pi\sigma_X\sigma_Y\sqrt{1-\rho_{XY}^{\ 2}}}\cdot$$

$$\exp\left[\frac{-1}{2\left(1-\rho_{XY}^{\ 2}\right)}\left\{\begin{array}{l}\left(\frac{x-\mu_X}{\sigma_X}\right)^2+\left(\frac{y-\mu_Y}{\sigma_Y}\right)^2\\ -2\rho_{XY}\left(\frac{x-\mu_X}{\sigma_X}\right)\left(\frac{y-\mu_Y}{\sigma_Y}\right)\end{array}\right\}\right] \qquad \textbf{Equation 2-30}$$

$$-\infty < x < +\infty; -\infty < y < +\infty;$$

$$-\infty < \mu_X < +\infty; -\infty < \mu_Y < +\infty;$$

$$\sigma_X > 0; \sigma_Y > 0; -1 \le \rho_{XY} \le +1$$

where $\mu_X, \mu_Y, \sigma_X, \sigma_Y, \rho_{XY}$ are the five parameters characterizing the function; ρ_{XY} is the *correlation coefficient* between X and Y. A typical bivariate normal distribution is illustrated in Figure 2-3. It should be noticed that the coefficient of correlation is a standardised measure of the **linear relationship** between two variates. Thus, although independence implies zero correlation, the reverse is not true: zero correlation does not **in general** imply independence for jointly distributed variates.

When $\rho_{XY} = 0$, Equation 2-30 can be written

$$f_{XY}(x,y) = \left\{ \frac{1}{\sqrt{2\pi\sigma_X{}^2}} \times \exp\left[-\frac{1}{2}\left(\frac{x-\mu_X}{\sigma_X} \right)^2 \right] \right\}$$
$$\times \left\{ \frac{1}{\sqrt{2\pi\sigma_Y{}^2}} \times \exp\left[-\frac{1}{2}\left(\frac{y-\mu_Y}{\sigma_Y} \right)^2 \right] \right\} \qquad \textbf{Equation 2-31}$$
$$= f_X(x;\mu_X,\sigma_X) \times f_Y(y;\mu_Y,\sigma_Y)$$

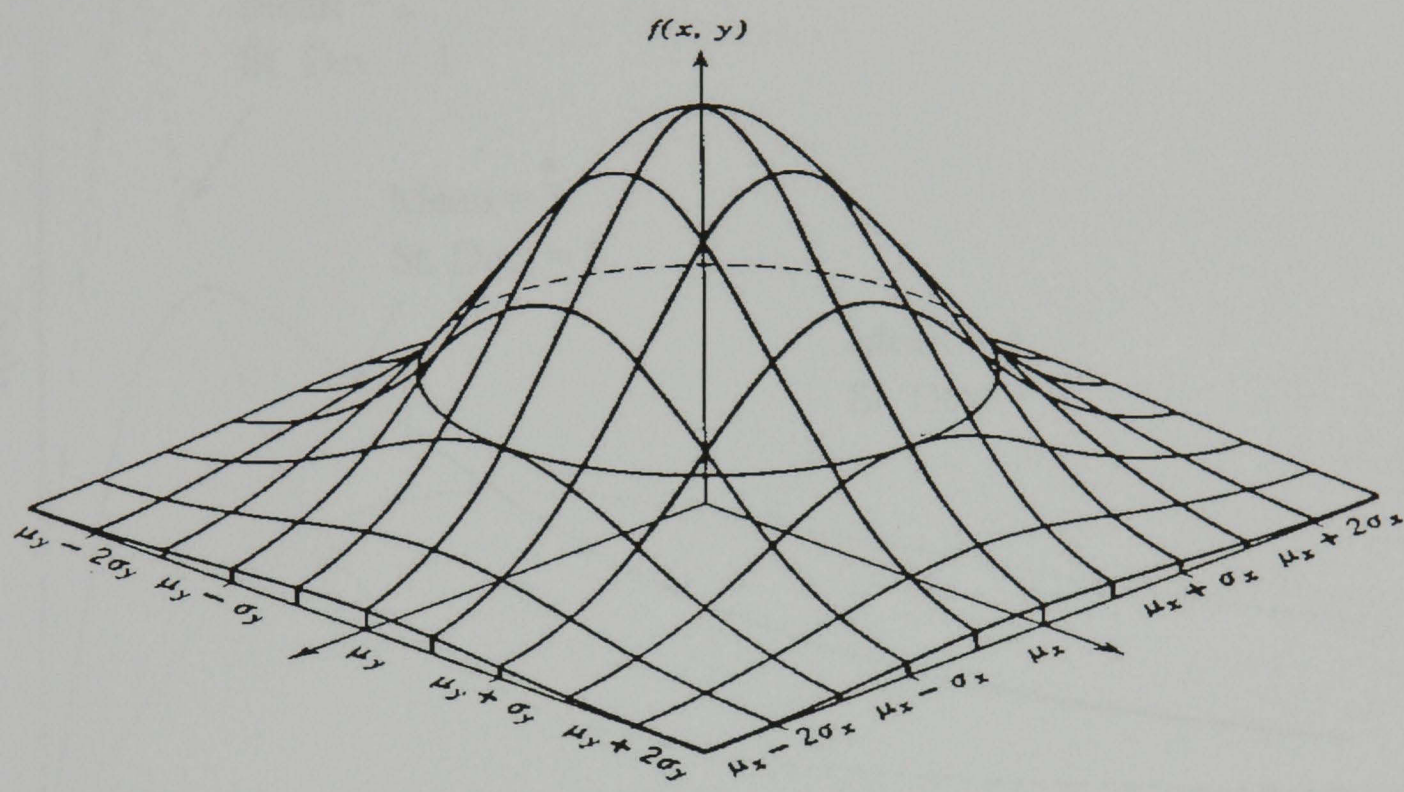

Figure 2-3: Bivariate normal density function (from Hahn & Shapiro 1967)

2.4.2 The logarithmic normal (*lognormal*) distribution

A random variable X has a logarithmic normal probability distribution if $\ln(X)$ (the natural logarithm of X) is normal, that is $\ln(X) = N(\mu,\sigma)$. In this case, the density function of X is (Saporta 1990):

$$f_X(x) = \frac{1}{\sigma\sqrt{2\pi x}} \exp\left[-\frac{1}{2}\left(\frac{\ln x - \mu}{\sigma} \right)^2 \right] \qquad \textbf{Equation 2-32}$$
$$0 \le x; -\infty < \mu < +\infty; \sigma > 0$$

where

$$E(X) = \exp\left(\mu + \frac{\sigma^2}{2}\right)$$
$$Var(X) = \exp\left(2\mu + \sigma^2\right)\left(\exp\sigma^2 - 1\right)$$

Equation 2-33

Examples of lognormal distributions are presented in Figure 2-4.

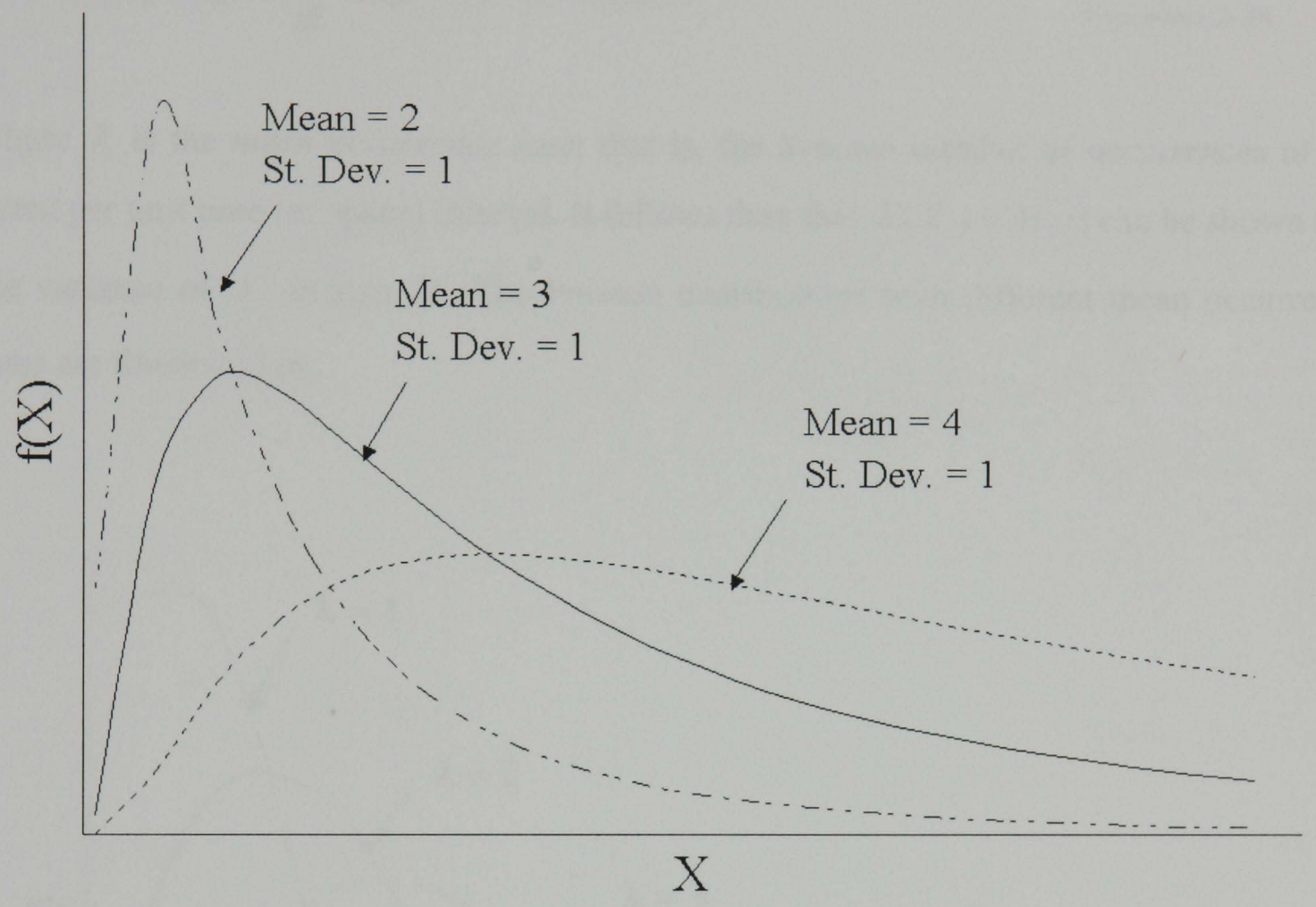

Figure 2-4: PDF of lognormal distribution for various mean values and constant standard deviation

2.4.3 The Poisson process and the Poisson distribution

The Poisson process is based on the following assumptions (Benjamin & Cornell 1970, Ang & Tang 1975):

- an event can occur at random and at any time or any point in space
- the occurrence(s) of an event in a given time (or space) interval is independent of that in any other non-overlapping intervals – assumption of **independence**
- the probability of occurrence of an event in a small interval Δt is proportional to Δt, and can be given by $\lambda\Delta t$, where λ is the mean rate of occurrence of the event (assumed to be constant) – assumption of **stationarity** ; and the probability of two

or more occurrences in Δt is negligible (i.e., of higher orders of Δt) – assumption of **non-multiplicity**.

On the basis of these assumptions, the number of occurrences of an event in t is given by the *Poisson distribution*; that is, if X_t is the number of occurrences in time (or space) interval t, then

$$P(X_t = x) = \frac{(\lambda t)^x}{x!}\exp(-\lambda t) \quad x = 0,1,2,... \qquad \textbf{Equation 2-34}$$

where λ is the *mean occurrence rate*; that is, the average number of occurrences of the event per unit time (or space) interval. It follows then that $E(X_t) = \lambda t$; it can be shown that the variance of X_t is also λt. The Poisson distributions with different mean occurrence rates are illustrated in .

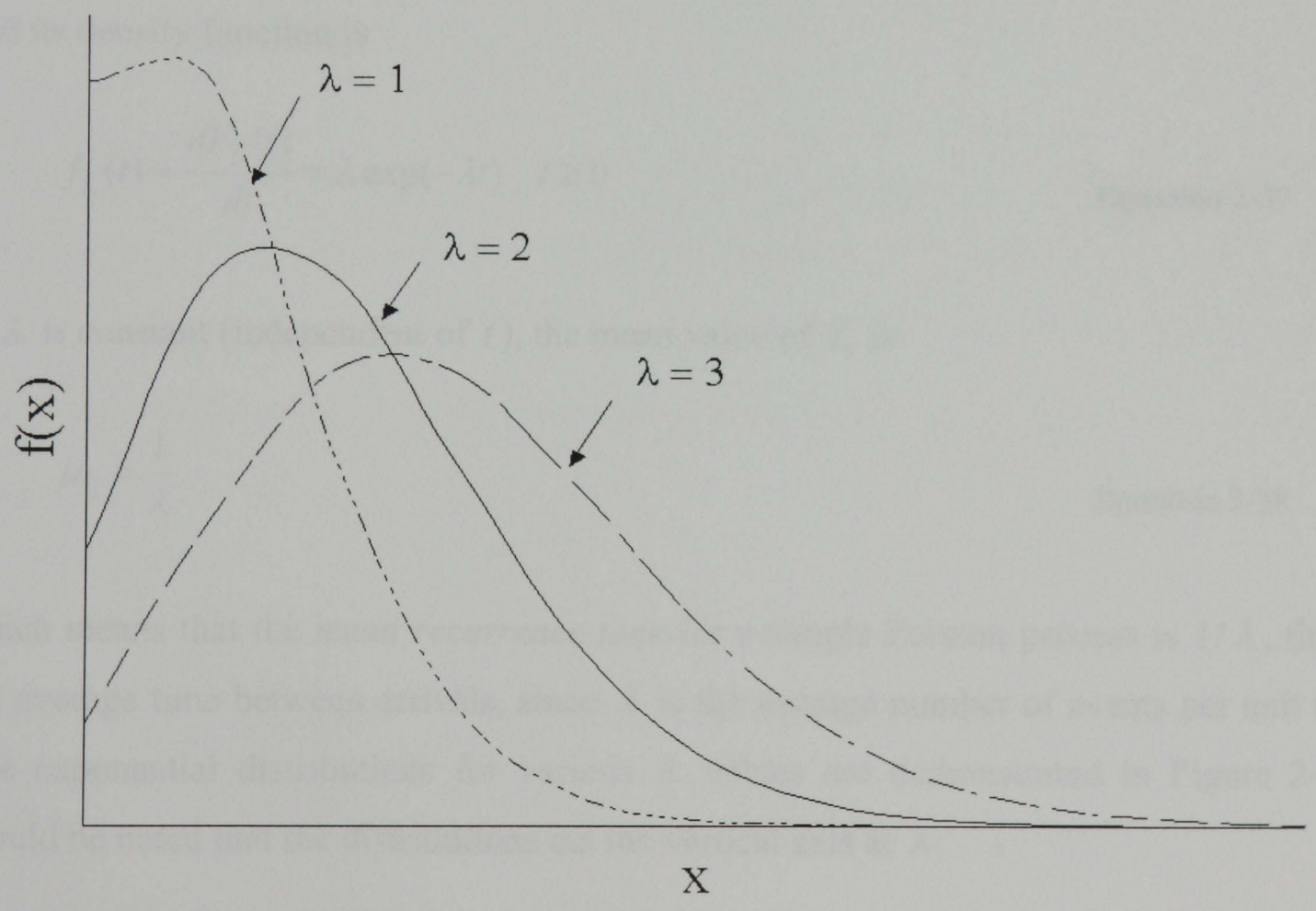

Figure 2-5: PDF of the Poisson distribution for different mean occurrence rate values

2.4.4 The exponential distribution

The *exponential distribution* (also known as the *negative exponential*) is related to the Poisson process as follows. If events occur according to a Poisson process, then the time T_1 until the first occurrence of the event has an exponential distribution. It is observed that $T_1 > t$ means that no event occurs in time t; hence, according to Equation 2-34,

$$P(T_1 > t) = P(X_t = 0) = \exp(-\lambda t)$$ **Equation 2-35**

T_1 is the *first occurrence time* in a Poisson process. However, since the occurrences of an event in non-overlapping time intervals in a Poisson process are statistically independent, T_1 is also the *recurrence time* or time between two consecutive occurrences of the event. The distribution function of T_1, therefore, is

$$F_{T_1}(t) = P(T_1 \le t) = 1 - \exp(-\lambda t)$$ **Equation 2-36**

and its density function is

$$f_{T_1}(t) = \frac{dF_{T_1}(t)}{dt} = \lambda \exp(-\lambda t) \quad t \ge 0$$ **Equation 2-37**

If λ is constant (independent of t), the mean value of T_1 is

$$\mu_{T_1} = \frac{1}{\lambda}$$ **Equation 2-38**

which means that the *mean recurrence time* for a simple Poisson process is $1/\lambda$, that is, the average time between arrivals, since λ is the average number of events per unit time. The exponential distributions for various λ values are demonstrated in Figure 2-6; it should be noted that the distributions cut the vertical axis at λ.

Due to the stationarity and independence properties of the Poisson process, $\exp(-vt)$ is the probability of no events in *any* interval of time of length t, whether or not it begins at time 0. In other words, the *inter-arrival* times of a Poisson process are independent and exponentially distributed. The Poisson process is often said to be "memory less", meaning that future behaviour is independent of its present or past behaviour.

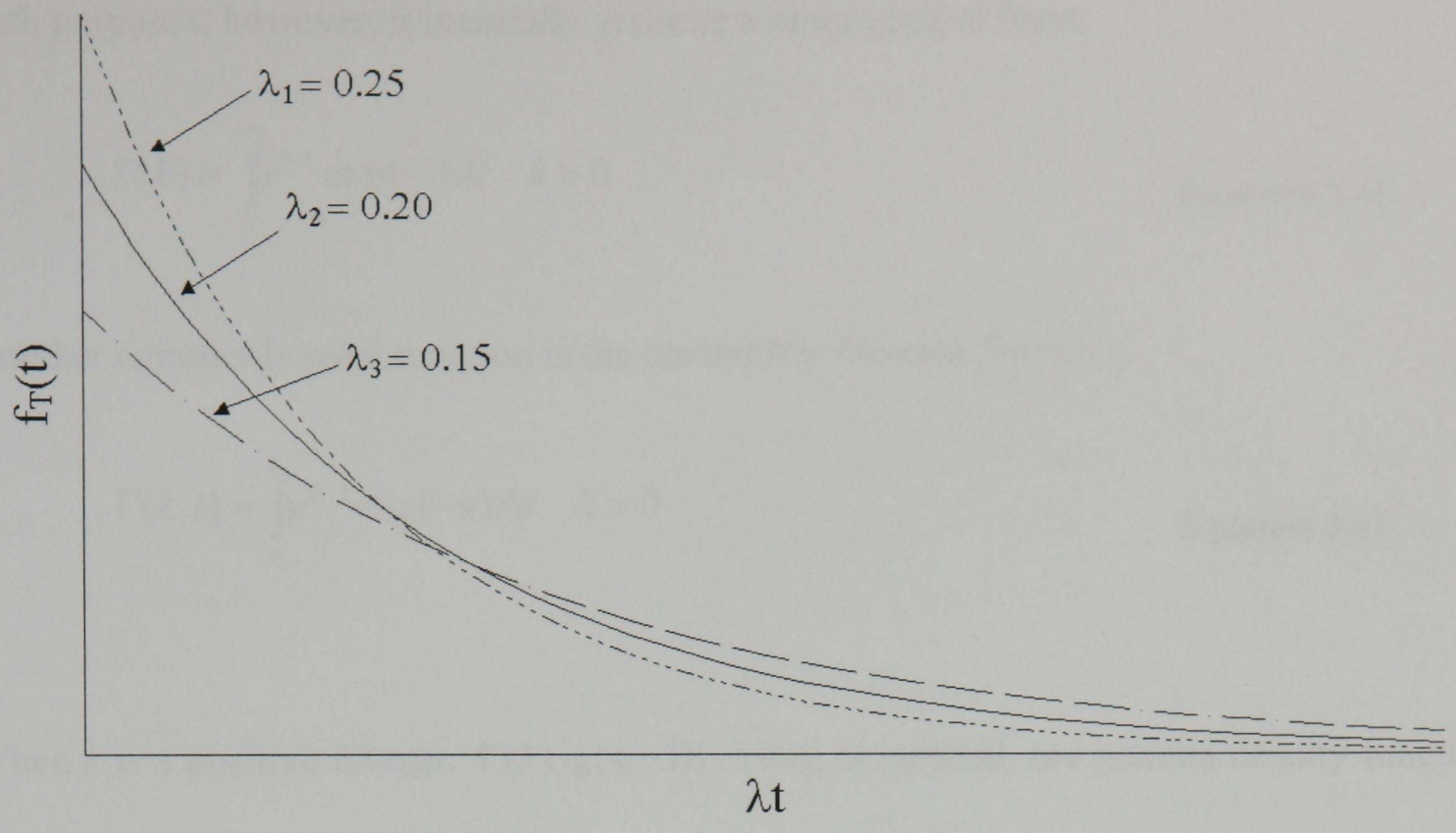

Figure 2-6: PDF of the exponential distribution for different λ values

2.4.5 The Gamma distribution

If the occurrence of an event constitutes a Poisson process, then the time until the *k*th occurrence of the event is described by the *gamma probability distribution*. Let T_k denote the time until the kth event; then $T_k \le t$ means that k or more events occur in time t. Hence, on the basis of Equation 2-34, the distribution function of T_k is (Benjamin & Cornell 1970, Ang & Tang 1975):

$$F_{T_k}(t) = \sum_{x=k}^{\infty} P(X_t = x)$$
$$= 1 - \sum_{x=0}^{k-1} \left(\frac{(\lambda t)^x}{x!} \exp(-\lambda t) \right) \qquad \textbf{Equation 2-39}$$

The corresponding density function is:

$$f_{T_k}(t) = \frac{\lambda(\lambda t)^{k-1}}{(k-1)!} \exp(-\lambda t) \quad t \ge 0 \qquad \textbf{Equation 2-40}$$

The gamma distribution is useful also as a general-purpose probability distribution. For such purposes, however, it is usually given in a more general form:

$$\Gamma(k) = \int_0^{+\infty} t^{k-1} \exp(-t)dt \quad k > 0$$

Equation 2-41

Another commonly used function is the *incomplete Gamma function*:

$$\Gamma(k,t) = \int_0^{t} u^{k-1} \exp(-u)du \quad k > 0$$

Equation 2-42

When k is a positive integer, $\Gamma(k) = (k-1)!$. Thus, in general, the gamma density function is:

$$f_T(t) = \frac{\lambda(\lambda t)^{k-1}}{\Gamma(k)} \exp(-\lambda t) \quad t \geq 0$$

Equation 2-43

Figure 2-7 illustrates the gamma distribution for various λ values and with constant k values. It should be emphasized that λ can be interpreted as the scale parameter and k as the shape parameter.

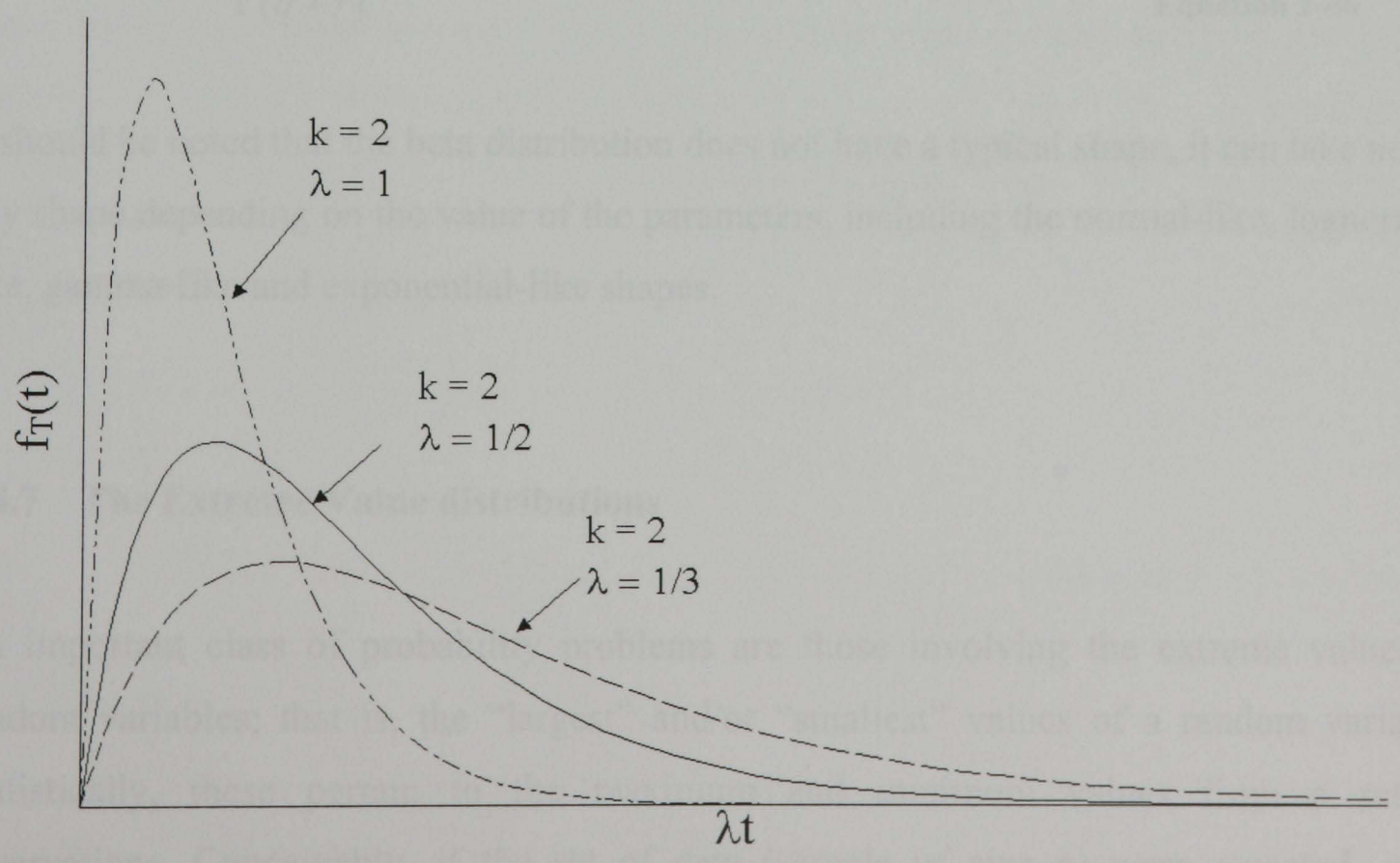

Figure 2-7: PDF of the gamma distribution for different λ values and with same k values

When k is restricted to integers, the gamma distribution is referred to as the *Erlang distribution* (Benjamin & Cornell 1970, Ang & Tang 1975). The exponential distribution is a gamma distribution with $k=1$, as illustrated previously.

2.4.6 The Beta distribution

Finally, a probability distribution appropriate for a random variable whose values are bounded, say between finite limits a and b, is the *beta distribution*. The density function of such a distribution is (Benjamin & Cornell 1970, Ang & Tang 1975):

$$f_X(x) = \frac{1}{B(q,r)} \frac{(x-a)^{q-1}(b-x)^{r-1}}{(b-a)^{q+r-1}} \quad a \le x \le b$$
$$= 0 \quad \textit{elsewhere}$$

Equation 2-44

in which q and r are parameters of the distribution, and $B(q,r)$ is the *beta function*:

$$B(q,r) = \int_0^1 x^{q-1}(1-x)^{r-1}\,dx$$

Equation 2-45

which is related to the Gamma distribution as follows:

$$B(q,r) = \frac{\Gamma(q)\Gamma(r)}{\Gamma(q+r)}$$

Equation 2-46

It should be noted that the beta distribution does not have a typical shape, it can take nearly any shape depending on the value of the parameters, including the normal-like, lognormal-like, gamma-like and exponential-like shapes.

2.4.7 The Extreme Value distributions

An important class of probability problems are those involving the extreme values of random variables; that is, the "largest" and/or "smallest" values of a random variable. Statistically, these pertain to the maximum and minimum values from a set of observations. Conceivably, if the set of data (sample of size n) were repeated, other maximum and minimum values will be obtained; thus, the possible largest and smallest

values comprise populations of their own. Therefore, these extreme values may also be modelled as random variables with respective probability distributions. Such distributions and their associated parameters have special characteristics that are unique to the extreme values. The subject of the statistics of the largest and smallest values is a subtopic within the broader subject of *order statistics*, that is, the statistics of the kth value from the maximum or minimum value.

The prediction of future conditions is often required in engineering planning and design, and may involve the prediction of the largest (or smallest) value. Extrapolation from previously observed extreme value data, is therefore necessary; for this purpose the asymptotic theory of statistical extremes often provides a powerful basis for developing the required engineering information. It is of interest and practical significance that the asymptotic form of an extremal distribution does not depend on the exact form of the initial distribution; rather it depends largely on the tail behaviour of the initial distribution in the direction of the extreme. The central portion of the initial distribution has little influence on the asymptotic form of the extremal distribution; the extremal parameters, however, will depend on the form of the initial distribution. A more detailed discussion is presented in the following chapter, in the section 'Prediction of extreme values'; this paragraph is merely an introduction to the subject with a brief description of the three distributions of extremes.

The Gumbel distribution

The extreme value from an initial distribution with an exponentially decaying tail (in the direction of the extreme) will converge asymptotically to the type I limiting form, that is the double exponential form. The Gumbel cumulative density function for maxima is given by

$$F(x) = \exp\left[-\exp\left(\frac{-(x-\lambda)}{\delta}\right)\right] \quad -\infty < x < +\infty; \delta > 0 \qquad \textbf{Equation 2-47}$$

where λ and δ are constants known as the location and scale parameters, respectively.

The Weibull distribution

If the extreme value is limited, that is, the largest value has a finite upper bound, or the smallest value has a finite lower bound, the corresponding extremal distribution will

converge (for large n) to the type III asymptotic form: the exponential form with upper bound. The Weibull cumulative density function for maxima is given by

$$F(x) = \begin{cases} \exp\left[-\left(\dfrac{\lambda - x}{\delta}\right)^{\beta}\right] & x \le \lambda; \delta > 0; \beta > 0 \\ 1 & otherwise \end{cases}$$

Equation 2-48

where λ, δ and β are constants known as the location, scale and shape parameters, respectively.

The Frechet distribution

If the extreme value from an initial distribution decays with a polynomial tail, it will converge to the Type II asymptotic form: the exponential form. The Frechet cumulative density function for maxima is given by

$$F(x) = \begin{cases} \exp\left[-\left(\dfrac{\delta}{x - \lambda}\right)^{\beta}\right] & x \ge \lambda; \delta > 0; \beta > 0 \\ 0 & otherwise \end{cases}$$

Equation 2-49

where λ, δ and β are constants known as the location, scale and shape parameters, respectively.

2.5 STATISTICAL INFERENCE

2.5.1 Estimating parameters from observational data

Once the distribution function of a random variable and the values of its parameters are known (or assumed), the probabilities associated with events defined by values of the random variable can be computed. The calculated probability is clearly a function of the values of the parameters, as well as of the assumed form of the distribution. From observational data, information about the probability distribution may be inferred, and its parameters estimated statistically. The techniques for deriving probabilistic information and for estimating parameter values from observational data are embodied in the methods

of statistical inference, in which information obtained from sampled data is used to make generalizations about the populations from which the samples were obtained. Figure 2-8 illustrates this concept.

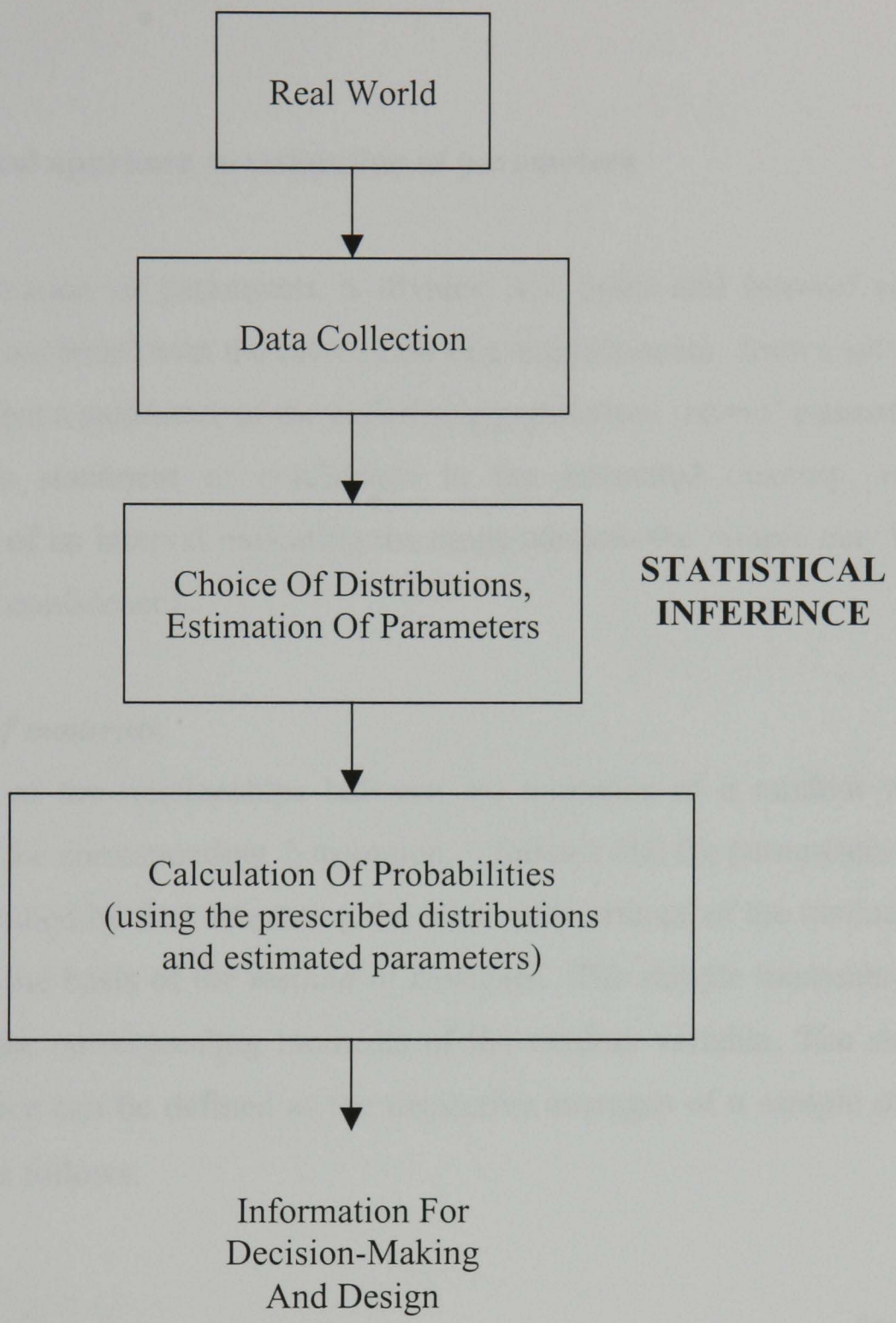

Figure 2-8: Role of statistical inference in decision-making process (Ang &Tang 1975)

It may be emphasised that even when the distribution function and its parameters for a random variable are known, the occurrence (or non-occurrence) of specific events cannot be predicted with certainty. At best, it can be said that an event will occur with an associated probability. The underlying uncertainty, in this case, is due to the inherent randomness of the natural phenomenon. However, uncertainty arises also from the inaccuracies in the estimation of the parameters and in the choice of the distribution. Uncertainties associated with errors of parameter estimation can be reduced by increasing

the amount of data, whereas the uncertainty associated with the inherent variability may remain unchanged or may even increase with additional data. More generally, errors would also include inaccuracies of modelling and prediction. In general, therefore, uncertainty is considered to be the result of (inherent or natural) variability as well as of prediction error.

2.5.2 Classical approach to estimation of parameters

Classical estimation of parameters is divided into *point* and *interval* estimation. Point estimation is concerned with the calculation of a single number, from a set of observational data, to represent a parameter of the underlying population. Interval estimation goes further to establish a statement of confidence in the estimated quantity, resulting in the determination of an interval indicating the range wherein the sample may be located (with the associated confidence).

The method of moments

On the basis of the relationships between the moments of a random variable and the parameters of the corresponding distribution, it follows that the parameters of a distribution may be determined by first estimating the mean and variance of the random variable. This, in essence, is the basis of the *method of moments*. The sample moments may be used as estimates of the corresponding moments of the random variable. The *sample mean* and *sample variance* can be defined as the respective averages of a sample of size n, namely $x_1, x_2, ..., x_n$, as follows:

$$\bar{x} = \frac{1}{n}\sum_{i=1}^{n} x_i \qquad \textbf{Equation 2-50}$$

and

$$s^2 = \frac{1}{(n-1)}\sum_{i=1}^{n}\left(x_i - \bar{x}\right)^2 \qquad \textbf{Equation 2-51}$$

Accordingly, $\bar{x}$ and s^2 are the *point estimates* of the population mean μ and population variance σ^2, respectively.

The method of maximum likelihood

In contrast to the method of moments, the maximum likelihood method provides a procedure for deriving the point estimator of the parameter directly. The likelihood of obtaining a particular sample value can be assumed to be proportional to the value of the probability density function evaluated at that sample value. Then, assuming a random sampling, the likelihood of obtaining *n* independent observations $x_1, x_2, ..., x_n$ is

$$L(x_1, ..., x_n; \theta) = f(x_1; \theta) f(x_2; \theta) ... f(x_n; \theta)$$

Equation 2-52

which is the *likelihood function* of observing the set $x_1, x_2, ..., x_n$. The *maximum likelihood function estimator* $\hat{\theta}$ is then the value of θ that maximises the likelihood function $L(x_1, ..., x_n; \theta)$. This estimator may be obtained by differentiating $L(x_1, ..., x_n; \theta)$ with respect to θ and setting the derivative equal to zero; that is, $\hat{\theta}$ is obtained as the solution to the following equation:

$$\frac{\partial L(x_1, ..., x_n; \theta)}{\partial \theta} = 0$$

Equation 2-53

Because of the multiplicative nature of the likelihood function, it is frequently more convenient to maximize the logarithm of the likelihood function instead; that is,

$$\frac{\partial \log L(x_1, ..., x_n; \theta)}{\partial \theta} = 0$$

Equation 2-54

Interval estimation of the mean

The point estimates obtained in the aforementioned methods do not convey information on the degree of accuracy of these estimates. For this reason, the interval over which a parameter may lie is often used to supplement the point estimate (a single number) of the same parameter. Such intervals are called the *confidence intervals*, and the method of estimation is known as *interval estimation*. In a general case, if we denote $(1-\alpha)$ as the specified confidence levels, and $\pm k_{\alpha/2}$ as the values of the standard normal variate with cumulative probability levels $\alpha/2$ and $(1-\alpha/2)$, respectively, it can be shown that:

$$P\left(\bar{x}-k_{\alpha/2}\frac{\sigma}{\sqrt{n}}<\mu\leq\bar{x}+k_{\alpha/2}\frac{\sigma}{\sqrt{n}}\right)=1-\alpha \qquad \textbf{Equation 2-55}$$

where σ is the known variance and n is the size of the sample. More properly, then, the interval estimated on the basis of a single sample of size n should be interpreted as follows: "There is a confidence of $(1-\alpha)$ that the estimated interval contains the unknown μ". Thus such an interval is called the $(1-\alpha)$ *confidence interval* for the mean μ, and is given by

$$\langle\mu\rangle_{1-\alpha}=\left(\bar{x}-k_{\alpha/2}\frac{\sigma}{\sqrt{n}};\bar{x}+k_{\alpha/2}\frac{\sigma}{\sqrt{n}}\right) \qquad \textbf{Equation 2-56}$$

It can be observed that the confidence interval for the mean depends on the standard deviation σ and on the sample size n. It is clear that as σ decreases or as n increases, the confidence interval becomes narrower for the same confidence level $(1-\alpha)$. This means that smaller population variance or larger sample size would increase the accuracy of the sample mean as the estimator of the population mean.

Using an approach similar to the establishment of the confidence interval for the population mean, the confidence interval for the population variance σ^2 may also be developed.

2.5.3 Empirical determination of distribution models and their validity

The probabilistic characteristics of a random variable phenomenon are sometimes difficult to discern or define. There are occasions when the required probability distribution has to be determined empirically (that is, based entirely on available observational data). If the frequency diagram (or histogram) for a set of data can be constructed, the required distribution may be determined by visually comparing a density function with the frequency diagram. Alternatively, the data may be plotted on *probability papers* prepared for specific distributions. When a theoretical distribution has been assumed, the validity of the assumed distribution may be verified or disproved statistically by goodness-of-fit tests.

Two such tests for distribution are widely available: the *chi-square* (χ^2) and the *Kolmogorov-Smirnov* ($K-S$) tests.

The use, construction and interpretation of probability paper is widely described through the relevant literature (e.g. Castillo 1988, Hahn & Shapiro 1967, Ang & Tang 1975). Figure 2-9 is an illustration of typical plots of extreme data on probability papers. The non-linearity of the data in the right tail on graph (a) means the distribution of GVW cannot be modelled by a Gumbel distribution of extremes; on the other hand, graph (b) shows that the extreme GVW's can be modelled using a Weibull distribution as the tail of the distribution is linear when plotted on Weibull probability paper.

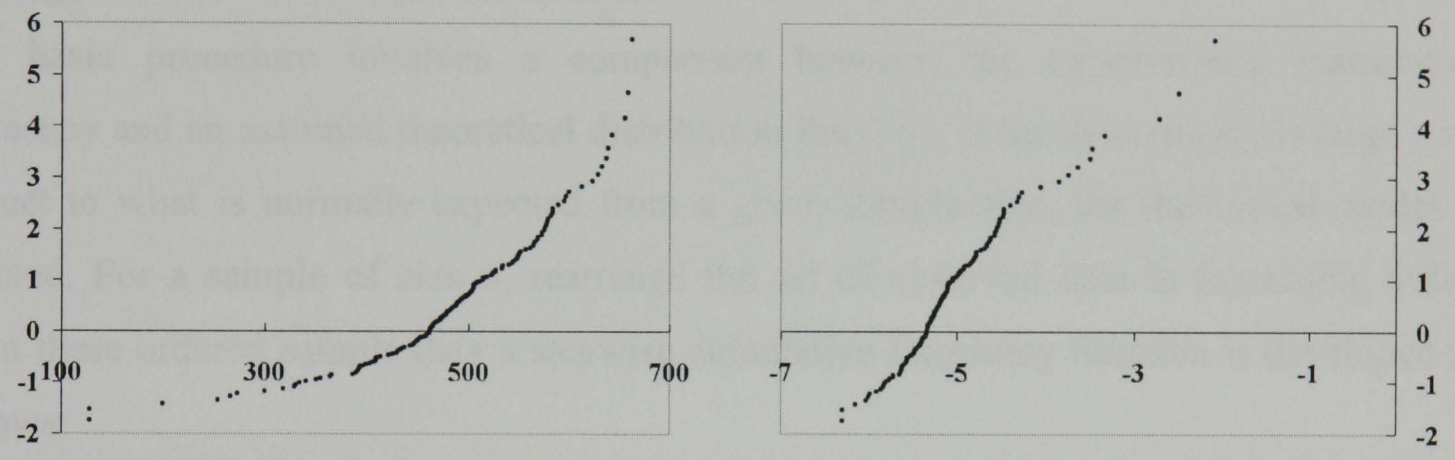

(a) (b)

Figure 2-9: Distribution of GVW (kN) of 6-axle trucks on (a) Gumbel probability paper and (b) Weibull probability paper

Chi-square test for distribution

Consider a sample of n observed values of a random variable. The chi-square goodness-of-fit test compares the observed frequencies $n_1, n_2, ..., n_k$ of k values (or in k intervals) of the variate with the corresponding frequencies $e_1, e_2, ..., e_k$ from an assumed theoretical distribution. The basis for appraising the goodness of this comparison is the distribution of the statistic:

$$\sum_{i=1}^{k} \frac{(n_i - e_i)^2}{e_i} \qquad \textbf{Equation 2-57}$$

which approaches the chi-square distribution with $(f = k-1)$ degrees of freedom as $n \to +\infty$ (Hoel 1962). However, if the parameters of the theoretical model are unknown

and must be estimated from the data, the above statement remains valid if the degree of freedom is reduced by one for every unknown parameter that must be estimated.
On this basis, if an assumed distribution yields:

$$\sum_{i=1}^{k} \frac{(n_i - e_i)^2}{e_i} < c_{1-\alpha,f} \qquad \textbf{Equation 2-58}$$

where $c_{1-\alpha,f}$ is the value of the appropriate chi-square distribution at the cumulative probability $(1-\alpha)$, the assumed theoretical distribution is an acceptable model at the *significance level* α (Benjamin & Cornell 1970, Ang & Tang 1975).

Kolmogorov-Smirnov test for distribution

The basic procedure involves a comparison between the experimental cumulative frequency and an assumed theoretical distribution function. If the discrepancy is large with respect to what is normally expected from a given sample size, the theoretical model is rejected. For a sample of size n, rearrange the set of observed data in increasing order. From these ordered sample data a stepwise cumulative frequency function is developed as follows:

$$S_n(x) = \begin{cases} 0 & x < x_1 \\ \dfrac{k}{n} & x_k \le x < x_{k+1} \\ 1 & x \ge x_n \end{cases} \qquad \textbf{Equation 2-59}$$

In the Kolmogorov-Smirnov test, the maximum difference between $S_n(x)$ and $F(x)$ over the entire range of X is the measure of discrepancy between the theoretical model and the observed data. Let the maximum difference be denoted by

$$D_n = \max_n \left| F(x) - S_n(x) \right| \qquad \textbf{Equation 2-60}$$

For a specified significance level α, the K-S test compares the observed maximum difference of D_n with the critical value D_n^{α}, which is defined by

$$P(D_n \le D_n^{\alpha}) = 1 - \alpha \qquad \textbf{Equation 2-61}$$

Critical values D_n^α at various significance levels α are tabulated widely for various values of n. If the observed D_n is less than the critical value D_n^α, the proposed distribution is acceptable at the specified significance level α; otherwise the assumed distribution is rejected.

2.5.4 Regression and correlation analysis

Regression analysis

When dealing with two or more variables, the functional relation between the variables is often of interest. However, if one or both variables (in a two-variable case) are random, there will be no unique relationship between the values of the two variables – given a value of one variable (the controlled variable), there is a range of possible values of the other- and thus a probabilistic description is required. If the probabilistic relationship between the variables is described in terms of the mean and variance of one random variable as a function of the value of the other variable, this analysis is called *regression analysis*.

When pairs of data for two variables, say X and Y, are plotted on a two-dimensional graph, the possible values of one variable, for example, Y, may depend on the value of the other variable X. For this reason, it would be inappropriate to analyse the data, say for Y, without due consideration of X. In general, the mean value of Y will depend on the value of X. If this relationship is linear, this is known as the *linear regression of Y on X*:

$$E(Y \mid X = x) = \alpha + \beta\, x \qquad \textbf{Equation 2-62}$$

Where α and β are constants, and the variance of Y may be independent of or a function of x. The best line is the one that passes through the data points with the least error. It can be obtained by minimizing the sum of the squared errors between each observed value and the straight line; this is known as the *method of least squares*.

Relationships between variables are not always linear, or may not always be adequately described by linear models. Experimental data for such variables may show a non-linear trend between the observed values of the variables. The determination of such non-linear relationships on the basis of observational data involves *nonlinear regression analysis*. The simplest type of nonlinear function for the regression of Y on X is

$$E(Y \mid x) = \alpha + \beta\, g(x)$$ **Equation 2-63**

where $g(x)$ is a predetermined non-linear function of x. For example, $g(x)$ may be $x + x^2$, $\exp(x)$, or $\ln(x)$. By defining a new variable $x' = g(x)$, Equation 2-63 becomes

$$E(Y \mid x') = \alpha + \beta\, x'$$ **Equation 2-64**

which is of the same mathematical form as the linear regression equation of Equation 2-62. If the observed data pair (x_i, y_i) is also transformed to $[g(x_i), y_i]$ or (x_i', y_i), the original problem of linear regression between x and y is thus converted to a linear regression between x' and y.

Correlation analysis

The study of the degree of linear interrelation between random variables is called *correlation analysis*. Mathematically, the correlation between two random variables X and Y is measured by the *correlation coefficient* defined as

$$\rho_{XY} = \frac{COV(X,Y)}{\sigma_X \sigma_Y}$$ **Equation 2-65**

Based on a set of observed values of X and Y, the correlation coefficient may be estimated by

$$\hat{\rho}_{xy} = \frac{1}{n-1} \frac{\sum_{i=1}^{n} (x - \bar{x})(y - \bar{y})}{s_x s_y}$$ **Equation 2-66**

where $\bar{x}$, $\bar{y}$, s_x and s_y are, respectively, the sample means and sample standard deviations of X and Y. The value of $\hat{\rho}_{xy}$ ranges from –1 to +1 and is a measure of the strength of linear relationship between the two variables X and Y. However, this coefficient is not 'robust'; in other words, it is very sensitive to extreme data points and can thus lead to (inappropriate) high values of correlations (Saporta 1990). It should also be emphasised that this coefficient does not account for non-linear relationship between variables. For these two reasons, great care has to be taken in using the coefficient of (linear) correlation. Figure 2-10 illustrates the above remarks explicitly: (a), (b) and (c) exhibit typical data sets and coefficient of correlations, (d) exhibits the lack of robustness of the coefficient of

correlation; (e) and (f) show perfectly correlated pairs of data but with coefficient of correlation equal to zero.

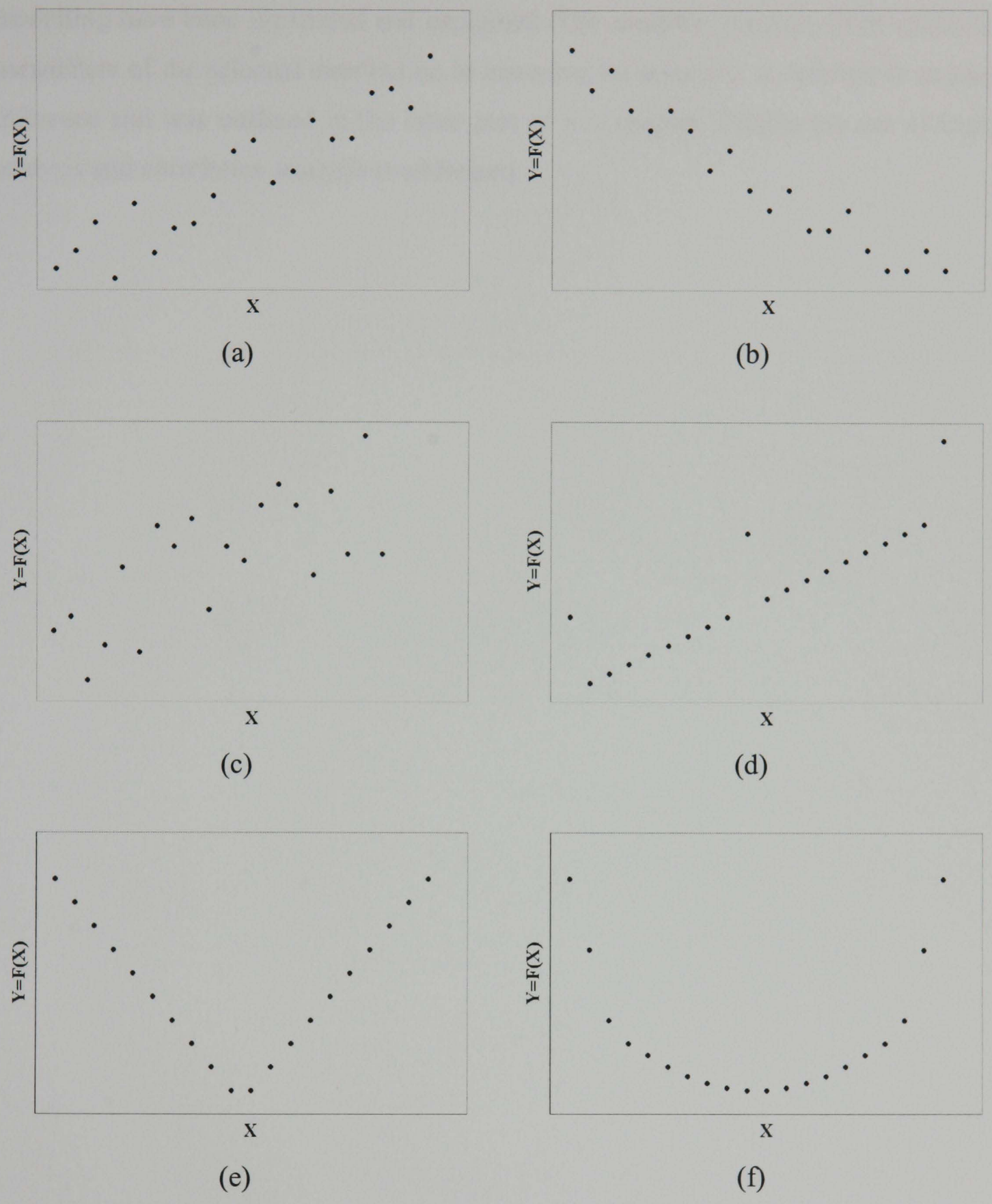

Figure 2-10: Example of data sets and their corresponding coefficient of correlation: (a) +0.94, (b) – 0.97, (c) +0.71, (d) +0.90, (e) 0.00 and (f) 0.00

2.6 CONCLUSIONS

The basics of the probability theory have been briefly reviewed so that they can later be used to derive relationships between variables and ultimately predict the value of other

variables with a certain degree of accuracy. Also, the concepts of random variable and function of random variable (in particular, *density function*) have been described. After that all the principal distributions used by various authors in traffic modelling and bridge load modelling have been illustrated and explained. The complete process, from estimating the parameters of the selected distribution to assessing its accuracy, is referred to as statistical inference and was outlined in the latter part of this chapter. Finally the use of regression analysis and correlation analysis is addressed.

Chapter 3

LITERATURE REVIEW

Chapter 3 LITERATURE REVIEW

3.1 INTRODUCTION

This chapter presents the literature related to the historical development of models for live loads on roads and bridges, along with the use of Weigh-In-Motion data, and the prediction of extreme effects; each of these three elements will be addressed in a distinct section. It should be emphasised that the aim of this thesis is the development of traffic load models for short to medium span bridges (i.e., 20 to 40m long), for both bi-directional and unidirectional traffics, and then the prediction of extreme effects; thus the discussions included herein will be motivated by this aim.

3.2 LIVE LOAD MODELLING

This section is divided into three parts, presenting the different approaches used over the years for modelling live load on roads and their applications to bridges. The first part deals with various Poisson processes used in order to model traffic and to ultimately predict the number of trucks present on a bridge. It also discusses the advantages and weaknesses associated with such processes. Then three case studies of renewal processes are presented in detail; each of which covers an area of particular interest in the scope of this thesis (short to medium span bridges under free-flowing conditions, opposing and adjacent lanes of traffic, modelling of groups of trucks). A number of fundamental ideas that will later be used in the development of new models are introduced. Finally, in the last part, more modern and complete models are described: they all simulate the flow of traffic over bridges and calculate the load effects induced in the structure as the vehicles traverse it. In some of these models, the extrapolation of short-term effects to longer periods is incorporated. However, although advanced, most of these models have limitations, which appear to be significant limitations in the study of short to medium span bridges.

3.2.1 Use of Poisson processes to model traffic flow

It was first suggested by Adams (1936) that the number of vehicles in light traffic passing a point in equal intervals of time follows a Poisson distribution. In a technical note, Breiman (1963) showed that 'in a strong sense the Poisson distribution is the only distribution leading to a stable traffic flow'. His main result was that, for a wide class of initial distributions, 'the passage of time brings a convergence to the Poisson distribution'. This result was announced at the Congress of the International Statistical Institute, in September 1961. At that time Herman & Weiss (1962) reported that they had each independently obtained similar results, using different approaches from the one adopted by Breiman (1963).

In the case of a Poisson model, the distribution of headways can be shown to be described by the negative exponential distribution. The Poisson distribution gives the probability that n vehicles arrive at a point during t seconds as

$$P_n(t) = \frac{e^{-qt}(qt)^n}{n!} \qquad \textbf{Equation 3-1}$$

where q is the mean number of vehicles arriving per second. The probability function for headways when the arrival or counting function is Poisson can be obtained as follows: the time interval t is treated as a Poisson variable in the Poisson expression for $P_0(t)$, which gives:

$$P_0(t) = e^{-qt} = e^{-t/\bar{h}} \qquad \textbf{Equation 3-2}$$

where $\bar{h}$ is the mean headway. This function gives the probability that no vehicle arrives in an interval t. The probability that some vehicle arrives in t is the same as the probability that a headway h_i is less or equal than t, namely,

$$P(h_i < t) = 1 - e^{-t/\bar{h}} \qquad \textbf{Equation 3-3}$$

This is a probability distribution function; by differentiation the probability density function can be obtained:

$$P'(h_i < t) = P(h_i = t) = \frac{1}{\bar{h}} e^{-t/\bar{h}} \qquad \textbf{Equation 3-4}$$

Modified Poisson process

While the Poisson and negative exponential distributions are very useful in traffic flow theories for light traffic, especially because of their mathematical simplicity, they have weaknesses in not taking account the limitations imposed by the physical size of vehicles (Gazis 1974, Haigt 1963). These limitations are especially significant for a single lane where overtaking is clearly impossible. One way to deal with the effects of these limitations is to replace the negative exponential headway distribution with its 'displaced' or 'shifted' version:

$$\begin{aligned} P(h_i = t) &= 0 && 0 \le t \le t_0 \\ &= \frac{1}{\bar{h}} e^{-t/\bar{h}} && t_0 \le t \\ P(h_i \le t) &= 0 && 0 \le t \le t_0 \\ &= 1 - e^{-t/\bar{h}} && t_0 \le t \end{aligned}$$

Equation 3-5

where t_0 is the minimum allowable headway. This is equivalent to saying that the probability of a headway, starting at $t = 0$, ending in the interval $(t, t+dt)$, provided that it did not end before time *t*, is

$$\begin{aligned} &0 && t \le t_0 \\ &1/\bar{h} && t_0 \le t \end{aligned}$$

Equation 3-6

The counting distribution for the displaced exponential headway distribution has been derived by Oliver (1962). It is given by the following equations:

$$\begin{aligned} P_n(t) &= 0 && 0 \le t < nt_0 \\ &= \frac{\Gamma[n; q(t - nt_0)]}{(n-1)!} && nt_0 \le t < (n+1)t_0 \\ &= \frac{\Gamma[n; q(t - nt_0)]}{(n-1)!} && (n+1)t_0 \le t \\ &\quad - \frac{\Gamma[n+1; q(t-(n+1)t_0)]}{n!} \end{aligned}$$

Equation 3-7

where $\Gamma(n;x)$ is the incomplete Gamma function of order *n* and argument *x*, which can be evaluated using:

$$\Gamma(n;x) = (n-1)!\left[1 - e^{-x}\left(\sum_{m=0}^{n-1} \frac{x^m}{m!}\right)\right] \quad n > 0$$

Equation 3-8

A similar approach has been adopted by Maillard & Gorse (1989), when they developed an expression for the number of vehicles present on a bridge assuming a Poisson process. Indeed, for short spans, they considered a shifted exponential distribution for the distributions of inter-arrival times, in order to avoid overlapping between trucks.

Another characteristic of vehicular traffic is its tendency to bunch when passing is hindered on a road with two-way traffic. One possible approach is to consider a traffic stream of moderate intensity, where some vehicles are free flowing and others are restrained in platoons behind one another. If the proportion of all vehicles in platoons is a, then the proportion that is free flowing is $1-a$, and a composite distribution of headways for all vehicles is given by (Gazis 1974):

$$P(h \geq t) = (1-a)\exp\left[\frac{-(t-t_1)}{\overline{h}_1 - t_1}\right] + a\exp\left[\frac{-(t-t_2)}{\overline{h}_2 - t_2}\right] \qquad \textbf{Equation 3-9}$$

where : t_1 is the minimum headway of free-flowing vehicles,

$\overline{h}_1$ is the mean headway of free-flowing vehicles,

t_2 is the minimum headway of restrained vehicles,

$\overline{h}_2$ is the mean headway of restrained vehicles.

Other processes

Studies (Haight 1963) indicated that as a model for vehicular arrangement, the Poisson process has a marked deficiency; the negative exponential probability density function for the inter-arrival times of vehicles prescribes higher probability for smaller inter-arrival times than for larger inter-arrival times. Actual traffic conditions require that the small inter-arrival time be improbable; i.e., the probability density function for inter-arrival time of vehicles approaches zero as the inter-arrival time approaches zero. The Gamma (or Pearson Type III) probability density function, given by

$$f_{T_k}(t) = \frac{v(vt)^{k-1}}{(k-1)!}\exp(-vt) \quad t \geq 0 \qquad \textbf{Equation 3-10}$$

has the required property (except when $k=1$, i.e. when the Gamma PDF reduces to the negative exponential). When k becomes larger, the Gamma PDF approaches the PDF of inter-arrival time for regular traffic conditions. By suitable choice of parameters λ and k,

the shape of the function can be changed considerably and was found to correspond well with various actual traffic conditions (Tung 1969).

Another distribution which has been found to fit headway data quite well in tunnels and on bridges as well as on streets and highways is the log-normal distribution (Gazis 1974). Larrabee (1979) compared the frequency of groups of k trucks, assuming that the k trucks arrive according to a renewal process with renewal PDF (i) exponential and (ii) lognormal. The results show that assuming truck arrivals to be Poisson increases the frequency of groups, at least for short and medium span bridges, and so is overestimating the probability of having a high number of vehicles present on a bridge at the same time.

Prediction of multiple presences of trucks on a bridge

The frequency of multiple-truck presence on a fixed length of highway has been studied at several highway locations by Desrosiers and Grillo (1973). Their first objective was to determine which of the following parameters have a significant effect on the probability of multiple presences: type of highway, length of bridge, time of day, total traffic volume, truck speed and truck volume. They concluded that the multiple presences of trucks is primarily dependent upon the length of the bridge and truck volume and it is almost independent of the type of highway, the time of the day, the total traffic volume, and truck speed.

The probabilities of multiple-presence events on a given length of bridge can be calculated using the probability distribution of headway distance. Based on observations of truck traffic moving on several highways, Goble et al. (1976) assume that the probability density of headway time in the short headway range is a constant equal to the average number of trucks per unit time q. They express their approximation as follows:

$$F(t) = 1 - \exp(-qt) \cong qt \qquad \textbf{Equation 3-11}$$

where $F(t)$ is the probability that the time between successive trucks is less than t. The assumed probability density q is the maximum ordinate of the negative exponential probability density function. Based on these assumptions, the calculated frequencies of headway time are slightly higher than the observed frequencies for most cases. The distribution of headway from zero to the length of the bridge is thus assumed to be a constant equal to the average number of trucks per unit of distance, which is also the reciprocal of the mean headway distance $\overline{h}$. Using this constant probability density and

assuming that headway distances are independent and identically distributed, the probability of multiple-truck events can be calculated. The probability of m or more trucks being on a length L conditional on at least one truck being present is given by (Harman & Davenport 1979):

$$P_m^* = \frac{(l_{m-1})^m}{L\bar{h}^{m-1}(m-1)!} \qquad \textbf{Equation 3-12}$$

where length l_{m-1} is shorter than the length L by the length of $m-1$ trucks. Because many, if not most, influence surfaces for bridges have large influence coefficients over only a small area, one truck is almost always present in this area when a peak value occurs. Therefore, it is rational to calculate the probabilities of multiple truck presence conditional on one truck being in a fixed location. Harman & Davenport (1979), when comparing the values given by Equation 3-12 with experimental data, have found that the number of multiple-truck events for spans less than 50 m is underestimated.

Bakht & Jaeger (1988) give a more accurate version of the above approach, in which they also consider the case of multiple lanes of traffic. Indeed, they state that, in sparse traffic, it is reasonable to assume that a Poisson distribution describes the multiple presence of trucks. For one lane of traffic, the probability of m trucks present on a highway segment of length L conditional on one truck being in a fixed location can be approximated by:

$$P_m = \frac{1}{(m-1)!}\left(\frac{L}{\bar{h}}\right)^{m-1}\exp\left(-\frac{L}{\bar{h}}\right) \qquad \textbf{Equation 3-13}$$

where $\bar{h}$ is the mean headway distance between trucks. However, it is important to use an idealisation of multiple truck presence which gives an exactly zero probability for impossible events, namely events with more trucks present than the number which would completely fill the specified highway length. Therefore, the basic Poisson distribution is modified because it gives small but finite probabilities for large (impossible) numbers of trucks in multiple presence events. In other words, the initial expression is modified in order to take into account the length of the trucks present on the bridge. The mean length occupied by a truck is denoted as $\bar{d}$. The free length of highway with m trucks on the highway length L is given by $L - m\bar{d} = L(1 - m\bar{d}/L)$. The adjusted free length is denoted by l_m and calculated by:

$$l_m = L(1 - m\bar{d} / L)^{\beta}$$ **Equation 3-14**

where β is the length parameter ($\beta \geq 0$). If this parameter is set to zero, the distribution reverts to a basic Poisson distribution. As β increases the adjusted free length decreases and the probability of multiple presence decreases. Thus the probability of m or more trucks of zero length on the adjusted free highway length l_m is given by:

$$P_m^* = 1.0 - \exp\left(-\frac{l_{m-1}}{\bar{h}}\right)\left[1.0 + \sum_{n=2}^{m-1}\frac{(l_{m-1})^{n-1}}{(m-1)!}\right] \quad m \geq 3$$ **Equation 3-15**

The modified Poisson probability of exactly m trucks present on length l conditional on a truck at a fixed location is then given by:

$$\tilde{P}_m = P_m^* - P_{m+1}^*$$ **Equation 3-16**

In the case of two or three lanes of unidirectional traffic, vehicles can change from one lane to another; therefore the independence of the lanes of traffic is questionable. To account for the additional space available for trucks, the authors suggest to modify the ratio $m\bar{d} / L$ in Equation 3-14 and to take it as $m\bar{d} / 2L$ for two lanes and $m\bar{d} / 3L$ for three lanes.

If the lanes of traffic were independent and the Poisson idealisation of traffic flow were accurate, multiple presence in two or more lanes could be calculated using a Poisson distribution with an arrival equal to the sum of the arrival rates for the individual lanes. In this study, the arrival rates of the single lanes are taken as the reciprocals of the effective mean truck headway distances obtained by fitting distributions to the data. The arrival rates are added and a 'combined mean truck headway distance' is calculated as the reciprocal of the sum. In their study, Bakht & Jaeger show that for moving traffic, multiple truck presence is more common than the modified Poisson distribution would indicate if the combined mean truck headway were used as the parameter of the distribution. One possible explanation is that multiple truck presence in adjacent lanes has positive dependence. This result shows the limitations of the modified Poisson model, which does not account for dependence between lanes of traffic (case of one-way traffic), and therefore underestimates the frequency of the critical multiple truck events.

3.2.2 Live load models using renewal processes: case studies

Tung (1969) studied the response of highway bridges to the passage of vehicles. In his study, the bridge is idealized as a damped linear system and the vehicles are assumed to be of the same type, have the same weight and travel at the same constant speed. A numerical technique is developed to compute the probability function and expected rate of threshold crossings of the bridge response. The above assumptions are, of course, unrealistic; however, they were introduced only for convenience of presenting the basic idea of the numerical technique. They may be removed by considering the influence function of the filtered renewal process as 'a random function, the sample of which represents the population of vehicle type and weight' (Tung 1969). Marcus (1974) used a filtered Markov renewal process in order to study the traffic noise, 'an environmental impact of urban highways whose properties depend significantly on statistical properties of the traffic on the highway'. These two examples, although relatively simple, show how the theory of renewal processes could be applied to model traffic flow and calculate its effects. In the following, three studies are presented in more detail. Each one is of particular interest as it introduces an approach and elements of modelling that will be studied later.

Larrabee's approach

In his doctoral thesis, Larrabee (1979) considers the topic of combinations of loads from different sources in terms of loads processes, and then shifts to the specific case of combining the load effects of multiple vehicles passing over a bridge. Indeed, a clear parallel between traffic loading on bridges and load combinations is the combining of the load effects of traffic in different lanes. Larrabee studies separately the case of free-flowing traffic and congested traffic. Only the results related to free-flowing traffic on short and medium span bridges are presented here.

The author assumes that trucks arrive according to a renewal process, which he considers reasonable for one lane in one direction. If two lanes in the same direction make equal contributions to the load effect, then the two lanes together can be modelled approximately as a renewal process. However, this must violate some physical constraints. The very short headways implied by the unshifted gamma or lognormal distributions are possible because trucks travelling in different lanes may overlap their lengths. However, two consecutive very short headways imply that the third truck is on top of one the first two. Larrabee

suggests modifying the second headway, by setting it to a minimum value, if the previous one was a very short one.

Except for very short influence lines, the principal vehicle random variable is total weight. Larrabee establishes the conditions under which the other random variables (truck type, length, axle weight, etc.) are of secondary importance. The concept of *effective weight* is introduced, as well the *random axle factor*, which is 'the ratio of the peak effect of a random truck to the peak effect of a truck with the same weight but with other properties specified'. The PDF of the axle factor is a function of the influence line of the bridge. The distribution of the axle factor for a variety of spans and influence lines is determined by simulation. The results of the simulations show that, in general, the PDF of the axle factor is a function of the slope of the influence line and truck type but is not a function of the length or overall shape of the influence line. This conclusion is of particular relevance in the scope of this thesis and should be emphasised.

Modelling trucks by the single random variable of total weight requires that the response of a truck crossing a bridge be described in time by a fixed pulse shape. It is then of interest to know what effect fixing the pulse shape of load effect has on the combined effect of two or more trucks. After calculations based on a number of influence lines and lengths, the author concludes that it is feasible to model the response of a truck crossing a bridge by a fixed pulse shape, and that 'the selection of that pulse shape should be based on an envelope of the random responses and not on the response of some arbitrary, fixed vehicle description'.

In order to calculate the bridge load effects due to truck groups, Larrabee used a simulation set up along the lines suggested by Davenport & Harman (1975). It is clear that at lower levels of load effect, the major contribution to the rate at which groups exceed some level is due to the more frequent single-truck groups. At higher levels, above the maximum load effect of a single truck, the major contribution to the rate is due to multiple truck events. It is not obvious, however, whether a certain size of a multiple truck group will dominate the total rate. Before running the simulations some preparations are required:

- determine an effective truck weight PDF by convoluting the truck weight PDF with the axle factor PDF and select a fixed pulse shape;
- compute the rate of occurrence of each group size;
- determine the distribution of headways conditioned on group size.

After these preparations, the simulation is done for each group size in its turn. The typical steps are:

- draw the random effective truck weights;
- draw the headways;
- compute the peak group effect;
- record this effect in a histogram.

After repeating these steps for all group sizes that occur with significant probability, the mean rate of exceedence of a specified level is computed.

Some of the conclusions drawn by the author from the results are of particular interest:

- the smaller groups make a larger contribution when the PDF of weight has a longer tail and the span decreases;
- at levels where the two-truck groups make the largest contribution, the upper tail of the truck weight distribution is critical;
- at larger group sizes, the results are less sensitive to the upper tail of the truck weight distribution.

Ghosn & Moses's approach

Most models are one-dimensional in the sense that they represent arrivals in only one lane. A more general Markov renewal process, which can represent a multilane system such as truck arrivals in several lanes, needs to be adopted. Restrictions on this model include the fact that truck properties such as Gross Vehicle Weight (GVW), truck type, etc., are independent of their arrival sequence. The authors concentrate on the study of two lanes of traffic in the same direction, which, again, is of particular interest here as a live load model will later be developed for the case of adjacent lanes of traffic.

Observing truck traffic arriving at a given point, such as the beginning of a bridge on a highway, three different lane position states or truck arrival events can be distinguished:

- a truck is in the slow lane;
- a truck is in the fast (/passing) lane;
- two trucks are side by side in both lanes.

The third is considered as a separate state since a renewal process does not permit an inter-occurrence time equal to zero; in other words, simultaneous occurrences are not possible in a renewal model. The Markov renewal process normally conditions the time of a new arrival on the time of arrival and the lane position of the previous truck. In order to avoid

possible overlapping between trucks, the Markov renewal process is modified so that each new truck arrival is conditioned on the two previous arrivals.

Since the arrival of a new truck event is conditioned on the previous two truck arrivals, one can study the whole renewal process by examining the arrival of the first three trucks on the bridge. These initial assumptions together with the theory of Markov renewal processes provide a set of equations that can be solved to calculate the characteristic function of the response. The characteristic function can then be inverted to calculate the probability density function of the stationary bridge response. Then the mean up-crossing rate is calculating according to Rice's formula (Rice 1954). Finally, the distribution of the lifetime maximum is calculated from the mean up-crossing rates assuming a Poisson arrival of the peaks, as suggested by Larrabee & Cornell (1979).

Although very attractive at first, this model is practically very difficult to implement for two reasons:

- the determination of the conditional probabilities of arrival of a truck in a given lane during a specified time interval, given the arrival of another truck in a pre-determined lane at a given time, is awkward;
- assuming that these probabilities can be determined accurately, the computations involved during the whole process (from the determination of the characteristic function of the bridge response, its inversion, the calculation of the upcrossing rates to, eventually, the probability distribution of maximum lifetime response) are extremely complicated and likely to induce significant.

Harman & Davenport (1979)

The authors developed a procedure to obtain a statistical prediction of the largest effects caused by traffic loading. In the calculation procedure developed, bridge loading is simulated, one event at a time and the frequency distributions of the structural effects are built up by repeating the simulation many times (Monte-Carlo approach). Direct simulation of traffic is not used because bridge loading events with only one truck present would predominate: the loading events are divided into five categories and each category is simulated separately. Loading events with more than one truck present are less frequent than single-truck events, but they are a primary interest of this study. Large numbers of these multiple-trucks events are simulated. It is important to note that the study was restricted to the static effects caused by traffic loading along one traffic lane only.

Static effects on bridge members are determined by passing idealized trucks over a series of influence lines, which are selected to be representative of the load-effect relationships for common bridges. The sensitivity of each effect to the multiple presence of vehicle is important in this study. Therefore, the influence lines are rated in accordance with a parameter that is an approximate measure of this sensitivity.

There are four important traffic parameters that influence the static effects caused by traffic:

- gross vehicle weight,
- vehicle type and axle spacing,
- distribution of GVW among axles
- multiple presence of vehicles.

By collecting relevant data (i.e. the first three traffic parameters mentioned above) at different weigh stations, idealized trucks can be derived. However, it is important to bear in mind that the data needs to be fully representative (in terms of weight distribution, type and frequency of trucks) in order to derive idealised, but appropriate, vehicles. For the simulation, each idealised truck is represented as a series of point loads, one corresponding to each axle.

For each truck arrangement, the trucks and their headways are selected randomly. A minimum distance of 7.32m is maintained between the last axle of one truck and the first axle of the following truck. Each truck arrangement is moved across each influence line in order to obtain the maximum effect. For each category of arrangement and for each influence line, the simulation is repeated until histograms of maximum effect are obtained. For each histogram, a cumulative frequency distribution of effects greater than or equal to a fixed effect is calculated. A curve having the form of a Gaussian function is fitted to each distribution by an iterative procedure. The fitting procedure is weighted to provide the best fit in the vicinity of the mean largest value calculated from the previous iteration. For one influence line there are five histograms, one for each category of truck arrangement. Using curves fitted to the histograms and the relative frequencies of the loading events obtained from traffic studies, the largest value distribution of the effect is calculated. The distribution is shown to be the product of five "largest value functions", each of which is determined uniquely by the corresponding category of loading events. From the largest value distribution, the mean largest effect and the coefficient of variation are calculated based on various periods up to a 50 year bridge lifetime.

Here are presented some of the main observations made by the authors regarding their results.

- Depending upon the sensitivity of an effect to multiple presence, some categories of truck arrangement have a negligible influence on the largest-value distribution.
- If an effect is sensitive to multiple presence, many arrangements of several trucks may have approximately equal influence on the largest value distribution. In other words, although one idealized live load can be calibrated to predict a mean largest effect, this simplification does not indicate that only one category of truck arrangement is likely to cause an effect of that magnitude.
- It is reasonable to assume that the mean largest effect based on one day is 75% of the corresponding mean largest effect based on 50 years and that between these two periods, the mean largest effect vary linearly with the logarithm of the period.

The three case studies discussed were developed in the 1970's. More recently, Croce & Salvatore (2001) introduced the most complete model of that type. They present a general theoretical stochastic traffic model, which is able, not only to reproduce actual traffic, but also to account for traffic interactions (e.g. several lanes of traffic). Each interval of the time history of actions on the structure can be considered to be the consequence of the transit of an appropriate convoy, characterized by its length and composition, so that each convoy can be associated with the maximum value of the time history interval related to it. Each convoy is composed of exactly 1, 2, …, n vehicles, and during its transit, no other vehicles can be present on the part of the bridge in question. In this way, all kinds of vehicle combinations are considered, and the traffic is represented exhaustively. Moreover, when the length of the given influence surface is greater than 30 m, the maximum values of the effects of a convoy depend almost exclusively on the total weight of the convoy. That is, the actual values of each axle load are assumed to be almost immaterial, so that each convoy can be substituted by its own weight, uniformly distributed on the total length of the convoy itself. By doing this, the model is applicable to bridge lengths greater than 30 m only. The maxima induced by traffic on several lanes, as well as those regarding combinations of traffic actions with other types of action, can be evaluated simply through the convolutions of the relevant PDF of maxima on a single lane, provided that the number of convoys travelling simultaneously on the lanes in question has already been determined. Therefore, although supposedly very general, this model suffers from two limitations:

- it is not applicable to bridge less than 30 m long;

- it requires previous knowledge of the number of convoys travelling simultaneously on several lanes.

Finally, there are two points that worth considering when studying traffic flow using stochastic processes with a view towards live load modelling:

- if truck arrivals are governed by a renewal process, then the inter-arrival times are independent. An alternative to a renewal model is one in which the vehicles may cluster together in pairs, triplets, etc. Therefore it might be important to test for clustering of trucks by examining the PDF of all consecutive pairs of headways. For clustering to occur, the probability of a short headway must be greater when the prior headway is also short;
- another interesting aspect of traffic flow is the possible correlation between weights of consecutive trucks caused by either slower trucks bunching together on hills or by trucks travelling together from a common starting point (although only larger spans would be affected by such correlation).

3.2.3 Simulation of traffic flow

A variety of models simulating traffic flow developed in the late 1980's and 1990's are now presented. It should be remembered that the scope of this thesis is the modelling of imposed traffic loadings on short to medium span bridges. Therefore, when discussing the following models, the emphasis is put on their ability to deal with such bridges rather long span ones.

In the late 1980's, Eymard & Jacob (1989) developed a software application called CASTOR (i.e. Calcul des Actions et Sollicitations du Trafic dans les Ouvrages Routiers). The main function of CASTOR is the calculation of effects (total load on a bridge, moment, shear force, etc.) induced in a bridge by the passage of traffic loads on the deck, and the statistical analysis of these effects through the use of histograms. CASTOR can be used to check the dimensioning of bridges under traffic loads, to calibrate design codes or for fatigue assessment. In terms of input, CASTOR requires a full traffic file and the knowledge of the influence line (or surface) to be considered. A traffic file is constituted by the succession of traffic records, each record representing a single vehicle. Each vehicle is fully described by the knowledge of the following elements:

- its exact arrival time at a fixed given point ;
- its lane and its direction of travel;
- its speed;
- its number of axles;
- its Gross Vehicle Weight (GVW) and its individual axle weights;
- its length (between first axle and last axle) and axle spacings.

The different vehicles types are distinguished according to their GVW; vehicles weighing less than 10 kN are referred to as cars, vehicles weighing between 10 and 35 kN are referred to as vans and vehicles above 35 kN are considered as trucks. Such traffic files can be obtained from Weigh-In-Motion (WIM) systems set up on any road or bridge. The traffic is recorded continuously for a period varying between a day and a few weeks (the main limitation being the size of the file generated as the recording period increases). The influence line (/surface) is defined longitudinally (/and transversely) by specifying the magnitudes of the influence line for a set of defined locations. The notion of influence line (/surface) assumes linearity and therefore a total effect induced by a set of axles is taken as the sum of the individual effects of the axles. The total time is discretised into a number of instants separated by constant time increments. For each distinct instant, and for each effect considered, the contributions of all the individual axles present on the structure are added, which gives the total effect for that instant. The outputs of the program consist of:

- The entire set of calculated effects for all the discretised instants (although this option is not recommended because of the very large size of the file generated)
- A set of histograms; including the histograms of successive local minima/maxima of an effect, level crossing histogram and 'rainflow' histogram (for fatigue).

In 1991, Bez & Hirt (1991) proposed a probability-based load model of highway traffic in which they used traffic simulation. The purpose of simulating traffic was to establish the statistical characteristics of the highway traffic load effects, in order to introduce them into the probabilistic analyses. The first step of the traffic simulation consists of choosing the characteristics of the structure which will support the traffic loads, namely the traffic system, the influence line, the type of cross-section (in order to take into account the lateral distribution of the loads) and the deck width (which is directly related the number of traffic lanes). On the basis of measured traffic and its statistical characteristics, namely:

- geometry of the vehicles (length, axle spacing)
- gross weight and its distribution to the axles

- distance between moving or stopped vehicles
- composition of the traffic (percentage of cars, single trucks, trucks with trailer and semi-trailers),

it is possible to simulate a traffic jam by a random generation of vehicles which are placed on the chosen influence line. This procedure is repeated over and over again, in order to simulate the number of traffic jams that could occur during the service life of the bridge. This leads to the extreme value of the traffic load effects. The simulation of this number of traffic jams is repeated by Bez & Hirt a number of times, in order to establish the statistical characteristics (mean and standard deviation) of the extreme value of the traffic load effects. As stated by the authors, the advantage of considering stopped traffic (yielding about the same results as slowly moving traffic) is that it is not necessary to take into account the dynamic effects, which is an area of research on its own. However, for relatively short spans (i.e. < 30 to 40 m), the dynamic effects are of primary importance and the congested configuration does not represent the critical loading situation, which therefore limits the immediate application of the present model.

Bez & Hirt's traffic simulation is done by means of a specially developed computer program, where the number of simulations of jams was taken to equal 50 000 (corresponds to about 4 jam situations per day during a service life of 50 years, on the basis of 250 working days per year), and the number of repetitions of the procedure to equal 50. The traffic characteristics used for the traffic simulation were established by field measurements of stopped and moving traffic in Switzerland between 1976 and 1988. In the simulations, a number of span lengths ranging from 20 to 100 m, lane widths (representing 1, 2, 3 and 4 lanes) and two different cross sections were considered. The bending moment at mid-span was the only effect calculated. The results of the simulations are expressed in terms of mean value and standard deviation. Obviously these simulations represent an enormous number of computations; however, by simulating the equivalent lifetime of the bridge, the extreme expected effects are obtained without having to extrapolate the results.

A very interesting model of simulation of real traffic flow is the one introduced by Vrouwenvelder & Waarts (1993). Indeed, they derived a complete traffic load model for the design of road bridges in which attention was given to the Ultimate, Service and Fatigue Limit Sates under both static and dynamic conditions. A statistical model, based on a set of measurements from the Netherlands, was derived for the calculation of axle loads (once the vehicle type and weight are given). A probabilistic traffic flow model was also

constructed in order to represent the three types of traffic (free, congested and full stop) and their respective characteristics (intensities, headway and speed distributions, etc.). Given these two models, design values can be obtained on single and multiple lanes for various influence lines.

The vehicles are distinguished by their type, defined by the number of axles and type of body (single body, semi-trailer, trailer). For a given vehicle type, the total load distribution of the weight is in most case a bimodal one. This shape of the distribution can be explained by assuming subpopulations of loaded and unloaded vehicles. In their study, the unloaded vehicles are modelled by truncated normal distributions. The authors then use different distributions to model the gross vehicle weights depending on the mode and limit state considered. The loaded part is modelled by truncated normal distributions for the analyses of fatigue limit state and by truncated Weibull for the other limit states. Given the vehicle type and its total weight W, the individual axle loads Q_i can be found from the following model:

$$Q_i = b_i + a_i W \qquad \textbf{Equation 3-17}$$

With $\sum b_i = 0.0$ and $\sum a_i = 1.0$. The (a_i, b_i) pairs of values should be regarded as average values; for some applications (e.g., short influence lines), it is necessary to include the statistical fluctuation around these values.

The traffic models consist of a long-term model and a short-term model. The long-term model describes the daily and hourly intensities and the duration of the type of traffic (i.e. free, congested or full stop). The short-term model describes in a probabilistic way the velocities and distances of individual cars, given the hourly averages. Each traffic type has its own short-term model. The static elastic behaviour of the bridge is characterized by means of influence lines. The simulated traffic is positioned above the influence line as an irregular set of point loads Q_i. After calculation of the load effect, the corresponding equivalent uniformly distributed load is calculated. The model also accounts for fatigue and dynamic analysis (by means of combined dynamic model for bridge/truck interaction). An interesting remark made by the authors is that the maxima of static and dynamic response in general do not occur at the same point in time. The case of multiple lanes is dealt with by applying multiplication factors, the values of which depend on the influence line considered.

'A complete model valid for every load effect (maximum load in a reference period, fatigue, frequent load for the verification of serviceability limit states), and for any situation (design of a new bridge or evaluation of an existing one), considering the most important correlations in actual traffic, is not available nowadays' commented Crespo & Casas (1997). Thus they decided to present a new model for the global analysis of traffic actions on roadway bridges. In order to make it feasible for use in the verification of most important limit states, the model includes an algorithm for the simulation of continuous flow of traffic, in order to be able to predict the effect of real traffic flow over the bridge as a function of time, and another for the extrapolation of maximum results from short periods to long return periods.

To account for the uncertainties in the traffic action, a statistical treatment was given to the most important variables involved in the problem. To characterize the statistics of those random variables from real traffic data records, several computational tools were developed. From the study of real traffic records, correlation matrices for the relation between the random variables total weight and weight per axle were computed for each vehicle type. In short span bridges, it is very important to represent the actual axle loads as accurately as possible. The model for the simulation of continuous flow of traffic was based on two different algorithms: one to create fictitious complete traffic records using the statistical properties extracted from the analysis of available real traffic data; and another one to manage the pass of all simulated vehicles over the bridge.

From the analysis of different real traffic records, the authors observed that the time interval between vehicles depends on the number of vehicles arriving at the registration point per unit time. No theoretical probability distribution function fits this random variable well for all traffic conditions and carriageway categories. After several studies, it is observed that the non-dimensional random variable 'actual time intervals between vehicles divided by average interval between vehicles' measured in different real traffic records, with different numbers of vehicles arriving at the registration point, showed uniform trends for each carriageway category. The authors thus decided to implement this new variable in the definition of the time intervals between all vehicles in the fictitious traffic record. One of the main advantages of that approach is that it is not necessary to hypothesize the nature of the time intervals distribution function, the CDF used for the sampling of this variable does not strongly depend on the traffic intensity, and this procedure allows the user to approximate, very accurately, real conditions for different

road categories. For the sampling of vehicles' velocities, a similar procedure was implemented.

Some major objectives of the model for the simulation of traffic flow over bridges were to account for the most important correlations between vehicles in one lane and different lanes, and to avoid overlapping between vehicles, since this is a very important source of error. To achieve these goals, some possibilities for the algorithm for the management of the crossing of vehicles over the bridge are: passing between vehicles, accelerations and decelerations and changes of vehicles' velocities at each computed instant. The dynamic bridge response to vehicle loading is taken into account by increasing the static effect of each vehicle by the impact factor. The impact factor is a deterministic value, but different values are considered based on the different truck types (light or heavy). Finally, the extrapolation of maximum effects within a period to a longer period is dealt with. The authors emphasise the importance of the accuracy in the extrapolation of results from the simulation of short periods to long intervals in order to get reliable results in the assessment of the safety of bridges. The fundamentals of the proposed methodology lay in the use of the Generalized Pareto Distribution (GPD) for the probabilistic definition of the tail of the variable of interest.

Bailey (1998) developed a simple method for the consideration of site-specific traffic loads as a function of parameters describing the bridge and traffic, referred to as site characteristics. The site-specific model of the frequency distribution of extreme traffic action effects is based on the results of a traffic simulation program. The simulation program generates random traffic loads for defined traffic conditions and determines the frequency distribution of maximum static effects for different structures. Axle weights, axle spacings and the distance between vehicles, are generated according to probability distributions that are adjusted in order to model different types of traffic and different traffic flow conditions. As a result, this approach enables the user to extend the scope of the study beyond recorded traffic types. Also, axle group weights are considered as single loads in order to increase the speed of simulations. The author states that the simplification has no significant influence on the effects calculated for spans greater than 30m.

Bailey finds that the frequency distributions of axle weights measured in traffic surveys are best modelled by the weighted sum of two beta distributions, one for each of the two peaks observed in the majority of the cases. Vehicle geometry is represented by the distance

between axle groups and the front and rear vehicle overhangs. Again these distances can best be modelled by beta distributions. A different distribution is used for each axle group spacing and overhang for each class of vehicle. The distance between vehicles is modelled differently for each of the three traffic flow conditions: free moving, congested and at rest. These frequency distributions are modelled by a beta distribution, the parameters of which vary as a function of traffic speed. Globally, the main traffic characteristics are all modelled by beta distributions, which obviously restricts the maximum GVW to a chosen limit. However, the following issue then arises: how to determine that limit, given that overloads regularly occur and must be accounted for?

A computer program was developed by Bailey for simulating the passage of traffic over bridges and determining the resulting frequency distributions for maximum load effects. For given traffic conditions and lane configuration, the program considers many bridges and effects at once (up to 64 influence lines). A stream of axles is generated for each lane and traffic is stepped over influence lines incrementally. At each step, the effect for each lane is calculated using an influence line and the combined effect of multiple lanes is calculated using lateral distribution factors. Frequency distributions of traffic action effects are compiled as the simulation progresses. The simulation program has been used to generate maximum traffic action effects for more than 1600 combinations of action effect type, bridge and traffic. The influence on traffic action effects of vehicle over-loading and weight restriction was also simulated. Simulations results are expressed in terms of the mean simulated maximum traffic action effects for different return periods, represented by the number of vehicles that pass over a bridge.

Conclusions

A number of approaches developed in the last four decades for modelling live loads on roads and bridges have been discussed. From simplistic to very advanced, from a simple Poisson process to full simulation of real traffic flow, the various models have improved over the years. Some of them are very complete and include both static and dynamic analysis of the traffic loads on bridges, for a large range of bridge lengths. However, most of these models come with their own limitations, the most common one being their restriction to bridges exceeding 30m in length.

3.3 USE OF FIELD MEASUREMENTS AND WEIGH-IN-MOTION DATA

Wilson et al. (1983) studied overtaking involving lorries and coaches on the M1 motorway in England during the summer of 1979. The authors were not only interested in the frequency of overtaking events but also in their type (e.g. full overtaking manoeuvre, vehicle remaining in its lane while passing another vehicle, etc.). In total, 14 two-hour observation periods were spent watching overtaking manoeuvres performed by lorries and coaches, between June 25 and July 13. The observer was equipped with a clipboard and a stopwatch. Although accurate in describing the overtaking manoeuvres, this technique is not suitable if one is interested in the real frequency of overtaking events over a continuous period of time (e.g. one full week). In addition, this technique does not provide any information on the actual weight of the vehicles observed. Another possible option is the use of static weighing scales, located on the side of the road or at control points. However, this technique does not provide full representative data as only a sample of the total traffic is weighed.

In 1992, a detailed study of heavy-good vehicles was undertaken by Pillot (1994) in order to obtain a database that would provide input data for models of polluting emissions. Two methods were used to obtain the various traffic variables required: a survey among drivers and video recording combined with weighing system. The latter approach is particularly interesting. Indeed, the heavy vehicles (over 20 kN in that study) are detected and the video-recorder is then automatically started to tape the passage of the detected vehicle. The system is managed through the use of a computer. Besides the video recording, a data file is generated, including the usual characteristics (arrival time, GVW, axle weights, number of axles, length, speed). Using this approach Pillot was able to obtain further information about the heavy vehicles (e.g. power, make) by analysing the video. However, the same methods could be equally applied to the study of critical loading events over a bridge and typical loading patterns.

3.3.1 The use of WIM data in bridge engineering

The use of field measurements and Weigh-In-Motion (WIM) data is well documented. In particular, knowledge of the traffic in terms of weight, frequency, composition, etc., is of great interest not only for engineers but also for legislators and tyre and truck

manufacturers. The main uses of road measurements in bridge engineering are (Prat 1997, O'Brien et al. 1998):

- calibration of traffic load models, including background studies to Eurocode;
- calculation of reduction factors for national conditions;
- dynamic Impact Factor;
- design of exceptional bridges (e.g. long span bridges);
- assessment of load on existing bridges;
- fatigue assessment of bridges;
- active control of traffic load on bridges.

One of the main advantages of WIM data is that statistical bias is reduced as there is no pre-selection of vehicles. A complete picture of the traffic is recorded for a continuous measurement period. The parameters governing traffic flow may be accurately modelled and realistic simulations can be performed in which multiple transverse and longitudinal presences are modelled as they occur, resulting in more realistic estimates of the governing load effects (O'Brien & Jacob 1996).

O'Connor et al. (1998) did a study in order to assess the accuracy of the current Ontario Highway Bridge Design Code (1991) live load model for the design of short to medium span highway bridges. The current model was derived from truck surveys carried out in Ontario in the mid 1970's and late 1980's. A major source of inaccuracy in the load model concerns the limitations on, and biases in the data, which was used in the calculation of characteristic load effects against which the load model was calibrated. In 1975, only trucks that appeared to be heavily loaded were stopped and weighed. This related to approximately every 3rd truck being weighed in sparse traffic and every 10th truck being weighed in dense traffic (Harman & Davenport 1979). The distribution of gross vehicle weight was therefore biased towards trucks travelling at, or close to, their legal weight limit. It is also reasonable to assume that heavily overloaded trucks deliberately avoided the weigh stations. Consequently, trucks which could be expected to induce the maximum load effect on the shorter span bridges were not recorded in the survey. The results of free flowing simulations performed on representative influence surfaces, using WIM data recorded in Ontario in 1995, are presented. Extrapolation of the calculated load effects is performed to determine characteristic values of the design of highway bridges in Ontario. The current load model is assessed by comparing the specified design effects with calculated characteristic effects. The authors concluded that, for one-lane bridges, the model is too light, whilst for two lanes it is too heavy. The inadequacy in the model is a

result of simulations performed, based upon a biased data set, where subjective assumptions were used to model the random variables governing traffic flow. Clearly the use of WIM data in simulations for code calibration is preferable.

Heavy motor vehicles represent a major load to highway bridge structures. Their weight and weight distribution over axles are limited by the regulations of the jurisdictions. However, vehicles exceeding these limits (i.e. overloads) may need to cross the bridges, mainly for economic reasons. In the U.S., these overloads are accommodated by the special permit system of the highway jurisdiction. Special permits can be given for a full year or for a few days. One of the issues associated with the operation of overload-permit systems has been the structural safety of highway bridges. It is well known that highway bridges may possess intended or unintended reserve strength, although they were designed for the standard loads at the time. This reserve strength can be utilized to accommodate occasional overloads. On the other hand, many bridges have deteriorated severely. As the demand for more and heavier overloads has been increasing; it becomes an imminent issue whether and/or how these overloads can be allowed to travel without jeopardizing the safety of bridges.

Fu & Hag-Elsafi (2000) presented a live (vehicular) load model for highway bridges including overloads. The model is used to assess the structural reliability of highway bridges subjected to overloads along with normal loads. Live load effect L_t due to vehicle traffic for a primary component of a highway bridge structure is modelled in a similar way to that of Moses and Ghosn (1985):

$$L_t = LmIg \qquad \textbf{Equation 3-18}$$

where the subscript t indicates the traffic being the source of the load effect, and L is the maximum static load effect due to vehicles with a typical configuration. L varies with the number, weights, and locations of heavy vehicles on the bridge. It is modelled as a lognormal random variable. In Equation 3-18, m is a modification factor covering the variation of vehicle configuration, I is a factor for impact due to dynamic effects of vehicle in motion; and g is a factor for load distribution to the bridge component. In essence, this model of L simulates the total load effect for the bridge component, including the effect of traffic volume. This volume is increased by the number of platoons of vehicles for a given period of time. To account for the effects of overloaded vehicles, the histogram of vehicle weight is constructed by adding histograms of both normal traffic and overloads. In that

way, the model is sufficiently flexible to include site-specific traffic information, when available. It can be applied to truck weight data obtained from any jurisdiction. In their study, the authors obtained the histogram of overloads from the statistics of the permits in the New-York State during 1991. In this model, the authors attempt to account for overloads in actual traffic by considering the permits issued for overloaded vehicles. However, this method remains inaccurate by neither considering the actual frequency of overloads nor considering actual measured weight (but theoretical permitted weight instead). Again, the need for complete unbiased data is recommended.

Laman & Nowak (1997) adopted a new approach for live load modelling by considering site-specific truck loads on bridges and roads. Indeed, truck loading is site-specific and depends on factors such as traffic volume, local industry and law enforcement effort. WIM data obtained for that study was collected at locations of different average daily truck traffic and different proximity to stationary weigh stations; each location corresponded to a different bridge structure. Truck axle weights, GVWs and axle spacing were obtained with a bridge WIM system. Tests indicated that the accuracy of measurements was good or very good for GVW (depending on the number of axles – the accuracy decreases as the number of axles increases). However, the accuracy for axle loads was not as good (±20%). The data obtained showed that between 40 and 80% of the truck population are five-axle vehicles, depending considerably on the location of the bridge. The recorded data also indicated that there were a number of illegally loaded trucks; maximum WIM truck weighs exceeded legal limits by as much as 63%. The recorded WIM data was processed to develop cumulative density functions of gross vehicle weight at each site. Axle weight distributions were also obtained. Important consideration was given to the proximity of stationary truck weigh stations. Indeed, it was expected that legal weight limit violations would occur with increasing frequency as the distance from state police controlled stations increased. The WIM data was checked against a large amount of available data (weighing stations and citation data). The truck weighing station data includes a very large number of trucks and represents the majority of highway traffic; however, it is biased. Very heavy trucks avoid weigh stations by using alternate routes or by operating during hours when the weigh station is closed. Although stationary truck weigh stations are a means of law enforcement, it is shown that overloaded vehicles generally do not pass through them. Citation data (i.e. data relative to overloaded vehicles) were provided by the Michigan State Police Division. The data covers one full year, which resulted in a large amount of

data. The data included number of axles, the axle loads, the axle spacing and the GVW, along with other information.

The author concludes that his study revealed a wide variation between sites, in terms of traffic composition and truck weights. Also, WIM measurements of trucks can be taken discretely during normal traffic conditions, resulting in unbiased data for a statistically accurate sample of truck traffic travelling on a particular highway. Another very interesting conclusion concerns the variation of GVW and axle weight with several factors, such as the proximity to stationary weigh stations, proximity to industrial areas and desirability and economics of the route for truck traffic between major metropolitan areas. Finally, the author observed a direct and negative correlation between law enforcement effort and the occurrence of overloaded trucks.

3.3.2 Dynamic load

In the scope of this thesis, only the static effects due to traffic loads on bridges will be considered. However, dynamic effects are critical when considering relatively short bridges. Therefore some elements that would help to understand and estimate the dynamic contribution to the total effect induced in the structure have been introduced. The emphasis has been put on the loading cases directly related to this research: multiple-truck presence, heavy truck (i.e. semi-trailer type rather than single body type). This introduction to dynamic load can be found in Appendix A.

3.3.3 Truck weight distributions

When considering traffic loads on road bridges, the most significant variable is certainly the distribution of truck weights. While easily derived when WIM data files are available, there are cases where such traffic files are not obtainable. Although WIM files are an exact picture of the actual traffic, they do not contain any information on future traffic (potential traffic growth, modification of weight limits, etc.). Research has thus been carried out in that field; some particular aspects are presented here: the prediction of probable vehicle

weight distribution and the effects that changing weight limits will have on the existing network.

Revising regulatory policies governing the physical and operating characteristics of heavy freight vehicles requires assessment of the implications of adopting alternative policies. Input variables required for the evaluation process exercise are characterised by a high degree of uncertainty. An important input variable is reliable estimates of the probable vehicle weight distributions under different weight limits and enforcement levels. The objective of the study by Fekpe (1995) and Fekpe & Clayton (1995) was to develop an improved methodology for predicting the probable weight distributions, pavement loading, and payloads under alternative weight limit and control policies. Two closely related aspects are addressed:

- understanding the relationship between intensity of enforcement of the weight regulations and the violation rate (i.e., number of trucks in violation as a percent of all trucks inspected);
- predicting the weight distributions for various truck types in terms of the weight limit and the intensity of enforcement.

The main purpose is to provide a reasonable weight prediction methodology that resolves much of the uncertainty about probable changes in weight distributions under alternative weight limits and enforcement strategies.

Fekpe & Clayton (1995) developed an enforcement intensity /violation rate model; it determines the maximum possible violation rate as a function of the level of enforcement and the method of enforcement. This model is incorporated into the weight prediction model through an enforcement correction factor. The underlying assumptions in the model are:

- trucks have definite load carrying capacities and therefore cannot be loaded indefinitely (even with no enforcement, the extent of overloading is constrained by technologies and dimensional limitations);
- the occurrence of overweight trucks is possible no matter how intensive the enforcement practice (there will always be offenders);
- generally, violation reduces with increasing intensity of enforcement.

The authors give the following equation in order to express quantitatively the above assumptions:

$$f(z) = A\exp(-0.10z)$$ **Equation 3-19**

where $f(z)$ is the violation rate (%); A is the maximum expected violation rate when enforcement is zero (a constant that depends on enforcement method); and z is the enforcement intensity (%) (number of trucks inspected as percent of all truck traffic).

The fundamental hypothesis of the GVW prediction model is that the GVW distributions of trucks can be related to and expressed as a function of the governing legal limits and the intensity of enforcement of the regulations. For a given GVW limit and level of enforcement measured by the violation rate, the GVW distribution can be predicted:

$$F(.) = \frac{1}{1+f(z)} P_r(x)$$ **Equation 3-20**

where $F(.)$ is the cumulative density function – the general form of GVW prediction model; $1+f(z)$ is the violation factor; and $P_r(x)$ is the probability of trucks operating less than or equal to given GVW x. The model is calibrated from static weight data collected in two Canadian provinces between 1989 and 1992, and is validated with new independent data not used in the development of the model. It was concluded that the model is sufficiently accurate in predicting GVW distributions and that these are stable in time and in space. The predicted GVW distribution is translated into axle weights on the basis of the weight split characteristics. It is shown that the proportion of the GVW supported on each axle unit of a given truck configuration is specific to that truck type and varies within a narrow range irrespective of the regulatory limit and the operating environment.

The application of the methodology is illustrated with the five-axle tractor semi-trailer in Europe. If the EU weight limits (40 t) are introduced in the U.K. (38 t), the pavement loading from this truck type measured by the truck load factor will increase by at least 22% above the current U.K. condition. The pavements may have to be upgraded to withstand the increased loading and tight weight control may be adopted in order to maintain the quality of the existing infrastructure. In Italy, the existing limit (44 t) is 10% higher than the proposed EU values; about 32% reduction in truck load factor is expected if EU limits were enforced or Italian trucks operate in the continent at EU limits. These results from Fepke & Clayton (1995) show that in a regional context, countries or jurisdictions allowing lower weight limits than proposed regional values, are likely to be more concerned about

the infrastructure impacts of allowing the higher limits. The issue of enforcement becomes more important under such circumstances.

On the one hand, bridge owners feel that they have to control the loading of highway bridges because of the general state of deterioration of the structures, and, on the other hand, the trucking industry feels that it is unfairly restricted by overly conservative bridge owners. These concerns clash when it comes to determining the safe load-carrying capacity of highway bridges. Ghosn (2000) developed truck weight regulations (i.e. new truck weight formula) using a bridge reliability model and Ghosn & Moses (2000) considered the consequences of adapting such a truck weight formula on the safety of the existing bridge network in terms of reliability and increases in the number of structural deficiencies if current rating procedures were maintained.

The overstress ratios used in the development of the actual truck weight formula were solely based on judgement without any consideration of the increased damage due to repeated load applications or the likelihood of overloads and simultaneous truck presence. It is widely accepted that a more rational approach to obtain the overload capacity of bridges should be developed based on structural reliability theory. The objective of Ghosn & Moses' paper is to present a reliability-based procedure to determine the optimal allowable loads on highway bridges considering static and dynamic effects. The usual application of reliability theory for bridges has been in determining the risks of the structures under current loads or the calibration of new design and evaluation codes. The problem of developing overload criteria and consequently obtaining a truck weight formula is an inverse problem. A new truck weight formula that regulates the weight of heavy trucks and axle groups was proposed in the first part of this two-paper sequence base on rational safety criteria (Ghosn 2000). In that paper a review of existing safety levels inherent in the use of current weight regulations was undertaken. Based on that review, a target reliability index of 2.5 is considered to be appropriate for use as a criterion for developing new national truck weight regulations. The procedure utilises a reliability analysis such that the projected truck load effect produces a uniform reliability index of 2.5 for bridges designed according to current AASHTO standards. The maximum live load moment envelope to produce the 2.5 target reliability index is calculated. The proposed truck weight formula is derived to satisfy this required live load moment envelope. The calibration of the proposed formula is executed to satisfy a target reliability index of 2.5 accounting for possible growth in the truck traffic and truck weights with time. In the

companion paper, it is demonstrated that the proposed formula is not sensitive to the statistical database used in the derivation if the target reliability index criterion is changed accordingly.

A major portion of the total cost impacts for new truck weight regulations is the effect on the existing bridge population. Various estimates state that, given current weight regulations, about 130 000 bridges are rated structurally deficient with an estimated $53 billion replacement or upgrading cost (TRB 1990). If a new truck weight regulation introduces higher legal loads, a larger number of structural deficiencies will result; this will increase the estimated replacement and upgrading costs. In their analysis, the authors assume that any bridge that is found to be deficient under a new legislation will have to be replaced (i.e., the possibility of upgrading, posting, or closing an existing bridge are not considered). The possibility of posting or closing bridges for extended periods has been ignored because these options will entail economic and productivity costs to the freight industry that may exceed the cost of replacing the affected structures.

Ghosn & Moses show that the increase in the number of deficiencies is about 3 to 6 times the current level of deficiencies. However, knowing that the proposed increases in the truck weights will result in a large increase in economic productivity, the increase in the number of deficiencies may be justified, at least for the primary bridge system. For example, the TRB truck weight study (TRB 1990) performed a complete comparison between levels of productivity and economic costs for bridges and highways and concluded that the increases in economic productivity would normally justify the costs of upgrading the existing bridge system. The problem appears to be with the secondary bridge system. The sheer number of deficiencies and the fact that many of these bridges may be located in areas with minimal economic activity, would create a big problem for any nationwide changes in truck regulations. The conclusion is that, if the proposed formula is adopted, it will increase the number of bridge deficiencies. It is also observed that the increase in the number of bridge deficiencies is uniformly spread over all span lengths. However, the expected number of bridge deficiencies could be reduced if different truck weight regulations were adopted or if different bridge safety criteria were used in the derivation of the truck weight formula.

Conclusions

The findings presented in this section show that reliable estimates of probable truck weight distributions can be obtained, allowing for enforcement level and changing weight limits. However, slight modifications in weight limits appear to have severe consequences in economical terms. Thus room should be made for such changes (e.g. increase in the weight limits) but these modifications, if they should occur, would probably be introduced progressively. Nonetheless, all the above results should be put into perspective when considering that sometimes a large proportion of heavy vehicles are well above the legal weight limits.

3.4 PREDICTION OF EXTREME VALUES

There exist many approaches to the problem of trying to estimate the extreme values of a stochastic process in time. The guiding principle in selecting a suitable approach is related to the fact that in many engineering applications, one typically seeks to determine the values with return periods that greatly exceed the length of the available data records. This tricky objective dominates any consideration of accuracy, confidence, interpretation, and practicality of the technique selected (Maes 1993). In the author's view, a balance must be struck between practicality and theoretical justification.

3.4.1 Tail equivalence

The characterisation of tails in random variables is of major concern in safety analysis such as structural reliability analysis or a quantitative risk analysis of an engineering system. One of the important questions raised is whether the tail is bounded or unbounded. Therefore, in a statistical analysis of a given set of data, it makes sense to use only the extreme small or large data in the tail modelling. This raises the important issue of the selection of thresholds above which 'tail behaviour' of the data can be justified. In general, thresholds close to the central data will bias the estimation towards the central values that are not informative on the tail. Excessively extreme thresholds will result in high estimation variances.

A key concept in characterising tail behaviour is that of tail equivalence (Resnick 1971, Castillo 1988). It provides a basic principle for deciding if two random variables X and Y

with cumulative distribution functions F_X and F_Y have the same ultimate tail behaviour. For the upper tail (or right tail), F_X and F_Y are tail equivalent if:

$$\lim_{t \to w} \frac{1 - F_X(t)}{1 - F_Y(t)} = 1 \qquad \textbf{Equation 3-21}$$

where w is the maximum value attained by both random variables (the value of w can be infinite). Therefore, in extrapolating a right-hand tail of an unbounded PDF for the purpose of estimating long-term extreme values, it is fully justified to consider that the tail is asymptotically equivalent to, or belongs to the domain of attraction of the (properly normalised) tail of one of the three extreme value distributions: the Gumbel, the Frechet or the Weibull distributions. This principle of tail equivalence is, strictly speaking, only valid for stochastically independent random variables. However, it can be extended to the extremes of general time series, provided some (weak) restrictions on the autocorrelation structure are satisfied (Leadbetter et al. 1983). This approach becomes increasingly justified when the sample size and (or) the level of the extreme increases, that is, as peaks become more and more independent.

3.4.2 Selection of an appropriate distribution

It is assumed that $(X_1, X_2, ..., X_n)$ are independent and identically distributed random variables coming from a continuous parent population with a cumulative distribution function $F(x)$ and probability density function $f(x)$. Castillo & Sarabia (1990) have shown that, 'when dealing with extremes, and n is large enough, the infinitely many degrees of freedom we have with the distribution $F(x)$ are reduced to three parametric families'. In other words, no matter what the exact parent distribution $F(x)$ is, one of the three distributions (Gumbel, Weibull and Frechet) can be used for approximating extremes (maxima or minima). Additionally, even though the limit of a given distribution belongs to one of the three families, in most cases they can be reduced to only two if we take into account the following two properties (Castillo 1988):

- a parent distribution with non-finite endpoint in the tail of interest cannot lie in a Weibull-type distribution domain of attraction;
- a parent distribution with finite endpoint in the tail of interest cannot lie in a Frechet-type distribution domain of attraction.

Thus, discussions between the choice of Gumbel versus Weibull, or Gumbel versus Frechet distributions for approximating extremes 'make no practical sense, because Gumbel distributions can be approximated, as closely as desired, by Weibull or Frechet distributions (the Gumbel families are in middle line between the Weibull and the Frechet families)' (Castillo & Sarabia 1990).

The most common problem in daily practice is the following: a sample is given, but no knowledge about $F(x)$ is available. Thus various methods can be used in order to select the appropriate limit distribution from the available data; among which: probability-paper, weighted least-squares and curvature methods. When using probability papers, the standard procedure consists of drawing the empirical cumulative distribution function and fitting a straight line to the whole range of data. In the case of extreme value problems, probability papers must be used in a different manner. In this case, it is known that the sample does not follow the prescribed extreme value distribution, but is only asymptotic to it. The practical method for determining the type of domain of attraction consists of the following steps:

- determine whether it is a problem of minima or maxima;
- draw the empirical CDF on the corresponding (maxima/minima) Gumbel probability paper;
- observe the curvature and the slopes of the CDF in the tail of interest. If the curvature is not negligible and the slope goes to zero or infinity, then reject the hypothesis that $F(x)$ lies in a Gumbel-type domain of attraction. Depending on the curvature, decide in favour of Weibull or Frechet. In case of maxima, convex downward (slope tending towards infinity) indicate Weibull-type and concave downward (slope tending towards zero) indicate Frechet-type.

Only the tail of the distribution governs the behaviour of the extremes of interest. Thus, the use of the other tail and central data will only disturb the estimation of limit distributions. Consequently, some data values must be excluded from the fitting procedure, and the rest of the data values must be given different weights. In selecting the weights, two important conflicting facts must be taken into consideration. On the one hand, estimated percentiles in the tail of interest have the largest variances. On the other hand, they approach the limit distribution values more closely. However, one thing is certain: data points in the tail of no interest must be given very small or null weights because for them both facts point in this direction.

The basic idea of the curvature method is to measure the curvature in the tail of interest by means of the ratio of the mean slopes in two neighbouring zones of the tail. To calculate the mean slopes of the zones, the curvature method proposes fitting two straight lines by least squares and using, as a measure of the curvature, the quotient of the slopes of these two lines. Again, the main issue lies in the selection of the number of tail values to consider.

Maes (1993) addresses the question of developing design criteria for thermal effects in concrete bridges, the objective being the determination of extreme temperature effects having specified return periods. In order to identify to which of the three extreme value tails the peak values belong, basic Gumbel plots are constructed: the peaks X_i, ordered decreasingly, are plotted against the double logarithm of their empirical cumulative distribution values η_i, where

$$\eta_i = -\ln(-\ln(p_i)) \qquad \textbf{Equation 3-22}$$

The Gumbel plot allows the type of extreme value distribution to be determined on the basis of the curvature of the right tail (as explained above). In view of the previous considerations, a straight-line approximation for the Gumbel type must account for the fact that peak values should be accorded more importance than the bulk of the data. In other words, there is no point in achieving a close fit to the entire data set at the expense of an unsatisfactory fit in the tail area. Since the interest lies in the extremes, an error minimisation scheme that emphasizes the tail data is needed. This can be achieved by a weighted least-squares technique, which involves minimising the following expression with respect to a and b:

$$\sum_{i=i^*}^{n} w_i \left[F(x_i \mid a,b) - p_i\right]^2 \qquad \textbf{Equation 3-23}$$

Where $F(x \mid a,b)$ represents the CDF of the Gumbel distribution with mode a and dispersion parameter b; the weights w_i, given by

$$w_i = \frac{1}{(1-p_i)^2} \qquad \textbf{Equation 3-24}$$

can be seen to decrease rapidly when i or x_i decreases. This means that the selection of the cut-off level i^* (which determines the number of peaks included in the analysis) becomes inconsequential. The choice of the weights w_i can be justified in many ways: the minimisation of Equation 3-23, which essentially represents a least-squares of the sum of relative errors of probability, can also be shown to coincide with a least-squares of the absolute error on return periods (Castillo 1988). Moreover, since the values of p_i are close to unity, it follows that the minimisation is equivalent to fitting the best straight line $\eta = (x - \hat{a})/\hat{b}$ through the $(n - i^* + 1)$ pairs of tail values (x_i, η_i). In the latter case, however, the choice of i^* has a critical impact on the resulting regression line. From this point of view, the tail-weighted least-squares procedure is clearly recommendable. In the case of the Weibull type, a best straight-line must be sought not between η and x, but between η and $[-\ln(\delta - x)]$, where δ is the location parameter of the Weibull distribution. Consequently, the analytical procedure consists of minimising the following sum of square errors, SSE:

$$SSE = \sum_{i=i^*}^{n} \{\eta_i - \gamma[-\ln(\delta - x_i) - \ln c]\}^2 \qquad \textbf{Equation 3-25}$$

with respect to the location parameter δ, the exponent γ, and the scale parameter c of the Weibull CDF. To avoid having to select the value of i^*, Equation 3-25 can easily be reformulated as a weighted least-squares procedure, similar to the Gumbel approach based on Equation 3-23. It follows from the analytical expressions of the Gumbel and the Weibull CDF that the characteristic value x_k, with a return period of k years (with n_{ext} extreme values per year), are respectively equal to

$$x_k = \hat{a} + \hat{b}\ln(n_{ext}k) \qquad \textbf{Equation 3-26}$$

$$x_k = \hat{\delta} - \hat{c}\left(\frac{1}{n_{ext}k}\right)^{1/\hat{\gamma}} \qquad \textbf{Equation 3-27}$$

In engineering, it is common to work with excesses over thresholds rather than maxima, in which case the generalized Pareto distribution arises as the limiting distribution (Dargahi-Noubary 1989, Caers & Maes 1998):

$$F_{GPD}(x) = 1 - \left(1 + \frac{\gamma}{\sigma}(x-u)\right)^{-1/\gamma} \qquad u < x < w$$ **Equation 3-28**

where

$$w = \infty \qquad \gamma \geq 0$$
$$w = u - \frac{\sigma}{\gamma} \qquad \gamma < 0$$ **Equation 3-29**

and u is a high threshold, σ is a positive scaling and γ is the so-called extreme value index. This extreme value index plays a key role in assessing the weight of the tail:

- when $\gamma > 0$, the tail is heavy (Pareto-like tail);
- when $\gamma = 0$, the tail is exponential-like, it includes all distributions having extremes belonging to the Gumbel domain of attraction for extreme values;
- when $\gamma < 0$ the tail is Beta-like, which includes the distributions having a finite upper bound.

In order to distinguish between central data and tail data, many practitioners use visual methods based on 'quantile plotting' or probability paper. An example of powerful quantile plot is the so-called generalised Pareto quantile-plot. In a sense, the GP quantile plot is similar to the Gumbel plot, with the difference that, in the GP plot, one always expects a linear behaviour, whereas the Gumbel plot is either linear, convex or concave. According to Caers & Maes (1998), the GP-plot seems more powerful since it is easier to detect linearity than to detect convexity or concavity. However, the challenge remains: how does one choose a 'good' treshold *u*, i.e., how many values should be included in the tail? Boos (1984) recommends that the ratio *k* (number of tail data) over *n* (total number of data) should be:

$$\frac{k}{n} = 0.02 \qquad 50 < n < 500$$
$$\frac{k}{n} = 0.1 \qquad 500 < n < 1000$$ **Equation 3-30**

Castillo (1988) suggested to use $k \cong 2\sqrt{n}$; while more recently, Hasofer (1996) recommended to use $k \cong 1.5\sqrt{n}$.

3.4.3 Prediction of extreme loads and load effects

Any probabilistic code calibration requires the determination of characteristic values of loads or load effects to keep the probability of structural failure below certain limits. This is especially true of the bridge loading codes that define the design loads for road bridges. The calibration of the vehicular loading models developed for the Eurocode are based on the results of extensive simulations using the available traffic data collected in the EU countries. However, such a calibration requires characteristic values of load effects related to Ultimate Limit State and Service Limit State, having specific probabilities of exceedance in the total lifetime of the bridges, together with the statistical parameters of the load effects. Because no traffic measurement is performed over periods longer than a few weeks, extrapolations of both loads and load effects are needed. The question is: how to extrapolate the computed maxima from one week to 100 years and determine the probability of the target values being exceeded?

Jacob et al. (1991) propose various methods of extrapolation depending on the load (axle load, vehicular load or load effect) to extrapolate:

- Extreme axle load and lorry load:
  - Method of the half-normal distribution
  - Method of the multi-modal Gumbel or Gaussian distributions
  - Method of the asymptotic extreme distributions
- Extreme total load on a lane length:
  - Method of the half-normal distribution
  - Method of Monte-Carlo simulation
  - Method of analytical modified Poisson model
  - Method of simulation and extrapolation of real traffics
  - Method of jam simulation program
- Extreme load effects:
  - Method of the half-normal distribution
  - Method of Monte-Carlo simulation
  - Method of Rice's formula
  - Method of simulation and extrapolation of real traffics
  - Method of jam simulation program.

Jacob & Maillard (1991) recommend the use of a particular method depending on the type of traffic (free or jammed):

- the load effects produced under free traffic, which have to be extrapolated over long time periods and magnified by dynamic impact factors;
- the load effects due to traffic jams including cars and lorries, generally occurring a small fraction of the time and at reduced speed, without dynamic magnification;
- the load effects due to traffic jams without cars, occurring only a few times during the bridge lifetime, under exceptional circumstances such as a demonstration or a queue behind a toll area or a border control.

The main interest of this thesis is in the free-traffic case, therefore only the methods relevant to that traffic type are now examined in more detail, namely (i) the half-normal method, (ii) the Rice's formula method and (iii) the simulation of real traffic flow. In (i), the traffic records are first used to compute the load effect time history and histograms with the help of CASTOR (Eymard & Jacob 1989). The main basic assumption in this method is that the upper tails of the distributions of the local extrema of the considered variables have a Gaussian shape. Then a half-normal PDF may be fitted to the part of the histogram corresponding to the decreasing upper tail. In (ii), the main assumption is that the load effect is a Gaussian stationary process. Rice's formula gives the level crossing distribution; its parameters are fitted to the level crossing histogram of the load effect computed by simulation (CASTOR) for a traffic record over a defined time period. Finally, in (iii), the extrapolation coefficients provided by the modified Poisson model for the total load on a lane are used to magnify the extreme load effects computed from one week of traffic. In the modified Poisson traffic model, the density of the total load on the bridge is obtained through an analytical convolution of the traffic flow process with the gross weight distribution described by a bimodal density with two Gaussian modes. Extrapolation coefficients are then computed from one week to 50 or 100 years, as the ratio between the corresponding total load fractiles; it has been shown by Jacob et al. (1991) that these coefficients do not depend on the span length. It is assumed that these coefficients remain valid for any load effect other than the total load on a span. These coefficients are applied to extrapolate the one-week extreme load effects computed by CASTOR under the recorded traffics.

The various methods presented are compared for the prediction of the extreme load effects having a return period of 1000 years, or a 10% probability of being exceeded within 100

years. Two load effects are considered: the total load on a lane length and the mid-span bending moment of a simply supported beam; and various lane lengths are considered, ranging from 20 to 200 m. The results are given in (Equivalent) Uniformly Distributed Load (UDL or EUDL). For lengths shorter than 40 to 50m, the maximum load is obtained under free traffic, after applying the impact factors; for lengths longer than 50m, congested traffic governs. For the total load on a span length, almost all the results agree with variations smaller than 10%. For the mid-span bending moment of a simply supported beam, the scattering is a little bit higher (Jacob et al. 1991). Also, triangular influence lines are more sensitive to the isolated vehicles than flat ones. Based on the work of Jacob & Maillard (1991), it is found that a good load model cannot be reduced to uniform distributed load, at least for short spans. Further developments of the above research are presented in O'Connor (2001); these developments include the re-calibration of the Eurocode 1, Part 3, Traffic Loads on Bridges (CEN 1994).

As mentioned earlier, one of the extrapolation methods consists of fitting Rice's formula to the tail of the level crossing histograms issued from the combination of weigh-in-motion records and influence surfaces. The practical problem related to that approach is the determination of the number of class intervals to be taken into account for fitting (Cremona 2001). During the Eurocode studies, the choice was made in an empirical manner by successive tests. One critical assumption in obtaining a good approximation of the tail is the choice of the value for the starting class interval at which the fitting is made. An intuitive approach consists in applying a statistical test between the fitting and the Rice formula, such as the Kolmogorov K-test. Following Cremona's results (Cremona 2001), the optimal fitting is obtained after a series of successive statistical tests based on the Kolmogorov test. The optimal fitting corresponds to the largest number of class intervals verifying a given confidence level for the Kolmogorov test. Extrapolation of traffic loads for any return period can then be deduced in a straightforward manner.

Finally, when a characteristic value is predicted by an extreme value analysis, a design engineer often takes it as a deterministic quantity and proceeds into structural design with few considerations of the reliability of that characteristic value. To fill the gap in the knowledge of the reliability of extremal estimates, Goda (1988) undertook a series of Monte-Carlo simulation studies. In these studies, 10 000 data sets were generated for each combination of sample size, censoring rate, and distribution functions. Each sample was analysed by a standard procedure in extremal statistics, and statiscal variability was

examined for the estimates obtained from the 10 000 samples. Several empirical formulas have been derived for the standard deviation of return values and the confidence interval of return period.

In O'Brien et al. (1995), one can find an example of application of these empirical formulas. In Northern Ireland the Foyle Bridge has been used experimentally for direct measurement of deflection statistics in free-flowing traffic and statistical extrapolation to calculate site-specific values. A technique suitable for non-specialists in statistics is presented for the verification of compliance with the extreme value type I statistical distribution and the calculation of the distribution parameters. Using probability paper, the parameters of the Gumbel distribution can be estimated. These parameters known, the design value of a load effect for a specified return period can easily be calculated. The accuracy of the characteristic value depends on the quantity of data used for its calculation. Goda's empirical formula is used to establish a margin of error to allow for variability in the result.

3.5 SUMMARY AND CONCLUSIONS

First, numerous approaches aimed at modelling live loads accurately on roads and especially bridges have been discussed. From the simple and manageable Poisson process to the more complex full simulation of real traffic flow, the various models kept improving over the years. However, no matter how advanced the models became, most of them have some limitations; the most commonly encountered one is an important limitation with regard to the scope of this thesis: these approaches are restricted to bridges over 30m long. Nonetheless, all the fundamentals that will later be used by the author to develop innovative models have been introduced through the detailed discussion of case studies.

In a second part, the benefits of using field measurements and Weigh-In-Motion data have been demonstrated. Some of these benefits include: more reliable modelling of the truck weights distribution, which include all the over-weight vehicles, and the possibility of obtaining accurate measurements of both static and dynamic effects due to the passage of trucks over a bridge. Finally, the use of extreme value distributions in order to predict extreme effects has been addressed. Various techniques for choosing the most appropriate

distribution have been presented. Then the use of different methods of prediction of extremes in the field of traffic loads is discussed.

Chapter 4

TRAFFIC DATA AND LOAD EFFECTS

Chapter 4 TRAFFIC DATA AND LOAD EFFECTS

4.1 INTRODUCTION

The first aim of this chapter is to present the Weigh-In-Motion (WIM) data files used in the development of the load models for assessing highway bridges. The description of the WIM files concentrates on a few crucial aspects: the traffic intensity, which is the determining factor in the frequency of loading events; the gross vehicle weight and axle weight distributions, which condition the severity of the loading events; and finally the truck geometry in terms of axle spacings, which is essential in the case of relatively short bridges. The static effects of the traffic actions (e.g., moment, shear) that are considered throughout this thesis are illustrated and the new concept of 'influence response' is introduced. The sensitivity of the influence responses corresponding to the various effects considered is then studied. Finally, in a third section, the traffic characteristics necessary for the development of a live load model are modelled. The results of the two former sections are used to make some assumptions that simplify the modelling process without introducing unreasonable simplifications.

4.2 DESCRIPTION OF MEASURED TRAFFIC FILES

4.2.1 Introduction

In the scope of this research, different traffic files have been used. These files all represent French traffic and have been generously given by the Laboratoire Central des Ponts et Chaussées (LCPC) of Paris. These traffic data files have been chosen as they were used for the recalibration of the Eurocode and are considered to be representative of European traffic (Bruls et al. 1996, O'Connor et al. 1998). The files were obtained using Weigh-In-Motion systems. General information is given about the different sites in Table 4-1. It

should be noted that only vehicles weighing at least 35 kN were recorded; in other words only the trucks were recorded. The cars were not recorded in order to limit the size of the traffic file and thus to record continuously a longer period of traffic. The speed limits and flow rates given in the table refer to trucks only; they do not include the cars. In Table 4-1, when the number of lanes recorded is less than the total number of lanes, it means that only the lanes corresponding to slower and heavier traffic were recorded, the 'outside' lanes.

Table 4-1: General information about the Weigh-In-Motion sites [(a) AHFR = Average Hourly Flow Rate , (b) ADFR = Average Daily Flow Rate]

Name of the site	Angers	Auxerre	A196	A296
Nature of the road	National Road	Motorway	Motorway	Motorway
Road name	RN23	A6	A1	A2
Location of the site	near Angers	near Auxerre	near Ressons	near Cambrai
Total number of lanes	3	4	6	4
Number of lanes recorded	2	4	4	4
Speed limit	80 km/h	110 km/h	110 km/h	110 km/h
Time of recording	April 1987	May 1986	Sept. 1996	Sept. 1996
Duration of recording	1 week	1 week	5 days	1 week
AHFR[(a)] during the week - Direction 1	64	139	349	126
AHFR[(a)] during the week - Direction 2	69	142	314	134
ADFR[(b)] during the week - Direction 1	1536	3336	8376	3024
ADFR[(b)] during the week - Direction 2	1656	3408	7536	3216

4.2.2 Traffic intensity

The traffic intensity can be described in terms of flow rates, usually taken as average hourly flow rates of trucks. It should be emphasised that only trucks are considered throughout this work. The data files represent one full week of data; however, the flow

rates of heavy good vehicles is very low during the week-ends as most of the trucks are not allowed to travel between Friday night and Sunday night on the French road network. Figure 4-1 illustrates the distribution of hourly flow rates over the day for a full week of traffic (Angers site). The truck flow rates during the weekend are very low in comparison with those during the weekdays. In addition, the flow rate distribution during the day appears to follow a pattern; this distribution is basically the same for any weekday. The only noticeable discrepancies are Friday afternoon or Monday morning, merely a consequence of the weekend beginning and finishing. Based upon the above observations, it is reasonable to assume that the distribution of flow rates over the day is the same for any of the weekdays and that the traffic of trucks during the weekend is negligible.

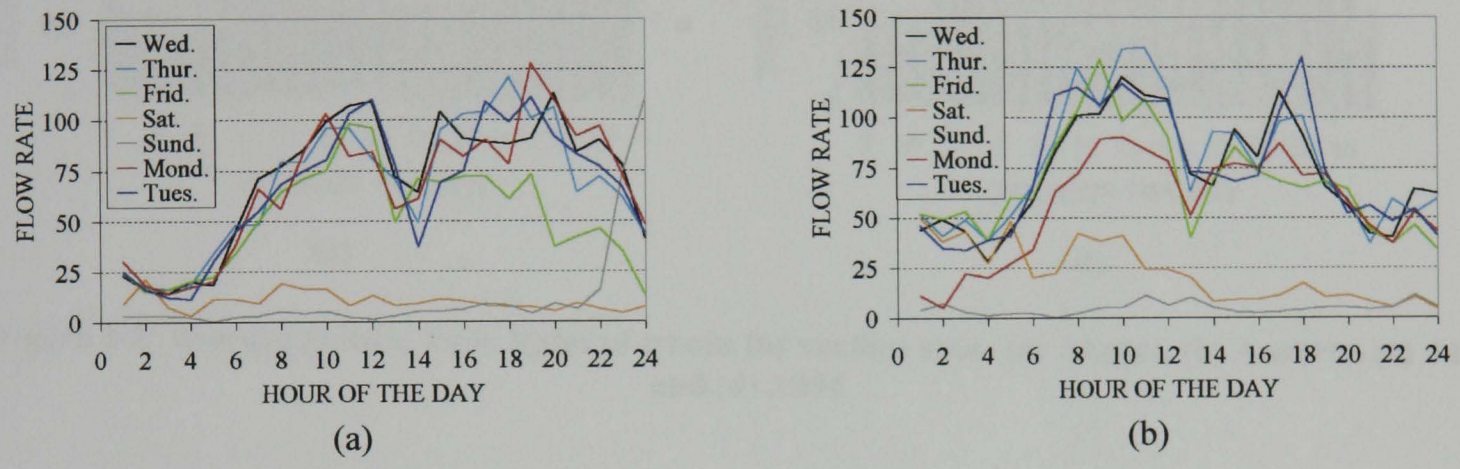

Figure 4-1: Average Hourly Flow Rates (trucks per hour) for each day of the week: (a) direction 1, (b) direction 2

The data is presented for 4 different sites: Angers, Auxerre, A196 and A296; and for each site both directions of traffic are presented separately (Figure 4-2). The 4 sites present different characteristics in terms of intensity, distribution over the day and distribution between the two directions of traffic. Angers shows two main peaks, one during the morning and one in the afternoon, with a period of lower traffic at lunchtime, and a period of very low traffic during the first few hours of the night. Although there are differences between the two directions, the general trend is the same. On the other hand, Auxerre exhibits different trends for each direction; in direction 1 the flow rates oscillate between 100 and 150 trucks per hour all day long, including the night, while direction 2 shows a little peak in the morning and a strong peak in the evening, around 22:00. On the A196, a similar observation can be made: for direction 2 the traffic is quasi-constant between 6:00 and 23:00 (with an average value of 300 trucks per hour), with a low between 24:00 and 5:00; direction 1 shows a traffic that increases from the early morning until about 13:00, remains around 450 trucks per hour until 16:00 and then decreases gradually.

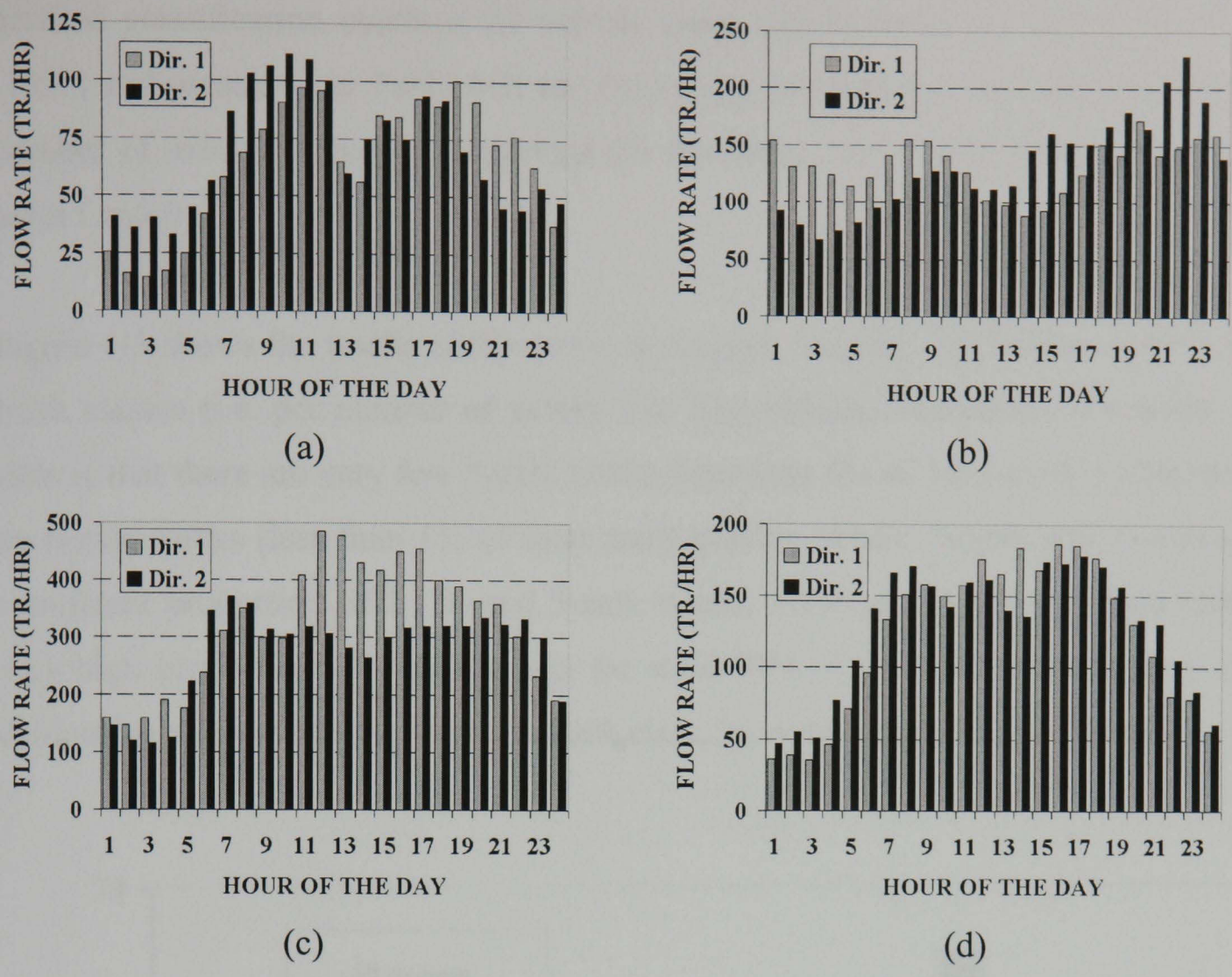

Figure 4-2: Average Hourly Flow Rates of trucks for various sites: (a) Angers, (b) Auxerre, (c) A196 and (d) A296

Finally, A296 exhibits the same trend for both directions throughout the day, increasing gradually from 4:00 until 8:00, oscillating around 150 trucks per hour until 19:00, before decreasing gradually until 24:00. In conclusion, the average hourly flow rates of trucks vary enormously from one site to another, and can also vary significantly from one direction to the other for certain sites. It is therefore recommended to consider the flow rates separately for the directions of traffic, as it is a variable that is not only site-specific but also direction-specific.

4.2.3 Traffic composition

Traffic composition can be described in different ways, from a simplistic distinction between cars and heavy vehicles to a detailed description of each vehicle type (function of number of axles and axle spacings). Two compositions are described hereafter: a simple one in which the vehicles are divided into 5 classes (2-, 3-, 4-, 5- and 6-axle vehicles) and a more detailed one in order to analyse the exact composition of the recorded traffics. The

detailed classification contains 21 vehicle types and is based on Crespo & Minguillon (1997) and presented in Table 4-2; the distinction between the vehicles is based upon the number of axles and the axle-spacings (in the table, 'S*ij*' refers to the spacing between axles *i* and *j*).

Figure 4-3 shows the traffic composition at Angers, Auxerre, A196 and A296, in terms of truck classes (i.e. per number of axles). The first obvious characteristic common to all 4 sites is that there are very few 3-axle trucks (less than 5% of total truck traffic) and nearly no 6-axle trucks (less than 1% of total truck traffic). While Angers and Auxerre reveal a significant proportion of 2-, 4- and 5-axle trucks, A196 and A296 are characterised by a very high proportion of 5-axle trucks (at least 60% of the total truck traffic). A further distinction can be made within each truck class, by considering the vehicle types.

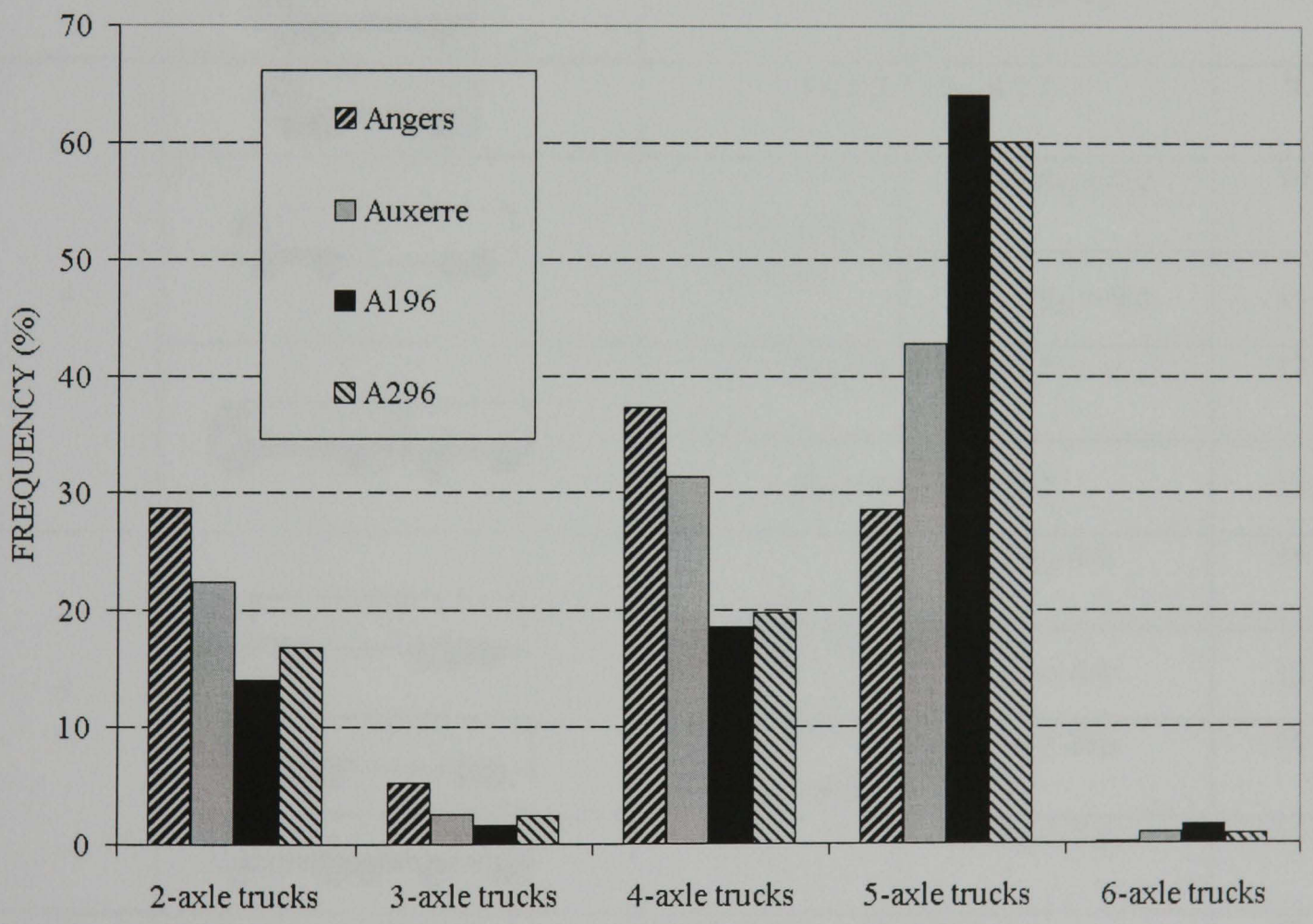

Figure 4-3: Traffic composition by truck class for various sites

Table 4-2: Detailed vehicle classification

No. Axles	Configuration			Vehicle type
2	*(Car)*	$S_{12} \leq 3.1$	$P \leq 35$ kN	1
	(Van)		$P > 35$ kN	2
	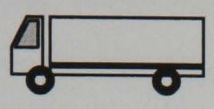	$3.1 < S_{12} \leq 3.6$		3
		$3.6 < S_{12} \leq 4.6$		4
		$4.6 < S_{12}$		5
3	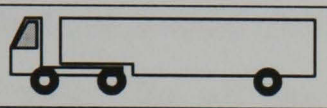	$S_{12} + S_{23} > 9.0$		6
	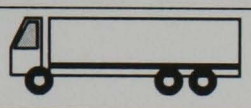	$S_{12} + S_{23} \leq 9.0$	$S_{12} > S_{23}$	7
	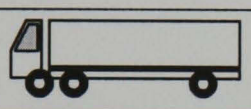		$S_{12} \leq S_{23}$	8
4	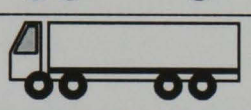	$S_{12} \leq 2.2$; $S_{34} \leq 2.2$		9
	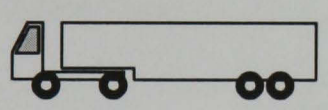	$2.2 < S_{12} \leq 4.0$ $S_{34} \leq 2.2$	$S_{12} + S_{23} \leq 9.0$	10
			$S_{12} + S_{23} > 9.0$	11
	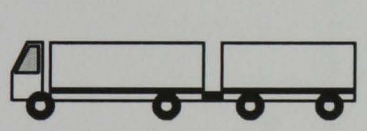	$S_{12} > 4.0$; $S_{34} \leq 2.2$		12
		$S_{12} > 4.0$; $S_{34} > 2.2$		13
5	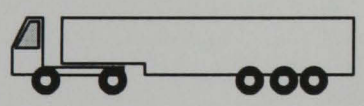	$S_{34} + S_{45} \leq 4.0$	$S_{12 \leq} 4.0$	14
			$S_{12} > 4.0$	15
	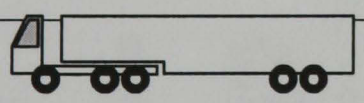	$S_{34} + S_{45} > 4.0$	$S_{34} > 2S_{45}$	16
	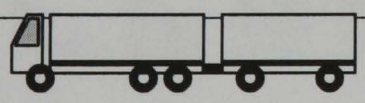		$S_{45} > 3.0$	17
6	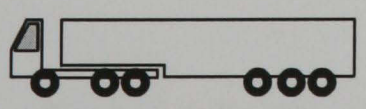	$S_{14} \leq 11.0$		18
		$S_{14} > 11.0$		19
	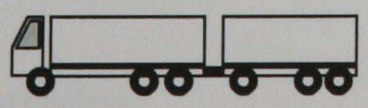	$S_{34} > 2.5$		20
		$S_{34} \leq 2.5$		21

Figure 4-4 shows the traffic composition for the 2-, 4- and 5-axle trucks representing respectively vehicle types 2 to 5, 9 to 13 and 14 to 17. Vehicle types corresponding to 3- and 6-axle trucks are not presented, as their proportion is very low, and vehicle type 9 (one body 4-axle truck) are not presented as their proportion is almost nil for the 4 sites considered. Most of the 4-axle trucks are represented by vehicle types 10 and 11, namely tractor/semi-trailer (with a tandem at the back). The only distinction between vehicle type 10 and 11 is in the distance between the 1st axle (i.e. 1st axle of the tractor) and the 3rd axle (i.e. the 1st axle of the semi-trailer). The vast majority of the 5-axle trucks correspond to vehicle type 14, namely the tractor/semi-trailer type (with a tridem at the back). Overall, for the 4 sites considered, between 55 and 70% of all the trucks consist of the tractor/semi-trailer; either the 4- or 5-axle version (i.e. with a tandem or a tridem). A table containing the numerical values for all the vehicle types for the various sites can be found in Appendix D.

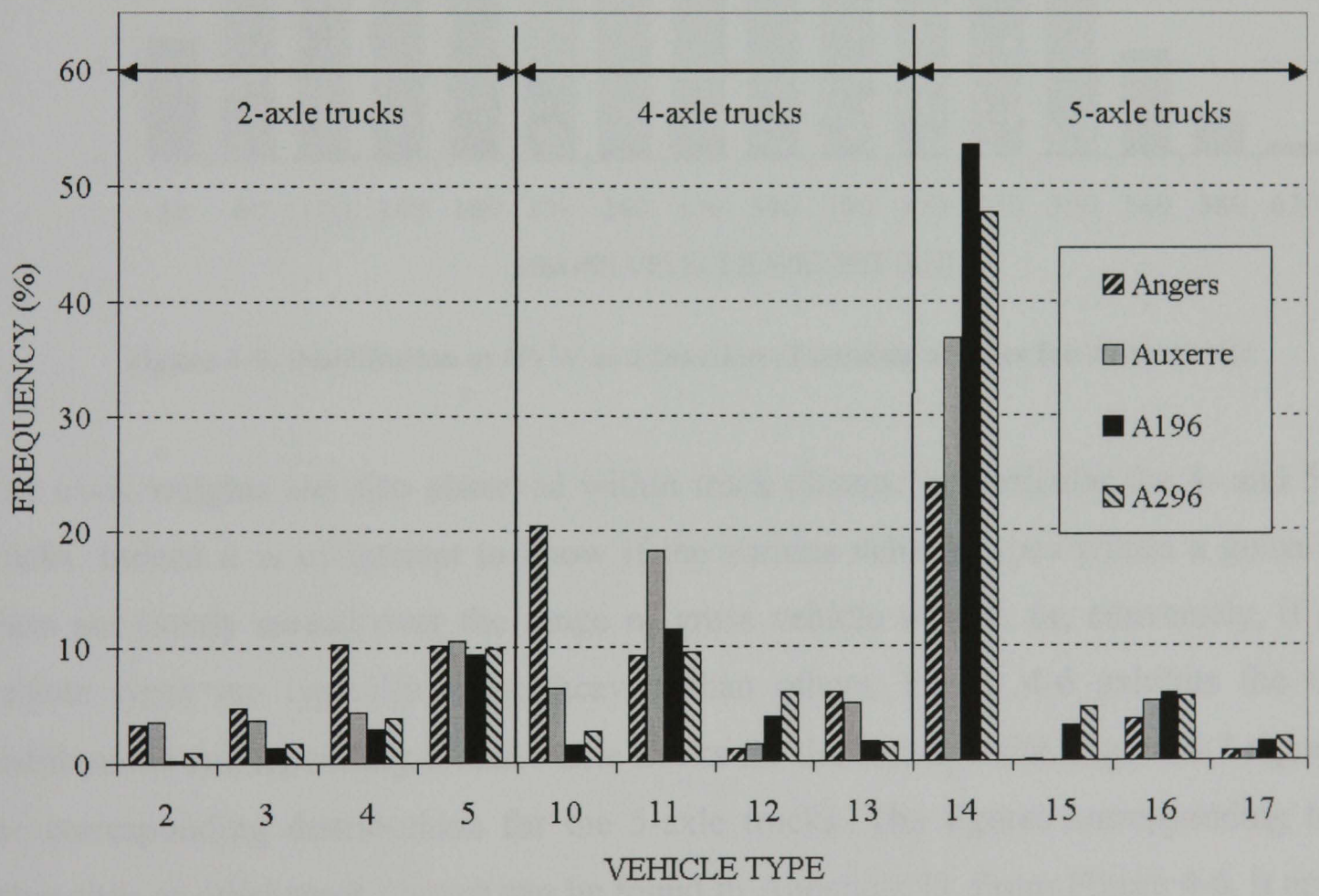

Figure 4-4: Traffic composition by truck type for various sites

4.2.4 Truck weights

The truck weights are observed not only in terms of frequency but also by considering truck classes, for the 4 different sites (cf. Figure 4-5). As expected, the 2- and 3-axle trucks

represent the first part of the histogram, namely the lighter trucks, while the 4-, 5- and 6-axle trucks correspond to the second part of the histogram: the heavier trucks. When moving towards the tail of the distribution, the 4-axle trucks become less frequent and the 5-axle trucks are dominant. Similar figures for the other sites can be found in Appendix D.

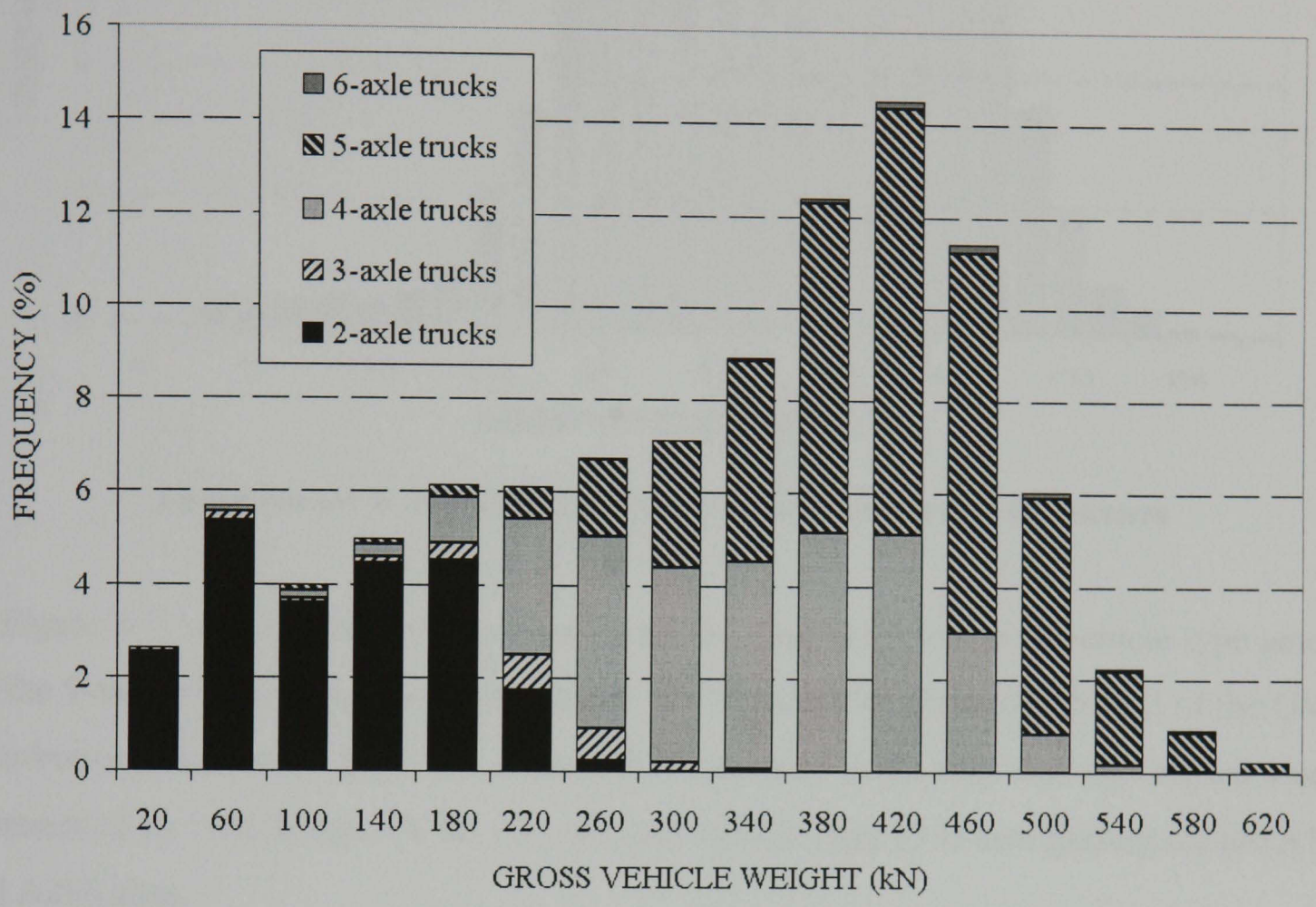

Figure 4-5: Distribution of GVW as a function of number of axles for Auxerre site

The truck weights are also observed within truck classes, in particular the 4- and 5-axle trucks. Indeed it is of interest to know if the various vehicle types within a given truck class are evenly spread over the range of gross vehicle weight, or, conversely, if some vehicle types are typically lighter/heavier than others. Figure 4-6 exhibits the GVW distributions corresponding to the 4-axle trucks for the Auxerre site. Figure 4-7 represents the corresponding distributions for the 5-axle trucks. The figures corresponding to the other sites or other truck classes can be found in Appendix D. From Figure 4-6, it appears that vehicle types 10 and 11 are the most heavily loaded 4-axle trucks, in comparison with vehicle type 12 and 13, which are lighter. When considering vehicle types 10 and 11, differences are observed between sites: Angers shows a higher proportion of vehicle type 10 in the tail of the distribution, while for Auxerre, A196 and A296, the most represented vehicle type towards the tail is vehicle type 11.

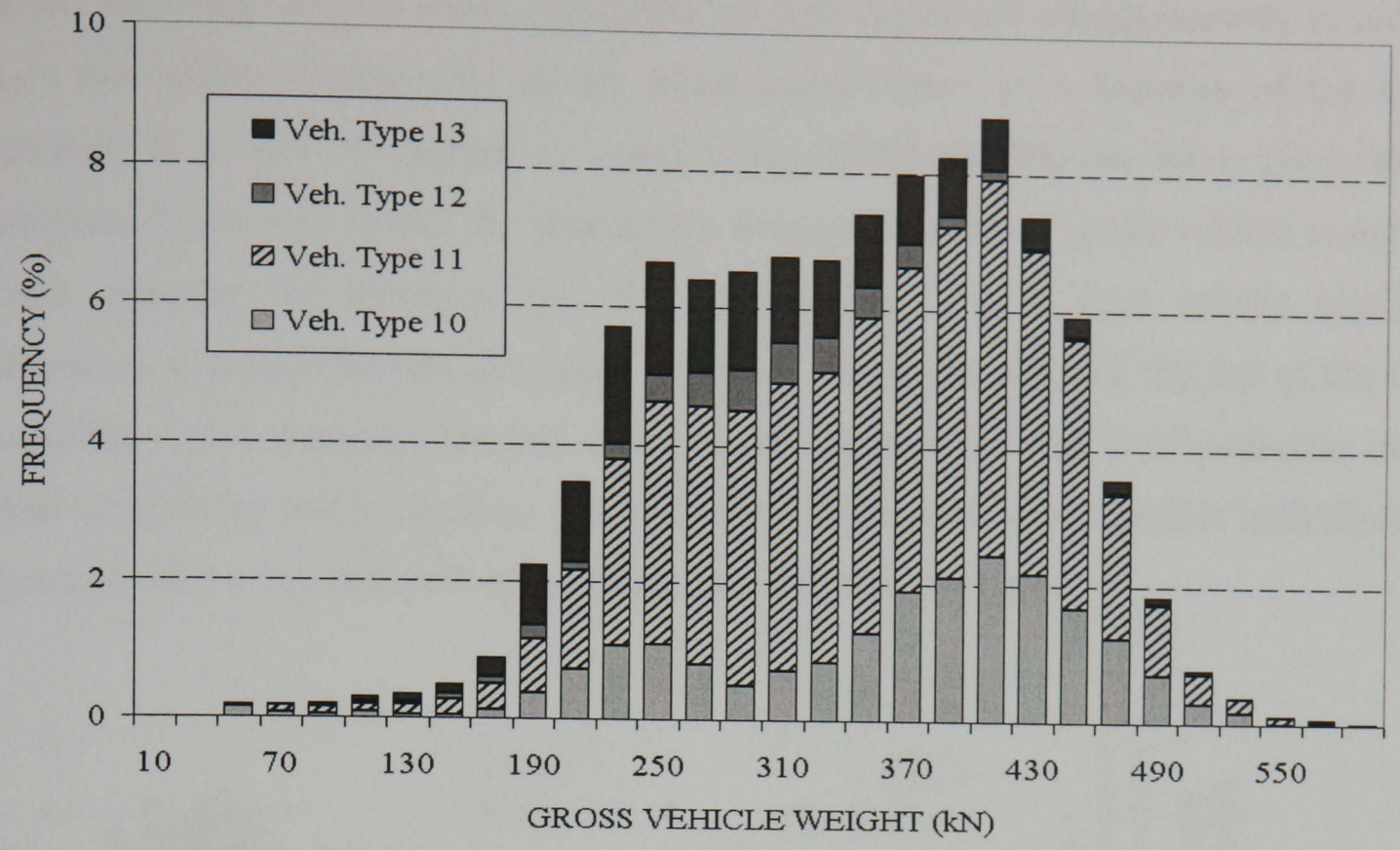

Figure 4-6: GVW distribution of 4-axle trucks by vehicle type for Auxerre

In Figure 4-7, vehicle type 14 is shown to be the most representative vehicle type among all the 5-axle trucks throughout the range of GVW, especially towards the tail of the GVW distribution. However, there are some (although very few) very heavily loaded trucks represented by vehicle type 16 for all sites, and vehicle type 15 is also present for the A196 and A296 sites.

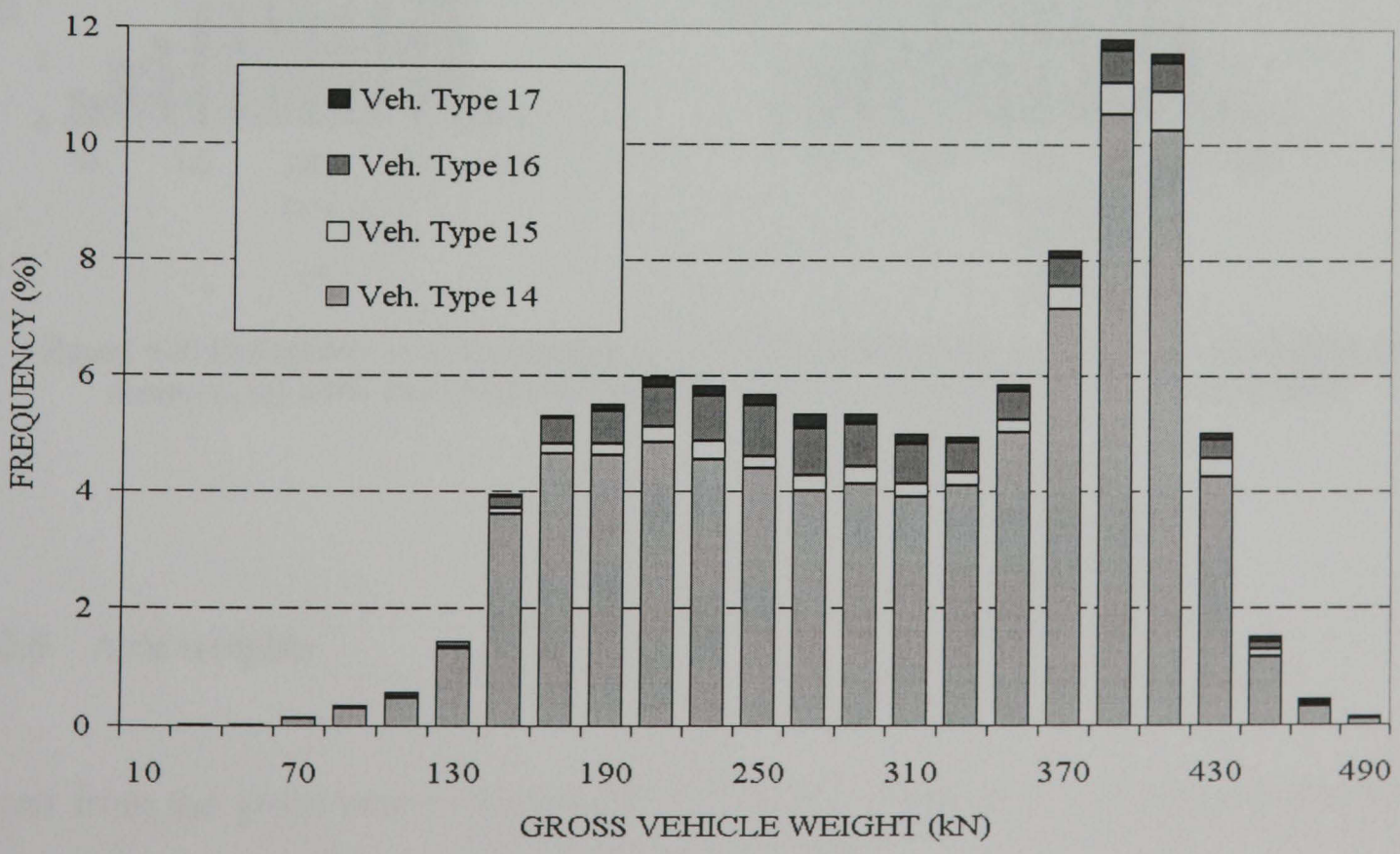

Figure 4-7: GVW distribution of 5-axle trucks by vehicle type for A196

So far, the truck weights were considered for both directions simultaneously in order to study the relative distribution of the truck classes/types as a function of the GVW. However, it is also of interest to consider the GVW distribution for a given site by direction. Figure 4-8 shows the probability density function of gross vehicle weight, all trucks included, by direction and for various sites. The 4 sites exhibit significant differences between the two directions of travel, especially towards the tail of the GVW distribution. It is generally the tail of the weight distribution that is of particular interest when considering traffic loading; it is therefore recommended to consider both directions separately as it is not only site-specific but also direction-specific.

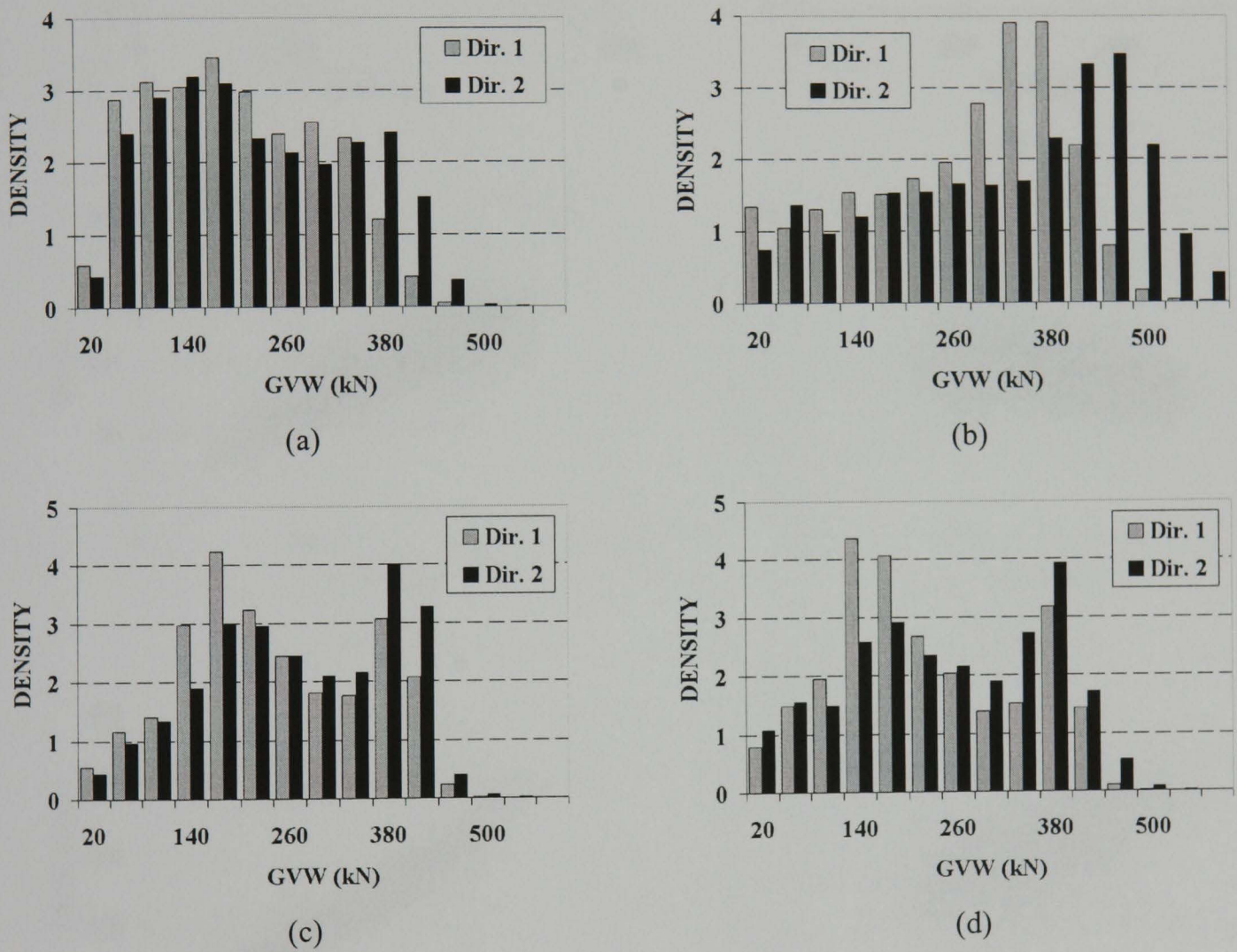

Figure 4-8: Probability density function of GVW by direction for various sites: (a) Angers, (b) Auxerre, (c) A196 and (d) A296; [*density values should be divided by a factor of 1000*]

4.2.5 Axle weights

Apart from the gross vehicle weight itself, it is also important to distinguish between the individual axle weights and group of axles' weights when considering relatively short bridges. It is common to describe the axle weight (or group of axles' weight) as a proportion of GVW carried by the axle (or group of axle) considered. Figure 4-9 shows the

weights of the two front axles and the back tridem of vehicle type 14 for the Angers site. Vehicle type 14 has been selected, as it is the most representative type for all the sites considered. Axle weights and tridem weights are shown in kN and in percentage of gross vehicle weight carried.

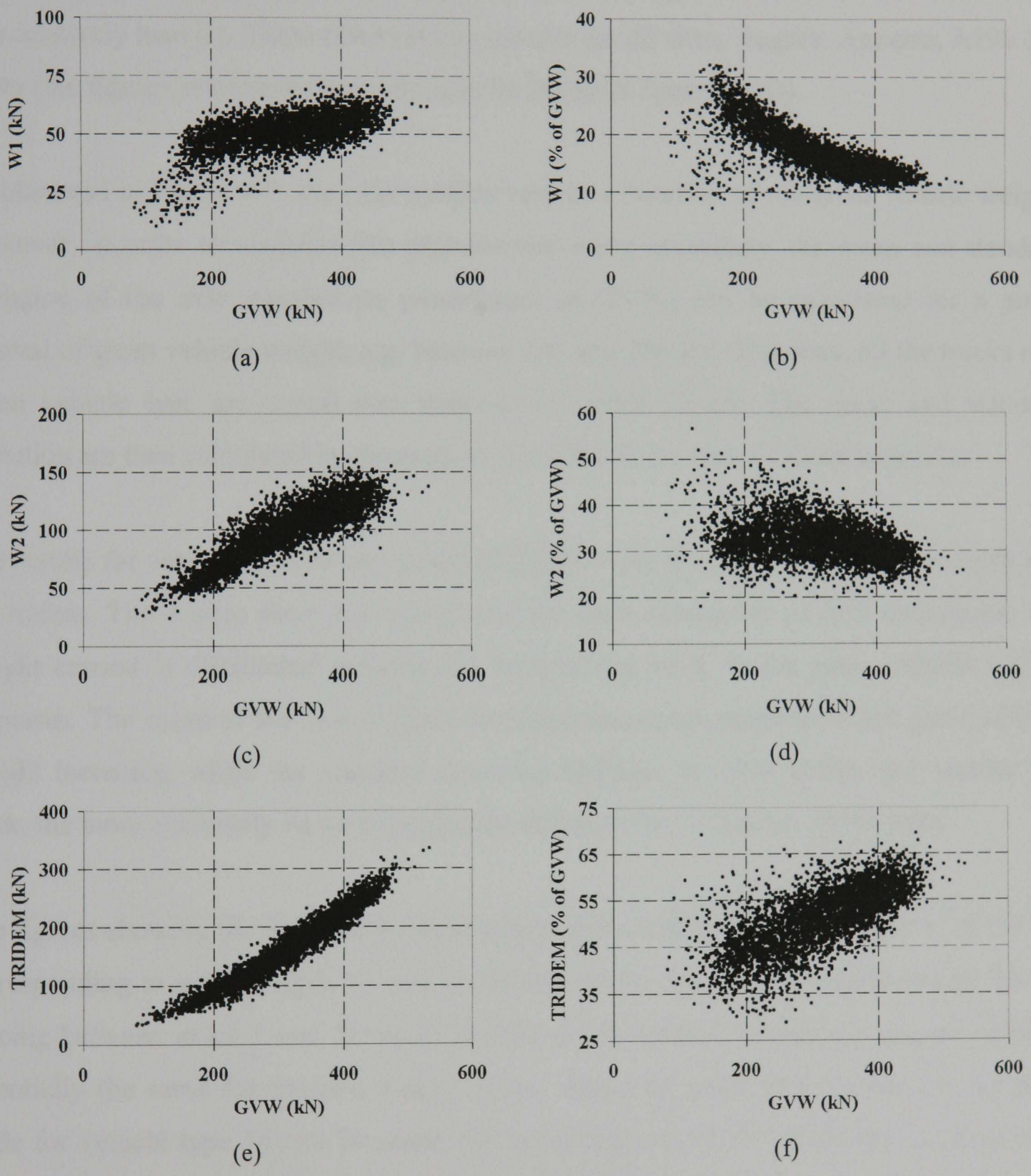

Figure 4-9: Axle Weights as a function of GVW for Vehicle Type 14 - Angers site [W1 = weight of 1st axle, W2 = weight of 2nd axle]

As anticipated, the axle and tridem weights increase as the gross vehicle weight increases. However, the weight of the 1st axle only increases slightly in comparison to the GVW, as illustrated by graph (b) in Figure 4-9. The percentage of GVW carried by the 1st axle weight actually decreases as the GVW increases, as does its spread. The weight carried by

the second axle gets higher as the GVW increases, while the percentage of weight carried by this axle remains fairly constant throughout the range of values of GVW, although its spread reduces as the truck weight increases. The tridem weight increases more rapidly than the GVW does, as shown by the percentage of GVW carried by the tridem, which keeps increasing, as the GVW gets higher. In other words, as the GVW increases, the axle weights change, the front of the truck getting relatively lighter while the back of the truck gets relatively heavier. These observations are true for all sites, Angers, Auxerre, A196 and A296 (the figures relative to these sites can be found in Appendix D).

As observed in Figure 4-9, the axle weights vary as a function of the gross vehicle weight. However, in order to visualise this phenomenon more accurately, the mean and standard deviation of the axle weights (as percentages of GVW) can be calculated for a given interval of gross vehicle weight, e.g. between 200 and 250 kN. This way, all the trucks of a given vehicle type are sorted into intervals of width 50 kN. The mean and standard deviation are then calculated by the method of moments for each of these intervals.

The results for vehicle type 14 are shown in Figure 4-10, for the first two axle weights and the tridem. The 4 sites show the same trend for each axle/group of axle considered: the weight carried is distributed towards the back of the truck as the gross vehicle weight increases. The mean of the axle weights increases/decreases regularly as the gross vehicle weight increases, while the standard deviation reduces. In other terms, the heavier the truck, the more accurately its axle weights are defined; this is true for all the sites.

The figures showing the mean of the front axle weights and tandem weight (in % of GVW) corresponding to vehicle types 10 and 11 (which are the same 4-axle trucks except for the spacing between axles 2 and 3) reveal that the distribution of weight among the axles is essentially the same for the two vehicle types. Also, the same observations as the ones made for vehicle type 14 can be made; the percentage of GVW carried by the front axle reduces while the percentage of GVW carried by the second axle tends to decrease very slightly and the tandem carries more and more of the weight as the gross vehicle weight increases. Again, the standard deviations decrease with increasing GVW.

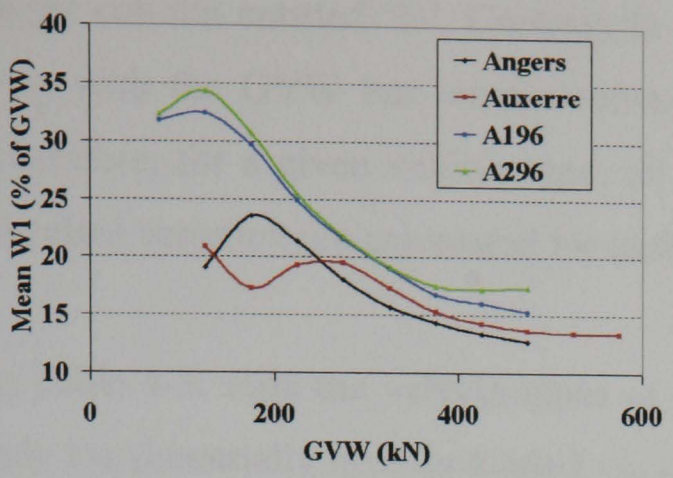

(a)

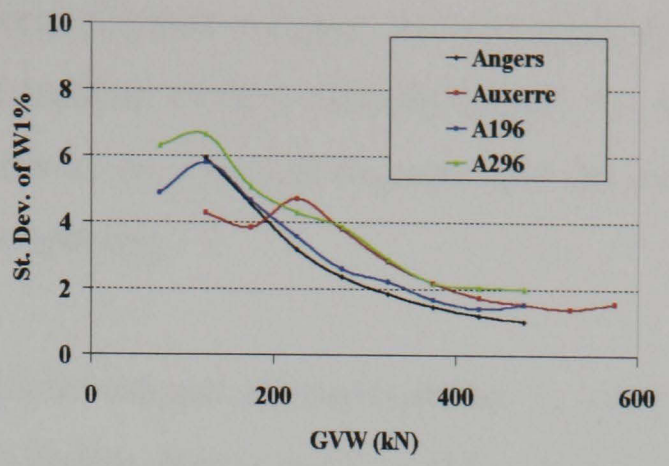

(b)

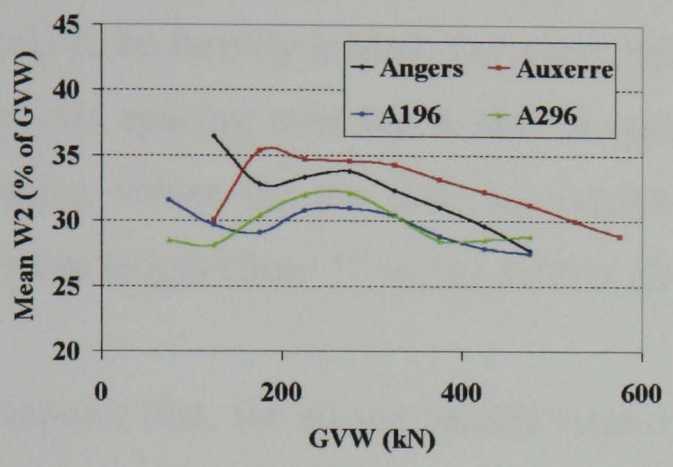

(c)

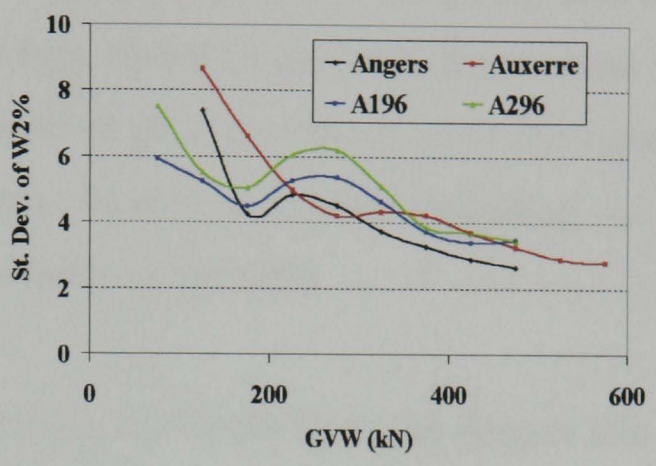

(d)

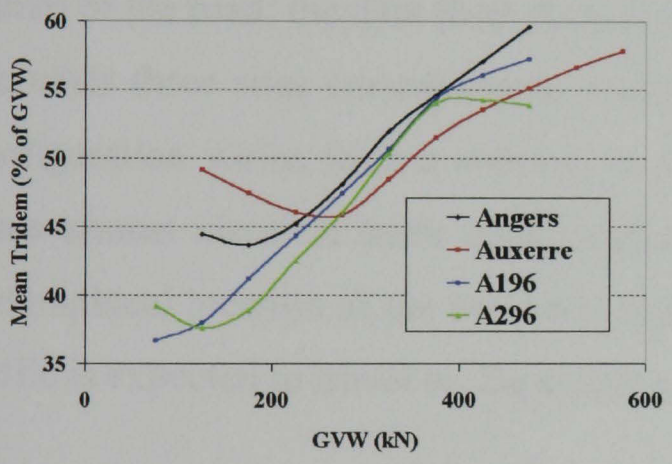

(e)

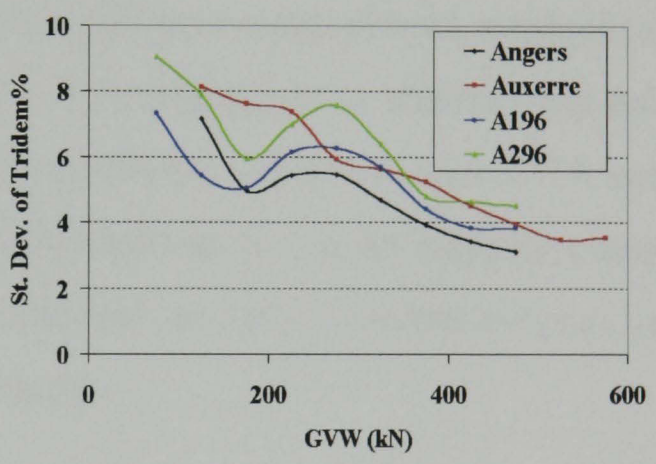

(f)

Figure 4-10: Mean and Standard Deviation of Axle Weights for Vehicle Type 14 as a function of GVW for various sites [W1 = weight of 1st axle, W2 = weight of 2nd axle]

4.2.6 Axle spacings

Another very important variable in traffic characteristics is the spacing between consecutive axles. When considering traffic loading for relatively short bridges, this variable can be critical. It is therefore important to know the values of axle spacings with accuracy. Table 4-3 shows the mean and standard deviation of axle spacings for different vehicle types and various sites. The relative frequency of the different vehicle types is expressed in terms of percentage of the total number of trucks for a given site and is shown

in the column entitled '%'. Contrary to the trend for axle weights, the axle spacings do not vary with the GVW but remain constant regardless of how heavily loaded the truck is. Therefore, for a given vehicle type, all the trucks are counted together and the mean and standard variation are calculated for each axle spacing.

In Table 4-3, only the vehicle types of particular interest are represented. In other words, only the potentially heavily loaded trucks are shown, that is the 4- and 5-axle trucks. Also shown is vehicle type 7, which is the most common of the 3-axle trucks and also the most likely to be heavily loaded. For every vehicle type shown in the table, the average value of the axle spacing over the 4 sites is represented to give an indication of the typical axle spacing values for the different vehicle types. Finally a column indicating the typical average length (from 1st to last axle) is also included in the table.

It appears that, for all the vehicle types presented, the trucks from the Angers site always exhibit smaller axle spacings than any other site. This distinction can be explained by the nature of the road: the data from Angers was recorded on a national road, while the data for the other three sites correspond to motorways. It is reasonable to assume that the traffic configuration varies from a national to a main motorway. The two sites A196 and A296 show almost identical truck configurations; this observation can be explained due to the geographical location of the two sites. Indeed, the two sites being closely located, the same traffic is expected to travel on these two motorways.

4.2.7 Speed distribution

The speed distribution is given as a function of the number of axles per truck. This enables to the overall distribution of speed between all trucks and also truck classes to be differentiated , in terms of spread for example. The speed distribution for the A196 site is illustrated in Figure 4-11; the figures for the other sites can be found in the Appendix D. For Angers, the average speed is around 67 km/hr with a large variance around that mean value; and that applies to all the truck classes. For A196 and A296, the average speeds are around 85 km/hr and 90 km/hr respectively, with a narrow spread except for the speed of the 2-axle trucks, which is widely spread towards higher speeds.

Table 4-3: Axle spacings (m) in terms of mean and standard deviation (respectively M* and SD) for some vehicle types (VT) and for various sites**

VT	Site	%	S12 (m)		S23 (m)		S34 (m)		S45 (m)		Av. Length
			M*	SD**	M*	SD**	M*	SD**	M*	SD**	
7	Angers	2.8	**3.64**	0.90	**1.19**	0.33					4.83
7	Auxerre	1.3	**4.96**	0.89	**1.24**	0.23					6.19
7	A196	0.8	**4.97**	0.76	**1.30**	0.23					6.27
7	A296	1.3	**5.02**	0.84	**1.28**	0.38					6.31
	Average		*4.65*	*0.85*	*1.25*	*0.29*					*5.90*
10	Angers	20.4	**3.00**	0.25	**4.97**	0.98	**1.27**	0.24			9.24
10	Auxerre	6.5	**3.17**	0.22	**5.11**	0.75	**1.47**	0.32			9.75
10	A196	1.5	**3.27**	0.44	**4.28**	0.79	**1.06**	0.36			8.61
10	A296	2.7	**3.32**	0.44	**4.22**	0.71	**1.08**	0.34			8.62
	Average		*3.19*	*0.34*	*4.64*	*0.81*	*1.22*	*0.32*			*9.06*
11	Angers	9.2	**3.13**	0.19	**6.28**	0.30	**1.21**	0.19			10.62
11	Auxerre	18.3	**3.25**	0.16	**6.30**	0.32	**1.40**	0.27			10.95
11	A196	11.4	**3.55**	0.19	**6.84**	0.50	**1.32**	0.20			11.70
11	A296	9.5	**3.61**	0.18	**6.99**	0.61	**1.36**	0.23			11.96
	Average		*3.39*	*0.18*	*6.60*	*0.43*	*1.32*	*0.22*			*11.31*
12	Angers	1.0	**4.78**	0.47	**5.38**	2.26	**1.20**	0.14			11.37
12	Auxerre	1.5	**4.91**	0.31	**6.34**	1.63	**1.25**	0.16			12.50
12	A196	3.9	**5.13**	0.47	**7.11**	0.47	**1.35**	0.24			13.58
12	A296	6.0	**5.22**	0.52	**7.26**	0.59	**1.32**	0.19			13.80
	Average		*5.01*	*0.44*	*6.52*	*1.24*	*1.28*	*0.18*			*12.81*
13	Angers	6.0	**4.50**	0.52	**4.59**	0.56	**4.34**	0.65			13.43
13	Auxerre	5.1	**4.89**	0.48	**5.02**	0.53	**4.73**	0.71			14.65
13	A196	1.8	**5.01**	0.53	**5.15**	0.67	**5.09**	0.72			15.25
13	A296	1.6	**5.03**	0.60	**5.35**	0.77	**5.05**	0.79			15.43
	Average		*4.86*	*0.53*	*5.03*	*0.63*	*4.80*	*0.72*			*14.69*
14	Angers	24.1	**3.02**	0.23	**5.01**	0.48	**1.12**	0.21	**1.12**	0.15	10.27
14	Auxerre	36.8	**3.24**	0.17	**5.40**	0.41	**1.21**	0.15	**1.21**	0.15	11.06
14	A196	53.6	**3.59**	0.17	**5.69**	0.46	**1.25**	0.07	**1.25**	0.08	11.78
14	A296	47.8	**3.66**	0.17	**5.71**	0.54	**1.29**	0.07	**1.29**	0.07	11.94
	Average		*3.38*	*0.19*	*5.45*	*0.47*	*1.22*	*0.12*	*1.22*	*0.11*	*11.26*
16	Angers	3.6	**4.29**	0.49	**4.13**	0.84	**3.80**	0.57	**1.15**	0.18	13.38
16	Auxerre	5.2	**4.35**	0.70	**4.12**	1.21	**4.31**	0.75	**1.27**	0.26	14.05
16	A196	5.9	**4.75**	0.49	**3.08**	1.66	**5.26**	1.12	**1.39**	0.25	14.47
16	A296	5.7	**4.83**	0.48	**3.03**	1.65	**5.46**	1.14	**1.40**	0.23	14.72
	Average		*4.55*	*0.54*	*3.59*	*1.34*	*4.71*	*0.90*	*1.30*	*0.23*	*14.15*
17	Angers	0.8	**3.53**	0.58	**2.21**	1.32	**3.65**	0.91	**4.44**	0.53	13.83
17	Auxerre	0.7	**4.16**	0.52	**1.61**	0.92	**4.40**	0.74	**4.60**	0.54	14.76
17	A196	1.5	**4.45**	0.36	**1.51**	0.83	**4.56**	0.65	**5.00**	0.38	15.52
17	A296	2.0	**4.57**	0.31	**1.37**	0.35	**4.79**	0.40	**5.03**	0.39	15.76
	Average		*4.18*	*0.44*	*1.67*	*0.86*	*4.35*	*0.67*	*4.77*	*0.46*	*14.97*

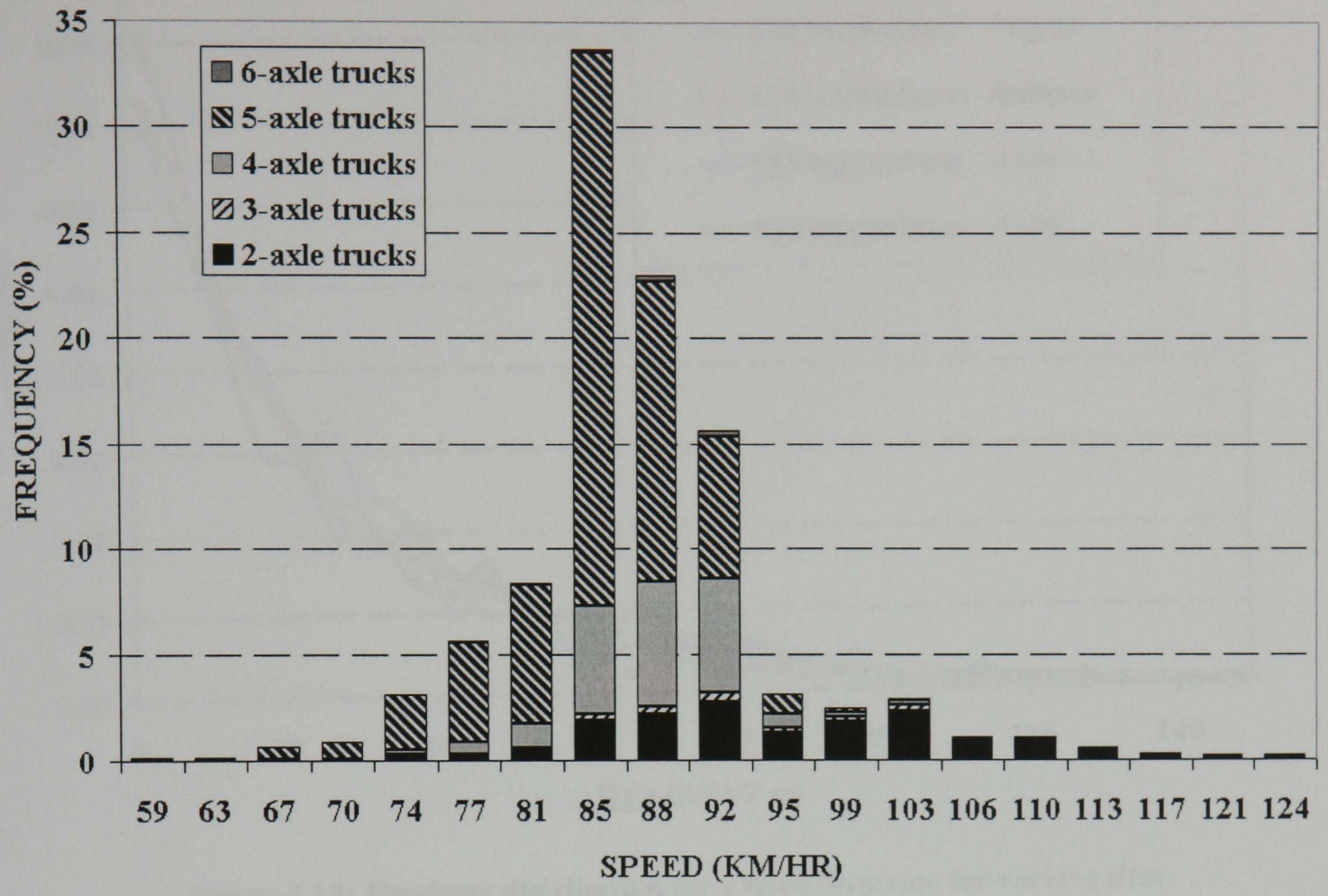

Figure 4-11: Speed distribution as a function of number of axles – A196 site

4.2.8 Headway distribution

The headway is normally defined as the time-interval between the arrivals of two consecutive vehicles at a fixed point (e.g. the sensors used to collect the WIM data). The headway distribution is, as for all the other traffic characteristics, a site-specific variable. In fact it is simply another way of expressing the flow rates. However, for a given value of flow rate, the headway distribution is not site-specific; its probability density function is very similar for all the sites, as illustrated in Figure 4-12. Therefore, all the headways are studied together, independently of their site of origin. Figure 4-13 shows the headway distributions corresponding to various flow rates, from 55 to 455 trucks per hour. Finally, Figure 4-14 presents the same distributions but in terms of normalised headways. A normalised headway, as suggested by Castillo & Minguillon (1997), is defined as the headway divided by the average headway (average hourly headway in the case of hourly flow rates).

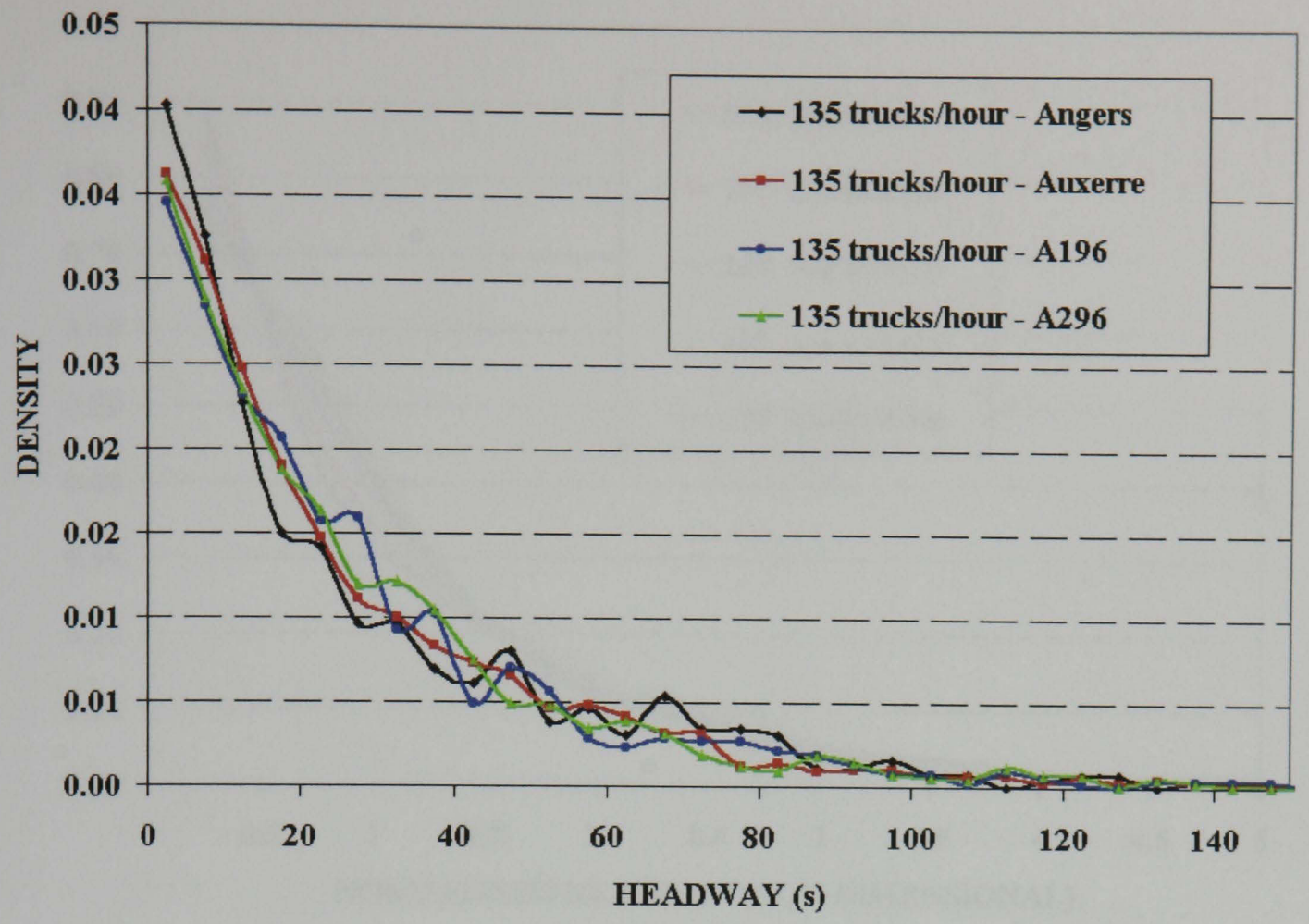

Figure 4-12: Headway distribution for a fixed flow rate for various sites

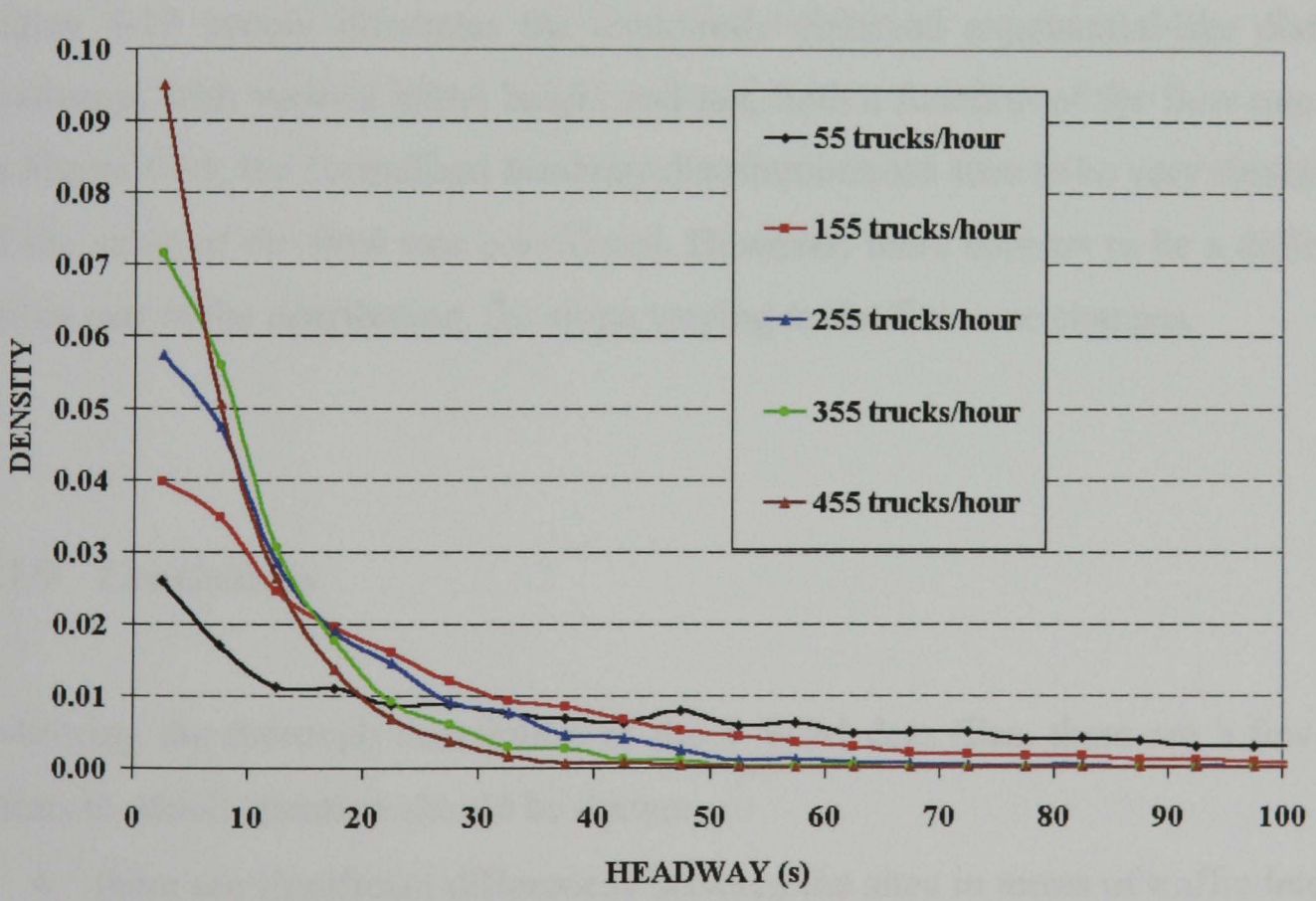

Figure 4-13: Headway distributions for various flow rates

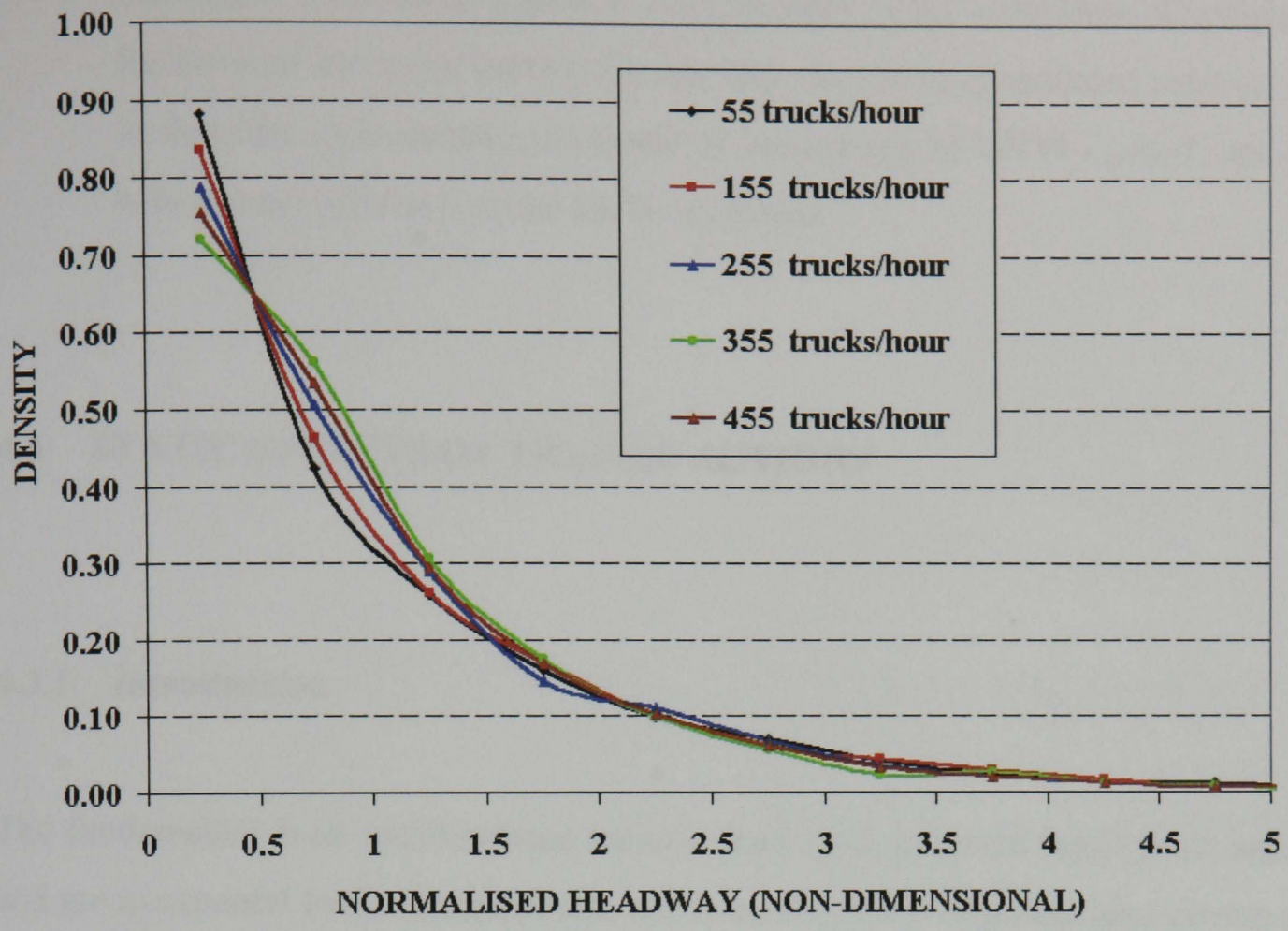

Figure 4-14: Normalised headway distributions for various flow rates

Figure 4-13 simply illustrates the commonly observed exponential-like distribution for headways, with various initial height and tail, both a function of the flow rate considered. In Figure 4-14, the normalised headway distributions are seen to be very similar, regardless of the value of the flow rate considered. However, there appears to be a difference in the initial part of the distribution, the slope varying as the flow rate changes.

4.2.9 Conclusions

Following the thorough description of the 4 WIM data files, there are a few noteworthy points to which attention should be drawn:

- there are significant differences between the sites in terms of traffic intensity, gross vehicle weight distribution, and, to a lesser extent, in the geometry of the trucks.
- there are also significant differences between the opposing directions of traffic, for any given site, in terms of traffic intensity and GVW distribution.
- the vast majority of heavy goods vehicles for these 4 sites consist of 4- and 5- axle trucks, namely the tractor/semi-trailer type.

- the weight distribution between axles changes as the gross vehicle weight increases, the back of the truck getting heavier (for the above mentioned trucks). In addition to that, the axle weights, in terms of percentage of GVW carried, are predictable with greater accuracy as the GVW increases.

4.3 STATIC EFFECTS OF TRAFFIC ACTIONS

4.3.1 Introduction

The fundamental load combinations include dead load, imposed load (static and dynamic) and environmental loads (temperature, wind, earthquake). Imposed load covers a range of forces produced by vehicles moving on the bridge. Traditionally, the static and dynamic effects are considered separately. The static response implies a load effect that is caused by the interaction between the weights of moving or stationary vehicles and bridge elastic response disregarding both bridge and vehicle inertial effects. In this study only the static effect is considered. A number of load effects and bridge lengths, for two different bridge types, will be considered in the development of the new models. These load effects are presented in this section, along with the concept of 'influence response' and the sensitivity of the load effects to traffic loading (in terms of truck configuration).

4.3.2 Influence lines

Two-lane simply supported and two-span continuous bridges ranging in total length from 20 m to 40 m are considered. In this study, six load effects are considered:

1. bending moment at mid-span of a simply supported bridge,
2. moment at central support of a two-span continuous bridge,
3. shear at left-end support of a simply supported bridge,
4. shear at right-end support of a simply supported bridge,
5. shear at left-end support of a two-span continuous bridge,
6. shear at right-end support of a two-span continuous bridge.

An influence line can be defined as a diagram that shows the variation of a load effect at a given position in a structure as a unit load travels across it. The influence lines corresponding to the load effects considered are illustrated in Figure 4-15. The value of each load effect is computed as the product of each axle load by the corresponding influence line ordinate at its position. The effect due to the presence of multiple trucks is calculated by simple superposition. Also, it should be noted that the effect of torsion is ignored in the scope of this research. The equations corresponding to the different influence lines are given in the Appendix C.

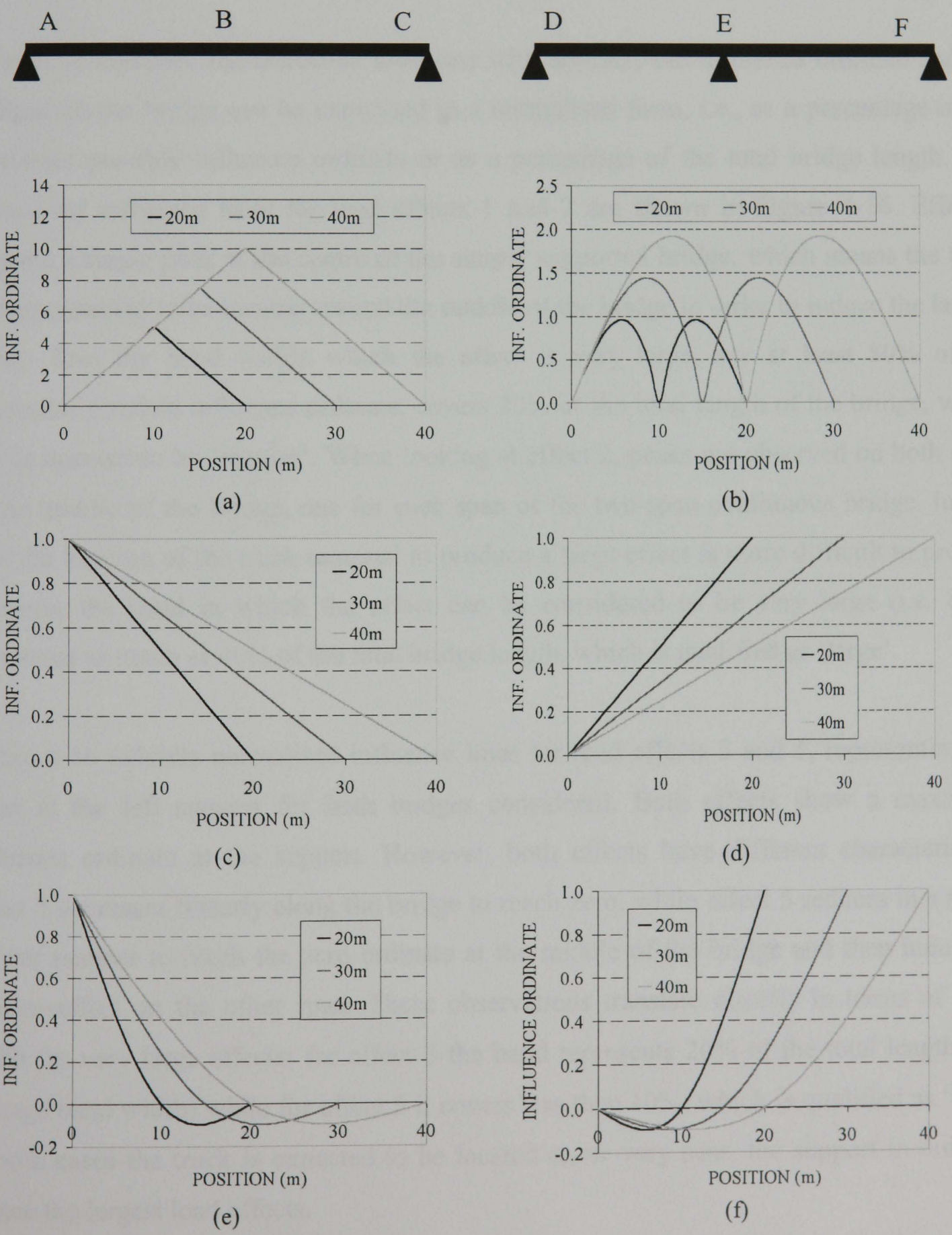

Figure 4-15: Table of influence lines: (a) Effect 1 - Bending Moment at B; (b) Effect 2 - Moment at E; (c) Effect 3 - Shear at A; (d) Effect 4 - Shear at C; (e) Effect 5 - Shear at D; (f) Effect 6 - Shear at F

It should be noted that all the load effects will be counted as positive, merely for practical convenience. However, part of the influence line corresponding to load effects 5 and 6 is counted negatively due to the nature of the influence line itself. Although the influence lines that correspond to the effects 3&4 and 5&6 (illustrated in Figure 4-15 (c) & (d) and in (e) & (f) respectively) are symmetrical, the load effect induced by a given truck will be different at both ends of the bridge. A trivial but nonetheless important observation is that the influence ordinate increases with the span for load effects 1 and 2, while it is always between 0 and 1 for the other load effects, independent of the bridge length.

In order to compare the influence lines one with another, the influence ordinate and the position on the bridge can be expressed in a normalised form, i.e., as a percentage of the maximum possible influence ordinate or as a percentage of the total bridge length. The normalised influence lines for load effects 1 and 2 are shown in Figure 4-16. Effect 1 presents a single peak at the centre of the simply supported bridge, which means the truck will be expected to be located around the middle of the bridge in order to induce the largest effect. Also the band within which the effect is very large, say at least 80% of the maximum possible influence ordinate, covers 20% of the total length of the bridge, which can be deemed to be 'regular'. When looking at effect 2, peaks are observed on both sides of the middle of the bridge, one for each span of the two-span continuous bridge. In that case the location of the truck required to produce a large effect is more difficult to predict. However the band in which the effect can be considered to be very large (i.e. 80%) represents as much as 40% of the total bridge length, which is qualified as 'large'.

Figure 4-16 exhibits normalised influence lines for load effects 3 and 5, representing the shear at the left support for both bridges considered. Both effects show a maximum influence ordinate at the support. However, both effects have different characteristics: effect 3 decreases linearly along the bridge to reach zero, while effect 5 reduces in a much steeper manner to reach the zero ordinate at the middle of the bridge and then induces a counter-effect on the other span. These observations translate directly in terms of band width for very large effects: for effect 3 the band represents 20% of the total length (i.e. average band width) while for effect 5 it covers less than 10%, which is qualified as 'low'. In both cases the truck is expected to be located at, or very near, the support in order to induce the largest load effects.

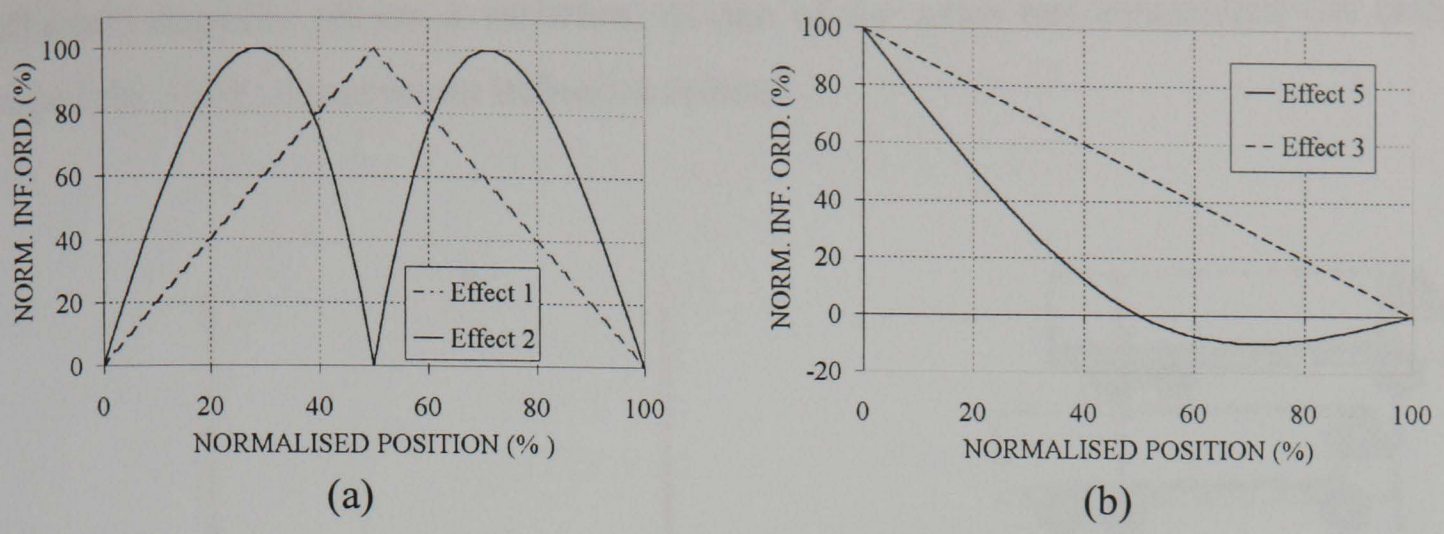

Figure 4-16: Normalised influence lines

4.3.3 Influence response

So far only a single unit load has been considered for the influence lines. However, the response of the bridge due the passage of a truck is far more interesting as it is extremely difficult to predict the response of a bridge under a truck load by knowing only the response induced by a single load. Thus the concept of 'influence response' has been introduced by the author. It is an extension of the concept of influence line but it deals with a complete truck rather than a single load. The truck is represented by its geometry, i.e. its axle spacings and its axle weights (in terms of percentage of GVW carried by each axle). Knowing the trucks characteristics, it is straightforward to calculate the response of the bridge for a given load effect, by simply superimposing the effects induced by each axle.

In order to demonstrate this concept explicitly, the example of influence response induced by a 3-axle truck is now developed. The truck adopted is similar to the vehicle type 7 defined in the previous chapter. Its characteristics have been taken as:

- W1 = 40 % of GVW = 0.4 and W2 = W3 = 30 % of GVW = 0.3
- S12 = 5 m and S23 = 1 m (where S12 and S23 are the spacing between axles 1 & 2 and 2 & 3 respectively).

This typical truck is moved along the bridge and the response is calculated repeatedly in order to obtain the influence response. Figure 4-17 illustrates the influence response corresponding to load effect 1 as the truck moves along the bridge. The important locations for that effect are both ends of the bridge as well as the middle of the bridge, represented by the red lines. Every time that one of the axles passes one of these locations, the

influence response shows a variation, as one of the axles has entered/left the bridge or passed the point of maximum influence ordinate.

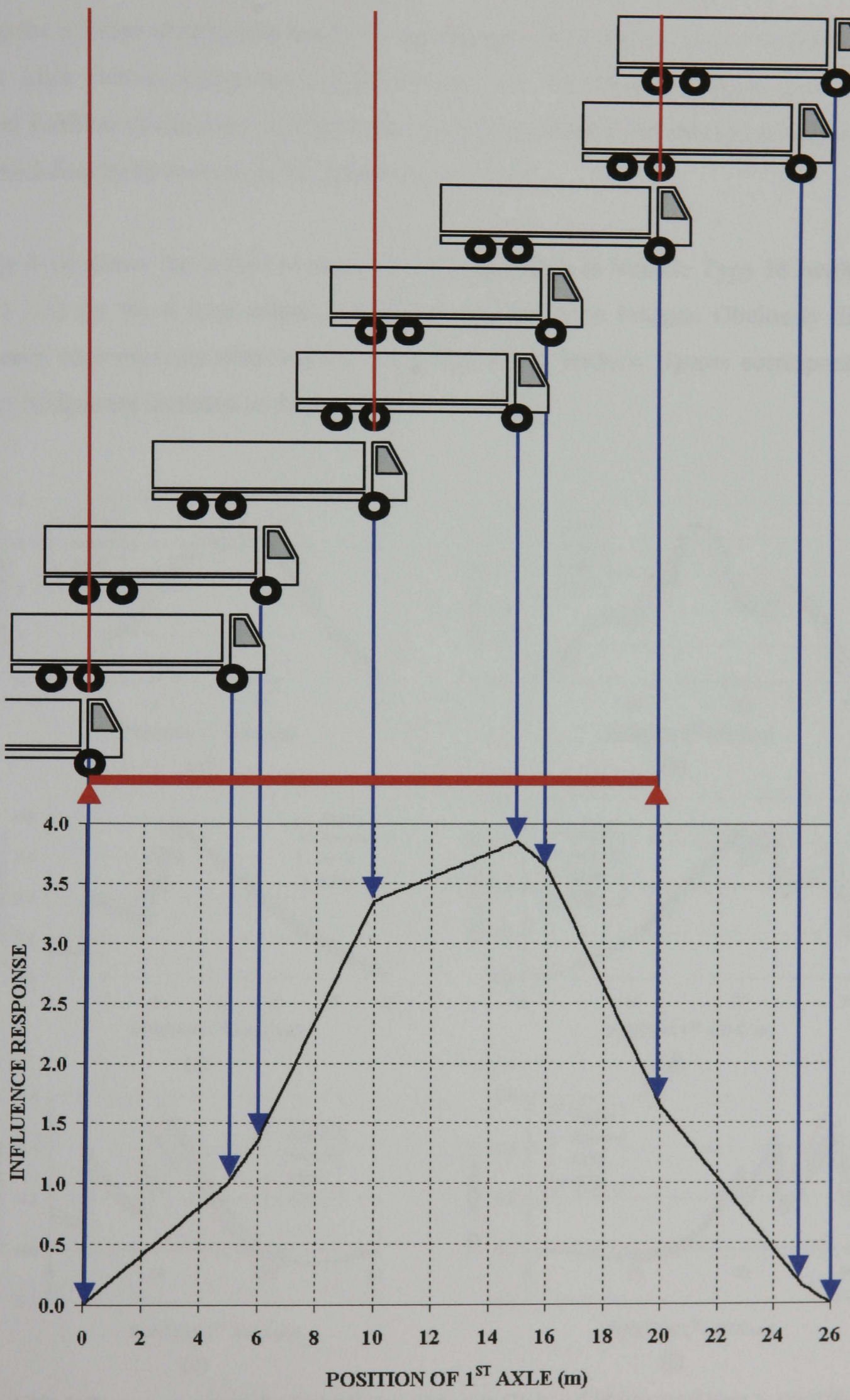

Figure 4-17: Illustration of the influence response concept

In this example, the maximum response due to the passage of the truck equals 3.8 and occurs when the last axle of the truck is exactly located at mid-span. The maximum effect is easily obtained by multiplying the maximum influence response by the truck GVW.

Using the concept of influence response, the response of the bridge due to the passage of a given truck (whose characteristics are known) can be obtained simply. Similarly the critical position of the truck on the bridge in order to induce the maximum load effect is obtained directly by looking at the influence response.

Figure 4-18 shows the influence responses corresponding to Vehicle Type 14 (with GVW = 525 kN) for the 6 load effects considered and for 20 m bridges. Obviously different influence responses are obtained for 30 m and 40 m bridges; figures corresponding to longer bridges are included in Appendix C.

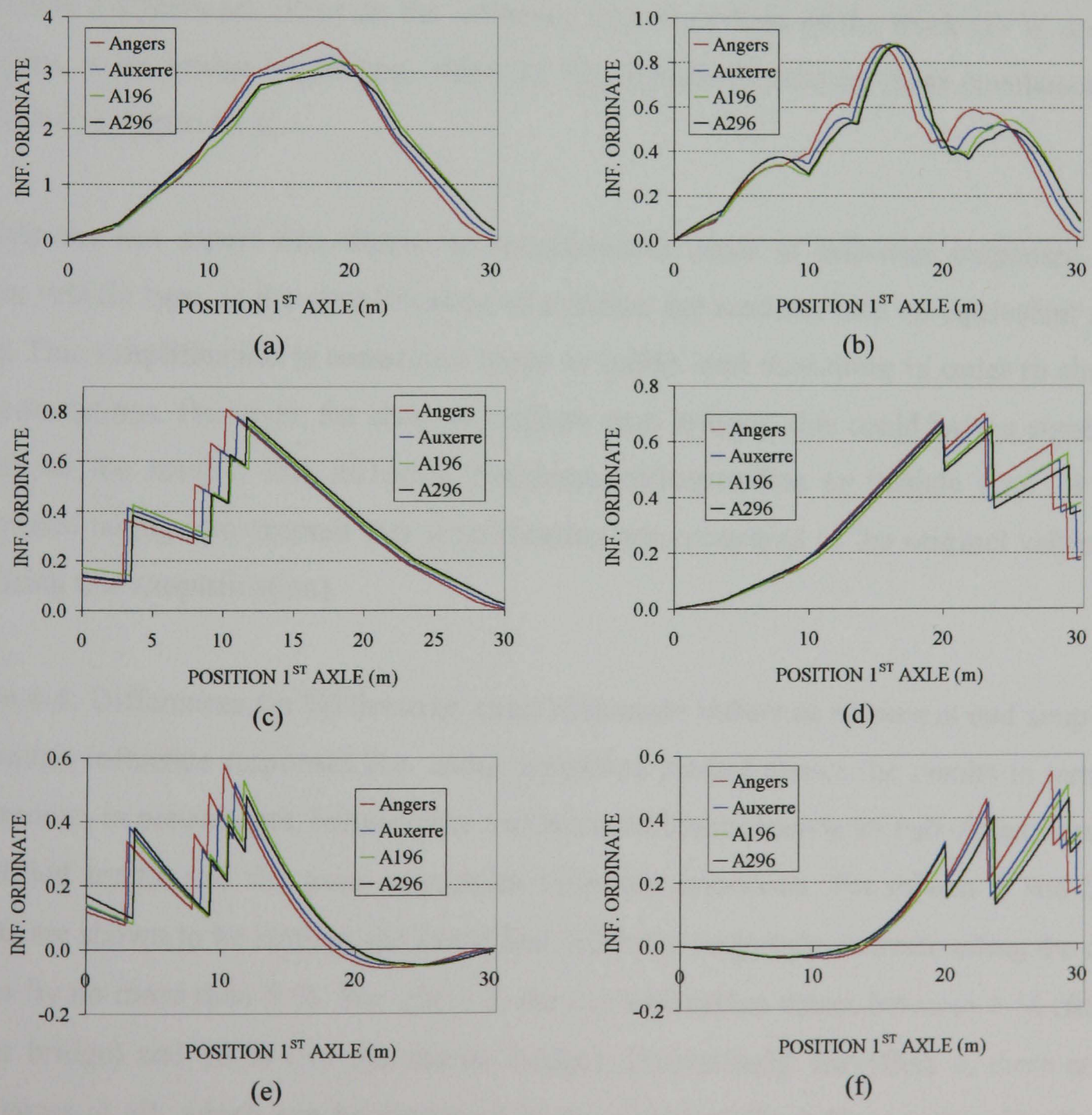

Figure 4-18: Influence responses for Vehicle Type 14 with GVW = 525 kN: (a) Effect 1; (b) Effect 2; (c) Effect 3; (d) Effect 4; (e) Effect 5; (f) Effect 6

As illustrated earlier in this chapter, the same vehicle types can have different typical axle weights depending on the GVW of the truck and different axle spacing depending on the site considered. As a consequence, variations are observed in the influence responses for the various sites (see Figure 4-18). The biggest differences are observed for the shortest bridges considered, i.e. the 20 m bridges. The one curve that seems to deviate from the three others corresponds to Angers. Its truck has shorter axle spacings, which explains the more noticeable discrepancies. However, as the bridge length increases, the relative variations get smaller and smaller between the different sites. The main conclusion is that the overall shape and order of magnitude is the same for all the sites, for a given truck weight.

When considering a given site and a particular vehicle type, the only variables that vary significantly are the axle weights. A sensitivity study revealed that the axle weights could have a significant effect on the influence response (e.g. effect 6). Another parameter that can have a significant effect on the influence line, regardless of the truck GVW and axle weights, is the bridge length (e.g. effect 2). The figures illustrating these conclusions can be found in Appendix C.

Finally the last aspect that should be considered in terms of influence responses, for a given vehicle type, is the simplification of a tridem (or tandem) into an equivalent single axle. This simplification is sometimes made in traffic load modelling in order to simplify the calculations. However, for short to medium span bridges, this could have a significant effect on the results. The influence responses corresponding to vehicle type 14 were calculated taking into account this simplification and compared to the original values (i.e. not using this simplification).

Table 4-4: Differences (in %) between exact maximum influence responses and simplified maximum influence responses [i.e. using simplified trucks] shows the results in terms of differences, in percentages, between the maximum influence responses calculated using the simplified trucks and the exact maximum influence responses. For effects 1 and 2 the results are shown to be similar, the simplified influence responses overestimating the exact values by no more than 5 %. For effect 3, the overestimation varies between 5 % (for the longer bridge) and 10 % (for the shorter bridge). Interestingly, for effect 4, there are no differences at all; which can be explained by the shape of the influence line. Finally, for effects 5 and 6, differences as high as +26 % are observed. Again the peakedness of the

influence lines explains these great variations; the influence response being extremely sensitive to every axle. However, one common observation can be made for all the effects: the differences between the simplified influence responses and the exact ones get smaller as the bridge length increases, which can be expected as the influence response becomes less sensitive to the exact position of the axles.

Table 4-4: Differences (in %) between exact maximum influence responses and simplified maximum influence responses [i.e. using simplified trucks]

Effect	Site	20 m Bridge GVW (kN)				30 m Bridge GVW (kN)				40 m Bridge GVW (kN)			
		225	**325**	**425**	**525**	**225**	**325**	**425**	**525**	**225**	**325**	**425**	**525**
1	Angers	0	0	2	3	0	0	1	2	0	0	1	1
1	Auxerre	0	0	1	2	0	0	1	1	0	0	1	1
1	A196	0	2	4	5	0	0	1	2	0	0	1	1
1	A296	0	3	4	4	0	0	1	1	0	0	1	1
		225	**325**	**425**	**525**	**225**	**325**	**425**	**525**	**225**	**325**	**425**	**525**
2	Angers	2	3	3	3	1	2	2	2	1	1	1	0
2	Auxerre	2	2	3	3	1	1	2	2	1	1	1	1
2	A196	2	3	3	3	1	2	2	2	1	1	1	1
2	A296	2	3	3	3	1	1	2	2	1	1	1	1
		225	**325**	**425**	**525**	**225**	**325**	**425**	**525**	**225**	**325**	**425**	**525**
3	Angers	7	7	7	7	4	4	4	5	3	3	3	3
3	Auxerre	8	8	8	8	5	5	5	5	3	3	3	3
3	A196	9	8	8	8	5	5	5	5	4	4	4	4
3	A296	9	9	9	9	5	5	5	5	4	4	4	4
		225	**325**	**425**	**525**	**225**	**325**	**425**	**525**	**225**	**325**	**425**	**525**
4	Angers	0	0	0	0	0	0	0	0	0	0	0	0
4	Auxerre	0	0	0	0	0	0	0	0	0	0	0	0
4	A196	0	0	0	0	0	0	0	0	0	0	0	0
4	A296	0	0	0	0	0	0	0	0	0	0	0	0
		225	**325**	**425**	**525**	**225**	**325**	**425**	**525**	**225**	**325**	**425**	**525**
5	Angers	20	23	22	22	14	14	13	13	9	9	9	9
5	Auxerre	19	25	24	24	15	15	14	14	10	10	10	10
5	A196	13	26	25	24	16	16	15	15	11	11	10	10
5	A296	6	26	25	25	17	16	16	15	11	11	11	11
		225	**325**	**425**	**525**	**225**	**325**	**425**	**525**	**225**	**325**	**425**	**525**
6	Angers	0	6	15	14	0	0	0	6	0	0	0	-1
6	Auxerre	0	4	17	17	0	0	0	0	0	0	0	0
6	A196	6	18	18	18	0	0	5	11	0	0	0	0
6	A296	0	19	19	19	0	0	3	3	0	0	0	0

So far, only one vehicle type has been considered, vehicle type 14. Although the most representative of all truck types in terms of frequency and in terms of heavy trucks, there are other truck types that can be heavily loaded. Therefore the influence responses corresponding to other vehicle types have been calculated. Typical trucks for each vehicle type of 4 or 5 axles have been used. Average axle spacings from the 4 sites have been used for vehicle types 12, 13, 16, 17 and 18. The most heavily loaded trucks that are relatively frequent for all vehicle types have been considered; that is the 325 kN one for the 4-axle truck and the 425 kN one for the 5-axle trucks. The 6-axle trucks are also included, as they resemble 5-axle trucks (vehicle type 14) with a tandem instead of the second axle. The maximum influence responses are shown in Appendix C, for the 6 load effects and for the 3 bridge lengths. It can be noticed that for all the effects and for all the spans the highest influences are always given by vehicle types 10 and 11 for the 4-axle trucks, and by vehicle type 14 for the 5- and 6-axle trucks (with one exception, for effect 2 on the 30 m bridge, where the maximum influence response given by vehicle type 18 is 2.7 % higher than the one given by vehicle type 14).

4.3.4 Conclusions

In this section, the static effects of traffic actions have been studied through the use of influence lines and influence responses. The main points on which emphasis should be put are:

- The influence lines characterising the load effects taken into account represent a variety of shapes and slopes that can be considered as representative, although not exhaustive, for this length of bridges (i.e. 20 m to 40 m long).
- The introduction of the concept of influence response of a bridge, induced by to the presence of unit weight truck. This concept will be extremely useful when considering critical loading events, in terms of locating the trucks inducing the largest possible effect and evaluating the intensity of the loading.
- The sensitivity of the influence responses (and, indirectly, the influence lines) to the various vehicle types, in terms of axle spacings and axle weights, has been studied. Essentially, the steeper the influence line and the shorter the bridge, the more sensitive the influence response is.

4.4 MODELLING THE TRAFFIC CHARACTERISTICS

4.4.1 Introduction

Following the thorough description of the traffic data and detailed analysis of the various load effects and their sensitivity to certain parameters such as the truck configuration (i.e. axle spacings and axle weights), it is now possible to model the traffic characteristics. A number of assumptions are made in order to restrict the number of characteristics to model and these are presented first. Then some crucial elements for the modelling of a probability density function are demonstrated. Finally the characteristics required to model the measured traffic files are derived using the previously introduced assumptions and modelling techniques.

4.4.2 Assumptions

The traffic composition is defined in terms of vehicle classes, i.e., as a function of the number of axles. The 6-axle trucks are included in the 5-axle class. Indeed, there are very few 6-axle trucks and they are very similar to the typical 5-axle trucks (vehicle type 14) in terms of GVW and truck configuration (axle-weights and axle-spacings). It is therefore reasonable to model the 6-axle trucks (vehicle type 17) using vehicle type 14.

It has been observed that Vehicle types 10 and 11 are in fact the same trucks apart from the spacing between axles 2 and 3; the axle weights (in % of GVW carried) are similar. Therefore there is no need to distinguish between vehicle types 10 and 11 in this study; from this point, this vehicle type will be referred to as vehicle types 10/11.

Each vehicle class is represented by one vehicle type, the 'most representative' one for that particular class. 'Most representative' is understood here to mean the most frequent in terms of GVW: the typical truck should represent the whole range of GVW for that class, and especially the right tail of the GVW distribution. Based on these assumptions and Figure 4-4, Figure 4-6 and Figure 4-7 the most representative trucks corresponding to the four vehicle classes are:

- for the 2-axle trucks, vehicle type 05;

- for the 3-axle trucks, vehicle type 07;
- for the 4-axle trucks, vehicle type 10/11;
- for the 5-axle trucks, vehicle type 14.

When modelling the most representative trucks for each vehicle class, the following assumptions are made:

- for the 2- and 3-axle trucks, i.e. VT 05 and VT 07, axle spacings and axle weights are modelled independently of the GVW;
- for the 4- and 5-axle trucks, i.e. VT 10/11 and VT 14, axle spacings are modelled independently of the GVW but axle weights are modelled as a function of the GVW.

As observed in the previous section, the axle weights for VT 10/11 and 14 change significantly with gross vehicle weight. Modelling the axle weights independently of the GVW could lead to unrealistic truck configurations with, for example, an extremely high (impossible) value for the front axle weight and extremely low (unrealistic) value for the tridem (in the case of a heavily loaded truck).

4.4.3 Modelling the probability density function of traffic characteristics

One important source of inaccuracy is the number of intervals selected to derive the density values. Formulae are given in the literature in order to have a reasonable estimate of the number of intervals to select as a function of n the number of values considered, such as the one given by Benjamin & Cornell (1970) where:

$$k = 1 + 3.3 \log_{10}(n)$$ **Equation 4-1**

However, even when using such estimates, the shape of the PDF can vary if different values of k are considered.

In Figure 4-19, the PDF of the spacing between axles 1 and 2 for vehicle type 10/11, using values for k ranging from 11 to 15, are presented. The overall shape of the distribution is similar for all the PDF's, with a main peak around 3.2 m. However, if the distribution using k=14 had been used, the main peak would be between 3.3 and 3.4 m, while the other

distributions would give a mean peak value of 3.2 m. One way to avoid this potential source of inaccuracy is to consider the densities corresponding to a wide range of intervals, as they all represent the same unique distribution, and to fit a distribution through all these points, as illustrated in Figure 4-20. By considering all the empirical density values and fitting a distribution to these data (cf. Figure 4-20 a), the various discrepancies are 'smoothed' out and a more robust trend is obtained. When compared to the initial distributions obtained using a particular value for *k*, the overall distribution is observed to be the 'average' of these distributions, (cf. Figure 4-20 b).

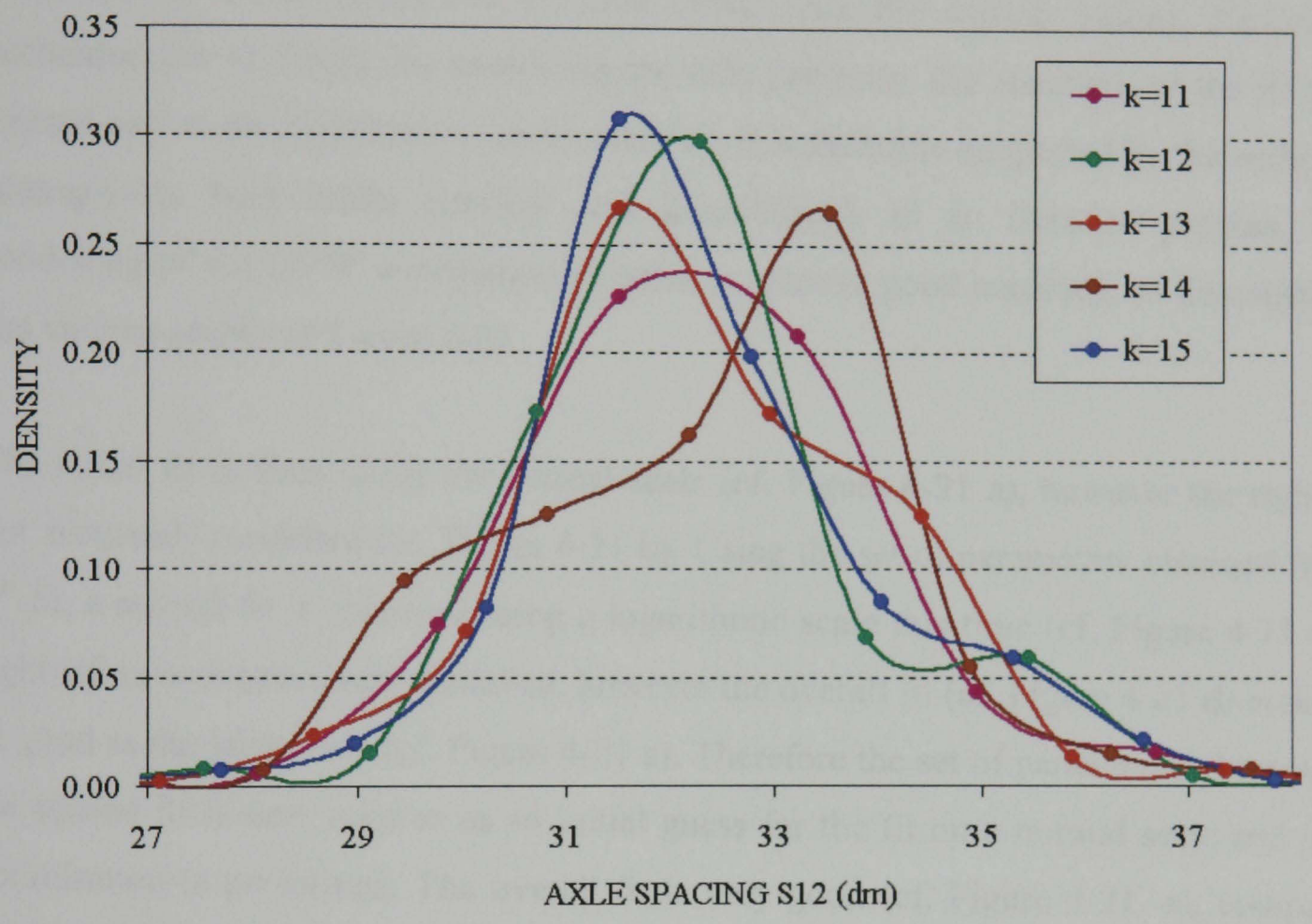

Figure 4-19 : Probability density function of spacing between axles 1 and 2 for vehicle type 10/11

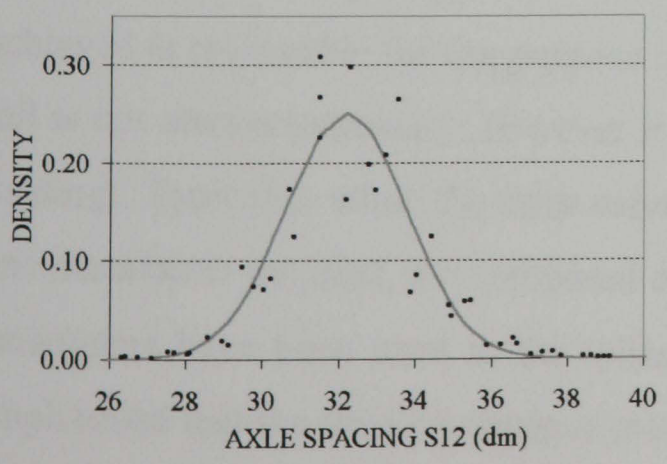

(a)

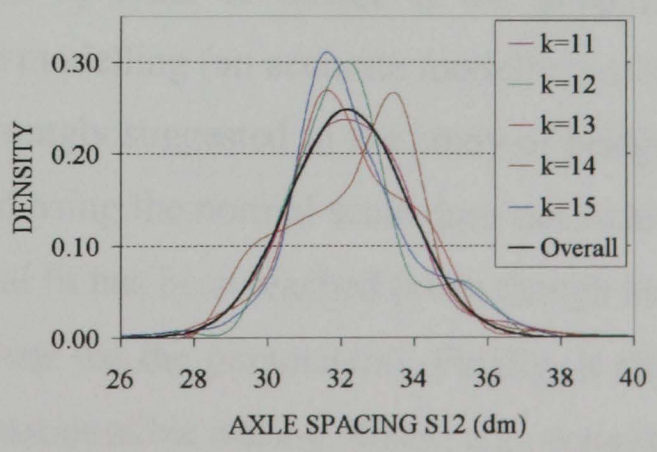

(b)

Figure 4-20: Probability density functions of spacing between axles 1 and 2

Another very important point is the modelling of the gross vehicle weight PDF, especially towards its right tail. Using the well-known technique of minimisation of the squares of the errors between the empirical distribution and the modelled distribution, a very accurate fit can easily be obtained overall, i.e. over the whole range of GVW values. However, the fit might not be very accurate in the region of the tails. Although an average fit is satisfactory for the left tail (the lighter trucks being of little importance in this study), the accuracy in the modelling of the right tail is of crucial importance. In order to optimise the fitting of the modelled distribution in the region of the tails, the logarithm of the density values (Maillard & Gorse 1989) can be used rather than the density values. However, this technique has its limits; by modelling the tails perfectly, the accuracy of the fit over the central part of the distribution can be affected. It is therefore suggested by the author to use alternatively both scales (normal and logarithmic), in an iterative process, for the modelling of the GVW distribution in order to achieve good accuracy, as demonstrated in the various graphs of Figure 4-21.

The initial fit is done using the normal scale (cf. Figure 4-21 a), however the right tail is not accurately modelled (cf. Figure 4-21 b). Using the set of parameters obtained from the 1st fit, a second fit is achieved using a logarithmic scale this time (cf. Figure 4-21 c). The right tail is now accurately modelled, however the overall fit (cf. Figure 4-21 d) is not quite as good as the initial one (cf. Figure 4-21 a). Therefore the set of parameters obtained from the second fit is now used to as an initial guess for the fit on a normal scale and another optimisation is performed. The overall fit is very good (cf. Figure 4-21. e), compared to (cf. Figure 4-21 a), but this time the fit in the region of the right tail has improved (cf. Figure 4-21 f). There is no simple criterion to decide whether or not the fit is sufficiently accurate; engineering judgement is required in order to decide if the goodness-of-fit achieved is reasonable for the purpose of the modelling (an accurate modelling of the right tail is not always necessary; however it is strongly suggested in the study of bridge traffic loading). Typically, when the error calculated using the normal scale does not reduce from one iteration to the next, the combined optimal fit has been reached (even though improved parameters have been used as the initial values for the parameters). Finally, it should be emphasised that the above technique is only one possible among others; e.g., weights could be imposed on the data in order to give more importance to the tail of the distribution.

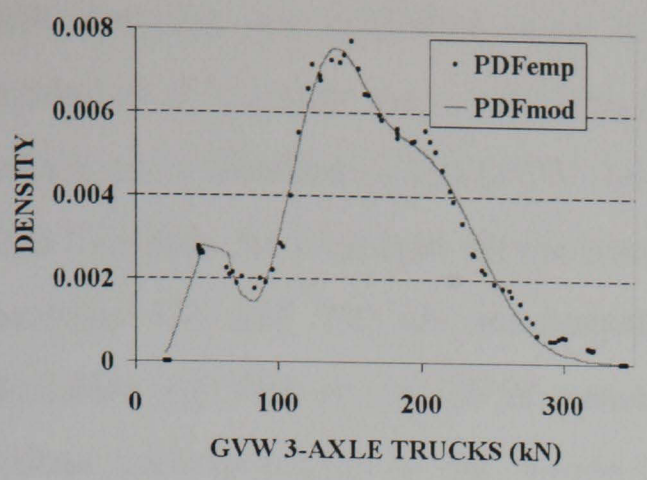

(a)

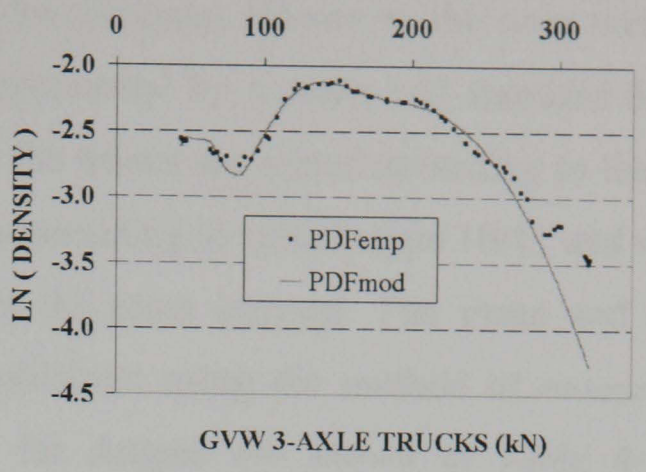

(b)

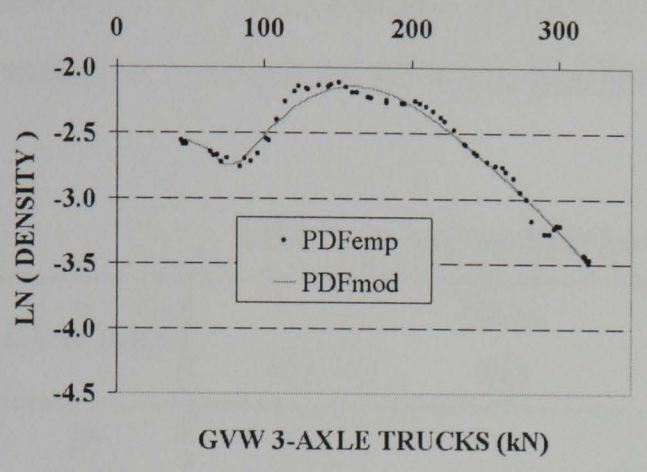

(c)

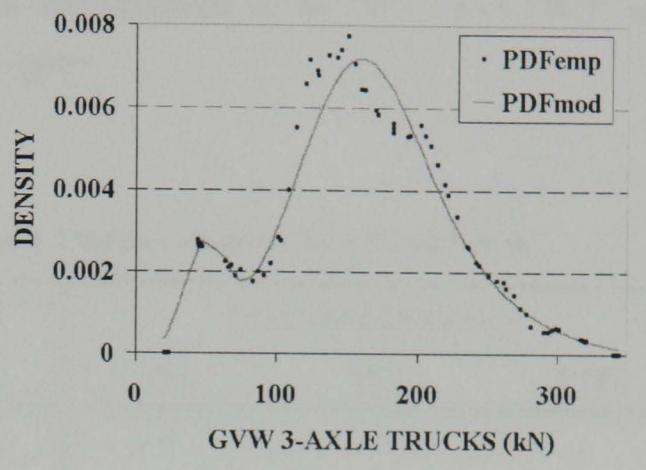

(d)

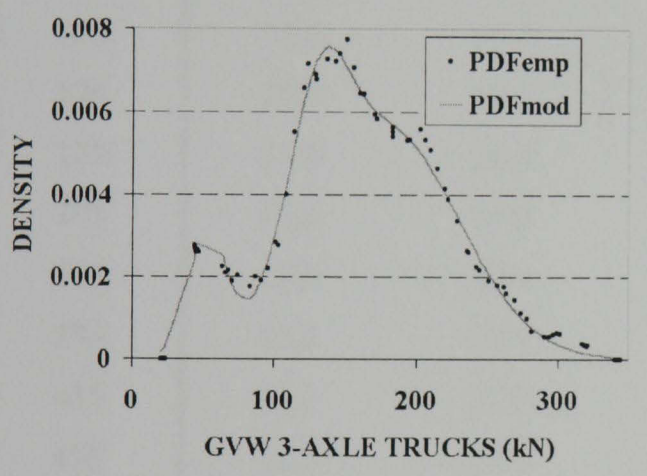

(e)

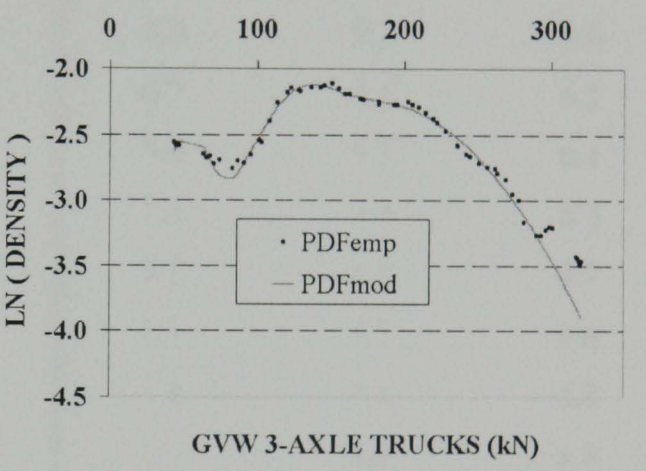

(f)

Figure 4-21: Modelling of the GVW probability density function using normal scale and logarithmic scale

Finally, it should be noted that most of the PDF's (i.e. GVW, axle weights and axle spacings) can be accurately modelled by the use of a normal distribution, or a combination of normal distributions (a limit of 3 modes has been selected in the scope of this thesis).

4.4.4 Modelling of typical trucks

The 2- and 3-axle trucks are modelled using vehicle types 05 and 07 respectively; the characteristics of which (axle spacings and axle weights) are modelled using normal distributions or a combination of normal distributions. For the 4- and 5-axle trucks, the

axle spacings are modelled using normal distributions. However, the axle weights are modelled differently: each axle weight is represented by a mean and standard deviation, which are a function of the GVW itself. All the trucks are sorted according to their GVW into intervals: for example, all the trucks corresponding to vehicle type 10/11 and weighing between 350 and 400 kN are considered in the same interval. The mean and standard deviation for that set of GVW values are obtained using the method of moments. The values corresponding to the 4-axle trucks for Angers are shown in Table 4-5 as an example. The axle weights of the front axles are referred to as 'W1' and 'W2' while the tandem at the back of the truck is referred as 'WT'.

Table 4-5: Axle weights for the 4-axle trucks (Angers) as a % of GVW

GVW (kN)	Mean			Standard Deviation		
	W1	W2	WT	W1	W2	WT
25	/	/	/	/	/	/
75	31.7	31.6	36.7	4.9	5.9	7.3
125	32.4	29.7	38.0	5.8	5.2	5.4
175	29.7	29.1	41.2	4.7	4.5	5.1
225	24.9	30.8	44.4	3.6	5.3	6.1
275	21.6	31.0	47.4	2.6	5.4	6.3
325	19.0	30.4	50.6	2.2	4.6	5.7
375	16.8	28.9	54.4	1.7	3.7	4.4
425	16.1	27.9	56.1	1.4	3.4	3.8
475	15.3	27.5	57.3	1.5	3.5	3.8
525	/	/	/	/	/	/
575	/	/	/	/	/	/

/ = data not available

In Table 4-6, the parameters of the normal distributions used to model the axle weights for the 3-axle trucks are presented for all sites. The distributions employed are typically bi/tri-modal; for each mode, the mode proportion, the mean and standard deviation are given. Finally, Table 4-7 exhibits the parameters of the distributions modelling the axle spacings for the 5-axle trucks (all sites): the distributions are uni/bi-modal. These tables only give examples of the distribution parameters used to model the various traffic characteristics; the complete set of tables representing all the truck classes and traffic types considered can be found in Appendix D.

Table 4-6: Parameters of the normal distributions representing the axle weights for 3-axle trucks (ρ = mode proportion, M*=mean, ST=standard deviation)**

	W1 (% of GVW carried)			W2 (% of GVW carried)			W3 (% of GVW carried)		
	ρ	M*	ST**	ρ	M*	ST**	ρ	M*	ST**
Angers	0.066	20.4	1.5	0.769	34.6	6.8	0.558	30.5	5.9
	0.522	26.0	4.9	0.227	39.2	2.2	0.442	37.7	3.5
	0.412	38.7	8.6	0.004	54.4	3.7			
Auxerre	0.515	26.6	2.1	0.132	31.8	5.7	0.714	23.2	2.3
	0.459	28.3	6.3	0.233	39.5	4.8	0.200	34.1	3.0
	0.025	21.5	43.3	0.635	50.3	3.0	0.085	40.8	2.3
A196	0.046	23.5	4.1	0.500	35.2	5.7	0.466	23.7	2.6
	0.570	31.6	3.4	0.462	44.0	3.6	0.534	28.3	7.2
	0.384	39.2	6.0	0.039	54.0	4.2			
A296	0.099	22.3	5.7	0.408	31.0	5.7	0.294	21.2	2.5
	0.462	32.1	4.5	0.535	45.3	4.9	0.706	26.5	8.7
	0.439	39.4	8.0	0.057	61.6	5.4			

Table 4-7: Parameters of the normal distributions representing the axle spacings for 5-axle trucks (ρ = mode proportion, M*=mean, ST=standard deviation)**

	S12 (m)			S23 (m)			S34 (m)			S45 (m)		
	ρ	M*	ST**	ρ	M*	ST**	ρ	M*	ST**	ρ	M*	ST**
Angers	0.041	2.3	0.1	0.133	4.2	0.6	1.000	1.1	0.2	1.000	1.1	0.2
	0.959	3.0	0.2	0.867	5.1	0.3						
Auxerre	1.000	3.2	0.2	0.041	4.2	0.3	1.000	1.2	0.2	1.000	1.2	0.1
				0.959	5.4	0.3						
A196	0.955	3.6	0.2	0.229	5.3	0.6	1.000	1.2	0.1	1.000	1.2	0.1
	0.045	4.1	0.0	0.771	5.8	0.3						
A296	1.000	3.7	0.2	0.320	5.3	0.7	1.000	1.3	0.0	1.000	1.3	0.1
				0.680	5.9	0.3						

Finally, Figure 4-22 shows the modelled PDF of truck weight (for the 4-axle trucks – direction 1) corresponding to the various sites considered. The variations between sites are obvious, apart from A196 and A296, which present similar distributions. The need to use site-specific (and direction-specific) data if accurate results are to be obtained is emphasised once again. The parameters corresponding to these distributions can be found in the Appendix D, together with the figures for the other truck classes.

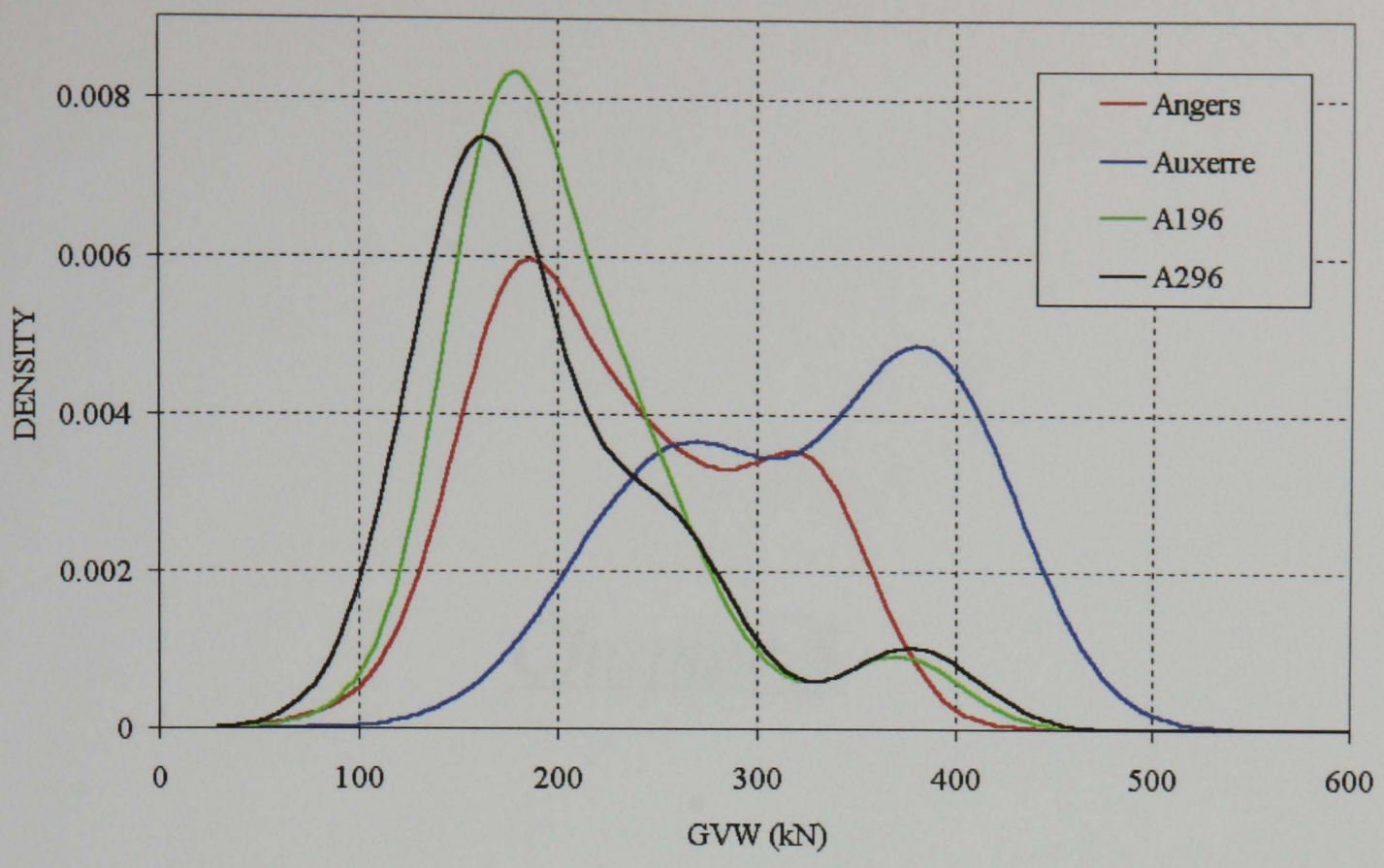

Figure 4-22: Modelled PDF of GVW for the 4-axle trucks for various sites (direction 1)

4.5 CONCLUSIONS

The first section concentrated on a thorough description of some WIM data files. A number of essential observations were made: the high variability of the traffic characteristics (GVW, truck configuration, traffic intensity) between sites, or even between directions for a given site. Also the vast majority of heavy vehicles consists of 4/5- axle trucks (tractor/semi-trailer type), whose weight distribution changes with the GVW, the back of the truck getting heavier. In the second part, the static effects of traffic actions have been studied through the use of influence lines and influence responses. The influence lines characterising the load effects taken into account represent a variety of shapes and slopes that can be considered as representative for this type of bridge (i.e. 20 m to 40 m long). The introduction of the concept of influence response of a bridge facilitates the prediction of the largest possible effect due to a truck (of known configuration). Also, the sensitivity of the influence responses to the various vehicle types revealed that, the steeper the influence line and the shorter the bridge, the more sensitive the influence response is. Finally, in a third part, the findings from the two previous sections along with some new modelling techniques, enabled the determination of distribution parameters that are used to model accurately the traffic characteristics. These characteristics will later be employed to generate traffic files and develop new load models.

Chapter 5

TRAFFIC GENERATION AND SIMULATION

Chapter 5 TRAFFIC GENERATION AND SIMULATION

5.1 INTRODUCTION

This chapter presents the various programs used and/or developed by the author throughout this thesis for traffic generation and simulation. All the programs have been written in the FORTRAN 90 language, apart from those dealing with the visualisation of the results, which were written in MATLAB Version 12. The two main programs developed by the author, GENERATETRAFFIC and SIMULTRAFFIC, are presented in detail. The program CASTOR, written by the Laboratoire Central des Ponts et Chaussees in Paris (Eymard & Jacob 1989), is also reviewed explicitly as it is used to validate SIMULTRAFFIC through comparison of the results given by the two programs. Finally, the programs developed to visualise the output data of SIMULTRAFFIC are briefly illustrated.

5.2 TRAFFIC GENERATION

From known traffic characteristics traffic records can be generated, and thus new traffic files assembled. The traffic characteristics are derived from one (or more) traffic measurement file(s) obtained at a specific measurement site. The traffic files generated are therefore representative of that site. This assumption is critical and one must ensure its validity before using the approach described herein. In addition, traffic files using characteristics obtained from different measurement sites can be mixed and artificial traffic files generated, which do not correspond to any particular measurement site but can be required for simulation purposes. For example, it is of interest to mix the heavy traffic (i.e. GVW) with high traffic intensity (i.e. flow rates) to study critical bridge loading, as critical loading events will then be both frequent and severe.

5.2.1 Input data

In order to generate traffic files, a number of input data are necessary:

- intensity of traffic (taken here in terms of Average Hourly Flow Rates per direction)
- traffic composition (in terms of percentage of trucks by class)
- speed distribution (per direction)
- Gross Vehicle Weight distribution (per class and per direction)
- truck characteristics: axle spacings and axle weights (per class)

All these data are input into the main program GENERATETRAFFIC via a subroutine and are stored in various arrays.

Traffic intensity

The average hourly flow rates (averaged over working days only) are stored in an array that contains entries representing 2[directions]*24[hours] entries. These will be the parameters used to generate the headways. The average hourly flow rates for each hour were averaged for the same hour over many days (see § 4.2.2).

Traffic composition

The traffic composition is stored in a 2[directions]*4[classes] array. The composition gives the proportion of trucks in each class, where each class corresponds to a different number of axles. As previously explained, the 6-axle trucks are included in the 5-axle truck class due to their extremely small number. Therefore, there are 4 classes, corresponding to the 2-, 3-, 4- and 5-axle trucks.

Speed distribution

The speed distribution is stored in a 2[directions]*2[parameters] array, where the two parameters are the mean and standard deviation of the normal distribution used to model the speed.

Gross Vehicle Weight distribution

The probability density functions of GVW corresponding to the 4 classes are stored in an array of 2[directions]*4[classes]*9[parameters]. For each probability density function, there can be as many as 9 parameters: 3 distinct modes with 3 parameters each (mode percentage, mean and standard deviation).

Truck characteristics – Axle spacings

The axle spacings are stored in a similar fashion as the PDF for the GVW, using an array of 4[classes]*4[spacings]*9[parameters)]. The same array is used for both directions (as the truck characteristics are considered to be basic characteristics associated with a truck type). There can be as many as 3 modes in order to model accurately the empirical distributions for axle spacings, as illustrated in the previous chapter in the modelling of the data section.

Truck characteristics – Axle weights

Depending on the number of axles (i.e. class) considered, two different types of information are required. For the 2- and 3-axle trucks, the axle weights (expressed as percentages of GVW carried by each axle) are considered to be constant and independent of the gross vehicle weight. However, for the 4- and 5-axle trucks, the axle weights are modelled as a function of GVW: the axle weights take different values as the GVW varies. For the 2- and 3-axle trucks, the characteristics for the axle weights are stored in an array of 2[classes]*3[number of axles]*9[parameters]. For the 4- and 5-axle trucks, an array 2[classes]*12[number of intervals]*3[number axles/axle groups]*2[parameters] is used. The number of intervals is 12, covering the range of GVW starting at 25 kN and finishing at 575 kN in intervals of 50 kN. The number of axles or group of axles is 3: the first two axles (corresponding to the tractor) and the tandem/tridem (corresponding to the semi-trailer). The number of parameters is 2: the mean and the standard deviation.

5.2.2 Generation of the traffic file

The main program that generates the traffic file calls 3 subroutines one after another. The first one generates the truck characteristics for all the trucks that will form the traffic file. The second one generates the arrival times of all the trucks and the third subroutine forms traffic records (combining the truck characteristics and the arrival times) and assembles the traffic file.

Generation of truck characteristics

The total number of trucks to be generated is estimated by summing the flow rates over a day and multiplying it by the number of days of traffic specified. The main steps in the subroutine GENERATETRUCKCHARACTERISTICS, which generates the trucks characteristics,

are described in Figure 5-1. The subroutine MULTIMODAL enables a number of variates that follow a multi-modal normal distribution of specified parameters to be generated.

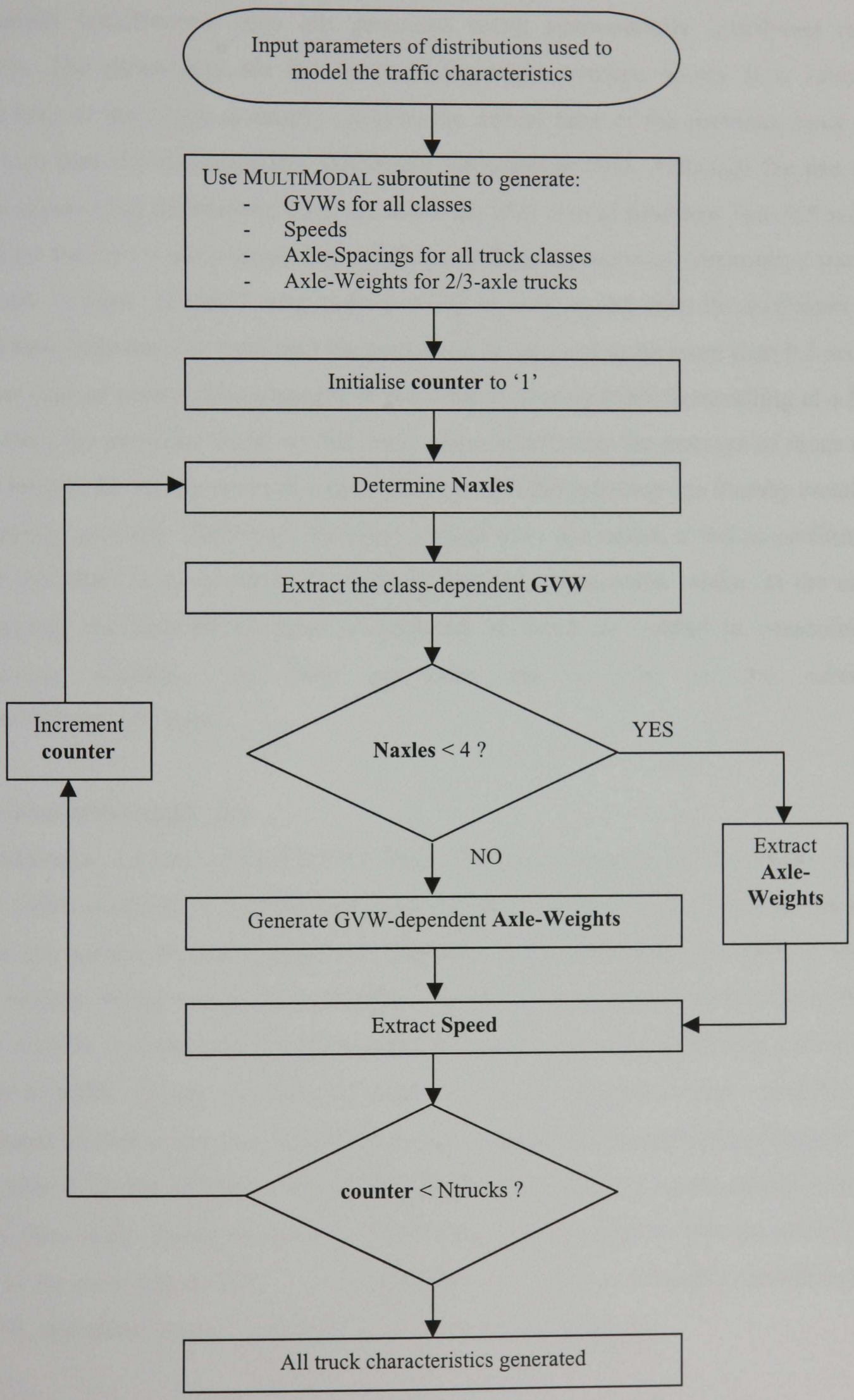

Figure 5-1: Flow chart of the subroutine GenerateTruckCharacteristics

Generation of arrival times

All the trucks having their proper characteristics defined, the next step is to generate arrival times for all the trucks. As the inter-arrival times have been modelled using the shifted exponential distributions, they are generated using exponentially distributed random numbers. The parameters are the direction-dependent average hourly flow rates. The arrival time of any truck is simply equal to the arrival time of the previous truck in the same lane plus the exponentially distributed inter-arrival time. Although the use of the shifted exponential distribution does not allow an inter-arrival time less than 0.5 seconds, great care has to be taken regarding possible overlapping between consecutive trucks. If the 'truck in front' is rather long and travelling at slow speed, then the minimum inter-arrival time between this truck and the next truck is required to be more than 0.5 seconds. Another case of potential overlapping is when the following truck is travelling at a higher speed than the previous truck; in that case, when simulating the passage of these trucks over a bridge, the following truck might catch up with the previous one thereby creating an overlapping scenario. Therefore, for every arrival time generated, a test is performed to ensure that there is no possible overlapping between consecutive trucks. In the case of overlapping, the inter-arrival time is increased as much as needed to overcome that overlapping scenario. All these operations are included in the subroutine GENERATEARRIVALTIMES.

Generation of the traffic file

The subroutine GENERATETRAFFICFILE takes the characteristics of the trucks and the arrival times generated previously and combines them to form traffic records. The traffic records are written chronologically, i.e., therefore the arrival times are used to sort the traffic records. When writing the traffic file, a specific format is used so that the traffic file can be read by CASTOR (this format is explained explicitly in the following section). The number of traffic records is indirectly determined by the number of days of traffic to be represented as well as the intensity of the traffic. In order to give an order of magnitude of the number of traffic records contained in a traffic file, Table 5-1 gives typical values for various flow rates. Trying to generate traffic files equivalent to one month of traffic can prove to be time and memory consuming (with the number of traffic records reaching 300,000), dependent on the number of lanes, intensity of traffic, etc.

Table 5-1: Typical number of traffic records contained in a traffic file as a function of the average daily flow rate

Average Daily Flow Rate (trucks/hour)	N° of trucks per day for 2 lanes	N° of trucks per week[(a)] for 2 lanes	N° of trucks per month[(b)] for 2 lanes
50	2,400	12,000	52,800
100	4,800	24,000	105,600
150	7,200	36,000	158,400
200	9,600	48,000	211,200
250	12,000	60,000	264,000
300	14,400	72,000	316,800
(a) a week means that the number of days is equal to 5 (only working days are accounted for)			
(b) a month means that the number of days is equal to 22 (only working days are accounted for)			

5.2.3 Modification of existing traffic files

Some of the measured traffic data files used in this thesis have been recorded to the nearest second, which is unfortunately not accurate enough when considering relatively short bridges. Indeed, in order to study in detail the different loading events, arrival times to the nearest hundredth of second are required. The exact position of the various trucks can then be determined. By considering the nearest second only, a lot of trucks have the same apparent arrival times, which is rather conservative for two parallel lanes of traffic (the two trucks being placed right beside each other).

In order to overcome that simplification, artificial hundredths of a second can be added randomly to the arrival times from the original file. Although they do not reproduce the 'real' arrival times (unknown in any case), they represent the randomness inherent in traffic data and, above all, enable accurate calculations to be made based upon these modified arrival times. A program, AddHundredthOfSecond, has been developed in order to artificially add hundredths of a second to the measured arrival times. Although simple, this operation requires the new arrival times to be sorted in chronological order and the traffic records to be rearranged to constitute the modified traffic file.

5.3 TRAFFIC SIMULATION USING CASTOR

5.3.1 Introduction

As briefly explained in chapter 3, CASTOR can generate a simulation of traffic over a bridge and can calculate the effects induced in the structure due to the passage of these traffic loads. In this section, the use of CASTOR is considered for traffic loading on short to medium span bridges (say <40m). For these bridges, the critical loading events typically consist of two to three trucks (as demonstrated in further chapters); the knowledge of the exact position of the trucks is crucial if accurate results are to be obtained. The details of CASTOR are now addressed, including its limitations when considering the case of traffic loading on relatively short bridges.

5.3.2 Running CASTOR

When running CASTOR, the user has to input a number of files and data. Apart from the traffic data file, the file(s) containing the details of the influence line(s) to be considered are also required. Some basic data have to be included too; such as the number of lanes and the time increment for the calculations. The last input data, but not the least, are the limits and the interval size for the level crossing histogram that will be used in the analysis of the effects calculated. The output data (i.e. the histograms of level crossing) depend on this input; therefore some initial calculations are necessary in order to estimate accurately these limits. The accuracy of the extrapolation based on the level crossing histogram will also slightly depend on this input data, which underlines the care that is required in determining these limits.

Another important point concerns the arrival times. Indeed, CASTOR assumes that these arrival times are 'correct' and are taken as given. However, if two traffic records show the same arrival time and the same lane, the trucks are still considered to be distinct (although they actually overlap each other). Thus the final results from CASTOR, although correct mathematically, are biased since two trucks cannot materially overlap. In other words, CASTOR allows overlapping of trucks if given as such by the input file. Another possible case of overlapping is when two trucks are not overlapping initially but will overlap at

some stage while crossing the bridge due to a significant difference in their speed. The typical example is when two trucks follow each other closely, in terms of arrival times, and the latter truck travels at a much higher speed than the former one. As CASTOR keeps the speeds constant over the bridge, the latter truck catches up with the former one and finally overlapping occurs, as illustrated in Table 5-2. In this example, 3 trucks are involved, all travelling in the same direction (2 trucks in the slow lane and 1 truck in the fast lane); only the two trucks located in the slow lane (lane 4) are of interest in this particular example (the truck in the fast lane is greyed out). While the 1st truck in the slow lane enters the bridge at time T, the other two trucks are still away from the bridge (the second truck in the slow lane being about 10m behind the first one). By the time the 2nd truck in the slow lane reaches the bridge, at T+0.70s, all the axles of the 1st truck are on the bridge. Finally, at T+1.31s, when the maximum value of the effect occurs, the 2nd truck has caught up with the 1st one and there is overlapping: the first two axles of the 2nd truck overly the back of the 1st truck (in the table the position of the overlapping axles are in bold). Although the example presented is very unlikely to happen, that is, to have two trucks closely positioned in the same lane and with a significant difference in speed, it is possible. The values employed here have been artificially exaggerated so as to clearly demonstrate the possibility of overlapping occurring during a traffic simulation using CASTOR.

Table 5-2: Axle positions of all trucks involved in a given crossing event – Load Effect 1 / 30m bridge

Truck	GVW (kN)	Naxles	Speed (m/s)	Lane	Axle W. (kN)	Axle Position (m) at: T	T+0.70s	T+1.31s	Effect (kN*m)
1	450	5	20.0	4	90	0.0	14.0	26.2	168
1	450	5	20.0	4	150	-3.3	10.7	22.9	522
1	450	5	20.0	4	70	-9.0	5.0	**17.2**	439
1	450	5	20.0	4	70	-10.2	3.8	**16.0**	481
1	450	5	20.0	4	70	-11.4	2.6	**14.8**	508
2	450	5	23.8	3	90	-11.9	2.1	19.3	473
2	450	5	23.8	3	150	-15.6	1.1	15.6	1061
2	450	5	23.8	3	70	-21.2	-4.5	10.0	343
2	450	5	23.8	3	70	-22.4	-5.7	8.8	301
2	450	5	23.8	3	70	-23.6	-6.9	7.6	260
3	450	5	30.0	4	90	-21.0	0.0	**18.3**	517
3	450	5	30.0	4	150	-24.3	-3.3	**15.0**	1104
3	450	5	30.0	4	70	-30.0	-9.0	9.3	319
3	450	5	30.0	4	70	-31.2	-10.2	8.1	278
3	450	5	30.0	4	70	-32.4	-11.4	6.9	237

These two possible cases of overlapping are a serious potential source of inaccuracy in the calculations, on the conservative side. When trying to develop an accurate site-specific model, accuracy is important and any potential source of error should be addressed. It is

therefore suggested by the author to check the initial traffic data file against any potential case of overlapping and to introduce slight modifications, such at slower speeds for certain trucks or modified arrival times, in the initial traffic file in order to avoid these cases of overlapping. To this end, the author developed a program CHECKTRAFFICFILE that takes the following steps:

- for all the vehicle in the same lane of traffic, check the speed of two consecutive vehicles
- if the speed of the second vehicle is higher than the speed of the first vehicle (i.e catching up with the vehicle in front), then overlapping could occur before the first vehicle has left the bridge. If overlapping occurs, the arrival time of the second vehicle is increased so as to avoid overlapping and to ensure a reasonable spacing between the two trucks
- if the speed of the second vehicle is lower than the speed of the first vehicle (i.e the vehicle in front going away from second vehicle), then overlapping could only occur when the first vehicle enters the bridge. If overlapping occurs, the arrival time of the second vehicle is increased so as to avoid overlapping and to ensure a reasonable spacing between the two trucks.

Other means could be used rather than modifying the arrival times, by only changing the speed of the 2nd vehicle for example. However, in order to ensure that the data is realistic, the modification of the arrival times is used because it enables the introduction of a minimum spacing between consecutive vehicles.

It should be emphasised that the fact that CASTOR allows for overlapping does not lessen its potential. The user simply needs to be fully aware of that specific, which can be efficiently overcome by the use of adequate pre-processing of the original data file.

5.3.3 Limitations of CASTOR

As mentioned in chapter 3, CASTOR allows the calculation of effects induced in a bridge by the passage of traffic loads on the deck. Among the possible output files, a number of extreme values (minima/maxima) of the effects can be written to a file. However, there are two limitations in the use of that option:

- the number of extreme values is limited to 10;

- a single loading event might induce more than one local extreme; CASTOR outputs the 10 absolute extreme effects regardless of whether they correspond to 10 different loading events or to only 3 different loading events with a few local extremes each.

In order to explicitly illustrate this limitation, Table 5-3 and Table 5-4 show the times at which the 10 maximum effects occur for the A196 file (direction 2 of traffic) for two different load effects and for a 30 m bridge. The rows shaded in grey represent the same events, as indicated by the times being identical except for the hundredths of second. In other words, in Table 5-3, the top 3 maximum effects are all induced by the same loading event; and so are maximum effects 5, 6 and 7.

Table 5-3: Times at which the 10 maxima occur for A196 direction 2 – Effect 2 – Span =30 m (from CASTOR)

	Effect	Day	Month	Hour	Hour	Minute	Second	Sec./100
10	1087	10	9	96	6	40	39	35
9	1087	10	9	96	19	14	45	18
8	1087	12	9	96	11	18	0	74
7	**1113**	**9**	**9**	**96**	**21**	**22**	**48**	**97**
6	**1116**	**9**	**9**	**96**	**21**	**22**	**48**	**95**
5	**1124**	**9**	**9**	**96**	**21**	**22**	**48**	**99**
4	1127	11	9	96	6	22	12	14
3	**1196**	**11**	**9**	**96**	**19**	**17**	**30**	**3**
2	**1201**	**11**	**9**	**96**	**19**	**17**	**30**	**1**
1	**1207**	**11**	**9**	**96**	**19**	**17**	**30**	**6**

Similarly, in Table 5-4, maximum effects 1, 3, 5, 6 and 8 are all induced by the same loading event; the maximum effects 2, 4 and 9 are induced by another loading event. From Table 5-4, the 10 maximum effects are induced by only 4 different loading events. Therefore, if it is of interest to know the maximum effect induced by each loading event, the output from CASTOR is not very satisfying as it does not distinguish between loading events, and furthermore the number of extreme effects that can be outputted is limited to 10. The multiple extreme effects induced by the same crossing event will be referred to as replicated effects.

Table 5-4: Times at which the 10 maxima occur for A196 direction 2 – Effect 3 – Span =30 m (from CASTOR)

	Effect	Day	Month	Hour	Hour	Minute	Second	Sec./100
10	649	9	9	96	21	22	49	23
9	662	11	9	96	19	17	30	42
8	**665**	**12**	**9**	**96**	**14**	**24**	**38**	**61**
7	666	11	9	96	16	10	23	98
6	**668**	**12**	**9**	**96**	**14**	**24**	**38**	**62**
5	**678**	**12**	**9**	**96**	**14**	**24**	**38**	**37**
4	**684**	**11**	**9**	**96**	**19**	**17**	**30**	**17**
3	**694**	**12**	**9**	**96**	**14**	**24**	**38**	**25**
2	**697**	**11**	**9**	**96**	**19**	**17**	**30**	**37**
1	**719**	**12**	**9**	**96**	**14**	**24**	**38**	**60**

Conclusions

The use of CASTOR has been illustrated in detail. The fact that CASTOR allows for overlapping between consecutive vehicles (if input as such in the original data file), and therefore could induce errors in the effects calculated, is not an issue since some adequate pre-processing of the traffic file eliminates that potential source of inaccuracy. However, in the scope of this research, CASTOR presents a limitation in that the main output available is the level crossing histogram, while the desired outputs are the maximum effects induced by each crossing event (CASTOR will only provide up to 10 distinct values – the most critical ones).

5.4 TRAFFIC SIMULATION USING SIMULTRAFFIC

A program, SIMULTRAFFIC, has been developed by the author for simulating traffic over a range of bridges, and calculating the effects induced in the structure as the traffic crosses it. The main objective is the study of the critical loading events for bridges less than 40m in length. Only significant loading events are to be considered; in other words, only multiple trucks event should be treated. However, for some particular effect, whose influence line presents an extremely narrow peak (and therefore is extremely sensitive to the exact location of the trucks), a single extremely heavily loaded truck might be as critical as a combination of trucks. This is particularly true when the flow rates are rather low and the crossing events are not so frequent. For this reason, the program has been developed in such a way as to account for single heavily loaded truck events (GVW > 500 kN) as well

as multiple truck events. SIMULTRAFFIC has been developed for use with traffic files containing two lanes of parallel or opposing traffic.

The general process followed by SIMULTRAFFIC is illustrated in Figure 5-2. After reading in the input data (namely the traffic file) and storing the data in two sets of arrays, a test is performed to identify potential crossing events. In the case of a crossing event, the load effects are calculated continuously as the trucks move along the bridge and the maximum value is recorded. This operation is repeated for each load effect treated. The process is terminated when all the trucks have been tested for crossing events. The development of the program is presented in more detail in the following sections.

The traffic data file needs to be written in a very specific format in order to be read correctly by the program. It is the same format as the one employed in CASTOR; as a result any traffic file can be used equally in both programs and part of the results can be compared. This specific format is given in Appendix E.

5.4.1 Testing for crossing event

A crossing event is defined as a loading event involving more than one truck. In other words, the program does not account for all the single-truck events. All the critical events will consist of at least two trucks present at the same time on the bridge (with the exception of extremely heavily loaded trucks). The first step consists in determining which of the two trucks, from the two lanes of traffic, reaches the bridge first; the first truck to do so is referred to as *initial truck*. The times at which the initial truck enters, and later leaves, the bridge are stored as *Ton* and *Tout*. Then the arrival times of the next trucks to arrive on the bridge, in either lane, are tested to check if these trucks actually reach the bridge before the initial truck has left. The number of trucks, *ntrucks*, constituting the crossing event is incremented every time a new truck reaches the bridge in time.

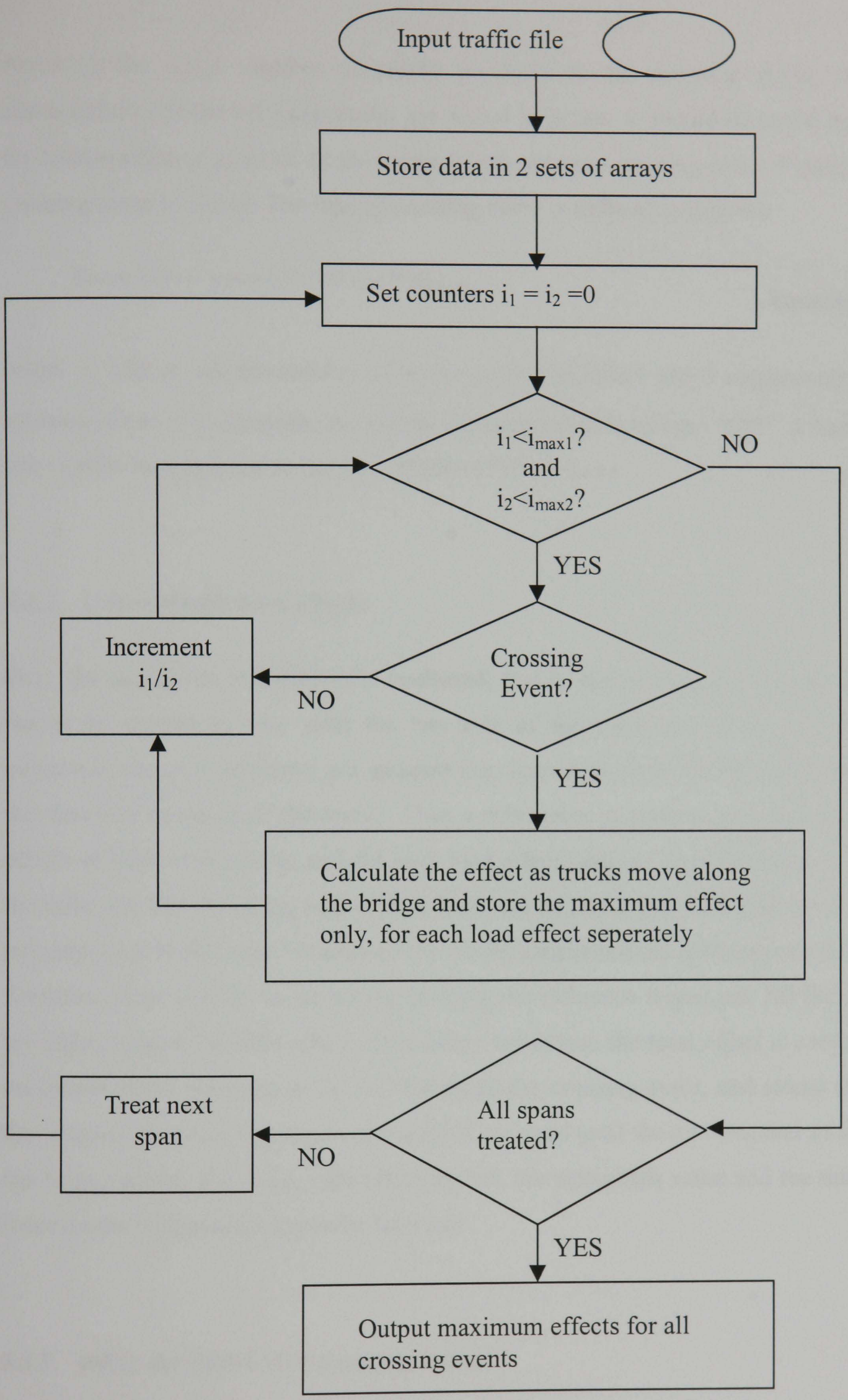

Figure 5-2: Flow chart describing the main program

Knowing the exact number of trucks involved in the crossing event, the relevant characteristics of the different trucks are stored in arrays. It should be noted that *Naxles* is the total number of axles of all the trucks involved in the crossing event. Finally the type of crossing event is stored. The type of crossing event is defined as follows:

$$EventType = ntrucks * 100 + n_1 * 10 + n_2 \qquad \textbf{Equation 5-1}$$

where n_1 and n_2 are the number of trucks present in lane 1 and 2 respectively during the crossing event. For example, the typical crossing event is of type '211': 2 trucks in total, one in slow lane and one in fast (i.e. 2*100+1*10+1=211).

5.4.2 Calculate the load effects

First, the number of calculations is evaluated; that is, the number of times the initial truck has to be moved by *incr* until the last axle of the truck leaves the bridge. At every increment, the axle positions are updated (i.e. incremented or decremented depending on the direction of travel of the truck). Then a subroutine is used to calculate the individual effects of each of the axles, and for each load effect treated. The calculation is done using the influence line for of the load effects. It should be noted that the influence responses are not employed in this case because all the trucks considered are different one from another. Therefore there will be no advantage in using the influence responses. All the axle effects are added to give the total effect. After every increment, the total effect is compared to the maximum effect obtained so far for that particular crossing event, and stored if it exceeds that maximum value. The above operation is repeated until the total number of calculations has been reached. For every load effect treated, the maximum value and the time at which it occurs are temporarily stored for later use.

5.4.3 Filter the duplicated crossing events

When updating the indices, to test for the next potential crossing event, only one of the two indices is updated at a time. For a given crossing event, the 1st truck to leave the bridge will be used as the criterion for choosing which index has to be updated (i.e. which lane has to be updated). Therefore, when considering the next crossing event, it is guarantied that the

truck that has just left the bridge will not be involved in that loading event. This criterion avoids any duplication of crossing events. However, this does not eliminate all the possible duplicates. The following example shows how difficult it can be to distinguish between crossing events. In Figure 5-3 (a), there are three trucks present on the bridge; the maximum effect for the crossing event (conditioned on the 3-axle truck still being present on the bridge) will be registered as the 3-axle truck is about to leave the bridge.

However, the 3-axle truck does not contribute to that maximum value of the effect by more than few percent; it only happens to be there when two heavily loaded trucks are present as well. When considering Figure 5-3 (b), the same two heavily loaded trucks induce the maximum effect, only hundredths of a second after the 3-axle truck has left the bridge. Therefore the maximum effects observed in the two configurations (a) and (b) are quasi-identical, as are the times at which they occur, the only difference being that in one case there is an extra-truck present on the bridge (although not contributing to the total effect in a significant manner). These two configurations can be considered as duplicated crossing events.

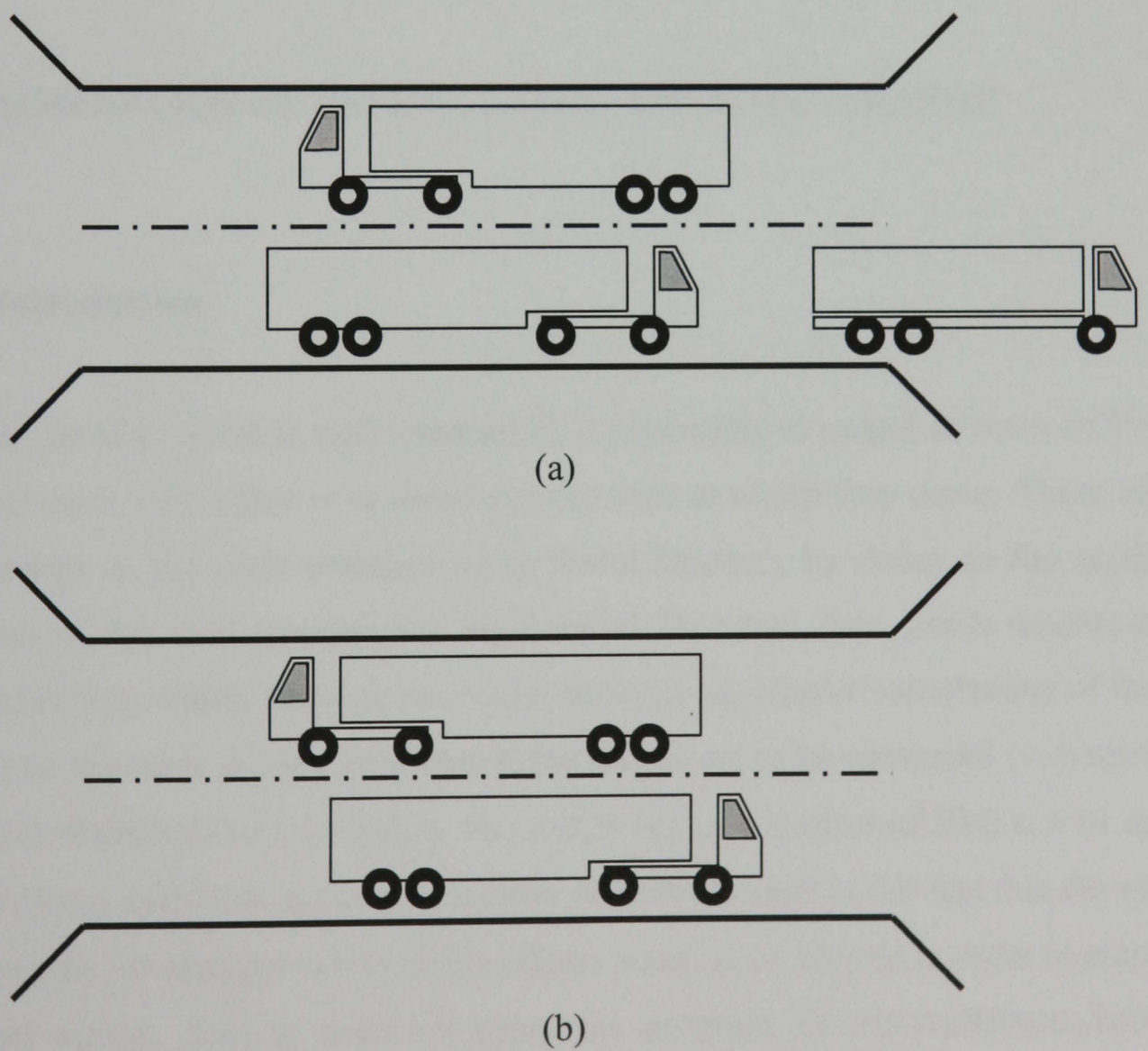

(a)

(b)

Figure 5-3: Example of duplicated crossing event

5.4.4 Output files

Various files can easily be generated depending on the required data. By default, all the maximum effects for the different load effects are written to files. These files are labelled in a systematic manner: 'E120_ID', where 'E1' stands for 'Load Effect 1', '20' refers to the bridge length and 'ID' is some identification number in order to distinguish between various simulations. For this project, runs of SIMULTRAFFIC typically generate 18 files, 'E120_ID' to 'E640_ID', corresponding to six load effects and three bridge lengths.

A file containing the ten extreme effects (for each load effect and bridge length), together with the time at which they occur, is also created. This file, written in the same format as the one used by CASTOR, enables a direct comparison between the results of the two programs. Other files can be outputted; for example, a file containing the details (GVW, axle weights and axle positions) of the trucks involved in the 20 most critical loading events for a given load effect and bridge length. These data can be used later when analysing the critical loading events.

5.5 COMPARISON BETWEEN CASTOR AND SIMULTRAFFIC

5.5.1 Introduction

Once the use of CASTOR is well understood, it is possible to output as many as 10 extreme values for each load effect considered and the time at which they occur. These values can be compared to the ones obtained using SIMULTRAFFIC; by doing so the accuracy and robustness of this new program can be assessed. However, two details deserve attention: the variable *pas*, which the time increment between successive calculations of the effects, needs to be the same in both programs if the results are to be compared (various values of *pas* induce slightly different results). The author suggests a value of 10 (i.e. 0.01 second) in order to obtain sufficient accuracy. Another important detail is the fact that the output file containing the 10 extreme values of the effects needs to be filtered in order to eliminate the replicated values. This is done by using the program ELIMINATEREPLICATEDVALUES, developed by the author.

5.5.2 Results

The results are compared in terms of percentage differences between the results obtained using SIMULTRAFFIC and CASTOR. Sometimes, these differences were not available due to the fact that some extreme effects were removed during the filtering of the replicated values. Also, very often the differences were found to be exactly 0; all these differences have been omitted from the table. Therefore, in Table 5-5, only the cases for which there was a difference are indicated. Tables showing the results for the other traffic files can be found in Appendix E.

Table 5-5: Differences (in %) between SIMULTRAFFIC and CASTOR for Angers ['-' = 0.00 and '/' = no difference available]

	Effect1			Effect2			Effect3		
	20m	**30m**	**40m**	**20m**	**30m**	**40m**	**20m**	**30m**	**40m**
1	-	-	-	0.07	0.05	0.06	-	-	-
2	-	-	-	0.05	0.03	0.07	-	-	-
3	-0.08	-	-	-	0.02	0.00	-	-	-
4	-	-	-0.02	0.02	0.02	0.08	-	-	-
5	-	-	-	0.04	0.06	0.08	-	-	-
6	-	-	-	/	0.05	-	-	-	-
7	-	-	-	/	0.04	0.08	-	-0.04	-
8	-	-	-0.02	/	/	-	/	-	-
9	-	-	/	/	/	/	/	/	/
10	-	-	/	/	/	/	/	/	/
	Effect4			**Effect5**			**Effect6**		
	20m	**30m**	**40m**	**20m**	**30m**	**40m**	**20m**	**30m**	**40m**
1	-	-	-	-	-	-	-	-	-
2	-	-	-	-0.03	-0.10	-	-0.03	-	-
3	-	-	-	-	-	-	-	-	-
4	-	-	-	-0.03	-	-	-	-	-
5	-	-	-	-0.03	-	-	-	-	-
6	-	-	-	-	-	-	-	-0.03	-
7	-	-	-	/	-	-	-	-0.03	-
8	-	/	/	/	/	-	-	-	-0.02
9	-	/	/	/	/	/	-	-	/
10	-	/	/	/	/	/	-	/	/

From the above tables, it can be observed that the differences (if any) are consistently less than 1%, usually no more than 0.1%, for the 4 different traffic files treated. Some load effects tend to show better results than others; load effect 1 shows extremely accurate results while load effect 2 presents greater discrepancies (although consistently very small). These discrepancies can be explained by the shape of its influence line, for which

the slopes on either site of the two local maxima are very steep. Therefore the slightest variation in axle position could induce a difference in the effect induced by that axle weight. Overall, for the three bridge lengths and six load effects considered, and for all the sites, the results obtained from SIMULTRAFFIC are the same as those from CASTOR. As the latter program is well established and widely cited in the literature, this provides evidence of the accuracy and robustness of the new program developed. Based on these results, SIMULTRAFFIC has been validated successfully.

5.6 CONCLUSIONS

All the programs used in the following chapters for the analysis and the development of models for site-specific traffic loading on short bridges have been presented and explained. First, the program GENERATETRAFFIC was presented; then the development of the program SIMULTRAFFIC has been addressed step by step. Its validation, through the comparison of its results with CASTOR results, has also been demonstrated. The development of these two programs was necessary in the scope of this research (notably because of the limitations of the existing programs) and was proven to be extremely valuable in the studies presented in the later chapters.

Chapter 6

BI-DIRECTIONAL TRAFFIC ANALYSIS AND MODELLING

Chapter 6 BI-DIRECTIONAL TRAFFIC ANALYSIS AND MODELLING

6.1 INTRODUCTION

This chapter deals with two opposing lanes of traffic, i.e.. lanes where traffic is travelling in opposite directions, on short to medium span bridges (20 to 40m long). Using the program GENERATETRAFFIC, a number of traffic files are generated, representative of various traffic types (i.e. various traffic weight and intensity). Full simulations are performed for all these files using SIMULTRAFFIC; details of the critical loading events are output, along with the maximum values for all the crossing events. By visualising the most critical events, a detailed analysis is performed and typical critical loading events are derived for each load effect and bridge length considered. Then, a simplified site-specific model is developed: its aim is to rapidly reproduce the critical events corresponding to a traffic type using basic information (such as average daily flow rate and GVW distribution).

6.2 TRAFFIC GENERATION

The use of a single traffic data file, even if taken as representative of a given site, cannot lead to robust and reliable results due to the inherent variability within traffic data. Indeed, for every single traffic data file considered for a specific site, variations in the results would be obtained. Results should not be greatly different but, by considering only one traffic file, biased results could be obtained if that particular file led to atypical (low or high) values of load effects. Thus the use of a number of traffic files is suggested in order to obtain reliable results.

Generally no more than one or two traffic data files are available for a given site. It is therefore required to generate artificial traffic files using the characteristics of an existing traffic file. The FORTRAN program described in the previous chapter, GENERATETRAFFIC, can be used to generate a number of traffic files using the characteristics of previously

analysed traffics (e.g. Angers, Auxerre, A196 and A296). There are two main components when considering traffic files for bridge loading: the traffic intensity (i.e. flow rates) and the truck weights (i.e. GVWs). These two components can have a different, but nonetheless significant, influence on the final results (i.e. the effects induced in the structure). Indeed, if the traffic intensity is very high but the traffic weight is rather low, there will be a great number of crossing events but most of them will not be critical. On the other hand, if the traffic weight is high and the traffic intensity is low, there will be only a few crossing events but these may prove to be extremely severe for the structure.

Based on this premise, it has been decided that a number of combinations (traffic intensity/traffic weight) should be considered to assess the relative importance of each component. The two components are referred to as Q (i.e. flow rate) and W (i.e. GVW) to which an index a, b or c is added that corresponds to increasing values of Q and W (i.e. $Qa < Qb < Qc$ and $Wa < Wb < Wc$). The two sets of three values that have been used for Q and W are: the GVW distribution of Angers, Auxerre and A196; and the flow rates of Angers, Auxerre and modified flow rates of A196. Indeed, the flow rates of A196 are extremely high and correspond to the slow lane of a very busy motorway; such flow rates are not realistic for a 2-lane main road. The values of the flow rates have been divided by a factor of 1.5 to make the values correspond to a multiple of the lowest traffic intensity considered (i..e Qa); therefore $Qb \approx 2*Qa$ and $Qc \approx 3*Qa$.

There are thus 9 possible combinations between the 2 sets of traffic intensity and weight. Figure 6-1, Table 6-1 and Table 6-2 show the characteristics and the names of the various combinations. It should be emphasised that Table 6-1 gives the average hourly flow rate per day as an indication of the traffic intensity; however the flow rates used to generate the traffic files are not constant over the day but different from one hour to another.

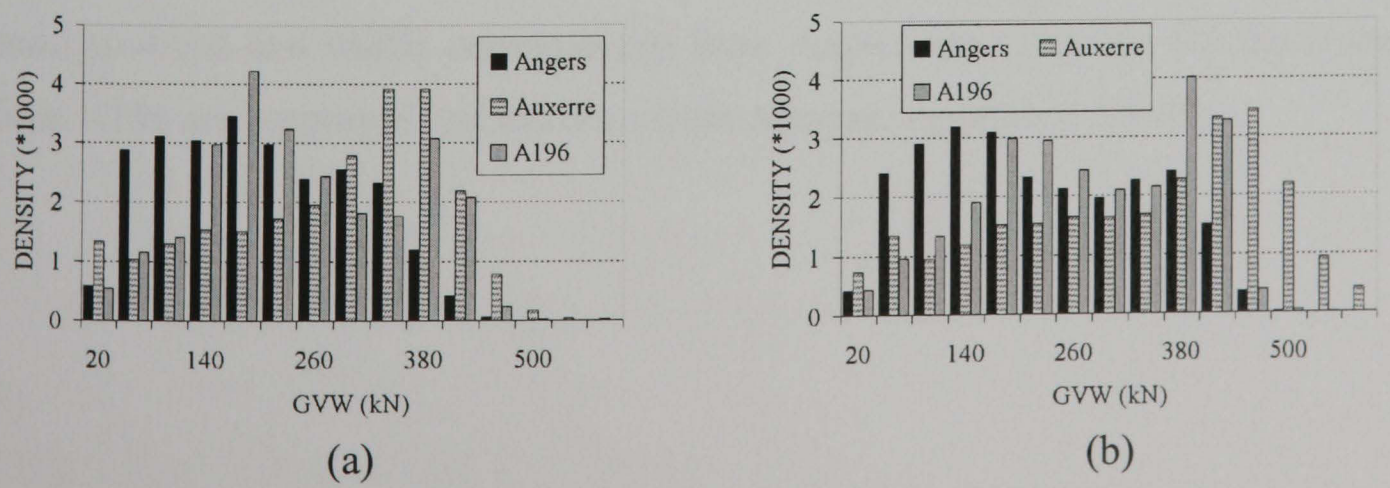

Figure 6-1: GVW histograms for various sites: (a) direction 1;(b) direction 2

Table 6-1: Average Dourly Flow Rate [ADFR] (trucks per hour) for various sites

Site	Angers	Auxerre	A196*
ADFR (trucks/hr) – Dir. 1	64	132	214
ADFR (trucks/hr) – Dir. 2	69	133	185
* = the initial flow rates corresponding to the A196 file divided by 1.5			

Table 6-2: File names for various combinations of traffic intensity and weight

		Traffic Weight (W)		
		Angers	**A196**	**Auxerre**
Traffic Intensity (Q)	**Angers**	QaWa	QaWb	QaWc
	Auxerre	QbWa	QbWb	QbWc
	A196*	QcWa	QcWb	QcWc
* = the initial flow rates corresponding to the A196 file divided by 1.5				

From Table 6-2 it appears that traffic types *QaWa* and *QbWc* correspond to the Angers and Auxerre sites (*QcWb* corresponds to the A196 site, with a reduction in the flow rates). All the other traffic combinations do not correspond to measured traffic but are artificial traffics. For each of the 9 possible combinations, 100 traffic data files of 1 week (i.e. 5 working days) were generated, which represents as many as 900 traffic data files. From the descriptions of the various traffic characteristics, the traffic type *QaWa* is the less severe (lowest intensity combined with lowest weight) of all while *QcWc* is the most severe (highest intensity combined with highest weight).

In addition, the truck configurations and the traffic composition employed in the generation of the various traffic types is the one corresponding to the selected *W* parameter. In other words, when *Wa* is selected, the traffic characteristics (i.e. truck configurations and traffic composition) from Angers are used; for *Wb* the characteristics from A196 are employed and the ones from Auxerre are utilised for *Wc*.

6.3 TRAFFIC SIMULATION

6.3.1 Calculation of the load effects

The program SIMULTRAFFIC, described in the previous chapter, has been used to simulate the passage of all the generated vehicles over bridges and calculate the load effects induced in the structure, either by the multiple presence of trucks or by a single very heavy truck. Each of the 900 traffic files, representing one week of traffic, has been used. The effects have been calculated for the six load effects and three bridge lengths considered; the maximum values corresponding to each crossing event have been stored for each load effect and bridge length. In order to avoid having too many values and mainly because only the critical effects are of interest, the 100 most critical effects for each 1-week file are considered. Finally, the results are regrouped in 10 sets; that is, the 100 files corresponding to the same traffic type (e.g. *QaWa*) are regrouped in 10 sets of 10 files each, every set representing a period of 10 weeks of traffic. Set 1 corresponds to files '_00' to '_09', set 2 to files '_10' to '_19', etc. Consequently, to every set there corresponds a number of 1000 critical effects (i.e. 10 files*100 critical effects) per load effect and per bridge length. In other words, for each of the 9 traffic types studied, there are 10 sets representing 10 weeks of traffic; 18 arrays (6 load effects * 3 bridge lengths) of 1000 critical values are associated with each set.

As explained earlier, variations can be observed between the results of different traffic files. Figure 6-2 presents the plot on Gumbel probability paper of the 10 sets of results, together with the average of the 10 sets, for bending moment at mid-span of a 20m simply supported bridge (i.e. load effect 1 in this study). Due to the nature of the probability paper, if the same number of values is plotted for different series, the ordinate values are the same for all the series. It is therefore possible to take the average of the 10 different 'x-values' for each of the 1000 'y-values' and constitute a set of average values. On Figure 6-2, it can be observed that the various sets present the same general trend, and only towards the right tail (i.e., the last 20 points or so) they exhibit perceptible differences, which correspond to the inherent variability in the traffic data referred to previously. However, in the Chapter 3, the tail of a distribution of extreme values was shown to be critical in the prediction of extrapolated values. It is therefore necessary to compare (i) the extrapolated values obtained by considering the average of the 10 sets separately and (ii) the extrapolated

values obtained by considering the set of average values in order to assess the validity of this assumption. For the method used in the calculation of the extrapolated values, the reader is referred to Appendix I.

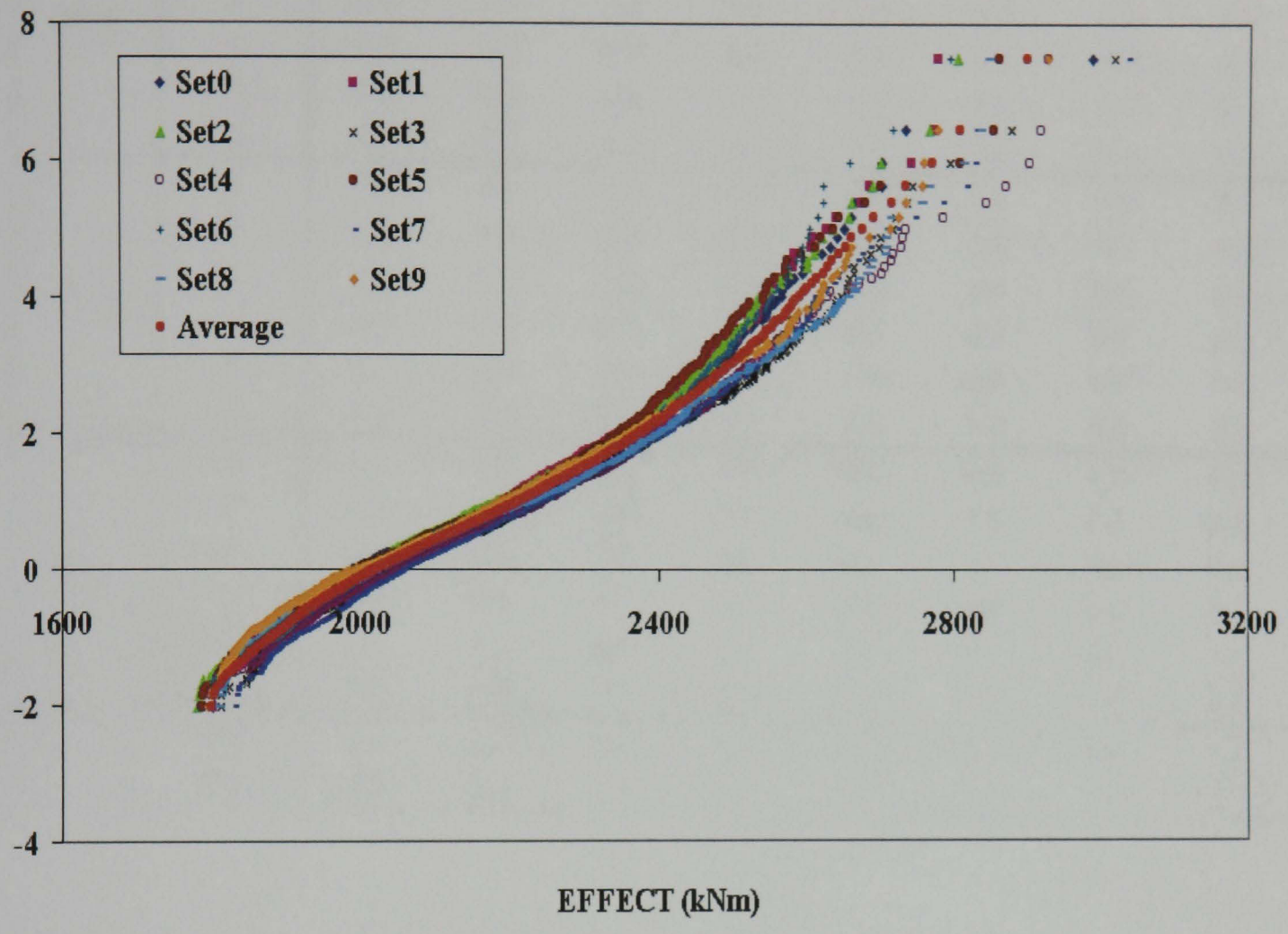

Figure 6-2: Gumbel Plot of 10 sets of data and their average for the bending moment at mid-span of a 20 m simply supported bridge

Table 6-3 presents the differences (in %) between the two extrapolated values obtained using (i) and (ii). For all the traffic types, the 3 bridge lengths and 6 load effects considered, the differences are always between –6.3% and +5.3%. These very small values for the differences verify that the above assumption is perfectly applicable. In other words, considering a set of average values for the critical effects in order to account for the natural variability in the traffic leads to the same results as considering all the sets separately. In addition, by considering the average of the 10 sets, a more robust trend can be obtained and used in later calculations. These average values, although not corresponding to a particular set of simulations, give representative values for the type of traffic considered.

Table 6-3: Differences (%) between Extrapolated Values from set of averaged effects and average of Extrapolated Values from each set

Bridge Length	Load Effect	Traffic Type								
		QaWa	QaWb	QaWc	QbWa	QbWb	QbWc	QcWa	QcWb	QcWc
20 m	1	-4.2	1.1	0.0	0.0	1.0	0.6	0.0	0.5	0.5
	2	-3.5	0.0	0.0	0.0	2.6	0.9	0.0	1.5	0.1
	3	-3.0	1.9	0.0	0.0	3.0	0.0	0.0	1.4	0.7
	4	-4.8	0.3	0.0	0.0	5.9	0.7	-4.8	0.8	0.6
	5	0.1	0.0	0.0	0.0	1.7	0.8	-3.5	1.1	0.1
	6	-1.3	-0.1	0.0	0.6	2.2	0.6	-0.1	0.5	0.7
30 m	1	0.0	0.0	0.0	0.3	1.0	0.0	0.0	0.5	0.4
	2	0.3	0.0	0.0	0.0	0.0	0.0	-0.1	-0.1	0.1
	3	1.6	0.0	0.0	0.9	1.4	0.4	0.0	0.0	0.9
	4	0.5	-3.8	0.0	0.6	0.8	0.2	0.0	0.2	0.1
	5	0.7	0.0	0.0	0.8	1.8	0.8	0.0	0.3	0.3
	6	0.3	0.0	0.0	0.0	3.1	0.0	0.0	0.6	0.2
40 m	1	0.4	0.0	0.0	0.0	0.8	0.0	0.0	0.2	0.1
	2	0.0	0.0	0.0	0.0	0.0	0.0	0.0	0.8	1.1
	3	0.0	0.4	0.0	0.0	0.4	0.1	0.0	0.5	0.0
	4	0.3	0.2	0.0	0.0	0.5	0.0	0.0	0.1	0.0
	5	1.0	1.1	0.0	0.0	2.4	0.3	0.0	1.1	0.0
	6	0.9	0.9	0.0	-6.3	1.6	0.6	0.1	1.4	1.1
	Max	1.6	1.9	0.0	0.9	**5.9**	0.9	0.1	1.5	1.1
	Min	-4.8	-3.8	0.0	**-6.3**	0.0	0.0	-4.8	-0.1	0.0

6.3.2 Results of the full simulations

Having values representative of 10 weeks of a given traffic type, it is possible to compare these values between different traffic types and to assess the influence of each parameter: traffic intensity and traffic weight. To do so, Gumbel plots (i.e. plots on Gumbel probability paper) of the 1000 most critical values have been generated. On each plot three series are represented: a fixed value of Q (/W) with the three possible values of W (/Q). Figure 6-3 presents the Gumbel plots for fixed traffic intensity (*Qa*) and varying traffic weight (*Wa*, *Wb* and *Wc*). It can be seen that the heaviest traffic induces higher values of effects, for each of the load effects considered. However, there is little difference between the two other traffic types, *QaWa* and *QaWb*. This observation is important because significant differences could be expected as the traffic *Wb* is significantly heavier than traffic *Wc* (see Figure 6-1). In that example, the lack of difference between the results is due to the variation in the truck geometry (axle weights and axle spacings) between the two traffic types. Traffic *Wa* consists of slightly shorter trucks than traffic *Wb*; therefore, although trucks from traffic *Wb* are heavier than those from traffic *Wa*, the total effect

induced in the structure is similar for both truck types. In other words, the effect induced by a lighter shorter truck is equivalent to that induced by a longer heavier truck (both trucks have the same vehicle type but different axle spacings).

This conclusion is confirmed by the influence responses examined in chapter 5. The maximum values reached by the representative trucks for vehicle type 14 for Angers can be up to 10% higher than those reached by the trucks (vehicle type 14) for A196 due to the variations in the truck configuration. Consequently, the effect induced by a typical truck from Angers can exceed the effect induced by a typical truck from A196 by as much as 10%, even though both trucks have the same GVW; or, the effect induced by a typical truck from Angers weighing, say, 400 kN, can be as great as the effect induced by a typical truck from A196 whose GVW is 10% higher, i.e., 440 kN.

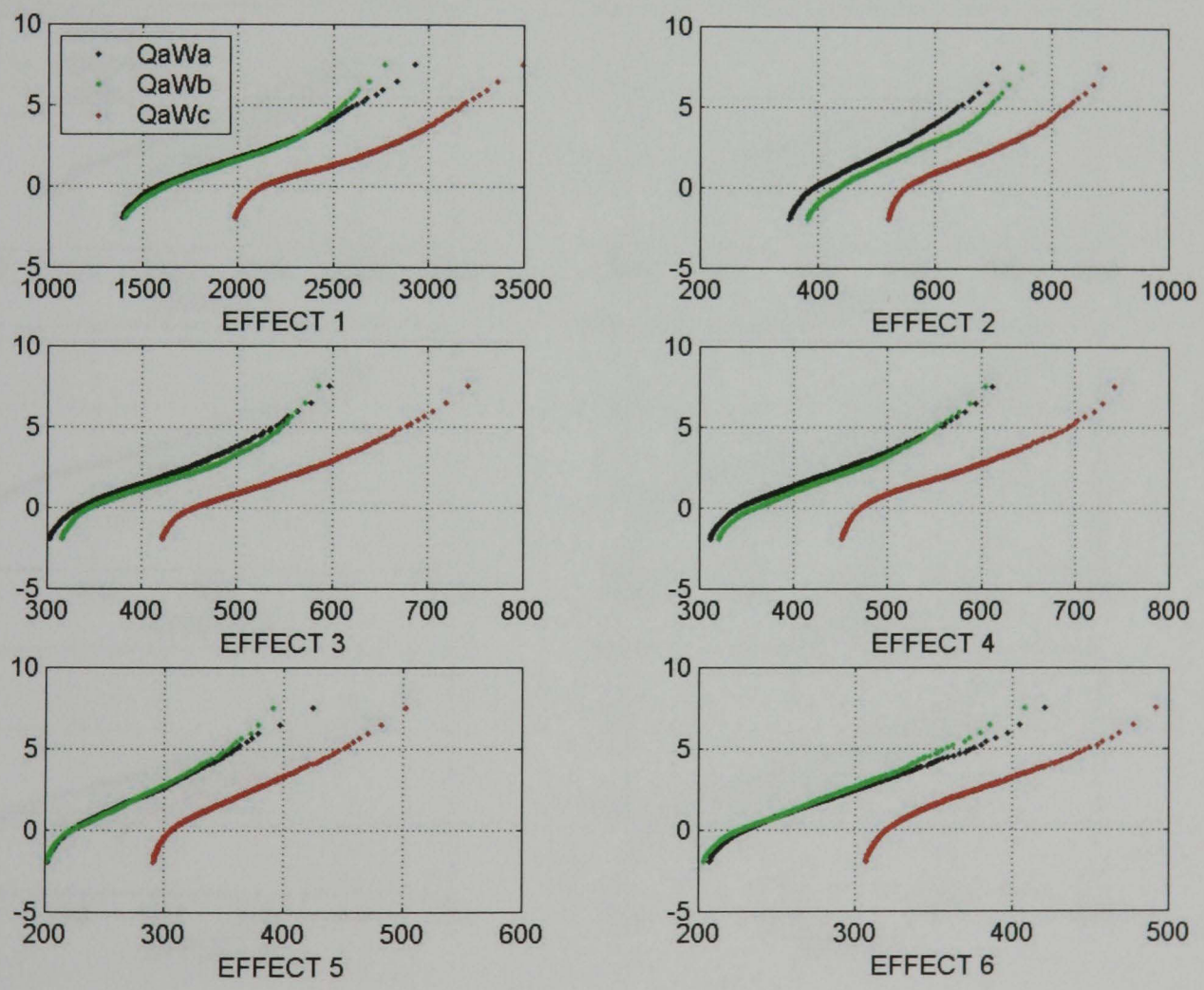

Figure 6-3: Gumbel plots of QaWa, QaWb and QaWc for 20m bridge

This observation is also valid for other bridge lengths (30 and 40m) and for other traffic intensities (*Qb* and *Qc*). As the bridge length increases, variations in the results from traffic *Wa* and traffic *Wb* become more noticeable, although not significant in comparison with

the initial difference in traffic weight. The plots corresponding to the above mentioned traffic types can be found in Appendix G.

The other important point to consider is the influence of the traffic intensity. The same procedure is used: for a given traffic weight, various traffic intensities are plotted together on the same Gumbel plots. Figure 6-4 presents the results for *QaWa*, *QbWa* and *QcWa* for 20m bridges. For each load effect, the same remark can be made: as the traffic intensity increases, the values of the maximum effect induced increase slightly and the range covered between the smallest and highest value decreases. This observation is explained by the simple fact that higher flow rates means higher likelihood of heavy trucks meeting at a critical location on the bridge. Again, the plots corresponding to other bridge lengths and traffic weight confirm these remarks. These plots can be found in Appendix G.

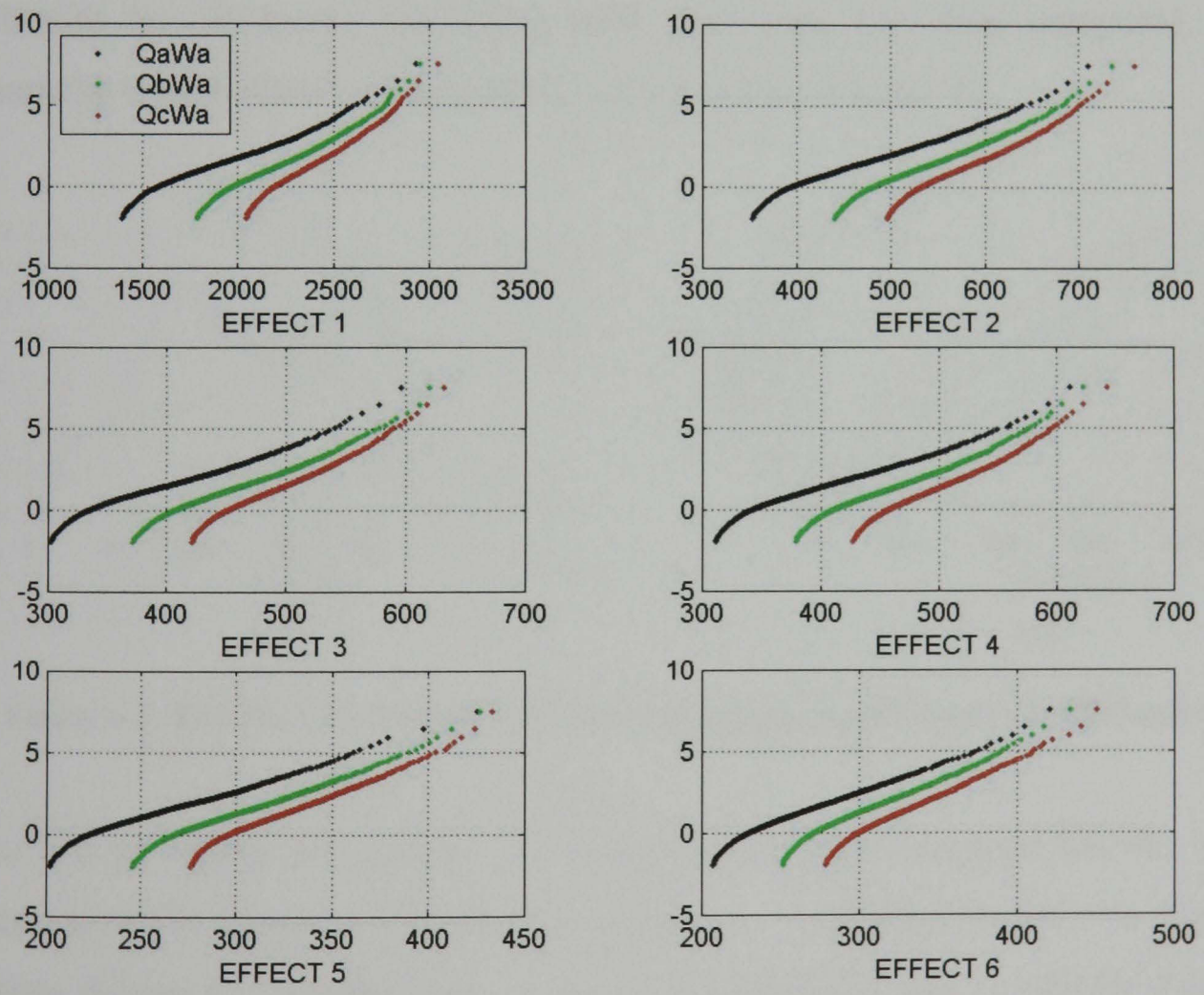

Figure 6-4: Gumbel plots of QaWa, QbWa and QcWa for 20m bridge

In conclusion, it is confirmed that higher values of traffic intensity, or traffic weight, generally means higher values of the effects induced in the bridge. However, the variations in truck geometry between various traffic types can have a significant influence; for example heavier traffic does not always mean higher effects (depending on the geometry

of the trucks). In the following section, a similar analysis is made in terms of extrapolated values.

6.3.3 Extrapolated values: results and comparative study

From the results of these simulations, the maximum values of load effect for each crossing event were obtained, for each bridge length and influence line considered. Extreme value distributions were fitted to the tail of the distribution of maxima; finally, extreme values corresponding to a 1000 years return period were determined.

For the generation of the traffic files, different GVW distributions were employed depending on the direction and class of trucks considered. However, in order to better appreciate the actual weights corresponding to the various traffic types, the GVW distribution for all trucks (including both directions) has been computed. Figure 6-5 presents the weight distributions corresponding to *Wa*, *Wb* and *Wc*.

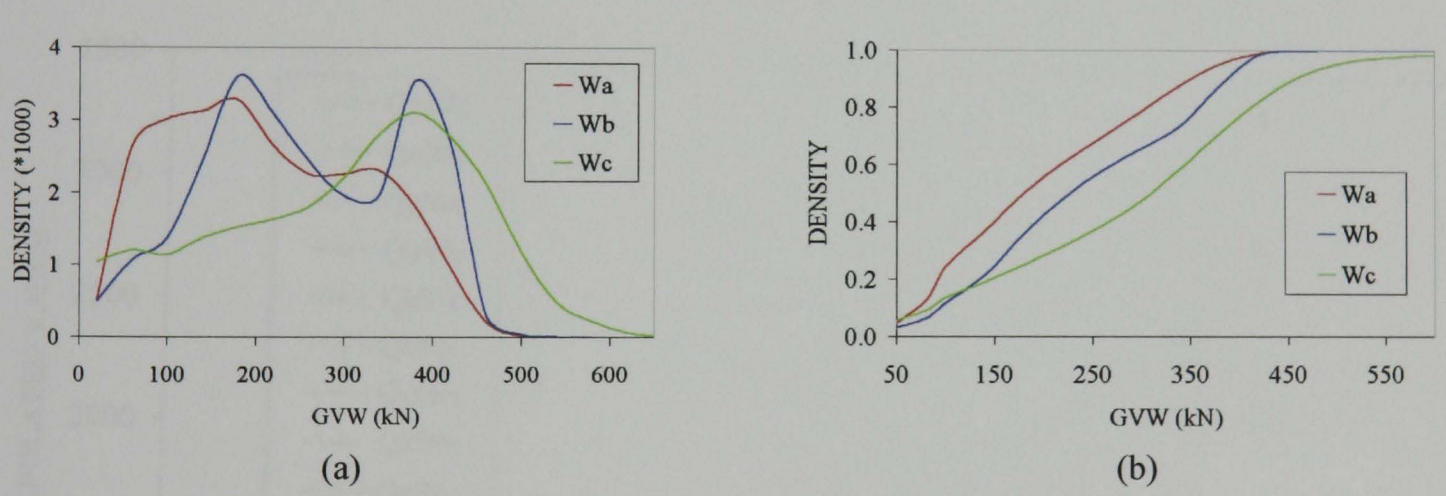

Figure 6-5: Distribution of weights for the bi-directional traffic types: (a) PDF and (b) CDF

Figure 6-6 to Figure 6-9 present the extrapolated values obtained for the various load effects and traffic types considered, as a function of the bridge length. The legend adopted for these figures is the following: a symbol is associated with a specific traffic intensity (circle for *Qa*, triangle for *Qb* and square for *Qc*), and a line style corresponds to a given traffic weight (solid line for *Wa*, dotted line for *Wb* and broken line for *Wc*). Tables containing all the extrapolated values, and ratios between extrapolated corresponding to the different traffic types and bridge lengths, are included in Appendix H, thus making possible a quantitative analysis. The extrapolated results corresponding to load effects 4 and 6 are not illustrated since they are almost identical to those for load effects 3 and 5.

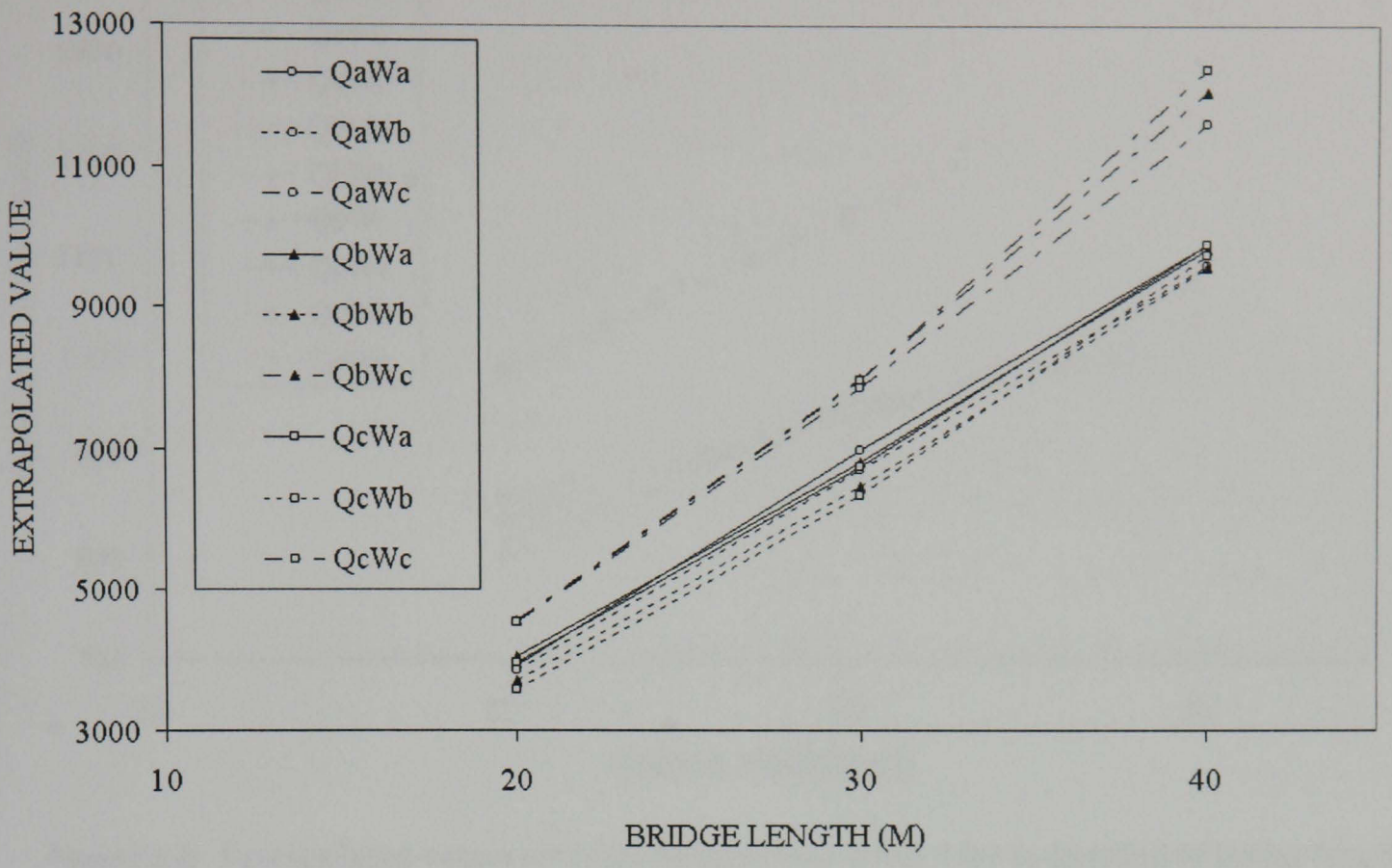

Figure 6-6: Extrapolated values corresponding to load effect 1 for in function of bridge length

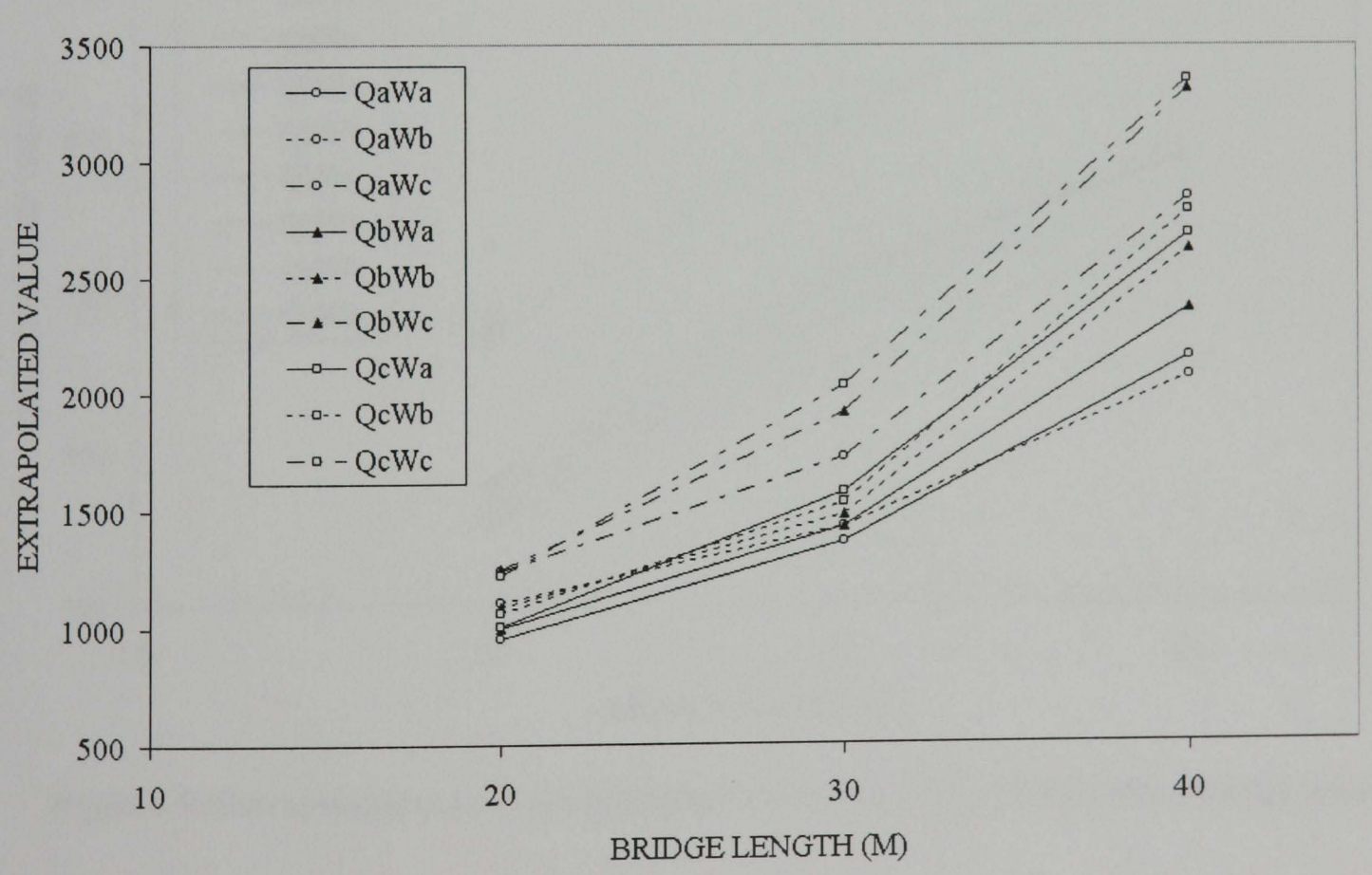

Figure 6-7: Extrapolated values corresponding to load effect 2 for in function of bridge length

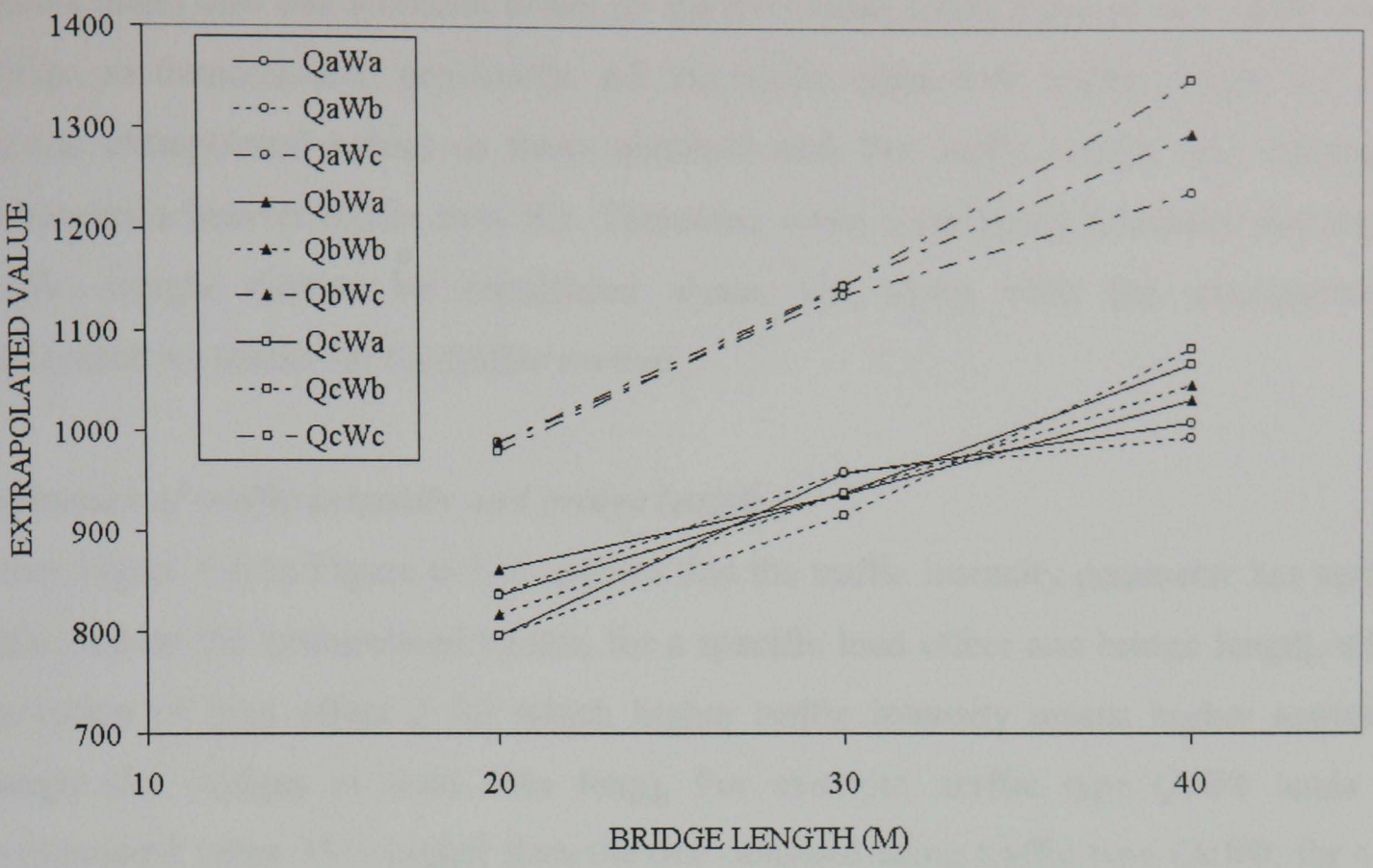

Figure 6-8: Extrapolated values corresponding to load effect 3 for in function of bridge length

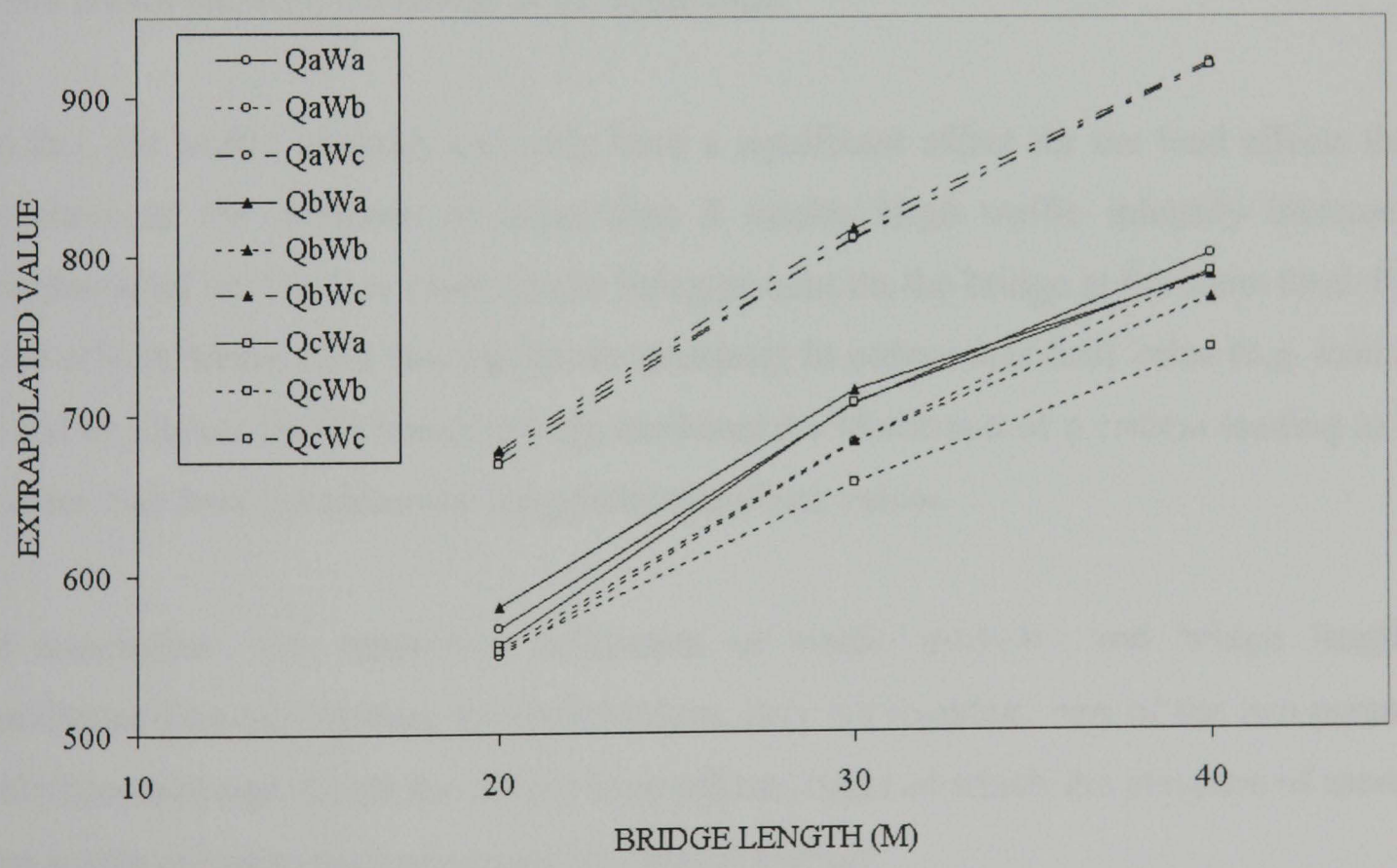

Figure 6-9: Extrapolated values corresponding to load effect 5 for in function of bridge length

Influence of traffic weight

The traffic weight is naturally a very influential parameter when evaluating the severity of a given traffic type in terms of bridge loading. The extrapolated values obtained for *Wc* are, on average, 20% higher than the ones obtained for *Wa* (for a fixed bridge length and given influence line). However, the configuration of the trucks (particularly the heavily

loaded ones) also has a crucial effect on the maximum loads induced in a relatively short bridge, as demonstrated previously. All the traffic types with traffic weight *Wb* lead to similar extrapolated values as those obtained with the traffic weight *Wa*, although *Wb* represents a heavier traffic than *Wa*. Therefore, when considering relatively short bridges, traffic weight cannot be considered alone, but along with the configuration of representative trucks for the traffic studied.

Influence of traffic intensity and bridge length

From Figure 6-6 to Figure 6-9, it appears that the traffic intensity parameter has very little influence on the extrapolated values, for a specific load effect and bridge length, with the exception of load effect 2 for which higher traffic intensity means higher extrapolated values (for bridges at least 30m long). For example, traffic type *QcWb* leads to an extrapolated value 35% higher than the one obtained using traffic type *QaWb*, for a 40 m bridge. This is due to the fact that this load effect is highly sensitive to the presence of 3 or more trucks on the bridge, and higher traffic intensity implies higher likelihood of 3 or more trucks crossing the bridge at the same time.

In fact, the traffic intensity can only have a significant effect for the load effects that are sensitive to the presence of more than 2 trucks. High traffic intensity increases the likelihood of having 3 or more trucks being present on the bridge at the same time. For the load effects where only two trucks are necessary to induce a critical value (e.g. load effect 5 and 6), higher traffic intensity only increases the likelihood of a critical loading to occur sooner, but does not affect the long-term maximum values.

In conclusion, the respective influences of traffic intensity and bridge length are conditioned on one another for such bridges; they act together. Any of the two parameters only becomes significant for certain load effects, those of which the presence of more than two trucks (or more than one truck per lane) is critical.

6.3.4 Frequency of crossing events

A study of the number of crossing events as a function of the traffic flow rates has been performed, based on the results of the full simulations. Indeed, the frequency of crossing events (per event type and per hour) is recorded during the simulations. From the analysis

of these results, it appears that only 50% of all the crossing events correspond to the meeting of two trucks from the two opposing lanes. Most of the remaining crossing events correspond to consecutive trucks in the same lane with no truck in the opposing lane; and finally there are some events involving one truck in one lane and two (or three) trucks in the other lane). The frequency of these latter events increases with the traffic intensity. All the results and details of this analysis can be found in Appendix I.

In addition, a site-specific formula has been derived in order to predict the number of meeting events (two trucks from the two opposing lanes) as a function of the traffic flow rates. This formula has been validated against the measured data and its accuracy assessed. There is a good agreement between the results. It is therefore possible to predict accurately the number of meeting events (if some characteristics of the site are known: average truck length, average speed and hourly flow rates). The development of this formula can also be found in Appendix I.

6.4 ANALYSIS OF THE CRITICAL LOADING EVENTS

Having performed the full simulations for the various traffic types, it is now of interest to consider the particular loading events that induce critical effects in the bridge and eventually determine typical patterns. The analysis of the critical loading events can be done through the detailed examination of the results of the traffic simulations. As mentioned earlier, the results of the simulations are grouped into sets, each of which represents a period of 10 weeks of traffic. Only the critical effects are of interest; for that reason the 20 most critical loading events will be considered, for each bridge length, effect and traffic type. A MATLAB program was used to plot these critical loading events. The visualisation of the results enables typical critical loading events to be derived. For obvious practical reasons, all the plots cannot be included in the body of this chapter; these plots can be found in Appendix J. The configuration of the various critical loading events may vary from one bridge length to another as a function of the influence line shape. Therefore the analysis, in order to be accurate, is done for each bridge length separately.

When considering 20m bridges, there cannot be more than two heavy (hence long) trucks present at the same time, one in each lane of traffic. The important information, knowing that only two trucks are involved, consists of their exact location. Table 6-4 presents the

typical critical loading events for various load effects. In order to visualise the typical events described in this table, the reader is advised to consult Appendix E that contains the figures showing the trucks on the bridge.

Table 6-4: Typical critical loading events for 20m bridges and various load effects

Load Eff.	Influence Line	No of trucks	Location of the trucks
1	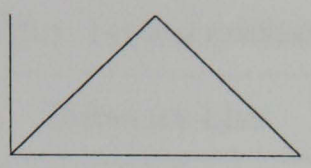	2	Both trucks have 4/5axles and have their 2nd axle or 3rd axle (1st axle of the trailer) near or at mid-span.
2	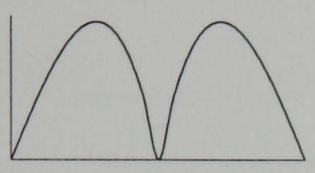	2	Both trucks have 4/5axles and have their front 2 axles on one span (near/at mid-span) and the tandem/tridem on the other (near/at mid-span).
3	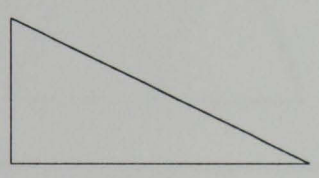	2	Both trucks have 4/5axles and one truck has its last axle at/near the left support while the other one has its 1st/2nd axle at/near the left support.
4	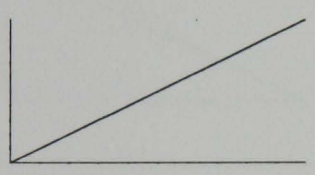	2	Both trucks have 4/5axles and one truck has its last axle at/near the right support while the other one has its 1st/2nd axle at/near the right support.
5	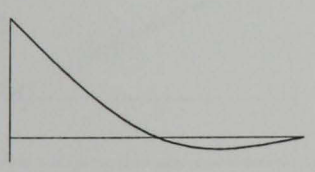	2	Both trucks have 4/5axles and one truck has its last axle at/near the left support (truck fully on the bridge) while the other one has its 2nd/3rd axle at/near the left support (truck partially on the bridge).
6	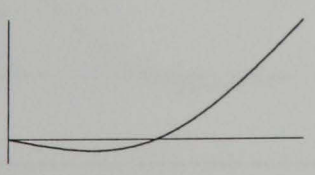	2	Both trucks have 4/5axles and one truck has its last axle at/near the right support (truck fully on the bridge) while the other one has its 2nd/3rd axle at/near the right support (truck partially on the bridge).

Depending on the load effect considered, the trucks are located near/at the centre of the bridge, or near/at the side support. Interestingly, for load effects 5/6, part of one of the two trucks is not present on the bridge; only the group of rear axles is. This is explained by the fact that the zone within which the influence line is substantial is very small. Therefore if the front of the truck is within that critical zone, then the back of the truck is not. The rear axles of truck carrying more weight than the front ones, the rear axles will have to be inside that critical zone.

Table 6-5 contains the details of the critical loading events for 30m bridges and various effects. Contrary to the case of 20m bridges, the bridges are now long enough to carry up to two trucks in each lane. The question is, when there are two trucks located in the same lane, do they induce a combined effect as severe as a single, heavily loaded truck (positioned at a critical location) would? Load effect 2 illustrates that point by presenting some critical loading events consisting of 3 trucks present on the bridge.

Table 6-5: Typical critical loading events for 30m bridges and various load effects

Load Eff.	Influence Line	No of trucks	Location of trucks
1	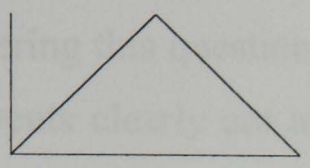	2	Both trucks have 4/5axles and have their 2nd axle or 3rd axle (1st axle of the trailer) near or at mid-span.
2	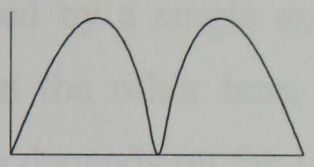	2(/3)	If 2 trucks, both have 4/5 axles and have their front axles on one span and the rear axles on the other; if 3 trucks, the whole trucks are located on one span each.
3	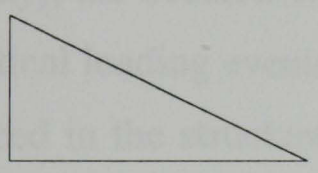	2	Both trucks have 4/5axles and one truck has its last axle at/near the left support while the other one has its 1st/2nd axle at/near the left support.
4	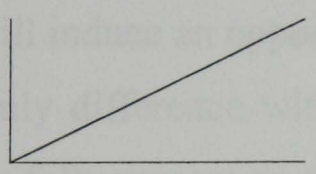	2	Both trucks have 4/5axles and one truck has its last axle at/near the right support while the other one has its 1st/2nd axle at/near the right support.
5	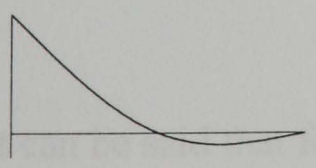	2	Both trucks have 4/5axles and one truck has its last axle at/near the left support (truck fully on the bridge) while the other one has its 2nd/3rd axle at/near the left support (truck partially on the bridge).
6	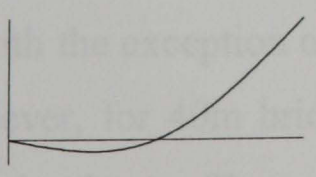	2	Both trucks have 4/5axles and one truck has its last axle at/near the right support (truck fully on the bridge) while the other one has its 2nd/3rd axle at/near the right support (truck partially on the bridge).

The characteristics of the critical loading events are basically the same as those observed for the 20m bridges, with the exception of load effect 2. When considering the influence line for that effect, it can be seen that there is just about enough space for a 4/5-axle truck to be located on one of the two spans. In other words, the occurrence of two consecutive

heavy (but relatively short) trucks is possible, these two trucks being at critical locations on the bridge (i.e. inducing critical effect values). However, if heavy but rather long trucks are present, the other configuration prevails: that is, the front axles on one side of the central support and the rear axles on the other side. It should be noted that 3-truck events are also critical loading events for load effects 3 and 4 if the traffic intensity is very high (e.g. *Qc* in this study).

Finally, the case of 40m bridges can be analysed. There is clearly enough space on the bridge for two trucks to be present simultaneously in either lane. The question is: are these 3-truck events as, or more, critical than the 2-truck ones? Table 6-6 goes some way towards answering this question, for the various effects considered. For load effects 1 to 4, the 3-truck events clearly are as critical as the 2-truck ones. Sometimes two consecutive trucks, with a reasonably heavy GVW, will induce a critical effect in the structure similar to that obtained by a single extremely heavy truck (along with the presence of another heavy truck in the other lane, for both cases). The occurrence of the different critical loading events depends on the traffic intensity; in the case of very high flow rates (such as *Qc* in this study), the occurrence of 3-truck events prevails. However, for load effects 5/6, the typical critical loading events are still made of 2 trucks only; the zone within which the effect is induced in the structure is still small (in comparison of the bridge length). More importantly, the presence of a third truck on the other span (away from the support considered) will induce an opposite effect that will counter-act the presence of the first two trucks. The only difference with the previous bridge lengths considered is that the two trucks are now fully present on the bridge (previously part of one of the two trucks was not present).

In summary, it can be said that for 20 and 30m bridges the critical loading events consist of two trucks (one in each lane of traffic) located at a critical location for the load effect considered (with the exception of load effect 2 on 30m bridge, where 3-truck events can be critical). However, for 40m bridges, the occurrence of 3-truck events become significant for some of the load effects (depending on the shape of their influence line). The occurrence of these events highly depends on the traffic intensity.

Table 6-6: Typical critical loading events for 40m bridges and various load effects

Load Eff.	Influence Line	No of trucks	Location of trucks
1	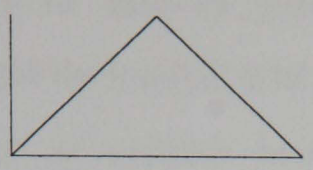	2/3	If two trucks, both trucks have 4 or 5axles and have their 2nd axle or 3rd axle (1st axle of the trailer) near or at mid-span. If three trucks, two trucks closely located one behind the other in one lane, third truck in the other lane near or at mid-span.
2	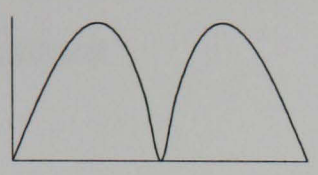	2/3	Independently of the number of trucks, all the trucks are located on span near/at the centre of the span.
3	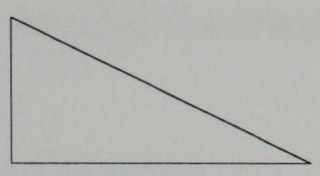	2/3	It 2 trucks, both have 4/5axles and one truck has its last axle at/near the left support while the other one has its 1st axle at/near the left support. If 3 trucks, same configuration with an extra truck just behind one of them.
4	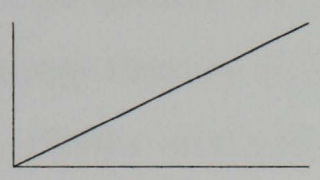	2/3	It 2 trucks, both have 4/5axles and one truck has its last axle at/near the right support while the other one has its 1st axle at/near the right support. If 3 trucks, same configuration with an extra truck just behind one of them.
5	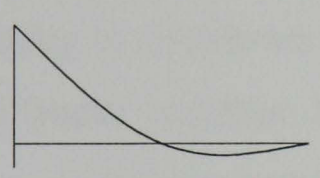	2	Both trucks have 4/5axles and one truck has its last axle at/near the left support (truck fully on the bridge) while the other one has its 1st/2nd axle at/near the left support (truck partially on the bridge).
6	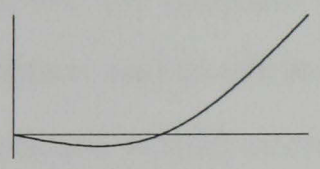	2	Both trucks have 4/5axles and one truck has its last axle at/near the right support (truck fully on the bridge) while the other one has its 1st/2nd axle at/near the right support (truck partially on the bridge).

6.5 DEVELOPMENT OF A SIMPLIFIED MODEL

From the above analysis of the critical loading events for the various load effects and bridge lengths considered, it has been observed that, in the vast majority of cases, there are two heavily loaded 4/5-axle trucks located at a critical location (for the load effect considered) on the bridge. It was therefore decided to attempt to derive a simplified model whose aim would be to reproduce similar loading events from the knowledge of the site specific traffic characteristics without having to generate entire traffic files and perform full traffic simulations. A very important point is that the simplified model is site-specific, that is, one or some of the parameters is directly related to data specific to the site

considered (i.e. traffic intensity and traffic weight). In order to develop this simplified model, two main components are required:

- sets of heavily loaded trucks, which implies a quantitative evaluation of 'heavily loaded' trucks;
- sets of critical locations for the various load effects and bridge lengths considered, which also implies a quantitative evaluation of these 'critical locations'.

6.5.1 Input data for the simplified model

Firstly, the determination of a 'heavily loaded' truck is dealt with. Two possible ways of accounting for the specific weight distribution of a given site are: the consideration of the cumulative density function (CDF) of all the trucks or the CDF of the 4/5-axle trucks only (i.e. the truck classes involved in the critical loading events). The former option can be thought to be more robust than the latter as it easier to consider all the trucks together rather than having to decide on whether to taken into account the 5-axle trucks only or the 4- and 5-axle trucks together. Indeed, depending on the traffic composition of the site, there will be a significant number of 4-axle trucks involved or very few. It is therefore difficult to decide on whether they should be considered or not. Having to consider the traffic composition and to obtain the CDF of GVWs per class before deciding which trucks to take into account would complicate the model. Therefore, in order to keep the model as simple as possible, the cumulative density function of all the trucks (per direction) will be used.

Figure 6-10 presents the cumulative density functions of all the trucks GVW for the three types of traffic weight considered. The variations between traffic types are obvious, and so are the differences between the two directions of traffic for a given traffic type. By selecting a fixed level of the CDF, for example 0.70, the following values of GVW are obtained for direction 1 and 2 respectively: for Qa, 255 and 290 kN; for Qb, 300 and 350 kN; and for Qc, 385 and 425 kN. The differences between traffic types and between directions for a given traffic type are significant: up to 170 kN and 50 kN respectively. These values confirm the necessity of using site-specific values if accurate results are to be obtained.

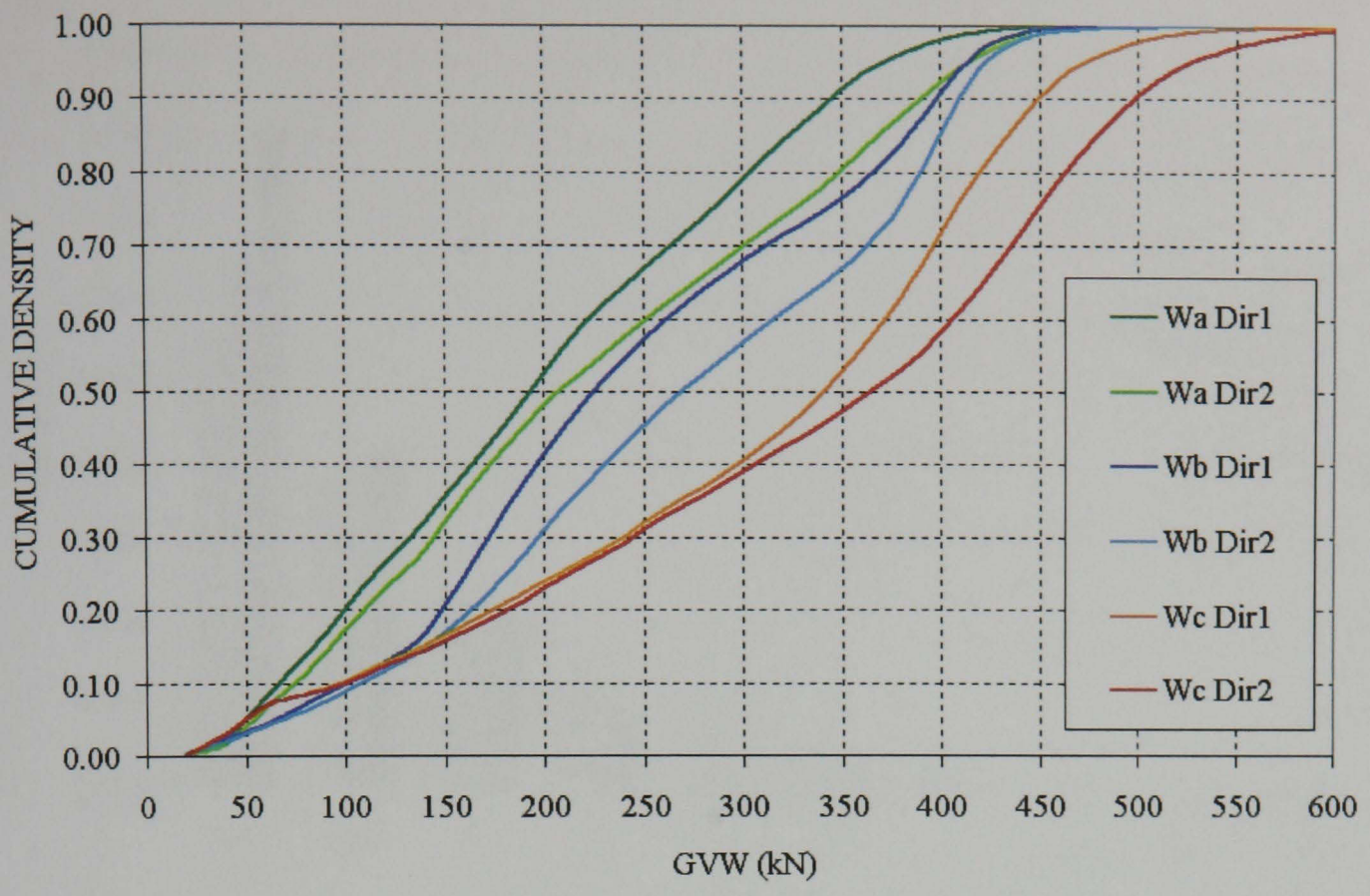

Figure 6-10: Cumulative Density Function of GVW for all the trucks for various traffic types

Sets of GVWs are required. Ideally, the density function of these GVWs should have a decaying tail, in order to reproduce the same trend as the one exhibited by the empirical distribution of GVWs. A simple way of obtaining such GVWs is to use the following formula:

$$GVW_i^{dir} = W^{dir} + DC \times [-\ln(R_i)] \qquad \textbf{Equation 6-1}$$

where W^{dir} is a site-specific constant value, DC (Decay Coefficient) is a constant value and R_i is a uniformly distributed random number ($0 < R_i < 1$). Basically, all the GVW_i^{dir} are higher than a fixed value, W^{dir}, and their PDF presents a decaying tail whose length depends on the value of the decay coefficient, DC. Figure 6-11 exhibits the probability density function corresponding to Equation 6-1 with $W^{dir} = 300kN$ and for various values of decay coefficient. As expected, the length of the tail increases with higher values of decay coefficient.

It should be emphasised that the W^{dir} will be determined in relation to the known CDF of truck weights for the traffic analysed. The idea behind the simplified model being developed is that, after calibration, the CDF level to be considered will be known and thus the determination of W^{dir} will be a simple operation.

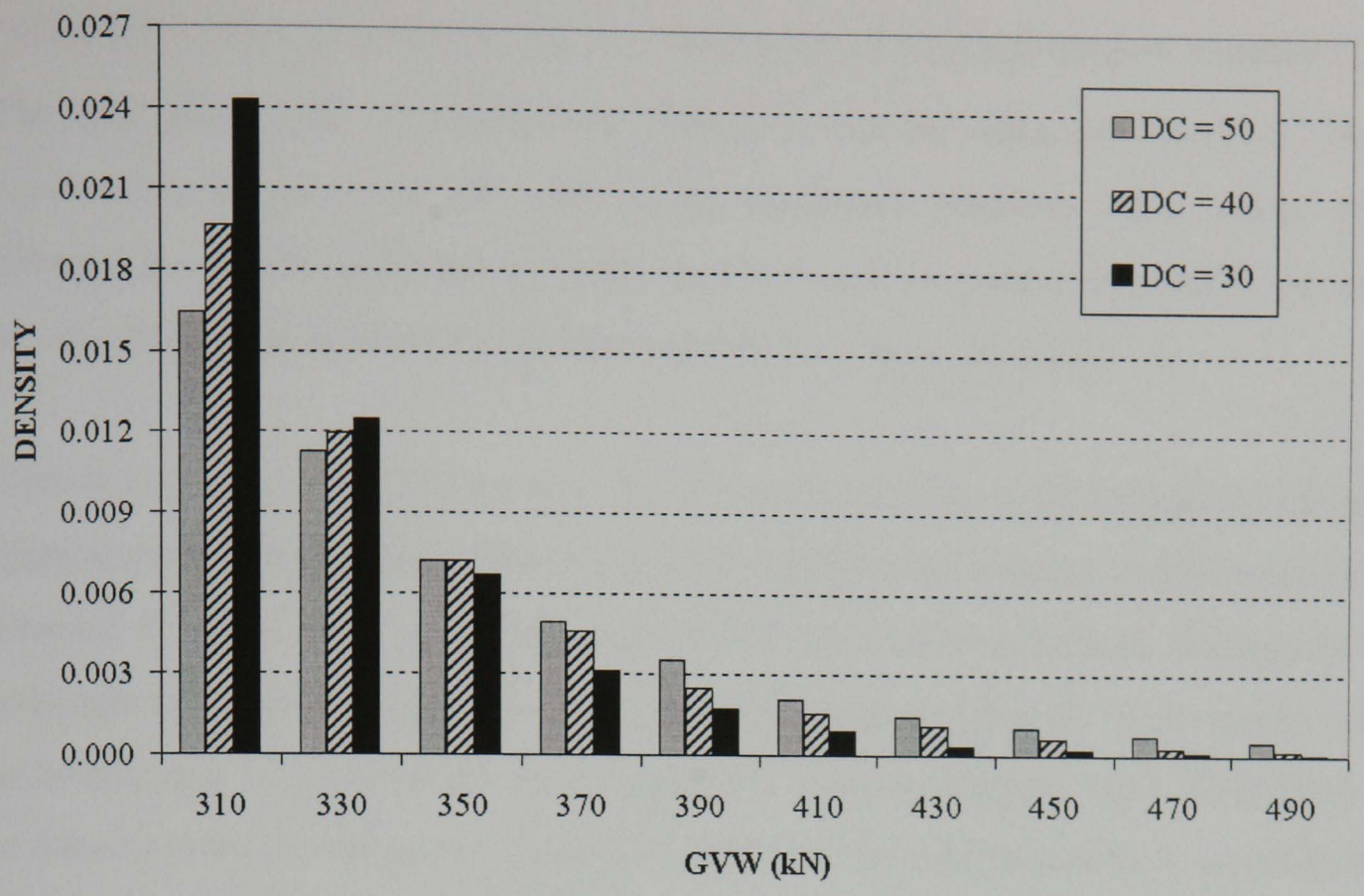

Figure 6-11: PDF of GVWs for different values of decay coefficient (DC) and with W = 300kN

The second step deals with the selection of critical locations for the trucks. As detailed in the previous section, these locations vary with the load effect considered and the bridge type/length considered. It would therefore be tedious to determine physical zones with exact dimensions for each of the load effect and bridge length treated. Indeed, there can be more than one critical zone as the bridge length increases, each zone having a different size (as evidenced by the saw-like shape of some influence responses in Chapter 4). There is a much simpler way of dealing with the critical locations. The meaning of a truck being located at a critical location is simply that this truck will induce a high effect, close to the maximum possible value that could be induced by that particular truck. Thus it is equivalent to expressing the presence of a truck at a critical location by saying that the truck induces an effect whose value is near its maximum possible value (e.g. between 80% and 100% of the maximum possible value). This way, there is no need to determine actual zones in which the trucks have to be located; it can simply be said that the truck induces an effect of X%.

The percentages can be generated as follows:

$$Perc_i = PercMin + (PercMax - PercMin) * R_i \qquad \textbf{Equation 6-2}$$

where *PercMin* and *PercMax* are the lower and upper bound of the effect (as % of maximum possible value) and R_i is a uniformly distributed random number ($0 < R_i < 1$). The two parameters *PercMin* and *PercMax* can be adjusted; however, *PercMax* is expected to be taken as 100, that is the maximum possible value, while *PercMin* is between 0 and 100, although *PercMin* really should be greater than 60/70 (an effect equal to, say, 50% of its maximum possible value is not really 'critical').

Considering the above idea in more detail, attention needs to be brought to the meaning of 'maximum possible value'. Obviously, every single truck induces a difference response. In Chapter 4, typical responses for given vehicle types were examined. It could be seen that, although the responses vary as a function of the axle weights (in % of weight carried) and axle spacings, the variations were small for a given vehicle type. Therefore a unique maximum possible value can be derived based on the configuration of a typical truck. This maximum possible value will thus be an average value, representative of all the 5-axle trucks. The configuration of the typical truck is based on the modelling of the vehicles described in chapter 4. The typical truck is naturally chosen as a 5-axle truck, vehicle type 14, as it is the one predominantly observed in the critical loading events.

The effect induced by any pair of trucks (i.e. any critical loading event), in the simplified model, can be calculated by:

$$Effect_i = \sum_{dir=1}^{2} GVW_i^{dir} * Perc_i^{dir} * MaxIR^{dir} \qquad \textbf{Equation 6-3}$$

where $MaxIR^{dir}$ is the maximum value of the influence response induced by the typical truck described above.

6.5.2 Simplified Model calibration

Knowing how to generate the two main components of the model, it is now time to calibrate the model; that is to determine a set of values for the parameters of the model to match the effects obtained using the full-scale simulations. There are mainly three parameters to evaluate, as follows:

- W^{dir}, (in terms of level of the CDF);

- the decay coefficient (DC);
- the percentages defining the critical zone: lower bound ($0 < PercMin < 100$) and upper bound (typically set equal to 100 - i.e., maximum possible value).

A MATLAB program was developed by the author in order to calculate the effects using the simplified model and to plot the results against the actual results of the full-scale simulations (referred to as measured effects). The input data required for the program are: the characteristics of the typical 5-axle trucks (axle spacings and axle weights) for the different traffic types so that the maximum influence response can be calculated; and the CDF data for the different traffic weights. Figure 6-12 shows the main steps of the program SIMPLIFIEDMODEL, which generates 1000 pairs of truck GVWs and truck locations (in terms of %) and calculate the effects induced by this 1000 pairs of trucks. The generation of effects using the simplified model is repeated 10 times to obtain a set of average values in a similar manner as the one adopted earlier.

After a number of trials with different sets of values for the various parameters, typical values were obtained in order to reach good agreement between measured effects and modelled effects. The main idea behind the calibration was that this simplified model had to be sufficiently robust so that one set of values for the model parameters would give accurate results for the different traffic types. The two main parameters to adjust were: the CDF level and the percentages for the lower/upper bounds of the critical zone. Indeed, it was found that the decay coefficient varies as a function of the CDF level; a result that could have been anticipated as the GVWs have to remain in a certain range, if the CDF level increases, then the decay coefficient has to be decreased.

It was also observed that the CDF level follows from,the traffic intensity. Indeed, as the flow rates increase, so does the likelihood of two heavy trucks crossing the bridge at the same time. The CDF level is the parameter that make the model site-specific, as it means to take the values of W^{dir} directly from the CDF. The other parameter, the lower bound of the percentage of the critical zone, is the one that allows the model to be adjusted to the sensitivity of the load effect considered. As observed in a previous section, the critical loading events exhibit differences as a function of the load effect considered (proportion of the truck present on the bridge, size of the critical zone, etc.). Appropriate values for the various parameters are presented in Table 6-7 and Table 6-8.

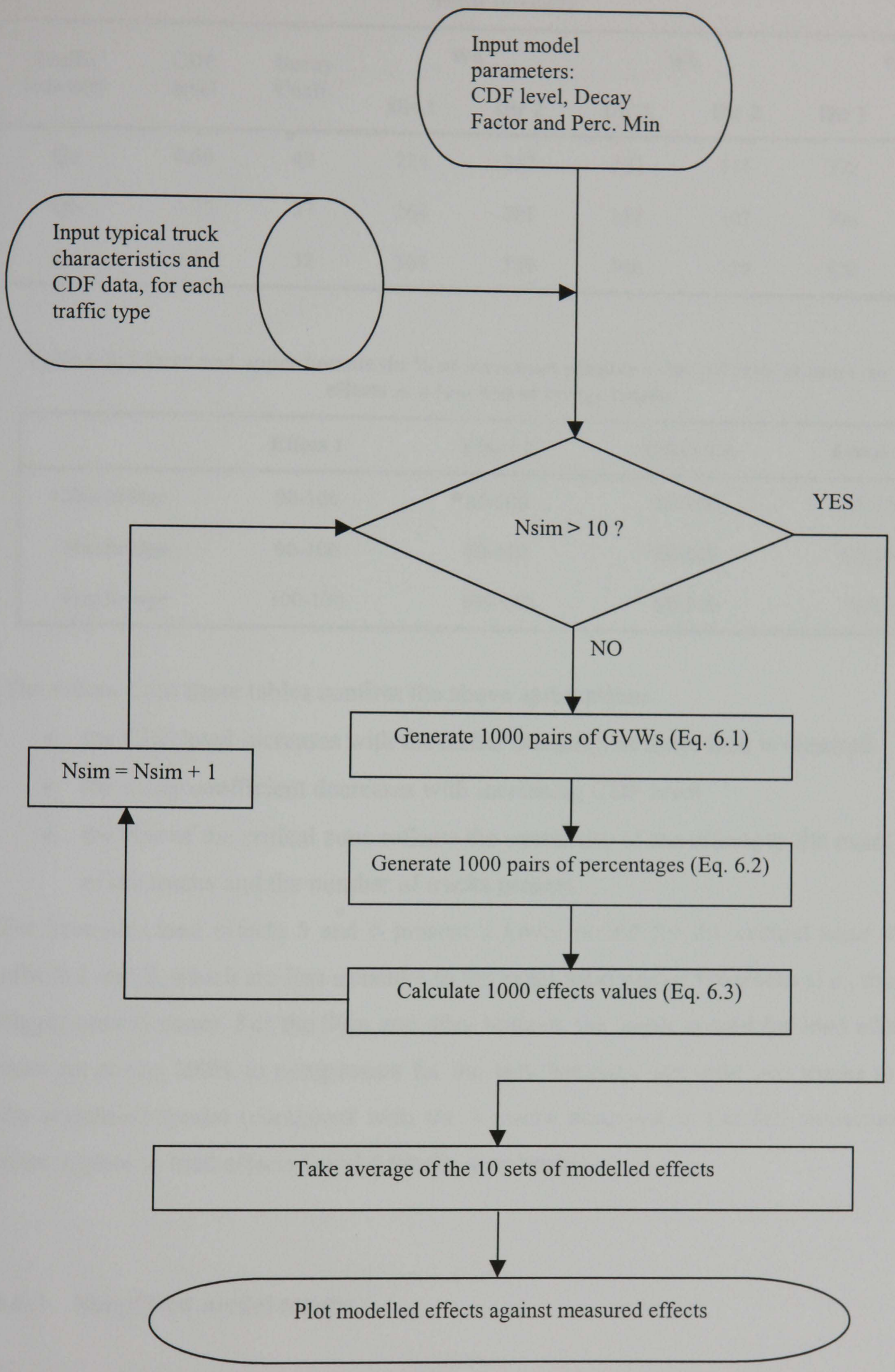

Figure 6-12: Flow chart of the Simplified Model program in MATLAB

Table 6-7: CDF levels, Decay Coefficient (kN) and W^{dir} (kN) for various traffic weights as a function of traffic intensity

Traffic Intensity	CDF level	Decay Coeff.	Wa		Wb		Wc	
			Dir 1	Dir 2	Dir 1	Dir 2	Dir 1	Dir 2
Qa	0.60	42	224	252	262	316	372	406
Qb	0.70	37	264	301	312	362	396	436
Qc	0.80	32	304	349	366	389	420	463

Table 6-8: Lower and upper bounds (in % of maximum possible value) of critical zones for various effects as a function of bridge length

	Effect 1	Effect 2	Effect 3/4	Effect 5/6
20m bridge	90-100	80-100	80-100	75-100
30m bridge	90-100	90-110	80-100	75-100
40m bridge	100-100	100-140	90-110	75-100

The values from these tables confirm the above assumptions:

- the CDF level increases with the traffic intensity, as more load is required
- the decay coefficient decreases with increasing CDF level
- the size of the critical zone reflects the sensitivity of the effects to the exact location of the trucks and the number of trucks present.

For example, load effects 5 and 6 present a lower bound for the critical zone than load effects 1 and 2, which are less sensitive to the exact locations of the trucks (i.e., they have a bigger critical zone). For the 30m and 40m bridges, the upper bound for load effect 2 has been set above 100% to compensate for the fact that there are only two trucks present in the simplified model (compared with the 3 trucks observed in the full simulations); the same applies to load effects 3 and 4 for the 40m bridge.

6.5.3 Simplified model results

Figure 6-13 presents the results of the simplified model for 20m bridges, corresponding to traffic type *QaWa*. The simplified model leads to results that are in good agreement with the measured values for all the load effects considered. The results for 30 and 40m bridges are similar to the ones presented in Figure 6-13, for traffic type *QaWa*. For traffic type *QaWb* and *QaWc*, good agreement is also observed (the plots can be found in Appendix

L). For the other traffic types, the results from the simplified model present a very good approximation to the measured results too (see Appendix K), using the same critical zones but higher CDF levels (to allow for the increase in traffic intensity, and therefore in critical GVWs).

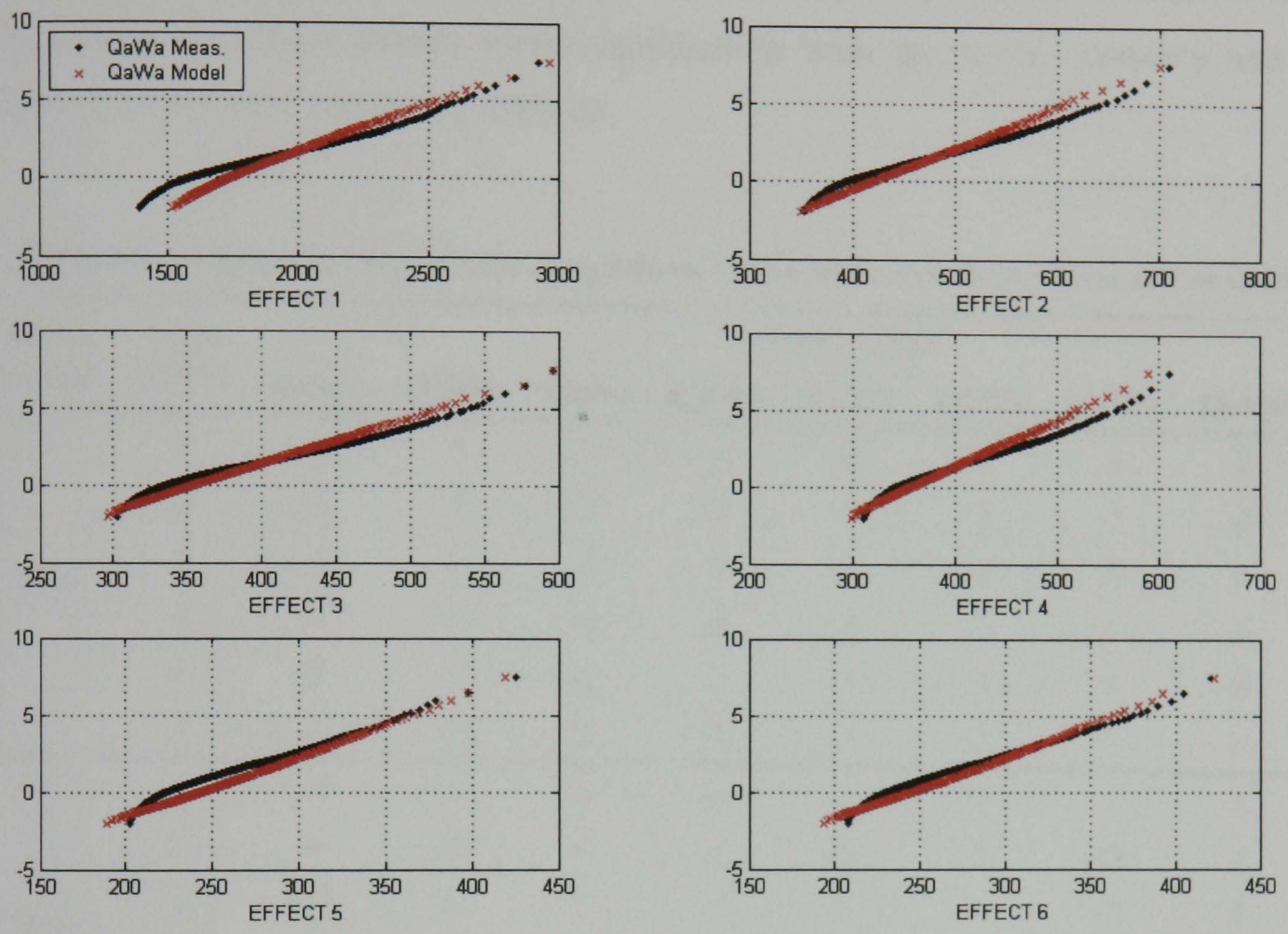

Figure 6-13: Measured results versus model results for 20m bridge, traffic type QaWa

However, good visual agreement is not sufficient to assess the actual accuracy and robustness of the model. Consequently extrapolated values were calculated based upon the measured effects and the modelled effects. Table 6-9 presents the differences (in %) between the extrapolated values calculated for both cases.

First, the results for the 20m bridges are considered. The differences observed vary between –9% and +5%, which shows a good agreement for the 9 traffic types and 6 load effects considered. For the 30m bridges, higher variations appear (i.e. between ±14%); however, all these higher values correspond to load effect 2. Indeed, as a function of the traffic intensity, there can only be only a few (e.g. traffic intensity *Qa*) or a great number (e.g. traffic intensity *Qc*) of 3-truck events; it is thus impossible to model accurately both cases (2-truck and 3-truck events). Also, depending on the configuration of the representative truck (length and weight distribution) for the traffic considered, the severity

of the 3-truck events varies, which explains the important differences observed between traffic types for the same load effect (i.e., load effect 2). However, for all the other load effects and traffic types, the variations are always between –10% and+4% for the 30m bridges. Again, these values illustrate a good agreement. Finally, the results for the 40m bridges reveal a good agreement too, with differences between ±10%, with the exception of load effect 2. For that load effect, the same phenomenon as described above occurs: the frequency of 3-truck events varies significantly with the traffic intensity and therefore renders an accurate modelling difficult.

Table 6-9: Differences (%) between extrapolated values from measured effects and modelled effects

Bridge Lenght	Load Effect	Traffic Type								
		QaWa	QaWb	QaWc	QbWa	QbWb	QbWc	QcWa	QcWb	QcWc
20m	1	-5	-7	2	-5	-2	-3	-1	2	-4
	2	-1	-9	-7	-7	-5	-7	-5	-2	-5
	3	-2	-2	-2	-7	0	-3	-3	5	-4
	4	-7	-6	-6	-6	-1	-5	1	2	-4
	5	2	-3	-1	1	-4	-3	4	0	-2
	6	-5	-4	-2	-2	-2	-4	0	-1	-4
30m	1	-10	-5	2	-3	2	-2	-2	5	-3
	2	0	**14**	4	-3	**11**	-8	**-11**	8	**-14**
	3	-10	-3	-5	-5	1	-4	-2	4	-5
	4	-5	-3	-4	-5	0	-6	-6	2	-8
	5	-3	-8	0	-7	-5	-2	-3	2	-3
	6	-8	-6	0	-6	-3	-2	-2	0	-4
40m	1	-3	6	2	-2	5	-3	0	4	-7
	2	10	**16**	3	3	-7	**-12**	-8	**-13**	**-11**
	3	-1	10	3	0	5	-2	-2	3	-9
	4	-3	4	3	0	3	-4	0	0	-9
	5	-10	-7	-4	-5	-3	-3	-2	0	-2
	6	-9	-8	-3	1	-2	-4	-3	2	-4

Overall, all the values are within between –14% and +16%, a figure that confirms the good agreement found by visual inspection; in addition, 85% of the values are within ±10%. In fact, if load effect 2 is considered apart from the other load effects, the agreement is very good, as the differences never exceed ±10%. In addition, the higher variations observed for load effect 2 are explained by the nature of the critical loading events, which changes as a function of the traffic intensity. However, the author believes that the model could be improved by introducing some modifications; for example, by accounting for the traffic

intensity in the determination of the critical zones, and not only on the shape of the influence line. On the other hand, any modification introduced is likely to complicate the model. Therefore, depending on the main objective of the model, a balance must be struck between accuracy, simplicity and robustness.

6.6 OVERVIEW AND CONCLUSIONS

The work described in this chapter concentrated on the detailed analysis of bi-directional traffic loading on relatively short bridges. The study was limited to bridges 20 to 40m long with two opposing lanes of traffic. A number of traffic data files corresponding to 9 traffic types (i.e. different traffic weight and intensity) have been generated and full simulations have been performed for all these traffic files. From the results of these simulations, typical critical loading events have been derived for each bridge length considered. In a second part, a site-specific simplified model has been developed in order to reproduce these critical loading events without having to perform full simulations. The model requires a knowledge of some site-specific data such as: the cumulative density function of truck weights, per direction, and the configuration of a representative truck for the critical loading events (typically a 5-axle truck, of tractor-trailer type).

In essence, the simplified model generates pairs of heavy trucks and places them at a critical location for the load effect and bridge length considered. The model has been calibrated against the results of the full simulations for the 9 traffic types studied by plotting the modelled effects versus the measured effects on Gumbel probability paper. Afterwards, the validation of the model has been achieved by comparing the extrapolated values obtained using the results from the full simulations and from the simplified model. The differences observed between the extrapolated values (corresponding to 1000 year return period) are reasonably small and demonstrate the validity and the accuracy of the model. Furthermore, the good agreement observed for the various traffic types shows the robustness of the simplified model. Finally, the relative inaccuracy observed for one of the load effects can be explained and could be reduced by modifying the model, which, however, would be more complex.

Chapter 7

UNIDIRECTIONAL TRAFFIC ANALYSIS AND MODELLING

Chapter 7 UNIDIRECTIONAL TRAFFIC ANALYSIS AND MODELLING

7.1 INTRODUCTION AND TERMINOLOGY

In the preceding chapter, the case of bridges carrying two lanes of bi-directional traffic was studied; however, this is not the only type of carriageway. Also very common are bridges for dual carriageways, which carry two or more lanes of traffic in the same direction. Their analysis requires special attention, as the lanes of traffic are not independent from one another: the presence of a vehicle in a certain lane is highly conditioned on the presence of another vehicle in the adjacent lane. This chapter concentrates on the study of short to medium span bridges (20 to 40m long) with two lanes of unidirectional traffic. In a first part, the traffic data used in this study is described and modelled for later use. Full simulations are then performed for a number of traffic files and typical critical loading events are derived. From there, a site-specific simplified model is developed; its aim is to reproduce accurately these critical events without having to perform full simulations. Based on the somewhat unsatisfactory results of this simplified model, further developments are implemented in order to improve on the accuracy and the simplicity of the initial model.

Throughout this chapter two unidirectional traffic lanes (i.e. two parallel lanes of flow in one direction) are considered. In order to simplify the notation, the lanes will be referred as the *slow lane* (i.e., the outside lane – containing most of the truck traffic) and the *fast lane* (i.e., the inside lane – normally used for overtaking). Therefore the truck travelling in the slow lane will be referred to as the *slow truck* while the truck travelling in the *fast lane* will be called the *fast truck*. In the same manner, any characteristic referring to the truck present in the slow (or fast) lane can be referred as *slow* (or *fast*) (e.g. 'Distribution of slow speeds means the distribution of speeds corresponding to the trucks in the slow lane). In this chapter the word "headway" has a different meaning than the commonly accepted one. Herein it always means the distance between the front axle of the fast truck and the front axle of the closest truck in the slow lane (see Figure 7-1).

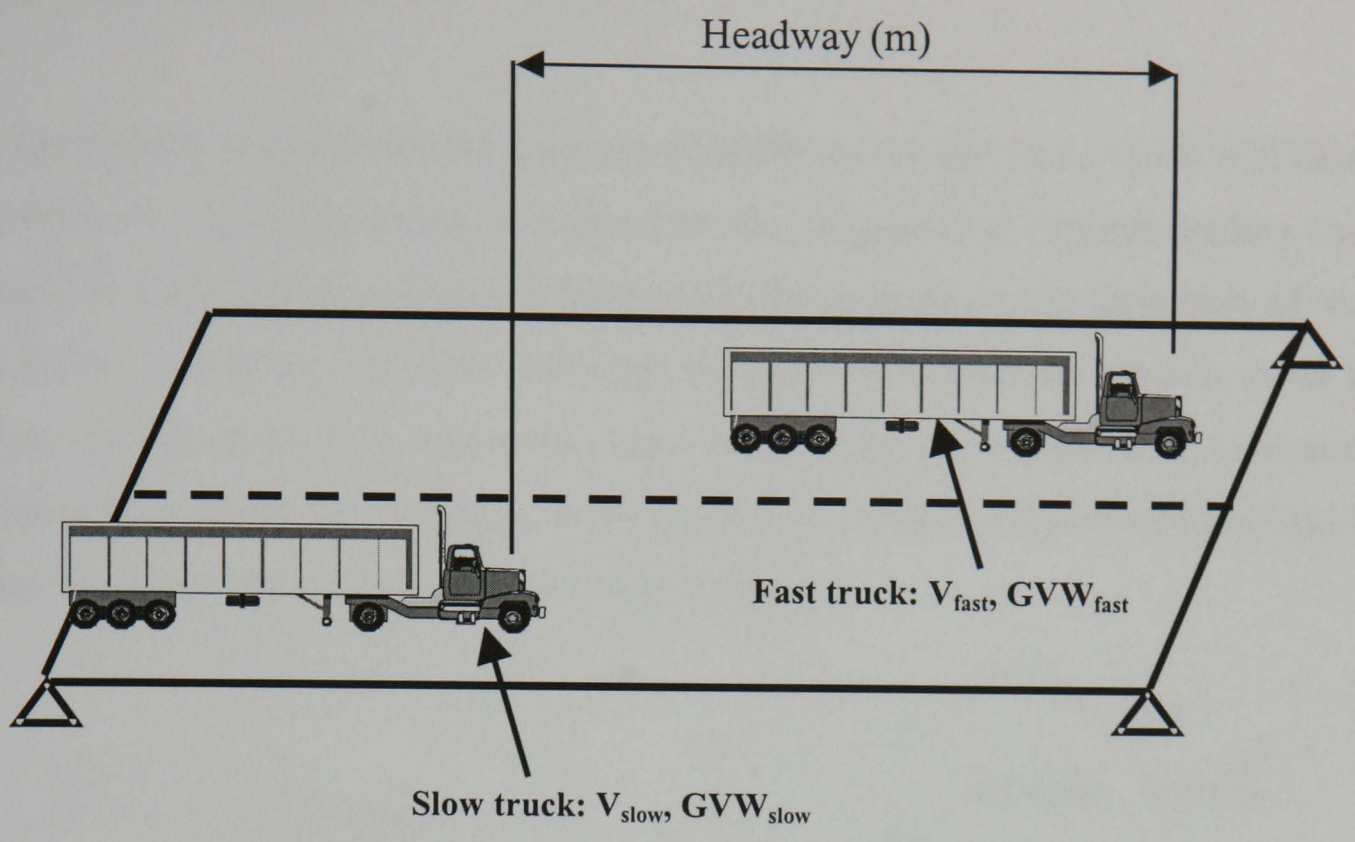

Figure 7-1: Typical overtaking event

7.2 TRAFFIC DESCRIPTION AND MODELLING

7.2.1 Traffic intensity

The first important traffic characteristic to be considered is the traffic intensity as it will determine the frequency of overtaking events. The hourly flow rates of trucks have been calculated over the week of traffic recorded for both directions; the representative values are obtained by averaging the values of flow rates for the 5 working days of the week (for each hour of the day separately). The weekend days were not included in the calculations because they were not representative of normal traffic in terms of composition and weights. Figure 7-2 shows the average hourly flow rates for the A196 for both directions. Although the overall volume of traffic is similar (~36 000 trucks in direction 1 and ~32 200 trucks in direction 2), the characteristics are different from one direction to another. Direction 1 shows fluctuations in traffic volume depending on the hour of the day: the lowest flow rates occurring in the early part of the morning (from 12am to 3am) while the highest values are reached at mid-day and in the late afternoon, the flow rates being 3 times higher than the lowest ones (450 trucks/hour against 150 trucks/hour). Direction 2

indicates a more consistent volume throughout the day. Apart from a low volume of traffic between 11pm and 5am, the hourly flow rates appear to be oscillating slightly around the value of 300 trucks/hour.

The second point of interest is the intensity of traffic in the fast lane, which will determine the number of overtaking events and therefore the frequency of critical loading cases (as explained in a later section). Figure 7-2 represent the average hourly flow rates of trucks in the slow lane and in the fast lane. Although the order of magnitude is much lower for the fast lane, the fast flow rates follow the same trend as the slow flow rates, increasing and decreasing throughout the day in the same manner. A relationship between total flow rates and fast flow rates will be examined in a later section.

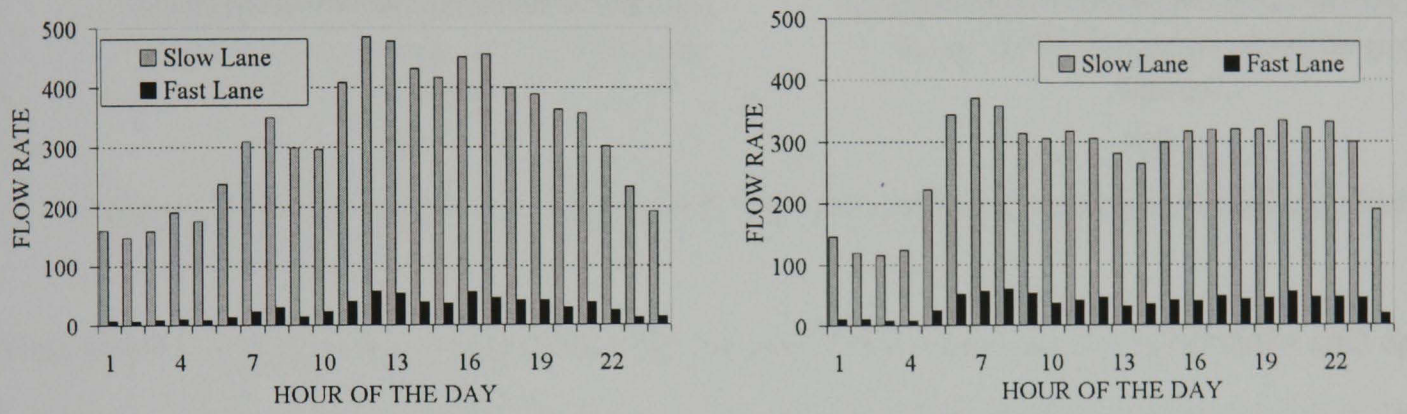

Figure 7-2: Average hourly flow rates of trucks per lane on the A1-1996: (a) direction 1 and (b) direction 2

7.2.2 Traffic weights

The probability density functions of all the gross vehicle weights for both directions were presented in Chapter 4. Both PDF's can be fitted by multi-modal normal distributions; both present two main peaks. The traffic was observed to be significantly heavier in direction 2. The histograms of GVW's for the different categories of truck (from 2-axle trucks to 5-axle trucks) were also presented in Chapter 4. Clearly the gross vehicle weight increases with the number of axles. An important difference is observed: the 5-axle trucks are significantly more heavily loaded than the 4-axle trucks (although the great majority of them consist of the same vehicle type, the tractor/trailer type). Therefore the tail of the gross vehicle weight distribution will mostly consist of 5-axle trucks.

In the case of parallel lanes of traffic, it is of interest to consider the distribution of truck GVW's per lane. Figure 7-3 presents the histograms of GVWs for the slow lane and for the fast lane separately. Both distributions have the same overall characteristics: bi-modal distribution with the same mean for the two modes, but different proportion for each mode from one distribution to the other. The slow lane distribution has a more pronounced second mode while the passing lane distribution has a higher first mode. Clearly, the lighter trucks overtake the heavier trucks.

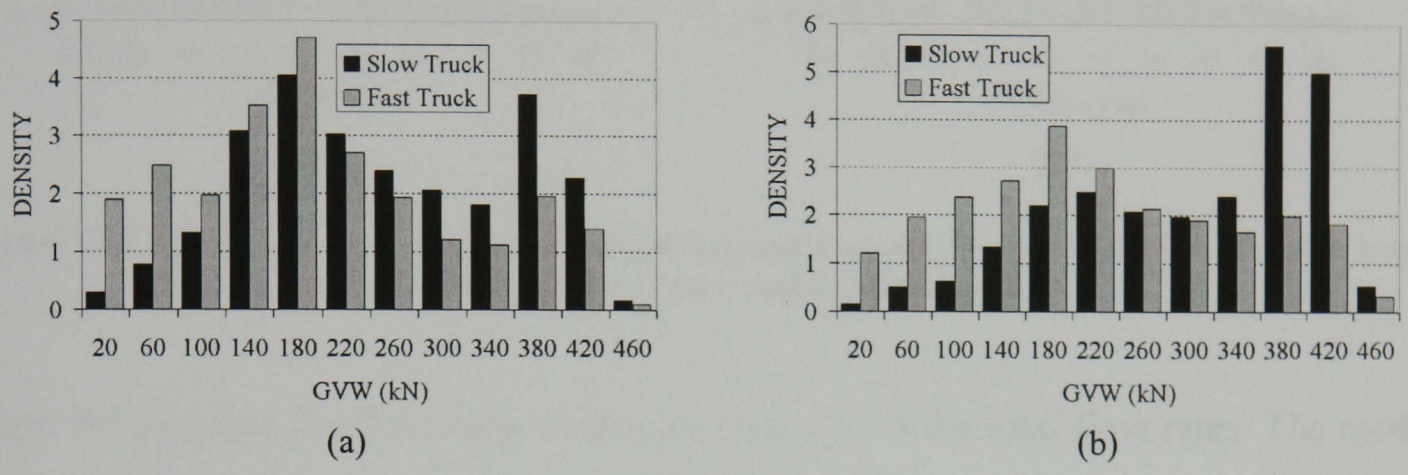

Figure 7-3: PDF of GVW's of trucks per lane on the A196: (a) direction 1 and (b) direction 2

Nonetheless the second mode of the fast lane distribution is quite significant and represents heavy trucks overtaking light (or heavy) trucks, the latter events inducing the most critical loading cases. Both directions have similar characteristics, with direction 2 showing the more noticeable variation between the two distributions (i.e., the two lanes).

7.2.3 Frequency of overtaking events

In Chapter 6 (i.e., for two opposing lanes of traffic), the governing loading cases for most of the load effects were proven to be two trucks beside or close to each other for relatively short bridges. In the case of unidirectional traffic, the lanes of traffic are not independent and the presence of a truck in the passing lane is due to the presence of another vehicle in the slow lane. In order to check that hypothesis in the measured traffic file A196, the distribution of headway (i.e., the distance between the front axle of any truck in the passing lane and the front axle of the closest truck in the slow lane) was derived.

Figure 7-4 shows that the majority of the trucks in the passing lane are within 30 m of a truck in the slow lane, which shows that they are passing (or have passed) that truck. Therefore it is a reasonable to assume that the number of overtaking events is directly

related to the number of trucks in the passing lane. Hence a relationship between the flow rates in the passing lane and the total flow rates was sought, in order to estimate the number of overtaking events.

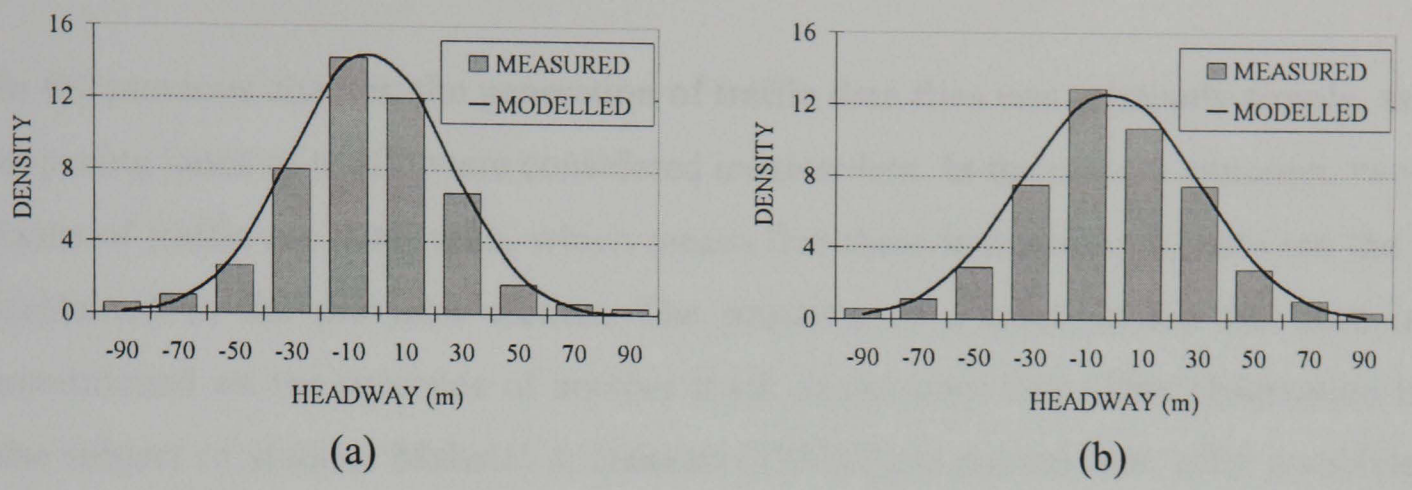

Figure 7-4: PDF of headway between passing truck and closest slow lane truck for direction 1 on the A196: (a) direction 1 and (b) direction 2

Figure 7-5 presents the flow rates of the fast lane versus the total flow rates. The modelled data correspond to the curve that was fitted to the measured data using the least squares technique. The curve used has an equation of the form:

$$Y = a\,X^{b}$$

Equation 7-1

Different values for the parameters *a* and *b* are obtained for the two directions of traffic.

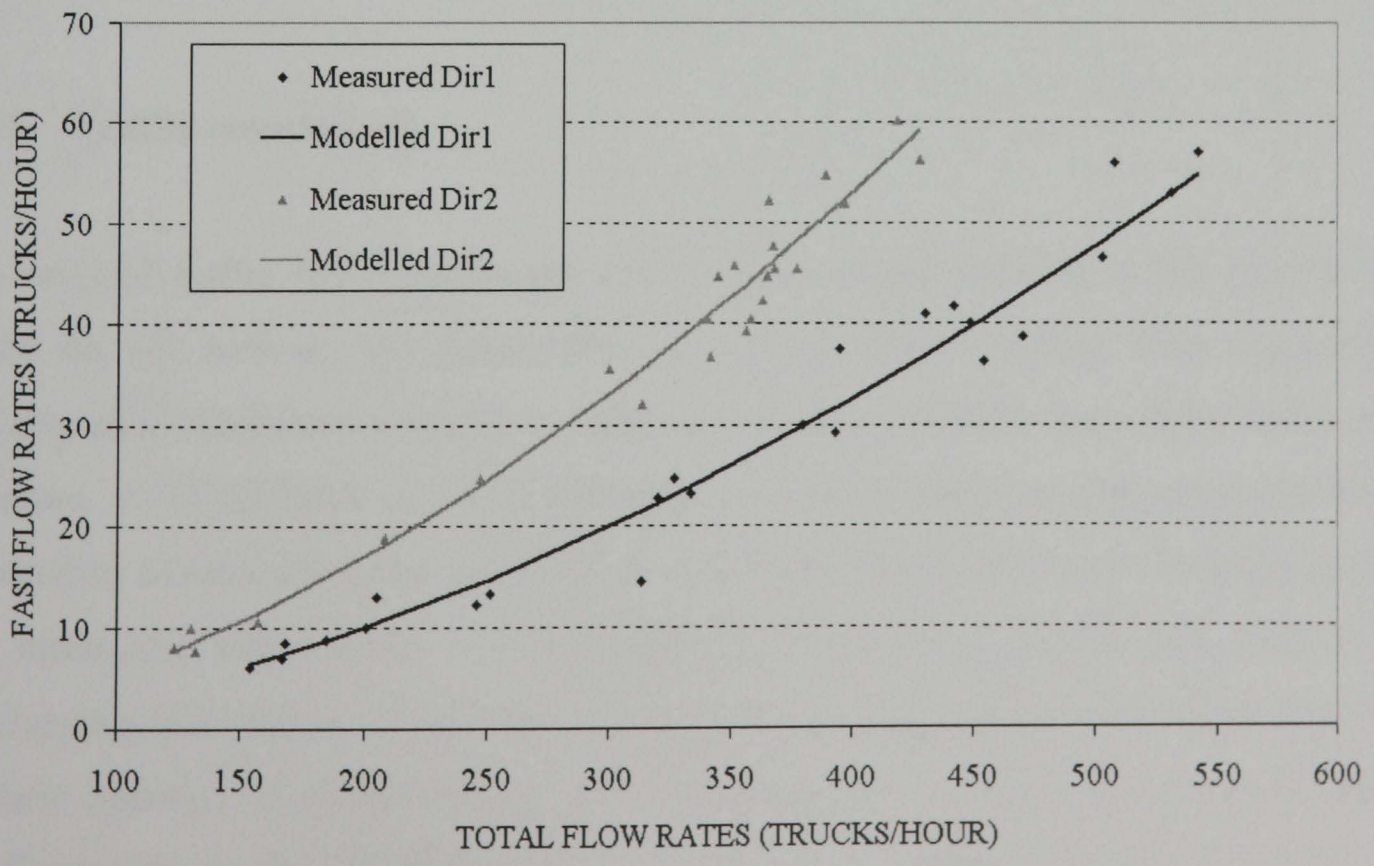

Figure 7-5: Fast Flow Rates against Total Flow Rates for direction 1 on the A196

7.3 TRAFFIC SIMULATIONS

7.3.1 Introduction

In the previous chapter, the generation of traffic data files was relatively simple, as the two opposing lanes of traffic were considered independent. In the present situation, two parallel lanes of traffic are dealt with, which means that there is dependence between the lanes as explained in the previous section. The presence of a truck in the fast lane is highly conditioned on the presence of another truck in the slow lane. This observation has been the subject of studies: Mahalel & Hakkert (1982) have proven that 'after a vehicle arrives in a certain lane, the tendency for the next vehicle to appear in the adjacent lane is greater than the unconditional probability for such a vehicle in that lane'. Models using Markov chains (Rorbech 1976, Mahalel & Hakkert 1982) can be used to generate unidirectional traffic where dependence between adjacent lanes is accounted for. However, the use of such models requires a knowledge of transition probabilities, which can be derived from the number of transitions of a vehicle between adjacent lanes (Anderson & Goodman 1957). This type of data was not available for the various sites studied in this thesis and thus traffic generation cannot be performed. Instead, the original traffic data were used; therefore the correlation between adjacent lanes is automatically accounted for in an appropriate manner.

7.3.2 Traffic simulations

The original traffic file contains the arrival times of the vehicles to the nearest second; hence do not indicate the hundredths of second. When dealing with relatively short bridges, exact times are required in order to calculate precisely the effects induced in the structure. A FORTRAN program has been written in order to add randomly generated hundredths of seconds to the measured arrival times. Great care has to be taken in defining the minimum inter-vehicle spacing between consecutive trucks, not only to avoid overlapping but also to avoid having two trucks directly behind each other (i.e. with no realistic spacing). A conservative value of 5m between the back axle of the 1st truck and the front axle of the 2nd truck was used, which gives approximately 2 to 3m for the minimum spacing between the rear of the 1st truck and the front of the 2nd truck.

The program previously developed, SIMULTRAFFIC, is used to run the complete traffic file over the bridges (with various span lengths and numbers of spans) and calculate the load effects induced. Only the multiple truck events are considered since just the tail of the distribution of the loading effects is of interest in this study.

In order to account for the inherent variability of the traffic data, a number of files are generated; each file is similar to the original file but with different hundredths of seconds. By averaging the results induced by a number of traffic files (20 in this study), a more robust trend is obtained (as explained in Chapter 6). The results obtained will therefore be representative of one week of traffic. Table 7-1 presents the average of the extrapolated values obtained by considering every traffic file separately and the extrapolated values obtained using the averaged effects; the differences are small (between –3.8% and +1.3%.), a result that confirms the validity of the above assumption. It should also be noted that two distinct analyses are carried out for each complete traffic file, i.e., one corresponding to each direction of traffic.

Table 7-1:Comparison between the average of the extrapolated values (Ave. EV) from a number of traffic files and the extrapolated values obtained from the averaged effects (EVave.)

Bridge Length	Load Effect	Direction 1			Direction 2		
		Ave. EV	EVave.	Diff. (%)	Ave. EV	EVave.	Diff. (%)
20 m	1	3935	3814	*-3.1*	3609	3609	*0.0*
	2	1093	1054	*-3.6*	1070	1070	*0.0*
	3	933	898	*-3.8*	717	719	*0.2*
	4	788	765	*-2.9*	891	872	*-2.1*
	5	581	580	*-0.2*	558	558	*0.0*
	6	561	562	*0.2*	571	572	*0.2*
30 m	1	6971	6971	*0.0*	6481	6489	*0.1*
	2	1559	1559	*0.0*	1620	1620	*0.0*
	3	1023	1023	*0.0*	913	913	*0.0*
	4	944	945	*0.1*	975	975	*0.0*
	5	742	742	*0.1*	592	593	*0.1*
	6	627	628	*0.1*	740	743	*0.4*
40 m	1	10290	10290	*0.0*	10359	10368	*0.1*
	2	2567	2567	*0.0*	3003	3009	*0.2*
	3	1092	1092	*0.0*	1119	1131	*1.0*
	4	1062	1062	*0.0*	1114	1128	*1.3*
	5	862	862	*0.0*	667	670	*0.4*
	6	726	726	*0.0*	841	841	*0.0*
	Max			***-3.8***			***-2.1***
	Min			***0.2***			***1.3***

7.3.3 Extrapolated values: results and comparative study

In a similar manner as employed in the preceding chapter, extrapolated values were obtained for unidirectional traffic. Before starting the analysis, it should be recalled that the representative trucks involved in the critical loading events are slightly shorter in direction 1 (although they belong to the same type as the ones observed in direction 2). Figure 7-6 illustrates the weight distributions for the two directions of traffic studied. Again, the GVW distributions are different from the slow lane to the fast lane; however, the two lanes have been considered together in Figure 7-6 simply to show that the traffic is heavier in direction 2.

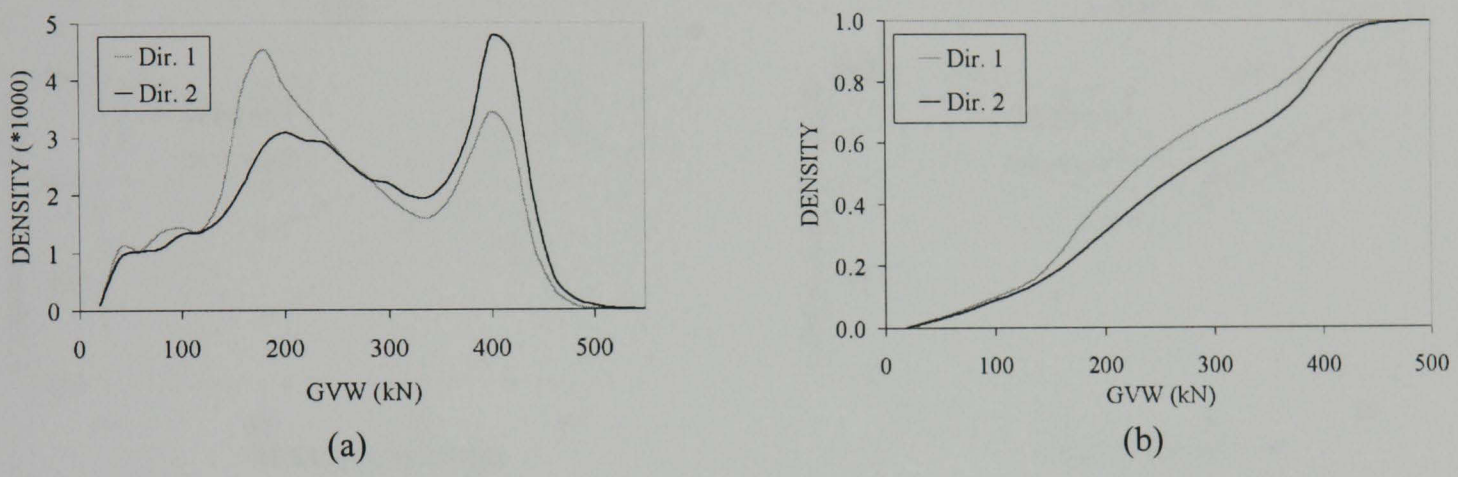

Figure 7-6: Distribution of weights for the unidirectional traffic types: (a) PDF and (b) CDF

Figure 7-7 presents the extrapolated values obtained for both directions and for the 6 load effects studied as a function of the bridge length. A number of observations can be made:

- Although the traffic is heavier in direction 2, the extrapolated values obtained for both directions are similar for the shortest spans (20 m); this is explained by the difference in truck geometry (the lighter, but slightly shorter, trucks of direction 1 induce the same effects as the heavier, but longer, trucks of direction 2).
- For the longer span (40 m), the influence of the traffic weight becomes dominant and the difference in truck geometry becomes less significant.
- For the load effects 3 to 6 (i.e. shear at the supports), the extrapolated values vary significantly depending on the direction of traffic considered. In one case only part of the trucks (the tridem at the back of the semi-trailer) is present on the bridge, or the whole truck is present but only the front is located at the critical position. In the other case the whole truck is present and has its heavier part located at the critical location.

In conclusion, the traffic weight needs to be considered together the geometry of the representative trucks since they both have a significant influence for short bridges; as the bridge increases in length, the traffic weight becomes more and more significant while the truck geometry naturally becomes less significant.

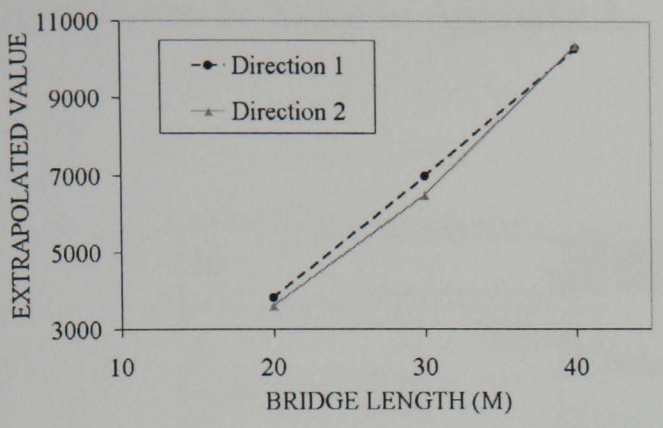

(a)

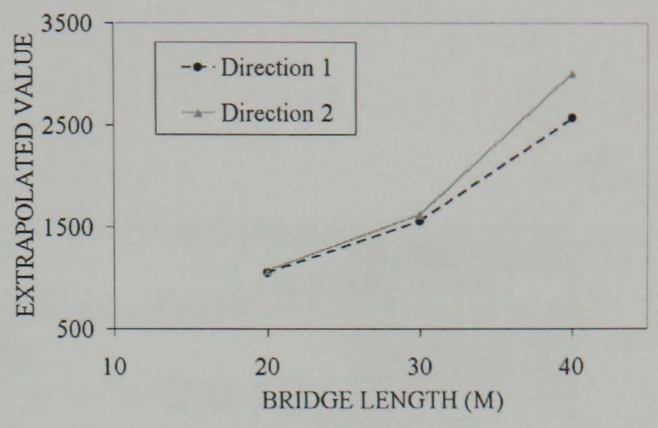

(b)

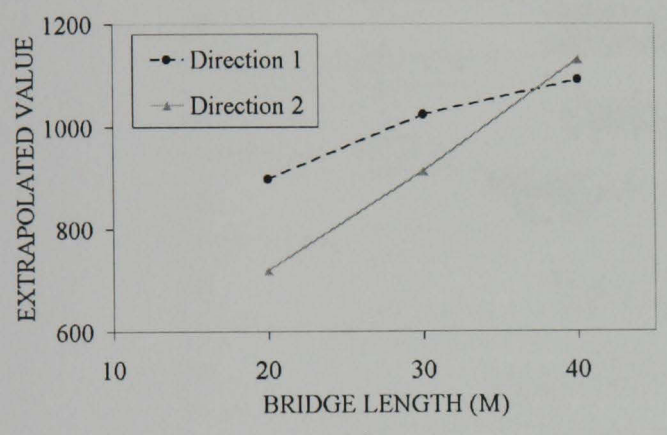

(c)

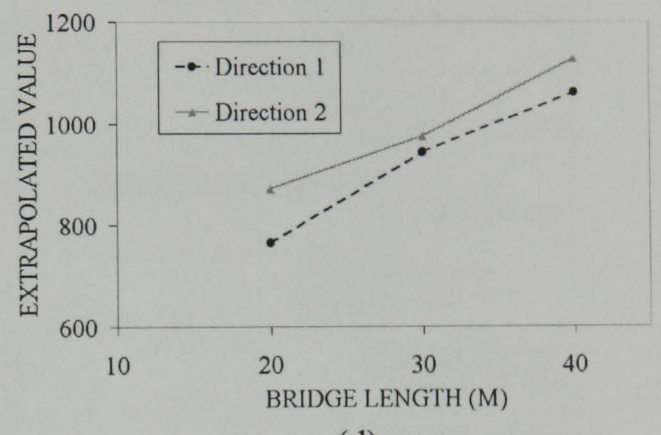

(d)

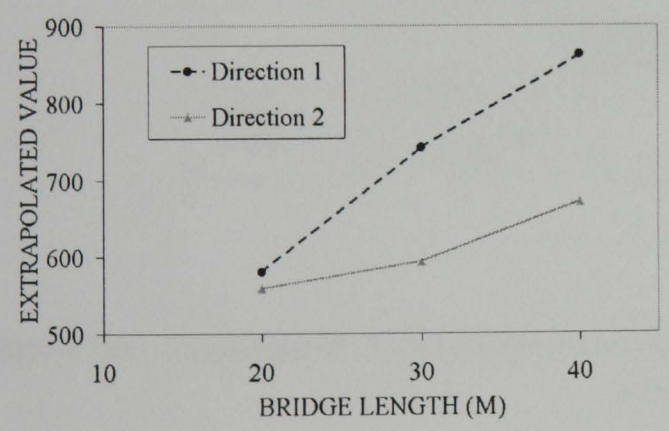

(e)

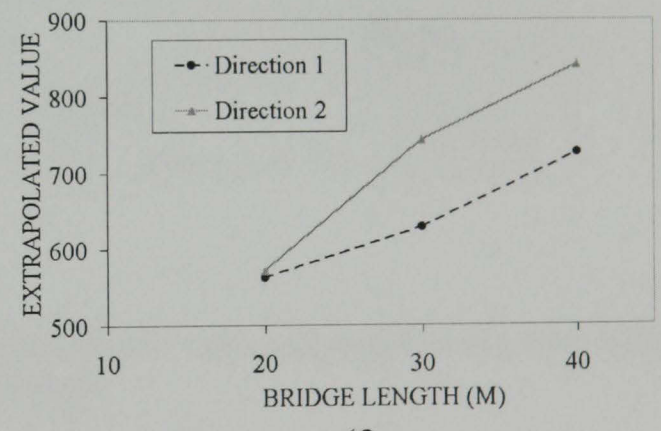

(f)

Figure 7-7: Extrapolated values corresponding to unidirectional traffic as a function of bridge length: (a) load effect 1, (b) load effect 2, (c) load effect 3, (d) load effect 4, (e) load effect 5 and (f) load effect 6

7.3.4 Critical loading events

In order to examine the characteristics of the trucks involved in the critical loading cases (e.g. location on the bridge, gross vehicle weight, number of axles, etc.), the program developed using MATLAB is used. This program draws the trucks on the bridge at their respective location for the 20 most critical events. The plots generated for the 20 measured

traffic files are analysed for each load effect and each span length in order to derive the typical critical loading cases. Output from this program was previously illustrated. However, in this chapter the two trucks involved in the critical loading events travel in the same direction and the configuration of these events can be different, at least for some load effects, as shown in Figure 7-8. All the plots for the various bridge lengths and the two directions can be found in Appendix L.

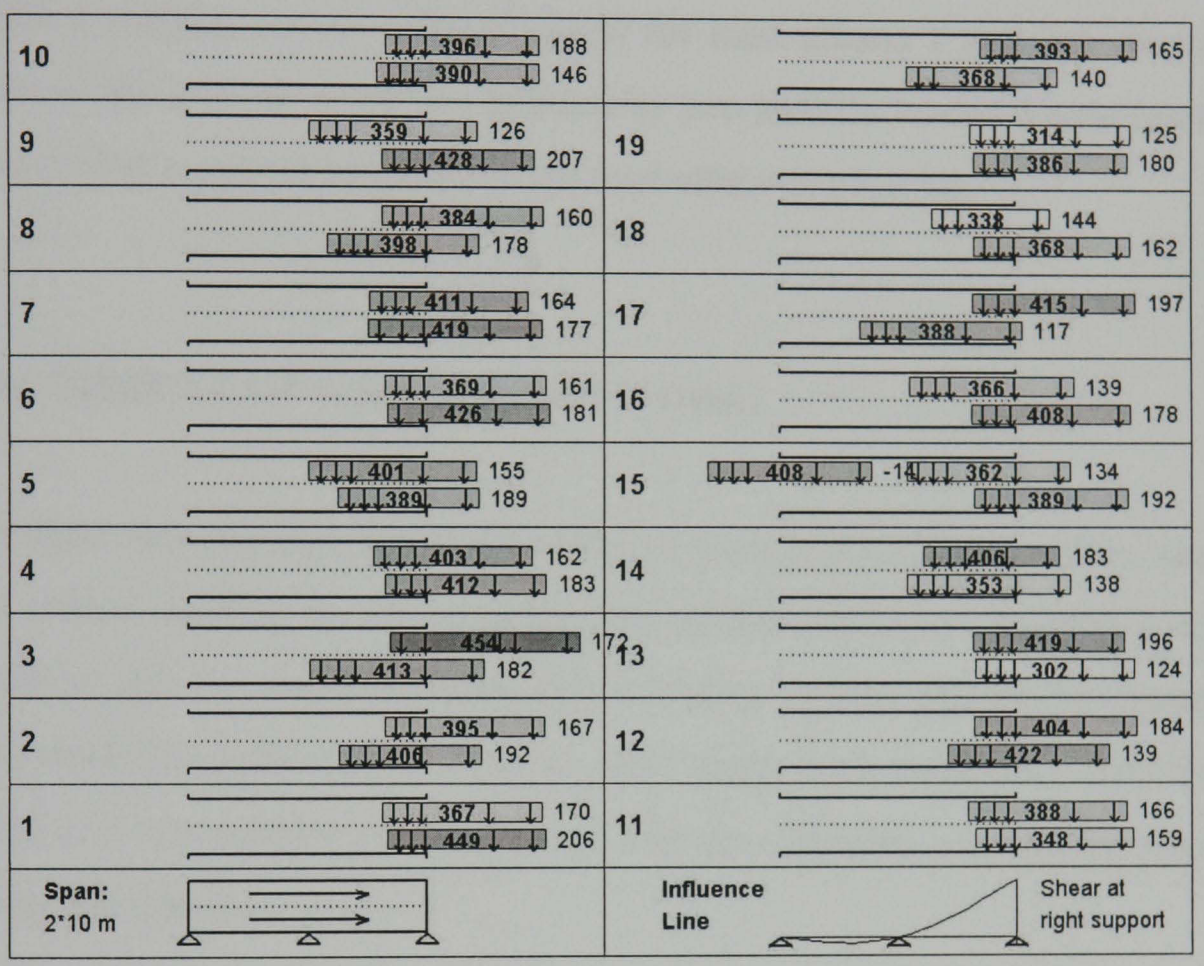

Figure 7-8: Output of the MATLAB program for the shear at the right-end support of a 20m two-span continuous bridge

The typical configurations for the overtaking events are very similar to those described in the previous chapter for the bi-directional traffic; hence there are not described in detail herein. The characteristics of these critical loading events, for each bridge length and load effect treated, can be found in Appendix M.

The characteristics of the typical events are essentially the same for the 20 and 30m long bridges, with the exception of load effect 6 for direction 1 (or load effect 5 for direction 2), for which the proportion of the trucks present on the bridge increases with the span (as the zone under which the effect is critical increases with the span). Almost all the trucks involved in these critical events are 5-axles trucks (vehicle type 14, i.e. 2-axle tractor + 3-

axle trailer); the remaining trucks being either 4-axle trucks or 5-axle trucks of a different type.

An important characteristic is that there are only two trucks involved in the loading events, with the exception of 40m bridges, for which the 3-truck events occur more and more frequently. For the 30m bridges, the simultaneous occurrence of 3 heavily loaded trucks can be critical (especially for load effect 2) but is a rare event. For the 40m bridges these 3-truck events are frequent but also more critical than the 2-truck events. This remark holds for load effect 2 mainly, and to a lesser extent for load effects 1 and 3/4. Based on this analysis, most of the critical events are induced by two heavily loaded 5-axle trucks beside each other located at a critical location for the load effect considered.

7.4 DEVELOPMENT OF A SIMPLIFIED MODEL

Having performed full simulations for a number of complete traffic data files, and having analysed the critical loading events, it is the aim of this section to develop a simplified model that will be able to reproduce these critical loading events. The traffic characteristics described and modelled in Section 7.2 can be used, along with some other data that needs to be modelled (e.g. the distribution of GVWs). The development is presented step by step in the following paragraphs.

7.4.1 Representative trucks

In order to develop a model that can simulate overtaking events without having to simulate a complete traffic file, typical 5-axle trucks need to be derived from the measured data. Two different types were derived, depending on their gross vehicle weight. The 1st type was based on all the 5-axle trucks corresponding to the 2nd mode of the GVW PDF while the 2nd type was based on the 5-axle trucks whose GVW is at least 95% of the CDF of GVW. In order to derive the characteristics of the typical trucks, normal distributions are fitted using the least squares technique and estimates of the mean and standard deviation are obtained. Table 7-2 shows the values of the typical axle-spacings (in metres).

Table 7-2: Axle-spacing (m) for the typical 5-axle truck

Dir	Sample	S12		S23		S34		S45	
		Mean	St. Dev.	Mean	St. Dev.	Mean	St. Dev.	Mean	St. Dev.
1	2nd Mode	3.47	0.14	5.63	0.28	1.18	0.08	1.18	0.08
1	95% CDF	3.52	0.18	5.61	0.32	1.15	0.09	1.16	0.08
2	2nd Mode	3.61	0.18	5.84	0.28	1.28	0.08	1.28	0.08
2	95% CDF	3.60	0.15	5.86	0.28	1.28	0.08	1.28	0.08

From Table 7-2, typical axle-spacings are observed to be quite similar for both samples. In addition, a difference can be noticed between the average truck lengths between directions: 11.46 m for direction 1 and 12.01 m for direction 2. Although small, this variation in the truck length between the two directions should not be neglected as it could induce significant differences in the load effects (due to the size of the bridges considered and their sensitivity to the truck location and truck configuration).

The axle weight distributions were also obtained for both directions separately; the results are presented in Figure 7-9. As for the axle spacings, variations appear between directions. Again, these differences are small, but could be significant due to the nature of the bridges considered.

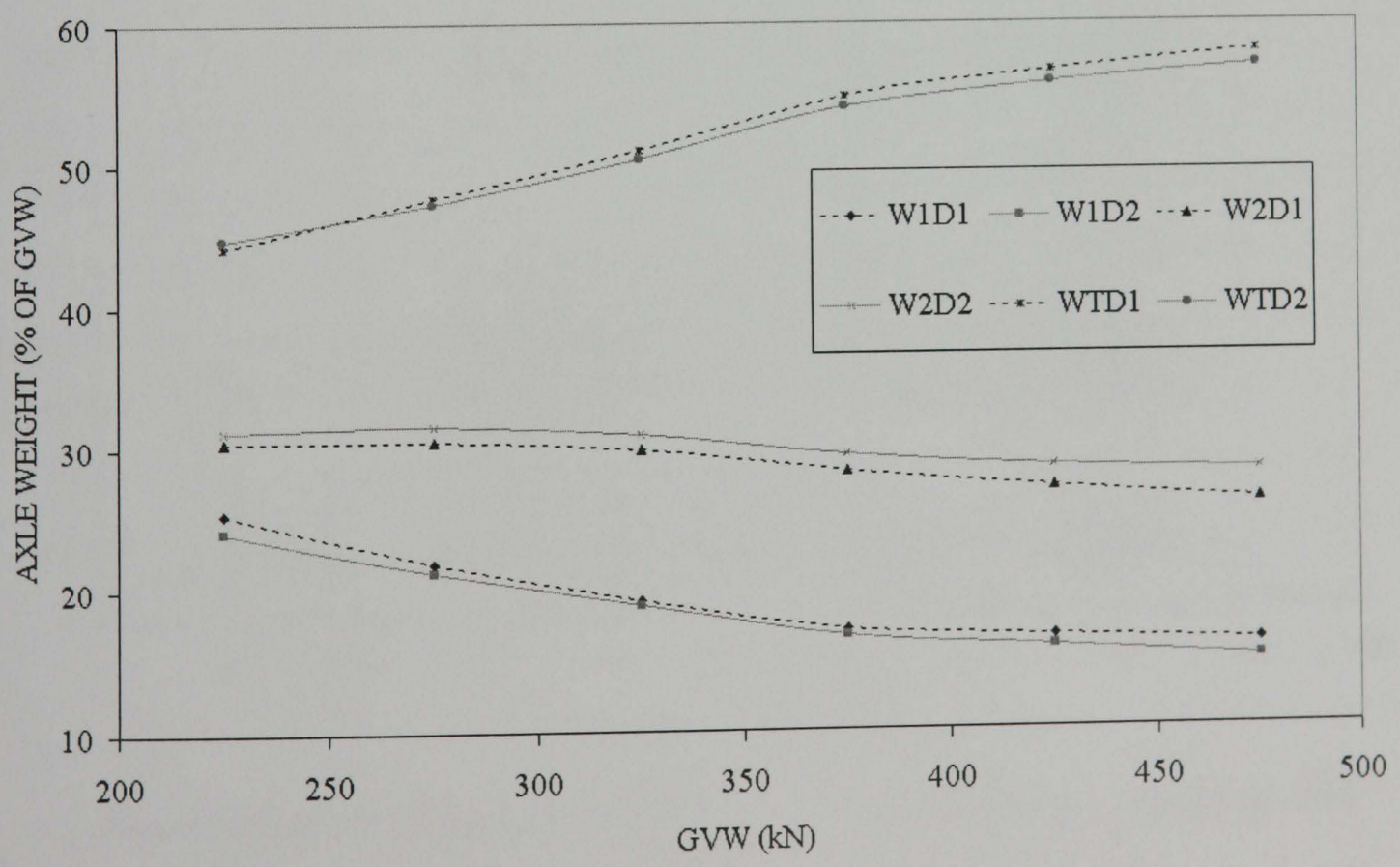

Figure 7-9: Axle-weights (as % of GVW) of vehicle type 14 for both directions as a function of GVW (kN).

In conclusion, the truck configuration appears to be direction-specific and will therefore be modelled as such in order to give results that are as accurate as possible.

7.4.2 Modelling truck weights

The characteristics of the typical trucks being known, their respective GVWs need to be determined. Unlike the case of bi-directional traffic, both lanes cannot be assumed to be independent. Thus the GVW's cannot be generated by simply using the GVW PDF's of the slow lane and fast lane. The dependency between lanes, and therefore between the overtaking truck's GVW and the slow truck's GVW, needs to be accounted for in the model. Figure 7-10 illustrates the GVWs of slow trucks and adjacent fast trucks, where adjacent is defined as being within one bridge length. Clusters of points can be observed. For example, there is a large number of overtaking events for which both trucks have a GVW of 180 kN (i.e. main peak of the graph); while there are extremely few events for which both trucks have a GVW of 330 kN.

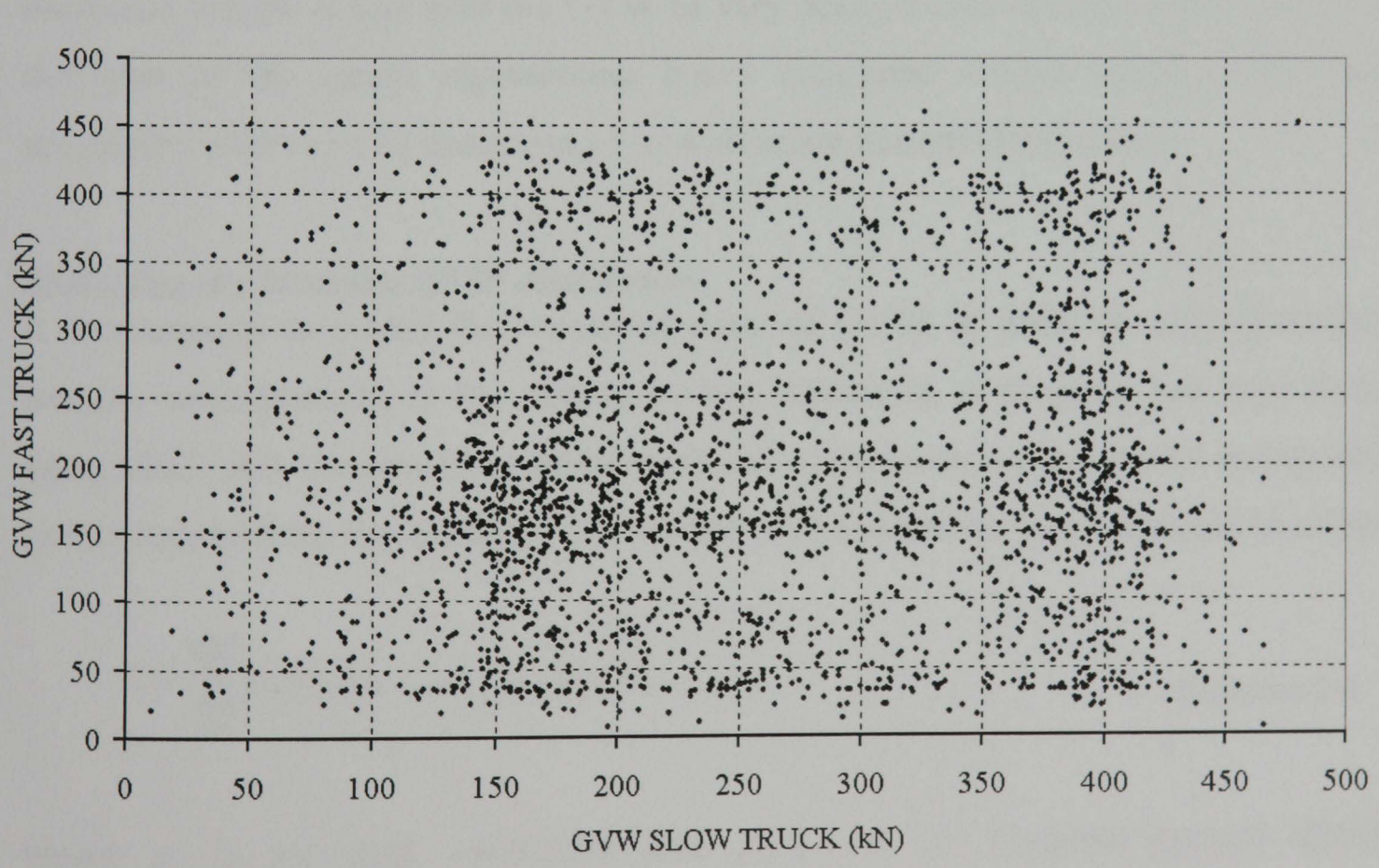

Figure 7-10: GVW of fast truck and GVW of slow truck in direction 1 on the A1-1996

A 3-dimensinoal (3D) graph is required in order to visualize the frequency of overtaking events for which the GVW of the fast truck is W2 kN given that the GVW of the slow

truck is W1 kN. Alternatively, a 2-dimensional (2D) contour plot can also be used in this analysis.

As explained in Chapter 2, a bivariate normal distribution is a function of 2 variables, but requires 5 parameters to be completely defined: mean and variance for both variables and the coefficient of correlation between the two variables. Furthermore, because there are a numbers of peaks to be modelled (i.e. a number of bivariate normal distributions), a coefficient needs to be applied to each distribution in order to keep the total volume beneath the surface equal to unity; that coefficient will be referred to as the *peak coefficient* and is between 0 and 1. Hence there are in fact 6 parameters to derive for each distribution. Assuming that there can be as many as 9 distributions (i.e., combination of 3 modes for GVW_{slow} and 3 modes for GVW_{fast}) required to model reasonably well the complete distribution, there would be 54 parameters to consider in the optimisation process, which practically and computationally would be too many. In the other hand, only the proportion of overtaking events for which the combined weight of the two trucks is very heavy, is of interest. Indeed, the events for which both trucks weigh 180 kN are not critical, even when both trucks are placed at the most critical location for the effect considered, as the combined weight is less than the GVW of very heavy trucks on their own. Therefore only that part of the graph representing heavy combined weight needs to be modelled accurately, which can be done using 3 or 4 bivariate normal distributions.

Modelling the bivariate GVW distribution

It is necessary to model the measured pairs of GVW in order to later generate truck weights corresponding to the critical loading situations. A program has been developed using MATLAB Version 12 to select a number of peaks on a contour plot and model them as bivariate normal distributions. The surface can be modelled as a combination of peaks:

$$S = \sum_{i=1}^{npeaks} p_i \cdot f_{XY}^{i}\left(x, y; \mu_X^i, \mu_Y^i, \sigma_X^i, \sigma_Y^i, \rho_{XY}^i\right) \qquad \textbf{Equation 7-2}$$

where p_i is the peak coefficient and $f_{XY}^{i}(\,)$ is the bivariate normal distribution corresponding to peak i. The MATLAB program developed is now presented, step by step:

1. Display the initial distribution as a 3D surface: calculate the bivariate distribution (i.e. density function in 3D) and plot it. An important parameter to be defined by the user is the grid spacing for both axes. The overall shape of the distribution remains the

same independent of the value selected for the grid spacing, but the shape is smoother for higher grid spacing values and patchier for smaller grid spacing values. Higher values are preferable since fewer peaks would be required to model the distribution.

2. Peak selection. Plot a contour graph of the bivariate distribution (see Figure 7-11) and ask user to select the location of the peak to be modelled, as well as the limits of the zone in which the optimisation will be performed for that peak. Initial estimates for the means of the two variables are taken as the X and Y coordinates of the peak. Inputting the limits of the zone for the optimisation is necessary as there is no simple way of estimating blindly how far the peak spreads in both directions. By overestimating or underestimating the size of the zone for the optimisation, the accuracy of the parameters being optimised could be greatly reduced.

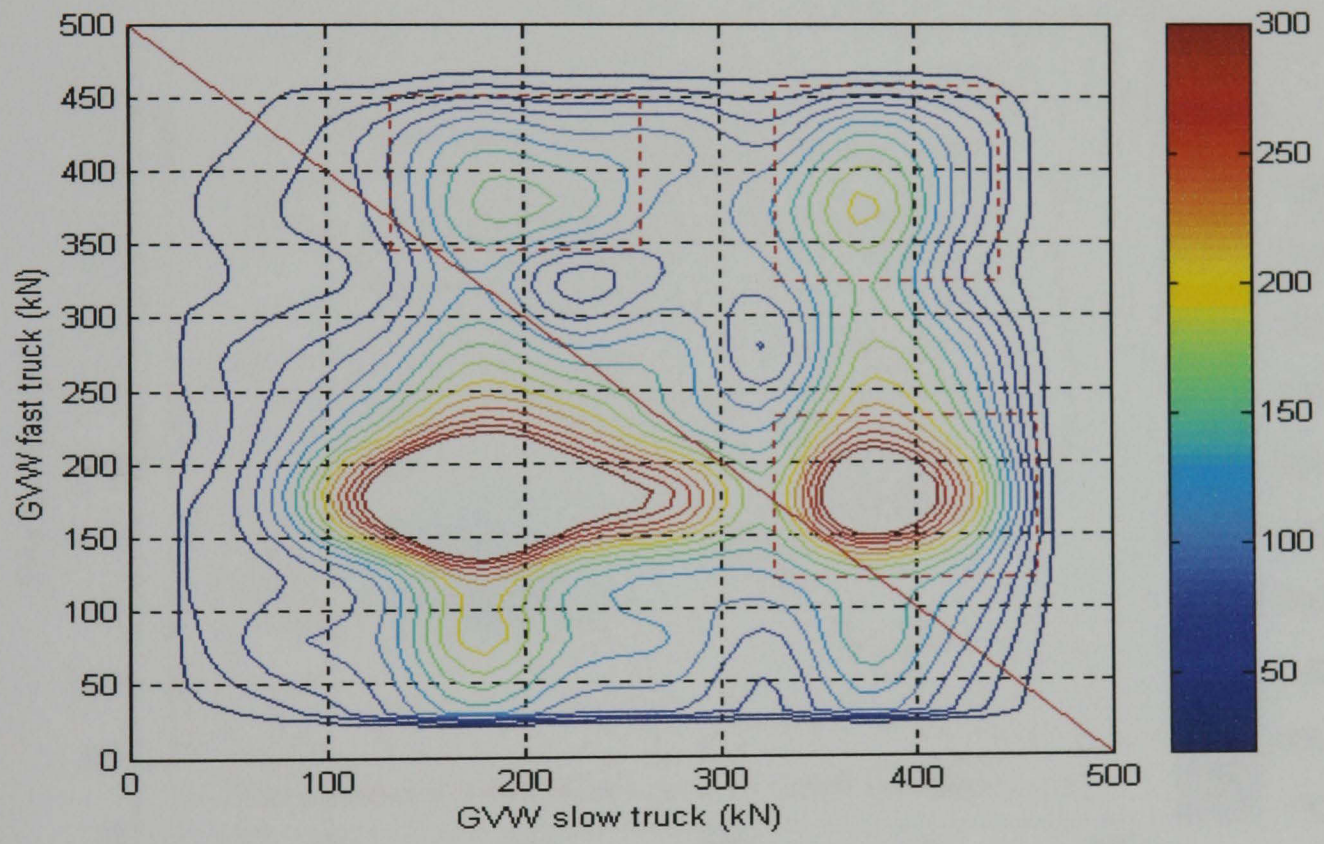

Figure 7-11: Contour plot of bivariate distribution of GVWs and selection of peaks

3. Peak modelling - estimation: perform the optimisation on 3 of the 6 parameters required to model a bivariate distribution: the variance of both variables and the weight coefficient. Initial guesses for these 3 parameters do not need to be very accurate; the optimisation will automatically converge towards the accurate values. The means and the coefficient of correlation are not optimised at first because their initial estimates are reasonably accurate; thus the optimisation process is speeded up.

4. Peak modelling - refinement: perform optimisation on the 6 parameters. All the parameters being well estimated, a complete optimisation can be performed that converges rapidly towards an accurate solution.

REPEAT STEPS 2 TO 4 UNTIL ALL CLEARLY IDENTIFIED PEAKS HAVE BEEN MODELLED

5. Assess the goodness of fit of the modelled distribution: compute the error between the measured distribution and the modelled one, and display it. Decide if any extra peak(s) can be identified and should be modelled, as illustrated in Figure 7-12. If this is the case, steps 2 to 4 are repeated. Each peak modelled will introduce an additional six variables.

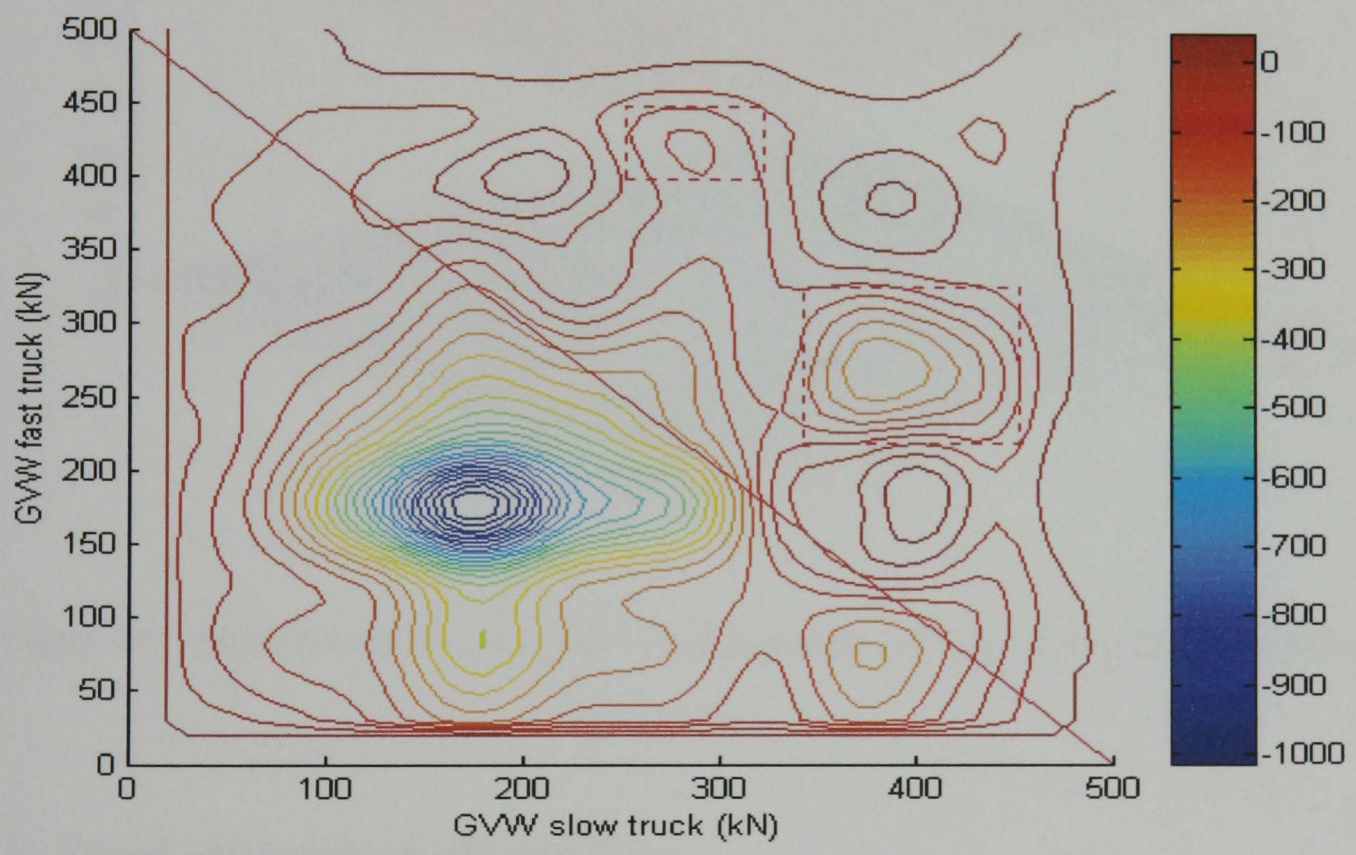

Figure 7-12: Contour plot of the error between modelled and empirical distribution with selection of extra peaks

6. Final optimisation: because the peaks have been modelled separately, once they add up, there might be some error between the measured distribution and the modelled one. The peak coefficients need to be optimised all at once, without varying the other parameters, in order to minimise the final error between the measured distribution and the modelled one.

7. Output the parameters of the modelled distribution: write the 6 parameters corresponding to each peak to a file (that will be used to generate GVWs and simulate passing events). The final result is presented in Figure 7-13; the measured bivariate distribution is in blue and the modelled distribution is in red. The main peak is missing (simply because it has not been modelled); the Z-axis does not have any significance on that plot, it is merely a means of showing the two surfaces on the same graph. Clearly, the three main peaks are well modelled.

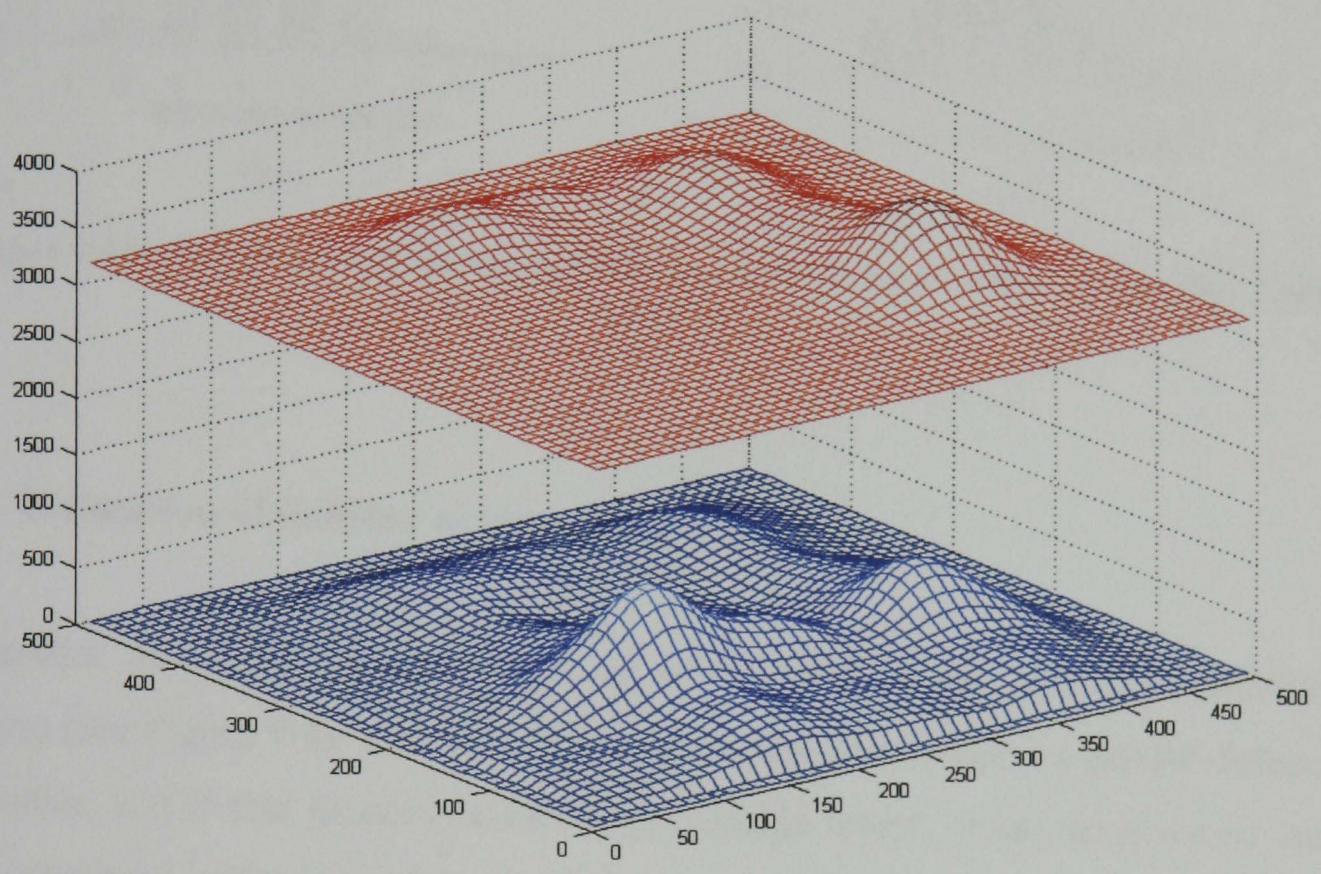

Figure 7-13: Modelled distribution (red) versus empirical distribution (blue) after optimisation

7.4.3 Speed and headway distributions

Knowing the GVW's distribution and the characteristics of the typical trucks, the last element necessary to model typical overtaking events accurately is the speed distribution of the two trucks. Rather than modelling the speed distribution separately for the slow lane and for the passing lane, it has been decided to model the speed distribution of the slow lane only and then to model the distribution of difference in speed between the fast truck and the slow truck. Using that method the speeds are modelled more accurately since the speed of the overtaking truck is not independent of the speed of the slow truck, but is a function of it. The Gumbel distribution (which, in this case, is not used a distribution of

extreme values but merely as regular distribution) was found to fit the histogram of speed differences accurately (cf. Figure 7-14). Once again, the overall shape of the distributions is the same for both directions, although the actual distributions are clearly different when observed more closely, which shows the direction-specific character of the measured data.

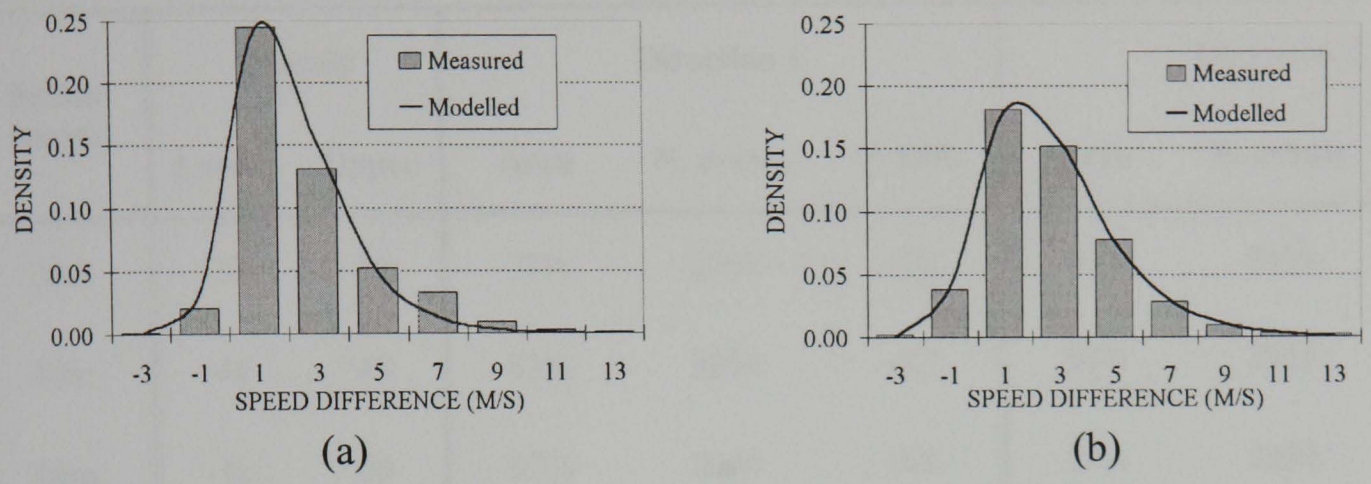

Figure 7-14: PDF of speed difference between adjacent trucks for A196: (a) direction 1 and (b) direction 2

7.4.4 Estimation of number of overtaking events

The number of overtaking events can be estimated from the modelled distribution of headways (see Figure 7-4). Indeed, if two adjacent trucks are within a certain distance from one another, and if that distance is less than a bridge length, it can be deduced that these trucks constitute a passing event. Also, the number of headways falling between given bounds can easily be calculated using the properties of the normal distribution used to model the empirical headway distribution. For a given bridge, the headway is required to satisfy the following equation,

$$-(L_{bridge} + L_{truck}) < headway < +(L_{bridge} + L_{truck}) \qquad \textbf{Equation 7-3}$$

, for an overtaking event to occur. In addition, the area under the normal curve (used to model the headway distribution) and between these two bounds represents the proportion of trucks present in the fast lane that will be involved in overtaking events. Furthermore, the number of trucks present in the fast lane can be estimated accurately from the equation fitted to the empirical data (see Figure 7-5). Finally the accuracy of the estimated number of overtaking events can be assessed by comparing it to the measured number of overtaking events. Table 7-3 presents the results for the two directions for A196: the column *area* corresponds to the proportion of headways included within the specified bounds, and *N.events* is the estimated number of overtaking events obtained by multiplying

the total number of trucks in the fast lane by the area. Finally *Diff* represents the error between the estimated number of overtaking events and the measured one obtained from the full simulations. It can be seen that the differences are small.

Table 7-3: Estimated number of overtaking events for various bridge lengths

Bridge length	Bounds		Direction 1			Direction 2		
	Lower	Upper	Area	N. events	% Diff.	Area	N. events	% Diff.
20m	-30	30	73%	2061	-0.6	66%	2415	-3.6
30m	-40	40	83%	2354	-4.7	80%	2915	-2.1
40m	-50	50	93%	2646	-3.0	89%	3250	-0.2

7.4.5 Simplified model to simulate critical overtaking events

This model is developed in order to simulate critical overtaking events only, rather than all the overtaking events, thereby greatly improving the computational efficiency. In the previous sections different distributions were modelled in order to represent accurately the characteristics of the critical loading events and the trucks involved in these events. This section explains how these distributions are used to simulate the critical overtaking events corresponding to a given traffic. Figure 7-15 describes the different steps followed in the simplified model developed.

At first, calculate the estimated number of overtaking events N_{events} that take place during the period of time considered, e.g., 1 week in this study. Generate N ($<N_{events}$) pairs of gross vehicle weights using the modelled joint PDF for GVWs; N is smaller than N_{events} because only some of the peaks are represented in the modelled distribution (the peaks corresponding to light pairs of trucks have not been modelled). Nonetheless the knowledge of N_{events} is necessary in order to calculate N, which is directly related to N_{events} through the peak coefficients applied to each modelled peak. Then N pairs of typical trucks are generated. Although all the trucks are based on the same vehicle type (e.g. 2-axle tractor + 3-axle trailer), they are all different one from another, the axle weights and axle spacings being generated using normal distributions of characteristics shown in Table 7-2 and Figure 7-9. Generate N headways, N slow speeds and N speed differences using the

modelled distributions outline in the previous paragraphs. There are now N pairs of trucks completely defined. The next step consists of the calculation of the effects induced in the bridge structure due to the pair of trucks as they move along the bridge. The values of the different effects are calculated every 0.01 seconds and the maximum values are recorded for each overtaking event treated. The calculations are carried out for each pair of trucks. Finally there are N maximum values recorded for each span and for each load effect considered.

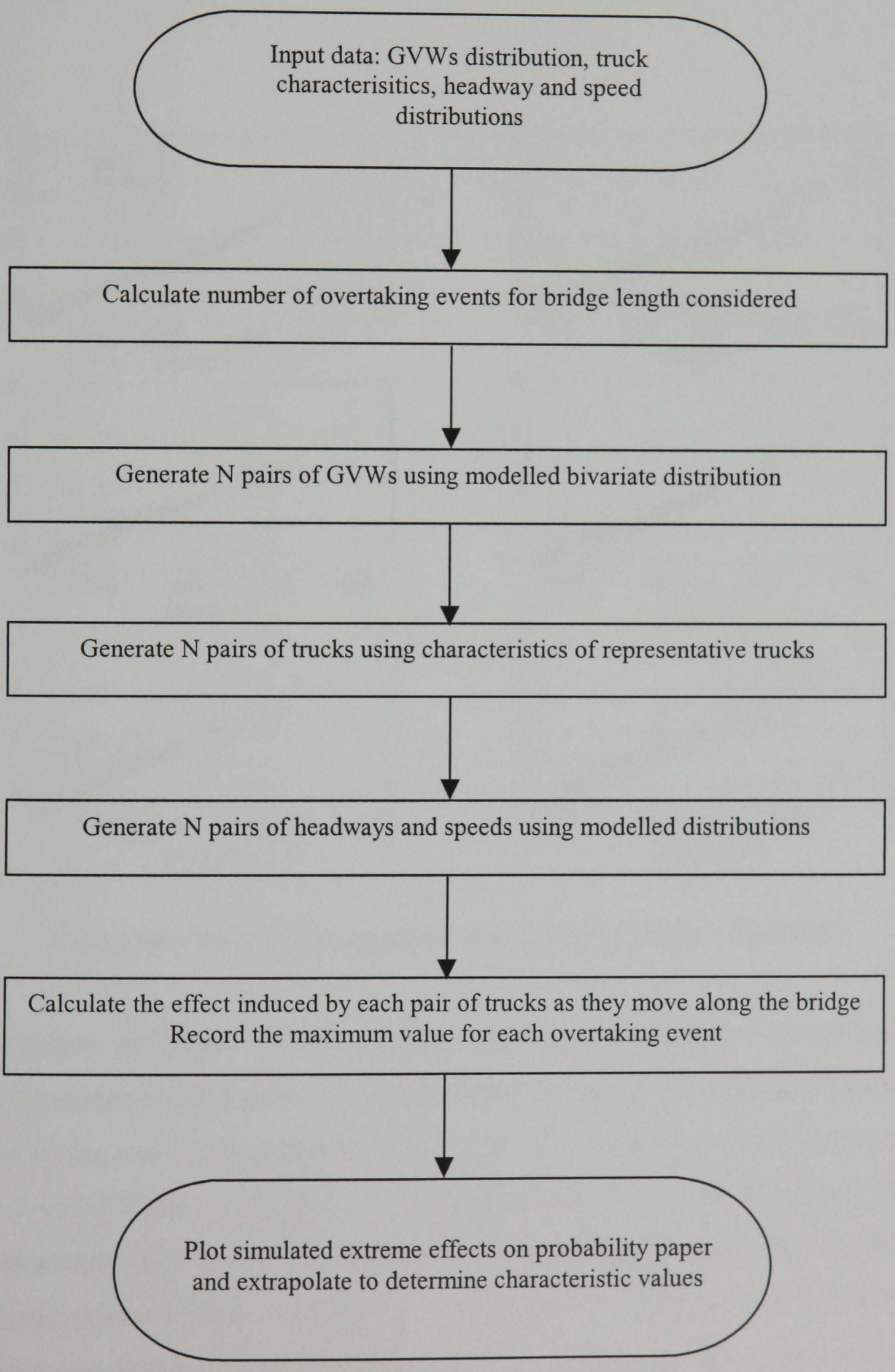

Figure 7-15: Flow chart of the simplified model

7.5 RESULTS OF THE SIMPLIFIED MODEL

The results obtained from the simplified model presented in the above section are now considered. The 100 most critical values for each load effect are plotted on Gumbel probability paper together with the measured effects. Figure 7-16 shows the results for 20m bridges, direction 1: very good agreement is observed for all the load effects considered. Similar agreement is found for direction 2 of traffic; the plots corresponding to other bridge lengths and for each direction can be viewed in Appendix N.

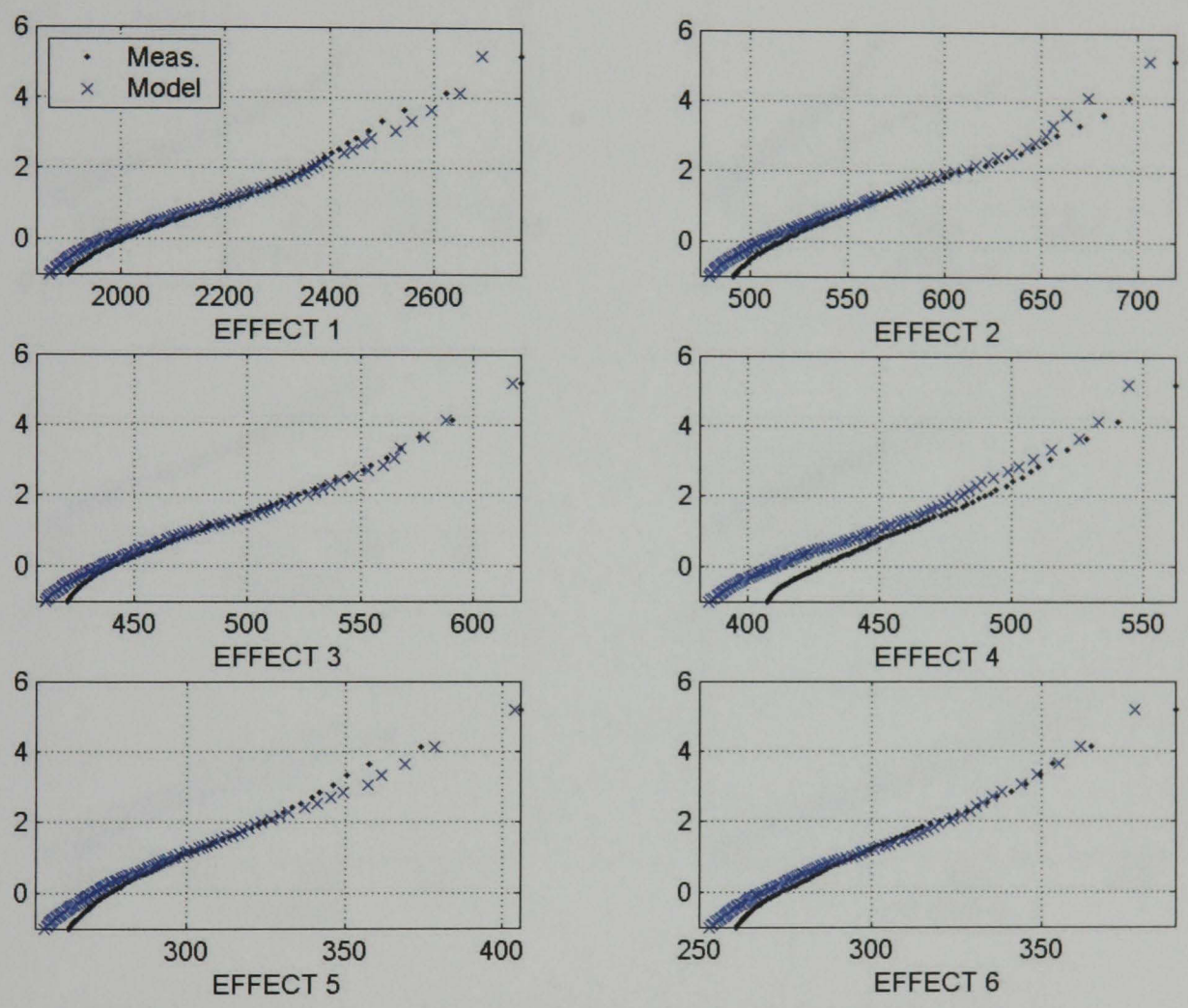

Figure 7-16: Results from simplified model for 20m bridges – Direction 1

For 30m bridges, the results are still satisfactory for all load effects but load effect 2, for which the occurrence of 3-truck events becomes frequent and critical. Although not as obvious as in the case of load effect 2, a similar observation can be made regarding load effects 1, 3 and 4 Figure 7-16. Some of the critical events (usually the most critical ones) are 3-truck events, that is why the results from the simplified model tend to diverge from the measured values towards the right tail of the plot. Figure 7-17 exhibits the results for 40m bridges: the observations made here above are confirmed. The simplified model fails to represent accurately the measured values of critical effects towards the tail of the plot,

for the trivial reason that only 2-truck events are modelled and cannot represent 3-truck events. However, distinctions should be made depending on the load effect considered: while only the tail of the distribution of critical effects is diverging for load effects 1, 3 and 4, the complete distribution is off from the measured one for load effect 2; and finally the model manages to predict accurately the critical events for load effects 5 and 6 as only 2 trucks are involved in that case. Figure 7-18 and Figure 7-19 illustrate the critical loading events corresponding to load effects 4 and 2 for the 40 m bridge.

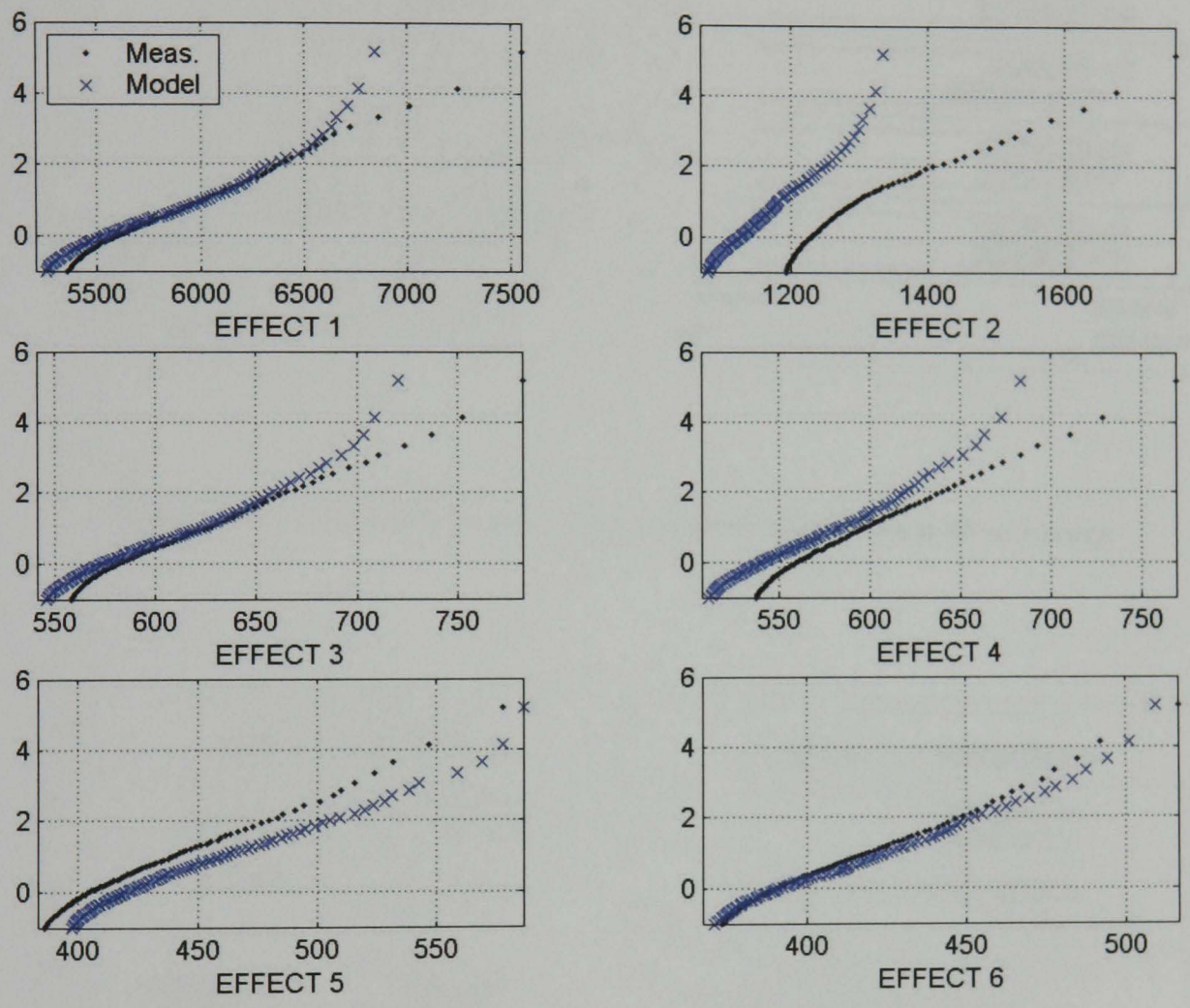

Figure 7-17: Results from simplified model for 40m bridges – Direction 1

Overall, the results obtained using the simplified model appear to be satisfactory for 20 and 30m bridges for all the load effects considered (with the exception of load effect 2 on 30m bridges). However, as the bridge length increases, so does the likelihood of having 3 trucks involved in the critical events, and the model becomes inadequate for most of the load effects. These conclusions are confirmed by Table 7-4, showing the extrapolated values obtained using the full simulations and the simplified model. The cells greyed out correspond to the cases where the error is becoming unsatisfactory, that is, where the model fails to represent the critical loading events consisting of 3 trucks.

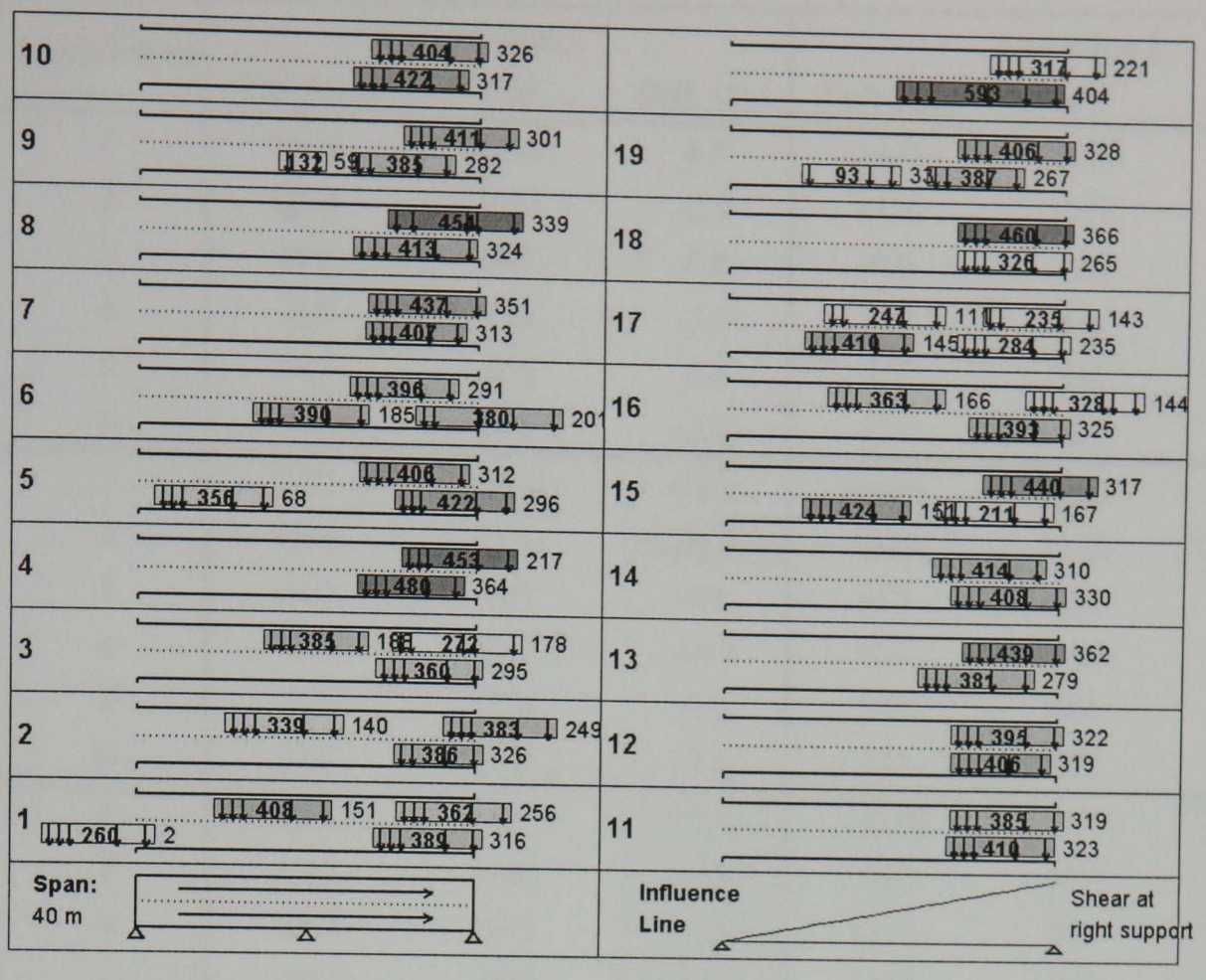

Figure 7-18: Critical loading events for load effect 4 on a 40 m bridge

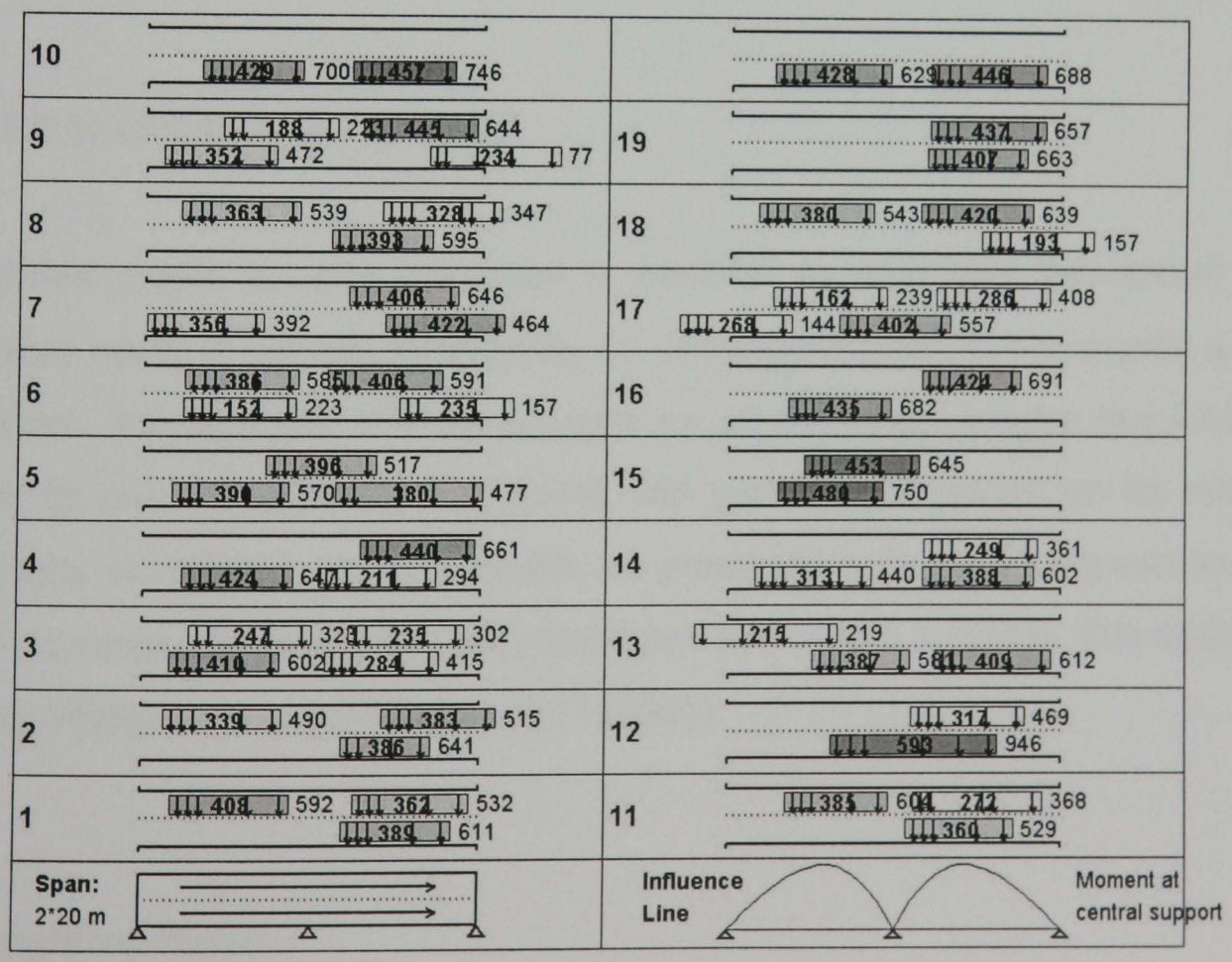

Figure 7-19: Critical loading events for load effect 2 on a 40 m bridge

Table 7-4: Extrapolated values from full simulations and simplified model (SM)

Bridge Length	Load Effect	Direction 1			Direction 2		
		Full Sim.	SM	Diff. (%)	Full Sim.	SM	Diff. (%)
20 m	1	3814	3849	*0.9*	3609	3723	*3.2*
	2	1054	1023	*-2.9*	1070	1013	*-5.3*
	3	898	907	*1.0*	719	770	*7.1*
	4	765	755	*-1.3*	872	878	*0.7*
	5	580	605	*4.3*	558	535	*-4.1*
	6	562	548	*-2.5*	572	581	*1.6*
30 m	1	6971	6212	*-10.9*	6489	6102	*-6.0*
	2	1559	1150	*-26.2*	1620	1170	*-27.8*
	3	1023	923	*-9.8*	913	838	*-8.2*
	4	945	843	*-10.8*	975	900	*-7.7*
	5	742	774	*4.3*	593	606	*2.2*
	6	628	574	*-8.6*	743	757	*1.9*
40 m	1	10290	8855	*-13.9*	10368	8752	*-15.6*
	2	2567	1684	*-34.4*	3009	1677	*-44.3*
	3	1092	952	*-12.8*	1131	891	*-21.2*
	4	1062	907	*-14.6*	1128	931	*-17.5*
	5	862	864	*0.2*	670	704	*5.1*
	6	726	692	*-4.7*	841	824	*-2.0*
	Max			*-34.4*			*-44.3*
	Min			*4.3*			*7.1*

7.6 SIMPLIFIED MODEL 2 AND 3

The simplified model initially developed is intended to reproduce the critical loading events as they occur in the full simulations. Its development and its use require a number of calculations. Furthermore, it is not accurate for all the bridge lengths and load effects considered. In order to simplify this model, and potentially improve on its robustness, variations were introduced; the new models are presented in the following section and are referred to as simplified model 2 (SM2) and simplified model 3 (SM3). The initial model will now be referred to as simplified model 1 (SM1).

7.6.1 Simplified Model 2

In the initial model, the truck locations (when the maximum value of the effect occurs) are the result of a combination of parameters: the initial headway when entering the bridge and

the relative speeds of the trucks. To avoid having to model the headway distribution and the speed distributions, and also to run the trucks over the bridge as in the full simulation, the actual critical locations can be represented by a percentage of the maximum possible value (see simplified model developed for the case of bi-directional traffic). Another advantage in using 'percentages' to express critical locations lies in the fact that the effects induced by a truck can exceed its theoretical maximum possible value (by fixing the percentage value above 100%). By doing so, the effects induced by two trucks could possibly match up to the values of the effects induced normally by three trucks. Thus a good agreement for all bridge lengths and load effects can be expected. The GVWs are still generated using the modelled bivariate normal distribution.

The model has been calibrated in order to give good agreement for both directions using the same set of values. It should be noted that the values for load effects 3/4 and 5/6 have to be switched from one direction to another. Indeed, for load effect 6 and direction 1 of traffic, only part of the trucks is located on the bridge, while for direction 2 this happens for load effect 5. Essentially, load effects 3/4 and 5/6 are symmetrical from one another for the two directions of traffic. Figure 7-20 presents the results for 20m bridges for direction 2; good agreement is observed for the six load effects treated. Similar agreement is also found for the other bridge lengths considered, including 40m, and for all the effects. All the plots can be found in Appendix N.

In Table 7-5, the lower and upper bounds used in SM2 are presented. For 30 and 40m bridges, the upper bounds can reach 110/120%, or even 150% in the case of load effect 2, i.e., to enable the two trucks to induce an effect superior to their theoretical maximum value (i.e., 100%) and thus reproduce the effect induced by a 3-truck events. As anticipated, a good agreement could be obtained for all bridge lengths and all effects because of these upper bounds enabling the replication of 3-truck events. However, it should be noted that, even for the 20m bridges, some of the upper percentages exceed 100%, although the critical loading events consist of two trucks only. In other words, either the trucks employed in SM2 are not as heavy as they ought to be or, the representative truck configuration used is not critical enough.

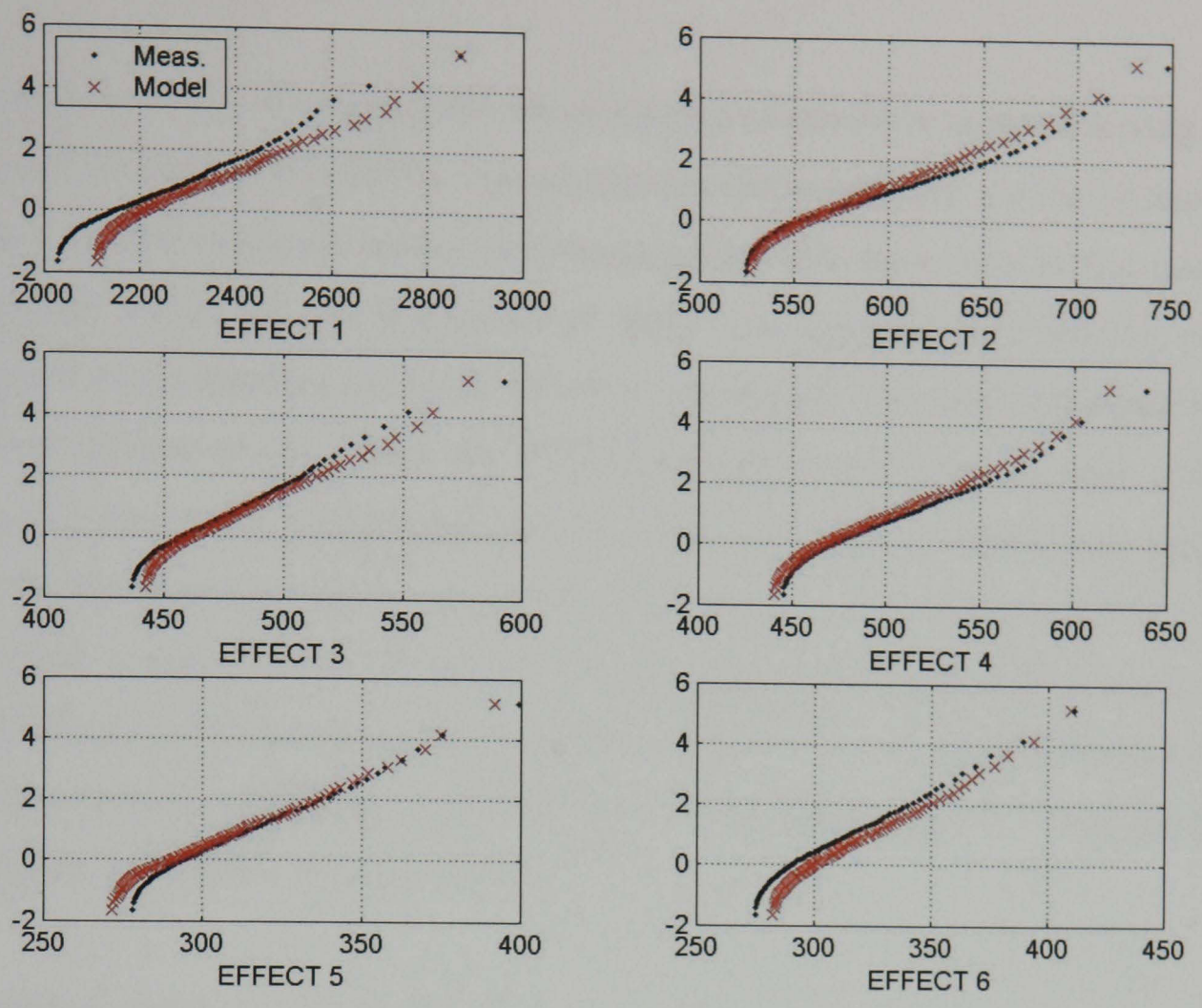

Figure 7-20: Results from SM2 for 20m bridges – Direction 2

Table 7-5: Lower and upper bounds (in %) of the critical zones for SM2 (direction 1)

Bridge length	Effect 1	Effect 2	Effect 3	Effect 4	Effect 5	Effect 6
20 m	50-110	30-102.5	35-102.5	50-107.5	30-100	40-100
30 m	50-110	35-115	40-107.5	45-110	25-110	45-105
40 m	45-117.5	10-145	30-115	35-115	25-110	45-105

The extrapolated values obtained using the full simulations and simplified model 2 are presented in a table in Appendix O. The differences observed are between –8.5% and +11.3%, which demonstrates the good agreement between this model and the full simulations (within the content of the problem, it is commonly agreed that differences in the results between ±15% and ±10% reveal good to very good agreement). In conclusion, the results obtained using the simplified model 2 are good.

7.6.2 Simplified Model 3

Another step in trying to simplify the initial simplified model is to avoid having to model the bivariate distribution of GVWs. Indeed, the derivation and then the use of this bivariate distribution do not make the model very manageable. The same idea as that described in the simplified model for the bi-directional traffic was adopted here: that is, to use the cumulative density function of the GVW of all the trucks. The only difference is that, in the case of unidirectional traffic, the CDFs have to be obtained per lane and not per direction. However, the computation of the CDFs is a much simpler task than that of deriving the bivariate distribution of GVWs. This third version of the simplified model is fundamentally a reproduction of that for bi-directional traffic, only with a small variation (i.e. the CDF of GVWs per lane). By doing so, the potential correlation between GVWs is ignored; however, by considering the CDF of GVW per lane separately rather than for both lanes together, reasonable accuracy should be achieved.

The simplified model 3 was calibrated for both directions simultaneously, using the same set of percentage values (and by switching the values for load effects 3/4 and 5/6 between the two directions). A good agreement was obtained for all load effects and bridge lengths considered, using a CDF level of 0.75 and a decay coefficient (DC) of 37kN for direction 1 (as illustrated in Figure 7-21). Slightly lower values were required for direction 2 (CDF level of 0.72 and DC of 35 kN); this difference is explained by the fact that the flow rates are higher in direction 1 (349 trucks/hour against 314 trucks/hour for direction 2), which increases the probability of having a heavier truck in direction 1.

Even though the actual correlation between the weights of adjacent trucks was ignored, satisfactory accuracy was found using simplified model 3. This can be explained by the fact that SM3 accounts for the GVW cumulative density function per lane. In conclusion, this simplified model 3 is simpler than the other two models, yet very accurate. Table 7-6 presents the values of lower and upper bounds found with SM3. As for SM2, some of the upper bounds are equal to 115% (up to 150% for load effect 2) for the longer bridges (i.e. 40m bridges), to compensate for the presence of only two trucks where three trucks should be present. This set of values gives good agreement for both directions of traffic.

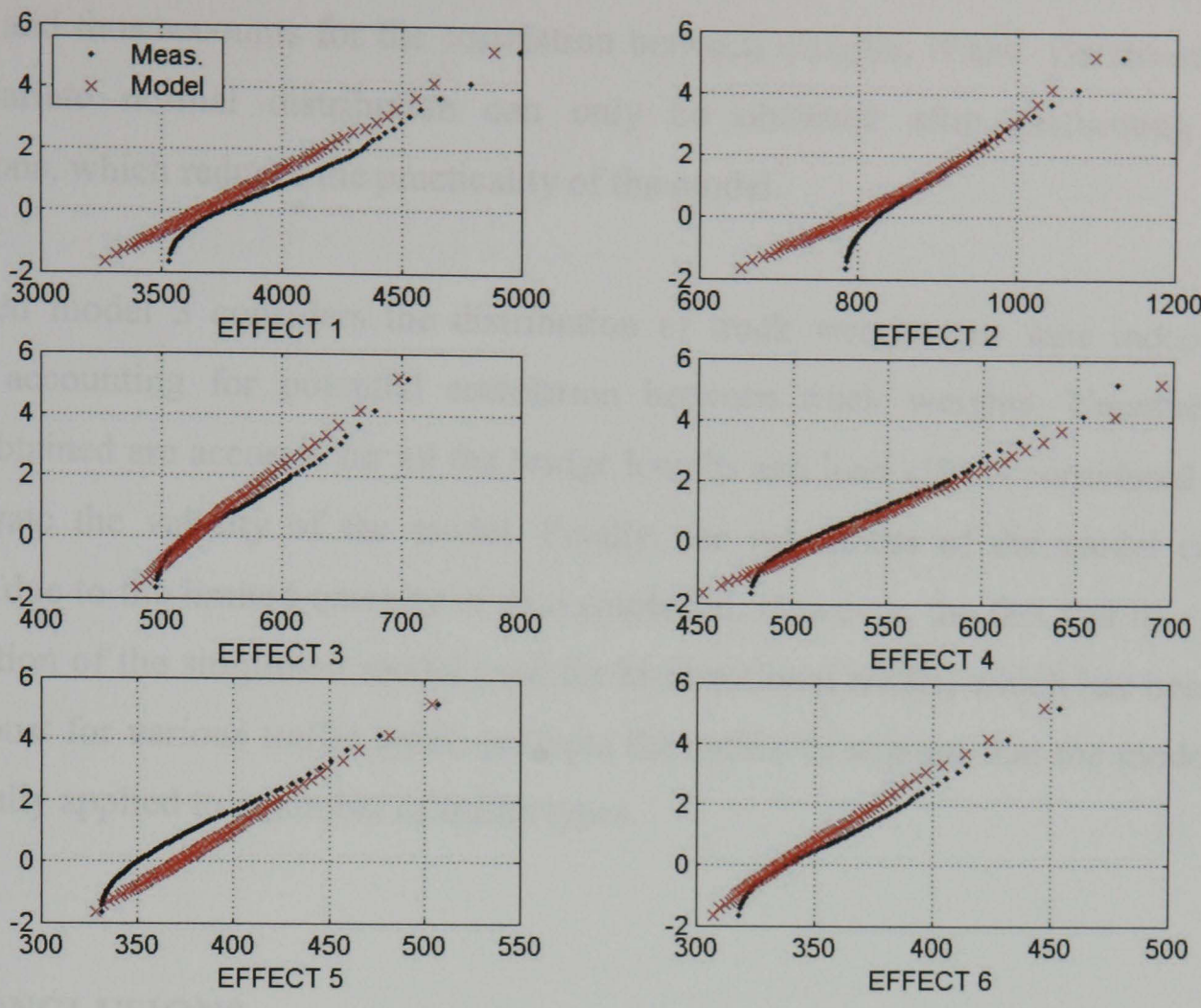

Figure 7-21: Results from SM3 for 20m bridges – Direction 1

Table 7-6: Lower and upper bounds (in %) of the critical zones for SM3 (direction 1)

Bridge length	Effect 1	Effect 2	Effect 3	Effect 4	Effect 5	Effect 6
20 m	100-105	70-100	80-100	95-100	70-100	80-100
30 m	100-105	90-115	90-100	95-100	70-100	90-100
40 m	100-110	80-150	100-110	100-100	70-100	95-95

The differences between the extrapolated values are between –9.2% and +7.9%; again, these values are reasonably small and confirm the good visual agreement found during the calibration process. The detailed results can be found in Appendix N.

7.6.3 Summary

Simplified models 2 and 3 have both shown good agreement when compared to the measured values for all the bridge lengths and load effects considered. Simplified model 2

uses the bivariate normal distribution derived from the measured data to model the truck weights and thus accounts for the correlation between weights, if any. On the other hand, this bivariate normal distribution can only be obtained after performing the full simulations, which reduces the practicality of the model.

Simplified model 3 considers the distribution of truck weights per lane independently, without accounting for potential correlation between truck weights. Nonetheless, the results obtained are accurate for all the bridge lengths and load effects considered and thus demonstrate the validity of the model. Finally, the robustness of the model cannot be assessed due to the limited quantity of data employed. However, the fact that this model is a replication of the simplified model used for bi-directional traffic, which has been shown to be robust for various traffic types, prompts the author to suggest that the model can be successfully applied to a number of traffic types.

7.7 CONCLUSIONS

The study of traffic loadings on relatively short bridges under unidirectional traffic conditions was the subject of this chapter. The analysis was restricted to two parallel lanes of traffic on 20 to 40m bridges. In a first part, Weigh-In-Motion data have been described and the relevant traffic characteristics have been modelled. Then full simulations have been performed on a number of traffic files and representative load effect values obtained for various bridge lengths and influence lines. The detailed analysis of the results from the full simulations enabled the characterisation of critical loading events, which in turn formed the basis for the development of a simplified model. This model was intended to reproduce the critical loading events as accurately as possible based on the knowledge of the site-specific characteristics (distribution of headways, speeds, etc.). In so doing, the bivariate distribution of GVWs for the trucks involved in the loading events has been derived. The results obtained were satisfactory for most of the load effects for 20 and 30m bridges but inadequate for the 40m bridges.

Subsequently, two other simplified models were developed, aiming at improving on the accuracy to cover all the bridge lengths and load effects considered. The results obtained were good and demonstrate the validity of these models. In particular, simplified model 3 is shown to be simple to employ and yet accurate (even though it did not take into account

potential correlation between the weights of adjacent trucks). The data used in the full simulations and in the development of the models were too limited to draw conclusions on the robustness of the model. However, based on the results of the preceding chapter in which a model similar to simplified model 3 was shown to be robust, it is suggested by the author that simplified model 3 could be successfully applied to other traffic types.

Chapter 8

CONCLUSIONS

Chapter 8 CONCLUSIONS

8.1 INTRODUCTION

In the introduction of this thesis, it was explained that the assessment of existing bridges is important for road authorities. Also, design codes were shown to be over conservative when applied to bridge assessment since they allow for uncertainty about the future loading and resistance of a structure. There was therefore a need for new methods that consider site-specific traffic loads as a function of parameters describing the bridge and traffic. The consideration of site data greatly reduces uncertainty and facilitates a more accurate assessment. In the case of road bridges, one of the most important sources of uncertainty is that associated with traffic loading.

The subject of this thesis was thus the analysis and modelling of relatively short existing bridges subjected to imposed traffic loading. In order to do so, a number of objectives were defined:

- To show how Weigh-In-Motion data can be utilised in an appropriate modelling of the traffic characteristics required for the generation of artificial traffic files and for the study of traffic loading on bridges.

- To analyse the critical loading situations due to imposed traffic on existing 2-lane bridges under various traffic conditions; namely, for a number of effects (moment and shear), bridge configurations (i.e., different bridge type and length) and traffic configurations (i.e., unidirectional and bi-directional).

- To develop site-specific simplified models able to reproduce the critical loading situations previously observed whilst keeping these models accurate, robust and easily applied by practicing engineers.

- To obtain the characteristic values for a number of load effects, bridge lengths and traffic types by extrapolating of the results from the full simulations of traffic files.

8.2 WEIGH-IN-MOTION DATA DESCRIPTION AND MODELLING

Following a description of some WIM data files recorded on the French network and described as representative of the European traffic, a number of essential observations were made:

- the traffic characteristics (e.g., GVW distribution, truck configuration and traffic intensity) vary significantly between sites, or even between directions for a given site;
- the vast majority of heavy trucks consist of 4/5- axle trucks of the same vehicle type (2-axle tractor + 2/3-axle semi-trailer);
- the weight distribution of this truck type changes with its gross vehicle weight: the back of the truck getting heavier; also, the weight distribution between the axles is known with more accuracy as the GVW increases.

The static effects of traffic actions have been studied through the use of influence lines and influence responses. The influence lines characterising the load effects represent a variety of shapes and slopes that can be considered as representative for this type of bridge (i.e. 20 m to 40 m long). The introduction of the concept of influence response of a bridge to a truck type facilitates the prediction of the largest possible effect due to a truck (of known geometry). Indeed, knowing which vehicle type a given truck corresponds to, and knowing its GVW, the influence response provides the maximum possible effect that this truck induces and its exact location in order to induce that maximum effect. In addition, the sensitivity of the influence responses to the various vehicle types confirmed that, the steeper the influence line and the shorter the bridge, the more sensitive the influence response was.

Finally, the findings from the two previous sections along with some suitable modelling techniques enabled the determination of statistical distribution parameters that are used to model accurately the traffic characteristics. For example, the GVW distributions were modelled using a linear combination of normal distributions, the parameters of which were optimised through an iterative process enabling a good overall fit to the empirical distribution as well as a good fit towards the right tail of the distribution (which clearly is the crucial part in the study of traffic loading). Also, the various truck types corresponding to a truck class (i.e. same number of axles) can be modelled by a single truck type, representative of this class of trucks in terms of GVW distribution and frequency.

8.3 GENERATION AND SIMULATION OF TRAFFIC FILES

The two programs, GENERATETRAFFIC and SIMULTRAFFIC, used in the next chapters for the analysis and the development of models for site-specific traffic loading on short bridges, have been presented and explained. First, the program GENERATETRAFFIC was developed in order to generate traffic files using traffic characteristics derived from measured WIM data. By combining the characteristics from different measured traffics (e.g. traffic intensity and traffic weight), the generation of artificial, but realistic, traffic files was possible. All the truck and traffic characteristics employed in these traffic files were generated using the modelled distributions derived in the preceding section.

Then the development of the program SIMULTRAFFIC was addressed. This program enables the passage of any traffic file on a bridge of specified length whilst calculating the effect induced in the structure for any load effect considered. For every bridge length and load effect studied, the program records the maximum load effect value corresponding to every crossing event identified (i.e. more than one truck being present on the bridge at a point in time). In addition, the details of the critical loading situations are recorded and outputted for later analysis. The program has been validated through the comparison of its results with the results from CASTOR, a well-established program (which has been used, for example, in the studies for the recalibration of the Eurocode).

8.4 BI-DIRECTIONAL TRAFFIC ANALYSIS AND MODELLING

Relatively short bridges (20 to 40 m long) subjected to two opposing lanes of traffic were studied. Data files corresponding to a period of one week of traffic were generated for nine different traffic types (corresponding to nine combinations of traffic weight and intensity). Full simulations were performed for all these traffic files; the results from ten distinct files were regrouped into sets representing a period of ten weeks of traffic each. To account for the inherent variability in traffic data, the values corresponding to ten sets of results were averaged in order to obtain representative values for the traffic type considered. The validity of this assumption has been verified by comparing the average of the extrapolated values with the results of extrapolating data made up from averaged effects from the different sets. Typical critical loading events were also derived for each bridge length considered, based upon the results of the full simulations. In addition, a formula to predict

the number of meeting events (i.e., two trucks from the two opposing lanes meeting on the bridge) as a function of the site-specific characteristics (i.e., flow rates, bridge length, average truck length and speed) has been derived and successfully validated against the measured number of meeting events.

From the full simulations, distributions of maximum load effect values were obtained and Gumbel distributions of extreme values were then fitted to the tail of those distributions for each of the traffic types studied. A method for estimating good initial values for the parameters of the extreme value distribution based on Castillo (1988) was employed; these initial estimates were then optimised using a weighted least-squares technique to obtain a good fit between the Gumbel distribution of extremes and the distribution of measured maximum effects. This combined approach proved to be fast and efficient. Extrapolated values corresponding to a 1000-year return period were then calculated using the Gumbel distribution and its optimised parameters.

A detailed analysis of the extrapolated values revealed that the dominant parameter was unsurprisingly the traffic weight, although its influence could be significantly reduced by the geometry of the representative trucks for the site considered. Indeed, for relatively short bridges, the exact position and weight of every axle is most significant, thus balancing the importance of the truck weights. The significance of the representative truck geometry should therefore be emphasised when considering the actual importance of the traffic weight since the latter depends on the former. In the same way, the influence of the traffic intensity is limited by the maximum length of the bridges studied. Indeed, for most of the load effects treated, the critical loading events consist of two trucks only; therefore the traffic intensity does not affect the magnitude of the extrapolated values. For the other load effects, sensitive to the presence of more than two trucks, the traffic intensity has a significant influence for bridges above 30 m.

A site-specific simplified model was developed in order to reproduce the critical loading events without having to perform full simulations. The model utilises site-specific data, such as: the cumulative density function of truck weights, per direction, and the configuration of a representative truck for the critical loading events (typically a 5-axle truck - 2-axle tractor + 3-axle trailer type). In essence, the simplified model generates pairs of heavy trucks and places them at a critical location for the load effect and bridge length considered using the appropriate influence response. The use of the influence response

makes it possible to express the critical location of a truck as a percentage of its maximum possible effect. This approach offers two clear advantages: the calculation of the load effect induced by a particular truck is straightforward and the effect induced by a given truck can be forced to exceed its theoretical maximum value if required (which is the case when 3-truck events are represented by two trucks only).

The model has been calibrated against the results of the full simulations for the nine intensity/weight combinations studied by plotting the modelled effects versus the measured effects on Gumbel probability paper. The validation of the model has been achieved by comparing the extrapolated values obtained using the results from the full simulations to those from the simplified model. The differences observed between the extrapolated values were reasonably small and demonstrate the validity and the accuracy of the model. Furthermore, the good agreement observed for the various traffic types shows the robustness of the simplified model. Finally, the relative inaccuracy observed for one of the load effects can be explained and could be reduced by modifying the model, which, however, would become more complex.

8.5 UNIDIRECTIONAL TRAFFIC ANALYSIS AND MODELLING

Next was the study of traffic loadings on relatively short bridges under unidirectional traffic conditions; the analysis was restricted to two parallel lanes of traffic on 20 to 40 m bridges. First, Weigh-In-Motion data were described with a view towards modelling the relevant traffic characteristics for later use. The generation of artificial traffic files was demonstrated to be a more complex problem in this traffic configuration because of the dependency between the two adjacent lanes of traffic. Although methods exist in the literature, the specific data required for these methods were not available in this study. Instead, slight alterations were applied to available measured arrival times using randomly generated hundredths of seconds and a number of distinct traffic files were thus obtained. Full simulations were then performed for all the traffic files and representative load effect values obtained for various bridge lengths and influence lines by averaging the effects obtained for each individual traffic file.

In a similar fashion to the bi-directional traffic study, extrapolated values were determined based upon the maximum load effects obtained in the full simulations. The effect of the

truck weights and truck configuration on the extrapolated values was assessed: the truck weight has unsurprisingly a crucial influence, but again, needs to be considered together with the truck geometry (which also has a significant effect for short bridges). The effect of the traffic intensity could not be assessed due to the limited data utilised. However, the author suggests that similar conclusions as previously drawn would apply, i.e., that the traffic intensity only has an important effect for certain load effects (sensitive to the presence of more than two trucks) and for bridges above 30 m.

The detailed analysis of the results from the full simulations enabled the characterisation of critical loading events, which in turn formed the basis for the development of a simplified model. This model was intended to reproduce the critical loading events as accurately as possible based on the knowledge of the site-specific characteristics, among which were: headway distribution, speed distributions, flow rates in the passing lane as a function of the flow rates in the slow lane. Also, the bivariate distribution of GVWs for the trucks involved in the passing events has been derived. The results obtained using the simplified model were satisfactory for most of the load effects for 20 and 30m bridges but inadequate for the 40m bridges, as the model failed to reproduce the 3-truck events.

Subsequently, two other simplified models were developed, aiming at improving on the accuracy to cover all the bridge lengths and load effects considered. Simplified model 2 used the bivariate normal distribution derived from the measured data to model the truck weights, and thus accounts for the correlation between weights (if any), along with critical locations for the trucks. After calibration of the model, good agreement was found between the results from the full simulations and those from the model.

Simplified model 3 considered the distribution of truck weights per lane separately, without accounting for potential correlation between truck weights. Again, the trucks are positioned at a critical location in order to induce a substantial effect. Nonetheless, the results obtained were accurate for all the bridge lengths and load effects considered and thus demonstrated the validity of the model. Finally, the robustness of the model could not be assessed due to the limited data employed. However, the fact that this model is similar to the simplified model used for bi-directional traffic, which was shown to be robust for various traffic types, prompts the author to suggest that the model could be successfully applied to a number of traffic types.

8.6 OVERVIEW AND SUGGESTIONS FOR FUTURE WORK

Overall, the simplified model developed for bi-directional traffic and its equivalent for unidirectional traffic (referred to in this thesis as simplified model 3) have shown good agreement with the results obtained from the full simulations. These models are accurate, as they make use of site-specific traffic data, and are easily applied because of their relative simplicity. The robustness of the simplified model for bi-directional traffic has been demonstrated for a variety of traffic types. However, the robustness of the model for unidirectional traffic could not be assessed and features among the suggestions for future work:

- The simplified models should be further validated using data for a range of sites; the arrival times of the vehicles for that data should be recorded to the nearest hundredth of a second.
- The simplified model developed for bi-directional traffic could possibly be improved on for certain load effects and span lengths; for example, by accounting for the traffic intensity in the determination of the critical locations to reflect the sensitivity of the effect to the 3- or 4-truck events for longer spans.
- The loading situations made up of more than two trucks were shown to be critical and frequent for a number of load effects on bridges of 30 m or more in length (for high traffic intensities). Further research could include 40 to 60 m bridges and the development of specific models for the loading events involving more than two trucks.
- The loading situations inducing critical static effects being known, the next major step would be to account for the dynamic interaction between the bridge and the trucks, i.e., to include in the calculations the dynamic component of the effects induced in the structure. The use of instrumented bridges would clearly enable experimental data to be collected, data that can later be used to calibrate and validate models.

References

REFERENCES

- ADAMS, W.F., (1936), *Road traffic considered as random services*, J. Inst. Civ. Engrs., 4, pp 121-130.
- ANG, A. H. S. and TANG, W.H., (1975), *Probability concepts in engineering planning and design, Volume I – Basic principles*, John Wiley & Sons.
- ANG, A. H. S. and TANG, W.H., (1984), *Probability concepts in engineering planning and design, Volume II – Decision, risk and reliability*, John Wiley & Sons.
- BAKHT, B and JAEGER, L.G., (1988), *Bridge design for multiple presence of vehicles*, Engineering Research and Development Branch, Ontario Ministry of Transportation and Communications, Downsview Ontario. Research Record SRR 88-05.
- BAILEY, S.F., O'BRIEN E.G. and ZNIDARIC, A., (2000), *Updating traffic load models for the assessment of existing road bridges,* Proceedings of Bridge Management Four - Inspection, maintenance, assessment and repair, University of Surrey, UK.
- BAILEY, S.F. and HIRT, M.A., (1996), *Site-specific models of traffic action effects for bridge evaluation*, Recent advances in bridge engineering, evaluation, management and repair, Barcelona – Spain - 15-17 July 1996.
- BAILEY, S.F., (1996), *Basic principles and load models for the structural safety evaluation of existing road bridges*, Ph.D. Thesis No. 1467, Ecole Polytechnique Fédérale de Lausanne, Switzerland.
- BEZ, R. and HIRT, M.A., (1991), *Probability-based load models of highway traffic*, Structural Engineering International, 2, pp 37-42.
- BOOS, D.D. (1984), *Using extreme value theory to estimate large percentiles*, Technometrics, 26, pp 367-393.
- BENJAMIN, J.R. and CORNELL, C.A., (1970), *Probability, statistics, and decision for civil engineers*, Mc Graw - Hill.
- BIRAN, A. and BREINER, M., (1995), *MATLAB for engineers*, Wokingham: Addison-Wesley.
- BORSE, G.J., (1997), *Numerical methods with MATLAB: a resource for scientists and engineers*, Boston : London : PWS.

- BREIMAN, L., (1963), *The Poisson tendency in traffic distribution*, Annals of Mathematical Statistics, Vol. 34, Issue 1, pp 308-311.
- BRULS, A., CALGARO J-A., MATHIEU, H. and PRAT, M., (1996a), *ENV 1991 Part 3: The main models of traffic loads on bridges – Background studies*, Proceedings of IABSE Colloquium, Delft, The Netherlands, IABSE-AIPC-IVBH, 215-228.
- BRULS, A., CROCE, P., SANPAOLESI, L. and SEDLACEK, G., (1996b), *ENV 1991 Part 3: Traffic loads on bridges –Calibration of load models for road bridges*, Proceedings of IABSE Colloquium, Delft, The Netherlands, IABSE-AIPC-IVBH, 439-453.
- CAERS, J. and MAES, M.A., (1998), *Identifying tails, bounds and end-points of random variables*, Structural Safety, 20, pp 1-23.
- CASTILLO, E. (1988), *Extreme value theory in engineering*, Academic Press, San Diego, 1988.
- CASTILLO, E. and SARABIA, J.M, (1990*), Engineering analysis of extreme value data: selection of models*, ASCE, Journal of Waterway, Port, Coastal and Ocean Engineering, Vol. 118, No. 2, March/April, 1992, pp 129-146.
- CEN (1994), *ENV1 1991-3 Eurocode 1: Basis of design and actions on structures, Part 3: Traffic load on bridges*, European Prestandard ENV 1991-3, Draft N119, European Committee for Standardisation TC250, Brussels.
- CHAMBERLAND, L. and RUSSELL, J., (1995), *FORTRAN 90: a reference guide*, Prentice Hall, London: Prentice-Hall International.
- CHAN, T.H.T. and O'CONNOR, C., (1990a), *Wheel loads from highway bridge strains: field studies*, ASCE, Journal of Structural Engineering, Vol. 116, No 7, July, 1990, pp 1751-1771.
- CHAN, T.H.T. and O'CONNOR, C., (1990b), *Vehicle model for highway bridge impact*, ASCE, Journal of Structural Engineering, Vol. 116, No 7, July, 1990, pp 1751-1771.
- CHAN, T.H.T. and YUNG, T.H., (2000a), *A theoretical study of force identification using pre-stressed concrete bridges*, Engineering Structures, 23, 2000, pp 1529-1537.
- CHAN, T.H.T. and YUNG, T.H., (2000b), *Moving force identification using an existing pre-stressed concrete bridge*, Engineering Structures, 23, 2000, pp 1529-1537.

- CINLAR, E., (1975), *Introduction to stochastic processes*, Prentice-Hall, Englewood Cliffs, New Jersey.
- CREMONA, C., (2000), *Optimal extrapolation of traffic loads effects*, Structural Safety, 23, pp 31-46.
- CRESPO-MINGUILON, C. and CASAS, J.R., (1997), *A comprehensive traffic load model for bridge safety checking*, Structural Safety, Vol. 19, No. 4, pp 339-359.
- DARGAHI-NOURABY, G.R., (1989), *New method for prediction of extreme wind speeds*, ASCE Journal of engineering mechanics, Vol. 115, No 4, April 1989.
- DAS, P.C., (1997), In DAS, P.C. (Ed.), The Safety of Bridges, Thomas Telford, London, pp3-6.
- DAVENPORT, A.G. and HARMAN, D., (1975), *A statistical approach to the description of vehicle loads for limit state design*, Colloquium on Highway Bridge Loading, Cambridge, England, April 1975.
- DESROSIERS, R.D. and GRILLO, R.J., (1973), *Estimating the frequency of multiple truck loading on bridges*, Final report for project 71-1, Civil Engineering Dept, The University of Connecticut, Storrs, CT.
- ELLIS, T.M.R., PHILIPS, I.R. and LAHEY, T., (1994), *FORTRAN 90 Programming*, Wokingham: Addison-Wesley.
- EYMARD, R. and JACOB, B., (1989), *Un nouveau logiciel: le programme CASTOR pour le Calcul des Actions et Sollicitations du Trafic dans les Ouvrages Routiers*, Bulletin de Liasion 164, Laboratoire Central des Ponts et Chaussées, Novembre/Décembre 1989.
- FEKPE, E., (1995), *Evaluating truck weight regulatory policies*, Canadian Journal of Civil Engineering, 22, pp 1235-1239.
- FEPKE, E. and CLAYTON, A., (1995), *Prediction of heavy-vehicle weight distributions*, ASCE, Journal of Transportation Engineering, Vol. 121, No. 2, March/April, 1995, pp 158-168.
- FLINT, A.R. and JACOB, B., (1996), *Extreme traffic loads on road bridges and target values of their effects for code calibration*, Proceedings of IABSE Colloquium, Delft, The Netherlands, IABSE-AIPC-IVBH, 215-228.
- FU, G. and HAG-ELSAFI, O., (2000), *Vehicular overloads: load model, bridge safety and permit checking*, ASCE, Journal of Bridge Engineering, Vol. 5, No 1, February 2000, pp 49-57.

- GAZIS, D.C., (1974), *Traffic science*, John Wiley &Sons, New York
- GHOSN, M., (1979), *Probabilistic approaches to bridge design loads*, Transportation Research Board, Transportation Research Record 711, pp 14-23.
- GHOSN, M. and MOSES, F., (1985), *Markov renewal model for maximum bridge loading*, Journal of the Engineering Mechanics Division, ASCE, 111(9), pp 1093-1104.
- GHOSN, M., (2000), Development of truck weight regulations using bridge reliability model, ASCE, Journal of Bridge Engineering, Vol. 5, No. 4, November, 2000, pp 293-303.
- GHOSN, M. and MOSES, F., (2000), *Effect of changing truck weight regulations on U.S. bridge network*, ASCE, Journal of Bridge Engineering, Vol. 5, No. 4, November, 2000, pp 304-310.
- GOBLE, G.G., MOSES, F. and PAVIA, A., (1976), *Applications of a bridge measurement system*, Transportation Research Board, National Research Council, Washington D.C., Transportation Record 579, pp 36-47.
- GODA, Y., (1988), *Numerical investigations on plotting formulas and confidence intervals of return values in extreme statistics*, (in Japanese), Report of Port and Harbour Research Institute, Vol. 27, No. 1, pp 31-92.
- GODA, Y., (1992), *Uncertainty of design parameters from viewpoint of extreme statistics*, Journal of Offshore Mechanics and Artic Engineering, Vol. 114, May 1992, pp 76-82.
- HAIGHT, F.A., (1963), *Mathematical theories of traffic flow*, Academic Press, New York.
- HAHN, G. J. and SHAPIRO, S.S., (1967), *Statistical models in engineering*, John Wiley & Sons.
- HANSELMAN, D. and LITTLEFIELD, B., (1996), *Mastering MATLAB: a comprehensive tutorial and reference*, Upper Saddle River, N.J: London: Prentice Hall.
- HARMAN, D.J. and DAVENPORT, A.G., (1979), *A statistical approach to traffic loading on highway bridges*, Canadian Journal of Civil Engineering, 6, pp 494-513.
- HASOFER, A.M. and LIND, N.C., (1974), *Exact and invariant second-moment code format*, ASCE, Journal of the Engineering Mechanics Division, Vol. 100, February, 1974, pp 111-121.

- HASOFER, A.M. (1996), *Parametric estimation of failure probabilities, Mathematical models for structural reliability analysis*, CRC Press, 1996.
- HAYNES, L., (1997), In DAS, P.C. (Ed.), The Safety of Bridges, Thomas Telford, London, pp3-6.
- HERMAN, R. and WEISS, G., (1962), *Statistical properties of low density traffic*, Quart. Appl. Math., 20, pp 121-130.
- HOSHIYA, M. and MARUYAMA, O., (1987), *Identification of running load and beam system*, ASCE, Journal of Engineering Mechanics, 113, pp 813-824.
- JACOB, B., BRULS, FLINT, MAILLARD and MERZENICH, (1991), *Methods for the prediction of extreme loads and load effects on bridges*, Report of Sub Group 8, Eurocode 1 On Actions, Part 12, Traffic Loads on Bridges, August 1991
- JACOB, B. and MAILLARD, J.B., (1991), *Probabilistic extrapolation and maximum load effect prediction for bridge code calibration*, Proceedings of ICASP 6, Mexico, pp865-871.
- KASCHNER, R., HAARDT, P., CREMONA, C., CULLINGTON D. and DALY, A.F., (2000), *Bridge Management in Europe (BRIME)*, Proceedings of Bridge Management Four - Inspection, maintenance, assessment and repair, University of Surrey, UK.
- LAMAN, J.A. and NOWAK, A.S., (1997), *Site-specific truck loads on bridges and roads*, Proceedings of the Institution of Civil Engineers Transportation Division, 123, May, pp 119-133.
- LANCASTER, P. and SALKAUSKAS, K., (1986), *Curve and surface fitting: an introduction*, Academic Press: London.
- LARRABEE, R.D., (1978), *Stochastic analysis of multiple loads: load combinations and bridge loads*, Ph. D. Thesis, Massachusetts Institute of Technology, United States.
- LARRABEE, R.D. and CORNELL, C.A., (1979), *Upcrossing rate solution for load combinations*, ASCE, Journal of the Structural Division, January 1979.
- LEADBETTER, M.R., LINDGREN, G. and ROOTZEN, H., (1983), *Extremes and related properties of random sequences and processes*, Springer-Verlag, New-York.
- LIND, N.C., (1971), *Consistent partial safety factors*, ASCE, Journal of the Structural Division, Vol. 97, June, 1971, pp 1651-1669.

- MAES, M.A., DILGER, W.H. and BALLYK, P.D., (1992), *Extreme values of thermal loading parameters in concrete bridges*, Canadian Journal of Civil Engineering, 19, pp 935-946.
- MAES, M., (1995), *Tail heaviness in structural reliability*, Proceedings of ICASP 1995, CERRIA-ICASP, Paris.
- MAILLARD, J-B. and GORSE, J-F., (1989), *Charges extrêmes de traffic sur les ponts: estimations pour divers modèles de traffic aléatoire*, Bulletin de liaison du Laboratoire Central des Ponts et Chaussées, 162, Juillet-Août 1989.
- MARCUS, A.H., (1974), *Effect of stochastic traffic flow on perceived noise*, in Proceedings of the 6th International Symposium on Transportation and Traffic Flow Theory, University of South Wales, Sidney, Australia, pp 231-243.
- MELCHERS, R.E., (1999), *Structural reliability analysis and prediction*, John Wiley & Sons, 2nd Edition.
- MENZIES, J.B., (1997), *Bridge failures, hazards and societal risk*, in *Safety of Bridges*, pp 36-41.
- MILLER, A., (196?), *On the theoretical justification of the random queues model for road traffic flow*, Proc. Cambridge Philos. Soc.
- MOSES, F. and GHOSN, M., (1985), *A comprehensive study of bridge loads and reliability*, Report FHWA/OH85/005, OhioDOT.
- NAKAMURA, S., (1996), *Numerical Analysis and graphic visualisation with MATLAB*, Upper Saddle River, N.J: Prentice Hall PTR.
- NOWAK, A.S. and LIND, N.C., (1979), *Practical bridge code calibration*, ASCE, Journal of the Structural Divison, vol. 105, December, 1979, pp 2497-2510.
- NOWAK, A.S., (1995), *Calibration of LRFD bridge code*, ASCE, Journal of Structural Engineering, Vol. 121, No.8, August, 1995, pp 1245-1251.
- O'BRIEN, E.J., BAILEY, S.F., O'CONNOR, A.J., ENEVOLDSEN, I. and ZNIDARIC, A., (1998), *Bridge applications of Weigh-In-Motion*, Proceedings of 2nd European conference on Weigh-In-Motion of road vehicles, Lisbon, Portugal, pp209-219.
- O'BRIEN, E.J., SLOAN, T.D., BUTLER, K.M. and KIRKPATRICK, J., (1995), *Traffic load 'fingerprinting' of bridges for assessment purposes*, The Structural Engineer, Vol. 73, No. 19, October 1995, pp 320-324.

- O'BRIEN, E.J. and JACOB, B.A., (1996), *Applications of Weigh In Motion*, 3rd Slovenian Congress on Roads and Transport, Road & Transport Research Association of Slovenia, Bled, Slovenia, pp 417-425.
- O'CONNOR, C. and SHAW, P.A., (2000), *Bridge loads: an international perspective*, Spon Press : London.
- O'CONNOR, C. and CHAN, T.H.T., (1988), *Dynamic wheel load from bridge strains*, ASCE, Journal of Structural Engineering, 114, ST8, pp 1703-1723.
- O'CONNOR, A.J., O'BRIEN, E.J. and LOOV, R.E., (1998a), *A review of the current Ontario highway bridge design code*, 5th International Conference on Short and Medium Span Bridges, Calgary, Alberta, Canada, pp 983-994.
- O'CONNOR, A.J., JACOB, B., O'BRIEN, E.J., and PRAT, M., (1998b), *Effects of traffic loads on road bridges – Preliminary studies for the re-assessment of the traffic load model for Eurocode 1 Part 3*, Proceedings of 2nd European conference on Weigh-In-Motion of road vehicles, Lisbon, Portugal, pp231-242.
- O'CONNOR, A.J., (2001), *Probabilistic traffic load modelling for highway bridges*, Ph. Thesis, Trinity College, Dublin.
- O'CONNOR, A.J., (1998), *Manual for use of CASTOR-LCPC*, Submitted to the Laboratoire Central des Ponts et Chaussees (LCPC), March 1998.
- OLIVER, R.M., (1962), *Distribution of gaps and blocks in traffic stream*, Operations Res., 10, pp 197-217.
- PARZEN, E., (1960), *Modern probability theory and its application*, John Wiley & Sons.
- PRAT, M., (1997), *The use of road traffic measurements in bridge engineering, in Proceedings of the Mid-term seminar of WAVE*, Delft, The Netherlands, September 1997.
- PILLOT, D., (1994), *Analyse fine des trafics lourds*, (in French), The Science of the Total Environment, 169, pp 103-111.
- PRESS, W.H., TEUKOLSKY, S.A., VETTERLING, W.T. and FLANNERY, B.P., (1992), *Numerical recipes in FORTRAN 90: the art of parallel scientific computing*, 2nd Edition, Cambridge University Press, U.K.
- RESNICK, S.I., (1971), *Tail equivalence and its applications*, Journal of Applied Probability, 8, pp 135-156.
- RICE, S.O., (1944), *Mathematical analysis of random noise*, Bell System Technical Journal, Vol. 23, 1944, pp 282-332 and Vol. 24, 1945, pp46-156.

- ROCHESTER, T.A., (1997), In DAS, P.C. (Ed.), The Safety of Bridges, Thomas Telford, London, pp3-6.
- RUEGG, A., (1989), *Processus stochastiques avec applications aux phenomenes d'attente et de fiabilite*, Presses Polytechniques Romandes, Lausanne, Suisse.
- SCHILLILNG, R.J. and HARRIS, S.L., (2000), *Applied numerical methods for engineers using MATLAB and C*, Brooks/Cole – Thomas Learning, Pacific Grove, U.S.
- SMITH, I.M., (1995), *Programming in FORTRAN 90: a first course for engineers and scinentists*, Chichester: Wiley.
- TRB (Transportation Research Board), (1990), *Truck weight limits: issues and options*, Special report 225, Washington D.C.
- TUNG, C.C., (1969), *Response of highway bridges to renewal traffic loads*, ASCE Journal of the Engineering Mechanics Division, 95, pp 41-57.
- VROUWENVELDER, A.C.W.M. and WAARTS, P.H., (1993), *Traffic load on bridges*, Structural Engineering International, 3, pp 169-177.
- WILSON, T., POSTANS, R. and GARROD, G., (1983), *Lorry and coach overtaking on the motorway*, Traffic Engineering and Control, June/July 1983, pp 311-314.

Appendix A

DYNAMIC LOAD

Appendix A - DYNAMIC LOAD

Information on axle weights is an important factor for pavement and bridge designs. Traditional methods use 'weigh-bridges' to weigh stationary vehicles and vehicles running at a crawl speed. However, the traditional methods to acquire axle weights are expensive and subject to bias. This prompted the need to develop a method to acquire axle loads from unbiased samples of vehicles. The first system to weigh-in-motion was the one developed in 1952. Subsequently, many systems have been developed. However, these systems measure static axle loads only. Hoshiya & Maruyama (1987) developed a system to identify a moving force on a simply supported beam. O'Connor and Chan (1988) proposed an advanced weighing system that can measure both static and dynamic axle load from bridge strain responses.

More recently, Chan & Yung (2000a, 2000b) developed to technique to identify moving force using an existing pre-stressed concrete bridge. The model was calibrated using field measurements and a control vehicle. All bridge responses were acquired when only one vehicle was on the tested span. The authors found that the gross vehicle weights and static axle loads were identified accurately (with errors less than 5%). The pre-stressing effects have to be taken into account for an optimal precision. Also the results showed that the amplification factor between static axle load and dynamic axle load could be as high as 3. However, more studies need to be performed to study other type of trucks (e.g. 5-axle semi-trailer) and also to analyse the dynamic response when multiple presence of trucks occur.

The literature suggests that the dynamic amplification of vehicle loads depends on a wide range of factors such as: the natural frequency of the bridge, the velocity of the vehicle, the bridge damping, the bearing damping, the vehicle damping, the dynamic response of the vehicle suspension system, and the road roughness. This wide range of factors and the complexity involved in their modelling make it extremely difficult to develop an accurate, but yet realistic, dynamic model able to represent both bridge and truck dynamic behaviour. Chan & O'Connor (1998a) have determined the values of *impact fraction I* through field measurements and use it to calibrate a simple vehicle model that may be used for further impact studies. The impact fraction I is defined by:

$$I+1=\frac{M_{dynamic}^{max}}{M_{static}^{max}}$$ **Equation A-1**

They concluded that 'a suitable dynamic design vehicle would have sinusoidally varying dynamic axle loads of the order of ± 10% superimposed on the specified equivalent static loads'. Also, the frequency of the dynamic loads should be set equal to the bridge frequency, with dynamic components in phase with respect to time. It should be noted that their study is restricted to central bending moments in simply supported beams and with the case of single vehicles.

The dynamic factor is defined as the total dynamic response divided by the maximum static response. Since the dynamic response and the static response vary differently, a high impact factor may not be due solely to a high dynamic response. Chan & O'Connor (1998a) introduce a new term, the *dynamic moment ratio*, defined as the quotient of the maximum dynamic moment and the product of the span length by the sum all the axle loads:

$$DMR=\frac{M_{dynamic}^{max}}{L*\sum_{i=1}^{Naxles} w_i}$$ **Equation A-2**

The benefit of using the dynamic moment ratio instead of the impact factor is that it does not involve the equivalent static bending moment. Additionally, the dynamic moment can easily be recovered by multiplying the DMR by the product of the span length by the sum all the axle loads. In the study, 20 bridges (seven small composite concrete slab and steel girder bridges, six pre-stressed concrete bridges formed of pre-cast box girder deck units and seven pre-stressed concrete girder bridges), spanning from 9 to 32 m, are considered. The simple model used by the authors is the one described above; factors such as the road roughness and prior excitation of the vehicle are taken to be transmitted into the amplitudes and the relative phase angles between the loads (Chan & O'Connor 1998b).

Among the main results, it has been found that the product of the span length by the first natural frequency of the bridge, Lf, is constant for the different type of bridges and span lengths considered. Furthermore the constant of 120 is a reasonable approximation for most bridges. In the study of the effects of a single dynamic load, the authors notice that the peak of the bending moment does not occur at the same time as the peak of the

dynamic load component. There is a time difference between the two maxima corresponding to a phase difference. For a system of multiple axles, superposition applies and the value of the bending moment at any point along the bridge at any time will equal to the summation of the values of the bending moment at that point caused at that time by the loads taken separately. It can be further deduced that, for a system of axle loads, the highest bending moments will occur if the local peaks of the separate BM-versus-time curves coincide. The authors find that in many cases the largest total bending moment is likely to occur when the last load is at the highest maximum. In effect the bridge stores the damped bending moments from the earlier axle loads and adds them to the effects of the later axle load. The authors also examine the case of tandem and tridem. They come to the conclusions that, in the study of high-impact or high-dynamic moment ratios, the axles within a group can be replaced by a single axle acting at the centre of the group.

Finally the authors look at the prediction of the dynamic effects for bridges of various spans, based on typical trucks (e.g. 5-axle semi-trailer) represented as three-axle load system. The results show that the impact factor approaches a constant value as the span increases, which is also the case for the dynamic moment ratio. Also, the actual maximum dynamic bending moment is increasing with the span although the impact factor is decreasing. The reduction in the impact factor is due to the relative increase in maximum static bending moment due the smaller ratios of axle spacing to span, with the longer spans. Therefore, studies made with a ±10% dynamic component of axle load suggest that high dynamic effects may occur not only in short span bridges but also in bridges of longer span. This conclusion, however, depends on the probability of occurrence of the following parameters:

- the coincidence of load frequencies with the first natural frequency of the bridge;
- the amplitude of the dynamic component of load;
- the phase angle relating the dynamic loads from successive axles.

The above discussion only introduces a few elements among the vast field of dynamics effects due to traffic loads on bridges. However, these elements constitute a base for considering in more details the dynamics effects induced by the critical loading events for short to medium span bridges described in this thesis, typically two heavily loaded trucks (semi-trailer type). Indeed, the dynamic effects for such bridges are thought to be critical; however, further research need to be performed in that field as so far mainly single truck

event were considered, sometimes two-trucks events have been dealt with but the two trucks were single body trucks.

APPENDIX B

DESCRIPTION OF TRAFFIC DATA

Appendix B DESCRIPTION OF THE TRAFFIC DATA

Table B-1: Traffic composition (%) for all sites in terms of vehicle types 219
Figure B-1: Distribution of GVW as a function of truck class for Angers site 220
Figure B-2: Distribution of GVW as a function of truck class for Auxerre site 220
Figure B-3: Distribution of GVW as a function of truck class for A196 site 221
Figure B-4: Distribution of GVW as a function of truck class for A296 site 221
Figure B-5: GVW distribution of 3-axle trucks by vehicle type for Angers 222
Figure B-6: GVW distribution of 3-axle trucks by vehicle type for Auxerre 222
Figure B-7: GVW distribution of 3-axle trucks by vehicle type for A196 223
Figure B-8: GVW distribution of 3-axle trucks by vehicle type for A296 223
Figure B-9: GVW distribution of 4-axle trucks by vehicle type for Angers 224
Figure B-10: GVW distribution of 4-axle trucks by vehicle type for Auxerre 224
Figure B-11: GVW distribution of 4-axle trucks by vehicle type for A196 225
Figure B-12: GVW distribution of 4-axle trucks by vehicle type for A296 225
Figure B-13: GVW distribution of 5-axle trucks by vehicle type for Angers 226
Figure B-14: GVW distribution of 5-axle trucks by vehicle type for Auxerre 226
Figure B-15: GVW distribution of 5-axle trucks by vehicle type for A196 227
Figure B-16: GVW distribution of 5-axle trucks by vehicle type for A296 227
Table B-2: Axle Weights as a function of GVW for Vehicle Type 14 - Angers site 228
Table B-3: Axle Weights as a function of GVW for Vehicle Type 14 - Auxerre site 229
Table B-4: Axle Weights as a function of GVW for Vehicle Type 14 – A196 site (direction 1) 230
Table B-5: Axle Weights as a function of GVW for Vehicle Type 14 – A196 site (direction 2) 231
Table B-6: Axle Weights as a function of GVW for Vehicle Type 14 – A296 site 232
Figure B-17: Mean of Axle Weights for Vehicle Type 10 and 11 as a function of GVW for various sites .. 233
Figure B-18: Mean and Standard Deviation of Axle Weights for Vehicle Type 11 as a function of GVW for various sites 234
Figure B-19: Speed distribution as a function of number of axles – Angers site 235
Figure B-20: Speed distribution as a function of number of axles – A196 site 235
Figure B-21: Speed distribution as a function of number of axles – A296 site 236

Table B-1: Traffic composition (%) for all sites in terms of vehicle types

No. Axles	Veh. Type	Angers	Auxerre	A196	A296
2	1	0.0	0.0	0.1	0.3
2	2	3.4	3.7	0.3	0.9
2	3	4.9	3.8	1.3	1.7
2	4	10.3	4.4	3.0	3.9
2	5	10.1	10.6	9.4	9.9
3	6	0.9	0.8	0.6	0.7
3	7	2.8	1.3	0.8	1.3
3	8	1.5	0.5	0.2	0.4
4	9	0.7	0.1	0.0	0.0
4	10	20.4	6.5	1.5	2.7
4	11	9.2	18.3	11.4	9.5
4	12	1.0	1.5	3.9	6.0
4	13	6.0	5.1	1.8	1.6
5	14	24.1	36.8	53.6	47.8
5	15	0.1	0.0	3.1	4.6
5	16	3.6	5.2	5.9	5.7
5	17	0.8	0.7	1.5	2.0
6	18	0.2	0.9	1.4	0.5
6	19	0.0	0.0	0.2	0.3
6	20	0.0	0.0	0.0	0.0
6	21	0.0	0.0	0.0	0.0
Misc.	22	0.0	0.0	0.0	0.1

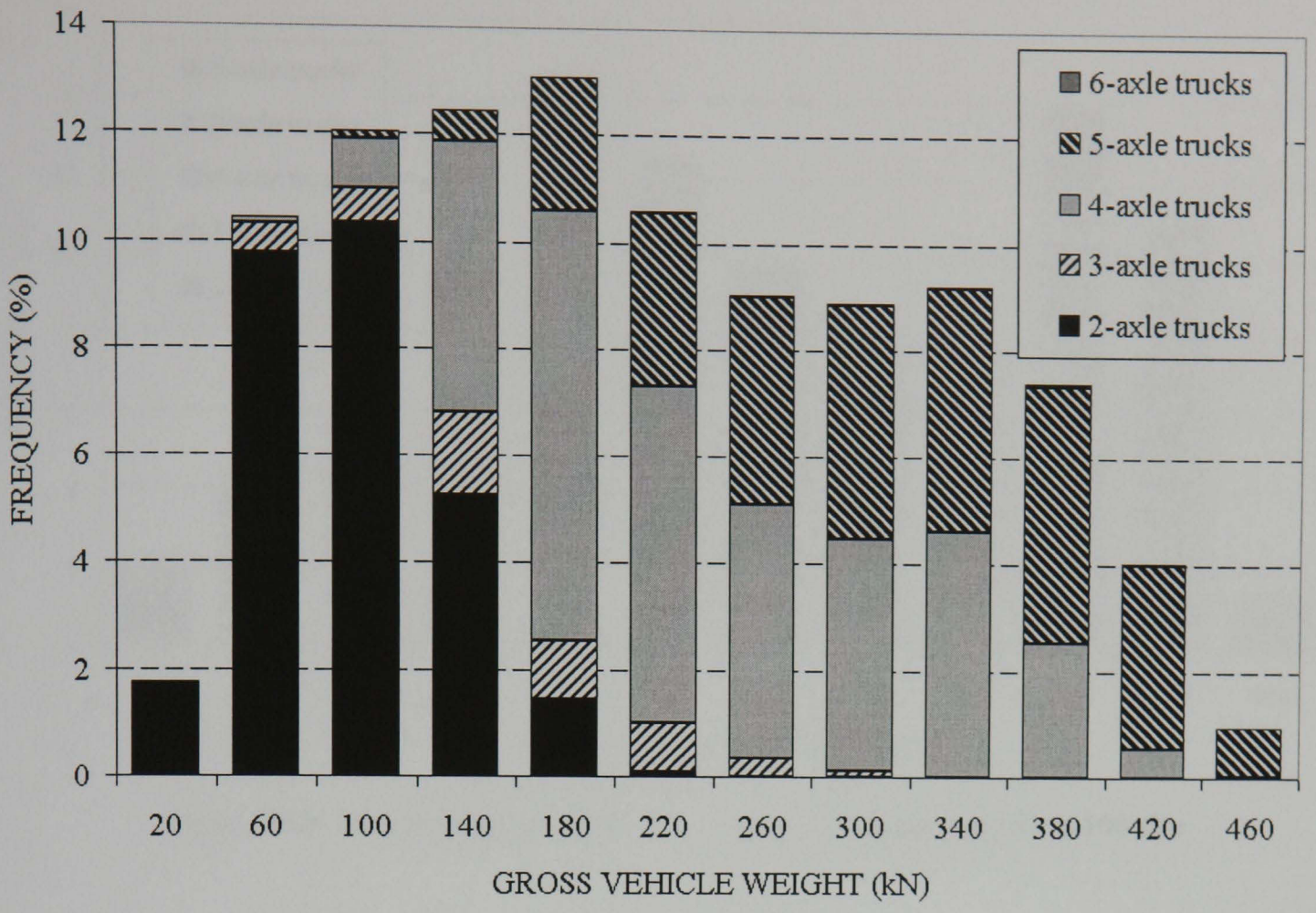

Figure B-1: Distribution of GVW as a function of truck class for Angers site

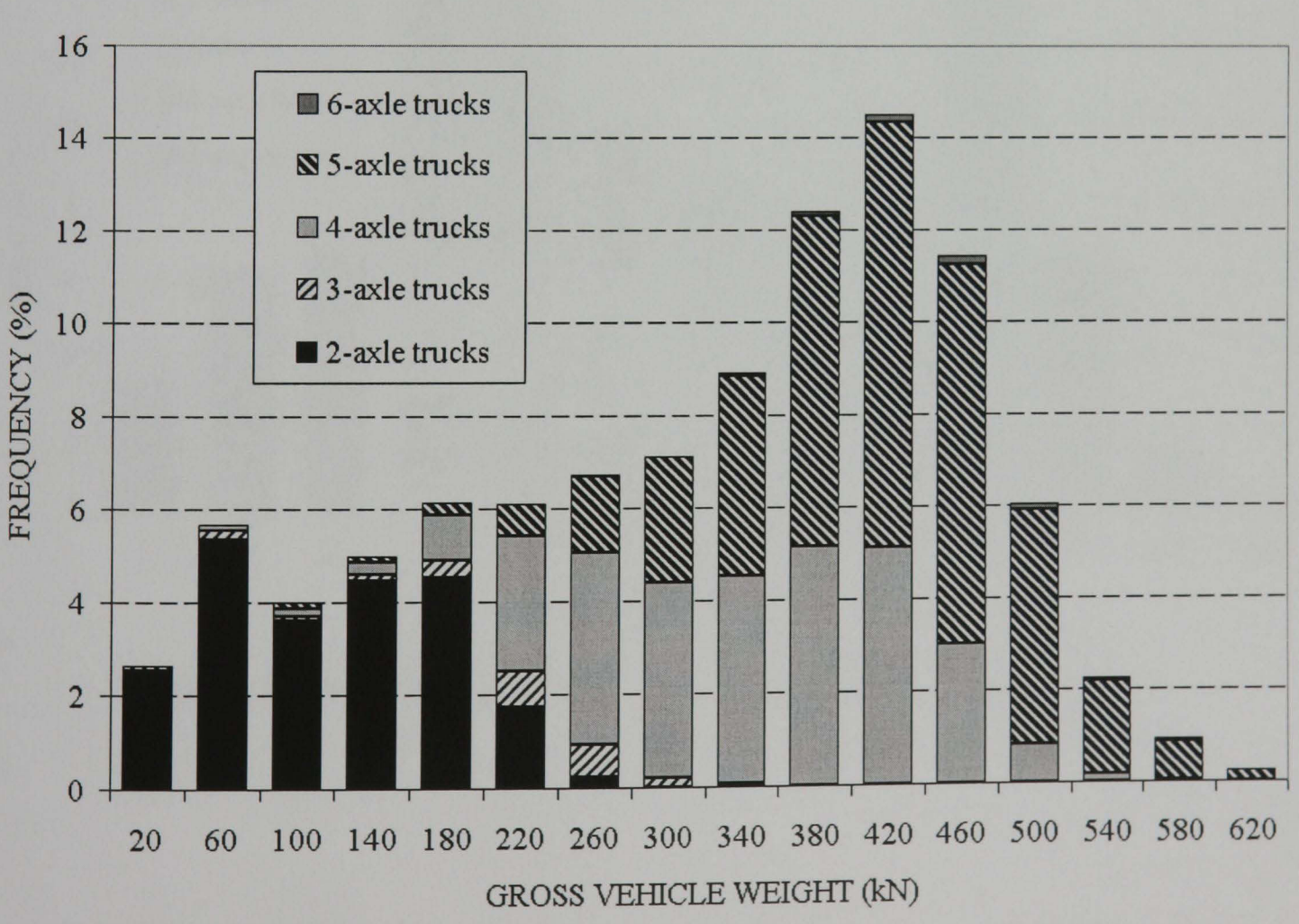

Figure B-2: Distribution of GVW as a function of truck class for Auxerre site

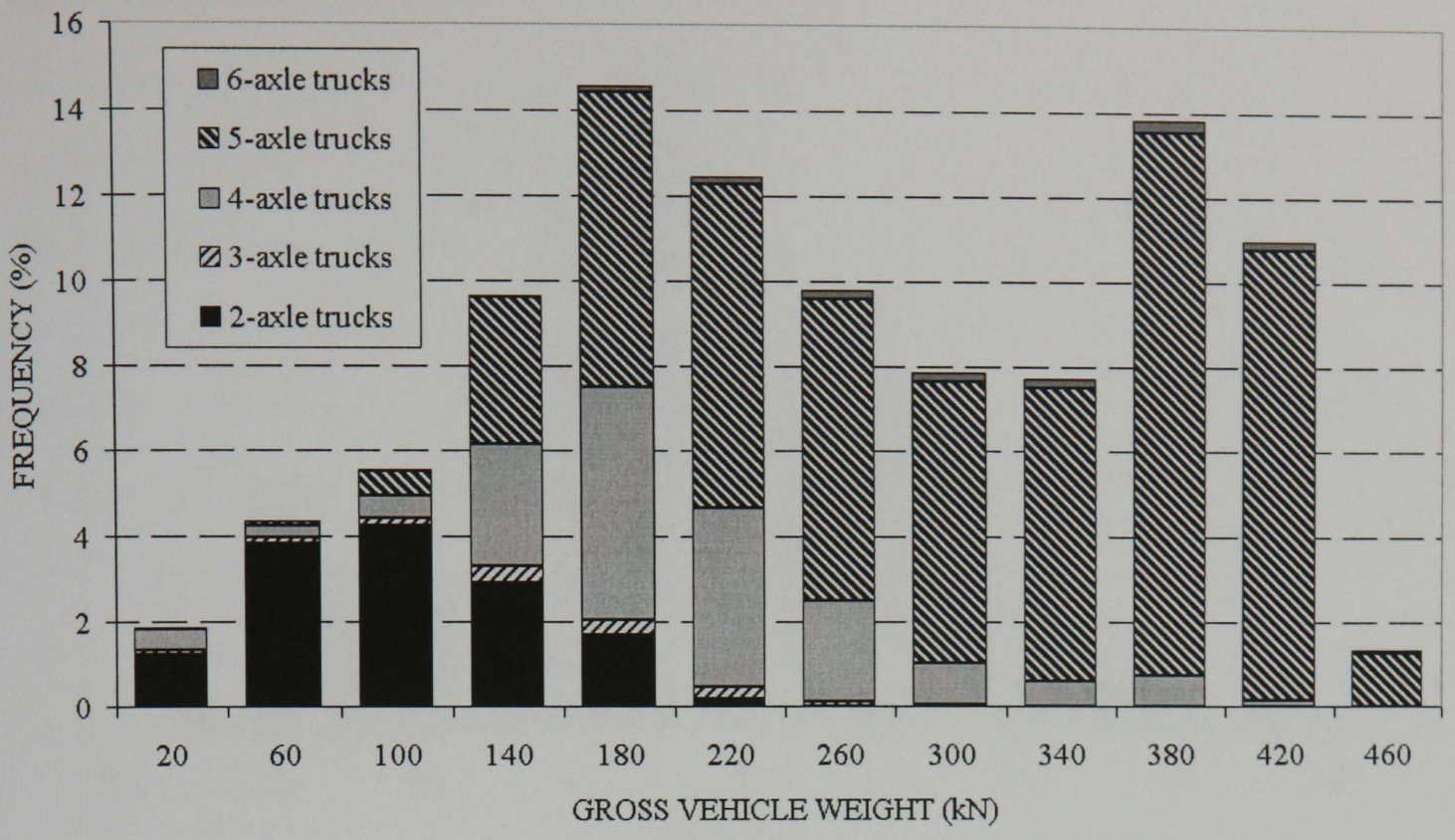

Figure B-3: Distribution of GVW as a function of truck class for A196 site

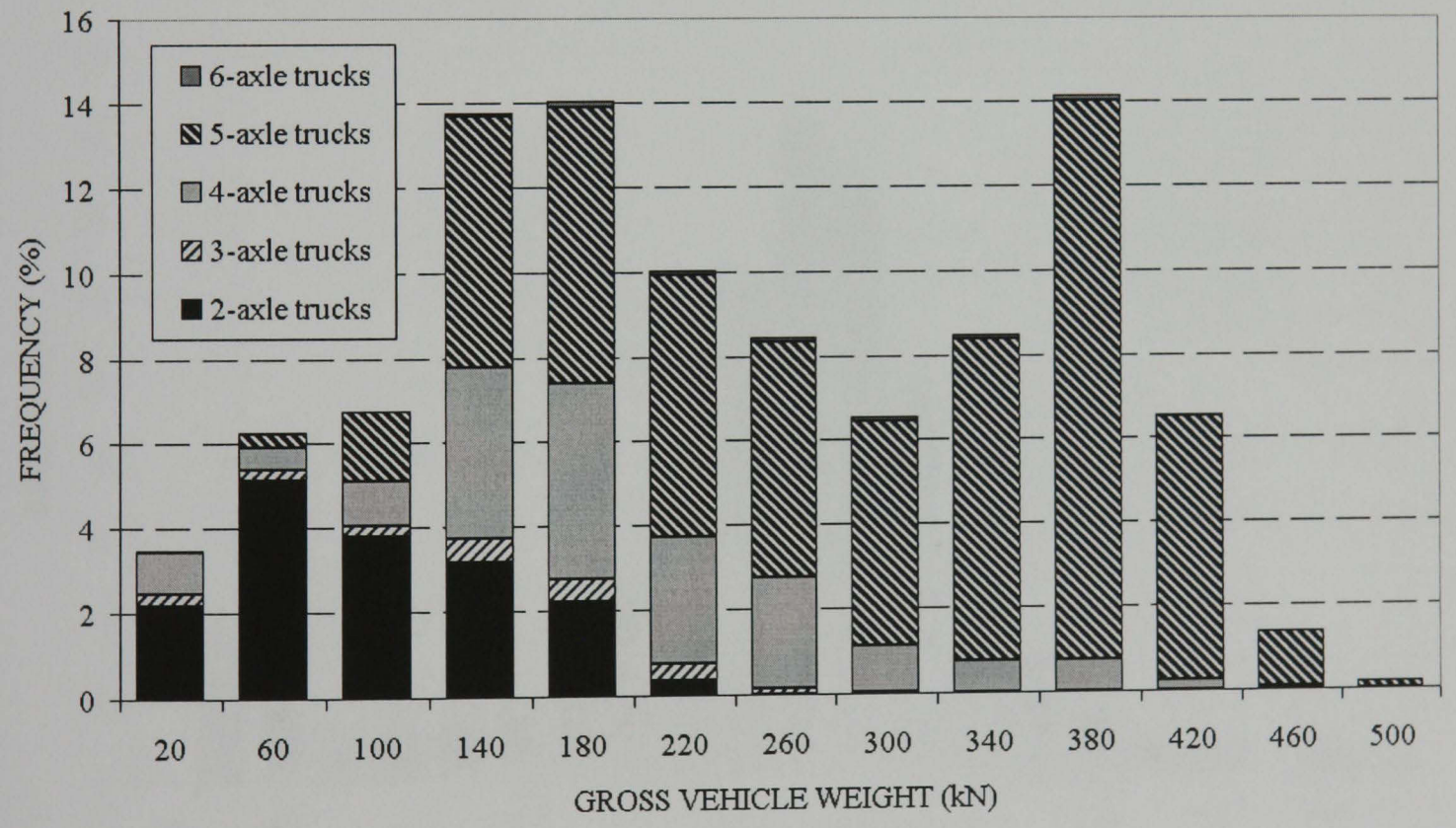

Figure B-4: Distribution of GVW as a function of truck class for A296 site

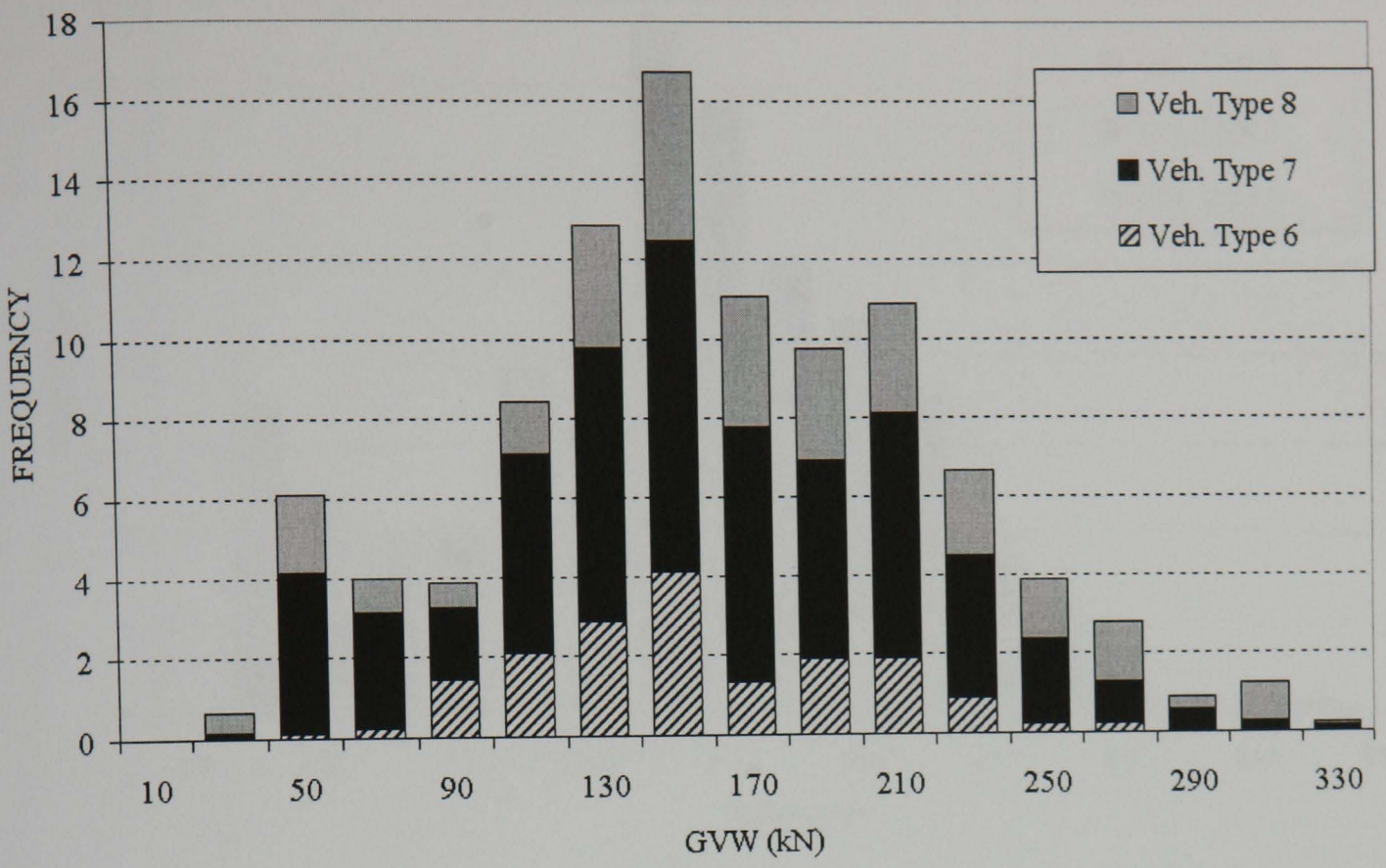

Figure B-5: GVW distribution of 3-axle trucks by vehicle type for Angers

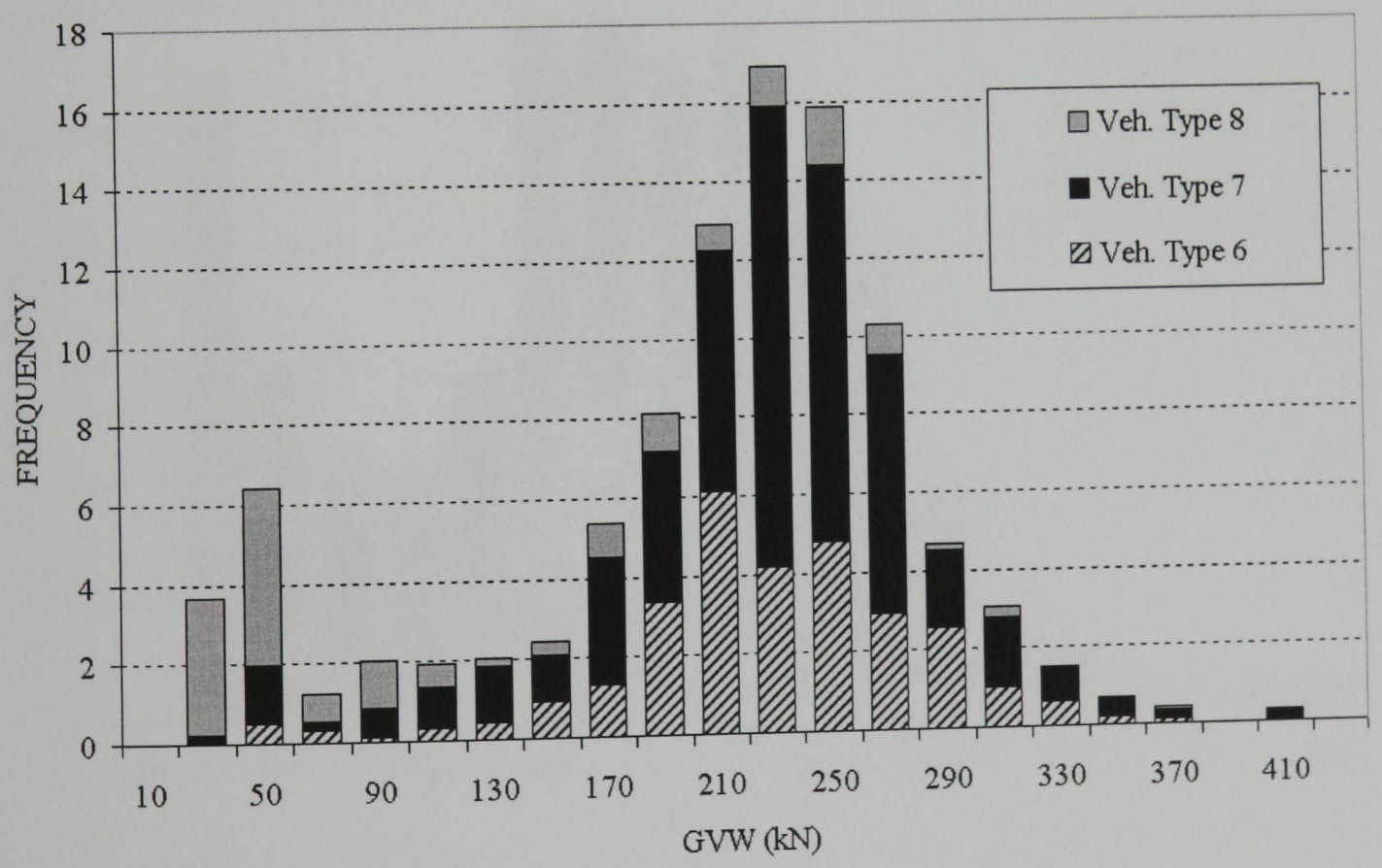

Figure B-6: GVW distribution of 3-axle trucks by vehicle type for Auxerre

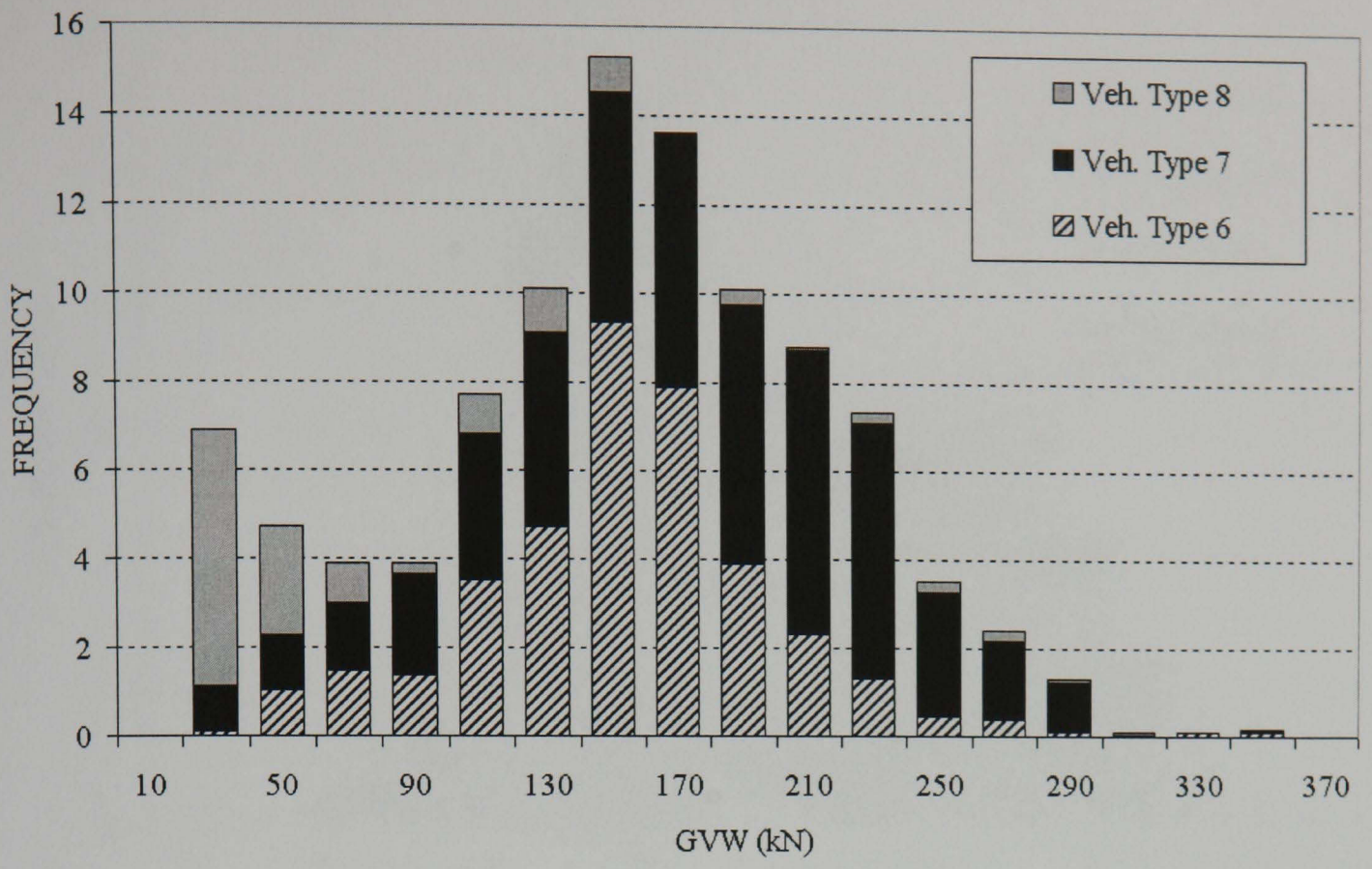

Figure B-7: GVW distribution of 3-axle trucks by vehicle type for A196

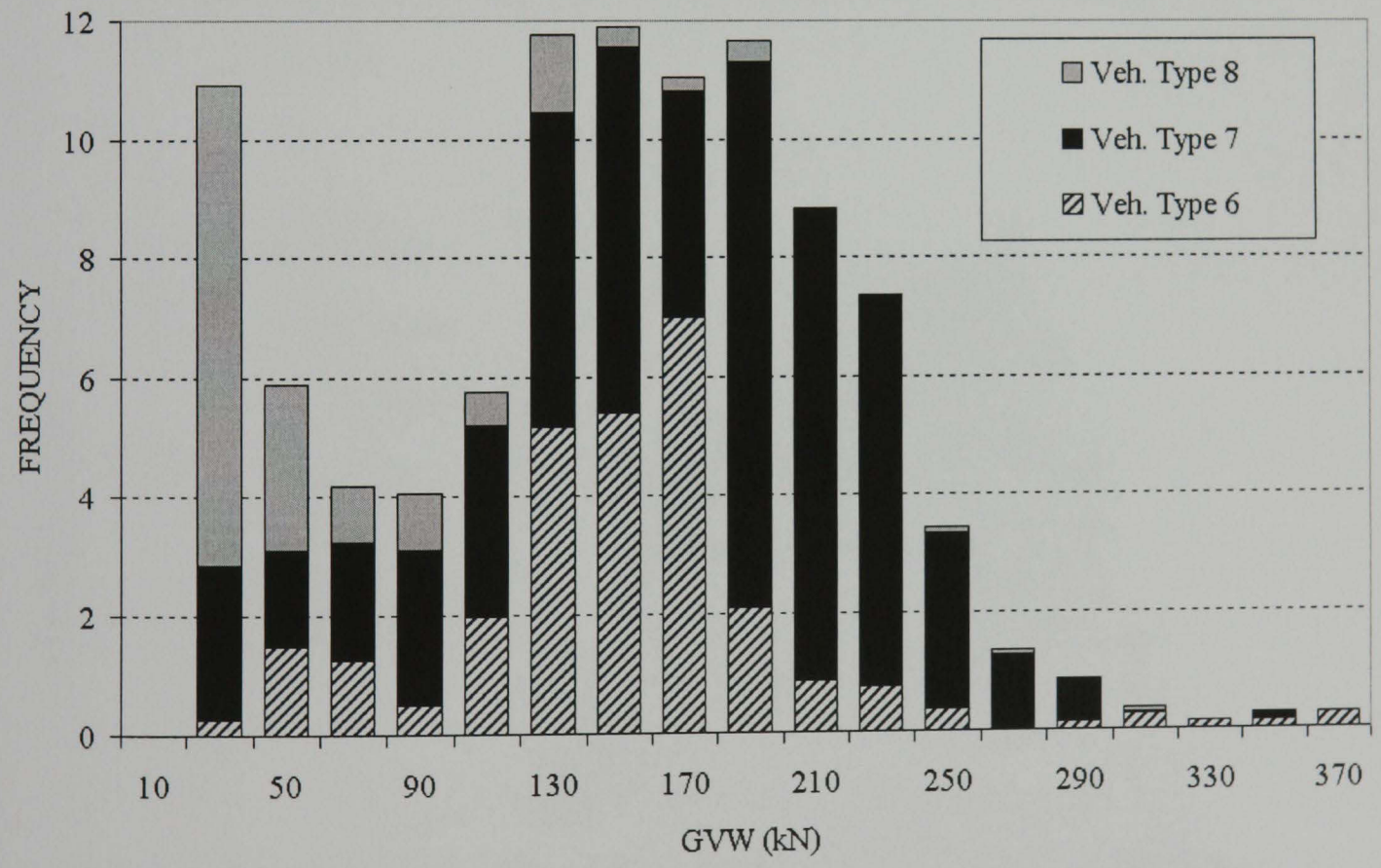

Figure B-8: GVW distribution of 3-axle trucks by vehicle type for A296

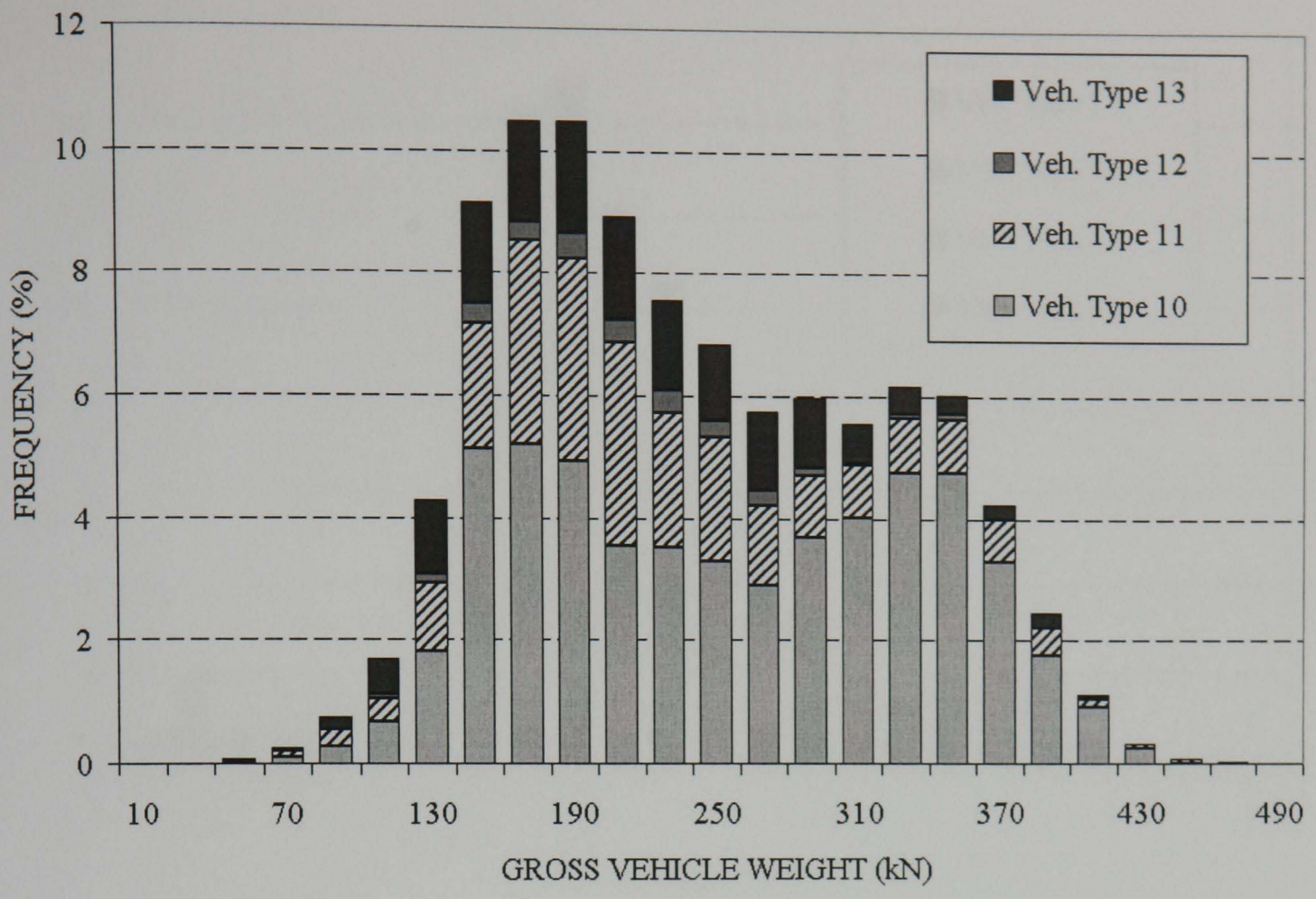

Figure B-9: GVW distribution of 4-axle trucks by vehicle type for Angers

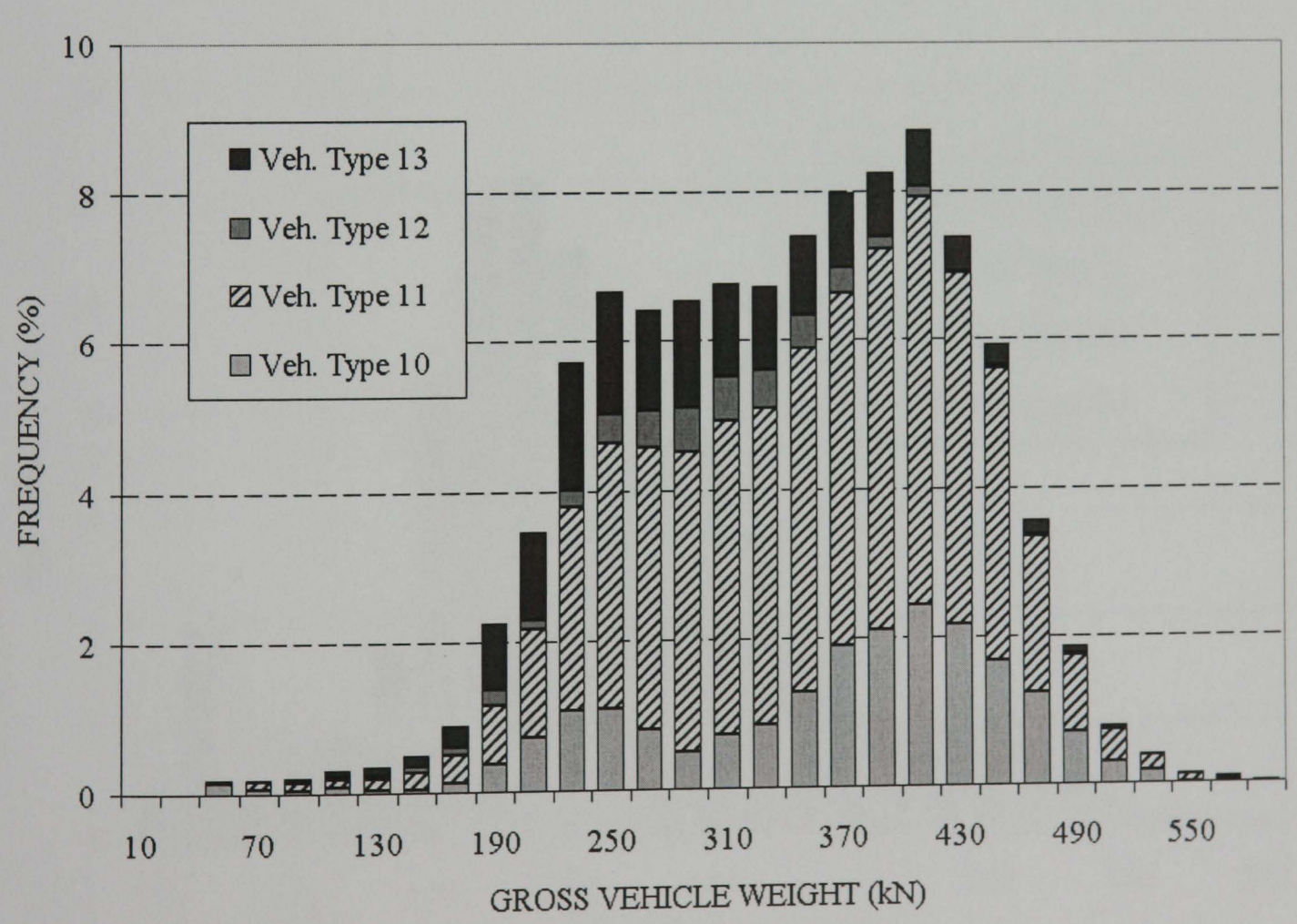

Figure B-10: GVW distribution of 4-axle trucks by vehicle type for Auxerre

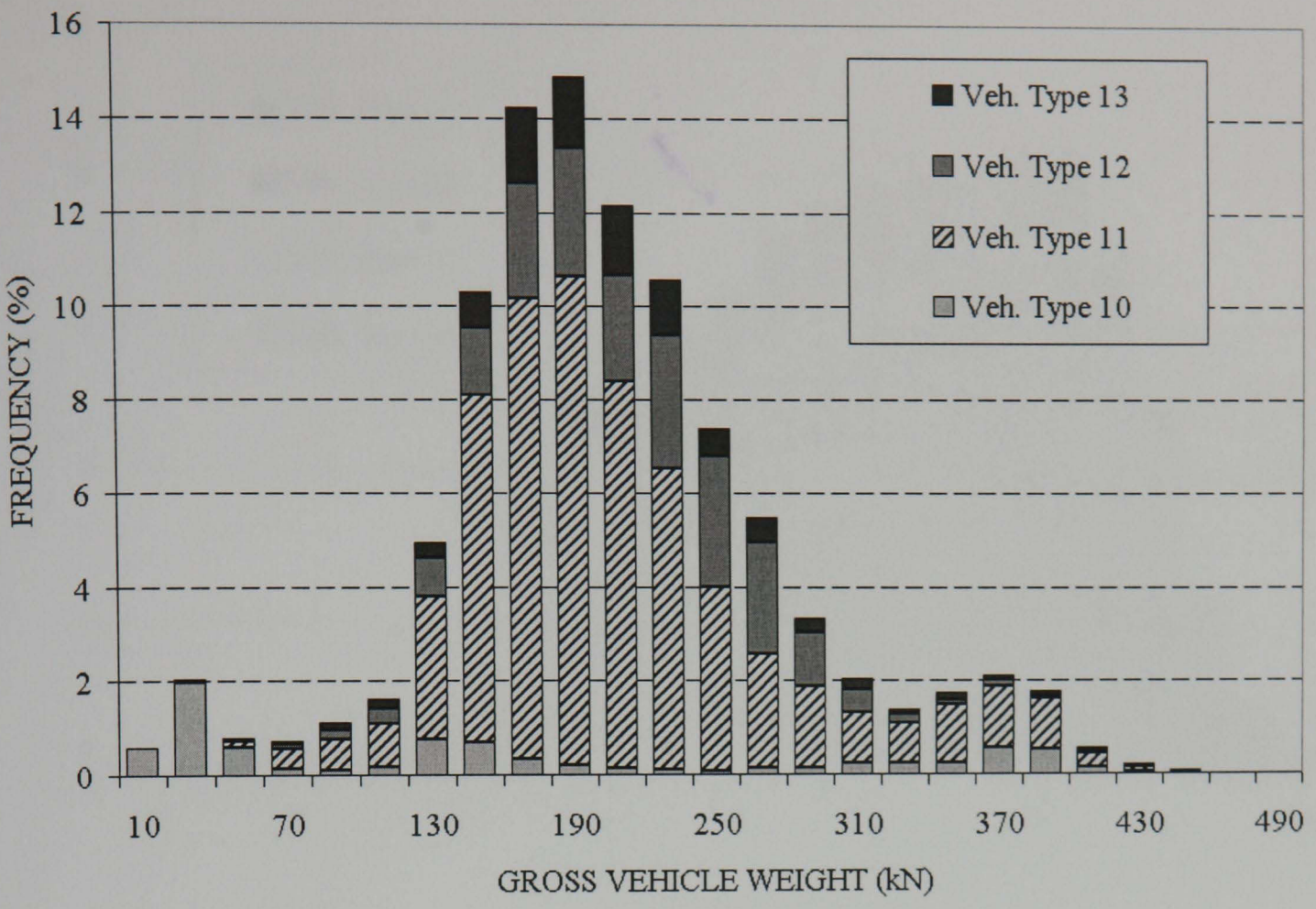

Figure B-11: GVW distribution of 4-axle trucks by vehicle type for A196

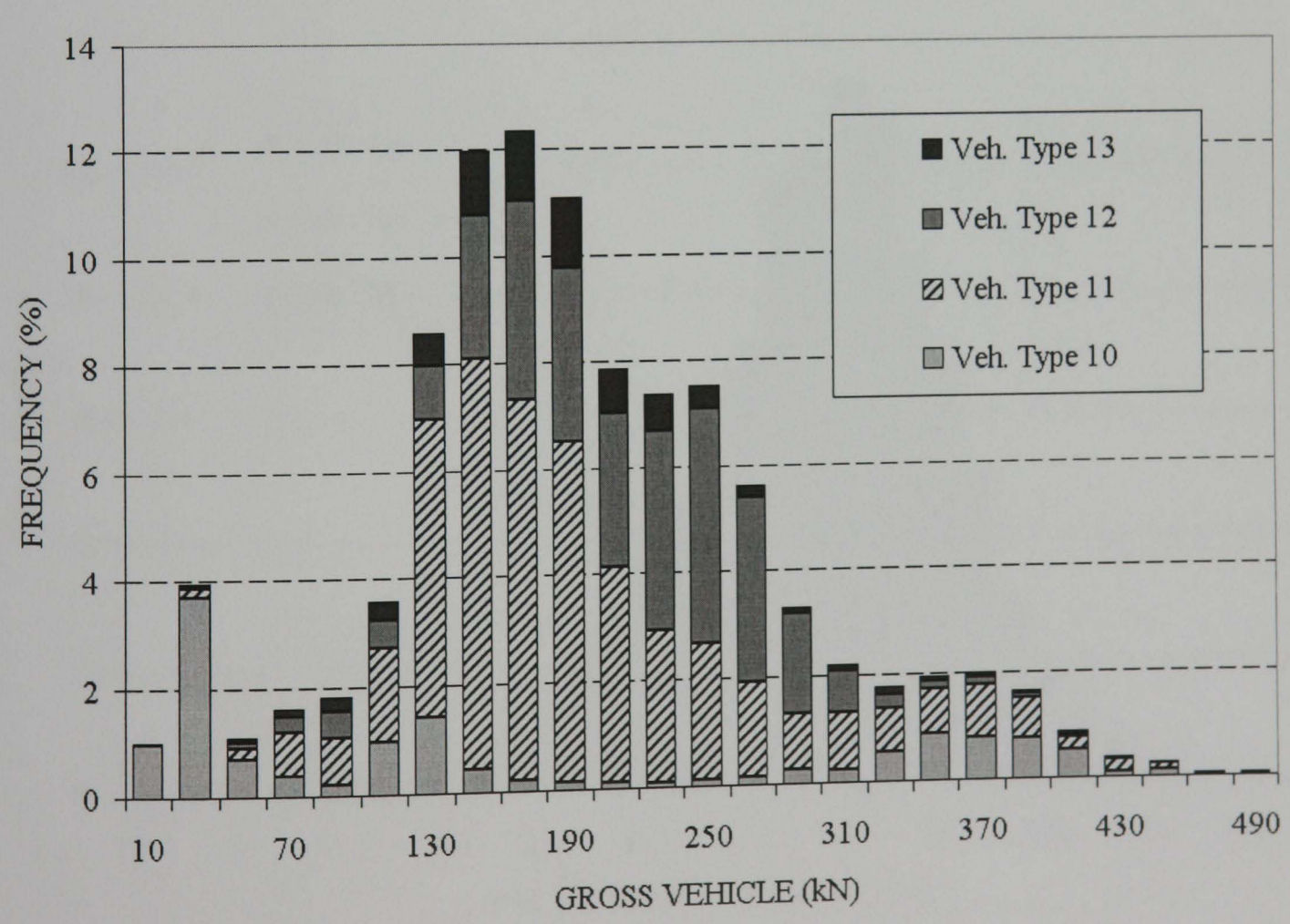

Figure B-12: GVW distribution of 4-axle trucks by vehicle type for A296

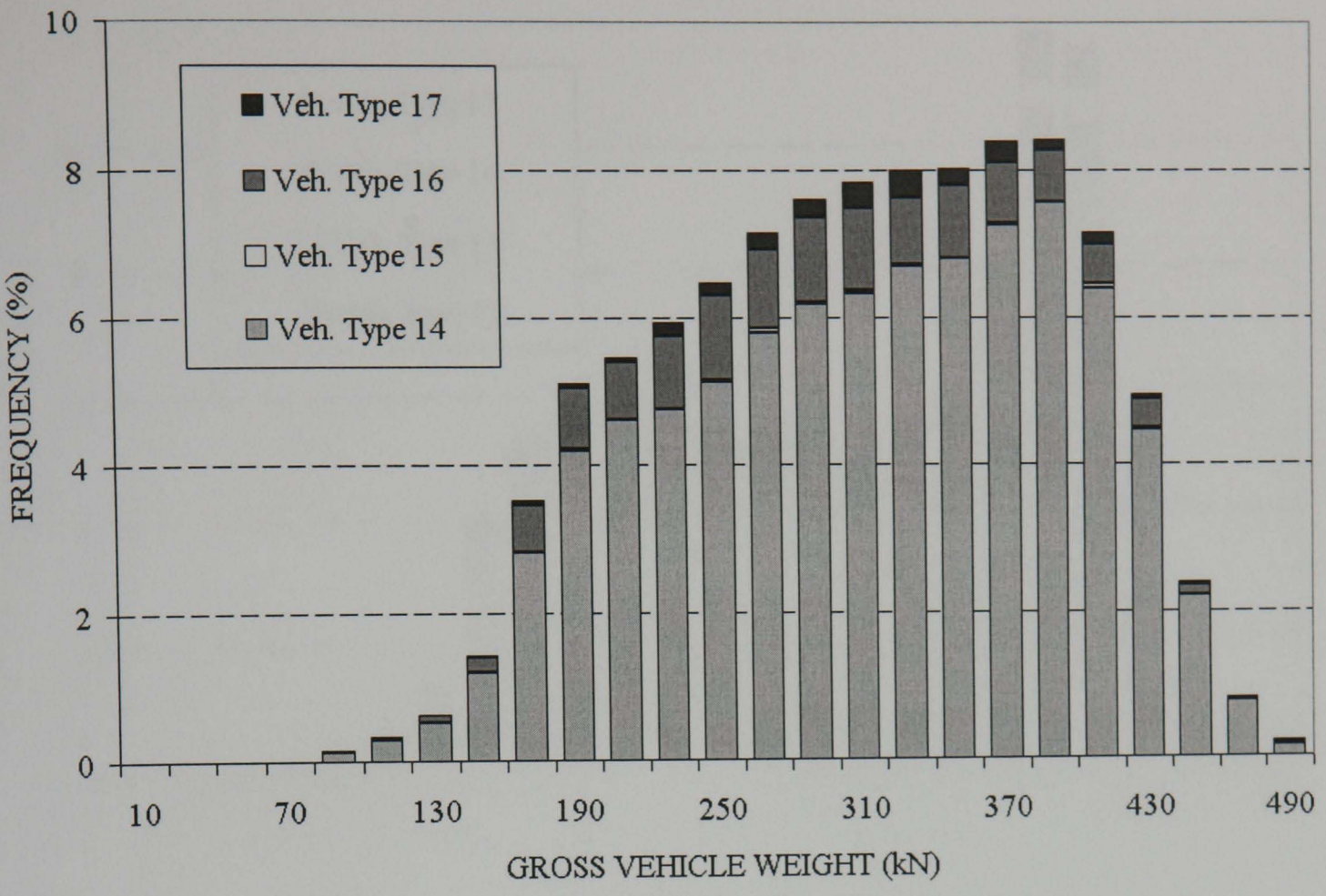

Figure B-13: GVW distribution of 5-axle trucks by vehicle type for Angers

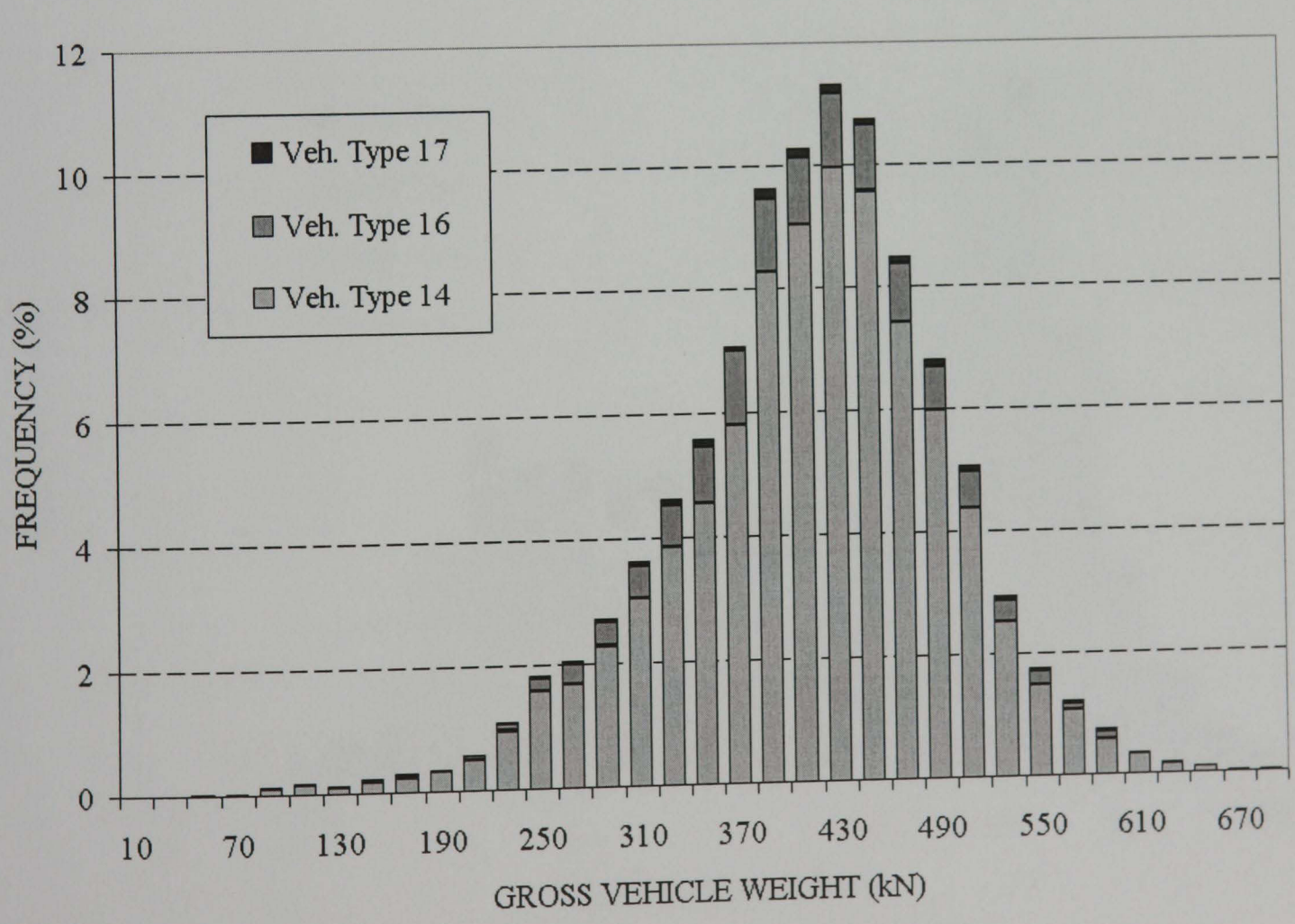

Figure B-14: GVW distribution of 5-axle trucks by vehicle type for Auxerre

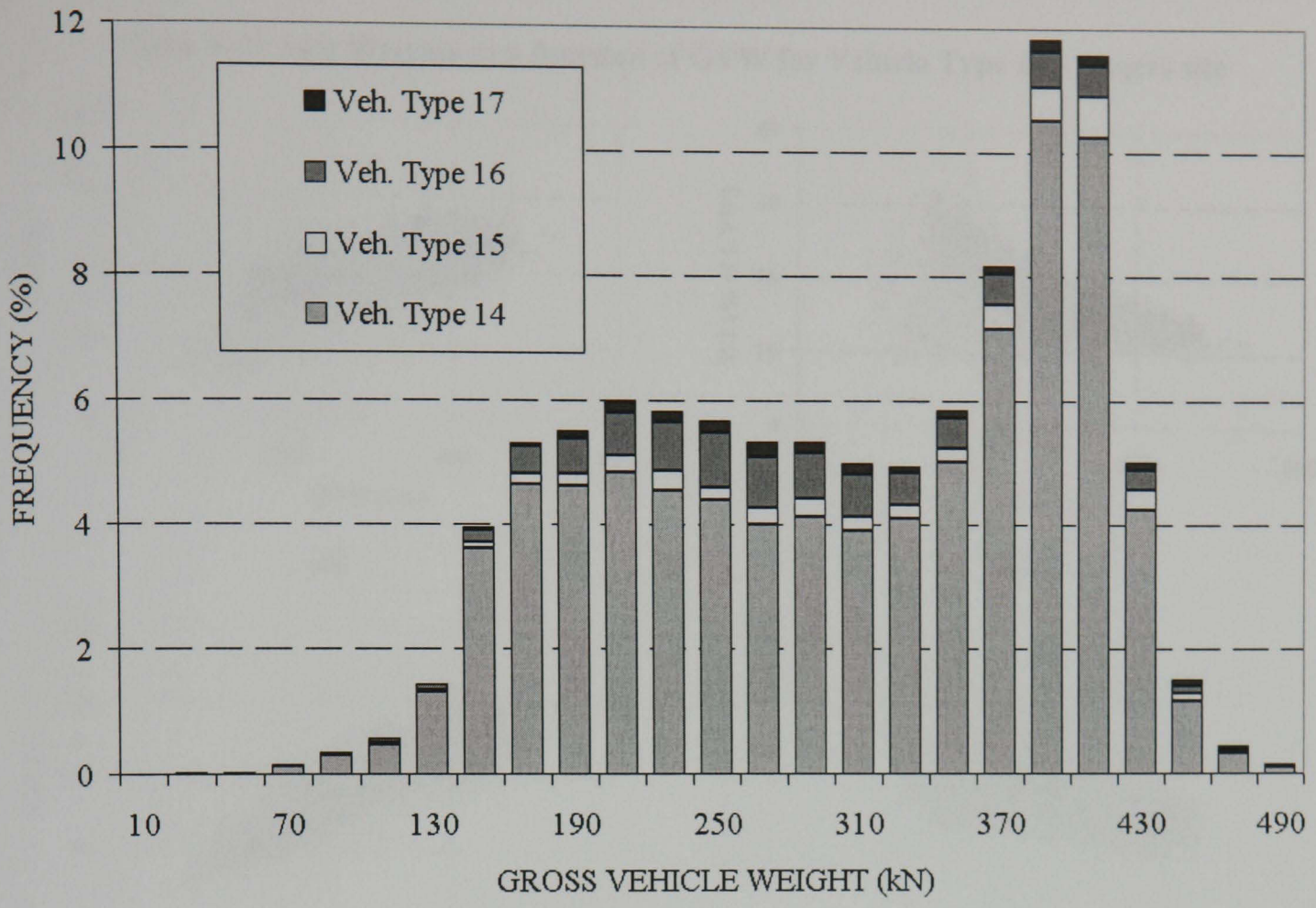

Figure B-15: GVW distribution of 5-axle trucks by vehicle type for A196

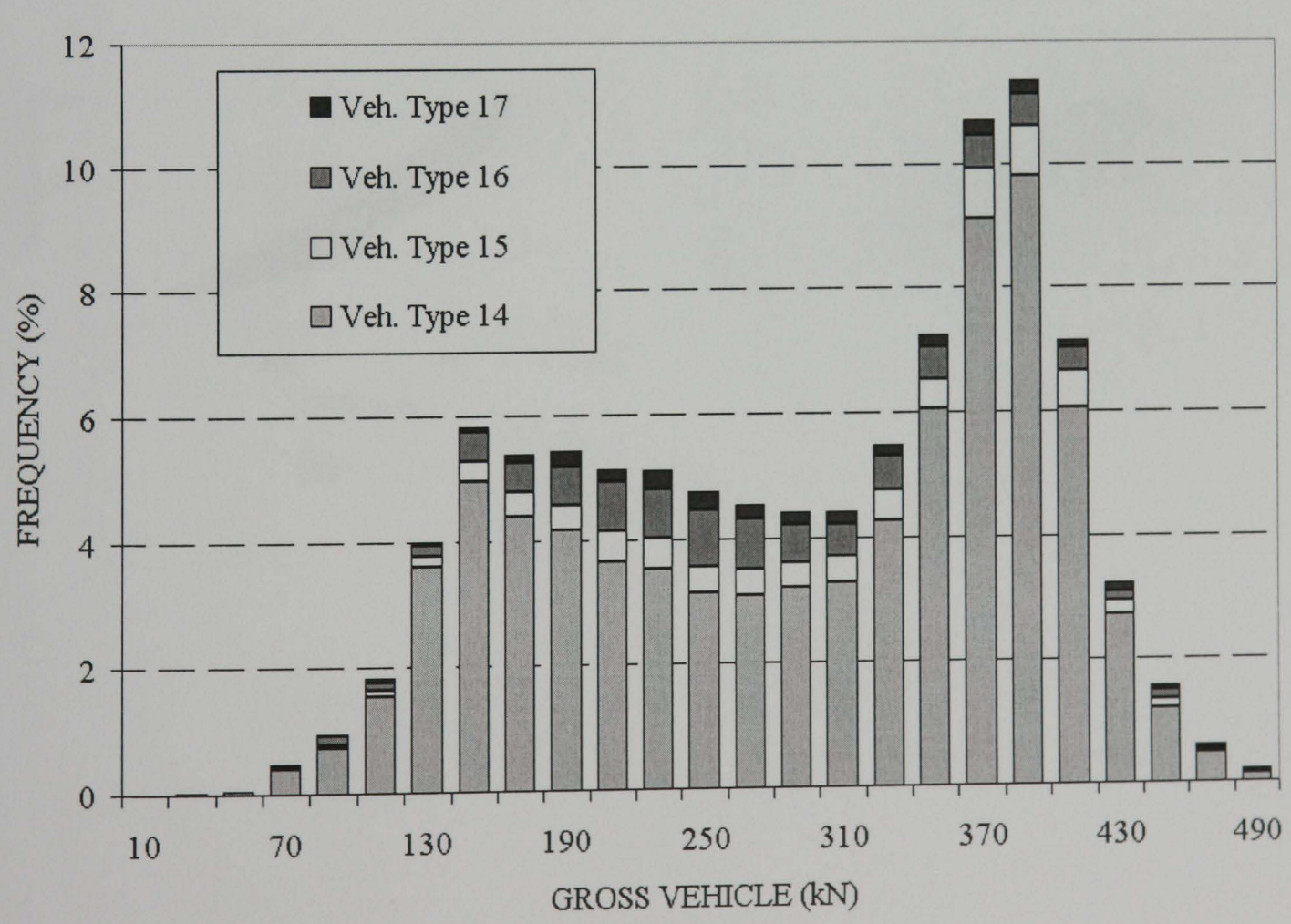

Figure B-16: GVW distribution of 5-axle trucks by vehicle type for A296

Table B-2: Axle Weights as a function of GVW for Vehicle Type 14 - Angers site

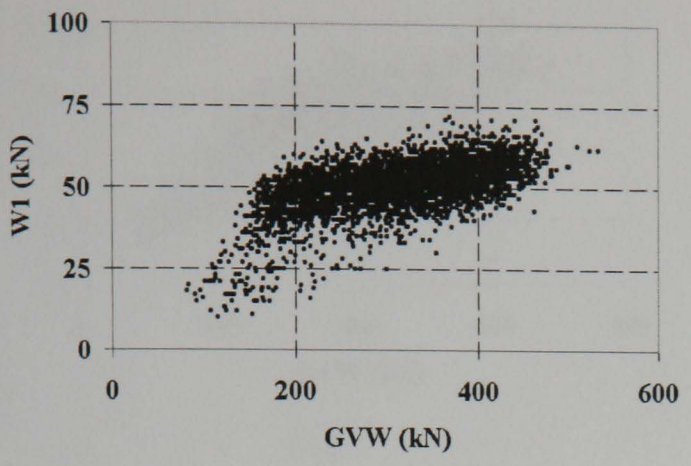

(a)

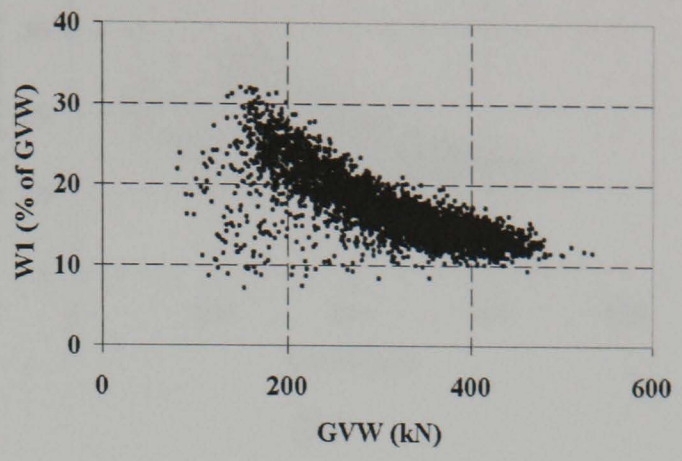

(b)

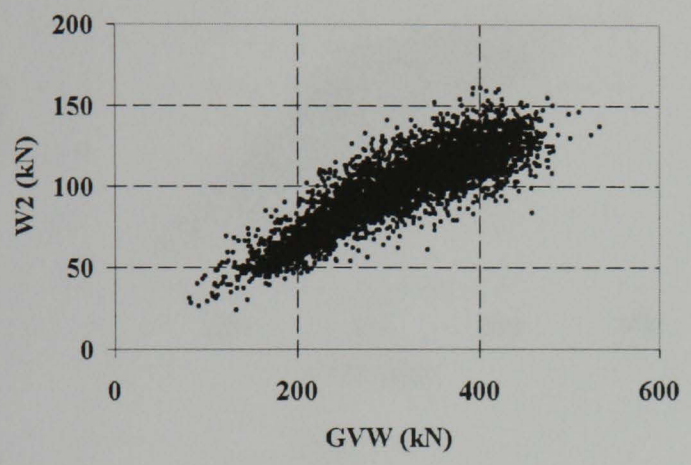

(c)

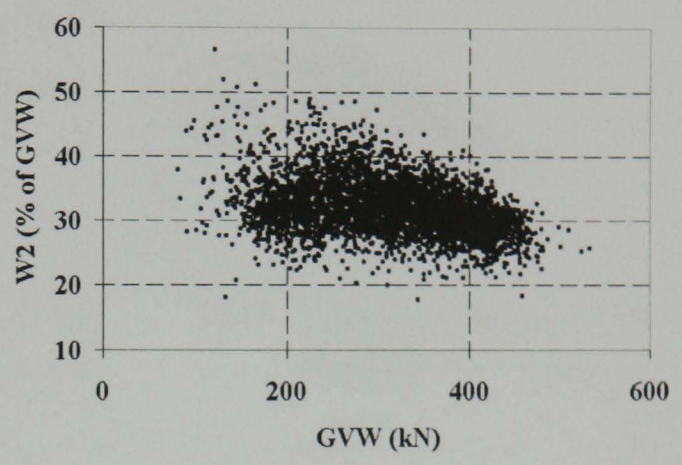

(d)

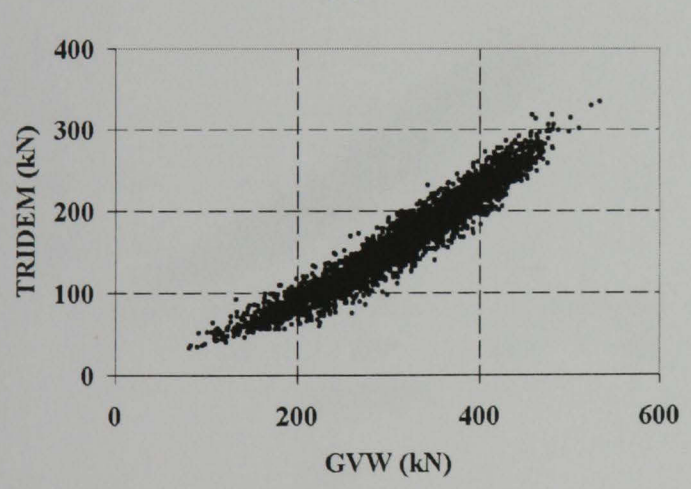

(e)

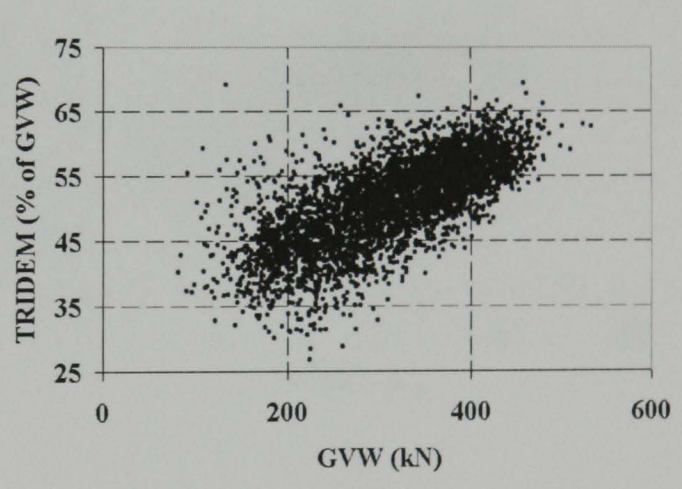

(f)

Table B-3: Axle Weights as a function of GVW for Vehicle Type 14 - Auxerre site

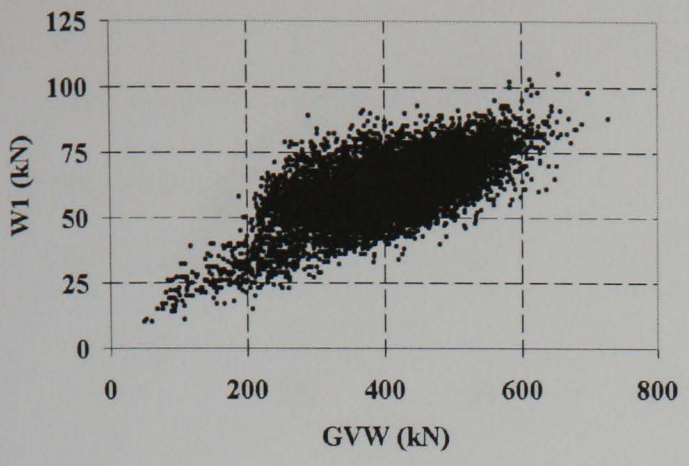

(a)

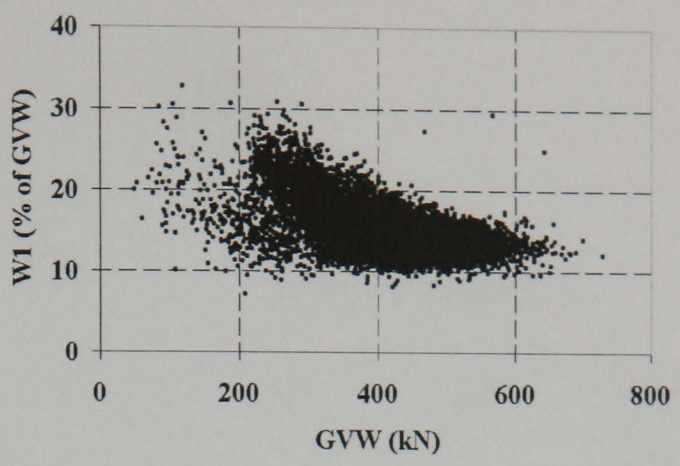

(b)

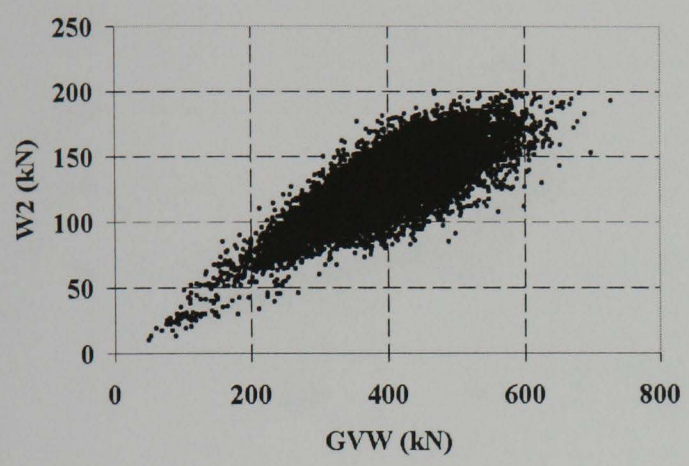

(c)

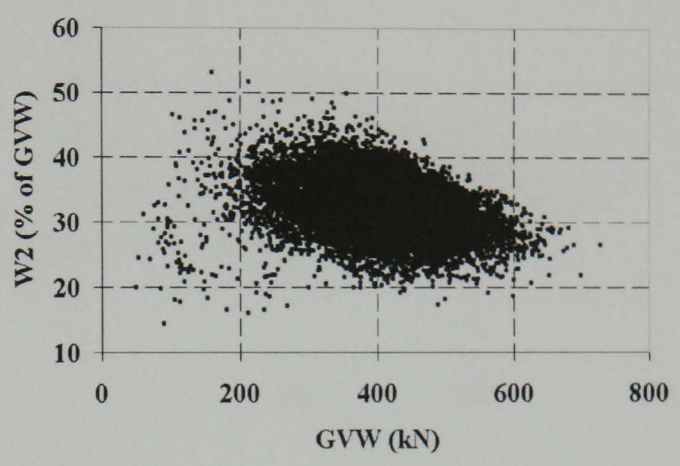

(d)

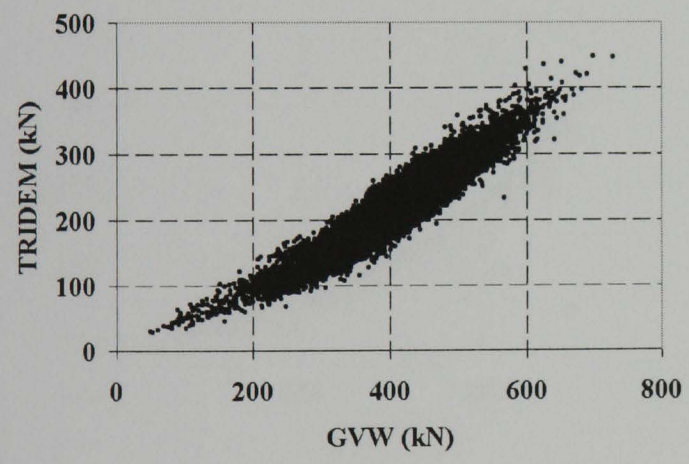

(e)

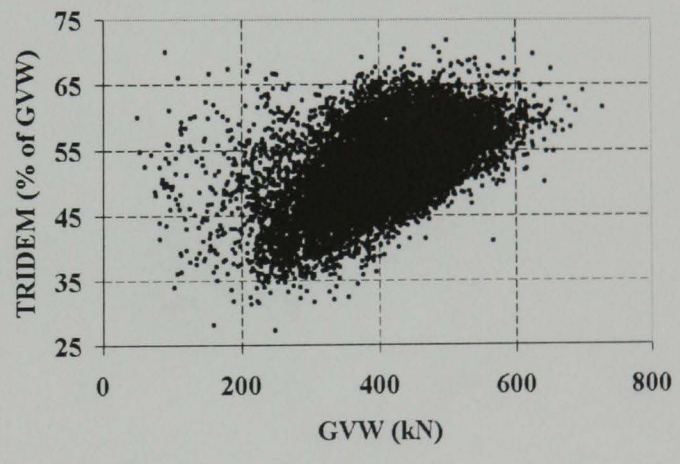

(f)

Table B-4: Axle Weights as a function of GVW for Vehicle Type 14 – A196 site (direction 1)

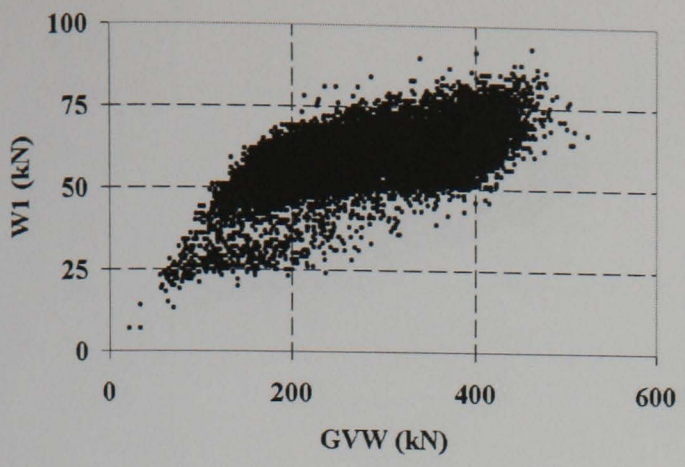

(a)

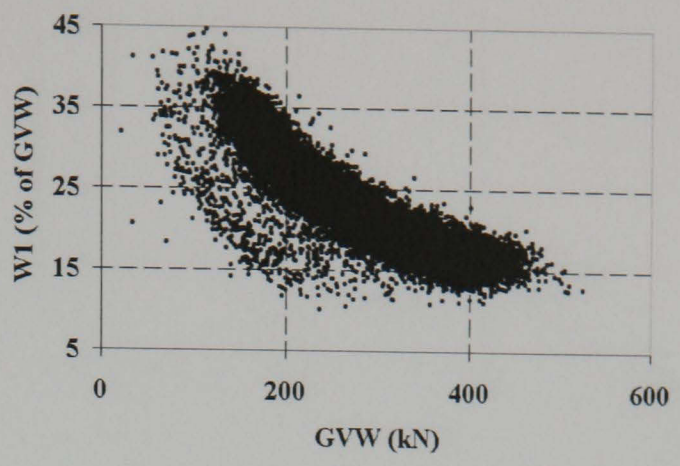

(b)

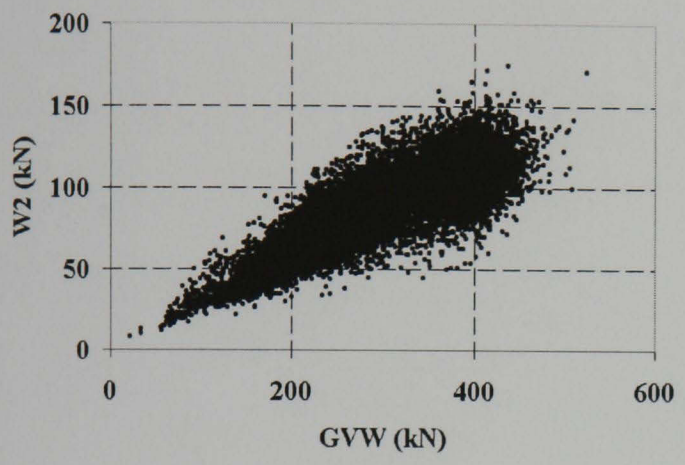

(c)

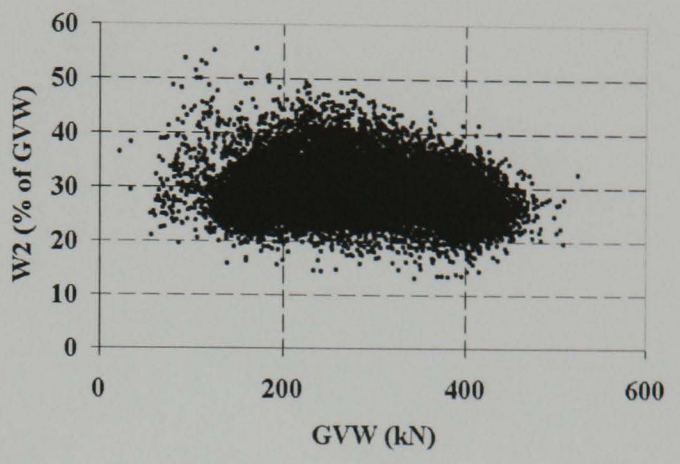

(d)

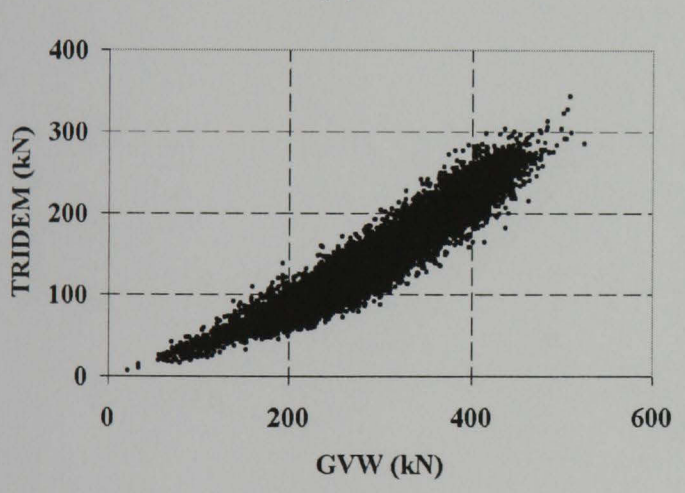

(e)

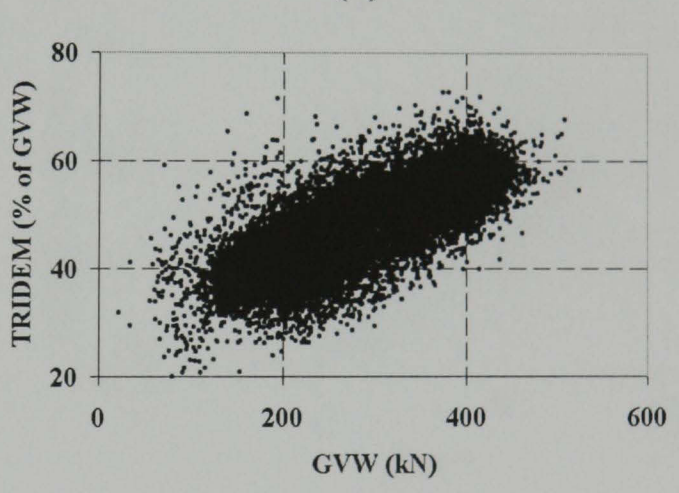

(f)

Table B-5: Axle Weights as a function of GVW for Vehicle Type 14 – A196 site (direction 2)

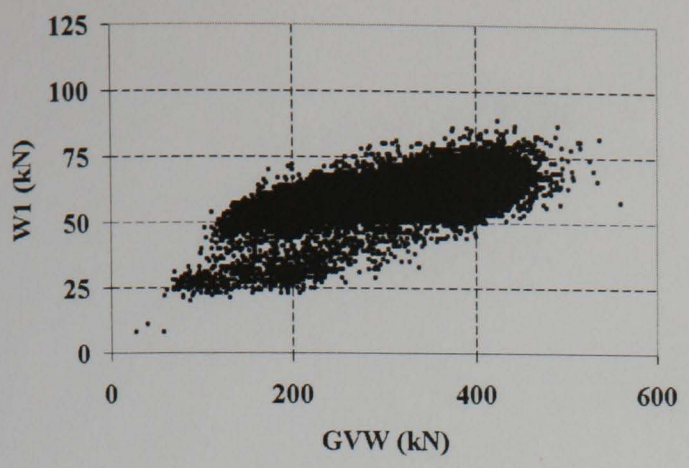

(a)

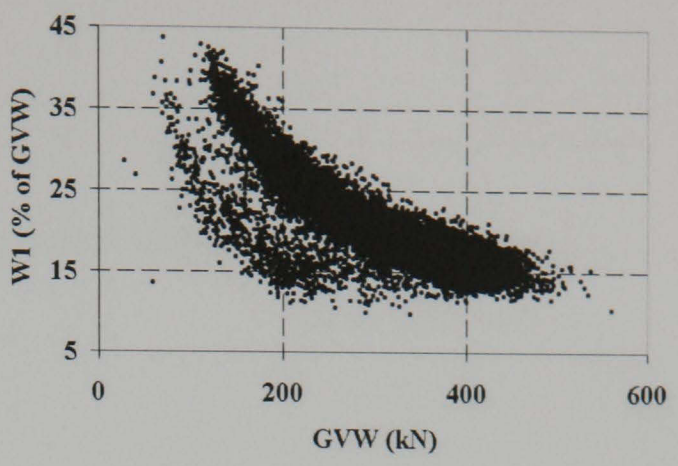

(b)

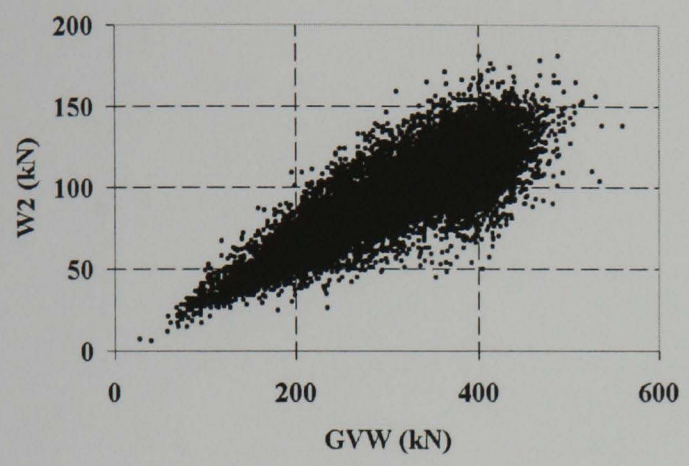

(c)

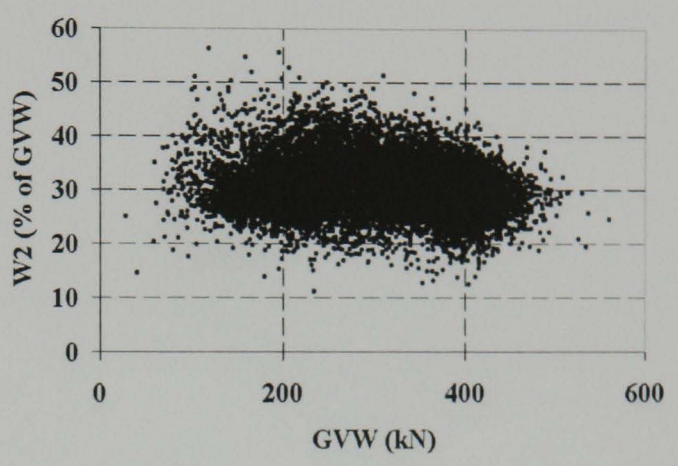

(d)

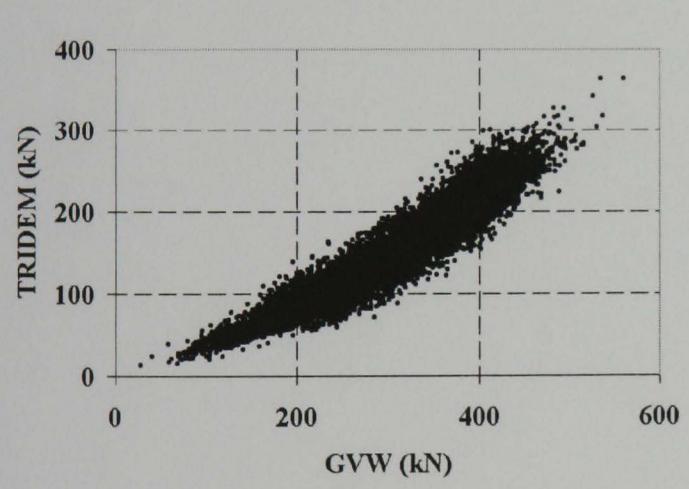

(e)

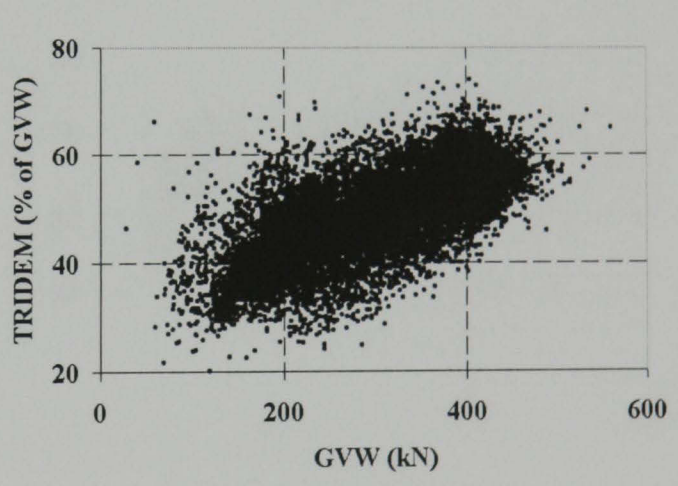

(f)

Table B-6: Axle Weights as a function of GVW for Vehicle Type 14 – A296 site

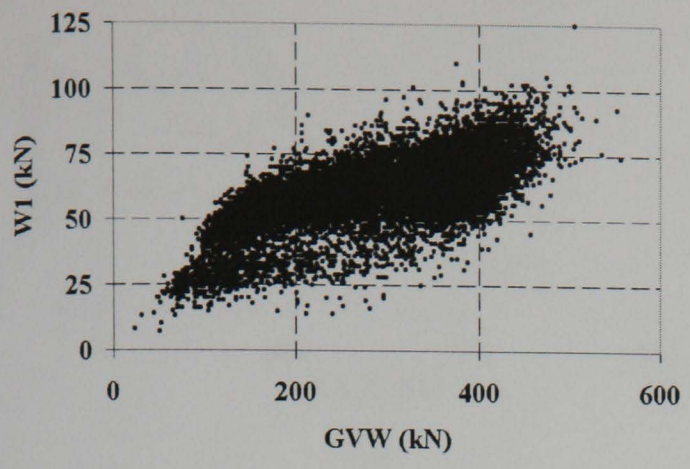

(a)

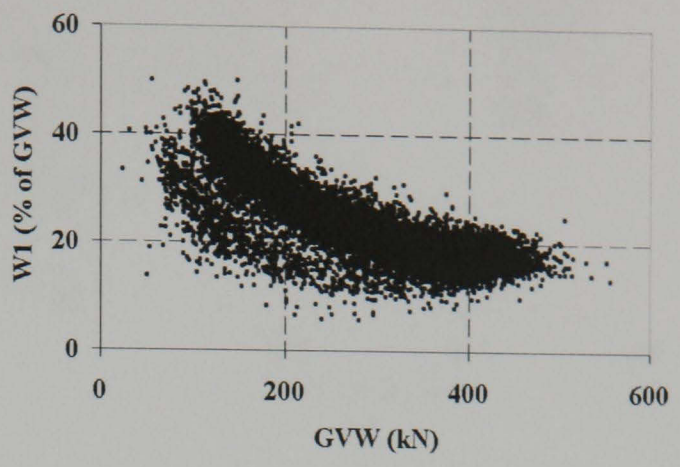

(b)

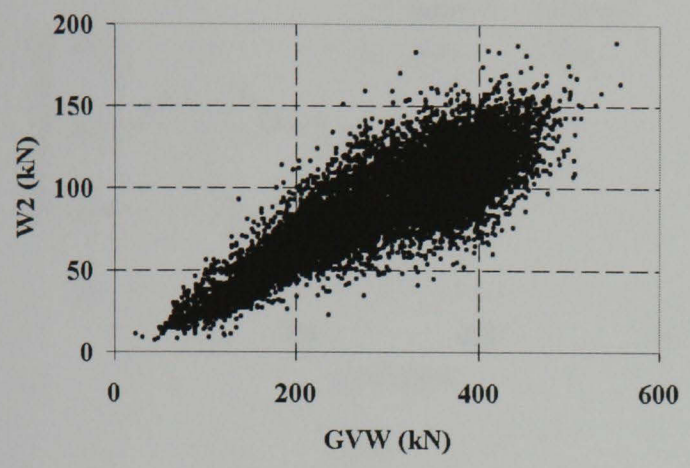

(c)

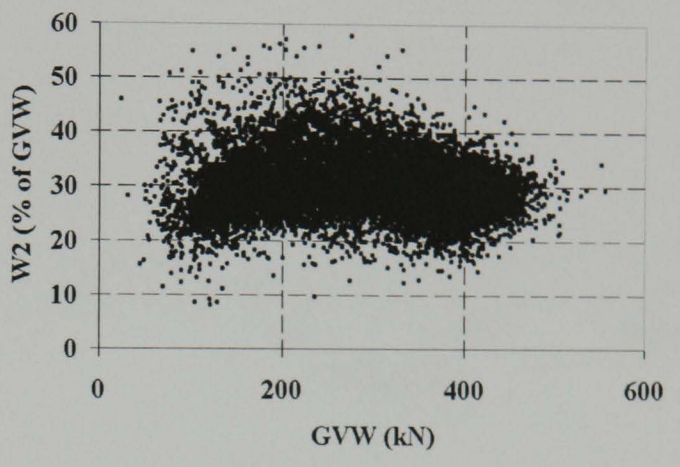

(d)

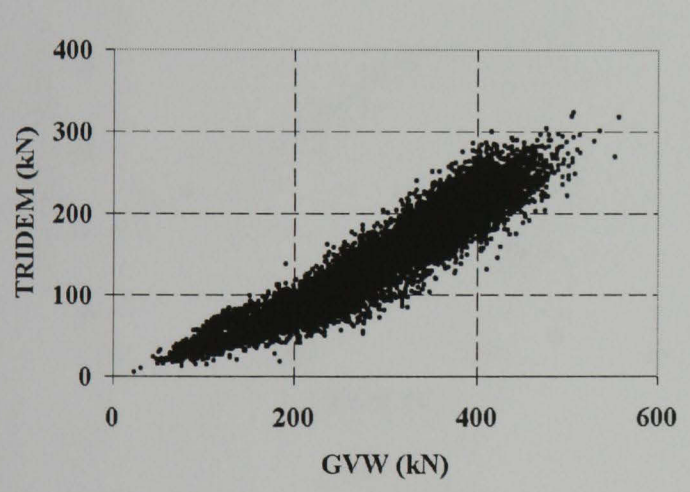

(e)

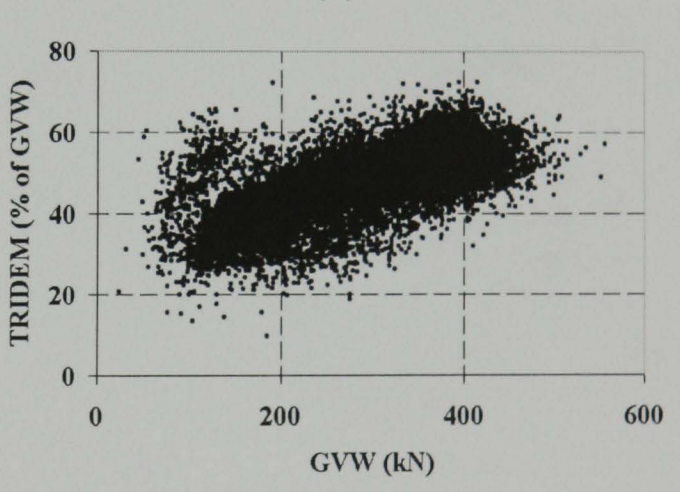

(f)

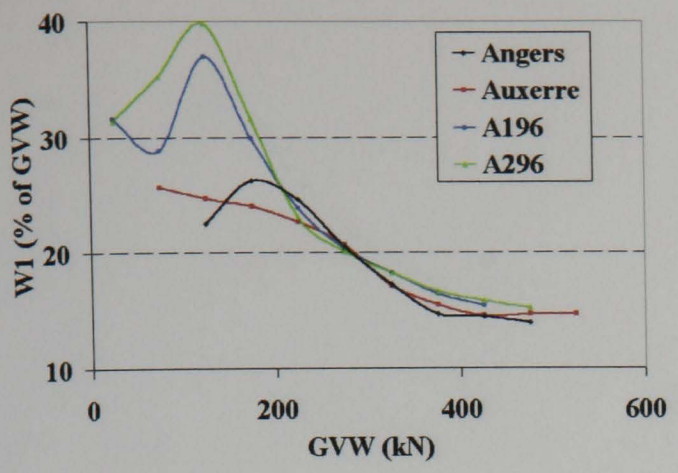

(a)

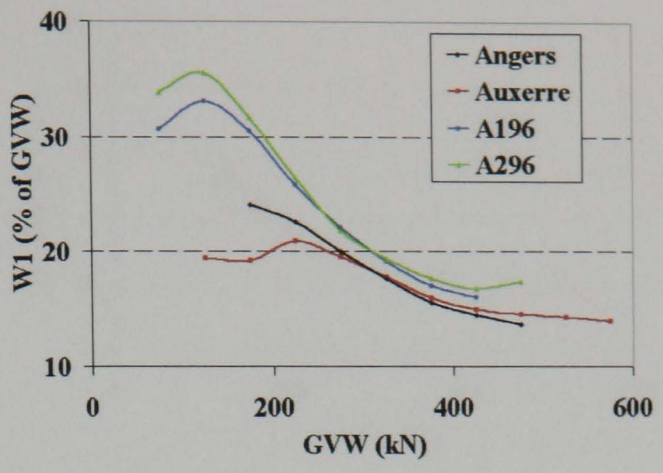

(b)

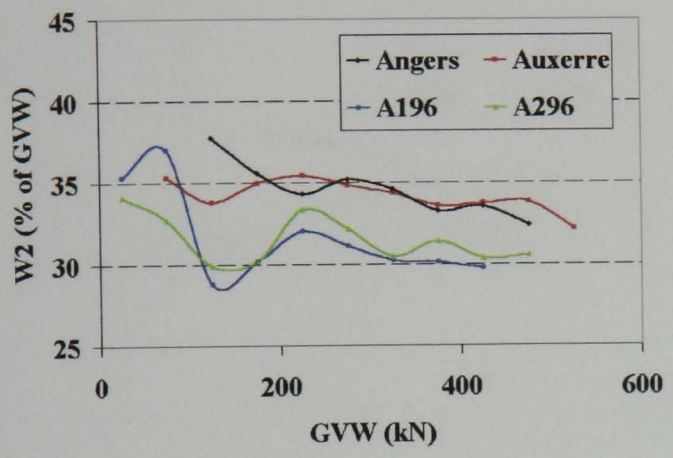

(c)

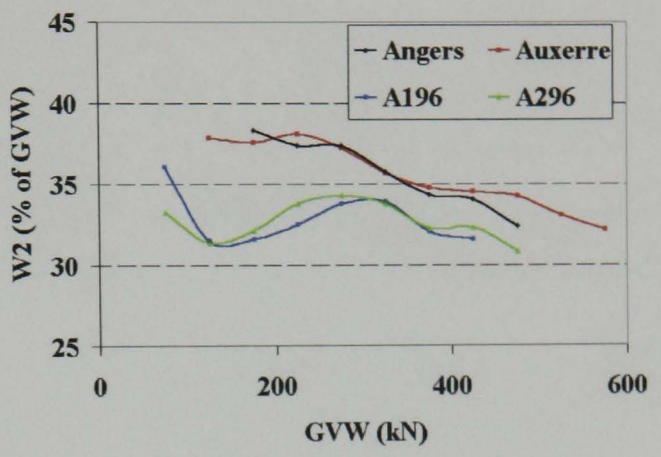

(d)

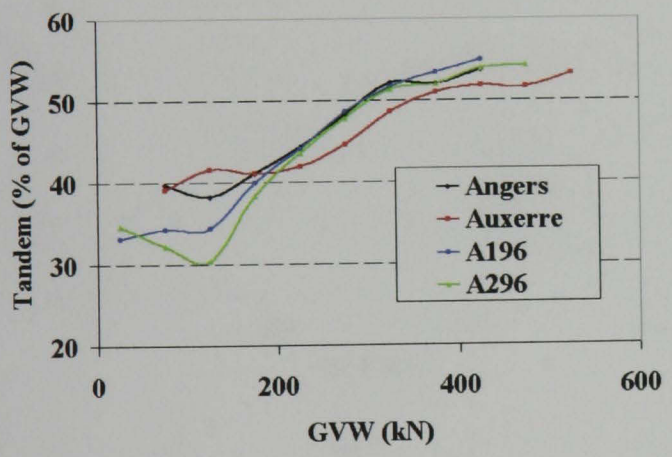

(e)

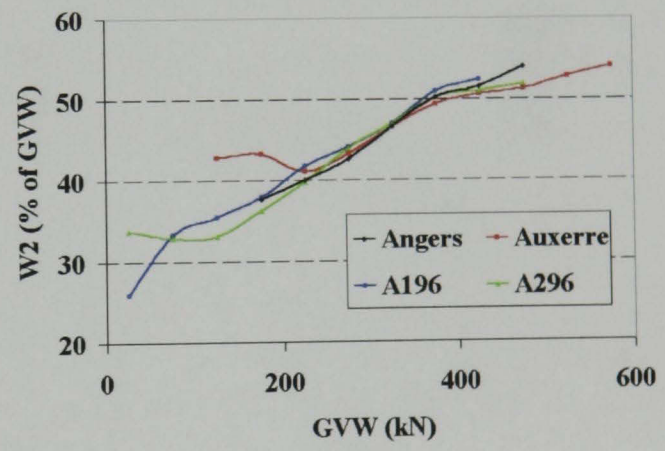

(f)

Figure B-17: Mean of Axle Weights for Vehicle Type 10 and 11 as a function of GVW for various sites

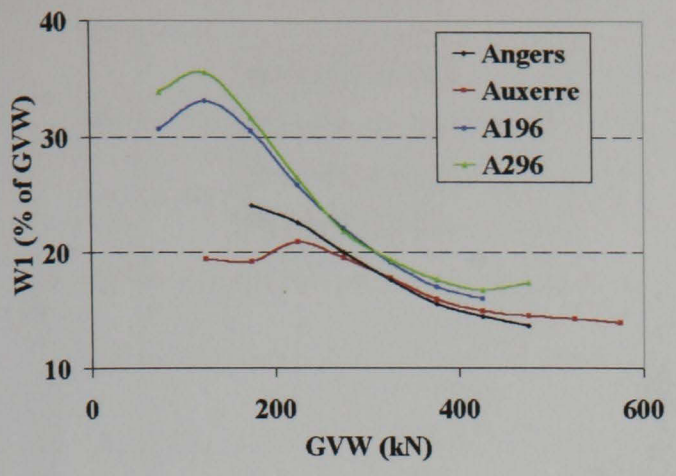

(a)

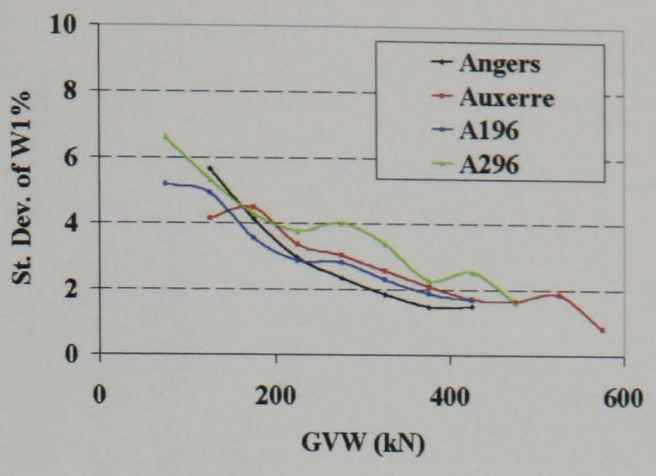

(b)

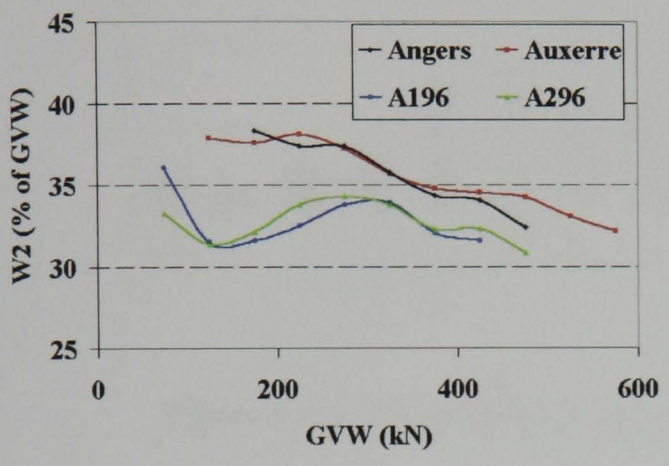

(c)

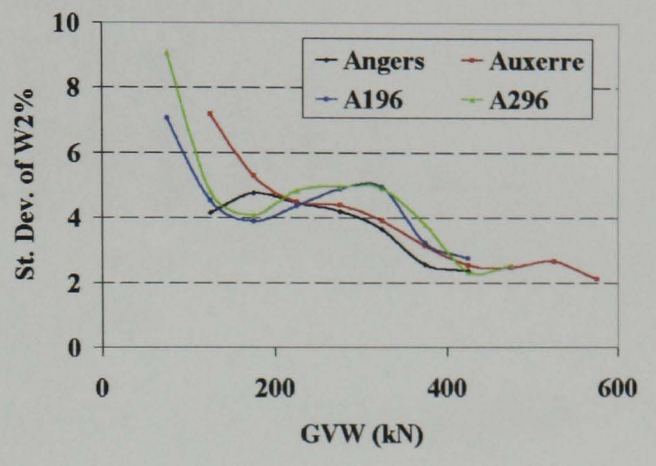

(d)

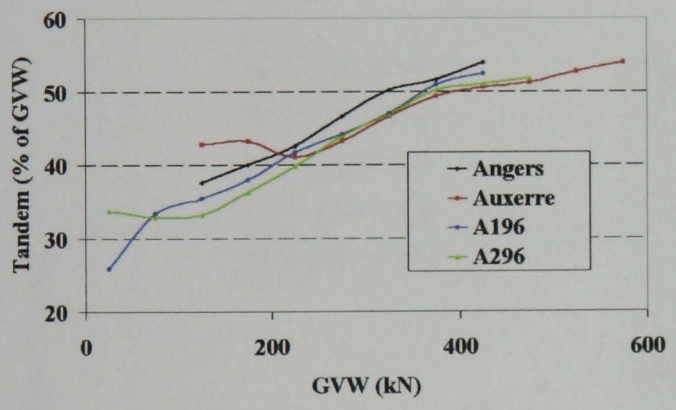

(e)

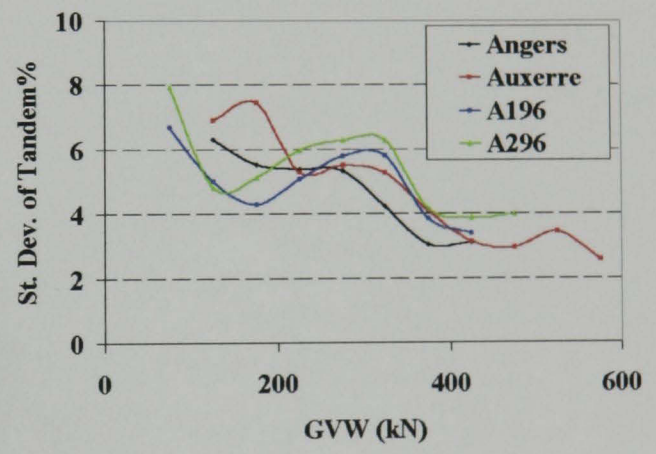

(f)

Figure B-18: Mean and Standard Deviation of Axle Weights for Vehicle Type 11 as a function of GVW for various sites

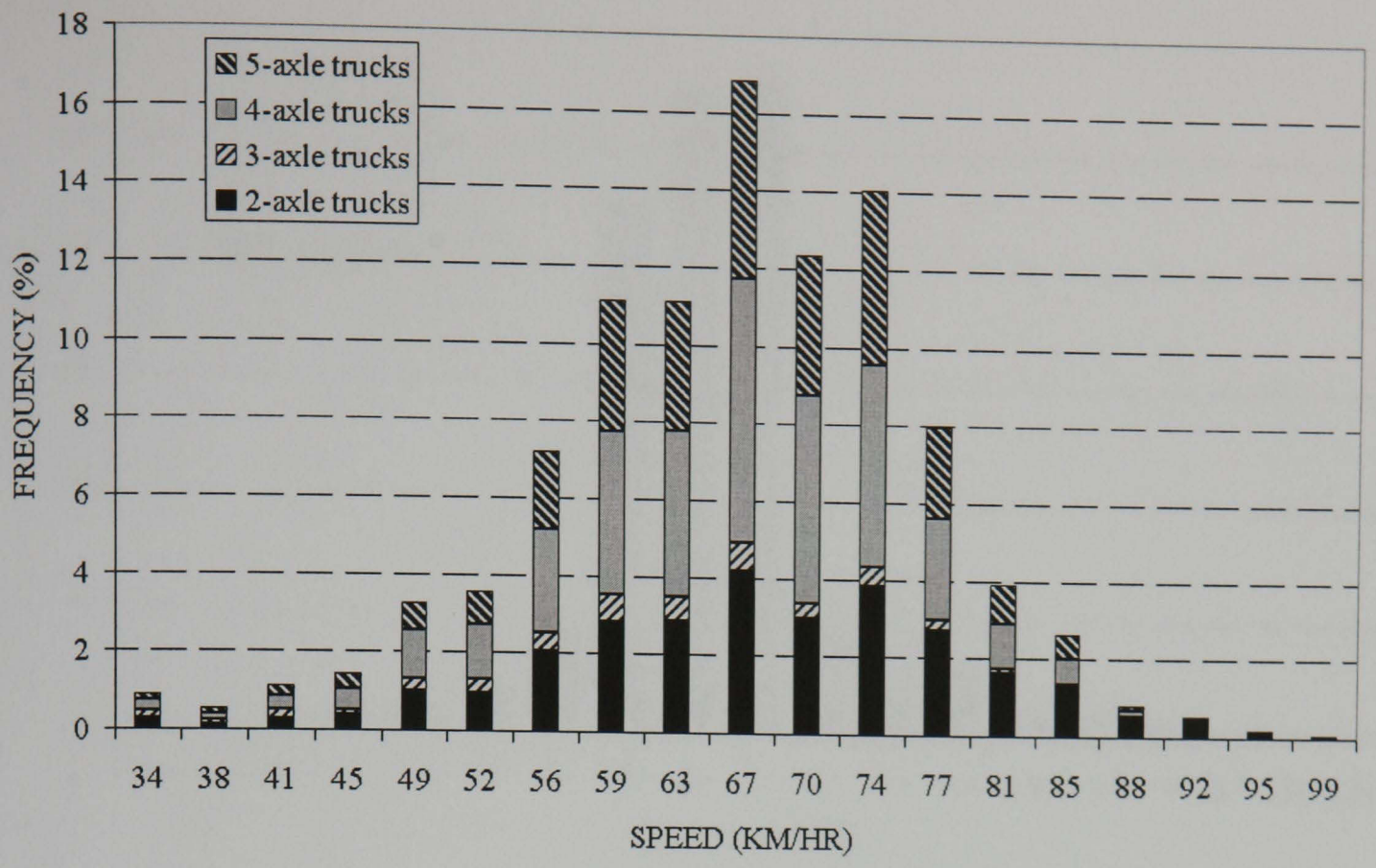

Figure B-19: Speed distribution as a function of number of axles – Angers site

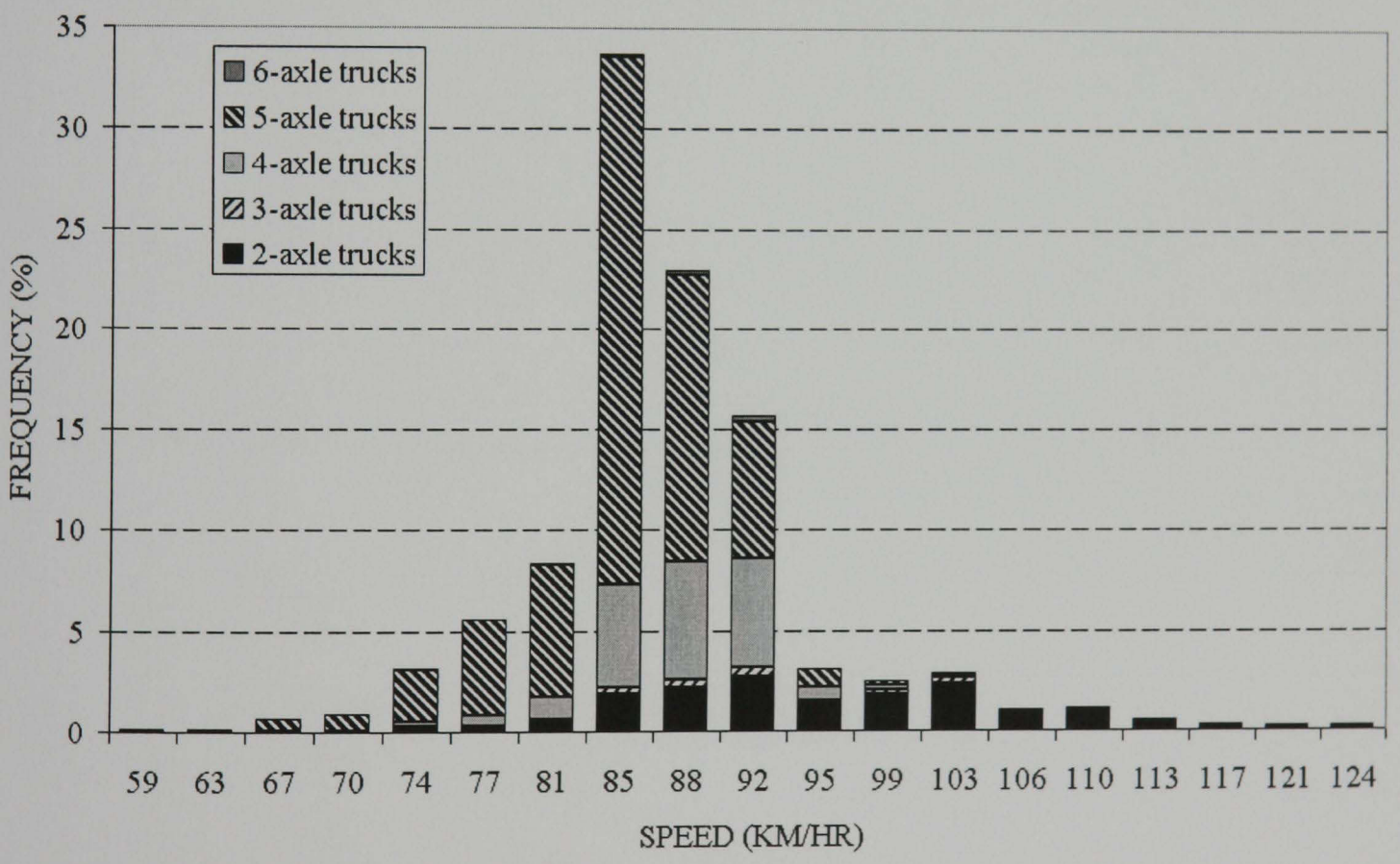

Figure B-20: Speed distribution as a function of number of axles – A196 site

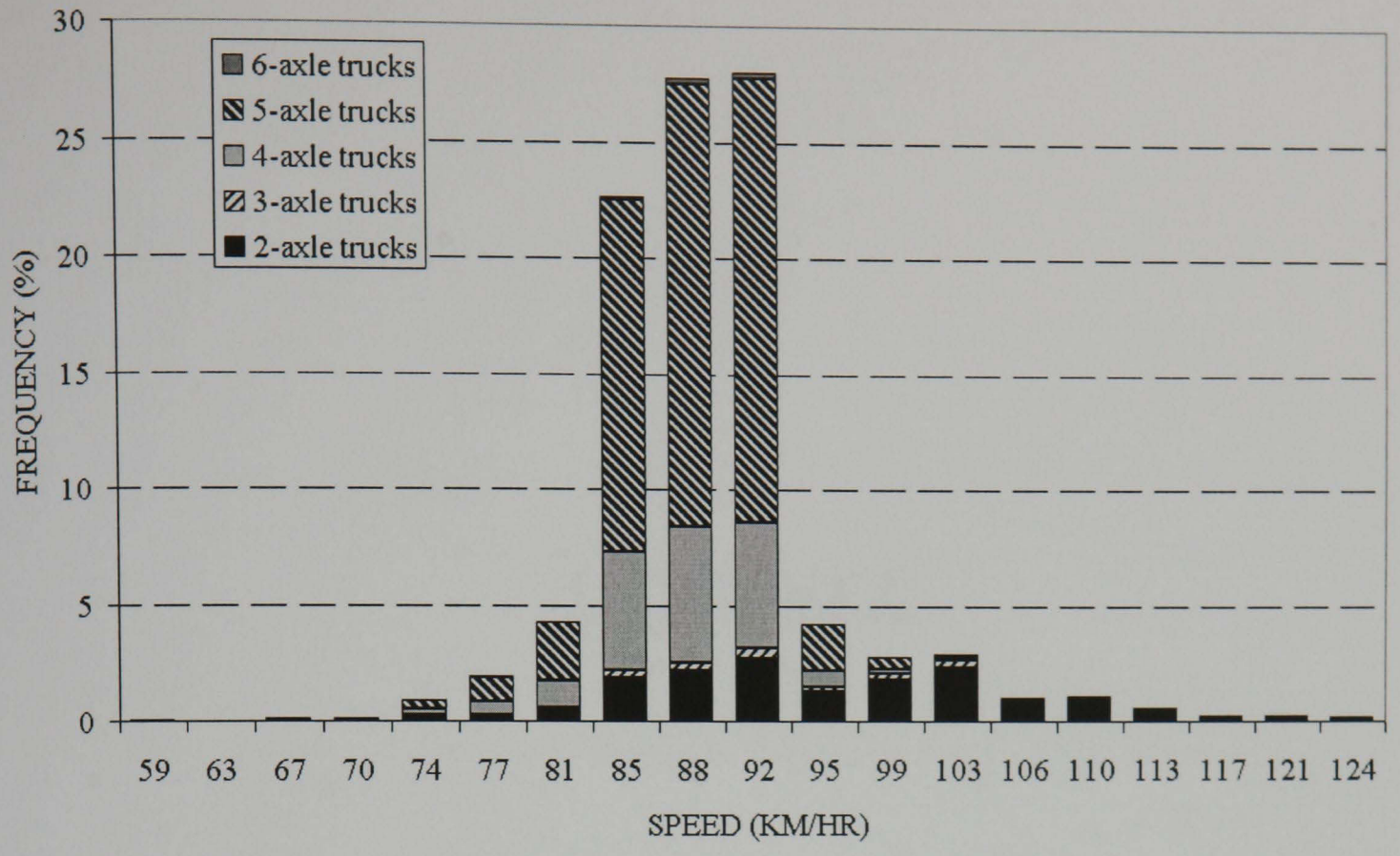

Figure B-21: Speed distribution as a function of number of axles – A296 site

APPENDIX C

STATIC EFFECTS OF TRAFFIC ACTIONS

Appendix C STATIC EFFECTS OF TRAFFIC ACTIONS

Equation C-1 239
Equation C-2 239
Equation C-3 239
Equation C-4 239
Equation C-5 239
Equation C-6 239
Table C-1: Maxima of influence responses for vehicle type 14 as a function of GVW for a 20m bridge and for various sites 240
Table C-2: Maxima of influence responses for vehicle type 14 as a function of GVW for a 30m bridge and for various sites 241
Table C-3: Maxima of influence responses for vehicle type 14 as a function of GVW for a 40m bridge and for various sites 242
Figure C-1: Influence responses for Vehicle Type 14 of various GVW: Auxerre - Effect 2 (a) 20m bridge, (b) 30m bridge and (c) 40m bridge; Angers – Effect 6 (d) 20m bridge, (e) 30m bridge and (f) 40m bridge 243
Figure C-2: Influence responses for Vehicle Type 14 - GVW 525 – for various sites: Effect 1 (a) 20m bridge, (b) 30m bridge, (c) 40m bridge; and Effect 4 (d) 20m bridge, (e) 30m bridge, (f) 40m bridge 244
Table C-4: Maximum influence responses for different vehicle types and for various bridge lengths 245

The equations corresponding to the different influence lines are given in Equation C-1 to Equation C-6respectively, where x refers to the position of the axle load considered and L refers to the total length of the bridge.

$$y = \left(\frac{x}{2}\right) \qquad x \le L/2$$

$$y = \left(\frac{L-x}{2}\right) \qquad x > L/2$$

Equation C-1

$$y = \left(\frac{x}{L^2}\right)\left(\frac{L^2}{4} - x^2\right) \qquad x \le L/2$$

$$y = \left(\frac{L-x}{L^2}\right)\left(\frac{L^2}{4} - (L-x)^2\right) \qquad x > L/2$$

Equation C-2

$$y = \left(1 - \frac{x}{L}\right)$$

Equation C-3

$$y = \left(\frac{x}{L}\right)$$

Equation C-4

$$y = \left(\frac{1}{L/2}\right)\left[\left(\frac{x}{L^2}\right)\left(\frac{L^2}{4} - x^2\right) + \frac{L}{2} - x\right] \qquad x \le L/2$$

$$y = \left(\frac{1}{L/2}\right)\left[\left(\frac{(L-x)}{L^2}\right)\left(\frac{L^2}{4} - (L-x)^2\right)\right] \qquad x > L/2$$

Equation C-5

$$y = \left(\frac{1}{L/2}\right)\left[\left(\frac{x}{L^2}\right)\left(\frac{L^2}{4} - x^2\right)\right] \qquad x \le L/2$$

$$y = \left(\frac{1}{L/2}\right)\left[\left(\frac{(L-x)}{L^2}\right)\left(\frac{L^2}{4} - (L-x)^2\right) - \frac{L}{2} + x\right] \qquad x > L/2$$

Equation C-6

Table C-1: Maxima of influence responses for vehicle type 14 as a function of GVW for a 20m bridge and for various sites

Effect	Site	Gross Vehicle Weight (kN)			
		225	**325**	**425**	**525**
1	**Angers**	3.282	3.302	3.417	3.550
1	**Auxerre**	3.158	3.115	3.191	3.275
1	**A196**	3.013	2.939	3.113	3.219
1	**A296**	3.033	2.902	3.023	3.039
		225	**325**	**425**	**525**
2	**Angers**	0.876	0.884	0.878	0.879
2	**Auxerre**	0.868	0.876	0.882	0.885
2	**A196**	0.889	0.900	0.908	0.912
2	**A296**	0.863	0.873	0.877	0.878
		225	**325**	**425**	**525**
3	**Angers**	0.749	0.783	0.795	0.810
3	**Auxerre**	0.735	0.746	0.767	0.778
3	**A196**	0.704	0.736	0.760	0.775
3	**A296**	0.693	0.732	0.749	0.751
		225	**325**	**425**	**525**
4	**Angers**	0.746	0.727	0.700	0.699
4	**Auxerre**	0.720	0.710	0.688	0.683
4	**A196**	0.715	0.683	0.659	0.658
4	**A296**	0.717	0.679	0.663	0.661
		225	**325**	**425**	**525**
5	**Angers**	0.473	0.515	0.551	0.582
5	**Auxerre**	0.468	0.462	0.503	0.525
5	**A196**	0.453	0.457	0.502	0.530
5	**A296**	0.466	0.452	0.484	0.487
		225	**325**	**425**	**525**
6	**Angers**	0.473	0.515	0.551	0.582
6	**Auxerre**	0.468	0.471	0.464	0.488
6	**A196**	0.421	0.433	0.480	0.507
6	**A296**	0.429	0.427	0.459	0.463

Table C-2: Maxima of influence responses for vehicle type 14 as a function of GVW for a 30m bridge and for various sites

Effect	Site	Gross Vehicle Weight (kN)			
		225	**325**	**425**	**525**
1	**Angers**	5.782	5.827	5.917	6.051
1	**Auxerre**	5.658	5.615	5.691	5.775
1	**A196**	5.513	5.439	5.613	5.719
1	**A296**	5.531	5.401	5.523	5.540
		225	**325**	**425**	**525**
2	**Angers**	1.161	1.150	1.142	1.148
2	**Auxerre**	1.194	1.188	1.183	1.186
2	**A196**	1.234	1.222	1.224	1.224
2	**A296**	1.238	1.227	1.228	1.228
		225	**325**	**425**	**525**
3	**Angers**	0.833	0.859	0.863	0.874
3	**Auxerre**	0.823	0.831	0.845	0.852
3	**A196**	0.803	0.824	0.840	0.850
3	**A296**	0.795	0.821	0.833	0.834
		225	**325**	**425**	**525**
4	**Angers**	0.831	0.821	0.800	0.790
4	**Auxerre**	0.814	0.807	0.792	0.785
4	**A196**	0.810	0.789	0.773	0.763
4	**A296**	0.811	0.786	0.775	0.774
		225	**325**	**425**	**525**
5	**Angers**	0.608	0.653	0.677	0.701
5	**Auxerre**	0.589	0.605	0.637	0.654
5	**A196**	0.549	0.595	0.631	0.652
5	**A296**	0.534	0.590	0.615	0.617
		225	**325**	**425**	**525**
6	**Angers**	0.603	0.604	0.593	0.588
6	**Auxerre**	0.568	0.576	0.580	0.573
6	**A196**	0.565	0.536	0.536	0.538
6	**A296**	0.569	0.532	0.531	0.532

Table C-3: Maxima of influence responses for vehicle type 14 as a function of GVW for a 40m bridge and for various sites

Effect	Site	Gross Vehicle Weight (kN)			
		225	**325**	**425**	**525**
1	**Angers**	8.282	8.352	8.418	8.551
1	**Auxerre**	8.158	8.115	8.191	8.275
1	**A196**	8.013	7.939	8.113	8.219
1	**A296**	8.030	7.901	8.023	8.040
		225	**325**	**425**	**525**
2	**Angers**	1.611	1.655	1.654	1.672
2	**Auxerre**	1.571	1.582	1.600	1.610
2	**A196**	1.504	1.531	1.554	1.573
2	**A296**	1.498	1.519	1.534	1.537
		225	**325**	**425**	**525**
3	**Angers**	0.875	0.897	0.898	0.905
3	**Auxerre**	0.868	0.873	0.884	0.889
3	**A196**	0.852	0.868	0.880	0.888
3	**A296**	0.846	0.866	0.875	0.876
		225	**325**	**425**	**525**
4	**Angers**	0.873	0.869	0.850	0.843
4	**Auxerre**	0.860	0.855	0.844	0.839
4	**A196**	0.858	0.842	0.830	0.822
4	**A296**	0.858	0.840	0.831	0.831
		225	**325**	**425**	**525**
5	**Angers**	0.697	0.735	0.752	0.770
5	**Auxerre**	0.682	0.695	0.720	0.733
5	**A196**	0.648	0.685	0.713	0.731
5	**A296**	0.636	0.680	0.700	0.702
		225	**325**	**425**	**525**
6	**Angers**	0.694	0.669	0.659	0.658
6	**Auxerre**	0.665	0.652	0.646	0.642
6	**A196**	0.661	0.623	0.607	0.614
6	**A296**	0.664	0.619	0.601	0.602

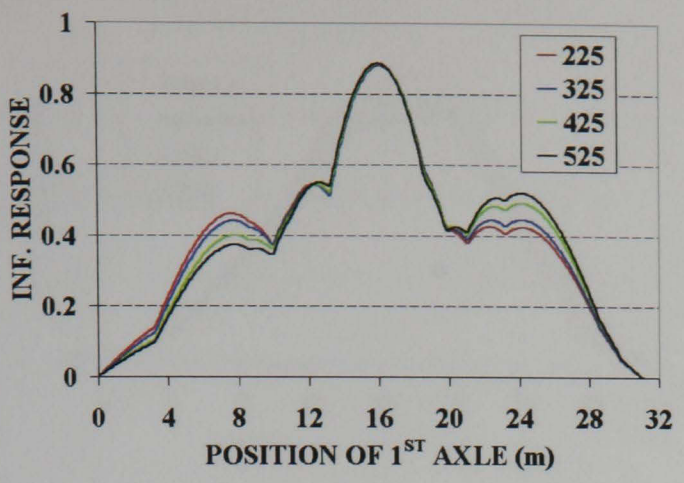

(a)

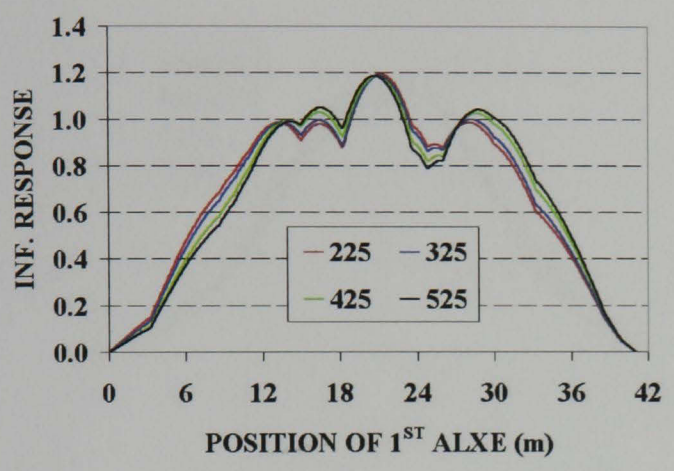

(b)

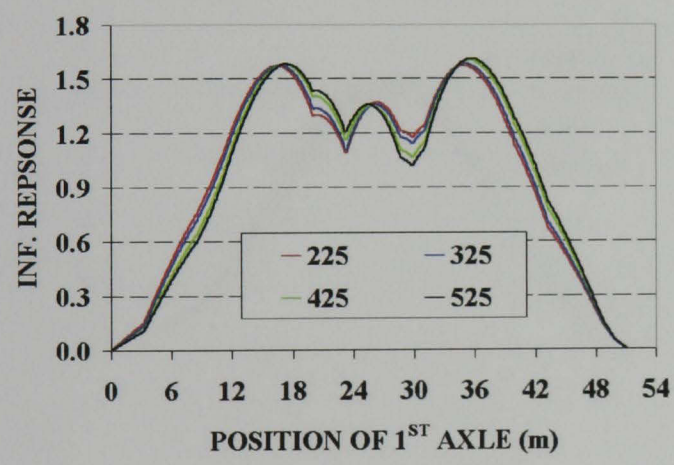

(c)

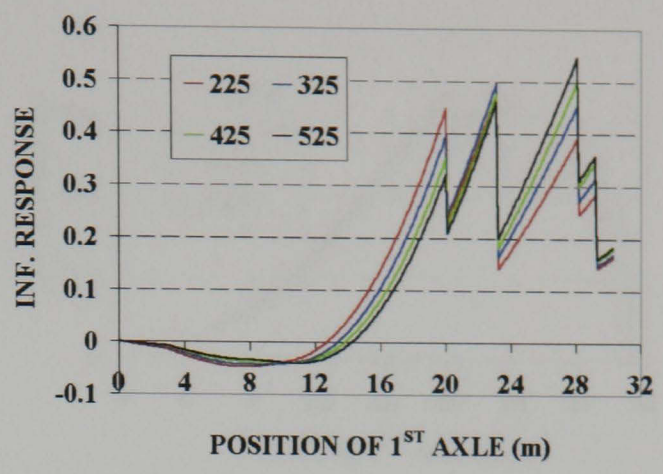

(d)

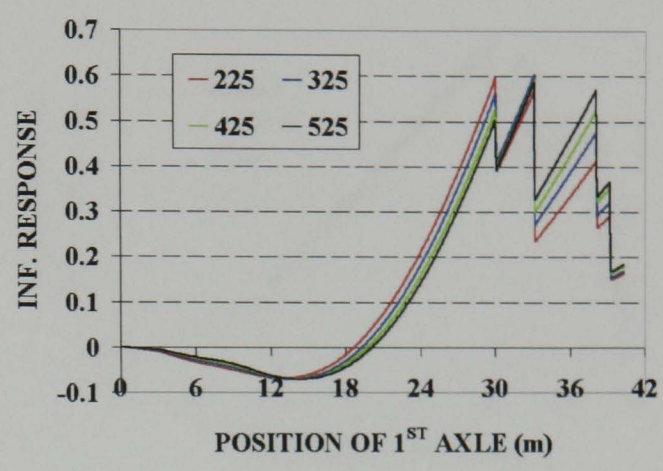

(e)

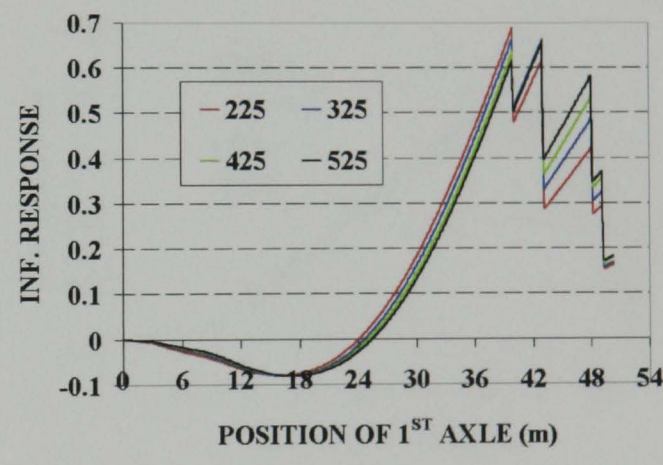

(f)

Figure C-1: Influence responses for Vehicle Type 14 of various GVW: Auxerre - Effect 2 (a) 20m bridge, (b) 30m bridge and (c) 40m bridge; Angers – Effect 6 (d) 20m bridge, (e) 30m bridge and (f) 40m bridge

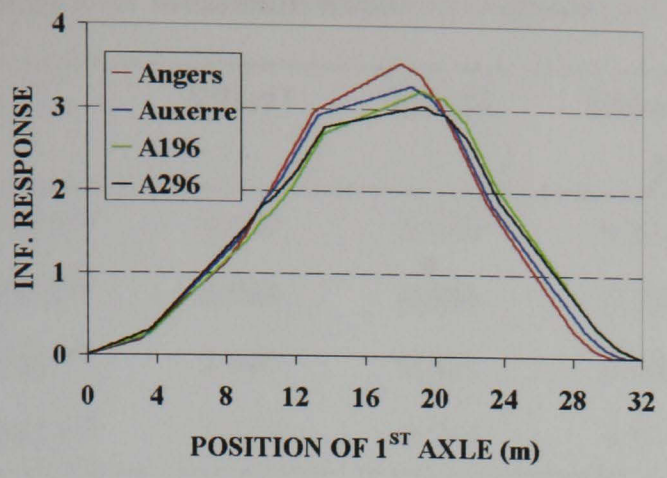

(a)

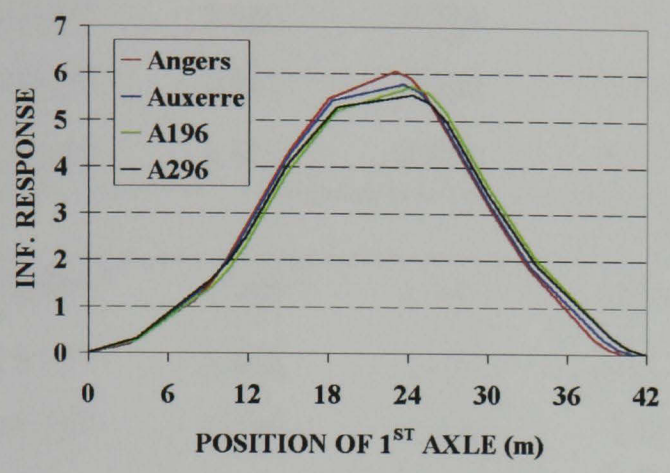

(b)

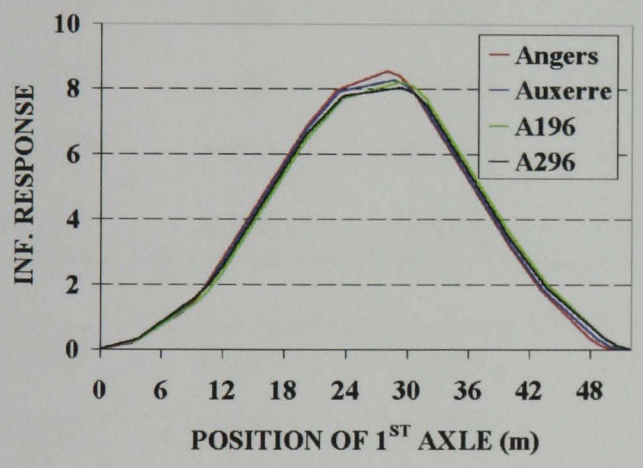

(c)

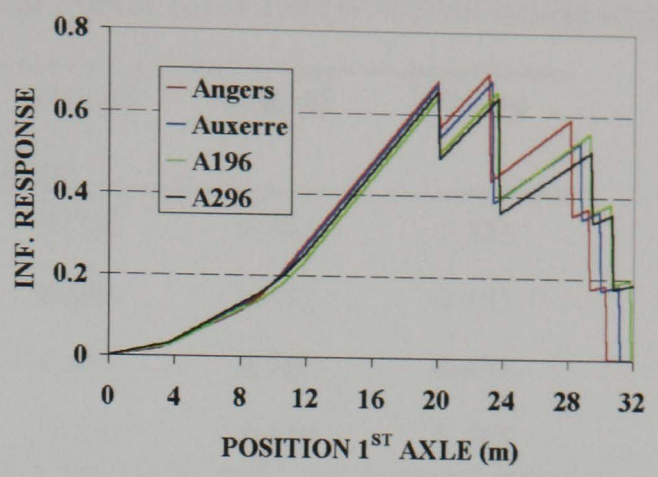

(d)

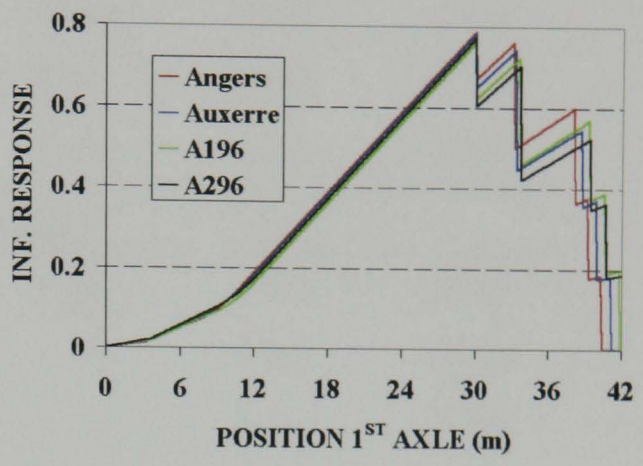

(e)

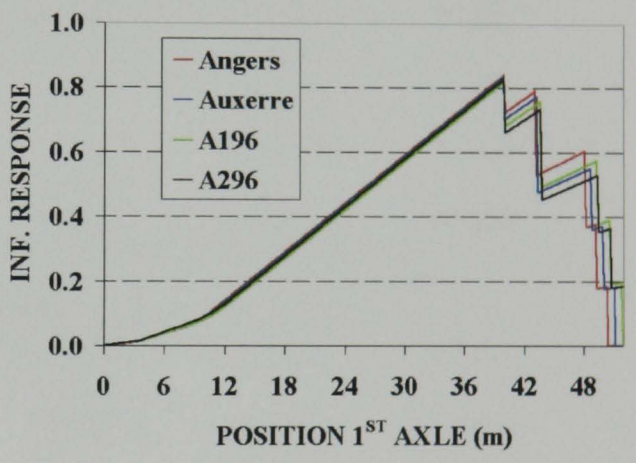

(f)

Figure C-2: Influence responses for Vehicle Type 14 - GVW 525 – for various sites: Effect 1 (a) 20m bridge, (b) 30m bridge, (c) 40m bridge; and Effect 4 (d) 20m bridge, (e) 30m bridge, (f) 40m bridge

Table C-4: Maximum influence responses for different vehicle types and for various bridge lengths

	Effect1	Effect2	Effect3	Effect4	Effect5	Effect6
			20 m bridge			
VT10[(a)]	3.449	0.848	0.824	0.738	0.605	0.523
VT11[(a)]	2.968	0.896	0.751	0.693	0.482	0.451
VT12[(b)]	2.980	0.821	0.702	0.663	0.460	0.453
VT13[(b)]	2.926	0.743	0.621	0.649	0.459	0.463
VT14[(c)]	3.186	0.886	0.768	0.678	0.510	0.489
VT16[(d)]	2.850	0.734	0.674	0.646	0.376	0.428
VT17[(d)]	2.951	0.738	0.616	0.643	0.431	0.435
VT18[(d)]	2.841	0.853	0.702	0.653	0.404	0.393
			30 m bridge			
VT10[(a)]	5.949	1.149	0.883	0.826	0.720	0.618
VT11[(a)]	5.468	1.247	0.834	0.795	0.616	0.552
VT12[(b)]	5.480	1.226	0.802	0.775	0.551	0.546
VT13[(b)]	5.426	1.158	0.747	0.766	0.494	0.555
VT14[(c)]	5.686	1.194	0.845	0.785	0.640	0.560
VT16[(d)]	5.350	1.162	0.782	0.748	0.513	0.540
VT17[(d)]	5.451	1.146	0.744	0.759	0.496	0.540
VT18[(d)]	5.341	1.226	0.802	0.768	0.549	0.520
			40 m bridge			
VT10[(a)]	8.449	1.689	0.912	0.869	0.786	0.684
VT11[(a)]	7.968	1.533	0.875	0.847	0.702	0.634
VT12[(b)]	7.980	1.465	0.851	0.831	0.648	0.603
VT13[(b)]	7.926	1.459	0.810	0.825	0.560	0.611
VT14[(c)]	8.186	1.586	0.884	0.839	0.721	0.628
VT16[(d)]	7.850	1.429	0.837	0.811	0.616	0.607
VT17[(d)]	7.951	1.467	0.808	0.819	0.566	0.605
VT18[(d)]	7.841	1.486	0.851	0.826	0.647	0.599

(a) corresponds to the averaged influence response of the 4 sites for GVW = 325 kN
(b) corresponds to the influence response of typical Veh. Type for the 4 sites and GVW = 325 kN
(c) corresponds to the averaged influence response of the 4 sites for GVW = 425 kN
(d) corresponds to the influence response of typical Veh. Type for the 4 sites and GVW = 425 kN

Appendix D

MODELLING OF THE TRAFFIC DATA

Appendix D MODELLING OF THE TRAFFIC DATA

Table D-1: Parameters of the normal distributions used to model the axle spacing for the 4 truck classes and for the 4 sites (ρ = mode proportion, M*=mean, ST**=standard deviation) 248
Table D-2: Parameters of the normal distributions used to model the axle weights for the 2- and 3-axle trucks and for the 4 sites (ρ = mode proportion, M*=mean, ST**=standard deviation) 249
Table D-3: Axle weights (in % of GVW carried) for the 4-axle trucks in function of GVW - Angers 249
Table D-4: Axle weights (in % of GVW carried) for the 4-axle trucks in function of GVW - Auxerre 250
Table D-5: Axle weights (in % of GVW carried) for the 4-axle trucks in function of GVW – A196 250
Table D-6: Axle weights (in % of GVW carried) for the 4-axle trucks in function of GVW – A296 251
Table D-7: Axle weights (in % of GVW carried) for the 5-axle trucks in function of GVW - Angers 251
Table D-8: Axle weights (in % of GVW carried) for the 5-axle trucks in function of GVW - Auxerre 252
Table D-9: Axle weights (in % of GVW carried) for the 5-axle trucks in function of GVW – A196 252
Table D-10: Axle weights (in % of GVW carried) for the 5-axle trucks in function of GVW – A296 253
Table D-11: Parameters of the normal distributions used to model the truck weights for the 4 truck classes and for the 4 sites – Direction 1 253
Table D-12: Parameters of the normal distributions used to model the truck weights for the 4 truck classes and for the 4 sites – Direction 2 254
Table D-13: Parameters of the normal distributions modelling the speed (m/s) for the 4 sites 254
Figure D-1: Modelled PDF of truck weights: (a) 2-axle trucks dir. 1, (b) idem dir. 2, (c) 3-axle trucks dir. 1, (d) idem dir. 2, (e) 4-axle trucks dir. 1, (f) idem dir. 2, (g) 5/6-axle trucks dir. 1, (h) idem dir. 2 255

Table D-1: Parameters of the normal distributions used to model the axle spacing for the 4 truck classes and for the 4 sites (ρ = mode proportion, M*=mean, ST=standard deviation)**

2-axle trucks	S12 (m)		
	ρ	M*	ST**
Angers	1.000	5.1	0.4
Auxerre	1.000	5.5	0.5
A196	1.000	5.7	0.6
A296	1.000	5.8	0.6

3-axle trucks	S12 (m)			S23 (m)		
	ρ	M*	ST**	ρ	M*	ST**
Angers	0.650	3.4	0.7	1.000	1.1	0.2
	0.268	3.4	0.1			
	0.081	6.1	0.6			
Auxerre	0.143	3.3	0.6	1.000	1.2	0.2
	0.252	4.4	0.4			
	0.605	5.4	0.2			
A196	0.135	3.7	0.2	1.000	1.3	0.1
	0.345	4.5	0.3			
	0.520	5.5	0.3			
A296	0.102	3.9	0.1	1.000	1.3	0.1
	0.623	4.9	0.9			
	0.275	5.6	0.2			

4-axle trucks	S12 (m)			S23 (m)			S34 (m)		
	ρ	M*	ST**	ρ	M*	ST**	ρ	M*	ST**
Angers	0.672	3.1	0.1	0.153	3.5	0.3	0.317	1.2	0.1
	0.328	3.0	0.4	0.386	5.5	0.9	0.598	1.2	0.2
				0.461	6.0	0.3	0.085	1.8	0.1
Auxerre	1.000	3.2	0.2	0.130	4.7	0.8	0.806	1.3	0.1
				0.616	6.2	0.5	0.194	1.9	0.1
				0.254	6.2	0.2			
A196	0.096	2.8	0.5	0.151	4.0	1.3	0.840	1.3	0.1
	0.884	3.6	0.2	0.658	7.0	0.3	0.072	0.7	0.1
	0.019	4.0	0.0	0.191	6.2	0.3	0.088	2.0	0.1
A296	0.071	2.8	0.2	0.206	4.0	0.6	0.728	1.3	0.1
	0.113	3.3	0.1	0.472	6.7	0.7	0.140	0.7	0.1
	0.816	3.7	0.1	0.322	7.1	0.3	0.132	2.0	0.1

5-axle trucks	S12 (m)			S23 (m)			S34 (m)			S45 (m)		
	ρ	M*	ST**	ρ	M*	ST**	ρ	M*	ST**	ρ	M*	ST**
Angers	0.041	2.3	0.1	0.133	4.2	0.6	1.000	1.1	0.2	1.000	1.1	0.2
	0.959	3.0	0.2	0.867	5.1	0.3						
Auxerre	1.000	3.2	0.2	0.041	4.2	0.3	1.000	1.2	0.2	1.000	1.2	0.1
				0.959	5.4	0.3						
A196	0.955	3.6	0.2	0.229	5.3	0.6	1.000	1.2	0.1	1.000	1.2	0.1
	0.045	4.1	0.0	0.771	5.8	0.3						
A296	1.000	3.7	0.2	0.320	5.3	0.7	1.000	1.3	0.0	1.000	1.3	0.1
				0.680	5.9	0.3						

Table D-2: Parameters of the normal distributions used to model the axle weights for the 2- and 3-axle trucks and for the 4 sites (ρ = mode proportion, M*=mean, ST=standard deviation)**

2-axle trucks	W1 (% of GVW carried)			W2 (% of GVW carried)		
	ρ	M*	ST**	ρ	M*	ST**
Angers	0.560	33.4	3.7	0.440	59.4	7.4
	0.440	40.6	7.4	0.560	66.6	3.7
Auxerre	0.316	30.9	2.5	0.317	69.1	2.5
	0.684	33.9	3.9	0.683	66.1	3.9
A196	1.000	40.9	6.9	1.000	59.1	6.9
A296	1.000	40.3	8.1	1.000	59.7	8.1

3-axle trucks	W1 (% of GVW carried)			W2 (% of GVW carried)			W3 (% of GVW carried)		
	ρ	M*	ST**	ρ	M*	ST**	ρ	M*	ST**
Angers	0.066	20.4	1.5	0.769	34.6	6.8	0.558	30.5	5.9
	0.522	26.0	4.9	0.227	39.2	2.2	0.442	37.7	3.5
	0.412	38.7	8.6	0.004	54.4	3.7			
Auxerre	0.515	26.6	2.1	0.132	31.8	5.7	0.714	23.2	2.3
	0.459	28.3	6.3	0.233	39.5	4.8	0.200	34.1	3.0
	0.025	21.5	43.3	0.635	50.3	3.0	0.085	40.8	2.3
A196	0.046	23.5	4.1	0.500	35.2	5.7	0.466	23.7	2.6
	0.570	31.6	3.4	0.462	44.0	3.6	0.534	28.3	7.2
	0.384	39.2	6.0	0.039	54.0	4.2			
A296	0.099	22.3	5.7	0.408	31.0	5.7	0.294	21.2	2.5
	0.462	32.1	4.5	0.535	45.3	4.9	0.706	26.5	8.7
	0.439	39.4	8.0	0.057	61.6	5.4			

Table D-3: Axle weights (in % of GVW carried) for the 4-axle trucks in function of GVW - Angers

GVW (kN)	Mean			Standard Deviation		
	W1	W2	WT	W1	W2	WT
25	/	/	/	/	/	/
75	20.9	39.8	39.3	5.2	6.9	7.3
125	25.6	36.5	38.0	5.4	4.8	5.7
175	23.9	35.5	40.7	4.3	4.6	5.2
225	20.3	36.1	43.6	3.6	4.6	5.4
275	17.4	34.9	47.7	3.0	4.1	5.5
325	14.8	33.4	51.8	2.1	3.1	4.1
375	14.5	33.6	51.9	1.5	2.6	3.2
425	13.9	32.4	53.7	1.3	2.3	3.1
475	/	/	/	/	/	/
525	/	/	/	/	/	/
575	/	/	/	/	/	/

/ = data not available

Table D-4: Axle weights (in % of GVW carried) for the 4-axle trucks in function of GVW - Auxerre

GVW (kN)	Mean			Standard Deviation		
	W1	W2	WT	W1	W2	WT
25	/	/	/	/	/	/
75	25.1	36.2	38.7	5.0	7.6	7.8
125	20.8	36.8	42.4	5.4	7.4	7.4
175	20.6	36.8	42.6	4.9	5.2	7.2
225	21.4	37.3	41.3	3.7	4.4	5.2
275	19.8	36.9	43.4	3.3	4.3	5.4
325	17.7	35.4	46.9	2.8	3.9	5.3
375	15.8	34.4	49.7	2.2	3.2	4.2
425	14.8	34.3	50.9	1.8	2.6	3.3
475	14.6	34.1	51.3	1.7	2.5	3.0
525	14.4	32.7	52.9	2.1	2.5	3.4
575	13.9	31.9	54.1	0.7	2.0	2.4

/ = data not available

Table D-5: Axle weights (in % of GVW carried) for the 4-axle trucks in function of GVW – A196

GVW (kN)	Mean			Standard Deviation		
	W1	W2	WT	W1	W2	WT
25	31.7	35.4	32.9	7.6	9.3	13.3
75	30.2	36.3	33.5	5.8	7.2	7.7
125	33.7	31.0	35.3	5.1	4.5	4.9
175	30.5	31.5	38.0	3.6	3.9	4.3
225	25.8	32.5	41.7	2.9	4.4	5.1
275	22.0	33.7	44.3	2.9	4.8	5.8
325	19.0	33.2	47.8	2.2	4.8	5.7
375	16.9	31.5	51.6	1.8	3.2	3.9
425	15.9	31.1	53.1	1.7	3.0	3.7
475	/	/	/	/	/	/
525	/	/	/	/	/	/
575	/	/	/	/	/	/

/ = data not available

Table D-6: Axle weights (in % of GVW carried) for the 4-axle trucks in function of GVW – A296

GVW (kN)	Mean			Standard Deviation		
	W1	W2	WT	W1	W2	WT
25	31.1	34.3	34.6	9.8	8.6	13.7
75	34.2	33.1	32.7	8.1	9.2	8.7
125	36.3	31.1	32.6	5.5	4.6	4.9
175	31.7	32.0	36.3	4.3	4.1	5.2
225	26.4	33.8	39.8	3.8	4.8	6.0
275	21.7	34.0	44.3	4.0	4.9	6.4
325	19.0	32.6	48.5	3.2	5.1	6.3
375	17.1	31.9	51.0	2.2	3.5	3.8
425	16.2	31.2	52.6	2.1	3.1	4.1
475	/	/	/	/	/	/
525	/	/	/	/	/	/
575	/	/	/	/	/	/

/ = data not available

Table D-7: Axle weights (in % of GVW carried) for the 5-axle trucks in function of GVW - Angers

GVW (kN)	Mean			Standard Deviation		
	W1	W2	WT	W1	W2	WT
25	/	/	/	/	/	/
75	/	/	/	/	/	/
125	19.1	36.5	44.5	6.0	7.4	7.2
175	23.6	32.8	43.7	4.6	4.2	5.0
225	21.4	33.4	45.3	3.2	4.8	5.4
275	18.1	33.8	48.1	2.4	4.5	5.5
325	15.7	32.3	52.0	1.8	3.8	4.7
375	14.3	31.0	54.6	1.5	3.3	3.9
425	13.4	29.6	57.1	1.2	2.9	3.4
475	12.7	27.7	59.6	1.0	2.7	3.1
525	/	/	/	/	/	/
575	/	/	/	/	/	/

/ = data not available

Table D-8: Axle weights (in % of GVW carried) for the 5-axle trucks in function of GVW - Auxerre

GVW (kN)	Mean			Standard Deviation		
	W1	W2	WT	W1	W2	WT
25	/	/	/	/	/	/
75	/	/	/	/	/	/
125	20.8	30.0	49.2	4.3	8.6	8.1
175	17.2	35.3	47.4	3.8	6.6	7.6
225	19.3	34.7	46.1	4.7	5.0	7.4
275	19.5	34.6	45.9	3.8	4.2	5.9
325	17.3	34.3	48.5	2.8	4.3	5.6
375	15.3	33.2	51.5	2.2	4.2	5.2
425	14.3	32.2	53.6	1.7	3.7	4.5
475	13.7	31.2	55.1	1.5	3.3	4.0
525	13.5	29.9	56.6	1.4	2.9	3.5
575	13.4	28.8	57.8	1.6	2.8	3.6

/ = data not available

Table D-9: Axle weights (in % of GVW carried) for the 5-axle trucks in function of GVW – A196

GVW (kN)	Mean			Standard Deviation		
	W1	W2	WT	W1	W2	WT
25	/	/	/	/	/	/
75	31.7	31.6	36.7	4.9	5.9	7.3
125	32.4	29.7	38.0	5.8	5.2	5.4
175	29.7	29.1	41.2	4.7	4.5	5.1
225	24.9	30.8	44.4	3.6	5.3	6.1
275	21.6	31.0	47.4	2.6	5.4	6.3
325	19.0	30.4	50.6	2.2	4.6	5.7
375	16.8	28.9	54.4	1.7	3.7	4.4
425	16.1	27.9	56.1	1.4	3.4	3.8
475	15.3	27.5	57.3	1.5	3.5	3.8
525	/	/	/	/	/	/
575	/	/	/	/	/	/

/ = data not available

Table D-10: Axle weights (in % of GVW carried) for the 5-axle trucks in function of GVW – A296

GVW (kN)	Mean			Standard Deviation		
	W1	W2	WT	W1	W2	WT
25	/	/	/	/	/	/
75	32.3	28.5	39.2	6.3	7.5	9.1
125	34.3	28.1	37.6	6.6	5.5	7.9
175	30.8	30.4	38.9	5.1	5.1	5.9
225	25.4	32.0	42.5	4.3	6.0	7.0
275	21.8	32.2	46.0	3.9	6.2	7.6
325	19.2	30.4	50.4	2.9	5.1	6.4
375	17.5	28.5	54.0	2.2	3.9	4.8
425	17.2	28.5	54.2	2.0	3.7	4.6
475	17.4	28.8	53.8	2.0	3.5	4.5
525	/	/	/	/	/	/
575	/	/	/	/	/	/

/ = data not available

Table D-11: Parameters of the normal distributions used to model the truck weights for the 4 truck classes and for the 4 sites – Direction 1

	2-axle trucks			3-axle trucks			4-axle trucks			5/6-axle trucks		
	ρ	M*	ST**	ρ	M*	ST**	ρ	M*	ST**	ρ	M*	ST**
Angers	0.153	44.2	6.5	0.069	51.2	9.7	0.583	231.1	61.9	0.274	199.9	36.7
	0.395	76.4	20.7	0.887	166.3	53.2	0.240	176.6	29.6	0.553	308.7	49.9
	0.453	117.4	30.5	0.043	268.4	34.7	0.177	331.0	30.1	0.173	383.2	35.4
Auxerre	0.064	43.8	2.3	0.060	85.2	23.2	0.000	258.9	125.4	0.160	296.2	55.1
	0.642	81.3	67.3	0.368	223.0	23.6	0.476	261.6	53.6	0.834	412.2	55.1
	0.294	163.0	26.2	0.572	220.7	51.2	0.524	386.6	45.2	0.006	604.3	56.4
A196	0.085	39.6	5.1	0.137	43.2	9.4	0.307	169.5	27.6	0.122	171.2	24.2
	0.631	82.6	29.6	0.688	156.1	40.9	0.625	208.6	50.5	0.553	257.6	72.1
	0.284	147.5	25.1	0.175	201.8	71.2	0.068	372.7	30.0	0.325	393.8	29.0
A296	0.423	57.1	29.5	0.126	41.8	8.1	0.685	161.4	36.9	0.285	157.8	37.3
	0.483	120.1	37.9	0.873	158.3	51.1	0.230	253.1	35.7	0.392	261.9	62.4
	0.094	163.8	12.8	0.001	280.6	9.1	0.085	378.2	33.1	0.323	387.7	26.7

Table D-12: Parameters of the normal distributions used to model the truck weights for the 4 truck classes and for the 4 sites – Direction 2

	2-axle trucks			3-axle trucks			4-axle trucks			5/6-axle trucks		
	ρ	M*	ST**	ρ	M*	ST**	ρ	M*	ST**	ρ	M*	ST**
Angers	0.143	46.5	8.0	0.093	56.4	12.4	0.493	243.6	64.6	0.160	205.3	40.1
	0.524	82.9	23.8	0.653	141.5	31.1	0.301	162.1	28.8	0.441	300.6	53.6
	0.333	132.3	31.8	0.254	218.5	33.4	0.206	361.9	31.6	0.399	400.4	35.9
Auxerre	0.177	41.5	5.5	0.094	99.1	28.1	0.037	265.4	140.2	0.149	293.8	59.6
	0.456	104.8	45.0	0.711	241.0	57.5	0.450	284.3	57.0	0.839	456.8	60.8
	0.367	188.0	31.4	0.195	252.7	16.4	0.514	425.4	48.9	0.012	583.1	25.2
A196	0.139	43.8	7.6	0.565	139.4	58.4	0.094	180.8	25.0	0.208	204.2	49.8
	0.612	91.7	30.4	0.147	156.8	13.8	0.818	209.7	60.4	0.424	310.6	71.7
	0.249	168.1	23.7	0.289	223.4	33.6	0.089	372.4	31.4	0.368	398.1	30.0
A296	0.301	41.8	10.5	0.198	37.3	15.7	0.077	21.4	21.1	0.384	203.1	69.0
	0.326	75.6	24.9	0.796	174.6	55.0	0.764	196.3	57.5	0.152	377.6	23.8
	0.373	151.9	37.3	0.007	350.0	9.9	0.159	339.1	59.5	0.464	366.4	55.5

Table D-13: Parameters of the normal distributions modelling the speed (m/s) for the 4 sites

	Angers		Auxerre*		A196		A296	
	Dir. 1	Dir. 2	Dir. 1	Dir. 2	Dir. 1	Dir. 2	Dir. 1	Dir. 2
Mean	19.5	18.1	24.8	22.2	23.6	23.9	24.2	25.1
St. Dev.	2.7	2.2	0.0	0.0	0.7	1.7	1.1	1.0

** in that traffic file all the speeds are equal*

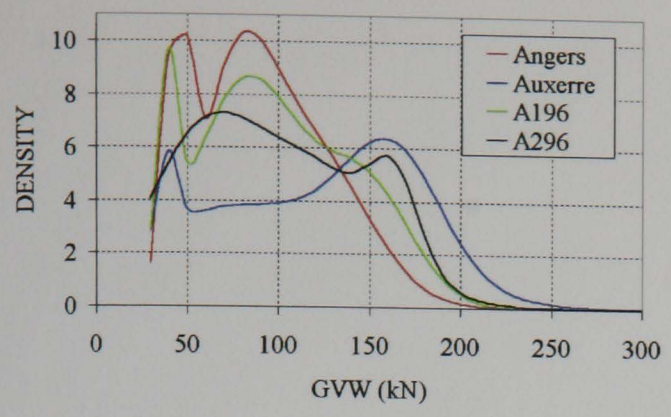

(a)

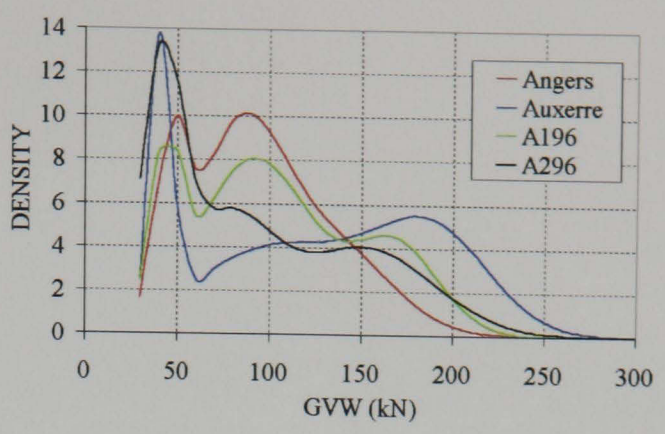

(b)

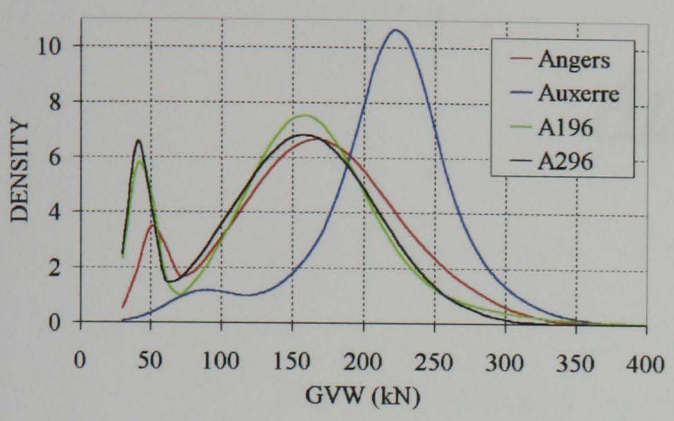

(c)

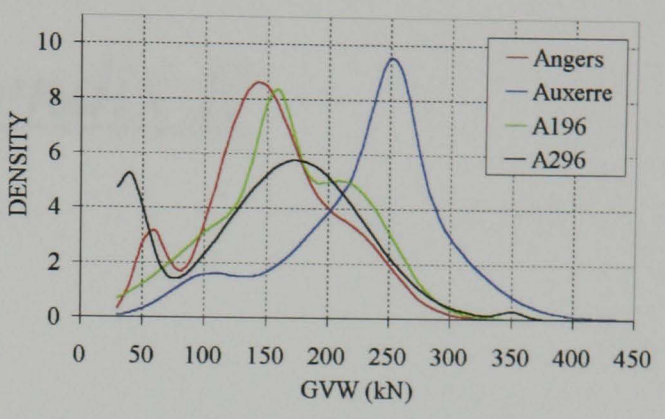

(d)

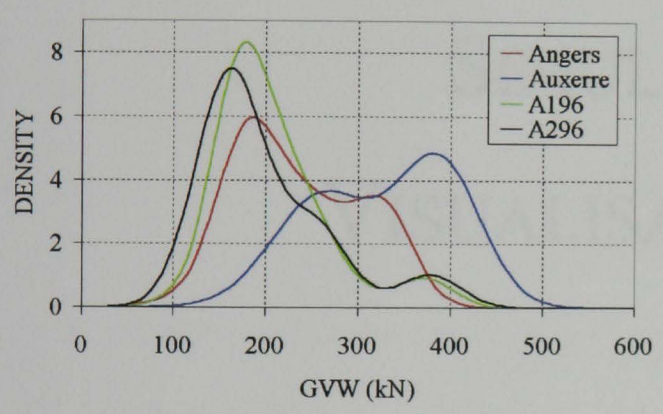

(e)

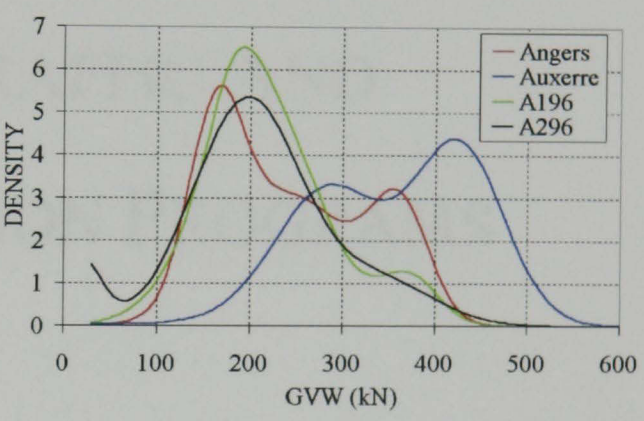

(f)

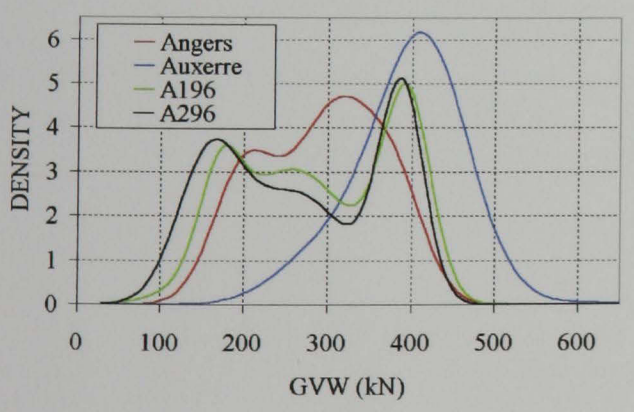

(g)

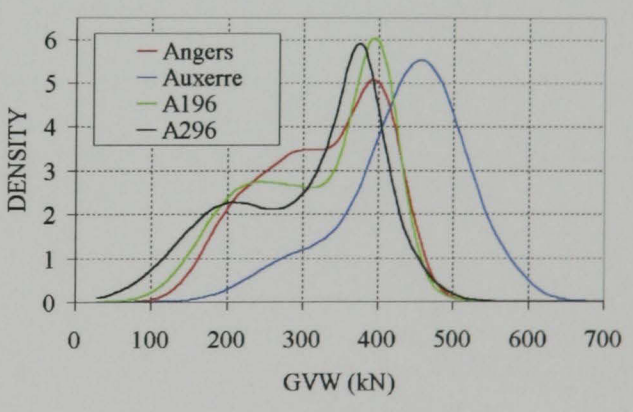

(h)

Figure D-1: Modelled PDF of truck weights: (a) 2-axle trucks dir. 1, (b) idem dir. 2, (c) 3-axle trucks dir. 1, (d) idem dir. 2, (e) 4-axle trucks dir. 1, (f) idem dir. 2, (g) 5/6-axle trucks dir. 1, (h) idem dir. 2

Appendix E

SIMULTRAFFIC AND VISUALISATION PROGRAMS

Appendix E SIMULTRAFFIC AND VISUALISATION PROGRAMS

E.1 PROGRAM SIMULTRAFFIC

E.1.1 Format of the data in the input file

Table E-1: Composition of a traffic record using the CASTOR format

Field	Format	Units	Description of the field
Head	I4	-	
Day	I2	-	
Month	I2	-	
Year	I2	-	
Hour	I2	-	
Minute	I2	-	
Second	I2	-	
Hundredth	I2	-	Hundredth of second
Speed	I3	dm/s	Speed of the truck
GVW	I4	kN	Gross Vehicle Weight
Length	I3	dm	Truck length (first to last axle)
Naxles	I1	-	Number of axles
Direction	I1	-	Direction of traffic
Lane	I1	-	Lane in which the truck is
Transverse	I3	dm	Transverse location of the truck
W1	I3	kN	Weight of the 1st axle
S12	I2	dm	Spacing between axles 1 and 2
W2	I3	kN	Weight of the 2nd axle
'-' = dimensionless			

E.1.2 Storage of the traffic data

The relevant details of the traffic records are stored into two sets of arrays, one for each lane of traffic considered. The different arrays employed are:

- 'T*i*': contains the arrival times of all the trucks in chronological order (for lane *i*);
- 'G*i*': contains the gross vehicle weights of all the trucks;
- 'L*i*': contains the lengths of all the trucks;
- 'N*i*': contains the number of axles of all the trucks;
- 'AW*i*': contains the axle weights of all the trucks;
- 'Sp*i*': contains the lengths of all the trucks.

For convenience, the arrival times are transformed into a single value number that corresponds to the arrival time in seconds. Trivially,

$$T_{arrival} = \text{day} * (24 * 60 * 60) + \text{hour} * (60 * 60) + \text{minute} * (60) + \text{seconde} + \text{hundredth of second} / 100$$

Equation E-1

However, attention has to be brought to the field 'day'. Indeed, it happens that the recording period starts at the end of one month and continues for few days during the next month. In that case the field 'day' goes from a high value (e.g. '31') to a low value (e.g.'1') and will induce the arrival times of the trucks in the next month to be less than the arrival times of the previously arrived trucks. In order to overcome that potential source of error, the days are artificially updated in the case of traffic files overlapping two months (e.g. '1' becomes '32' if the last day of the previous month was '31').

The full storage of the data is done at the beginning of the program, until the traffic data file has been read through completely. All the abovementioned arrays will have N*i* rows, where N*i* is the total number of trucks in lane *i*.

E.1.3 Testing for crossing events

The process of testing for crossing events is described in Figure E-1.

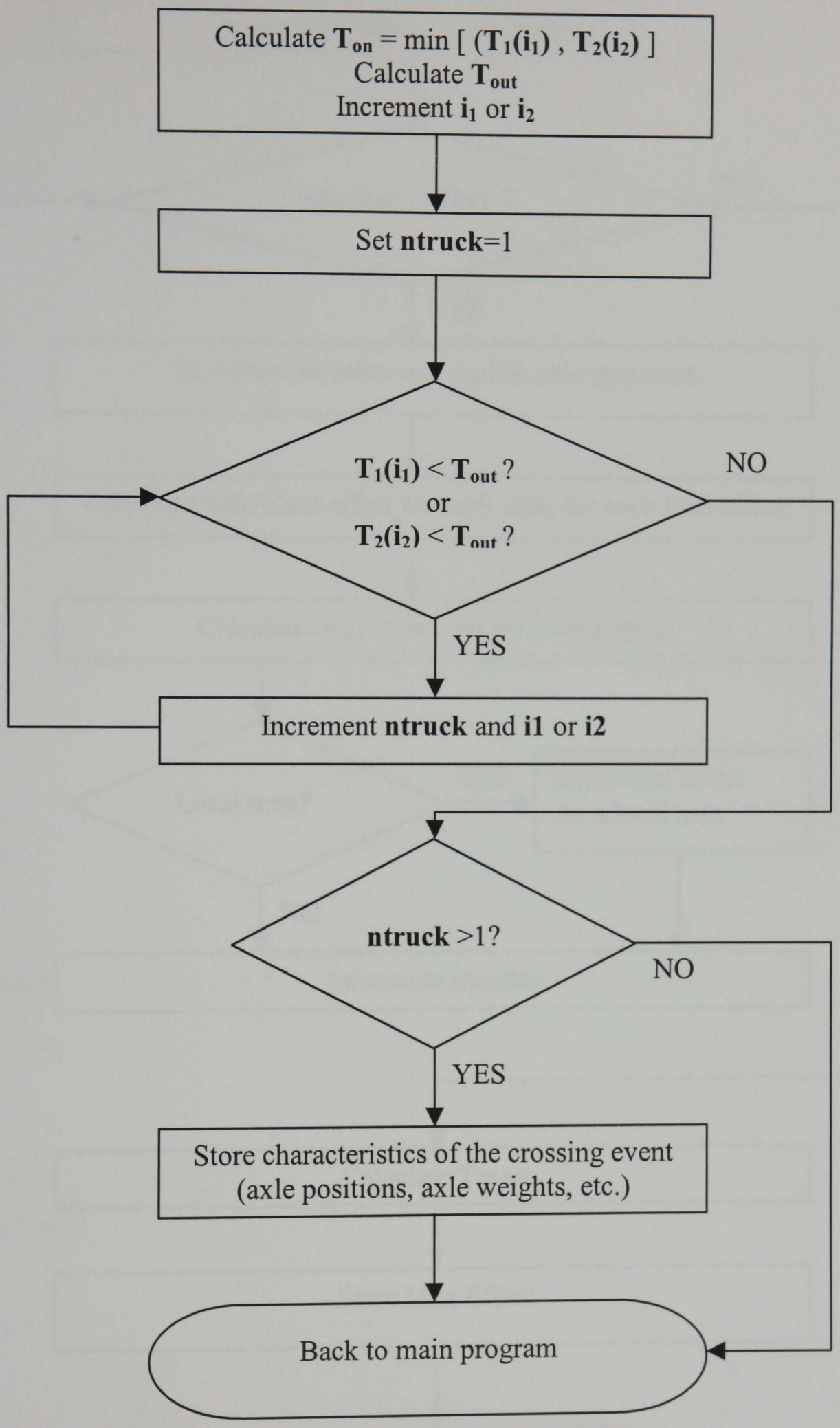

Figure E-1: Flow chart describing the process of testing for crossing events

E.1.4 Calculating the effects

The process of calculating the load effects is described in Figure E-2.

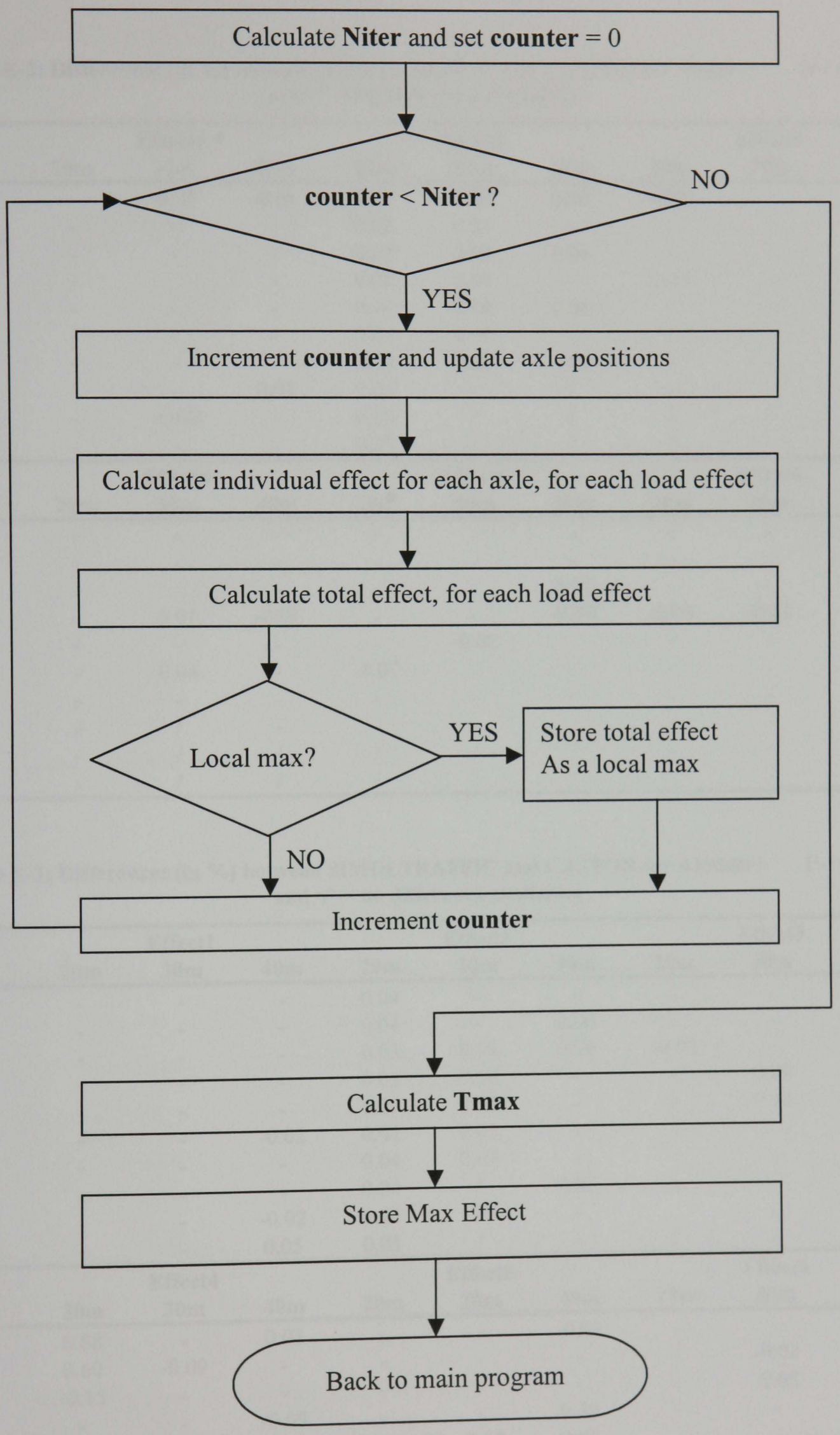

Figure E-2: Flow chart describing the process of calculating the maximum effects for a crossing event

E.1.5 Results

Table E-2: Differences (in %) between SIMULTRAFFIC and CASTOR for Auxerre ['-' = 0.00 and '/' = no difference available]

	Effect1			Effect2			Effect3		
	20m	30m	40m	20m	30m	40m	20m	30m	40m
1	-	-0.03	-0.08	0.04	0.08	0.05	-0.06	-	-0.06
2	-	-	-	0.02	0.08	-	-	-	-
3	-	-	-	0.02	0.09	0.06	-	-	-
4	-	-	-	0.02	0.09	-	-0.11	-	-
5	-	-	-	0.04	0.09	0.06	-	-	-
6	-	-	-	0.04	0.09	-	-	-	-
7	-	-	-	0.04	0.09	0.06	-	-	-
8	-	-	0.03	0.04	-	/	-	-	-
9	-	-0.02	-	0.04	/	/	-	-	/
10	-	-	-	0.05	/	/	/	-	/
	Effect4			**Effect5**			**Effect6**		
	20m	30m	40m	20m	30m	40m	20m	30m	40m
1	-	-	-	-	-	-	-	-	-
2	-	-	-	-	-	-	-	-	-
3	-	-	-	-	-	0.07	-	-	-0.02
4	-	0.01	-0.01	-	-	-0.22	-0.05	-0.02	-
5	-	-	-	-	-0.02	-	-	-	-0.02
6	-	0.04	-	-0.07	-	-	-	-	-
7	-	-	-	-	-	-	-	-	-0.03
8	-	/	-	-	-		-	-	-
9	-	/	/	/	/	/	-	/	/
10	-	/	/	/	/	/	-	/	/

Table E-3: Differences (in %) between SIMULTRAFFIC and CASTOR for A196dir1 ['-' = 0.00 and '/' = no difference available]

	Effect1			Effect2			Effect3		
	20m	30m	40m	20m	30m	40m	20m	30m	40m
1	-	-	-	0.04	-	-	-	-	-0.04
2	-	-	-	0.04	-	0.06	-	-	-0.06
3	-	-	-	0.03	0.10	0.06	-0.02	-	-
4	-	-	-	0.03	0.10	-	-	0.20	-
5	-	-	-	0.03	0.06	-	-	0.15	-
6	-	-	-0.02	0.01	0.05	-	-	-	-0.06
7	-	-	-	0.04	0.03	-	-	-	-
8	-	-	-	0.04	/	0.07	-	-	-
9	-	-	-0.02	0.04	/	-		-	/
10	-	-	0.05	0.03	/	-	/	/	/
	Effect4			**Effect5**			**Effect6**		
	20m	30m	40m	20m	30m	40m	20m	30m	40m
1	0.88	-	0.03	-	-	-0.09	-	-	0.09
2	0.60	-0.09	-	-	-	-	-	-0.02	-0.02
3	-0.15	-	-	-	-	-	-	-0.02	-0.27
4	-	-	-0.09	-	-	0.39	-	-	-
5	-	-	-	-0.03	-0.02	0.65	-	-	-
6	/	-	-	-	-	0.51	-	-	-
7	/	-0.02	/	-	-0.02	0.37	-	/	/
8	/	-	/	-0.08	-	0.32	-	/	/
9	/	/	/	/	-	0.48	/	/	/
10	/	/	/	/	/	/	/	/	/

Table E-4: Differences (in %) between SIMULTRAFFIC and CASTOR for A196dir2 ['-' = 0.00 and '/' = no difference available]

	Effect1			Effect2			Effect3		
	20m	30m	40m	20m	30m	40m	20m	30m	40m
1	-	-	-	0.04	-	0.05	-	-	-
2	-	-	-	0.03	-	-	-	-	-
3	-	-	-	0.04	0.09	0.06	0.24	-	-
4	-	-	-	0.03	0.09	-	-0.02	-	-
5	-	-	-	0.04	-	0.06	-	/	-
6	-	-	-	0.03	0.09	0.06	-	/	/
7	-	-	/	0.03	-	0.06	-	/	/
8	-	-	/	0.04	0.10	-	-0.02	/	/
9	-	-	/	0.03	/	0.06	/	/	/
10	-	0.02	/	0.03	/	-	/	/	/
	Effect4			**Effect5**			**Effect6**		
	20m	30m	40m	20m	30m	40m	20m	30m	40m
1	-	-	-	-	-	-0.02	-	-	-
2	-	-	0.37	0.15	-0.02	-	-	-	-
3	-	-	-	-	-	-	-	-	-
4	-	-	-	-	-	-	-	-	-0.02
5	-	0.56	-	-	-0.02	-0.02	-	-	-
6	-	-	-	-	-	-0.02	-0.03	-	-
7	-	-	-	-	-0.02	0.08	-	-	-
8	-	/	/	-	-	0.02	-0.03	-	-
9	/	/	/	-	-	0.49	-0.03	/	/
10	/	/	/	-0.03	-	/	/	/	/

E.2 VISUALISATION OF THE CRITICAL LOADING EVENTS

All the output files generated by SIMULTRAFFIC are merely a succession of numbers and, intrinsically, not very visual. In order to make the results easier to read and more meaningful, two programs have been developed by the author using MATLAB Version 12. These two programs enable the visualisation of the output data, which in turn makes the analysis and interpretation of the results an easier task.

Plotting the trucks for the critical loading events

From SIMULTRAFFIC an output file is generated, containing the relevant details of the trucks involved in the most critical loading events. The data are stored in an array, every row corresponding to a distinct truck; a typical crossing event involves two trucks and will therefore be represented by two rows in the array. The array is the main input to the program PLOTTRUCKSFORGIVENEFFECT, which itself outputs a plot showing the 20 most critical loading events, and the various trucks involved at their respective locations. Also indicated on the plot (see Figure E-3) are the gross vehicle weights of the trucks and their

number of axles (represented by their wheels). The trucks are filled with different shades of grey varying in function of the GVW of the truck (darker grey indicates heavier truck). Finally the individual contributions of each truck to the combined effect are also represented on the plot.

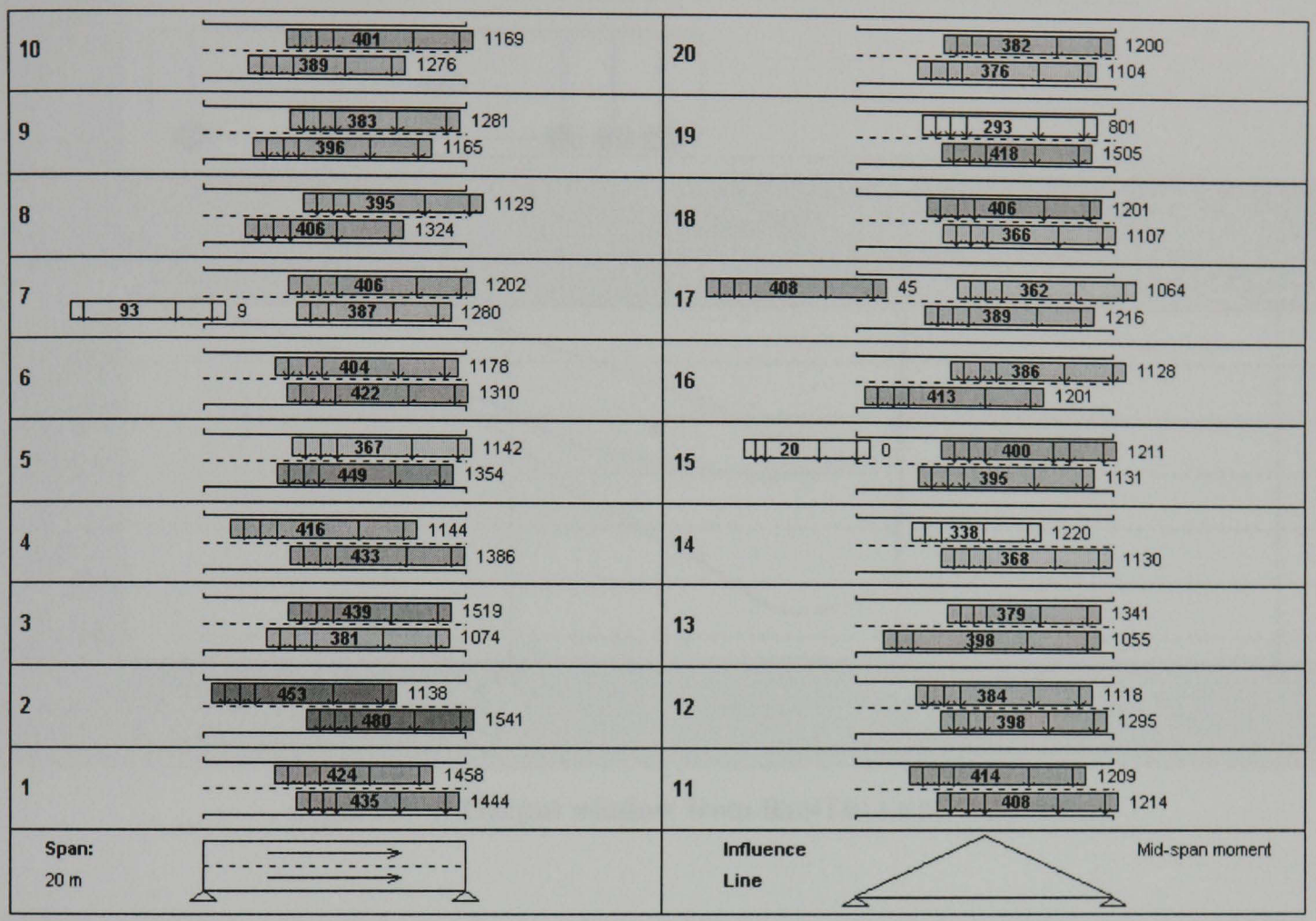

Figure E-3: Output of the program PLOTTRUCKSFORGIVENEFFECT

From Figure E-3, it can be seen that the interpretation of the results is greatly facilitated by the visualisation of these results, as the trucks can be observed directly without having to be 'imagined'. Detailed discussions and interpretations of what are the typical critical loading events are included in the next two chapters.

Running the trucks over the bridge

Another useful program has been developed by the author in order to visualise the combined effect induced by the trucks involved in a crossing event as they move along the bridge. Indeed, it can be awkward to realise by how much each truck contributes towards the combined effect, and also how this combined effect varies as the trucks traverse the bridge. The program RUNTRUCKSOVERBRIDGE simulates the passage of the trucks involved in a given crossing event while, at the same time, displaying both the individual and the combined effect (as illustrated in Figure E-4).

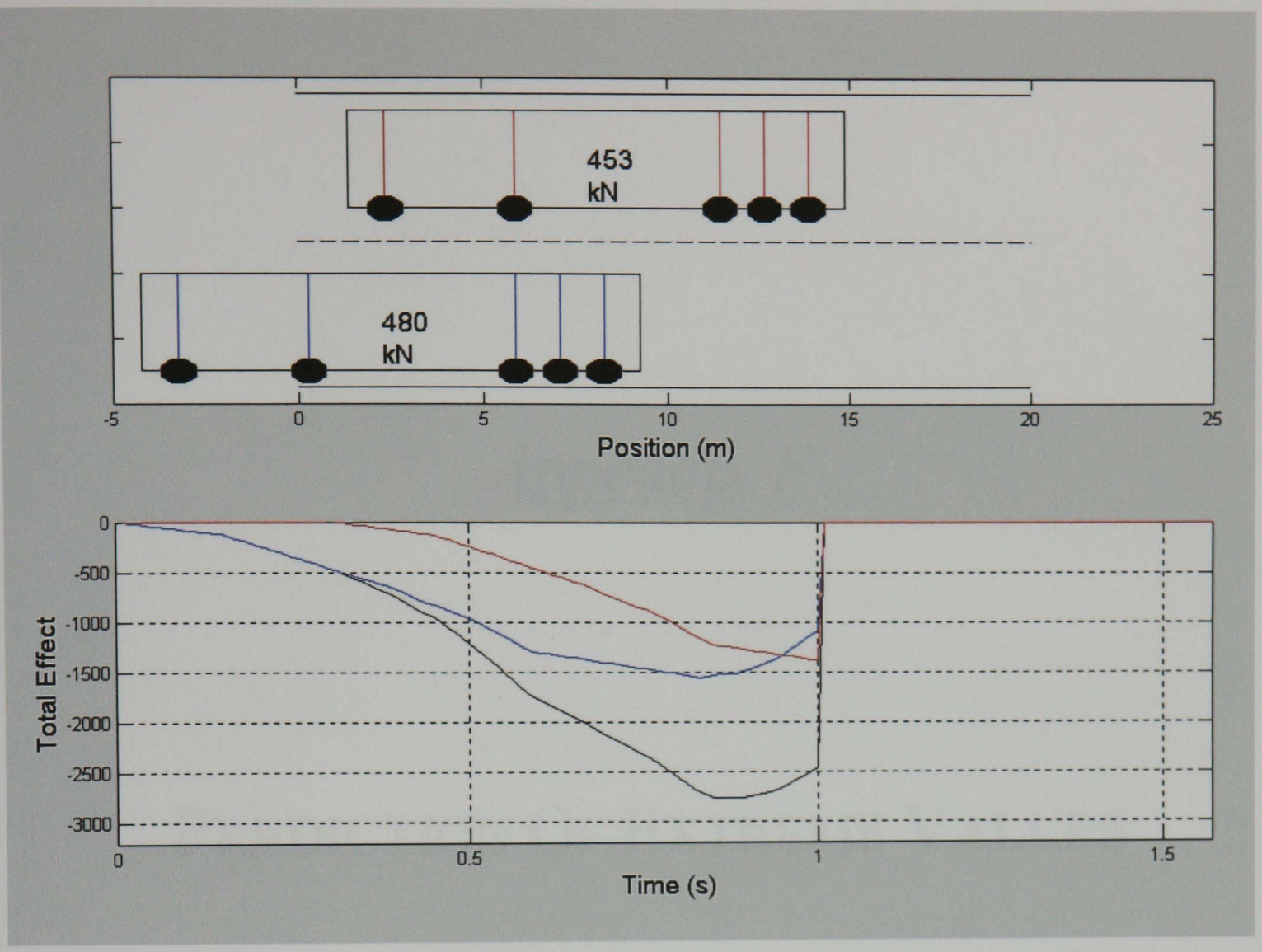

Figure E-4: Output window from RUNTRUCKSOVERBRIDGE

In Figure E-4 the blue line corresponds to 480kN truck and the red line to the 453kN truck. The figure is a 'print screen' of the program while it is running; the execution of the program only stops once both trucks have left the bridge completely. From Figure E-4 it appears that the blue truck has past the critical location (mid-span for that load effect) while the red is reaching it; however, the combined maximum has already been attained as the magnitude of the effect induced by the blue truck reduces quicker than the magnitude of the red truck increases (which is justified by the difference in GVW).

Appendix F

PREDICTION OF EXTREME VALUES

Appendix F PREDICTION OF EXTREME VALUES

F.1 INITIAL ESTIMATES FOR GUMBEL DISTRIBUTION

This method was developed by Castillo (1988) and is called the percentile method. Any variate following a Gumbel distribution for maxima can be expressed as:

$$x_i = \lambda + \delta u_i \qquad \textbf{Equation F-1}$$

where

$$u_i = \ln\left(-\ln\left(1 - G(x_{(i)})\right)\right) \qquad \textbf{Equation F-2}$$

and if $G(x_{(i)})$ the cumulative density function at x_i is approximated by $\left((i-1/2)/n\right)$ then Equation F-1 can be rewritten as:

$$x_i = \lambda + \delta \ln\left(-\ln\left(1 - \frac{i-0.5}{n}\right)\right) \qquad \textbf{Equation F-3}$$

For any pair (k_1, k_2) of integers smaller than n, it can be written:

$$\sum_{i=k_1}^{k_2} x_i = \lambda(k_2 - k_1 + 1) + \delta \sum_{i=k_1}^{k_2} \ln\left(-\ln\left(1 - \frac{i-0.5}{n}\right)\right) \qquad \textbf{Equation F-4}$$

A linear system of two equations can be obtained and solved using the following equations:

$$\begin{bmatrix} B_1 \\ B_2 \end{bmatrix} = \begin{bmatrix} A_{11} & A_{12} \\ A_{21} & A_{22} \end{bmatrix} \qquad \textbf{Equation F-5}$$

$$B_1 = \sum_{i=k_1}^{\text{int}[(k_1+k_2)/2]} x_i \qquad \textbf{Equation F-6}$$

$$A_{11} = \text{int}\left[(k_1 + k_2)/2\right] - k_1 + 1$$

Equation F-7

$$A_{12} = \sum_{i=k_1}^{\text{int}\left[(k_1+k_2)/2\right]} \left[\ln\left(-\ln\left(1 - \frac{i-0.5}{n} \right) \right) \right]$$

Equation F-8

$$B_2 = \sum_{i=\text{int}\left[(k_1+k_2)/2+1\right]}^{k_2} x_i$$

Equation F-9

$$A_{21} = k_2 - \text{int}\left[(k_1 + k_2)/2 + 1\right] + 1$$

Equation F-10

$$A_{22} = \sum_{i=\text{int}\left[(k_1+k_2)/2+1\right]}^{k_2} \left[\ln\left(-\ln\left(1 - \frac{i-0.5}{n} \right) \right) \right]$$

Equation F-11

Finally, good initial estimates are derived using the following equations:

$$\lambda_{ini} = \left(B_1 A_{22} - B_2 A_{12}\right)/D$$

Equation F-12

and

$$\delta_{ini} = \left(B_2 A_{11} - B_1 A_{21}\right)/D$$

Equation F-13

where

$$D = \left(A_{11} A_{22} - A_{12} A_{21}\right)$$

Equation F-14

This approach can be used efficiently for any distribution of extremes (Gumbel, Weibull or Frechet) and for problems of minima or maxima by transforming the initial variates appropriately (cf. Castillo 1988). Typically, when the right tail (i.e. problem of maxima),

$k_2 = n$ and $k_1 = n - n_{tail}$ (where n is the total number of data and n_{tail} is the number of values from the tail considered for the estimation of the parameters).

F.2 OPTIMISATION OF THE EXTREME VALUE DISTRIBUTION PARAMETERS

F.2.1 Method for optimising the parameters

The next step consists in optimising the parameters of the extreme value distribution selected; this optimisation is done through minimisation of the error between the distribution and the measured data. As mentioned in the literature review, the right tail (in a problem of maxima) of the distribution is the most important part and therefore should be given more weight in the optimisation process. Among the various weighted lest-squares methods proposed by Castillo (1988), the one thought to be the most suitable for this study is the tail equivalence one. The function to be minimised is:

$$\sum_{i=k_1}^{k_2}\left[\frac{1}{(1-p_i)^2}\left(p_i - G(x_{(i)};\theta)\right)^2\right] \qquad \textbf{Equation F-15}$$

where p_i is the plotting position, $G(x_{(i)})$ is the cdf of $x_{(i)}$ and θ is the vector of parameters characterising the distribution (e.g. $[\lambda, \delta]$ for a Gumbel distribution).

This minimisation can be done using the POWELL subroutine from the FORTRAN Numerical Recipes (reference). This subroutine uses the *conjugate directions* method; basically it carries out one-dimensional minimisations along favourable direction in a N-dimensional space. One of its advantages is that the knowledge of the function to be minimised suffices, its derivative is not required. In addition, it can easily be adapted to multi-dimensional problems (bi-dimensional for Gumbel and tri-dimensional for Weibull/Frechet).

It should be note that all the extrapolation performed correspond to a return period of 1 000 years (i.e. a lifetime of 50 years and a probability of exceedance of 5%), as commonly used in the design and assessment of bridges (Flint & Jacob 1991, Bruls *et al.* 1991).

F.2.2 Sensitivity to the number of data

An important aspect to consider in the optimisation of the parameters (and consequently in the extrapolation of extreme values) is the sensitivity to the number of data selected in the tail. Various numbers have been considered for the extrapolation, based upon Castillo (1988): $\sqrt{n}$, $2\sqrt{n}$ and $3\sqrt{n}$ (where n is the number of meeting events for the period of traffic considered). Using the formula developed in Appendix H, the number of meeting events is estimated for a period of 10 weeks of traffic; the optimisation procedure is then applied to each traffic type, considering the appropriate number of data to select in the tail from Table F-1. As illustrated in the table, there can be as little as 64 values to consider, and as many as 813, depending on the traffic type (mainly traffic intensity) and the span.

Table F-1: Number of points selected in the tail for various traffic types

		Wa			Wc			Wb		
		20m	30m	40m	20m	30m	40m	20m	30m	40m
Qa	$\sqrt{n}$	71	83	93	64	74	83	66	75	84
	$2\sqrt{n}$	142	166	186	128	148	166	132	150	168
	$3\sqrt{n}$	213	249	279	192	222	249	198	225	252
Qb	$\sqrt{n}$	135	157	177	122	141	158	124	143	160
	$2\sqrt{n}$	270	314	354	244	282	316	248	286	320
	$3\sqrt{n}$	405	471	531	366	423	474	372	429	480
Qc	$\sqrt{n}$	208	242	271	187	216	242	191	220	245
	$2\sqrt{n}$	416	484	542	374	432	484	382	440	490
	$3\sqrt{n}$	624	726	813	561	648	726	573	660	735

After estimating good initial estimates, the optimisation process was performed for each traffic type and bridge length, using successively): $\sqrt{n}$, $2\sqrt{n}$ and $3\sqrt{n}$ values in the tail. The results are presented in Table F-2 to Table F-4 for the various traffic intensities *Qa*, *Qb* and *Qc*. For each traffic type, the extrapolated value obtained by using $2\sqrt{n}$ data in the right tail is given, along with the differences (in %) between this value and the extrapolated values obtained when using $\sqrt{n}$ and $3\sqrt{n}$ points in the tail.

From Table F-2, the maximum differences observed for all the load effects, bridge lengths and traffic types considered, are –12% and +11%. As a general rule, higher extrapolated value are obtained when the number of data selected in the tail increases. Only in few cases the extrapolated value is lower than the one obtained when using fewer points in the tail. Also, the variations tend to be higher between the extrapolated values obtained using $2\sqrt{n}$ and $\sqrt{n}$ than the ones obtained when using $2\sqrt{n}$ and $3\sqrt{n}$ points.

Table F-2: Extrapolated values in function of number of points selected in the tail (traffic int. Qa)

Bridge Length	Load Effect	QaWa			QaWb			QaWc		
		EV *	D**	D***	EV *	D**	D***	EV *	D**	D***
20 m	1	3921	-4	3	3852	-11	7	4539	-6	4
	2	957	-3	2	1112	-10	1	1245	-9	4
	3	795	-2	2	837	-12	6	988	-6	3
	4	828	-2	2	845	-9	4	1029	-7	3
	5	566	-3	1	549	-7	2	675	-3	0
	6	581	-2	-1	557	-4	1	668	-5	0
30 m	1	6988	-8	-1	6718	-10	7	7875	-5	3
	2	1366	-1	2	1429	-4	2	1723	2	0
	3	959	-7	-3	961	-10	-4	1135	-4	4
	4	942	-6	-1	917	-5	2	1122	-7	4
	5	706	-7	2	682	-10	-3	810	-3	2
	6	718	-6	2	675	-8	3	821	-6	4
40 m	1	9912	-7	5	9598	-7	7	11606	-3	2
	2	2154	4	-1	2071	11	-3	2845	2	-3
	3	1009	-6	2	995	-6	4	1237	-4	2
	4	1018	-3	1	1011	-7	3	1230	-4	2
	5	800	-8	2	788	-12	5	921	-3	2
	6	795	-7	2	788	-10	3	935	-6	4
Average (%)			**-4**	**1**		**-7**	**3**		**-4**	**2**
Min. Diff. (%)			**-8**	**-3**		**-12**	**-4**		**-9**	**-3**
Max. Diff. (%)			**4**	**5**		**11**	**7**		**2**	**4**

* extrapolated value using $2\sqrt{n}$ values in the tail

** difference in the extrapolated values when using $2\sqrt{n}$ and $\sqrt{n}$ values in the tail

*** difference in the extrapolated values when using $2\sqrt{n}$ and $3\sqrt{n}$ values in the tail

Table F-3 shows the same results as the previous table for other traffic types, the ones for which the traffic intensity is *Qb*. The maximum differences observed are –10% and +9%.

Again, the overall trend is an increase in the extrapolated value as the number of data selected in the tail increases. Finally Table F-4 presents similar results for traffic types with traffic intensity *Qc*. The same observations can be made; the maximum differences observed is are –7% and +5%.

Table F-3: Extrapolated values in function of number of points selected in the tail (traffic int. Qb)

Bridge Length	Load Effect	QbWa			QbWb			QbWc		
		EV *	D**	D***	EV *	D**	D***	EV *	D**	D***
20 m	1	4041	-7	3	3714	-6	5	4550	-2	1
	2	997	-5	2	1087	-10	-8	1247	-4	3
	3	862	-7	2	816	-6	-3	989	-3	2
	4	851	-6	2	829	-7	-5	1007	-4	2
	5	580	-4	1	553	-4	-3	678	-2	0
	6	589	-4	0	557	-4	1	684	-3	0
30 m	1	6822	-5	3	6476	-5	-2	8010	-2	1
	2	1428	1	0	1483	1	1	1919	1	-2
	3	938	-5	2	940	-5	-2	1145	-3	1
	4	963	-5	0	941	-5	-2	1146	-4	2
	5	714	-5	2	683	-5	-2	816	-3	1
	6	714	-6	0	680	-6	-5	830	-4	-2
40 m	1	9830	-4	2	9588	-2	0	12058	-1	0
	2	2366	3	-2	2624	4	-5	3317	-3	-2
	3	1032	-3	1	1047	-2	0	1295	-1	1
	4	1030	-1	1	1040	-2	0	1303	-1	0
	5	787	-5	-3	772	-8	-5	921	-2	2
	6	748	0	9	760	-6	4	934	-3	2
Average (%)			**-4**	**1**		**-4**	**-2**		**-2**	**1**
Min. Diff. (%)			**-7**	**-3**		**-10**	**-8**		**-4**	**-2**
Max. Diff. (%)			**3**	**9**		**4**	**5**		**1**	**3**

* extrapolated value using $2\sqrt{n}$ values in the tail

** difference in the extrapolated values when using $2\sqrt{n}$ and $\sqrt{n}$ values in the tail

*** difference in the extrapolated values when using $2\sqrt{n}$ and $3\sqrt{n}$ values in the tail

In conclusion, the extrapolated values calculated are quite sensitive to the number of data selected in the tail; in general, the extrapolated values increases slightly as the number of data considered increases. For all the predictions of extreme values in this study, a fixed value of $2\sqrt{n}$ has been selected.

Table F-4: Extrapolated values in function of number of points selected in the tail (traffic int. Qc)

Bridge Length	Load Effect	QaWa			QaWb			QaWc		
		EV *	D**	D***	EV *	D**	D***	EV *	D**	D***
20 m	1	3951	-4	1	3581	-3	-2	4543	-1	0
	2	1008	-5	0	1067	-7	-7	1227	-2	1
	3	836	-4	1	795	-5	-4	980	-1	0
	4	803	1	5	808	-4	-3	996	-2	1
	5	556	1	4	552	-2	0	669	-1	0
	6	586	-1	0	554	-1	0	677	-1	-1
30 m	1	6751	-4	1	6355	-2	1	7974	-1	0
	2	1580	4	0	1535	2	-1	2032	1	-3
	3	939	-3	1	917	-3	2	1144	0	0
	4	953	-3	-2	932	-3	2	1152	-1	0
	5	707	-4	-4	657	-3	1	811	0	0
	6	705	-4	-5	665	-4	1	824	-2	-1
40 m	1	9907	-3	-2	9760	0	0	12383	-1	-1
	2	2688	0	-2	2788	-3	-1	3354	-3	-1
	3	1068	-1	-1	1083	0	-1	1349	0	-1
	4	1056	-1	0	1090	1	-1	1373	0	-1
	5	788	-3	0	740	-3	2	919	0	0
	6	785	-2	1	747	-3	1	924	-2	-1
Average (%)			**-2**	**0**		**-2**	**-1**		**-1**	**-1**
Min. Diff. (%)			**-5**	**-5**		**-7**	**-7**		**-3**	**-3**
Max. Diff. (%)			**4**	**5**		**2**	**2**		**1**	**1**

* extrapolated value using $2\sqrt{n}$ values in the tail

** difference in the extrapolated values when using $2\sqrt{n}$ and $\sqrt{n}$ values in the tail

*** difference in the extrapolated values when using $2\sqrt{n}$ and $3\sqrt{n}$ values in the tail

Appendix G

PLOTS OF THE MEASURED EFFECTS FOR BI-DIRECTIONAL TRAFFIC

Appendix G PLOTS OF THE MEASURED EFFECTS FOR BI-DIRECTIONAL TRAFFIC

Figure G-1: Gumbel plots of QaWa, QaWb and QaWc for 20m bridges 275
Figure G-2: Gumbel plots of QaWa, QaWb and QaWc for 30m bridges 275
Figure G-3: Gumbel plots of QaWa, QaWb and QaWc for 40m bridges 276
Figure G-4: Gumbel plots of QbWa, QbWb and QbWc for 20m bridges 276
Figure G-5: Gumbel plots of QbWa, QbWb and QbWc for 30m bridges 277
Figure G-6: Gumbel plots of QbWa, QbWb and QbWc for 40m bridges 277
Figure G-7: Gumbel plots of QcWa, QcWb and QcWc for 20m bridges 278
Figure G-8: Gumbel plots of QcWa, QcWb and QcWc for 30m bridges 278
Figure G-9: Gumbel plots of QcWa, QcWb and QcWc for 40m bridges 279
Figure G-10: Gumbel plots of QaWa, QbWa and QcWa for 20m bridges 279
Figure G-11: Gumbel plots of QaWa, QbWa and QcWa for 30m bridges 280
Figure G-12: Gumbel plots of QaWa, QbWa and QcWa for 40m bridges 280
Figure G-13: Gumbel plots of QaWb, QbWb and QcWb for 20m bridges 281
Figure G-14: Gumbel plots of QaWb, QbWb and QcWb for 30m bridges 281
Figure G-15: Gumbel plots of QaWb, QbWb and QcWb for 40m bridges 282
Figure G-16: Gumbel plots of QaWc, QbWc and QcWc for 20m bridges 282
Figure G-17: Gumbel plots of QaWc, QbWc and QcWc for 30m bridges 283
Figure G-18: Gumbel plots of QaWc, QbWc and QcWc for 40m bridges 283

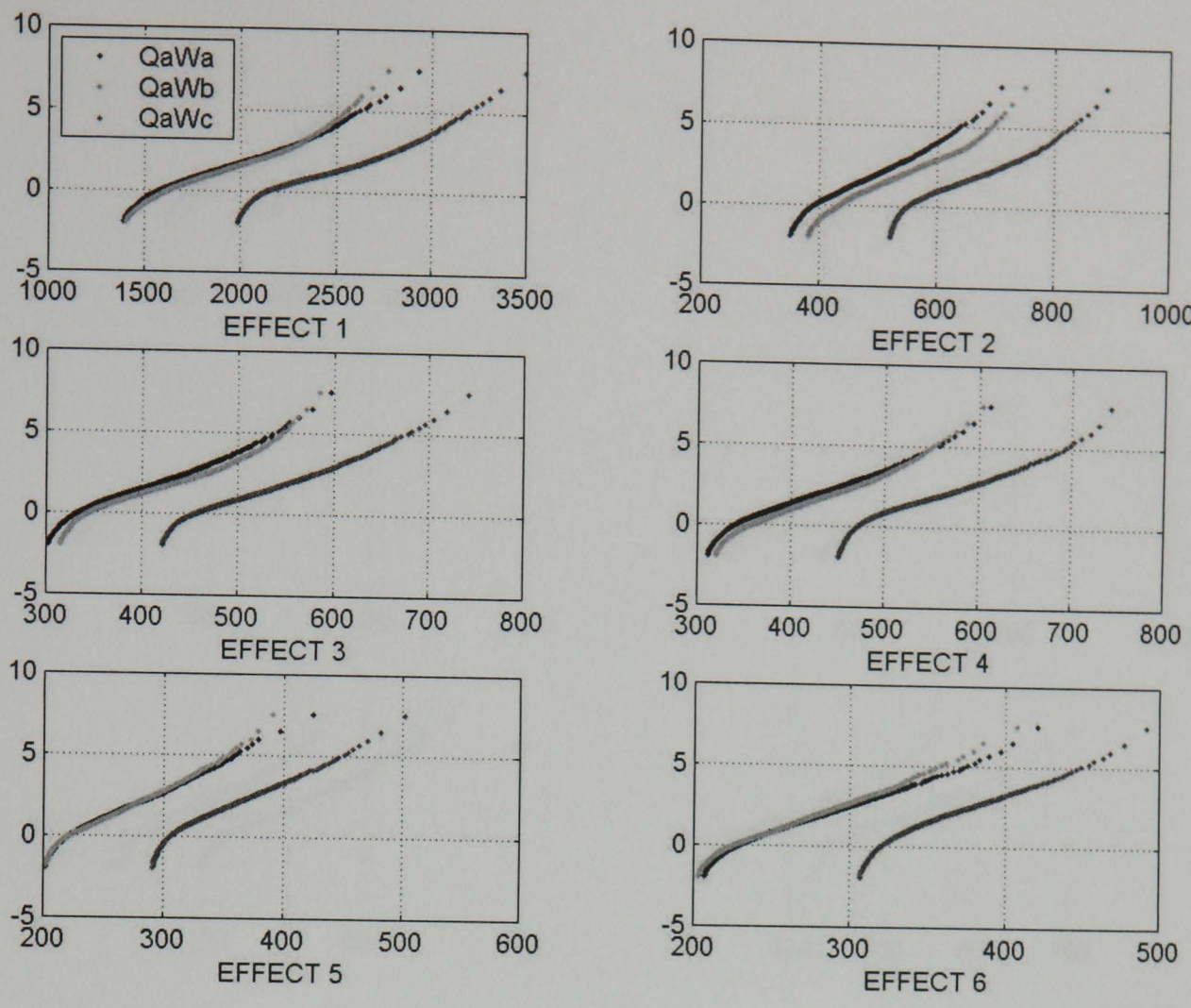

Figure G-1: Gumbel plots of QaWa, QaWb and QaWc for 20m bridges

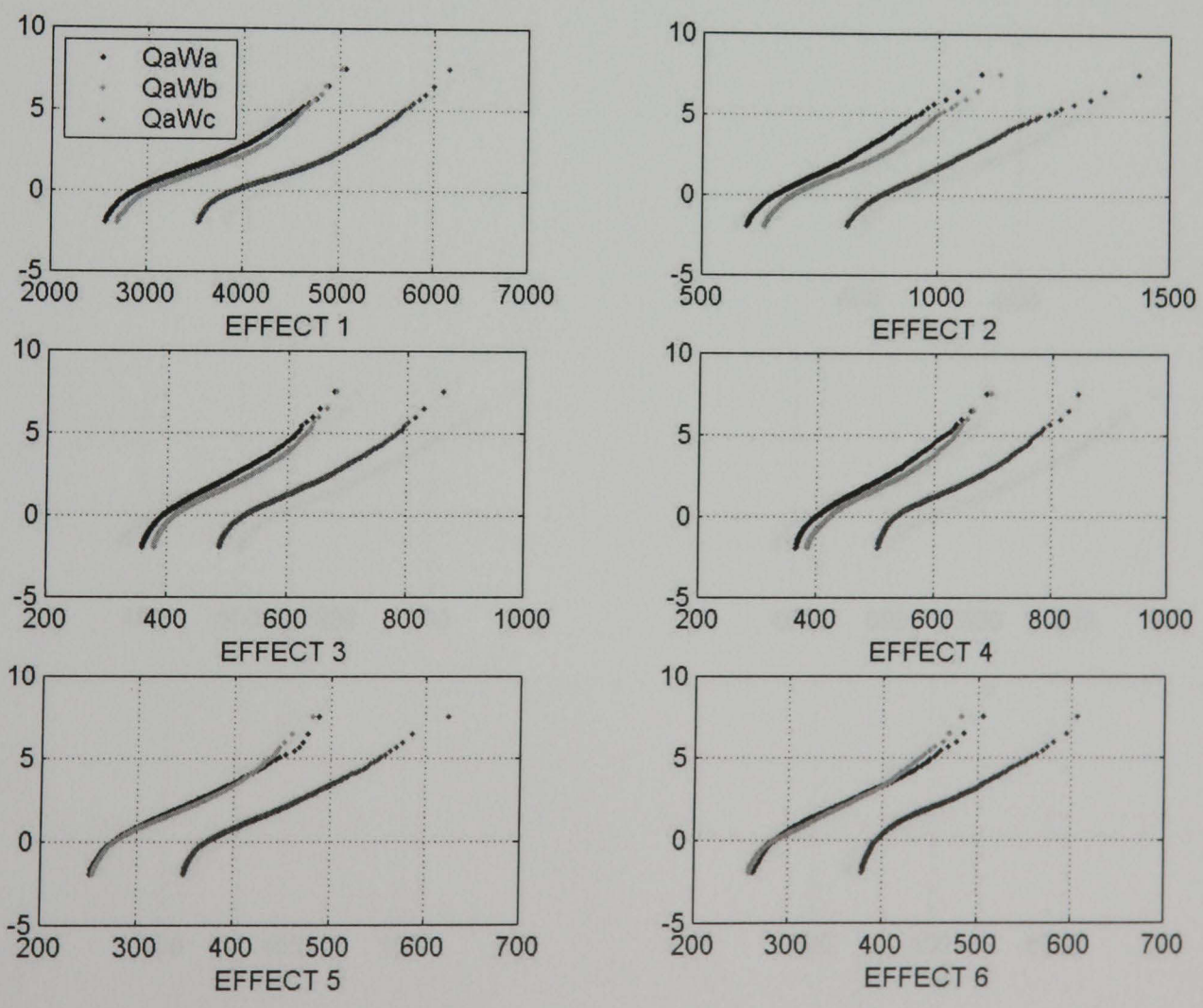

Figure G-2: Gumbel plots of QaWa, QaWb and QaWc for 30m bridges

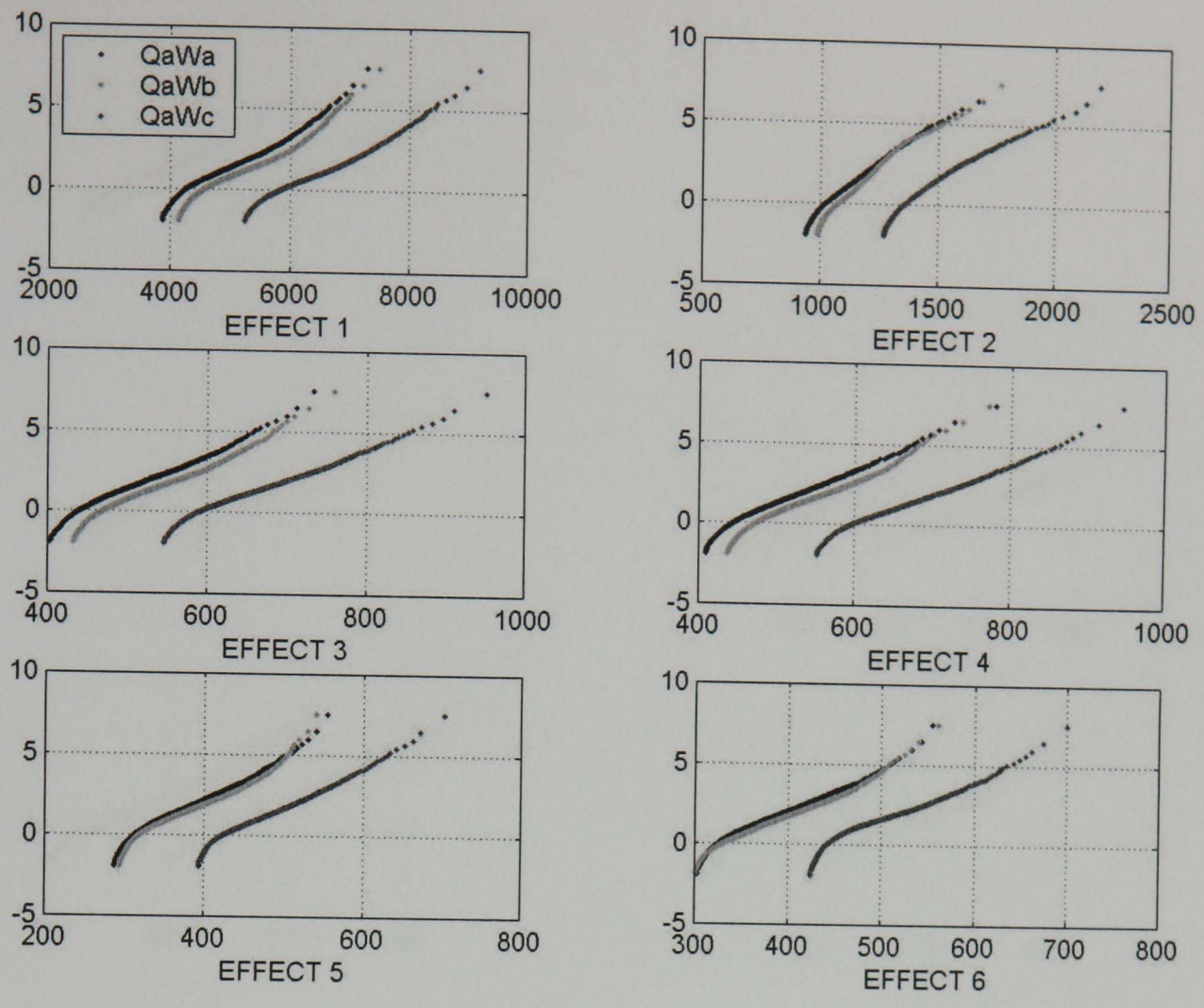

Figure G-3: Gumbel plots of QaWa, QaWb and QaWc for 40m bridges

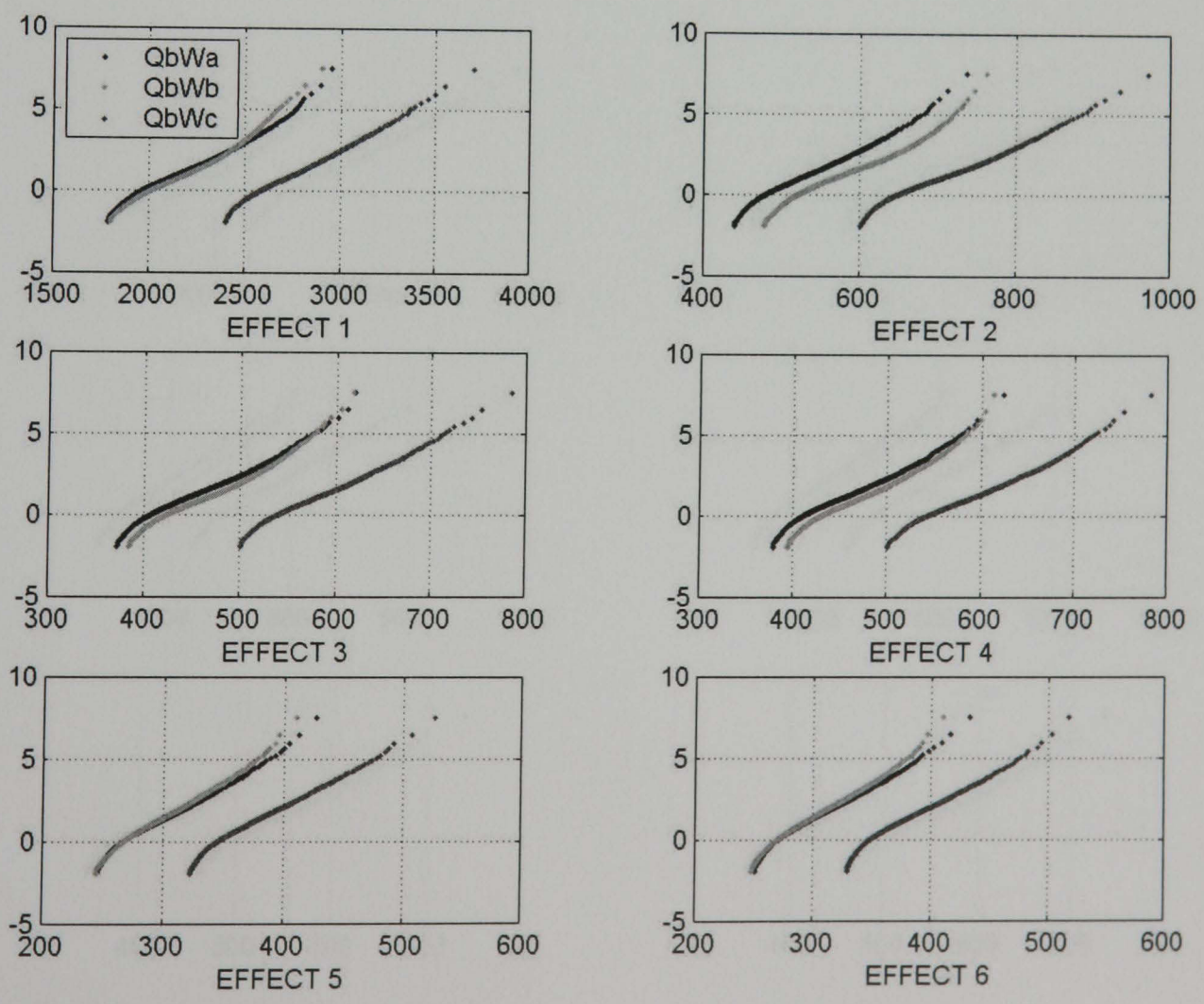

Figure G-4: Gumbel plots of QbWa, QbWb and QbWc for 20m bridges

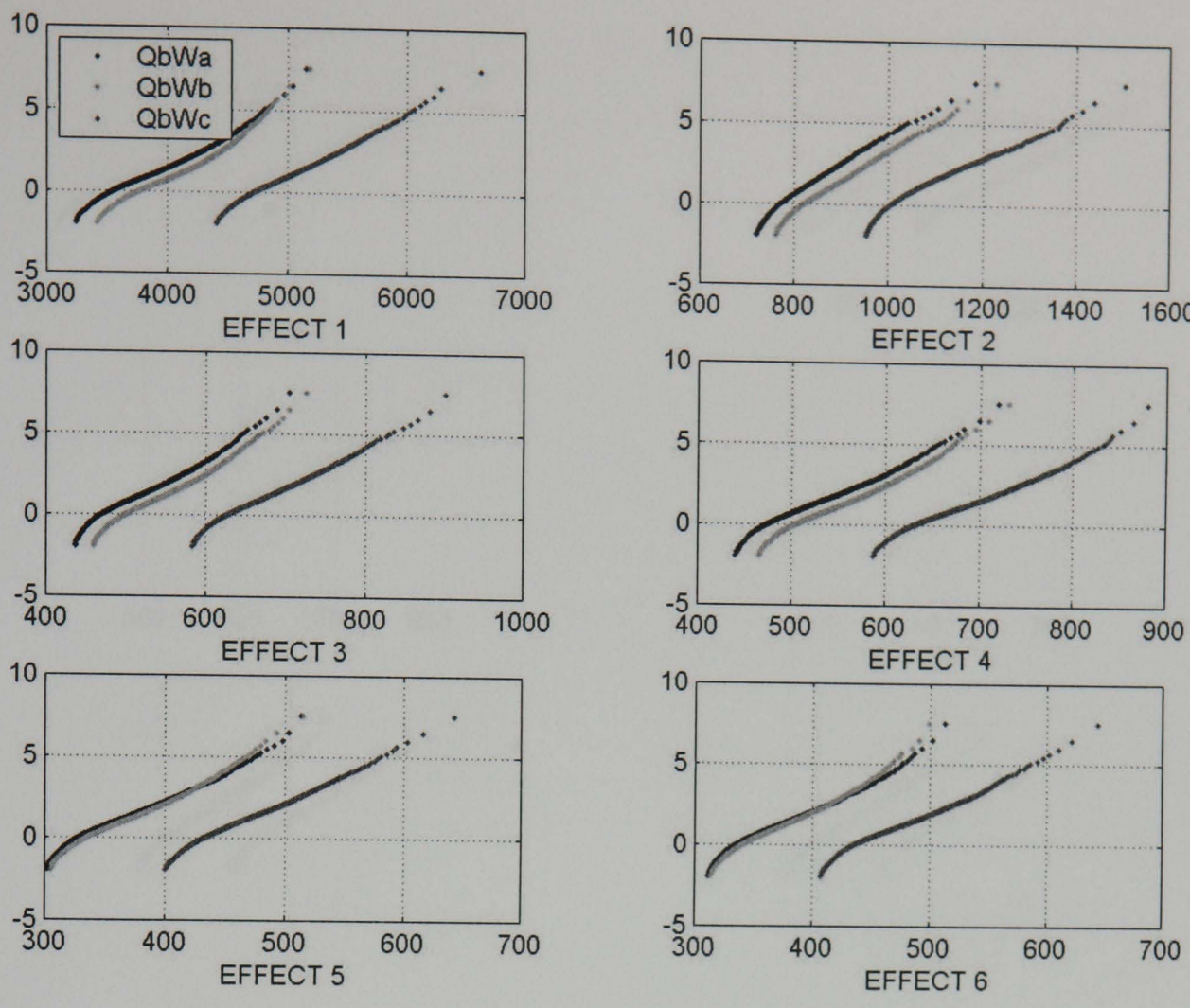

Figure G-5: Gumbel plots of QbWa, QbWb and QbWc for 30m bridges

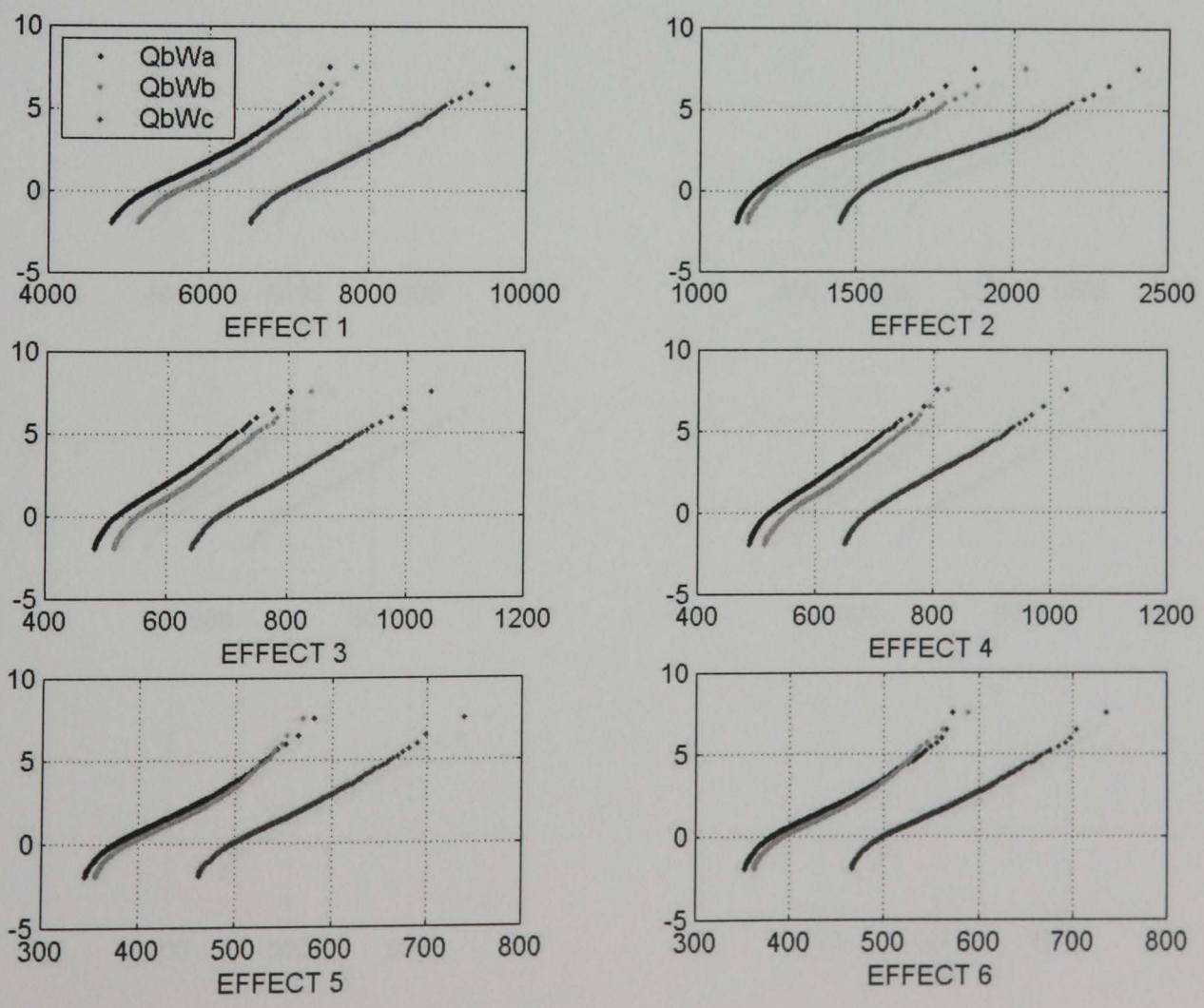

Figure G-6: Gumbel plots of QbWa, QbWb and QbWc for 40m bridges

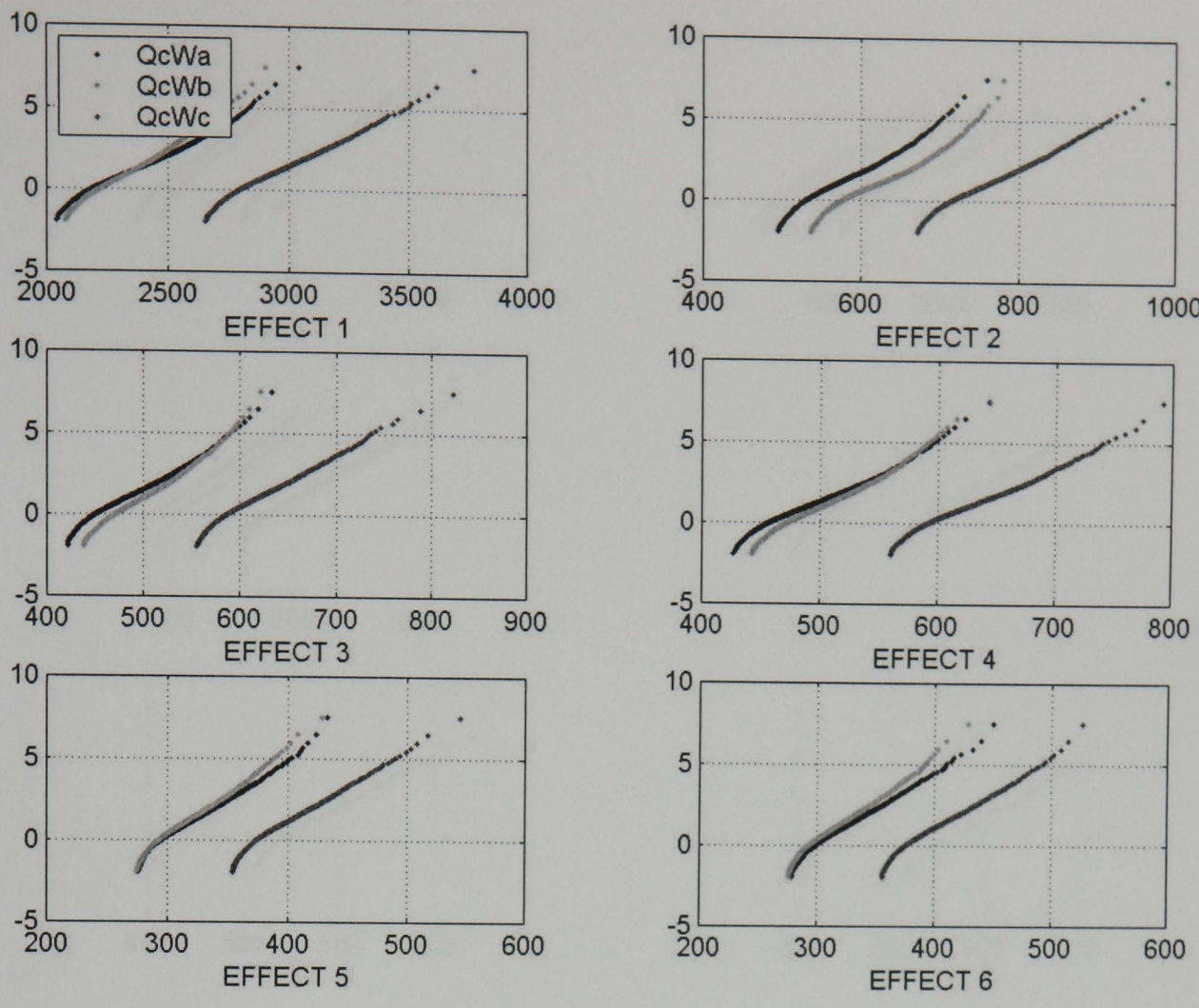

Figure G-7: Gumbel plots of QcWa, QcWb and QcWc for 20m bridges

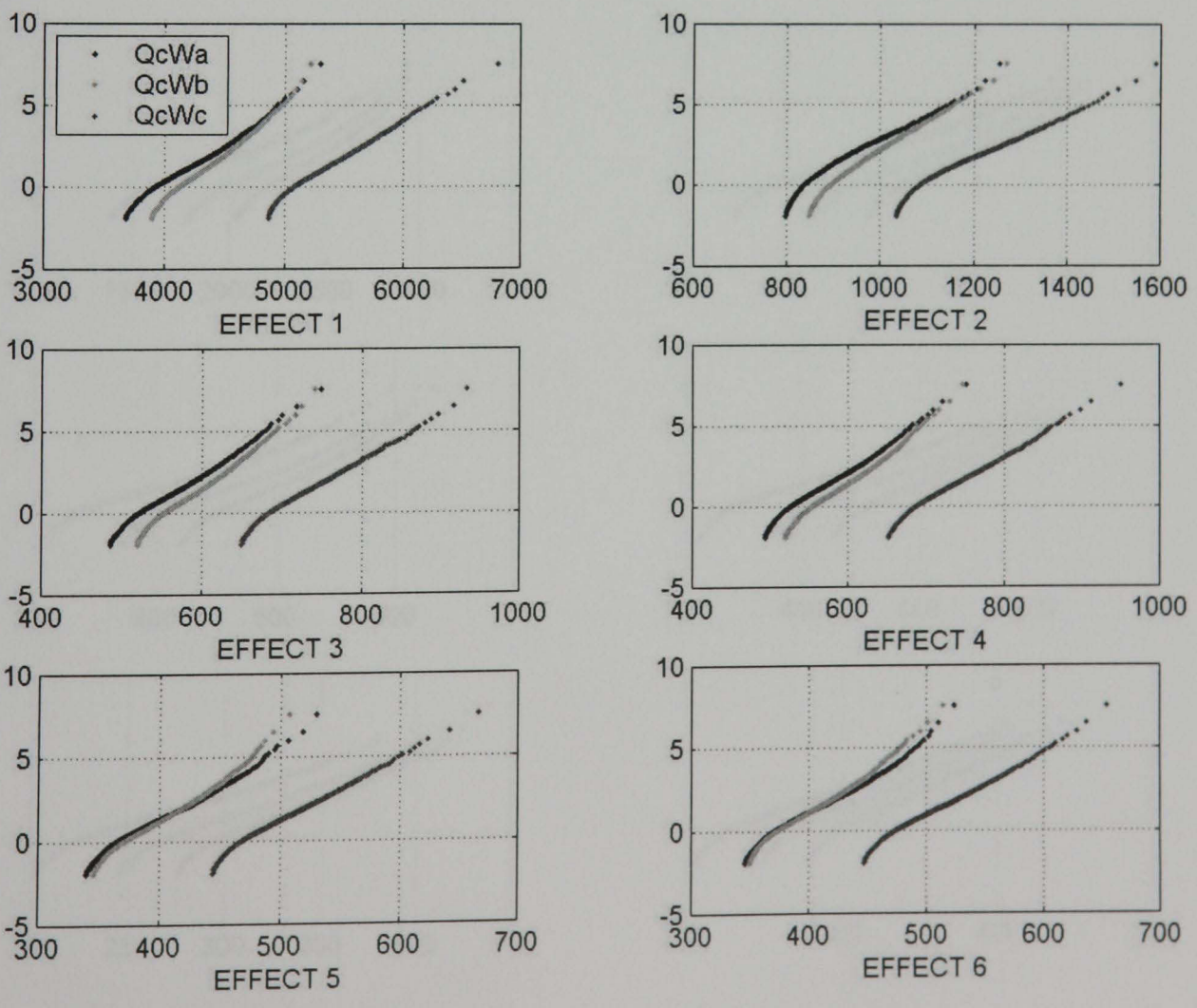

Figure G-8: Gumbel plots of QcWa, QcWb and QcWc for 30m bridges

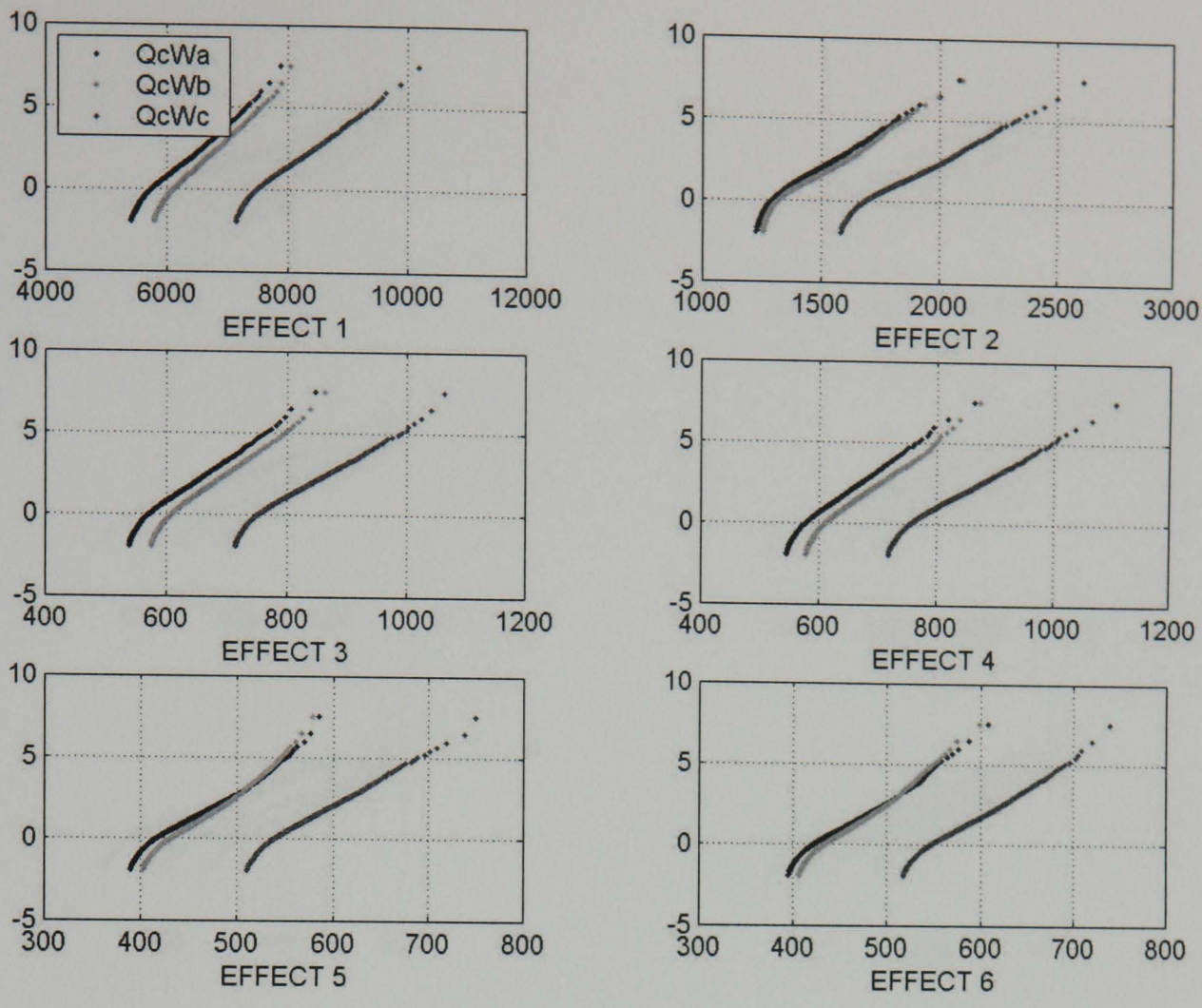

Figure G-9: Gumbel plots of QcWa, QcWb and QcWc for 40m bridges

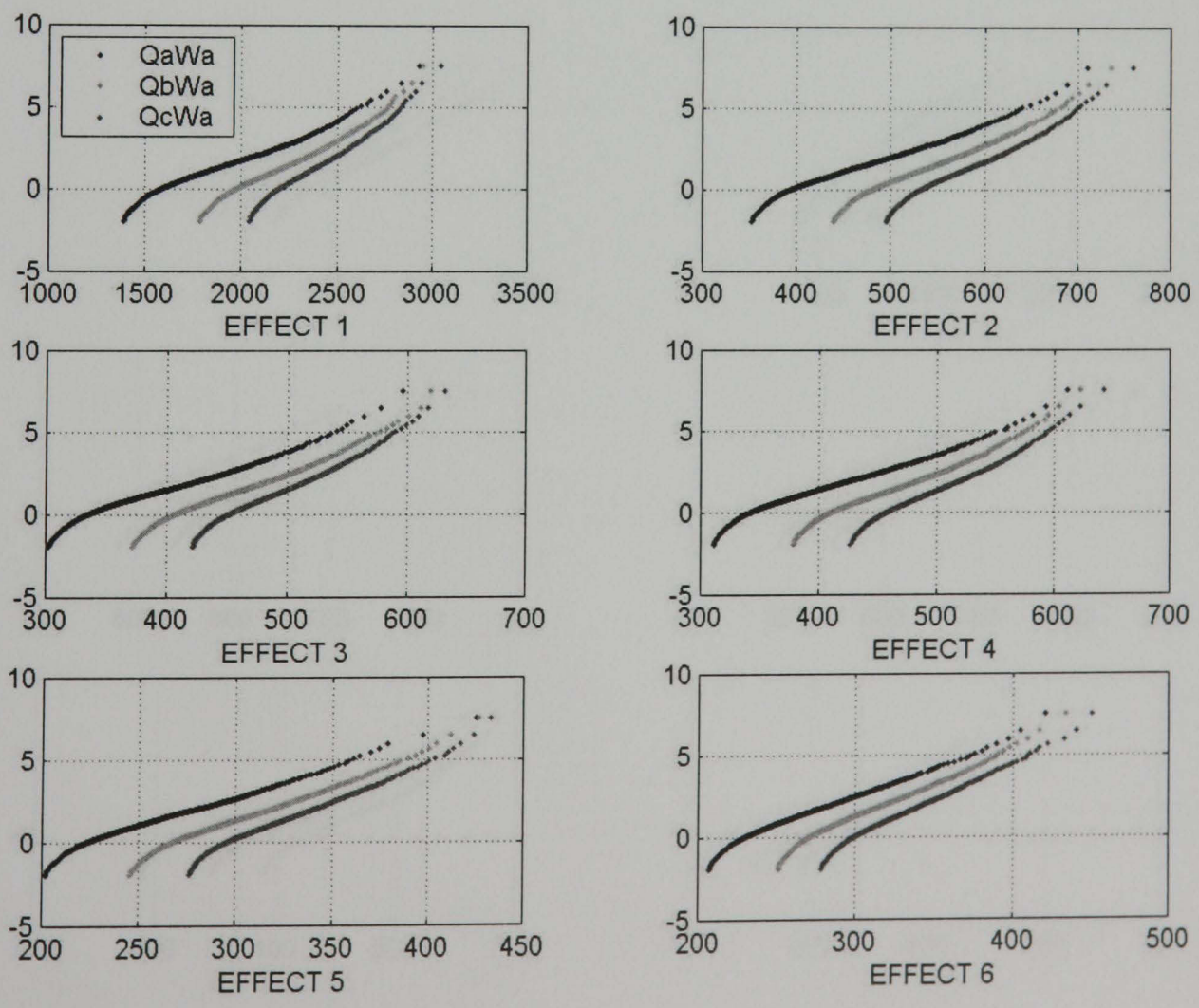

Figure G-10: Gumbel plots of QaWa, QbWa and QcWa for 20m bridges

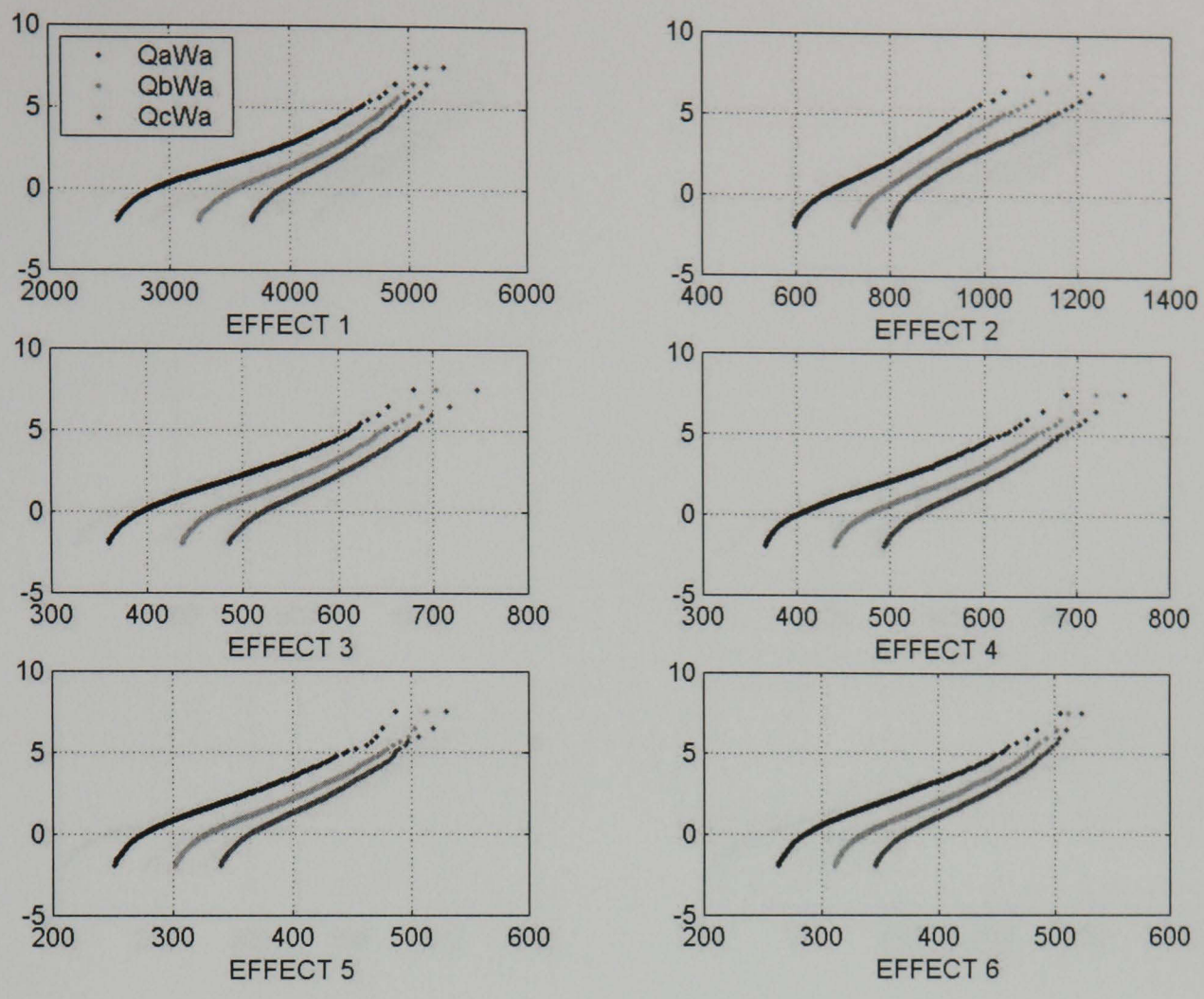

Figure G-11: Gumbel plots of QaWa, QbWa and QcWa for 30m bridges

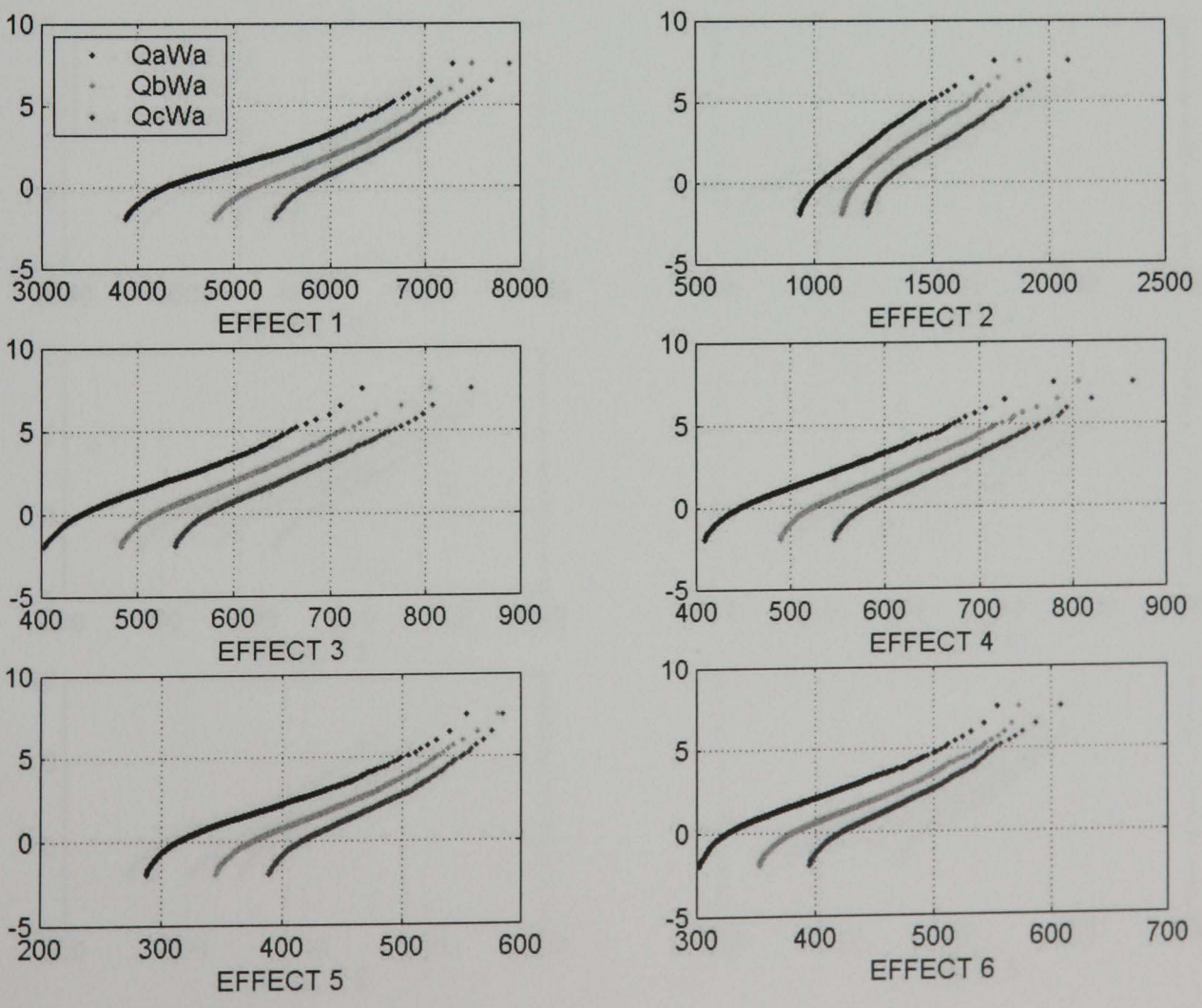

Figure G-12: Gumbel plots of QaWa, QbWa and QcWa for 40m bridges

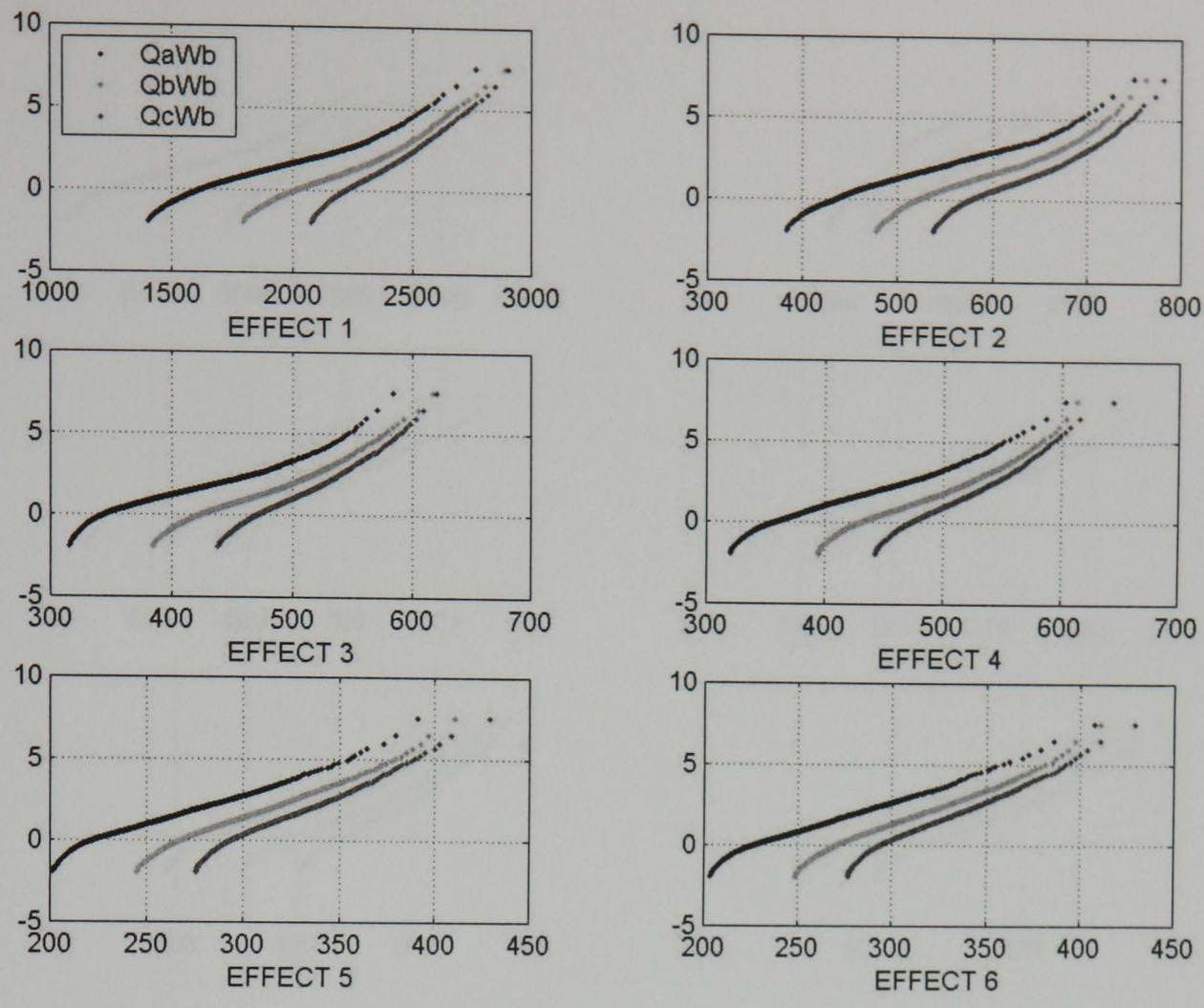

Figure G-13: Gumbel plots of QaWb, QbWb and QcWb for 20m bridges

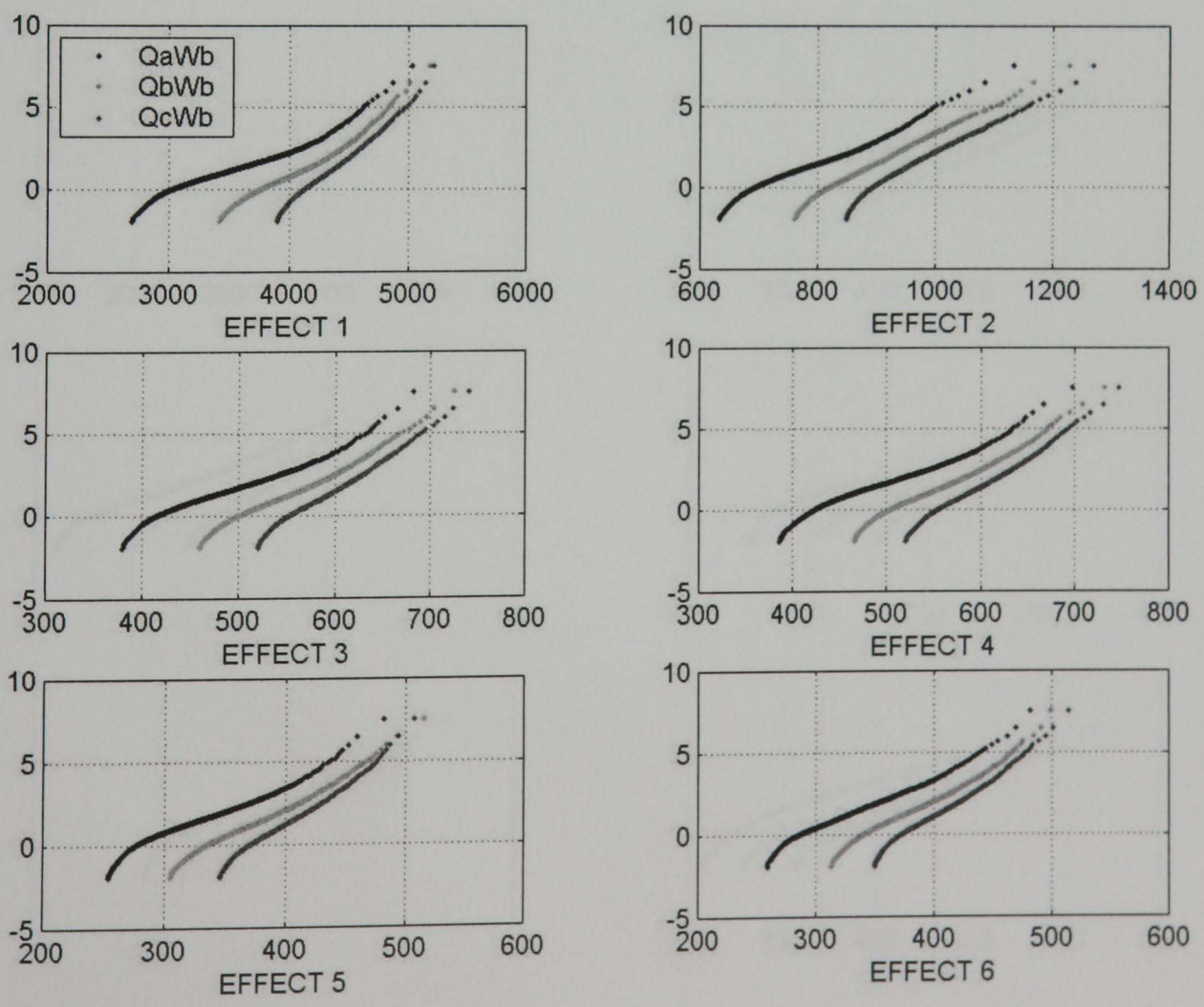

Figure G-14: Gumbel plots of QaWb, QbWb and QcWb for 30m bridges

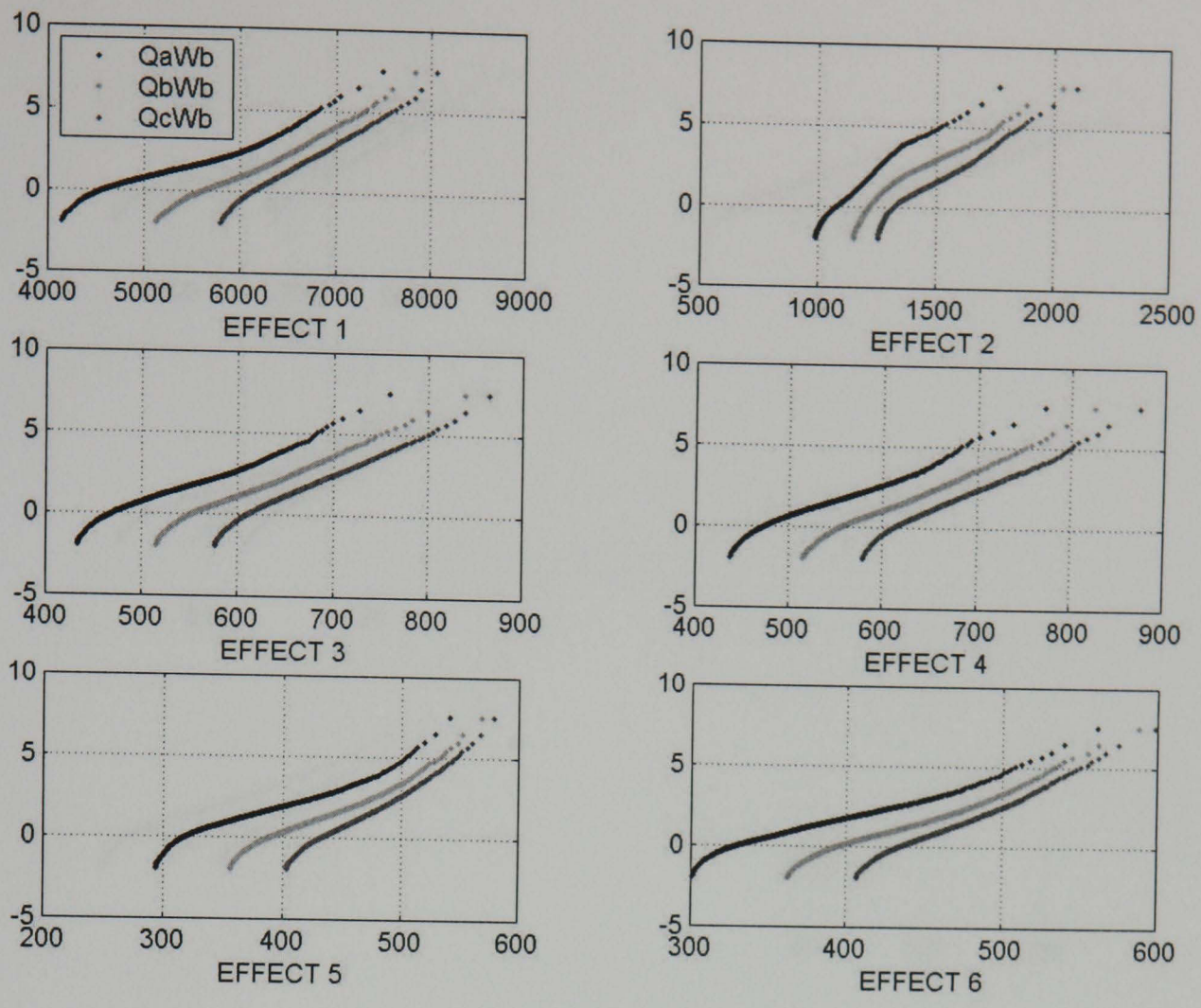

Figure G-15: Gumbel plots of QaWb, QbWb and QcWb for 40m bridges

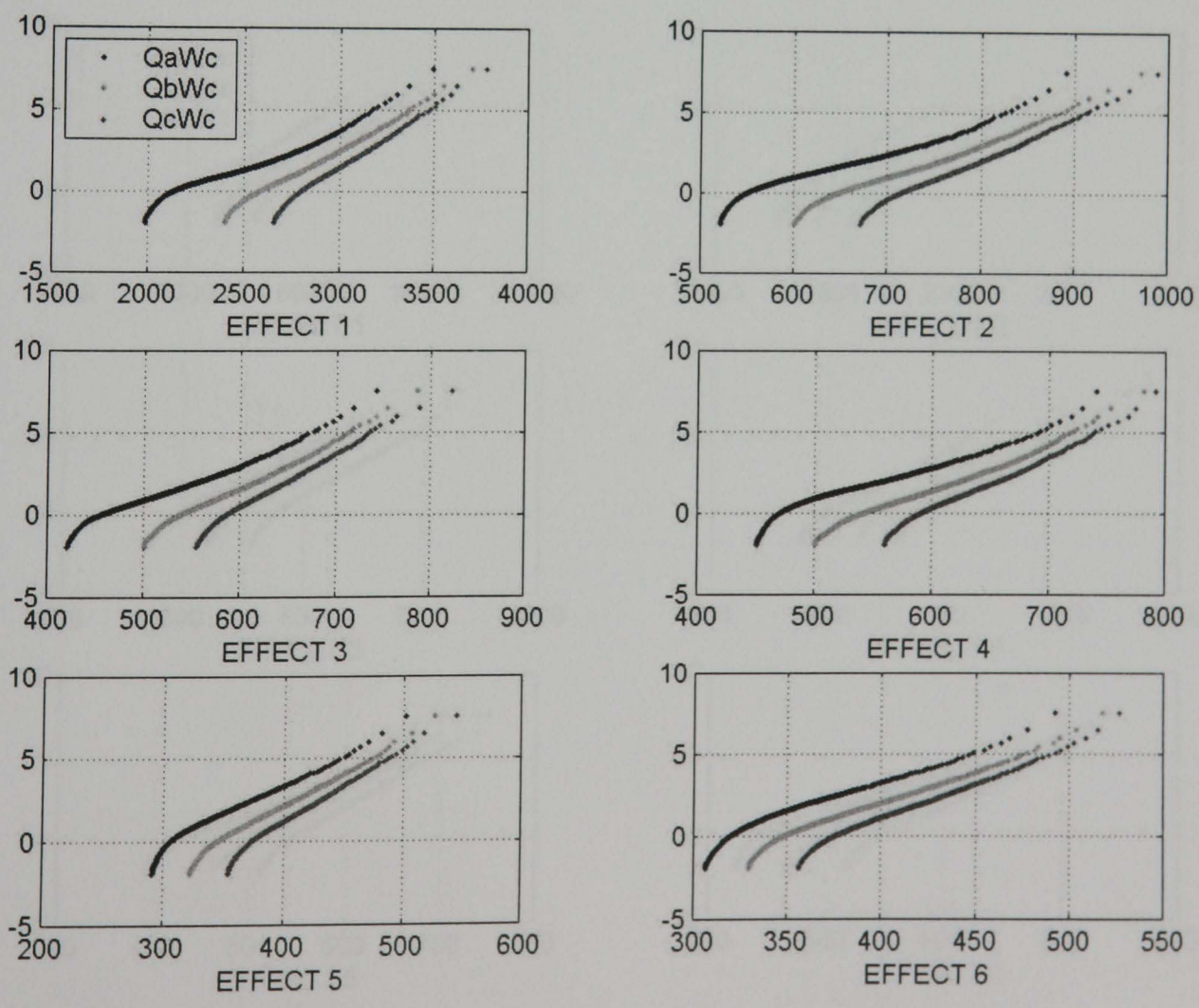

Figure G-16: Gumbel plots of QaWc, QbWc and QcWc for 20m bridges

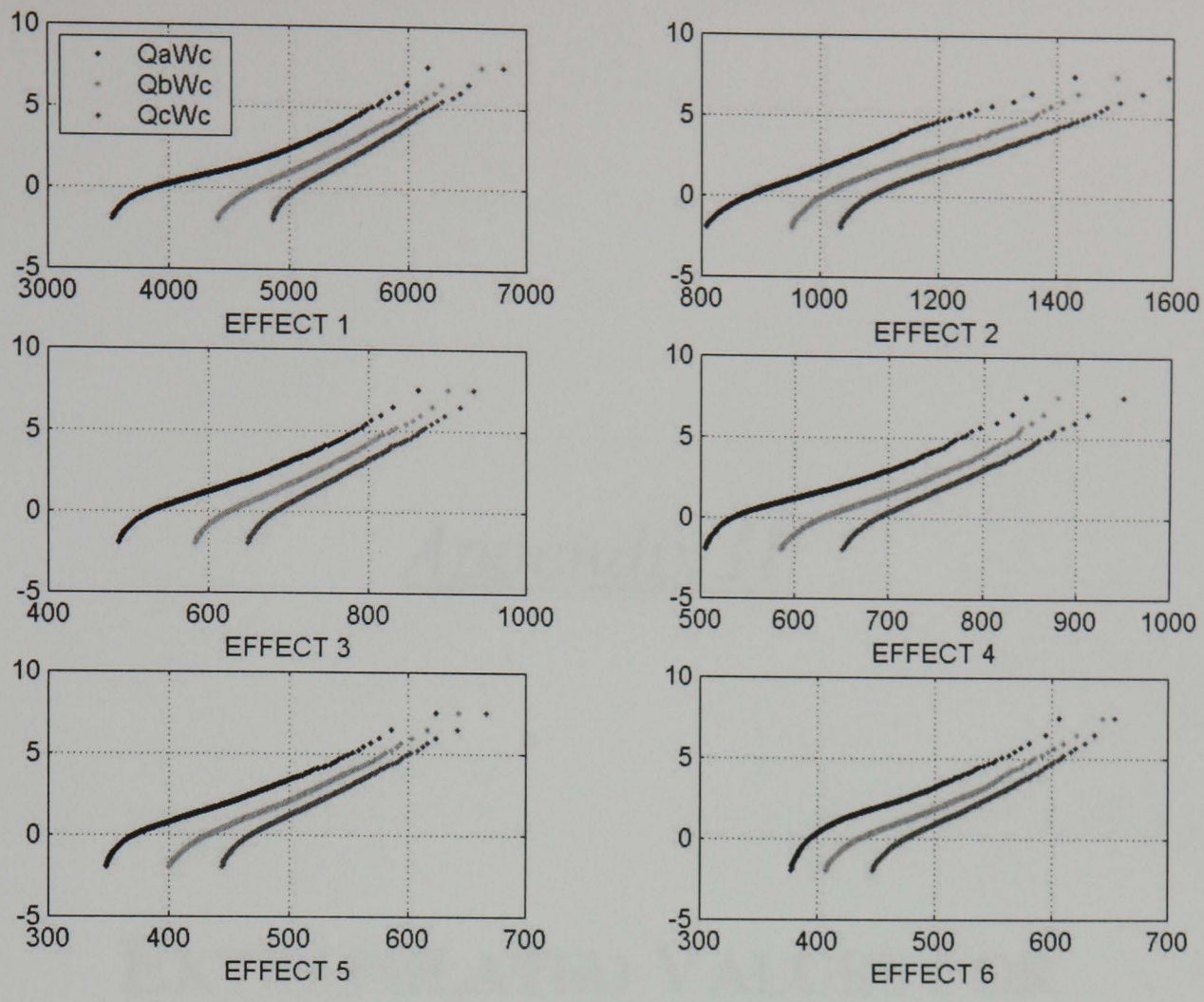

Figure G-17: Gumbel plots of QaWc, QbWc and QcWc for 30m bridges

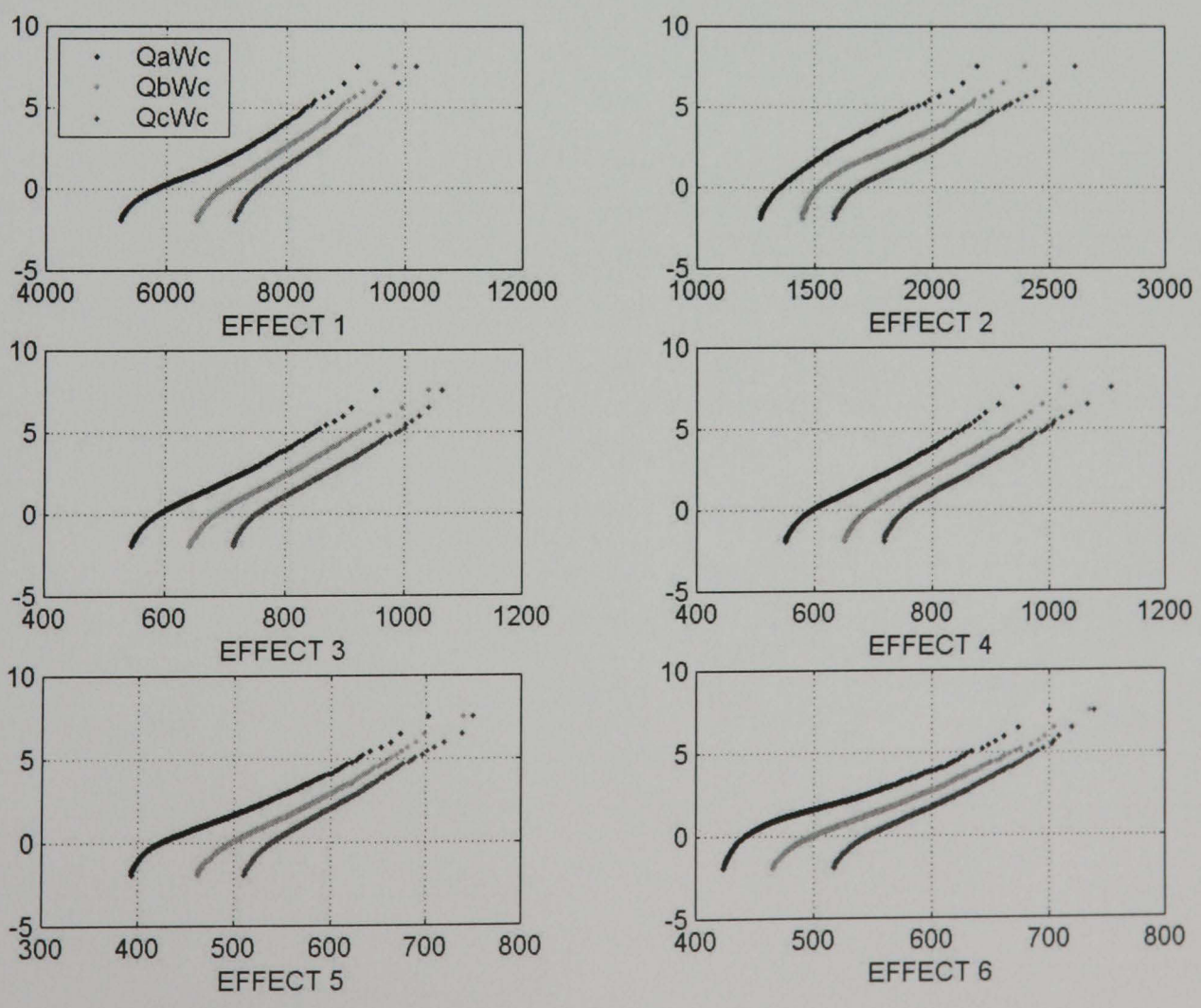

Figure G-18: Gumbel plots of QaWc, QbWc and QcWc for 40m bridges

Appendix H

EXTRAPOLATED VALUES FOR BI-DIRECTIONAL TRAFFIC

Appendix H EXTRAPOLATED VALUES FOR BIDIRECTIONAL TRAFFIC

Table H-1: Comparison of extrapolated values for constant traffic intensity and various traffic weights

Load Effect	Bridge Length	Traffic type								
		QaWa	Rab	Rac	QbWa	Rbb	Rbc	QcWa	Rcb	Rcc
1	20	*3921*	0.98	1.16	*4041*	0.92	1.13	*3951*	0.91	1.15
	30	*957*	1.16	1.30	*997*	1.09	1.25	*1008*	1.06	1.22
	40	*795*	1.05	1.24	*862*	0.95	1.15	*836*	0.95	1.17
2	20	*828*	1.02	1.24	*851*	0.97	1.18	*803*	1.01	1.24
	30	*566*	0.97	1.19	*580*	0.95	1.17	*556*	0.99	1.20
	40	*581*	0.96	1.15	*589*	0.95	1.16	*586*	0.95	1.16
3	20	*6988*	0.96	1.13	*6822*	0.95	1.17	*6751*	0.94	1.18
	30	*1366*	1.05	1.26	*1428*	1.04	1.34	*1580*	0.97	1.29
	40	*959*	1.00	1.18	*938*	1.00	1.22	*939*	0.98	1.22
4	20	*942*	0.97	1.19	*963*	0.98	1.19	*953*	0.98	1.21
	30	*706*	0.97	1.15	*714*	0.96	1.14	*707*	0.93	1.15
	40	*718*	0.94	1.14	*714*	0.95	1.16	*705*	0.94	1.17
5	20	*9912*	0.97	1.17	*9830*	0.98	1.23	*9907*	0.99	1.25
	30	*2154*	0.96	1.32	*2366*	1.11	1.40	*2688*	1.04	1.25
	40	*1009*	0.99	1.23	*1032*	1.01	1.25	*1068*	1.01	1.26
6	20	*1018*	0.99	1.21	*1030*	1.01	1.27	*1056*	1.03	1.30
	30	*800*	0.99	1.15	*787*	0.98	1.17	*788*	0.94	1.17
	40	*795*	0.99	1.18	*748*	1.02	1.25	*785*	0.95	1.18
Average			**1.00**	**1.20**		**0.99**	**1.21**		**0.98**	**1.21**
Standard Deviation			**0.05**	**0.06**		**0.05**	**0.07**		**0.04**	**0.05**

Rab = Ratio of the extrapolated value of QaWb to the extrapolated value of QaWa

Rac = Ratio of the extrapolated value of QaWc to the extrapolated value of QaWa

Rbb = Ratio of the extrapolated value of QbWb to the extrapolated value of QbWa

Rbc = Ratio of the extrapolated value of QbWc to the extrapolated value of QbWa

Rcb = Ratio of the extrapolated value of QcWb to the extrapolated value of QcWa

Rcc = Ratio of the extrapolated value of QcWc to the extrapolated value of QcWa

Table H-2: Comparison of extrapolated values for constant traffic weight and various traffic intensities

Load Effect	Bridge Length	Traffic type								
		QaWa	Rba	Rca	QaWb	Rbb	Rcb	QaWc	Rbc	Rcc
1	20	*3921*	1.03	1.01	*3852*	0.95	0.93	*4539*	1.00	1.00
	30	*6988*	0.98	0.97	*6718*	0.93	0.95	*7875*	1.02	1.01
	40	*9912*	0.99	1.00	*9598*	0.97	1.02	*11606*	1.04	1.07
2	20	*957*	1.04	1.05	*1112*	1.14	0.96	*1245*	1.00	0.99
	30	*1366*	1.05	1.16	*1429*	1.09	1.07	*1723*	1.11	1.18
	40	*2154*	1.10	1.25	*2071*	1.22	1.35	*2845*	1.17	1.18
3	20	*795*	1.08	1.05	*837*	1.03	0.95	*988*	1.00	0.99
	30	*959*	0.98	0.98	*961*	0.98	0.95	*1135*	1.01	1.01
	40	*1009*	1.02	1.06	*995*	1.04	1.09	*1237*	1.05	1.09
4	20	*828*	1.03	0.97	*845*	1.00	0.96	*1029*	0.98	0.97
	30	*942*	1.02	1.01	*917*	1.00	1.02	*1122*	1.02	1.03
	40	*1018*	1.01	1.04	*1011*	1.02	1.08	*1230*	1.06	1.12
5	20	*566*	1.02	0.98	*549*	0.98	1.01	*675*	1.00	0.99
	30	*706*	1.01	1.00	*682*	0.97	0.96	*810*	1.01	1.00
	40	*800*	0.98	0.99	*788*	0.97	0.94	*921*	1.00	1.00
6	20	*581*	1.01	1.01	*557*	0.96	0.99	*668*	1.02	1.01
	30	*718*	0.99	0.98	*675*	0.95	0.99	*821*	1.01	1.00
	40	*795*	0.94	0.99	*788*	0.96	0.95	*935*	1.00	0.99
Average			**1.02**	**1.03**		**1.01**	**1.01**		**1.03**	**1.03**
Standard Deviation			**0.04**	**0.07**		**0.07**	**0.10**		**0.05**	**0.06**

Rba = Ratio of the extrapolated value of QbWa to the extrapolated value of QaWa

Rca = Ratio of the extrapolated value of QcWa to the extrapolated value of QaWa

Rbb = Ratio of the extrapolated value of QbWb to the extrapolated value of QaWb

Rcb = Ratio of the extrapolated value of QcWb to the extrapolated value of QaWb

Rbc = Ratio of the extrapolated value of QbWc to the extrapolated value of QaWc

Rcc = Ratio of the extrapolated value of QcWc to the extrapolated value of QaWc

Load Effect	Bridge Length	QcWc	QcWb	QcWa	QbWc	QbWb	QbWa	QaWc	QaWb	QaWa	Ave.	St Dev	Min.	Max.
1	20	*4543*	*3581*	*3951*	*4550*	*3714*	*4041*	*4539*	*3852*	*3921*				
	30	1.76	1.77	1.71	1.76	1.74	1.69	1.73	1.74	1.78	**1.74**	**0.03**	**1.69**	**1.78**
	40	2.73	2.73	2.51	2.65	2.58	2.43	2.56	2.49	2.53	**2.58**	**0.10**	**2.43**	**2.73**
2	20	*1227*	*1067*	*1008*	*1247*	*1087*	*997*	*1245*	*1112*	*957*				
	30	1.66	1.44	1.57	1.54	1.36	1.43	1.38	1.29	1.43	**1.45**	**0.11**	**1.29**	**1.66**
	40	2.73	2.61	2.67	2.66	2.41	2.37	2.29	1.86	2.25	**2.43**	**0.28**	**1.86**	**2.73**
3	20	*980*	*795*	*836*	*989*	*816*	*862*	*988*	*837*	*795*				
	30	1.17	1.15	1.12	1.16	1.15	1.09	1.15	1.15	1.21	**1.15**	**0.03**	**1.09**	**1.21**
	40	1.38	1.36	1.28	1.31	1.28	1.20	1.25	1.19	1.27	**1.28**	**0.06**	**1.19**	**1.38**
4	20	*996*	*808*	*803*	*1007*	*829*	*851*	*1029*	*845*	*828*				
	30	1.16	1.15	1.19	1.14	1.14	1.13	1.09	1.09	1.14	**1.13**	**0.03**	**1.09**	**1.19**
	40	1.38	1.35	1.32	1.29	1.25	1.21	1.20	1.20	1.23	**1.27**	**0.07**	**1.20**	**1.38**
5	20	*669*	*552*	*556*	*678*	*553*	*580*	*675*	*549*	*566*				
	30	1.21	1.19	1.27	1.20	1.24	1.23	1.20	1.24	1.25	**1.23**	**0.03**	**1.19**	**1.27**
	40	1.37	1.34	1.42	1.36	1.40	1.36	1.36	1.44	1.41	**1.38**	**0.03**	**1.34**	**1.44**
6	20	*677*	*554*	*586*	*684*	*557*	*589*	*668*	*557*	*581*				
	30	1.22	1.20	1.20	1.21	1.22	1.21	1.23	1.21	1.24	**1.22**	**0.01**	**1.20**	**1.24**
	40	1.36	1.35	1.34	1.37	1.36	1.27	1.40	1.41	1.37	**1.36**	**0.04**	**1.27**	**1.41**

Table H-3: Comparison of extrapolated values for various traffic types in function of bridge length

Appendix I

FREQUENCY OF CROSSING EVENTS FOR BI-DIRECTIONAL TRAFFIC

Appendix I FREQUENCY OF CROSSING EVENTS FOR BI-DIRECTIONAL TRAFFIC

I.1 ANALYSIS OF THE NUMBER OF MEETING EVENTS

In the program SIMULTRAFFIC, all the crossing events identified were classified in function of their configuration. The classification is simply based on the number of trucks present in each lane for the crossing event detected. Table I-1 presents the different event types used in the classification.

Table I-1: Definition of the various event types

Event Type	Total number of trucks involved in the event	Number of trucks in lane 1	Number of trucks in lane 2
211	2	1	1
202	2	0	2
220	2	2	0
312	3	1	2
321	3	2	1
303	3	0	3
330	3	3	0
422	4	2	2
413	4	1	3
431	4	3	1
999*	/	/	/

*= miscellaneous type – does not correspond to any of the pre-defined event types

Table I-2 shows the average number of crossing events corresponding to one week of traffic, for various traffic types and bridge lengths. These values represent the average value for 100 traffic files (as there are 100 distinct traffic files for each traffic type considered). A number of observations can be made from Table I-2 (it should be reminded that $Qa < Qb < Qc$):

- the total number of crossing events increases rapidly with the traffic intensity
- the number of crossing events involving more than 2 trucks increases with the span and with the traffic intensity
- for a specified traffic intensity, the number of crossing events is higher for *Wa* than for *Wb* and *Wc*; this is due to the fact that the trucks travel slower for *Wa*, and

therefore spend more time on the bridge, which increases their probability of being present on the bridge while another truck is present at the same time.

Table I-2: Number of crossing events (per type and per week) for various traffic types and bridge lengths

Event Type	QaWa			QaWb			QaWc		
	20m	30m	40m	20m	30m	40m	20m	30m	40m
211	485	641	791	416	541	660	404	528	648
202	176	266	353	151	220	286	166	239	311
220	229	308	376	206	266	323	186	242	299
312	8	17	28	6	11	18	6	12	21
321	11	21	33	8	15	23	8	14	22
303	0	2	4	8	1	3	0	2	4
330	0	3	8	0	3	6	0	3	5
422	0	0	1	0	0	0	0	0	1
413	0	0	0	0	0	0	0	0	0
431	0	0	1	0	0	1	0	0	0
999	0	0	1	0	0	1	0	0	0
Total	909	1258	1596	797	1058	1321	771	1041	1311
Event Type	QbWa			QbWb			QbWc		
	20m	30m	40m	20m	30m	40m	20m	30m	40m
211	1655	2149	2600	1437	1836	2207	1388	1799	2179
202	606	893	1156	518	741	950	579	820	1043
220	785	1044	1255	727	922	1110	655	841	1016
312	46	95	158	35	68	110	37	71	115
321	66	123	189	49	87	133	44	80	125
303	1	11	27	0	7	17	1	9	23
330	1	20	44	1	20	36	2	17	31
422	1	4	10	1	3	6	1	3	6
413	1	1	3	1	1	2	1	1	2
431	0	2	6	1	2	4	0	2	3
999	0	2	1	1	2	0	0	2	0
Total	3162	4344	5449	2770	3686	4575	2708	3644	4543
Event Type	QcWa			QcWb			QcWc		
	20m	30m	40m	20m	30m	40m	20m	30m	40m
211	3686	4663	5504	3205	4031	4758	3131	3970	4714
202	1081	1571	1995	940	1322	1657	1058	1471	1841
220	2098	2692	3134	1961	2408	2826	1746	2172	2568
312	142	287	466	106	203	324	113	218	348
321	252	468	705	199	342	511	182	318	480
303	3	24	61	1	15	39	2	24	55
330	6	94	207	6	96	170	7	82	147
422	8	24	51	5	14	29	5	14	31
413	0	4	12	5	2	7	0	3	9
431	1	15	41	1	11	27	1	10	24
999	1	1	7	1	1	3	1	1	4
Total	7278	9843	12182	6428	8445	10350	6246	8283	10222

For the traffic types with traffic intensity *Qc*, the significant variations between the statistics for the event types 202/220 and 303/330 can be explained by the fact that the flow rates are much higher in direction 1 than in direction 2 for a number of hours during the day.

Table I-3 presents the same results in terms of frequency. The most common crossing event is the event type involving 2 trucks (one in each of the two opposing lanes); it represents between 45 and 53% of all the crossing events. Most of the remaining events correspond to event types 202 and 220 (between 15 and 31%); finally there are few events involving 3 or 4 trucks (between 0 and 6% depending on the traffic intensity).

Table I-3: Frequency of crossing events (in %) per event type for various traffic types and bridge lengths

Event Type	QaWa			QaWb			QaWc		
	20m	30m	40m	20m	30m	40m	20m	30m	40m
211	53	51	50	52	51	50	52	51	49
202	19	21	22	19	21	22	22	23	24
220	25	24	24	26	25	24	24	23	23
312	1	1	2	1	1	1	1	1	2
321	1	2	2	1	1	2	1	1	2
303	0	0	0	1	0	0	0	0	0
330	0	0	0	0	0	0	0	0	0
Event Type	**QbWa**			**QbWb**			**QbWc**		
	20m	**30m**	**40m**	**20m**	**30m**	**40m**	**20m**	**30m**	**40m**
211	52	49	48	52	50	48	51	49	48
202	19	21	21	19	20	21	21	23	23
220	25	24	23	26	25	24	24	23	22
312	1	2	3	1	2	2	1	2	3
321	2	3	3	2	2	3	2	2	3
303	0	0	0	0	0	0	0	0	0
330	0	0	1	0	1	1	0	0	1
Event Type	**QcWa**			**QcWb**			**QcWc**		
	20m	**30m**	**40m**	**20m**	**30m**	**40m**	**20m**	**30m**	**40m**
211	51	47	45	50	48	46	50	48	46
202	15	16	16	15	16	16	17	18	18
220	29	27	26	31	29	27	28	26	25
312	2	3	4	2	2	3	2	3	3
321	3	5	6	3	4	5	3	4	5
303	0	0	0	0	0	0	0	0	1
330	0	1	2	0	1	2	0	1	1

I.2 PREDICTION OF NUMBER OF MEETING EVENTS

From the previous section, it was observed that there are a number of different types of crossing events, however, the crossing events that are of particular concern when studying traffic loading imposed on relatively short bridges are of type 211. It is therefore of interest to estimate the number of meeting events (2 trucks from the 2 opposing lanes meeting on the bridge) based on the knowledge of the flow rates.

I.2.1 Development of a formula to predict the number of meeting events

Using the axioms of probability, a formula has been derived in order to estimate the number of meeting events during one hour, assuming that the site characteristics are known. Basically, for any truck entering an empty bridge in lane 1 at instant t, there will be a meeting event if a truck in lane 2 reaches the bridge before the truck in lane 1 has left the bridge at instant $t+\Delta t_1$, if Δt_1 is the time taken by truck 1 to cross the bridge. The probability that a truck in lane 2 arrives in interval Δt_1 is the same as the probability that a headway (i.e., the inter-arrival time between vehicles) is less or equal than Δt_1, and is approximately defined as:

$$P(\overline{h_2} < \Delta t_1) = 1 - e^{-\frac{\Delta t_1}{\overline{h_2}}} \cong \frac{\Delta t_1}{\overline{h_2}} \qquad \textbf{Equation I-1}$$

where $\overline{h_2} = 3600 / Q_2$ (Q_2 being the number of trucks per hour in lane 2) and Δt_1 can be estimated using the following formula:

$$\Delta t_1 = \frac{(L^{bridge} + L_1^{truck})}{V_1^{truck}} \qquad \textbf{Equation I-2}$$

where L^{bridge} and L_1^{truck} are the bridge length and the average truck length for lane i (m)

V_1^{truck} is the average speed for lane i (m/s).

The simplification introduced in Equation I-1 is considered reasonable for the relatively low value of flow rates employed throughout this thesis (i.e., flow rate < 400 trucks/hour). There will also be a meeting event if a truck had entered the bridge in lane 2 in the interval $[t-\Delta t_2, t]$. The probability of a truck arriving in lane 2 in interval Δt_2 can be estimated

using Equation I-1. Therefore, the probability of having a meeting event given that a truck enters the bridge in lane 1 at time *t* can be estimated by:

$$\frac{\Delta t_1}{h_2} + \frac{\Delta t_2}{h_2} \cong 2\frac{\Delta t_1}{h_2} = 2\frac{\Delta t_{average}}{h_2} \quad as\ \Delta t_2 \cong \Delta t_1 = \Delta t_{average} \qquad \textbf{Equation I-3}$$

(since the average truck length and speed are similar for both lanes for a given traffic type). Therefore, for all the trucks arriving to the bridge during one hour, the total number of meeting events N can be approximately estimated by:

$$N = Q_1\left(2\frac{\Delta t_{average}}{h_2}\right) = Q_1\left(2\frac{Q_2 \Delta t_{average}}{3600}\right) = \frac{2Q_1Q_2(L^{bridge} + L^{truck}_{average})}{3600V^{truck}_{average}} \qquad \textbf{Equation I-4}$$

where Q_i is the number of trucks per hour in lane *i*,

$\Delta t_{average}$ is the average time taken by a truck to cross the bridge,

$L^{truck}_{average}$ is the average truck length for both lanes (m),

$V^{truck}_{average}$ is the average speed for both lanes (m/s).

The expression in Equation I-4 is only an estimation of the number of meeting events involving two trucks since it does not account for the possibility of two trucks following each other closely and thus slightly overestimates the number of meeting events. However, the following section shows that the accuracy of the formula developed is reasonable.

I.2.2 Validation of the formula

In order to validate this formula, the empirical results were analysed in more detail. Figure I-1 presents the average number of meeting events per hour as a function of the product of the flow rates for a 20m bridge. The three traffic types (same traffic intensity, different traffic weight) exhibit the same linear trend, which agrees with Equation I-4, and also reveal slightly different slope values depending on the traffic type, which also agrees with the traffic-specific aspect of Equation I-4 (the average truck length and speed are function of the selected traffic).

In Figure I-1, straight lines (forced to go through the origin) were fitted to the measured data using the least-square technique. The slope of the lines correspond to the multiplying factor *k* [if Equation I-4 is expressed as $N = k(Q_1Q_2)$] by:

$$k = \frac{2(L^{bridge} + L^{truck}_{average})}{3600 V^{truck}_{average}}$$

Equation I-6

Table I-4 presents the values of the multiplying factor *k* obtained for the measured data and using Equation I-6. The differences are small, between –1.5% and +6.1%; which confirms the validity of the formula developed.

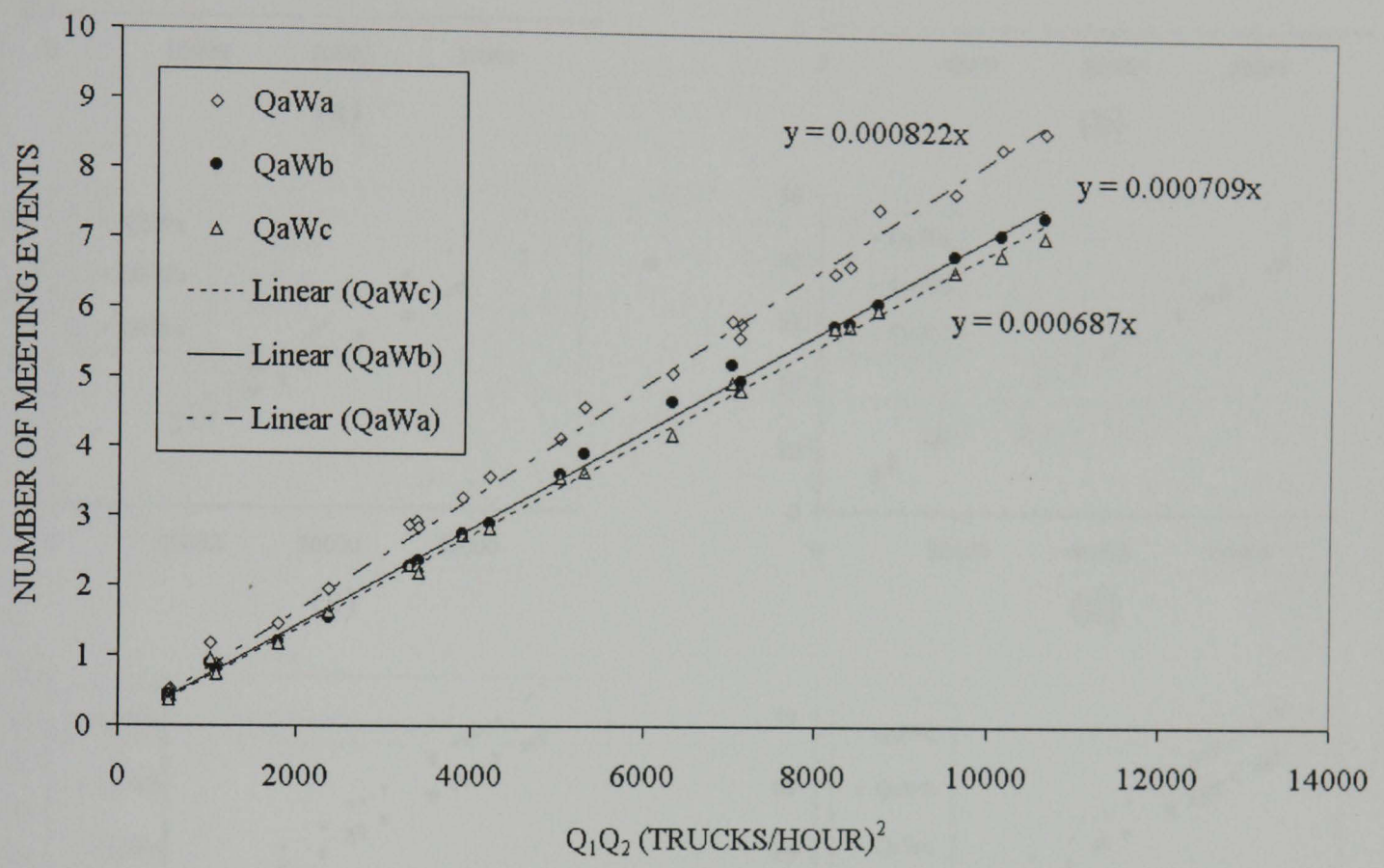

Figure I-1: Number of meeting events (per hour) in function of the product of hourly flow rates Q1 and Q2

Table I-4: Values of multiplying factor *k*

	Wa	Wc	Wb
Average Truck Length (m)	8.49	9.78	11.08
Average Speed (m/s)	18.37	23.70	23.68
Modelled *k* (*1 000 000)	862	698	729
Empirical *k* (*1 000 000)	822	709	687
Difference (%)	4.8	-1.5	6.1

Figure I-2 shows the plots for other traffic types with higher traffic intensity; the same observation applies to all the figures: there is an obvious linear relationship between the number of meeting events and the product of flow rates. The distinction between the traffic types is still noticeable, mainly between *Wa* and the other two traffic types *Wb&Wc*.

Again, this difference is mathematically explained by the slower speed corresponding to type *Wa*.

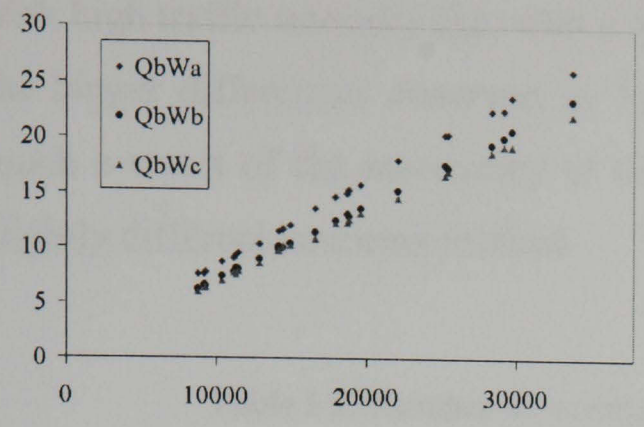

(a)

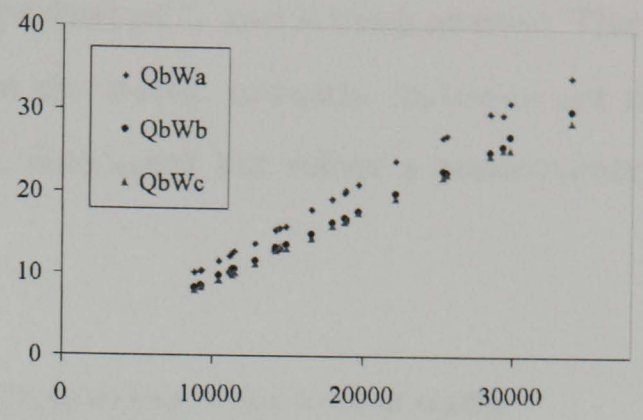

(b)

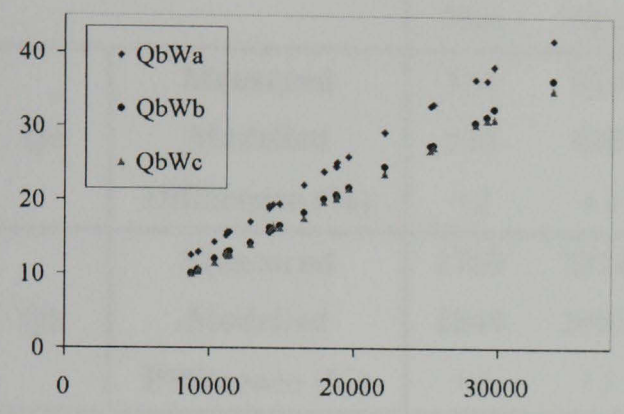

(c)

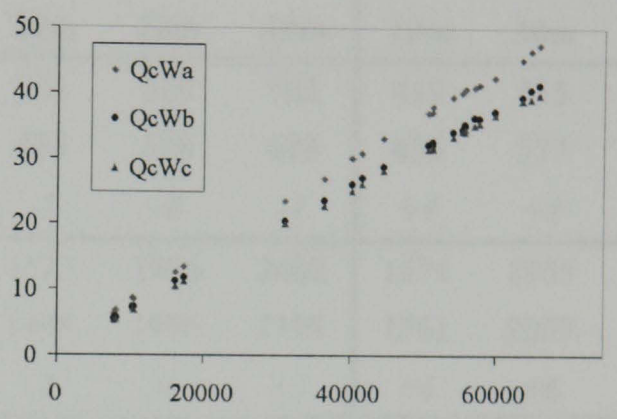

(d)

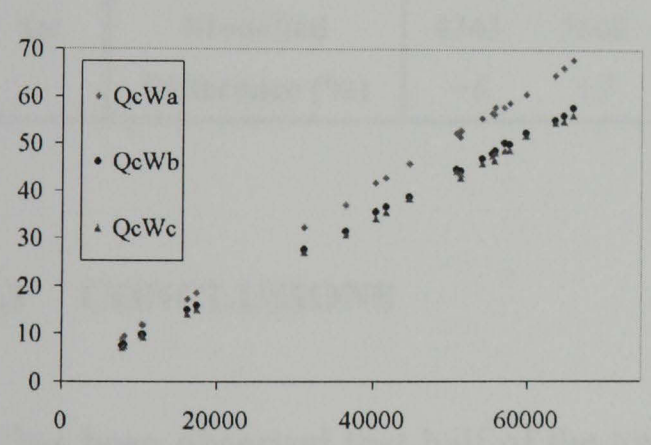

(e)

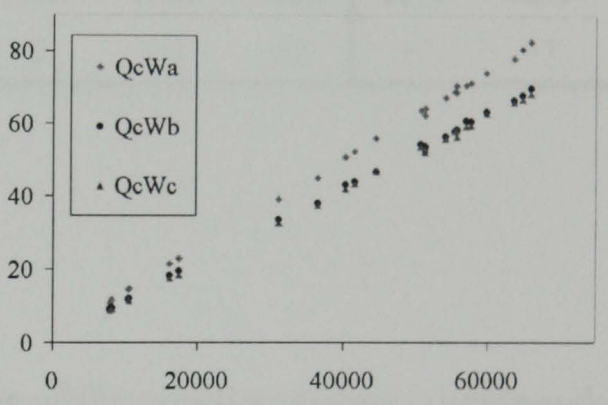

(f)

Figure I-2: Number of meeting events (per hour) in function of the product of flow rates (Q1xQ2) for various traffic intensities: (a) Qb – 20m bridges, (b) Qb – 30m bridges, (c) Qb – 40m bridges, (d) Qc – 20m bridges, (e) Qc – 30m bridges and (f) Qc – 40m bridges

Finally, the total number of meeting events corresponding to a full week of traffic can be estimated using Equation I-5. These estimated values are compared to the measured values obtained from the full simulations for all the traffic types and bridge lengths considered in Table I-5. The agreement is good: all the estimated values are within –3 and +9% of the measured numbers. The differences between modelled and measured number of meeting events increase with the traffic intensity; the formula of Equation I-5 tend to overestimate the number of meeting events. However, this phenomenon can be explained by the way that the meeting events are counted in SIMULTRAFFIC. For example, if an event

corresponds to the event type 321/312 or 422/431/413, it is counted once only; however, it corresponds to more than one event in reality. Consequently the measured number of meeting events obtained from SIMULTRAFFIC is slightly underestimated for traffic types with high traffic intensity (i.e. with a higher proportion of 3- and 4-truck events). Therefore the bigger differences observed in Table I-5 as the traffic intensity increases are not so much a result of the inaccuracy of the formula developed but rather a consequence of a slightly different counting method.

Table I-5: Number of meeting events corresponding to one week of traffic

		Wa			Wc			Wb		
		20m	**30m**	**40m**	**20m**	**30m**	**40m**	**20m**	**30m**	**40m**
Qa	**Measured**	504	679	854	431	568	702	419	555	691
	Modelled	516	696	877	418	558	698	436	577	717
	Difference (%)	*+2*	*+3*	*+3*	*-3*	*-2*	*-1*	*+4*	*+4*	*+4*
Qb	**Measured**	1769	2374	2966	1523	1996	2462	1471	1955	2430
	Modelled	1844	2491	3139	1494	1996	2498	1561	2063	2565
	Difference (%)	*+4*	*+5*	*+6*	*-2*	*0*	*+1*	*+6*	*+6*	*+6*
Qc	**Measured**	4090	5460	6779	3520	4604	5655	3432	4533	5605
	Modelled	4343	5868	7392	3519	4701	5882	3676	4858	6041
	Difference (%)	*+6*	*+7*	*+9*	*0*	*+2*	*+4*	*+7*	*+7*	*+8*

I.3 CONCLUSIONS

It has been observed that half of the total number of the crossing events corresponds to the basic meeting event type (i.e. 2 trucks from 2 opposing lanes meeting). The majority of the other crossing events consist of two trucks following each other in the same lane. In addition, there are some events involving 3 or 4 trucks; the proportion of these events increase with the traffic intensity. In a second part, a formula for predicting the number of meeting events (2 trucks from 2 opposing lanes meeting) has been developed and validated. The formula uses site-specific characteristics (hourly flow rates, average truck length and speed). Comparisons with the measured numbers of meeting events show good agreement for various traffic types and bridges lengths.

APPENDIX J

PLOTS OF THE CRITICAL LOADING EVENTS FOR BI-DIRECTIONAL TRAFFIC

Appendix J PLOTS OF THE CRITICAL LOADING EVENTS FOR BI-DIRECTIONAL TRAFFIC

Traffic type 'QaWb' – Set 0

10	415 1130 468 1376		449 1332 377 1059
9	372 1252 436 1258	19	420 1159 440 1247
8	446 1422 398 1135	18	392 1106 411 1301
7	383 1131 436 1441	17	375 1057 423 1349
6	409 1284 406 1293	16	490 1443 273 967
5	414 1160 462 1437	15	387 1164 447 1256
4	417 1261 430 1336	14	456 1242 384 1179
3	452 1393 400 1205	13	428 1402 392 1022
2	436 1435 453 1188	12	405 1185 439 1241
1	381 1036 579 1621	11	399 1266 418 1196
Span: 20 m		Influence Line	Mid-span moment

10	398 343 377 322		418 356 356 299
9	379 316 414 350	19	386 331 381 324
8	356 305 419 361	18	384 318 397 338
7	400 334 397 333	17	380 327 386 332
6	409 332 406 344	16	417 318 430 342
5	375 318 423 360	15	415 312 468 350
4	383 325 436 360	14	336 287 437 376
3	399 345 402 349	13	392 328 411 335
2	387 324 447 376	12	361 307 412 356
1	446 380 398 329	11	376 325 384 338
Span: 2*10 m		Influence Line	Moment at central support

10	409 304 396 233		405 292 406 223
9	421 317 388 222	19	426 337 336 179
8	414 318 397 223	18	460 329 337 189
7	445 335 317 207	17	458 273 402 245
6	396 299 401 246	16	353 252 373 266
5	452 345 400 202	15	359 263 404 259
4	415 307 231 4 394 235	14	442 305 412 217
3	420 285 440 273	13	414 240 462 290
2	422 313 413 272	12	377 262 431 270
1	437 325 429 269	11	408 297 405 238
Span: 20 m	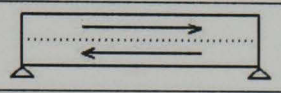	Influence Line	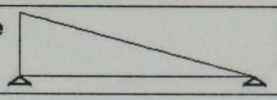 Shear at left support

10	345 206 459 341		428 253 365 270
9	393 233 421 320	19	345 214 406 309
8	406 262 438 293	18	402 210 425 315
7	324 222 454 336	17	418 254 381 272
6	399 242 419 320	16	312 202 441 327
5	436 227 453 343	15	417 273 357 257
4	404 241 470 343	14	432 241 399 294
3	398 255 464 332	13	424 246 397 292
2	441 293 434 308	12	467 233 418 309
1	381 210 579 426	11	414 235 425 312
Span: 20 m	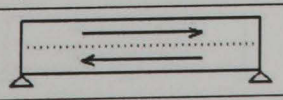	Influence Line	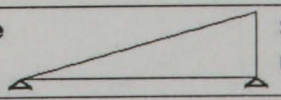 Shear at right support

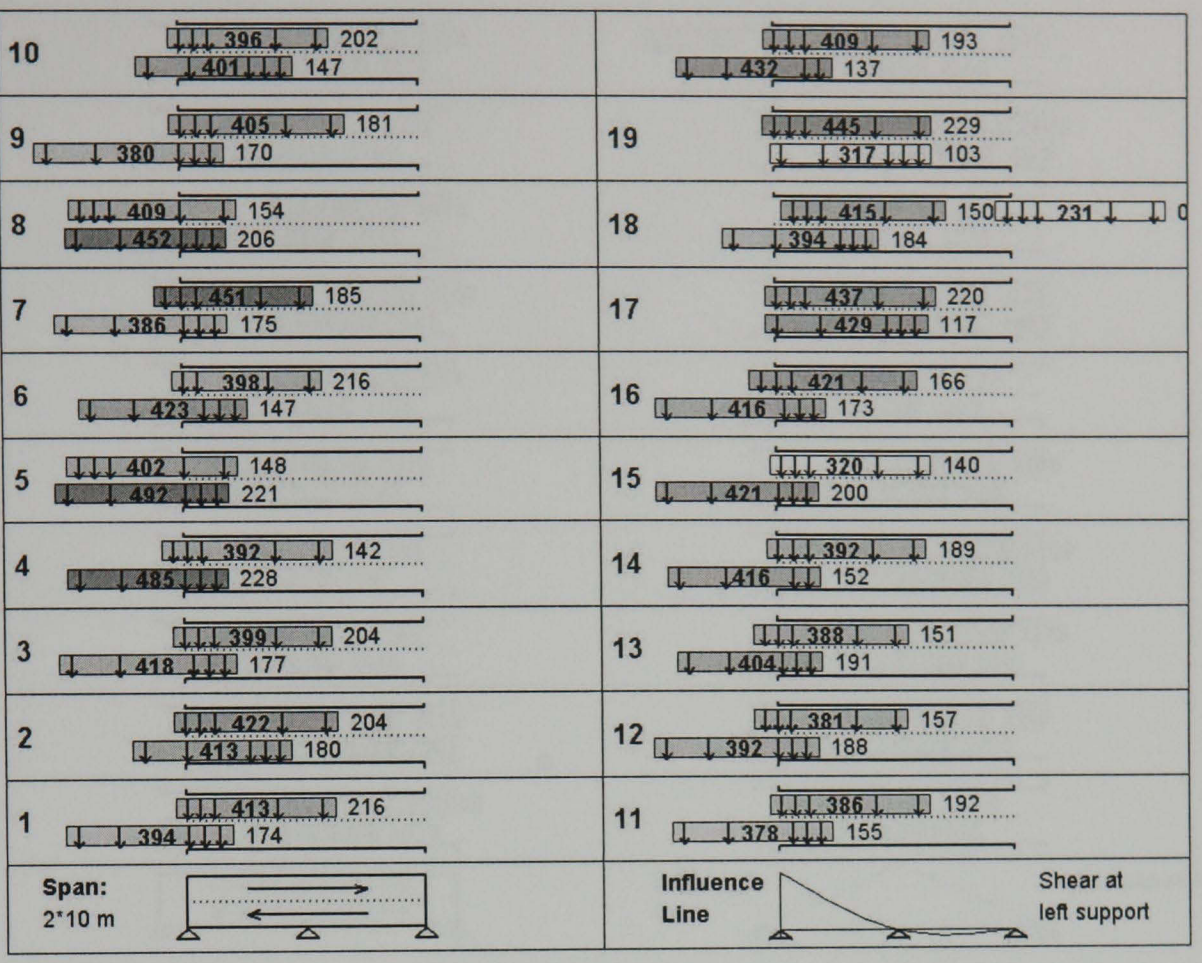
10
396 202
401 147
9
405 181
380 170
8
409 154
452 206
7
451 185
386 175
6
398 216
423 147
5
402 148
492 221
4
392 142
485 228
3
399 204
418 177
2
422 204
413 180
1
413 216
394 174
Span:
2*10 m
409 193
432 137
19
445 229
317 103
18
415 150 231
394 184
17
437 220
429 117
16
421 166
416 173
15
320 140
421 200
14
392 189
416 152
13
388 151
404 191
12
381 157
392 188
11
386 192
378 155
Influence
Line
Shear at
left support

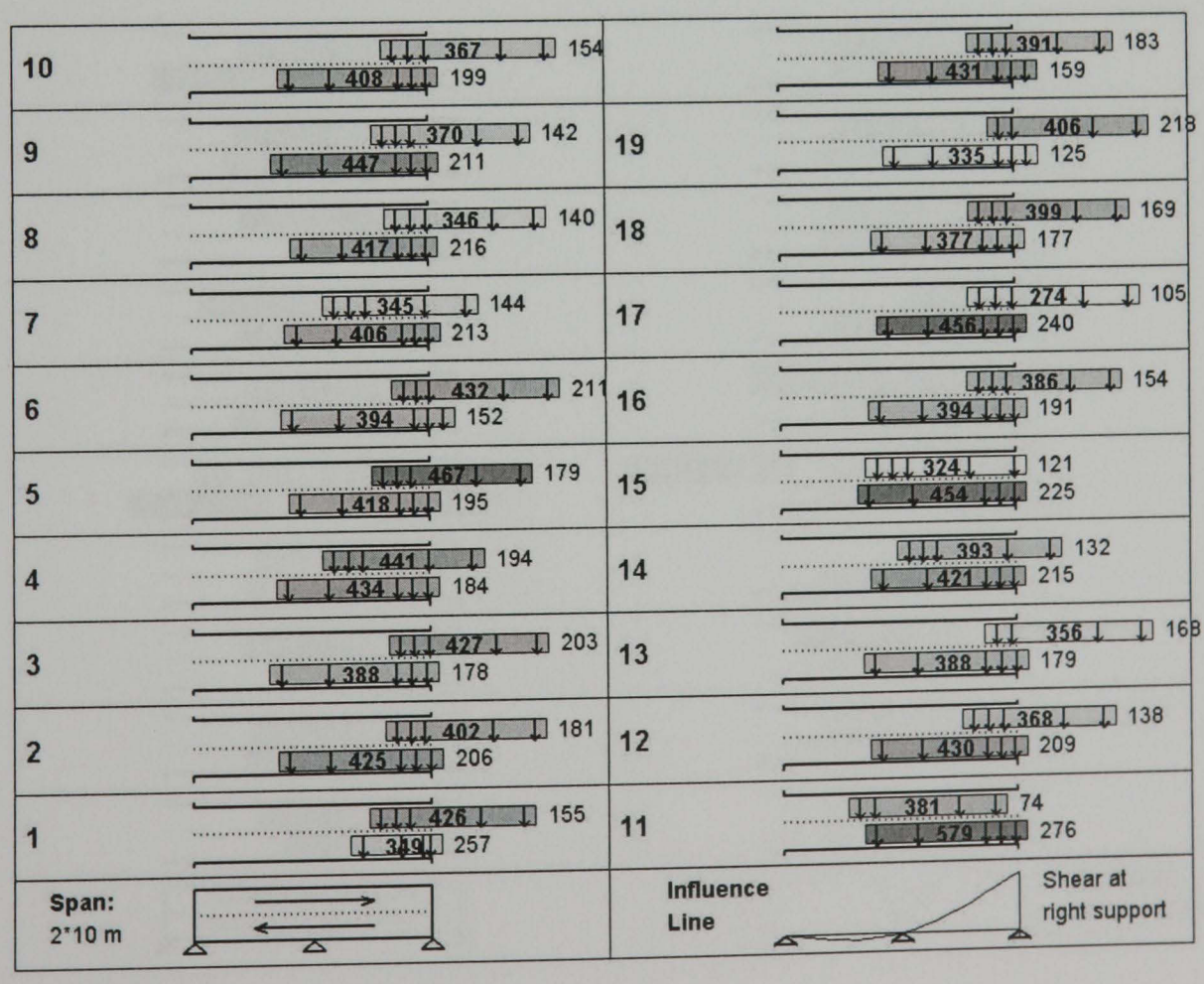
10
367 154
408 199
9
370 142
447 211
8
346 140
417 216
7
345 144
406 213
6
432 211
394 152
5
467 179
418 195
4
441 194
434 184
3
427 203
388 178
2
402 181
425 206
1
426 155
349 257
Span:
2*10 m
391 183
431 159
19
406 218
335 125
18
399 169
377 177
17
274 105
456 240
16
386 154
394 191
15
324 121
454 225
14
393 132
421 215
13
356 168
388 179
12
368 138
430 209
11
381 74
579 276
Influence
Line
Shear at
right support

10	405 2173 439 2334		169 63 375 1979 423 2380
9	409 2272 406 2289	19	398 2080 464 2343
8	383 2071 436 2515	18	449 2419 377 2020
7	415 2166 468 2462	17	428 2473 392 1985
6	446 2517 398 2116	16	420 2179 440 2282
5	417 2273 430 2382	15	387 2115 447 2356
4	452 2526 400 2187	14	404 2105 470 2372
3	414 2169 462 2565	13	456 2379 384 2099
2	436 2519 453 2301	12	399 2245 418 2235
1	381 2010 579 3029	11	372 2150 436 2343
Span: 30 m	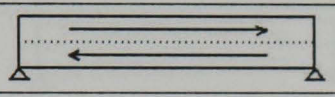	Influence Line	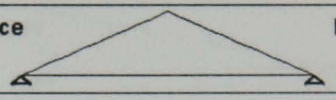 Mid-span moment

10	437 545 429 419		379 455 414 487
9	449 532 377 434	19	386 470 381 473
8	456 569 384 407	18	376 464 384 481
7	414 423 462 557	17	345 388 459 558
6	399 490 402 504	16	242 220 375 298 387 428
5	297 285 448 377 392 337	15	169 9 375 457 423 485
4	446 519 398 482	14	436 430 453 523
3	415 519 468 486	13	452 483 400 471
2	387 467 447 541	12	365 423 169 47 419 487
1	381 477 579 591	11	385 473 388 489
Span: 2*15 m	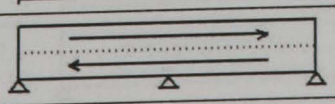	Influence Line	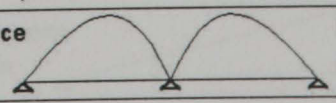 Moment at central support

10	398 333 423 288		425 348 389 257
9	398 326 450 295	19	451 372 386 235
8	401 326 394 200 218 95	18	297 218 448 339 392 52
7	449 363 395 263	17	396 319 419 292
6	411 333 386 294	16	387 316 465 295
5	409 300 432 329	15	387 294 432 317
4	399 326 418 305	14	388 304 404 310
3	413 332 394 299	13	437 350 402 266
2	445 312 456 333	12	400 316 446 301
1	392 318 485 369	11	392 301 416 320
Span: 30 m		Influence Line	Shear at left support

10	426 314 [illegible] 296		434 315 375 286
9	381 140 579 473	19	330 260 425 343
8	403 286 402 328	18	438 313 359 291
7	370 251 447 364	17	346 256 417 349
6	381 240 457 384	16	356 269 320 157 386 178
5	427 321 388 305	15	403 268 416 337
4	388 293 413 335	14	403 271 409 335
3	391 286 431 349	13	368 253 430 354
2	402 286 425 349	12	374 260 431 348
1	467 316 418 343	11	408 294 393 316
Span: 30 m		Influence Line	Shear at right support

10	409 257 341 180		428 250 379 176
9	389 251 393 188	19	413 266 394 161
8	402 234 492 206	18	411 241 386 186
7	396 228 419 214	17	437 249 402 179
6	409 246 452 198	16	371 229 390 199
5	388 231 432 214	15	382 233 347 196
4	438 268 394 180	14	397 254 384 176
3	449 263 395 193	13	425 258 389 174
2	392 232 485 230	12	398 242 450 190
1	421 255 439 233	11	375 225 429 207
Span: 2*15 m	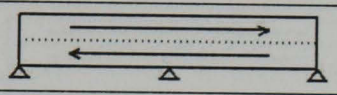	Influence Line	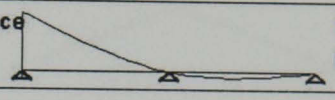 Shear at left support

10	389 175 407 251		394 192 443 219
9	330 179 425 247	19	391 161 431 251
8	274 132 456 297	18	402 152 425 260
7	403 187 409 247	17	426 184 341 228
6	364 193 498 241	16	337 150 410 266
5	373 156 432 283	15	399 179 398 238
4	374 194 431 251	14	430 189 372 230
3	438 238 359 211	13	346 150 417 269
2	373 165 474 289	12	368 166 448 258
1	424 217 419 250	11	388 180 413 245
Span: 2*15 m	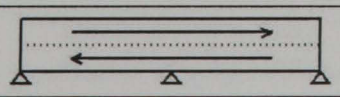	Influence Line	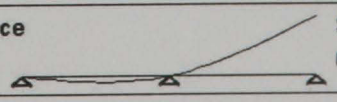 Shear at right support

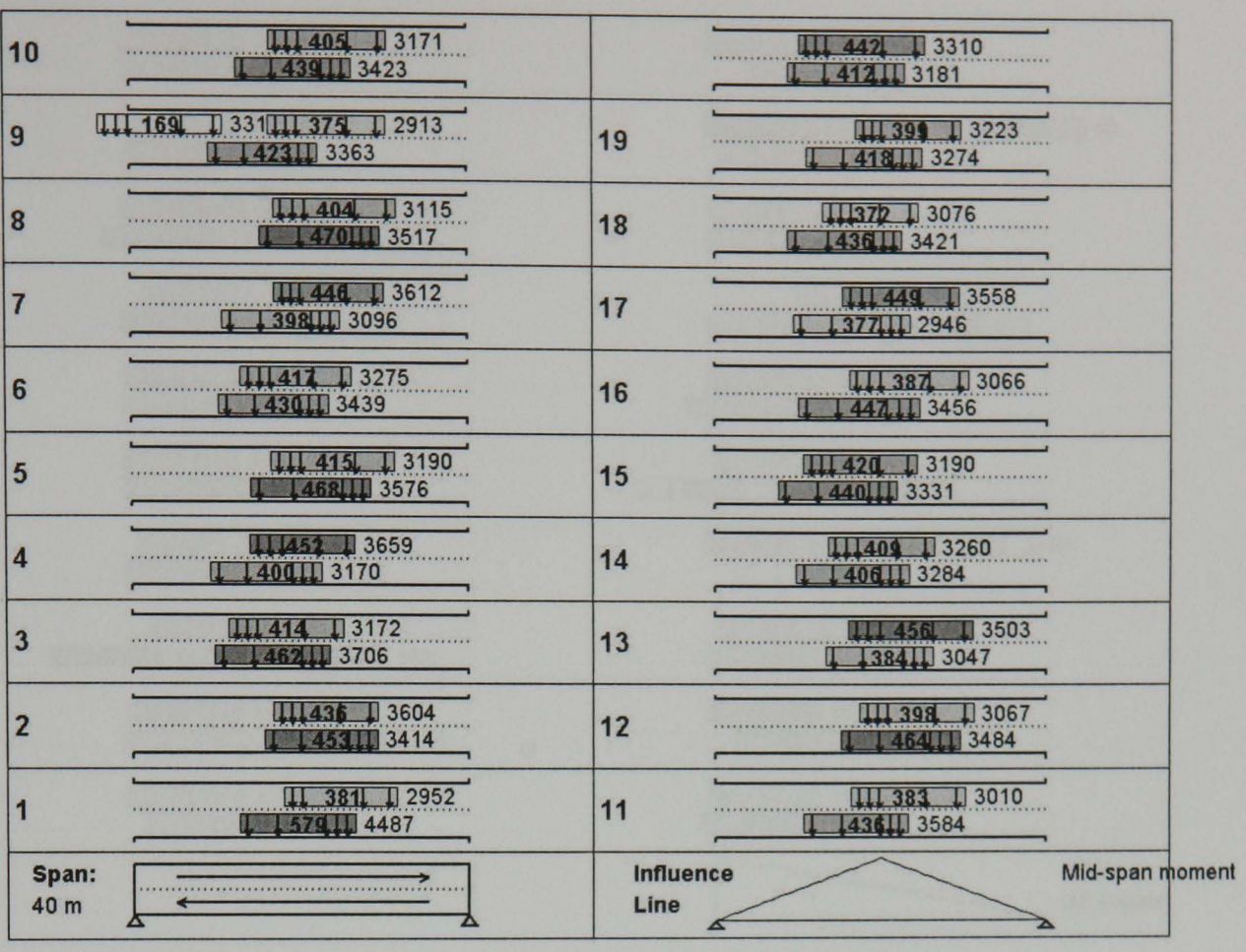
10
405 3171
439 3423
9
169 331 375 2913
423 3363
8
404 3115
470 3517
7
446 3612
398 3096
6
417 3275
430 3439
5
415 3190
468 3576
4
452 3659
400 3170
3
414 3172
462 3706
2
436 3604
453 3414
1
381 2952
579 4487
Span:
40 m
Influence
Line
Mid-span moment
442 3310
412 3181
19
399 3223
418 3274
18
372 3076
436 3421
17
449 3558
377 2946
16
387 3066
447 3456
15
420 3190
440 3331
14
409 3260
406 3284
13
456 3503
384 3047
12
398 3067
464 3484
11
383 3010
436 3584

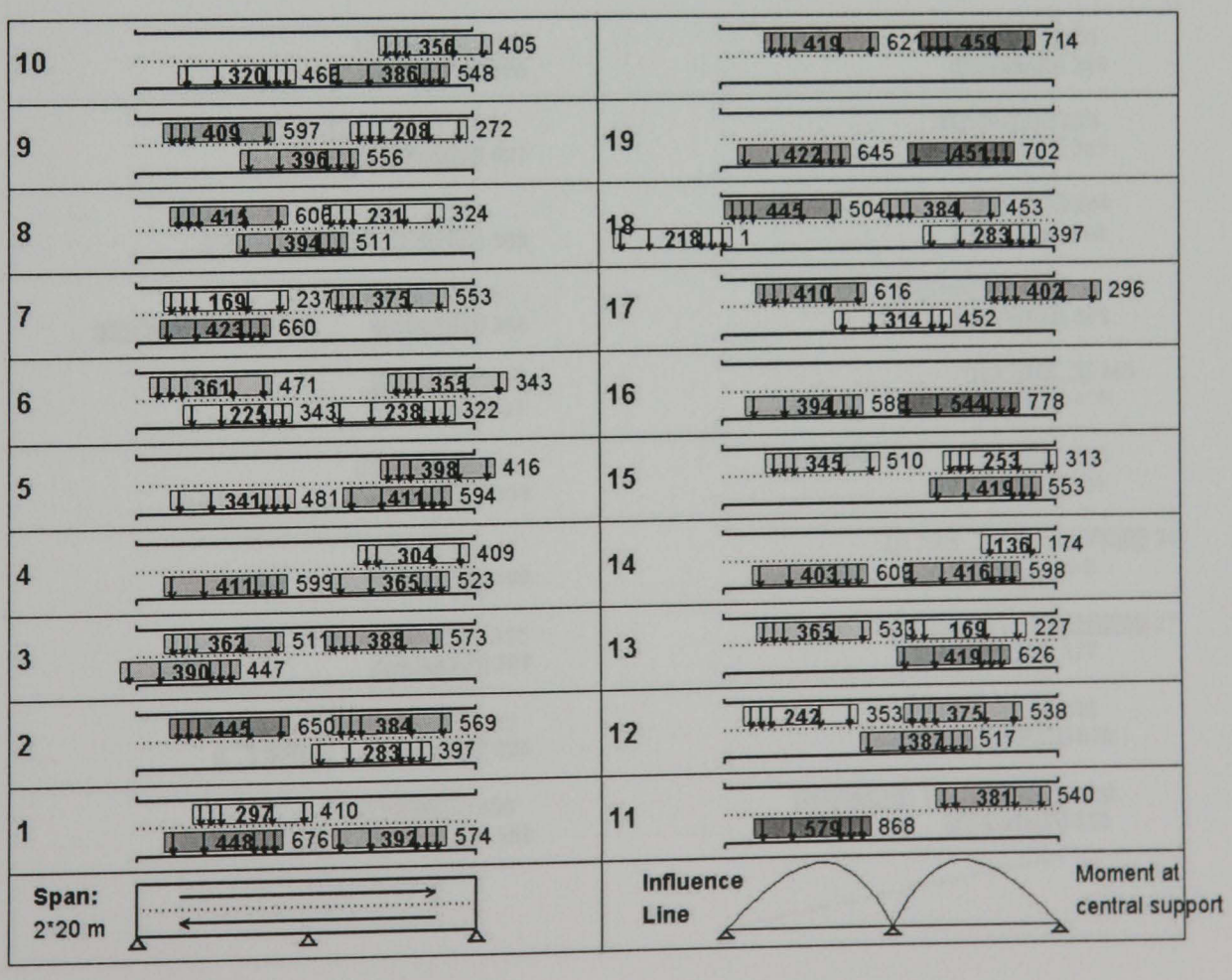
10
356 405
320 468 386 548
9
409 597 208 272
396 556
8
413 606 231 324
394 511
7
169 237 375 553
423 660
6
361 471 355 343
225 343 238 322
5
398 416
341 481 411 594
4
304 409
411 599 365 523
3
362 511 388 573
390 447
2
445 650 384 569
283 397
1
297 410
448 676 392 574
Span:
2*20 m
Influence
Line
Moment at
central support
419 621 459 714
19
422 645 451 702
18
445 504 384 453
218 1 283 397
17
410 616 402 296
314 452
16
394 588 544 778
15
345 510 253 313
419 553
14
136 174
403 609 416 598
13
365 533 169 227
419 626
12
242 353 375 538
387 517
11
381 540
579 868

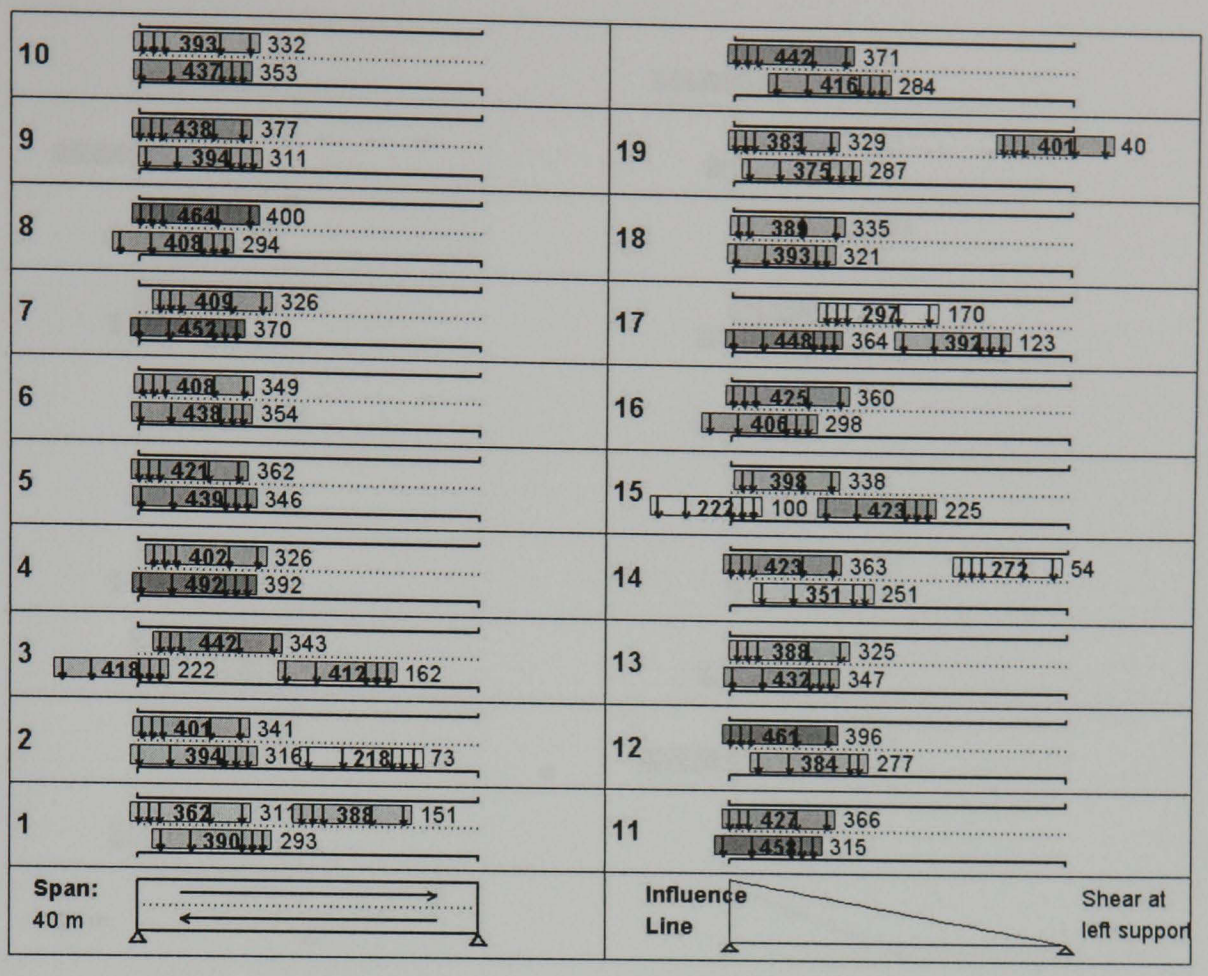
10
393 332
437 353
9
438 377
394 311
8
464 400
408 294
7
409 326
452 370
6
408 349
438 354
5
421 362
439 346
4
402 326
492 392
3
442 343
418 222
412 162
2
401 341
394 316
218 73
1
362 31
388 151
390 293
Span:
40 m
442 371
416 284
19
383 329
401 40
375 287
18
384 335
393 321
17
297 170
448 364
392 123
16
425 360
406 298
15
398 338
222 100
423 225
14
423 363
272 54
351 251
13
388 325
432 347
12
461 396
384 277
11
422 366
454 315
Influence
Line
Shear at
left support

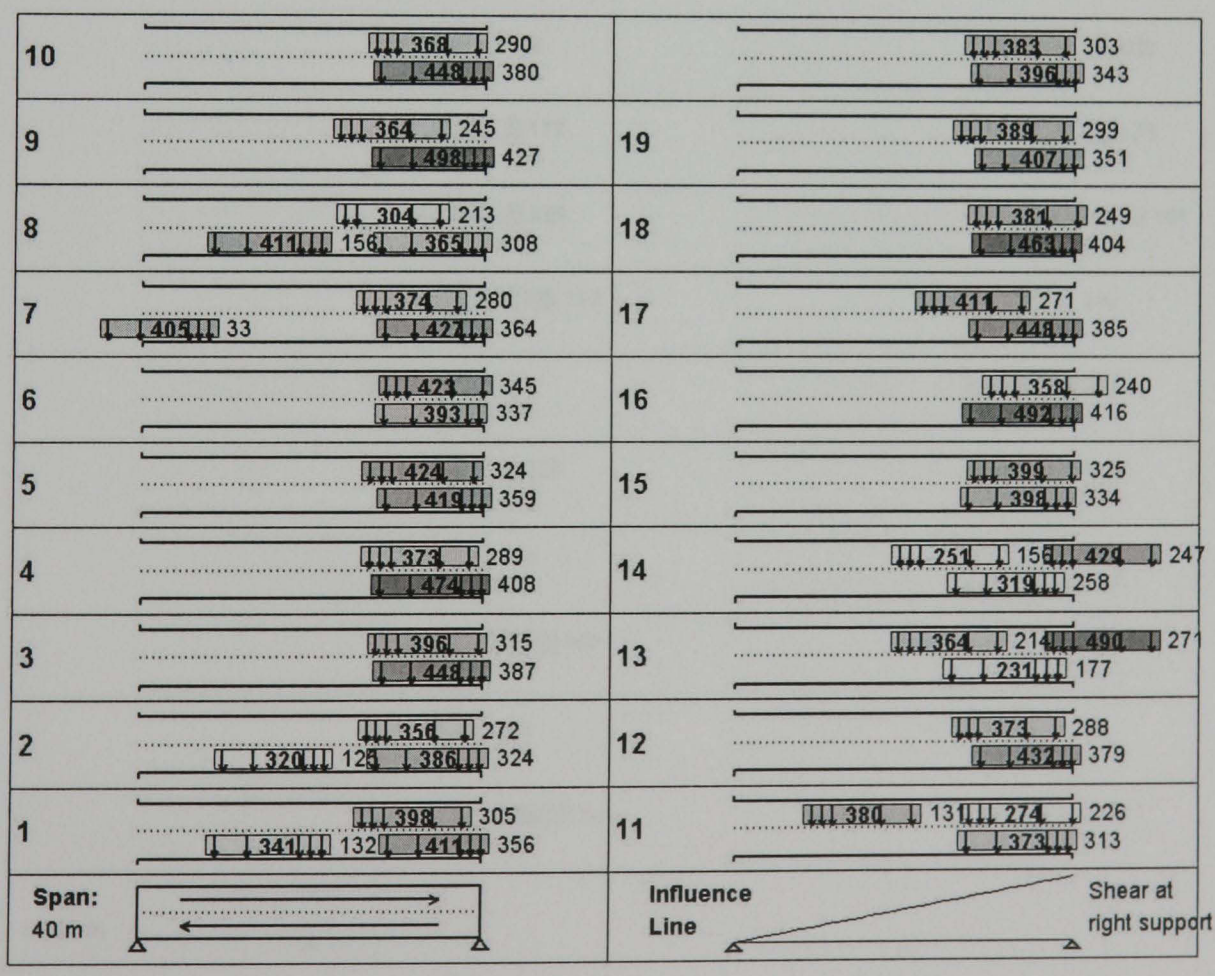
10
368 290
448 380
9
364 245
498 427
8
304 213
411 156
365 308
7
374 280
405 33
427 364
6
423 345
393 337
5
424 324
419 359
4
373 289
474 408
3
396 315
448 387
2
356 272
320 125
386 324
1
398 305
341 132
411 356
Span:
40 m
383 303
396 343
19
389 299
407 351
18
381 249
463 404
17
411 271
448 385
16
358 240
492 416
15
399 325
398 334
14
251 156
429 247
319 258
13
364 214
490 271
231 177
12
373 288
432 379
11
380 131
274 226
373 313
Influence
Line
Shear at
right support

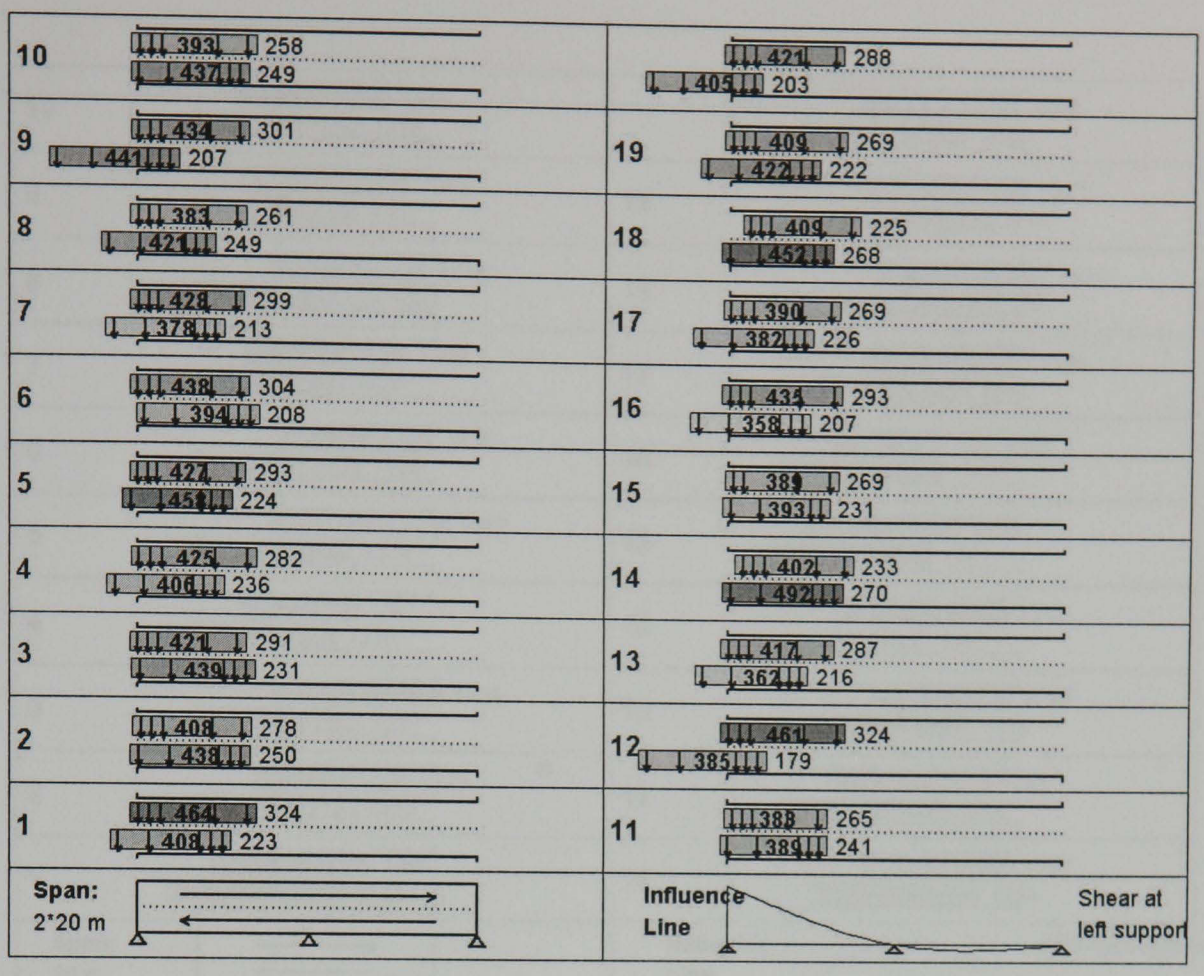
10
393 258
437 249
9
434 301
441 207
8
383 261
421 249
7
428 299
378 213
6
438 304
394 208
5
427 293
451 224
4
425 282
406 236
3
421 291
439 231
2
408 278
438 250
1
464 324
408 223
Span:
2*20 m
19
421 288
405 203
409 269
422 222
18
409 225
452 268
17
390 269
382 226
16
435 293
358 207
15
389 269
393 231
14
402 233
492 270
13
417 287
362 216
12
461 324
385 179
11
388 265
389 241
Influence
Line
Shear at
left support

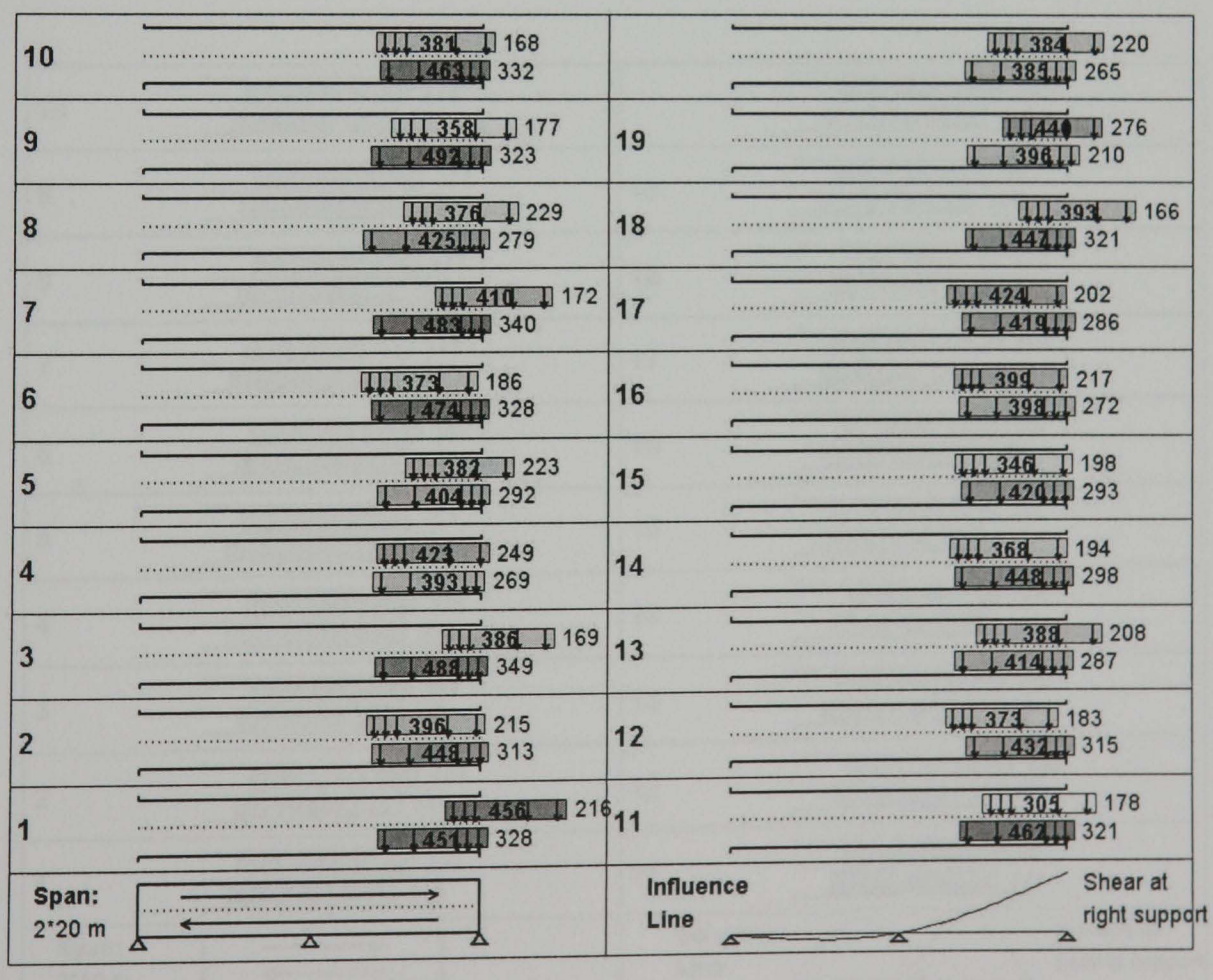
10
381 168
463 332
9
358 177
492 323
8
376 229
425 279
7
410 172
483 340
6
373 186
474 328
5
382 223
404 292
4
423 249
393 269
3
386 169
489 349
2
396 215
449 313
1
456 216
451 328
Span:
2*20 m
19
384 220
385 265
440 276
396 210
18
393 166
447 321
17
424 202
419 286
16
399 217
398 272
15
346 198
420 293
14
368 194
448 298
13
388 208
414 287
12
373 183
432 315
11
305 178
467 321
Influence
Line
Shear at
right support

Traffic type 'QbWb' –Set 0

10	427 1346 421 1276		386 1235 450 1322
9	426 1245 436 1387	19	443 1271 409 1288
8	418 1373 433 1269	18	510 1582 360 985
7	449 1325 423 1327	17	406 1196 442 1370
6	426 1375 417 1286	16	384 1095 452 1473
5	414 1257 476 1408	15	398 1129 486 1447
4	393 1391 475 1310	14	423 1217 383 1367
3	466 1426 406 1277	13	370 1218 464 1377
2	401 1303 443 1425	12	444 1353 425 1244
1	427 1254 559 1733	11	435 1373 430 1224
Span: 20 m	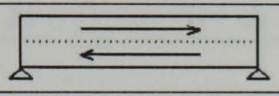	Influence Line	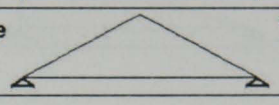 Mid-span moment

10	373 318 460 399		404 353 388 340
9	435 372 405 345	19	426 361 406 338
8	438 377 397 344	18	386 322 450 379
7	370 318 471 406	17	403 344 408 358
6	416 361 420 364	16	419 364 388 338
5	411 351 434 376	15	384 331 430 371
4	436 376 412 352	14	418 338 433 365
3	426 367 417 362	13	409 352 406 352
2	466 401 406 349	12	411 334 446 374
1	414 352 476 411	11	441 371 403 340
Span: 2*10 m	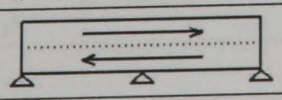	Influence Line	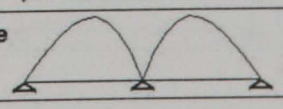 Moment at central support

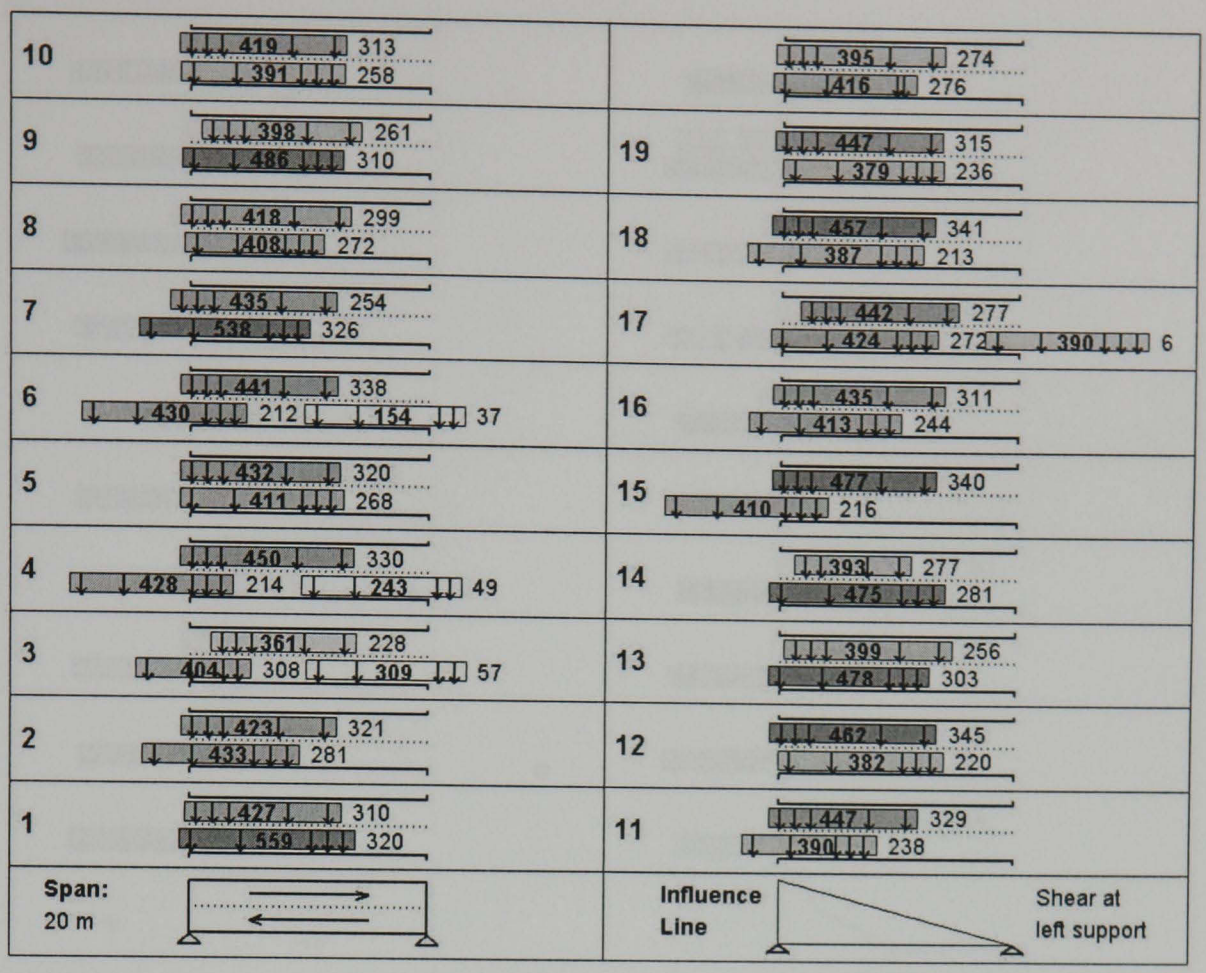
10
419 313
391 258
9
398 261
486 310
8
418 299
408 272
7
435 254
538 326
6
441 338
430 212 154 37
5
432 320
411 268
4
450 330
428 214 243 49
3
361 228
404 308 309 57
2
423 321
433 281
1
427 310
559 320
Span:
20 m
19
395 274
416 276
19
447 315
379 236
18
457 341
387 213
17
442 277
424 272 390 6
16
435 311
413 244
15
477 340
410 216
14
393 277
475 281
13
399 256
478 303
12
462 345
382 220
11
447 329
390 238
Influence
Line
Shear at
left support

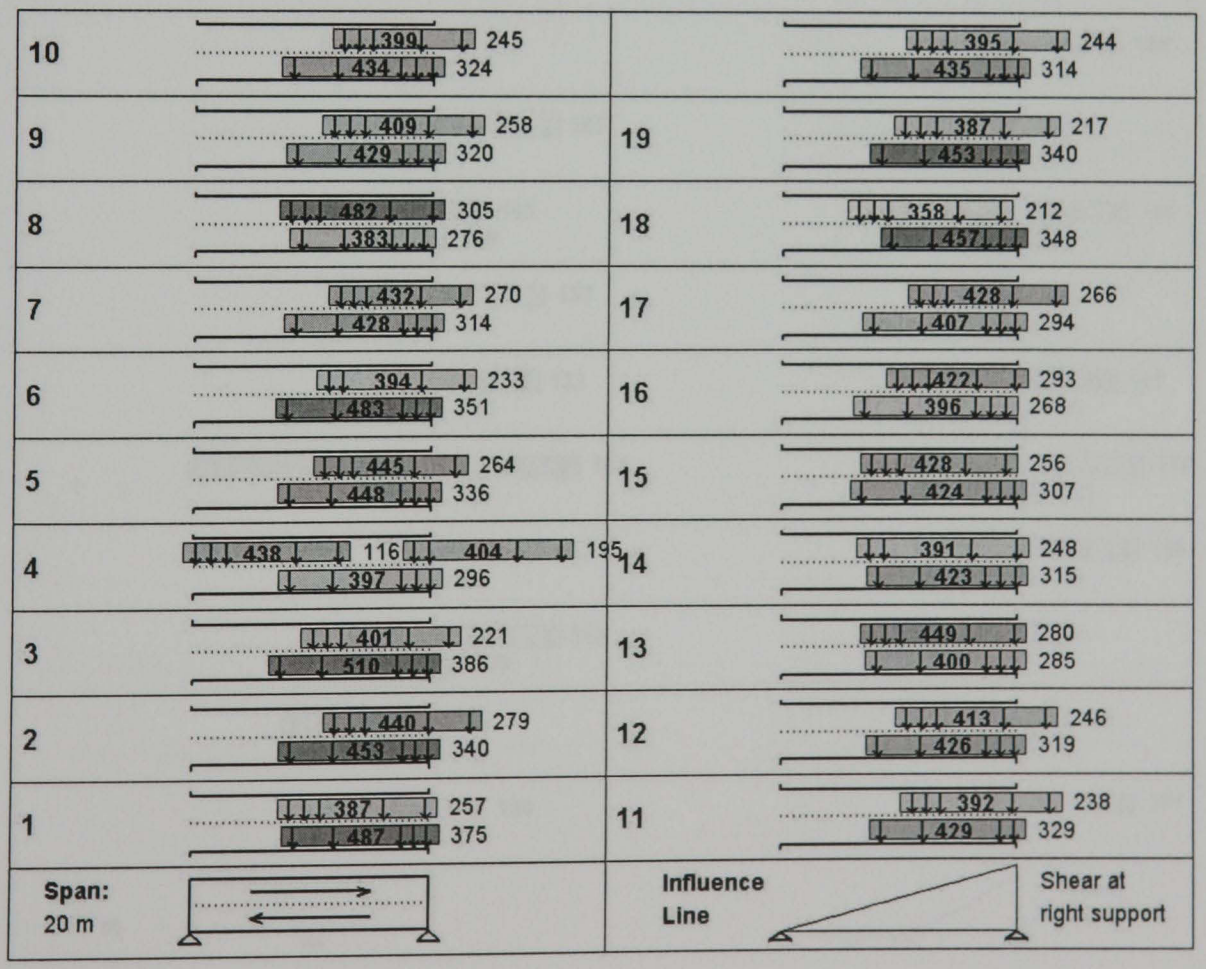
10
399 245
434 324
9
409 258
429 320
8
482 305
383 276
7
432 270
428 314
6
394 233
483 351
5
445 264
448 336
4
438 116 404 195
397 296
3
401 221
510 386
2
440 279
453 340
1
387 257
487 375
Span:
20 m
19
395 244
435 314
19
387 217
453 340
18
358 212
457 348
17
428 266
407 294
16
422 293
396 268
15
428 256
424 307
14
391 248
423 315
13
449 280
400 285
12
413 246
426 319
11
392 238
429 329
Influence
Line
Shear at
right support

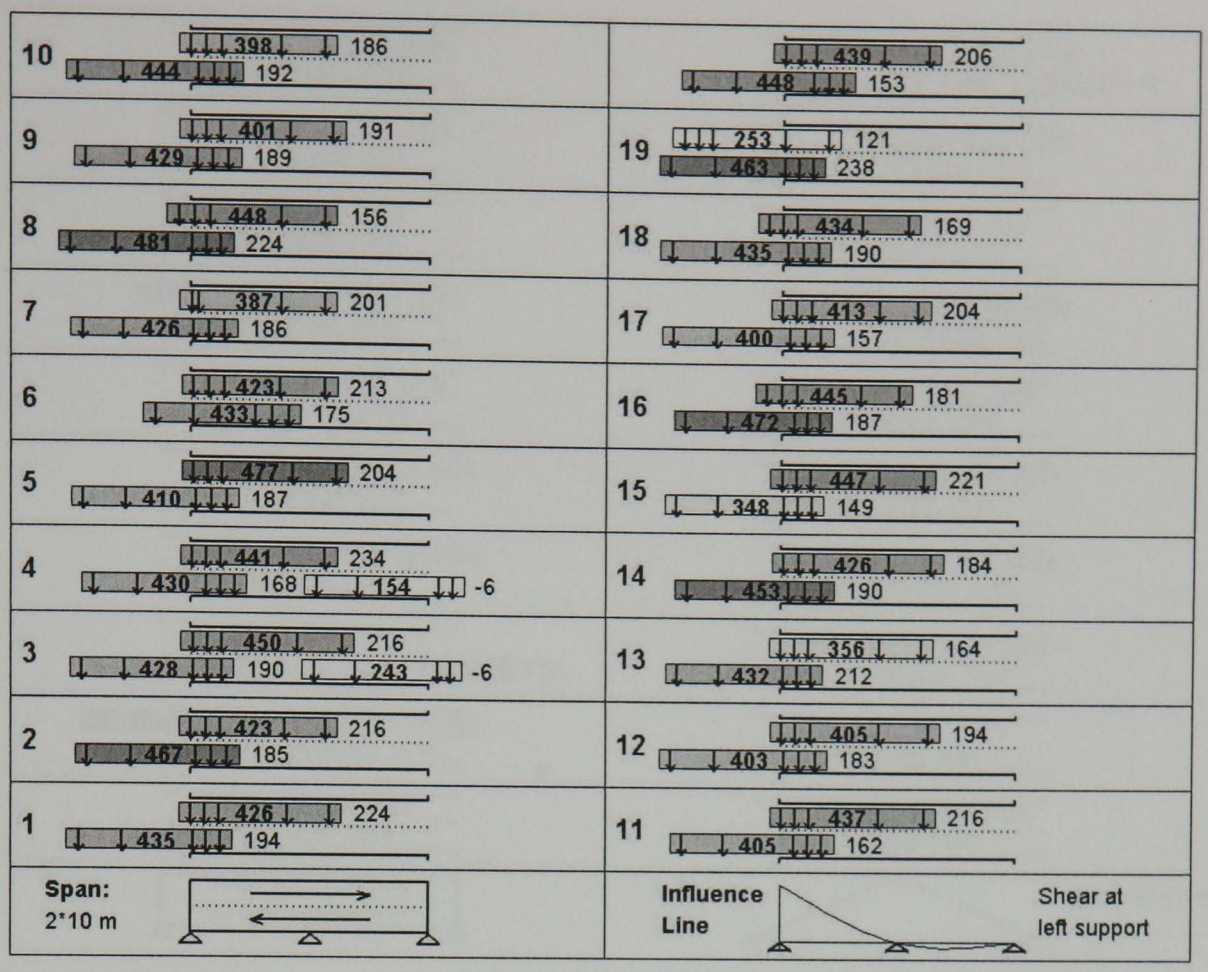
10
398 186
444 192
9
401 191
429 189
8
448 156
481 224
7
387 201
426 186
6
423 213
433 175
5
477 204
410 187
4
441 234
430 168
154 -6
3
450 216
428 190
243 -6
2
423 216
467 185
1
426 224
435 194
Span:
2*10 m
439 206
448 153
19
253 121
463 238
18
434 169
435 190
17
413 204
400 157
16
445 181
472 187
15
447 221
348 149
14
426 184
453 190
13
356 164
432 212
12
405 194
403 183
11
437 216
405 162
Influence
Line
Shear at
left support

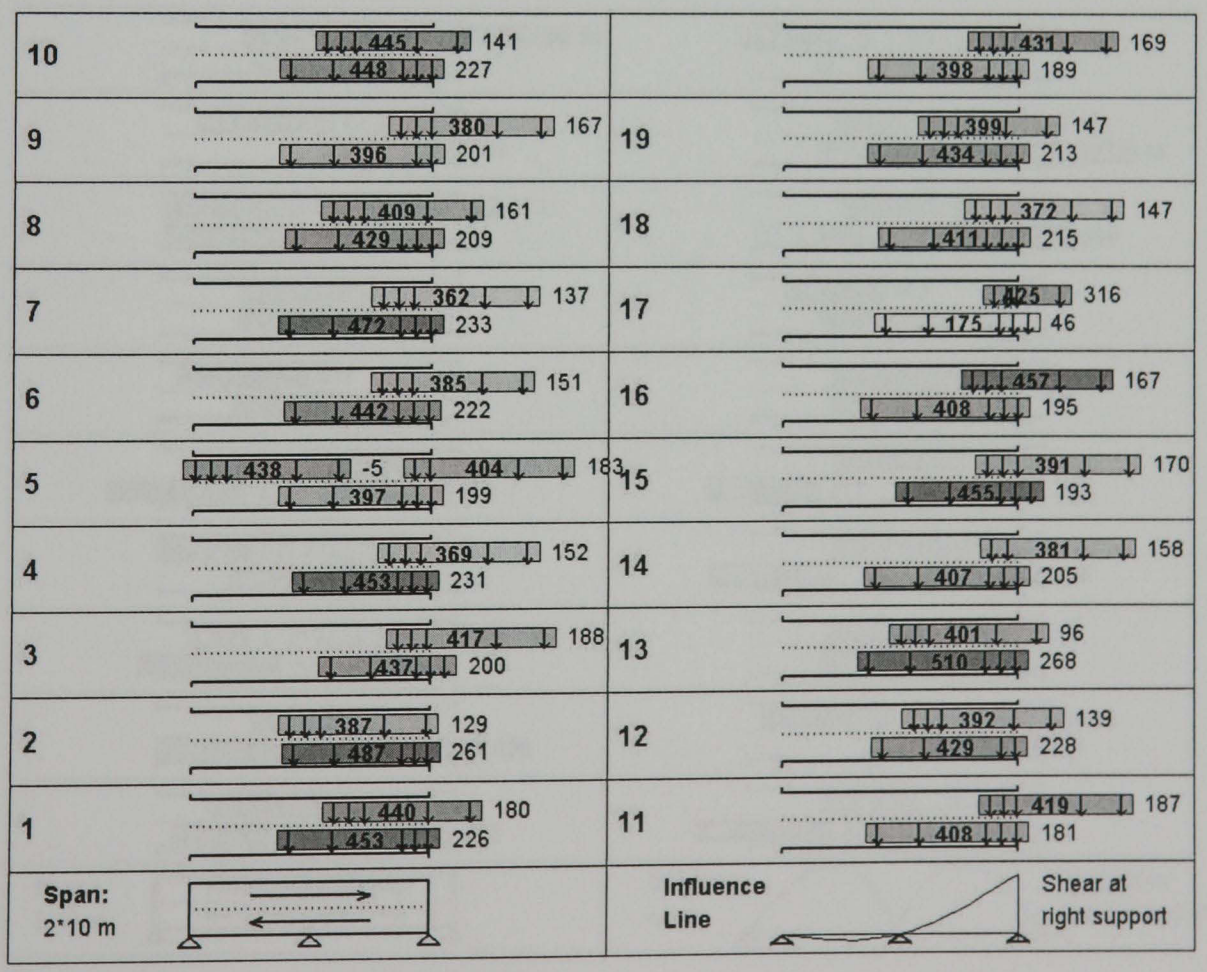
10
445 141
448 227
9
380 167
396 201
8
409 161
429 209
7
362 137
472 233
6
385 151
442 222
5
438 -5
404 183
397 199
4
369 152
453 231
3
417 188
437 200
2
387 129
487 261
1
440 180
453 226
Span:
2*10 m
431 169
398 189
19
399 147
434 213
18
372 147
411 215
17
425 316
175 46
16
457 167
408 195
15
391 170
455 193
14
381 158
407 205
13
401 96
510 268
12
392 139
429 228
11
419 187
408 181
Influence
Line
Shear at
right support

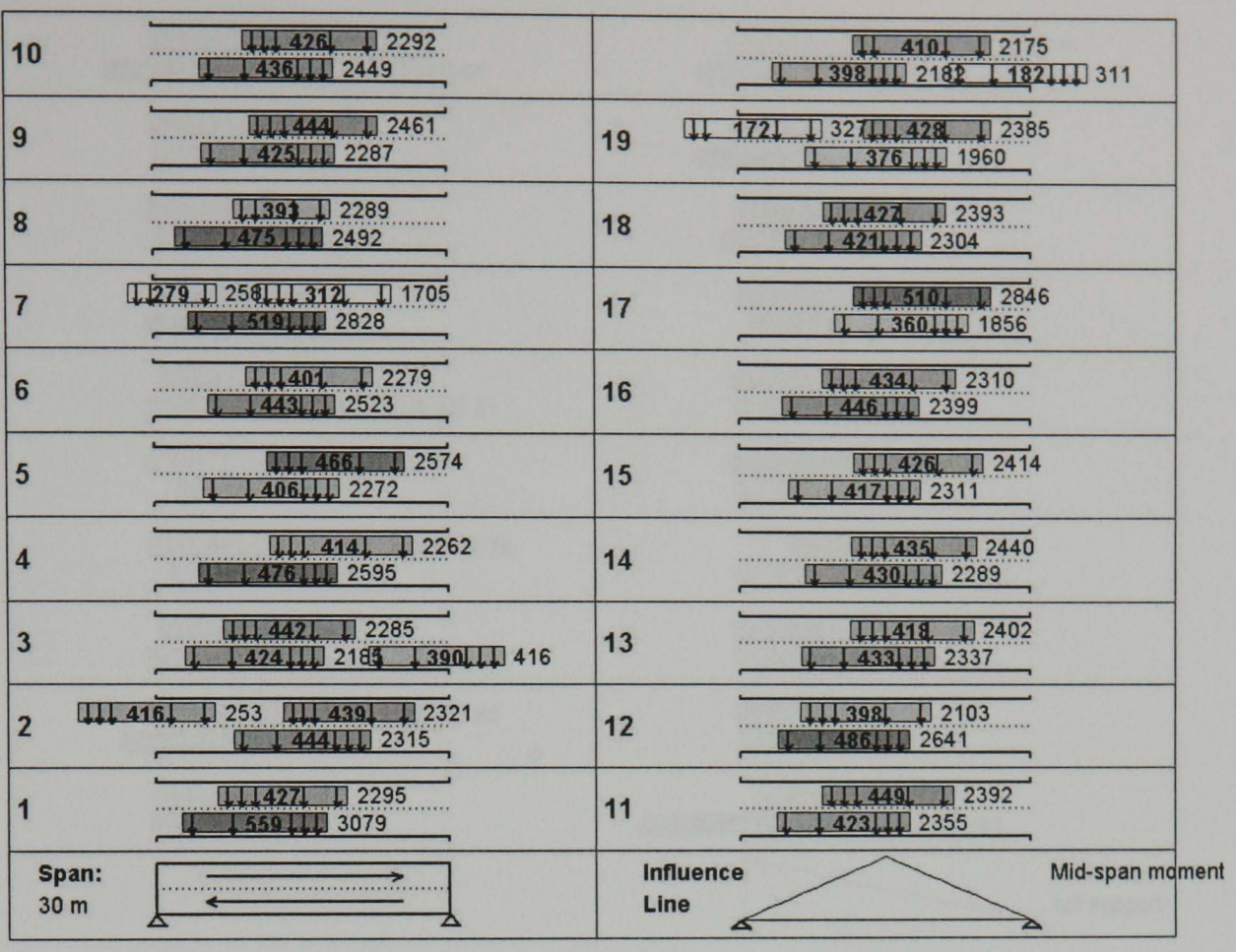
10
426 2292
436 2449
9
444 2461
425 2287
8
393 2289
475 2492
7
279 258 312 1705
519 2828
6
401 2279
443 2523
5
466 2574
406 2272
4
414 2262
476 2595
3
442 2285
424 2185 390 416
2
416 253 439 2321
444 2315
1
427 2295
559 3079
Span:
30 m
410 2175
398 2182 182 311
19
172 327 428 2385
376 1960
18
427 2393
421 2304
17
510 2846
360 1856
16
434 2310
446 2399
15
426 2414
417 2311
14
435 2440
430 2289
13
418 2402
433 2337
12
398 2103
486 2641
11
449 2392
423 2355
Influence
Line
Mid-span moment

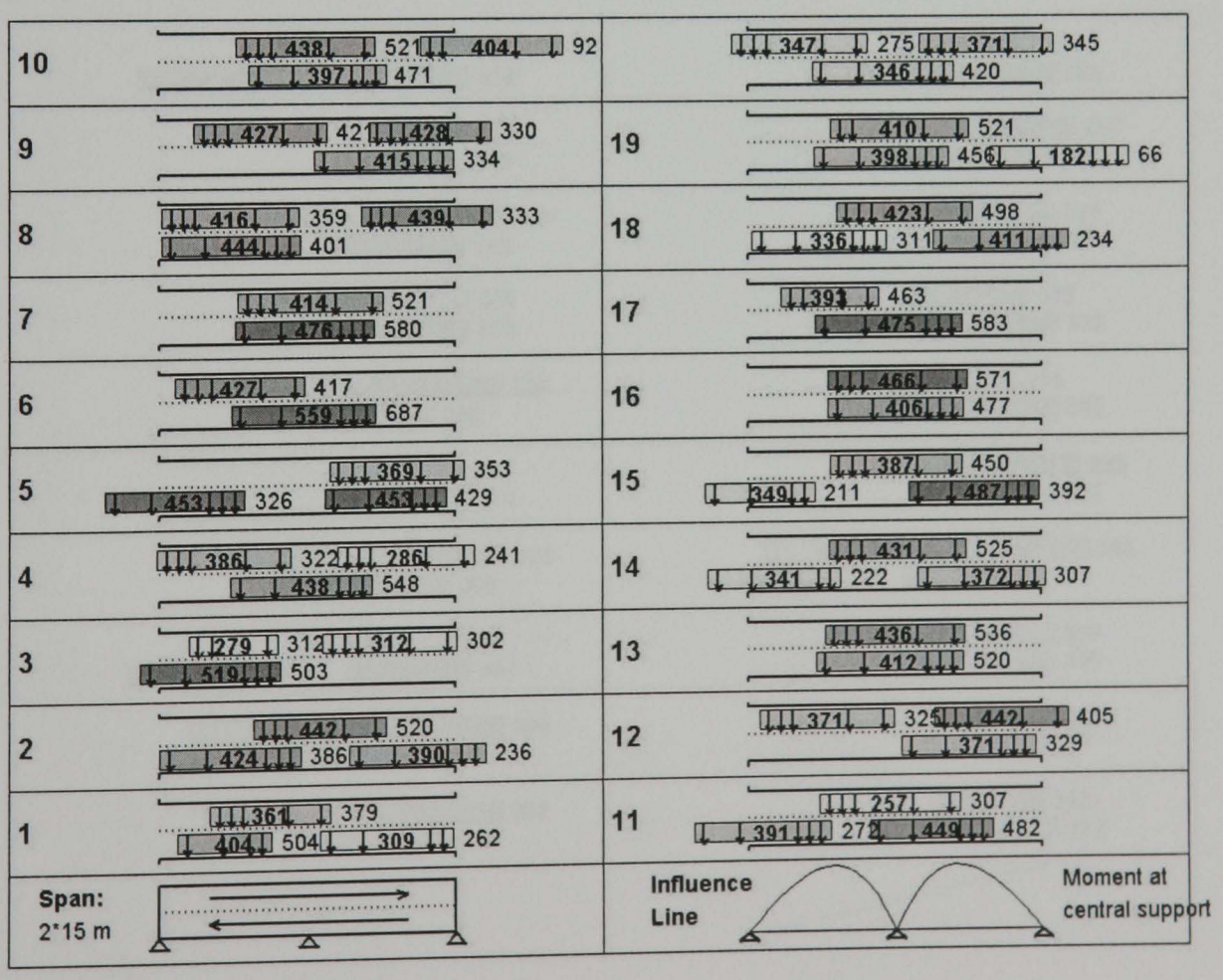
10
438 521 404 92
397 471
9
427 421 428 330
415 334
8
416 359 439 333
444 401
7
414 521
476 580
6
427 417
559 687
5
369 353
453 326 453 429
4
386 322 286 241
438 548
3
279 312 312 302
519 503
2
442 520
424 386 390 236
1
361 379
404 504 309 262
Span:
2*15 m
347 275 371 345
346 420
19
410 521
398 456 182 66
18
423 498
336 311 411 234
17
393 463
475 583
16
466 571
406 477
15
387 450
349 211 487 392
14
431 525
341 222 372 307
13
436 536
412 520
12
371 325 442 405
371 329
11
257 307
391 272 449 482
Influence
Line
Moment at
central support

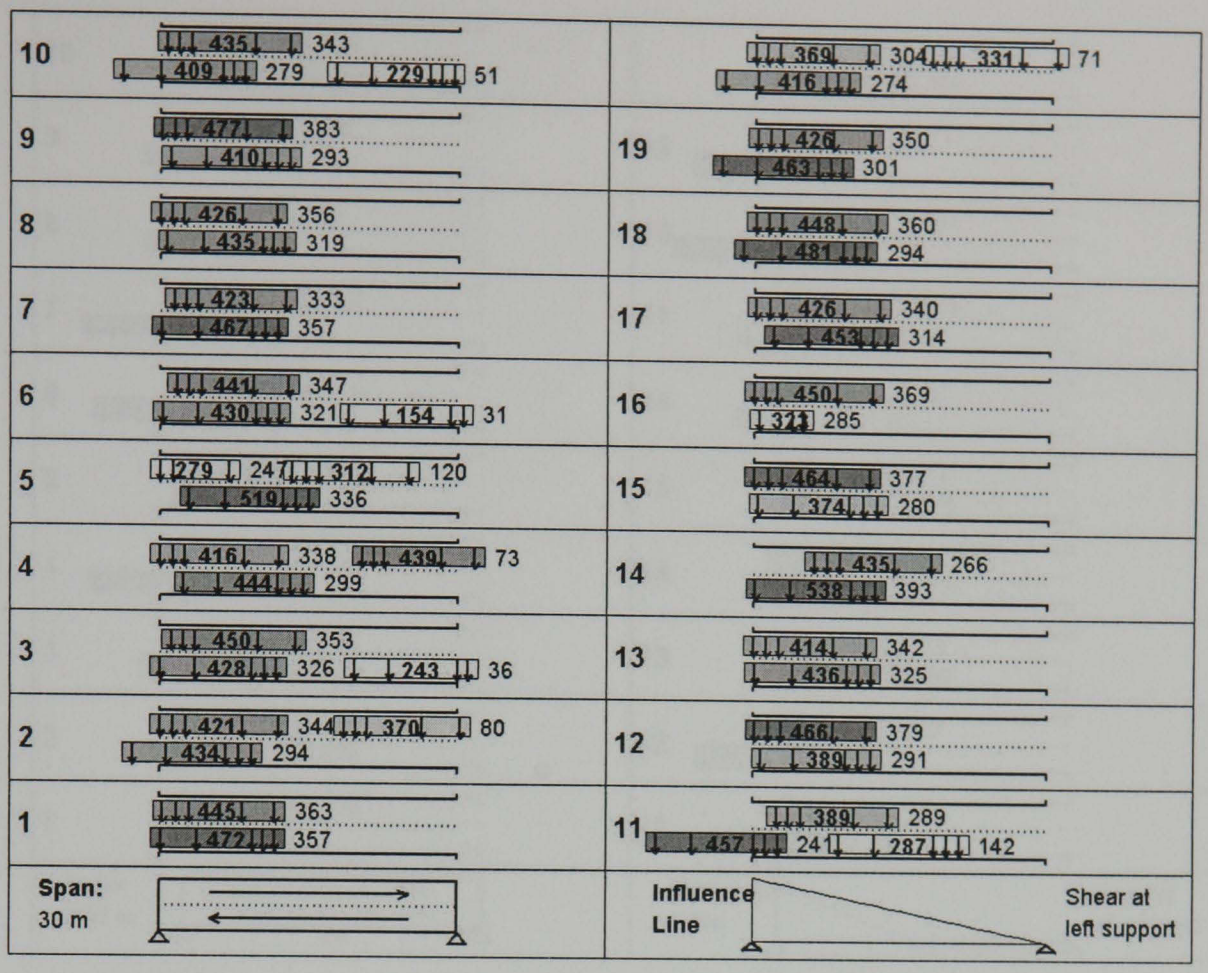
10
435 343
409 279 229 51
9
477 383
410 293
8
426 356
435 319
7
423 333
467 357
6
441 347
430 321 154 31
5
279 247 312 120
519 336
4
416 338 439 73
444 299
3
450 353
428 326 243 36
2
421 344 370 80
434 294
1
445 363
472 357
Span:
30 m
19
369 304 331 71
416 274
426 350
463 301
18
448 360
481 294
17
426 340
453 314
16
450 369
321 285
15
464 377
374 280
14
435 266
538 393
13
414 342
436 325
12
466 379
389 291
11
389 289
457 241 287 142
Influence
Line
Shear at
left support

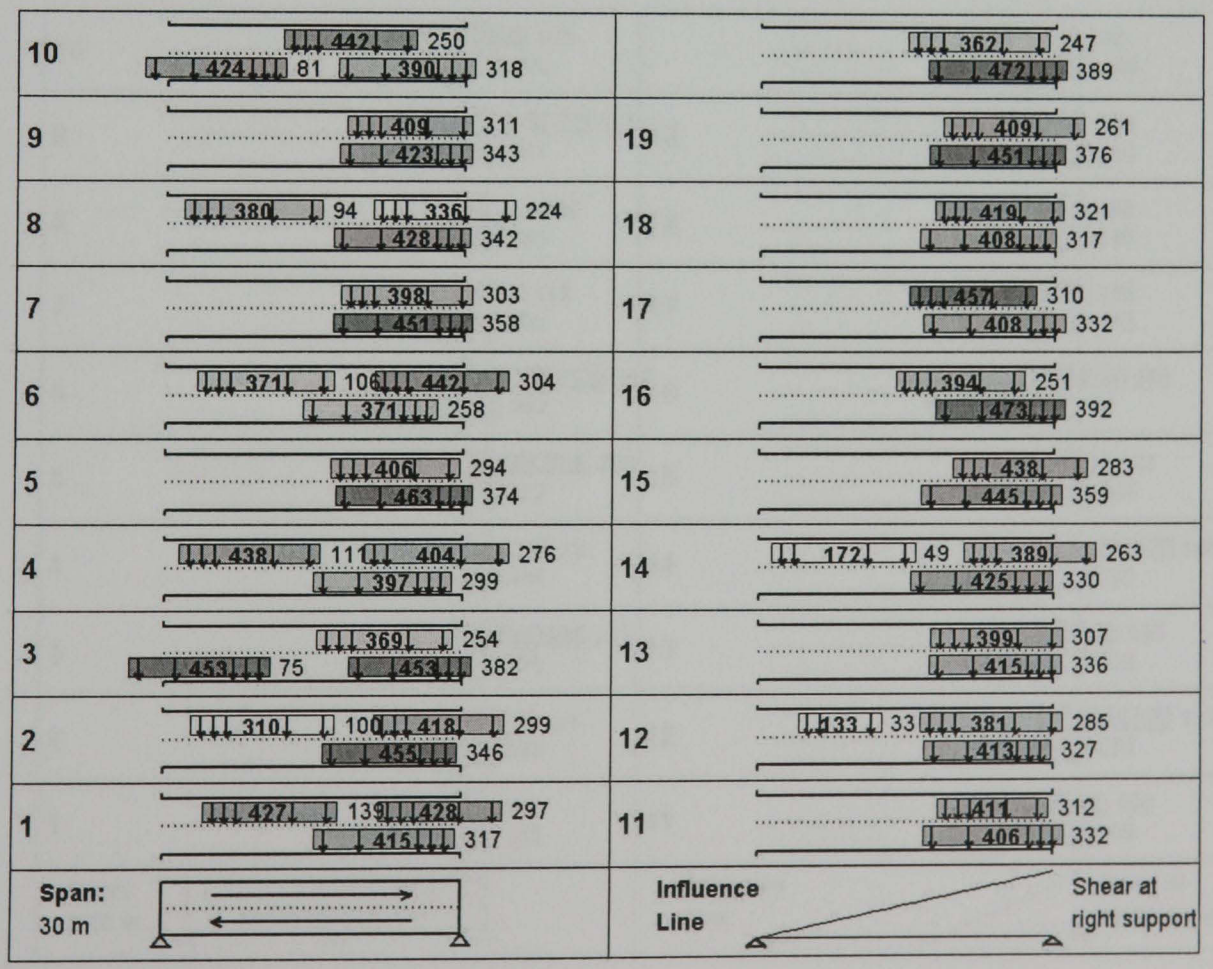
10
442 250
424 81 390 318
9
409 311
423 343
8
380 94 336 224
428 342
7
398 303
451 358
6
371 106 442 304
371 258
5
406 294
463 374
4
438 11 404 276
397 299
3
369 254
453 75 453 382
2
310 100 418 299
455 346
1
427 139 428 297
415 317
Span:
30 m
19
362 247
472 389
409 261
451 376
18
419 321
408 317
17
457 310
408 332
16
394 251
473 392
15
438 283
445 359
14
172 49 389 263
425 330
13
399 307
415 336
12
133 33 381 285
413 327
11
411 312
406 332
Influence
Line
Shear at
right support

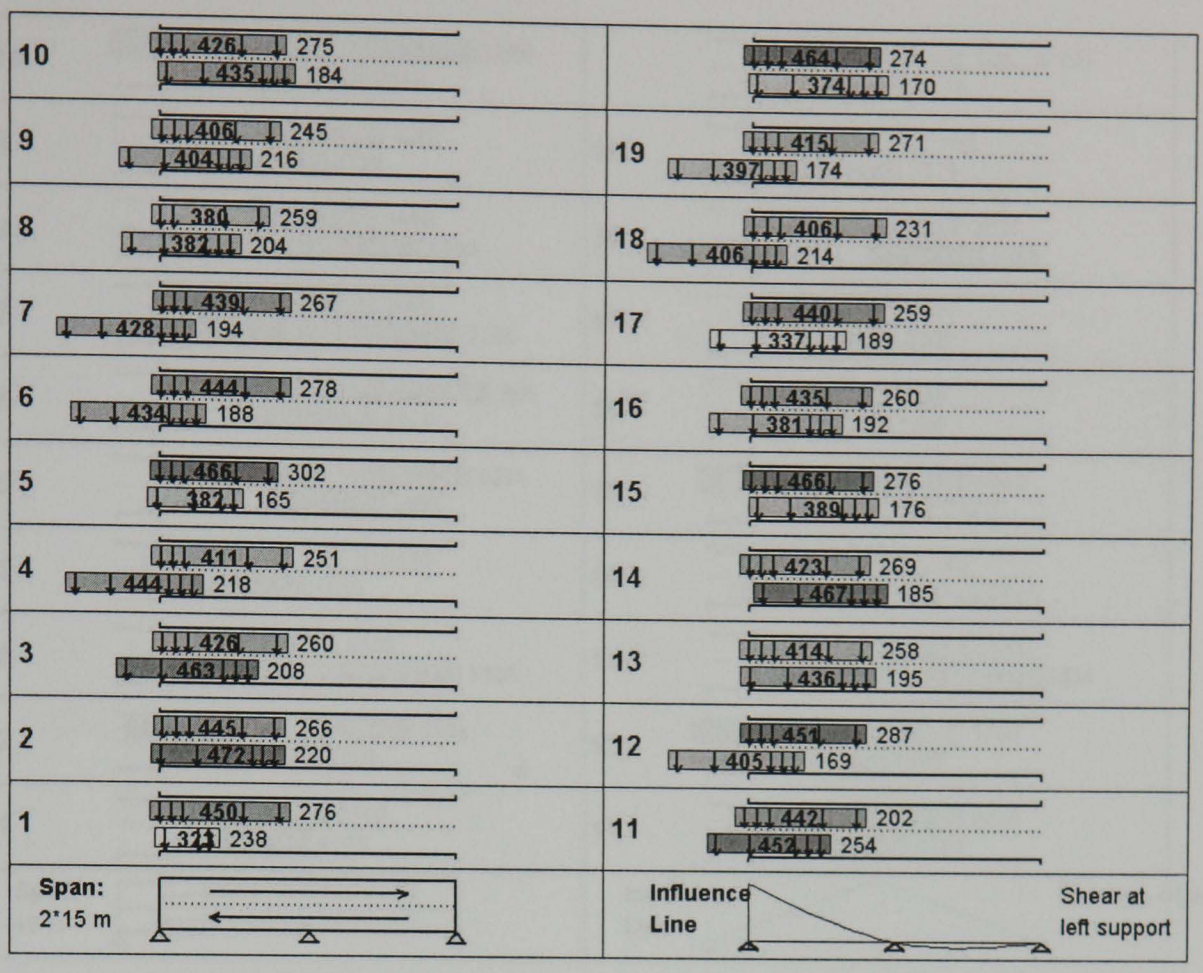
10
426 275
435 184
9
406 245
404 216
8
380 259
382 204
7
439 267
428 194
6
444 278
434 188
5
466 302
382 165
4
411 251
444 218
3
426 260
463 208
2
445 266
472 220
1
450 276
321 238
Span:
2*15 m
19
464 274
374 170
19
415 271
397 174
18
406 231
406 214
17
440 259
337 189
16
435 260
381 192
15
466 276
389 176
14
423 269
467 185
13
414 258
436 195
12
451 287
405 169
11
442 202
452 254
Influence
Line
Shear at
left support

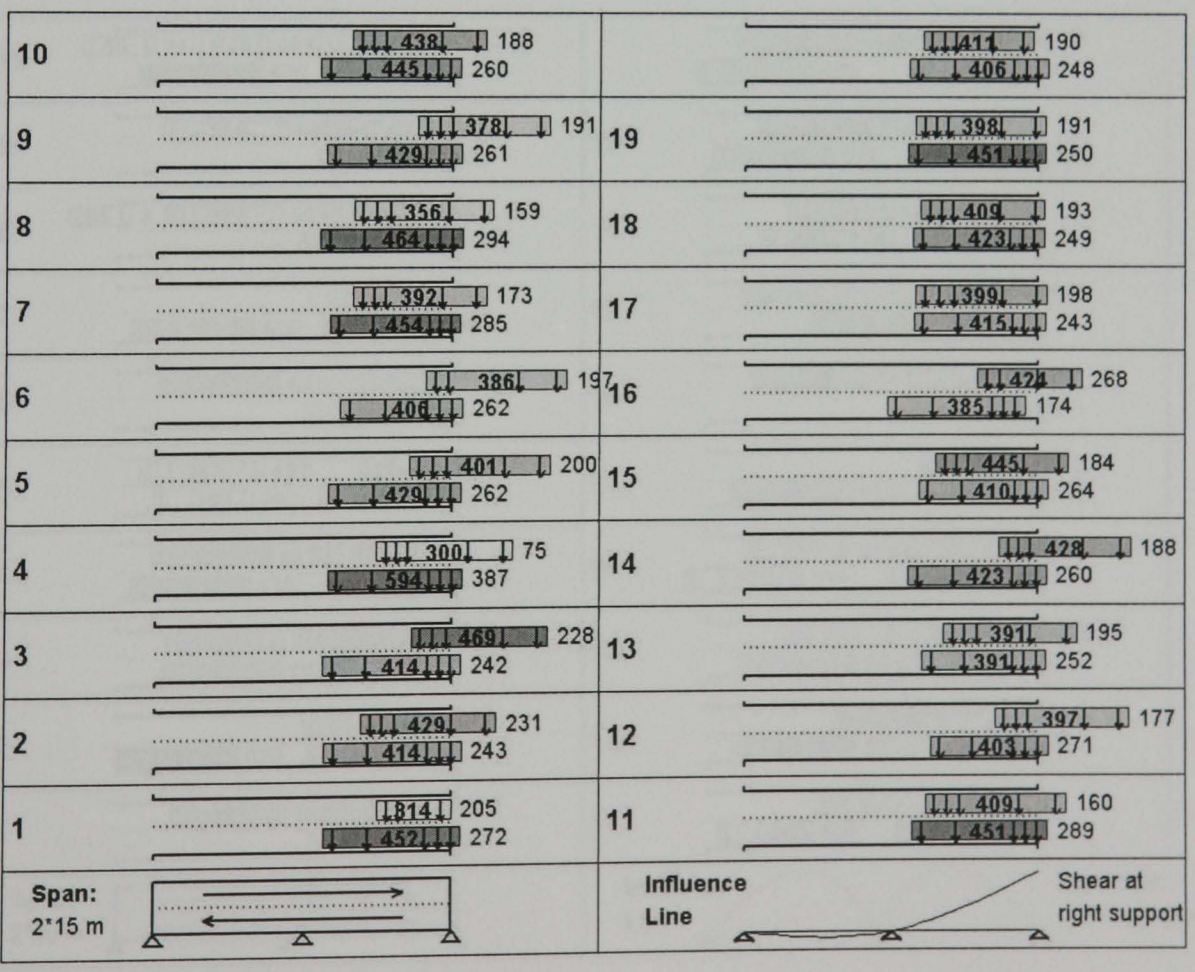
10
438 188
445 260
9
378 191
429 261
8
356 159
464 294
7
392 173
454 285
6
386 197
406 262
5
401 200
429 262
4
300 75
594 387
3
469 228
414 242
2
429 231
414 243
1
414 205
452 272
Span:
2*15 m
19
411 190
406 248
19
398 191
451 250
18
409 193
423 249
17
399 198
415 243
16
424 268
385 174
15
445 184
410 264
14
428 188
423 260
13
391 195
391 252
12
397 177
403 271
11
409 160
451 289
Influence
Line
Shear at
right support

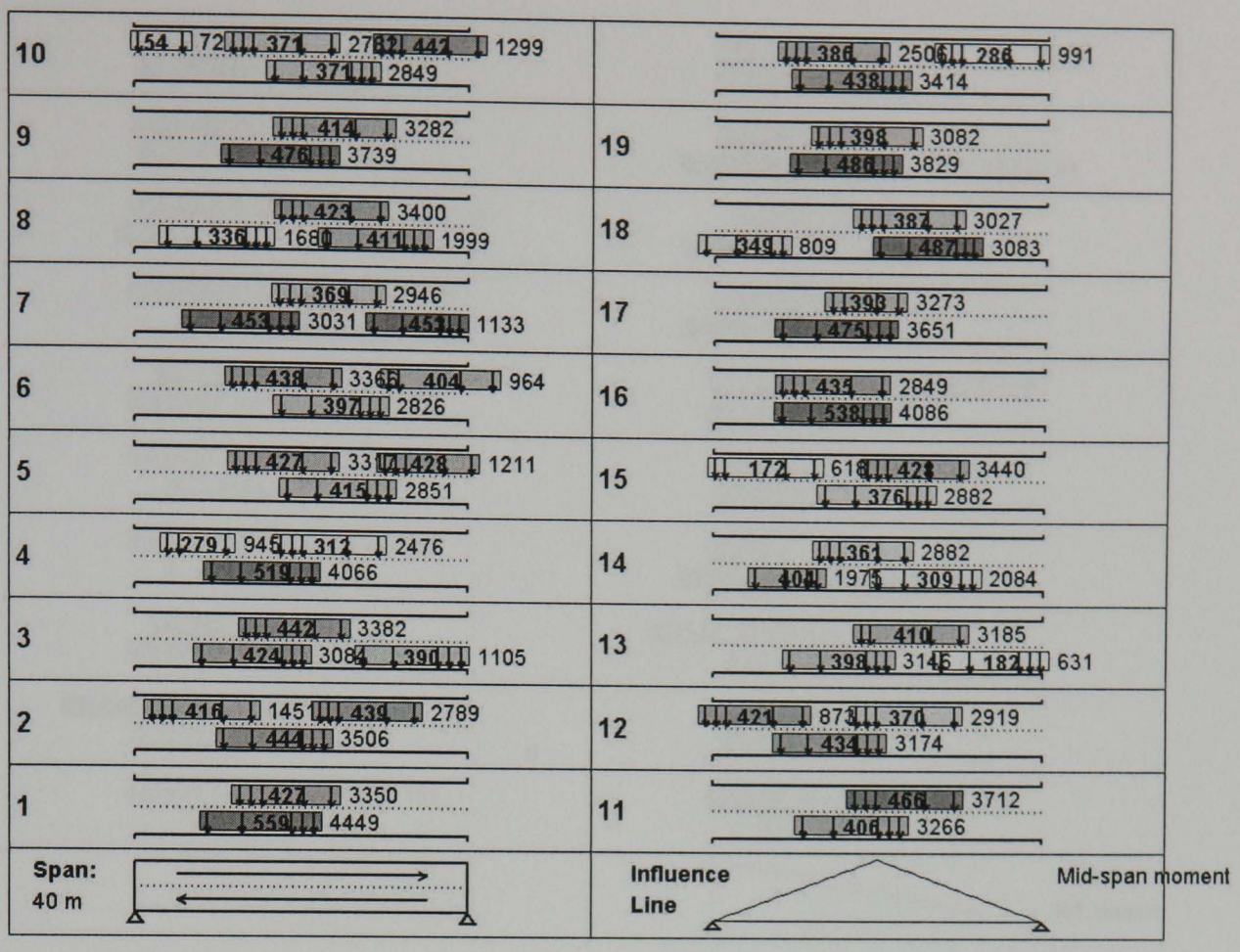
10
54 72 371 2782 447 1299
371 2849
9
414 3282
476 3739
8
423 3400
336 1680 411 1999
7
369 2946
453 3031 453 1133
6
438 3365 404 964
397 2826
5
427 3312 428 1211
415 2851
4
279 945 312 2476
519 4066
3
442 3382
424 3084 390 1105
2
416 1451 439 2789
444 3506
1
427 3350
559 4449
Span:
40 m
19
398 3082
486 3829
18
387 3027
349 809 487 3083
17
398 3273
475 3651
16
435 2849
538 4086
15
172 618 428 3440
376 2882
14
361 2882
404 1975 309 2084
13
410 3185
398 3145 182 631
12
421 873 370 2919
434 3174
11
466 3712
406 3266
Influence
Line
Mid-span moment

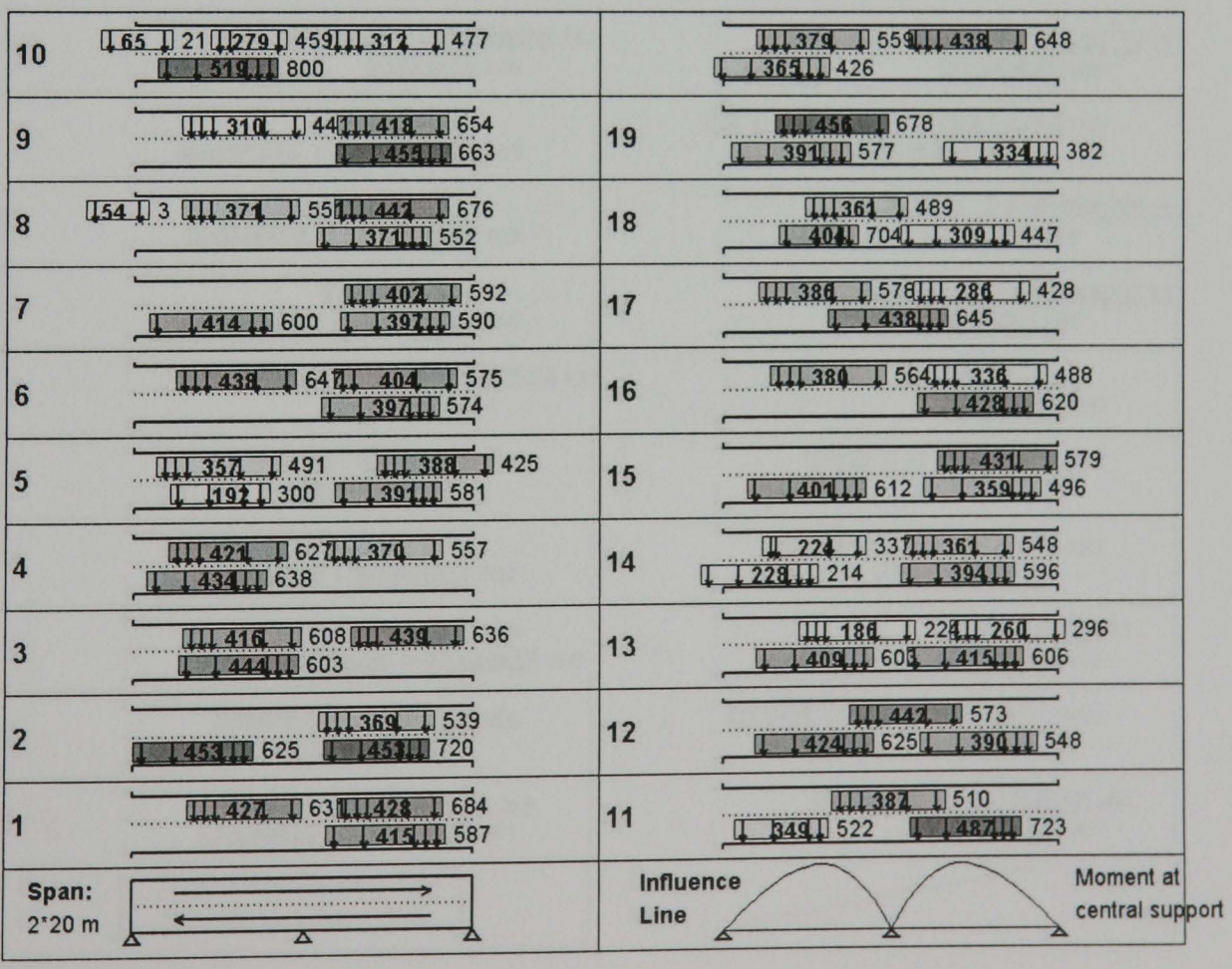
10
65 21 279 459 312 477
519 800
9
310 441 418 654
459 663
8
154 3 371 551 442 676
371 552
7
402 592
414 600 397 590
6
438 647 404 575
397 574
5
357 491 388 425
192 300 391 581
4
421 627 370 557
434 638
3
416 608 439 636
444 603
2
369 539
453 625 453 720
1
427 634 428 684
415 587
Span:
2*20 m
19
456 678
391 577 334 382
18
361 489
404 704 309 447
17
386 578 286 428
438 645
16
380 564 336 488
428 620
15
431 579
401 612 359 496
14
224 337 361 548
228 214 394 596
13
186 224 260 296
409 606 415 606
12
442 573
424 625 390 548
11
387 510
349 522 487 723
Influence
Line
Moment at
central support

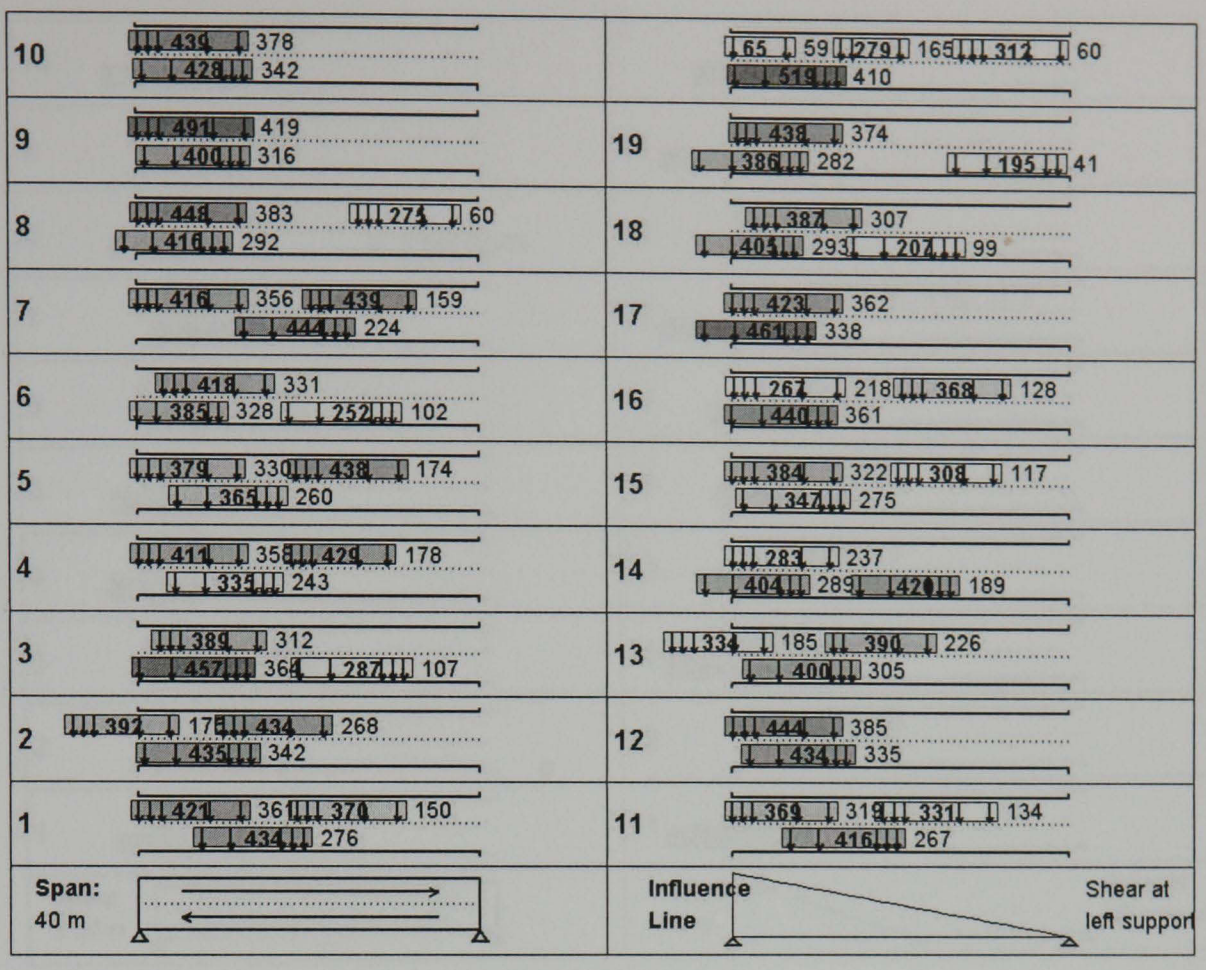
10
439 378
428 342
9
491 419
400 316
8
448 383
275 60
416 292
7
416 356
439 159
444 224
6
418 331
385 328
252 102
5
379 330
438 174
365 260
4
411 358
429 178
335 243
3
389 312
457 368
287 107
2
392 175
434 268
435 342
1
421 361
370 150
434 276
Span:
40 m
65 59
279 165
312 60
519 410
19
438 374
386 282
195 41
18
387 307
405 293
207 99
17
423 362
461 338
16
267 218
368 128
440 361
15
384 322
308 117
347 275
14
283 237
404 289
420 189
13
334 185
390 226
400 305
12
444 385
434 335
11
369 319
331 134
416 267
Influence
Line
Shear at
left support

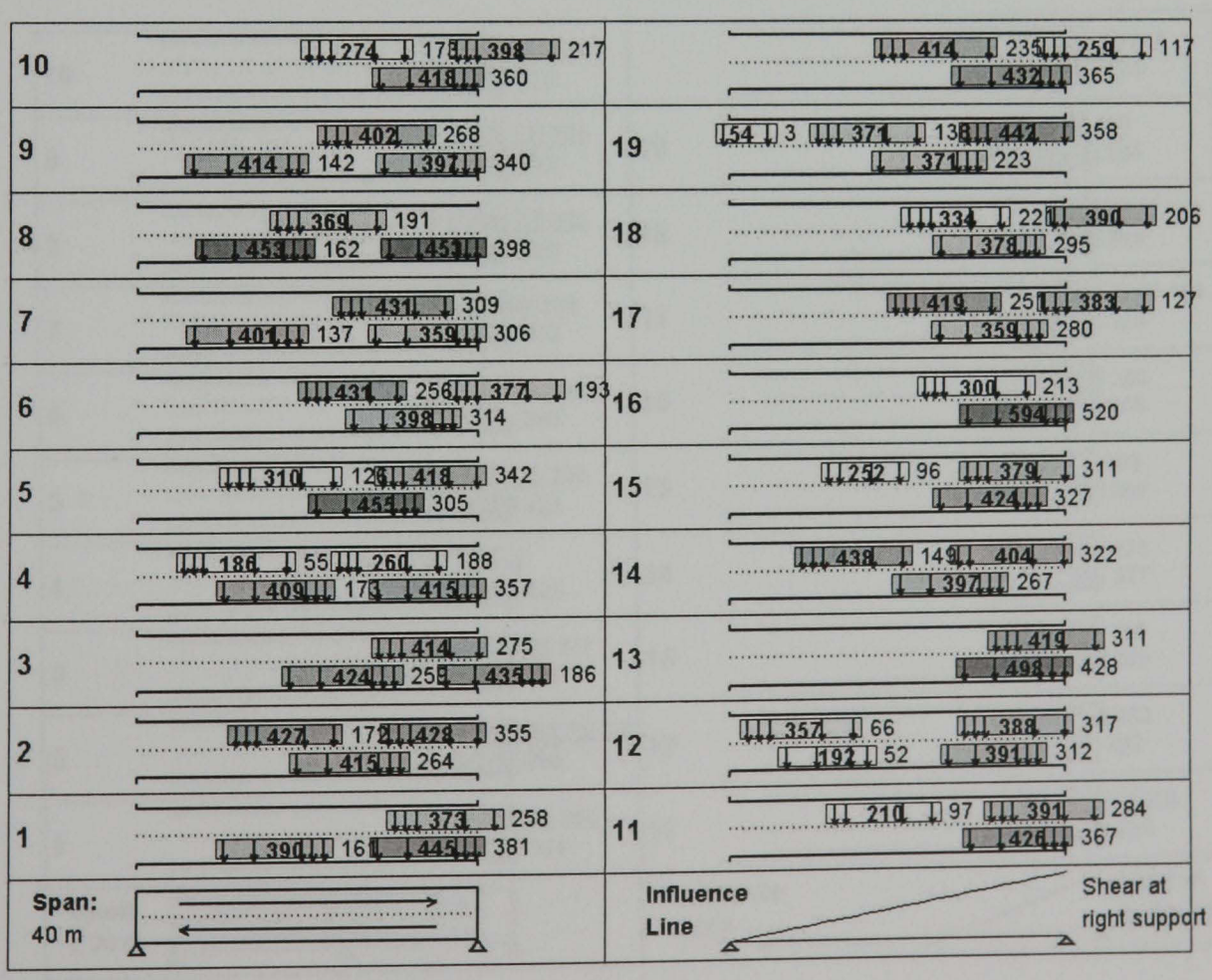
10
274 175
398 217
418 360
9
402 268
414 142
397 340
8
369 191
453 162
451 398
7
431 309
401 137
359 306
6
431 256
377 193
398 314
5
310 126
418 342
454 305
4
186 55
260 188
409 173
415 357
3
414 275
424 259
435 186
2
427 172
428 355
415 264
1
373 258
390 16
445 381
Span:
40 m
414 235
259 117
432 365
19
54 3
371 138
442 358
371 223
18
334 221
390 206
378 295
17
419 25
383 127
359 280
16
300 213
594 520
15
252 96
379 311
424 327
14
438 149
404 322
397 267
13
419 311
498 428
12
357 66
388 317
192 52
391 312
11
210 97
391 284
426 367
Influence
Line
Shear at
right support

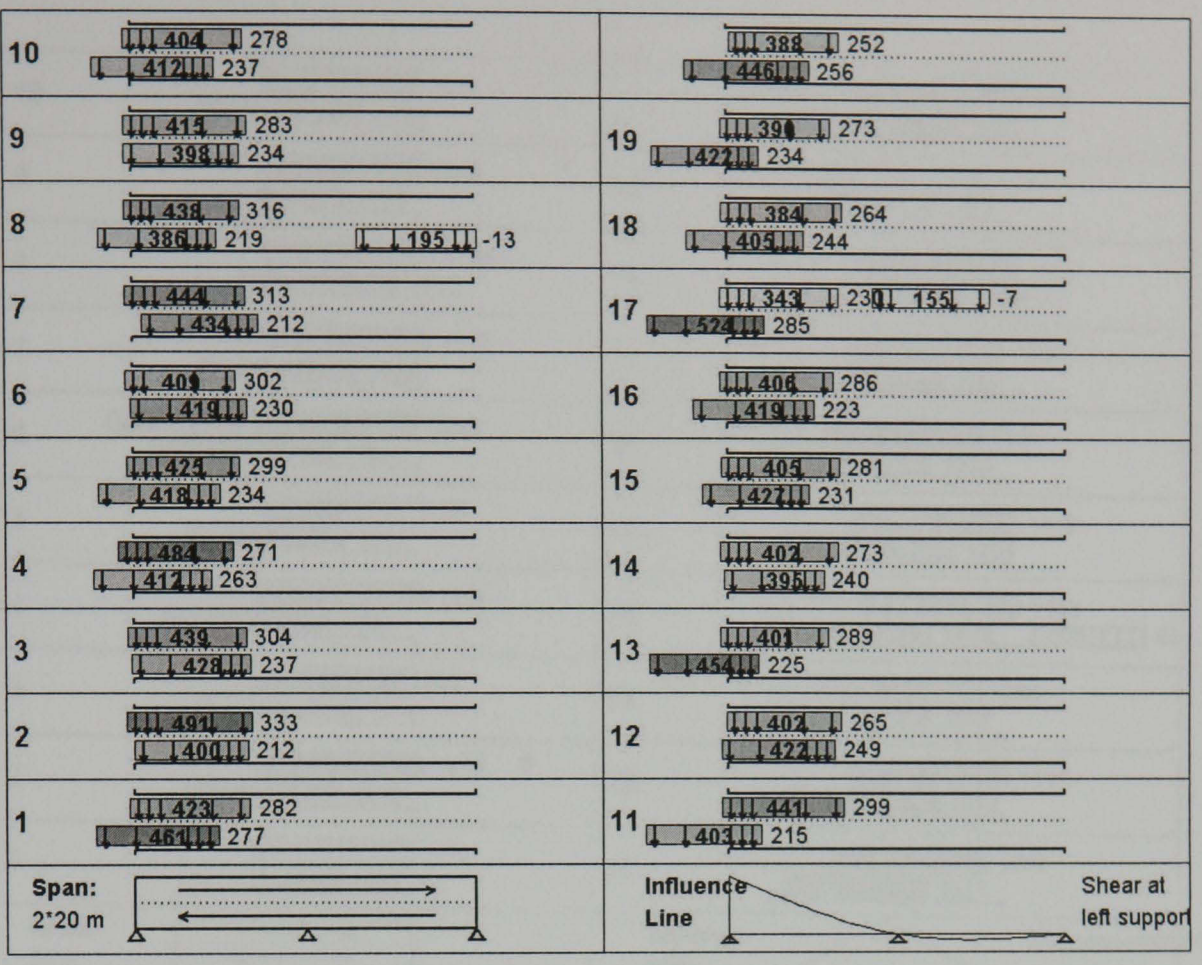
10
404 278
412 237
388 252
446 256
9
415 283
398 234
19
390 273
422 234
8
438 316
386 219
195 -13
18
384 264
405 244
7
444 313
434 212
17
343 230
155 -7
524 285
6
401 302
419 230
16
406 286
419 223
5
425 299
418 234
15
405 281
427 231
4
484 271
412 263
14
402 273
395 240
3
439 304
428 237
13
401 289
454 225
2
491 333
400 212
12
402 265
422 249
1
423 282
461 277
11
441 299
403 215
Span:
2*20 m
Influence
Line
Shear at
left support

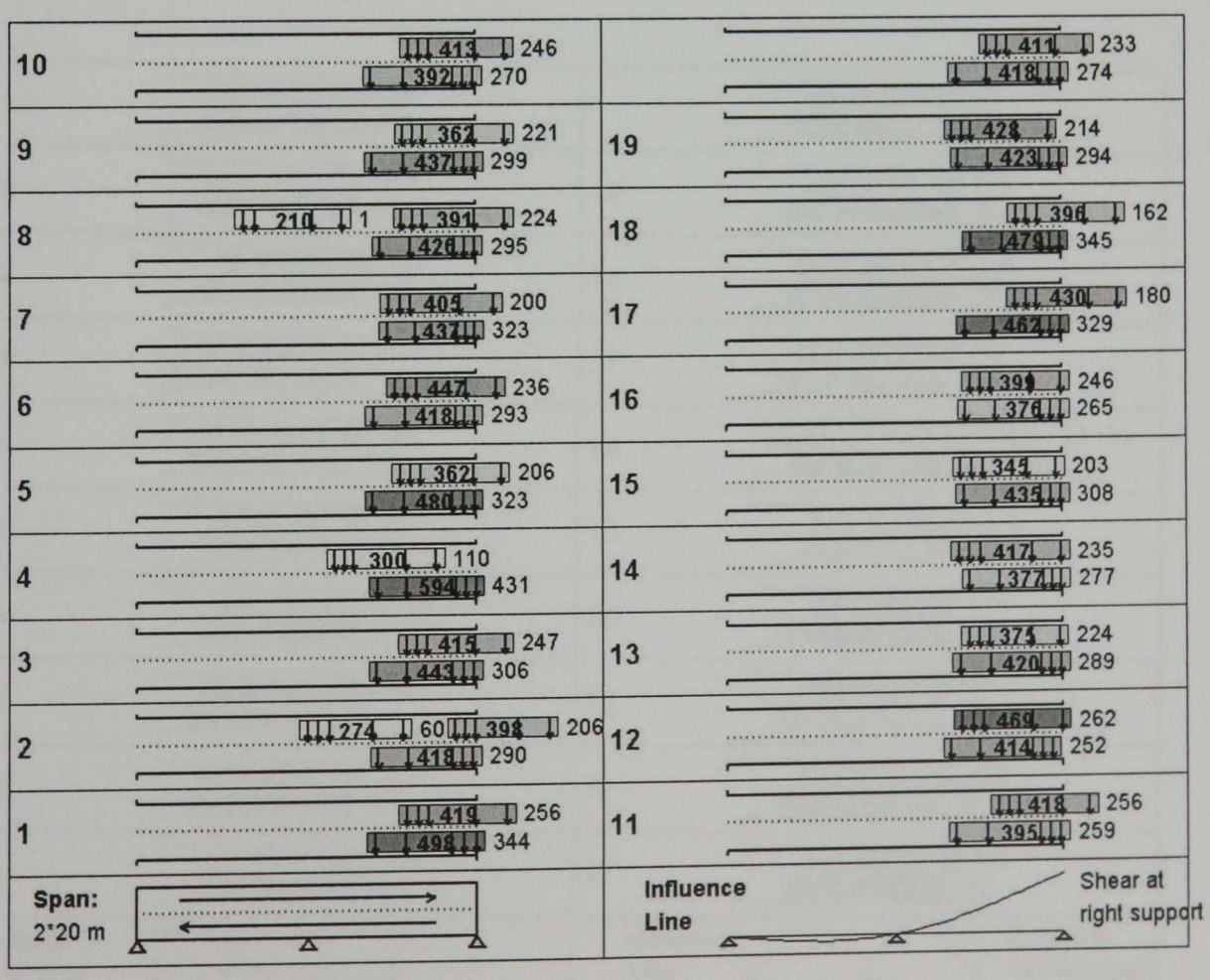
10
413 246
392 270
411 233
418 274
9
362 221
437 299
19
428 214
423 294
8
210 1
391 224
426 295
18
396 162
479 345
7
405 200
437 323
17
430 180
462 329
6
447 236
418 293
16
391 246
376 265
5
362 206
480 323
15
345 203
435 308
4
300 110
594 431
14
417 235
377 277
3
415 247
443 306
13
375 224
420 289
2
274 60
398 206
418 290
12
469 262
414 252
1
419 256
498 344
11
418 256
395 259
Span:
2*20 m
Influence
Line
Shear at
right support

Traffic type 'QcWb' –Set0

10	453 1420 415 1253		384 1200 473 1438
9	415 1249 444 1432	19	414 1133 484 1506
8	425 1296 478 1395	18	473 1496 393 1148
7	370 1117 523 1590	17	412 1366 426 1283
6	98 23 429 1349 464 1351	16	432 1321 434 1333
5	420 1408 434 1331	15	439 1366 435 1293
4	382 1120 527 1709	14	383 1143 461 1472 320 44
3	442 1523 435 1308	13	367 1064 495 1597
2	473 1418 452 1475	12	397 1191 462 1472
1	429 1372 393 1588	11	424 1298 406 1371
Span: 20 m	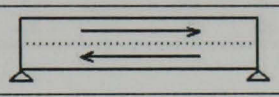	Influence Line	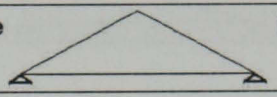 Mid-span moment

10	442 355 435 376		412 344 426 367
9	289 246 559 489	19	378 317 463 395
8	453 383 415 355	18	390 339 434 376
7	429 353 464 386	17	442 382 386 333
6	468 400 403 343	16	251 139 358 138 522 440
5	415 361 444 384	15	439 365 435 353
4	370 302 523 443	14	384 314 473 404
3	444 385 425 365	13	420 347 434 375
2	382 325 527 460	12	383 328 461 397
1	473 404 452 382	11	397 336 462 389
Span: 2*10 m	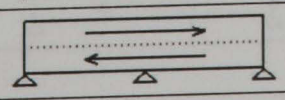	Influence Line	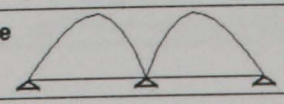 Moment at central support

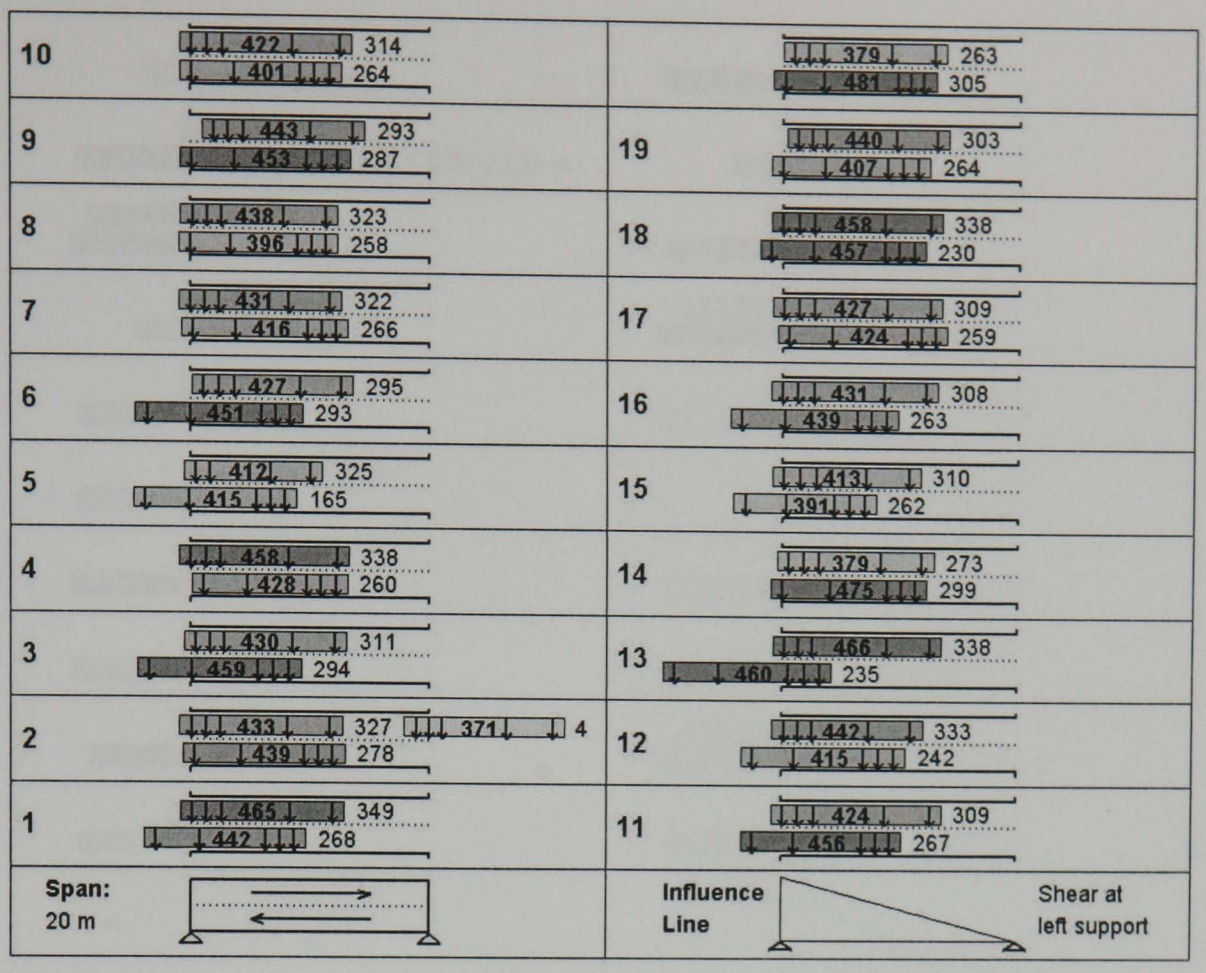
10
422 314
401 264
9
443 293
453 287
8
438 323
396 258
7
431 322
416 266
6
427 295
451 293
5
412 325
415 165
4
458 338
428 260
3
430 311
459 294
2
433 327
371 4
439 278
1
465 349
442 268
Span:
20 m
19
379 263
481 305
19
440 303
407 264
18
458 338
457 230
17
427 309
424 259
16
431 308
439 263
15
413 310
391 262
14
379 273
475 299
13
466 338
460 235
12
442 333
415 242
11
424 309
456 267
Influence
Line
Shear at
left support

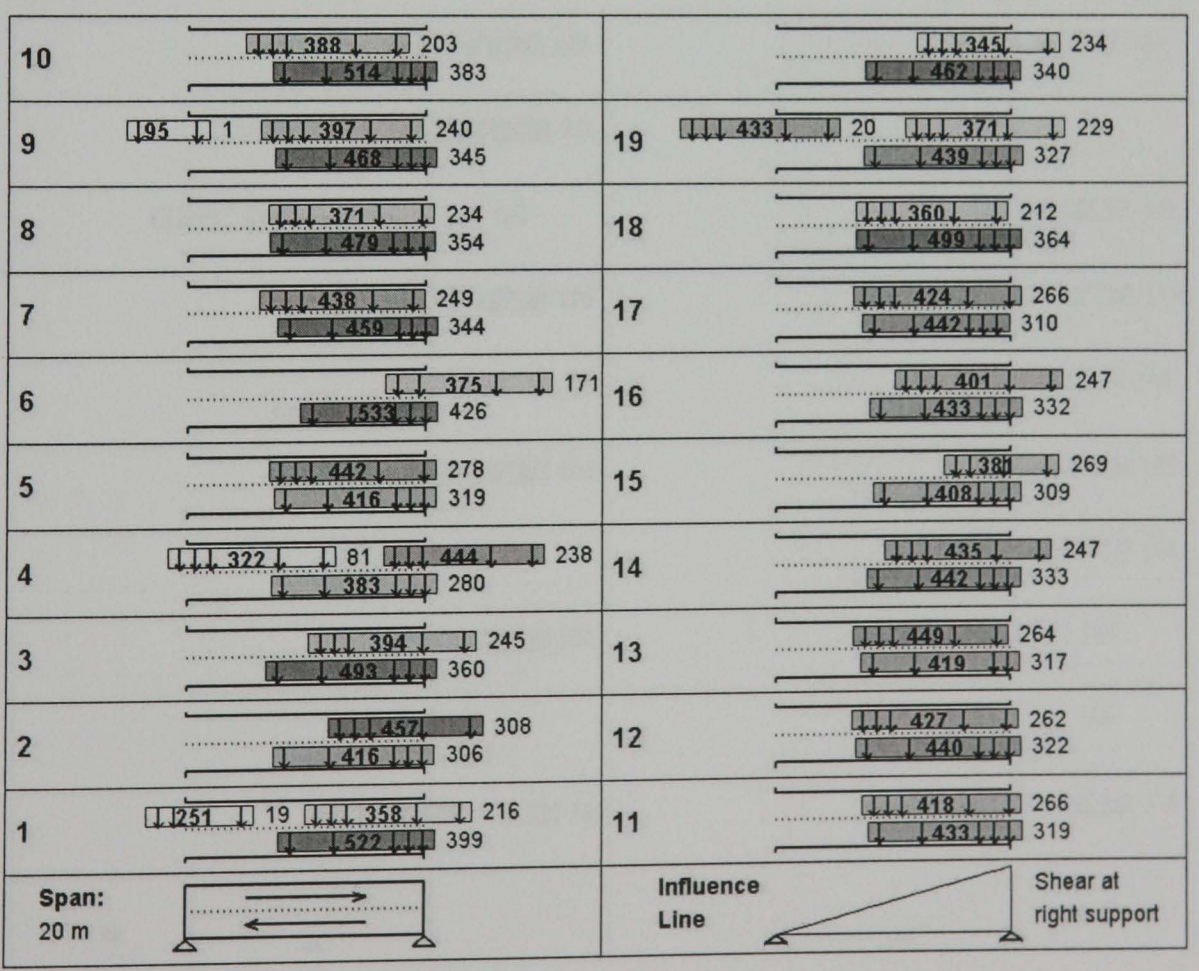
10
388 203
514 383
9
95 1
397 240
468 345
8
371 234
479 354
7
438 249
459 344
6
375 171
533 426
5
442 278
416 319
4
322 81
444 238
383 280
3
394 245
493 360
2
457 308
416 306
1
251 19
358 216
522 399
Span:
20 m
19
345 234
462 340
19
433 20
371 229
439 327
18
360 212
499 364
17
424 266
442 310
16
401 247
433 332
15
380 269
408 309
14
435 247
442 333
13
449 264
419 317
12
427 262
440 322
11
418 266
433 319
Influence
Line
Shear at
right support

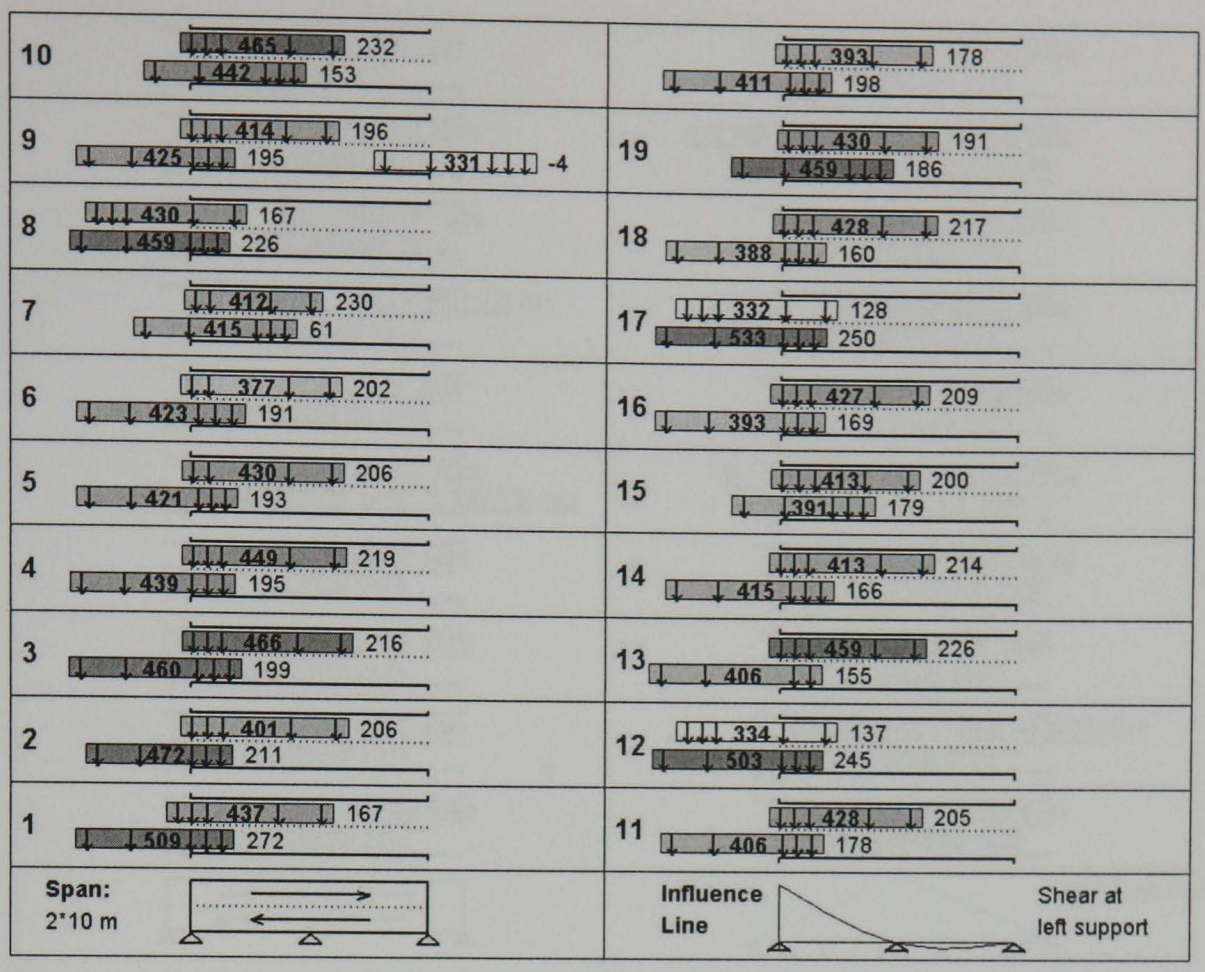
10
465 232
442 153
9
414 196
425 195
331 -4
8
430 167
459 226
7
412 230
415 61
6
377 202
423 191
5
430 206
421 193
4
449 219
439 195
3
466 216
460 199
2
401 206
472 211
1
437 167
509 272
Span:
2*10 m
19
393 178
411 198
19
430 191
459 186
18
428 217
388 160
17
332 128
533 250
16
427 209
393 169
15
413 200
391 179
14
413 214
415 166
13
459 226
406 155
12
334 137
503 245
11
428 205
406 178
Influence
Line
Shear at
left support

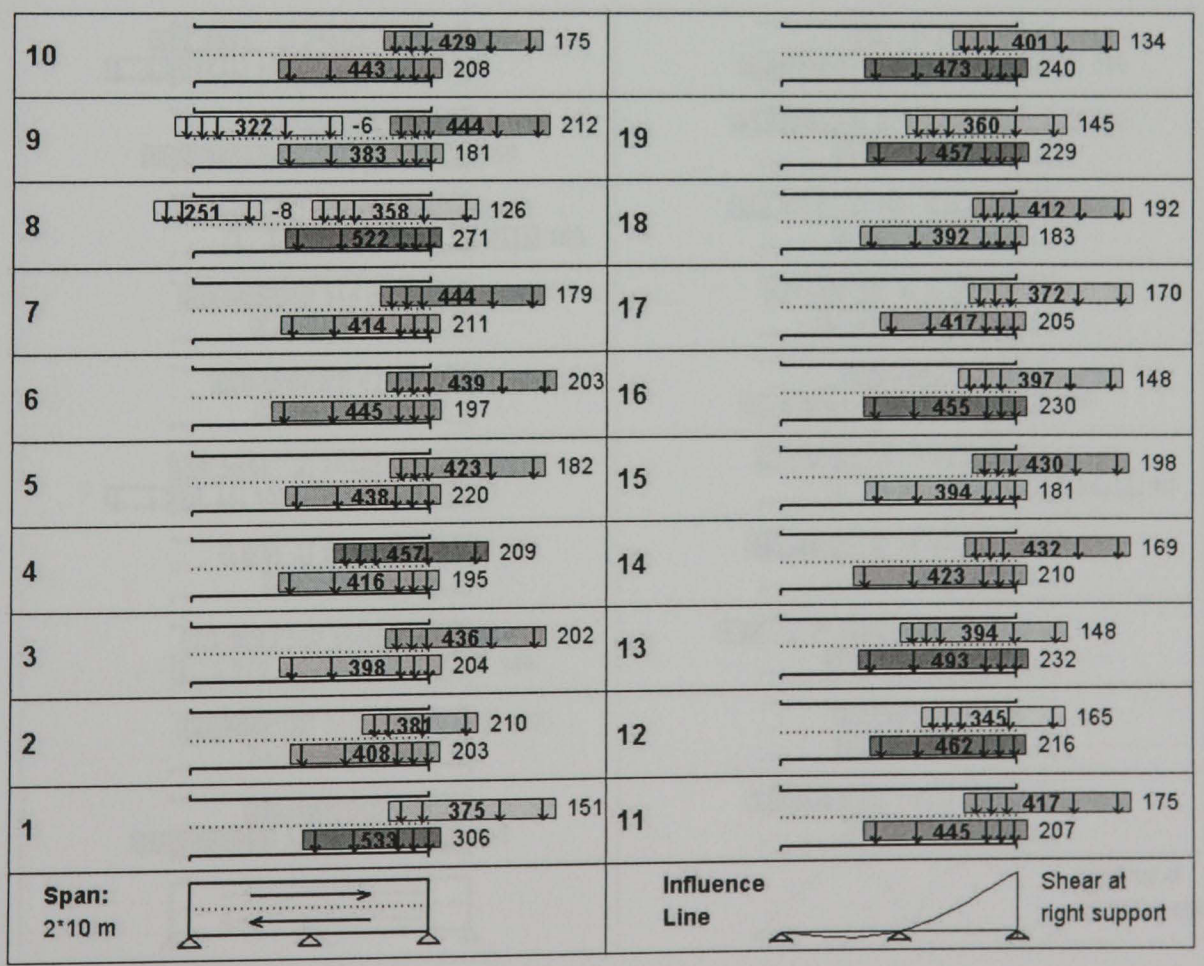
10
429 175
443 208
9
322 -6 444 212
383 181
8
251 -8 358 126
522 271
7
444 179
414 211
6
439 203
445 197
5
423 182
438 220
4
457 209
416 195
3
436 202
398 204
2
381 210
408 203
1
375 151
533 306
Span:
2*10 m
19
401 134
473 240
19
360 145
457 229
18
412 192
392 183
17
372 170
417 205
16
397 148
455 230
15
430 198
394 181
14
432 169
423 210
13
394 148
493 232
12
345 165
462 216
11
417 175
445 207
Influence
Line
Shear at
right support

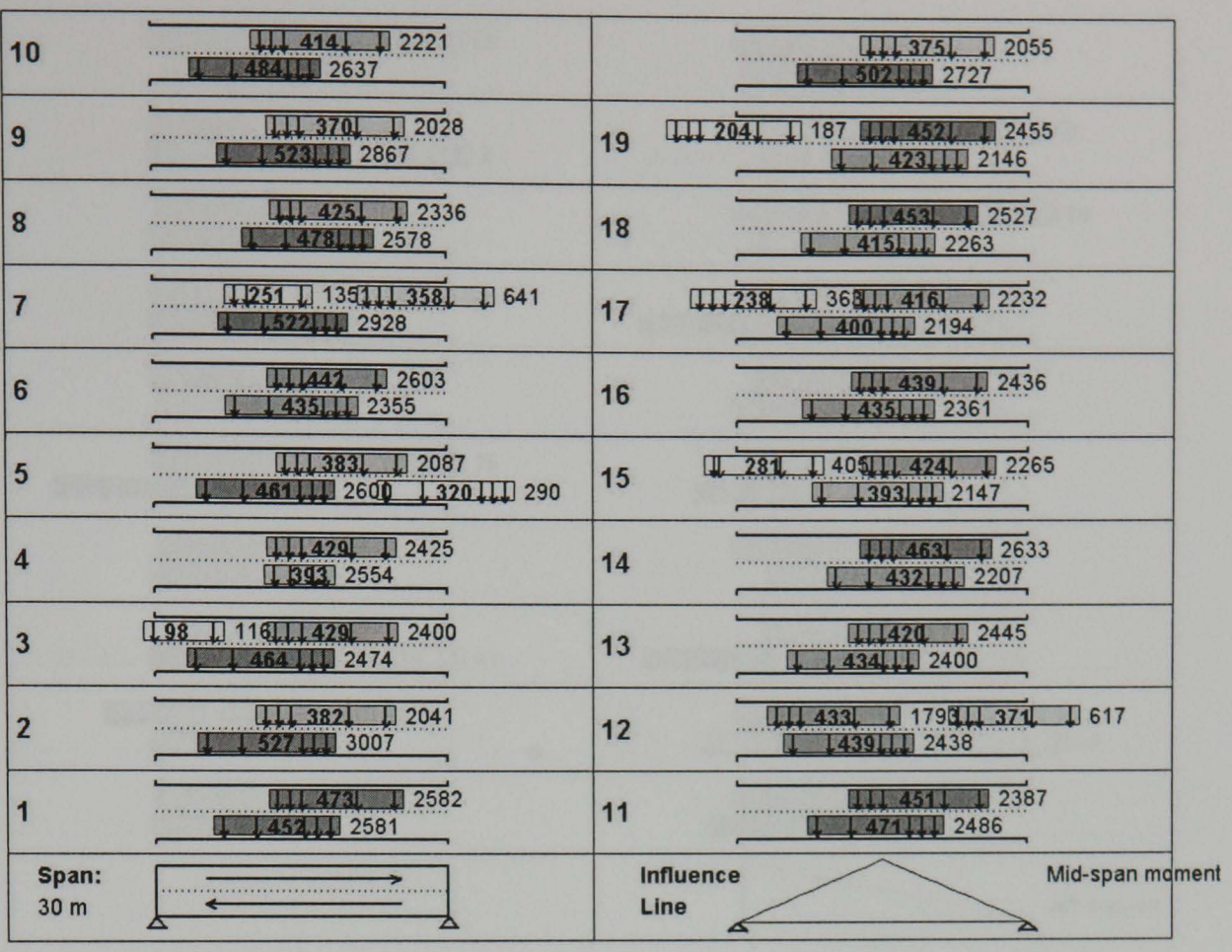
10
414 2221
484 2637
9
370 2028
523 2867
8
425 2336
478 2578
7
251 135 358 641
522 2928
6
442 2603
435 2355
5
383 2087
461 2600 320 290
4
429 2425
393 2554
3
98 116 429 2400
464 2474
2
382 2041
527 3007
1
473 2582
452 2581
Span:
30 m
19
375 2055
502 2727
204 187 452 2455
423 2146
18
453 2527
415 2263
17
238 368 416 2232
400 2194
16
439 2436
435 2361
15
281 405 424 2265
393 2147
14
463 2633
432 2207
13
420 2445
434 2400
12
433 1798 371 617
439 2438
11
451 2387
471 2486
Influence
Line
Mid-span moment

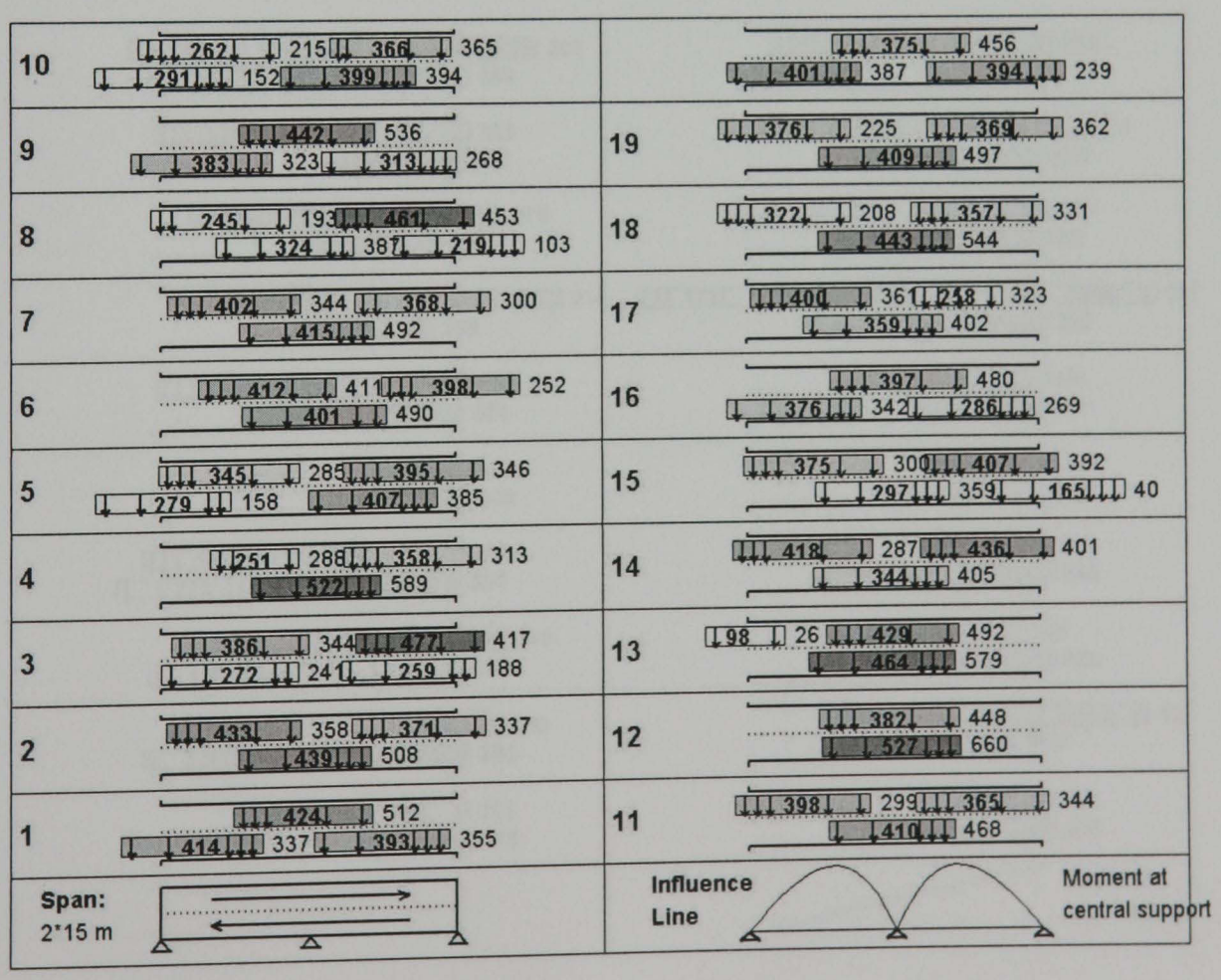
10
262 215 366 365
291 152 399 394
9
442 536
383 323 313 268
8
245 193 461 453
324 387 219 103
7
402 344 368 300
415 492
6
412 411 398 252
401 490
5
345 285 395 346
279 158 407 385
4
251 288 358 313
522 589
3
386 344 477 417
272 241 259 188
2
433 358 371 337
439 508
1
424 512
414 337 393 355
Span:
2*15 m
19
376 225 369 362
409 497
18
322 208 357 331
443 544
17
400 361 258 323
359 402
16
397 480
376 342 286 269
15
375 300 407 392
297 359 165 40
14
418 287 436 401
344 405
13
98 26 429 492
464 579
12
382 448
527 660
11
398 299 365 344
410 468
Influence
Line
Moment at
central support

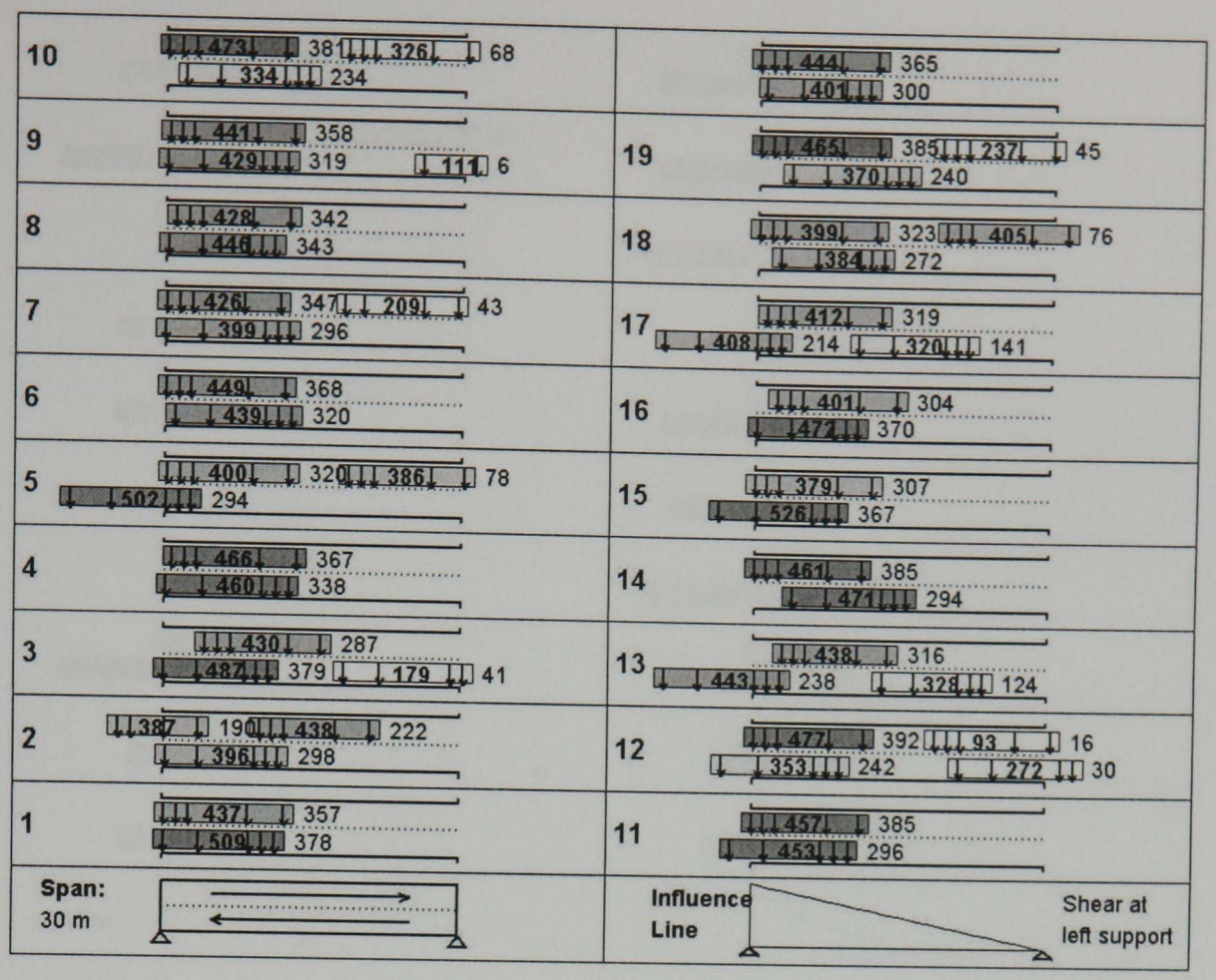
10
473 38 326 68
334 234
9
441 358
429 319 111 6
8
428 342
446 343
7
426 347 209 43
399 296
6
449 368
439 320
5
400 320 386 78
502 294
4
466 367
460 338
3
430 287
487 379 179 41
2
387 190 438 222
396 298
1
437 357
509 378
Span:
30 m
19
444 365
401 300
19
465 385 237 45
370 240
18
399 323 405 76
384 272
17
412 319
408 214 320 141
16
401 304
472 370
15
379 307
526 367
14
461 385
471 294
13
438 316
443 238 328 124
12
477 392 93 16
353 242 272 30
11
457 385
453 296
Influence
Line
Shear at
left support

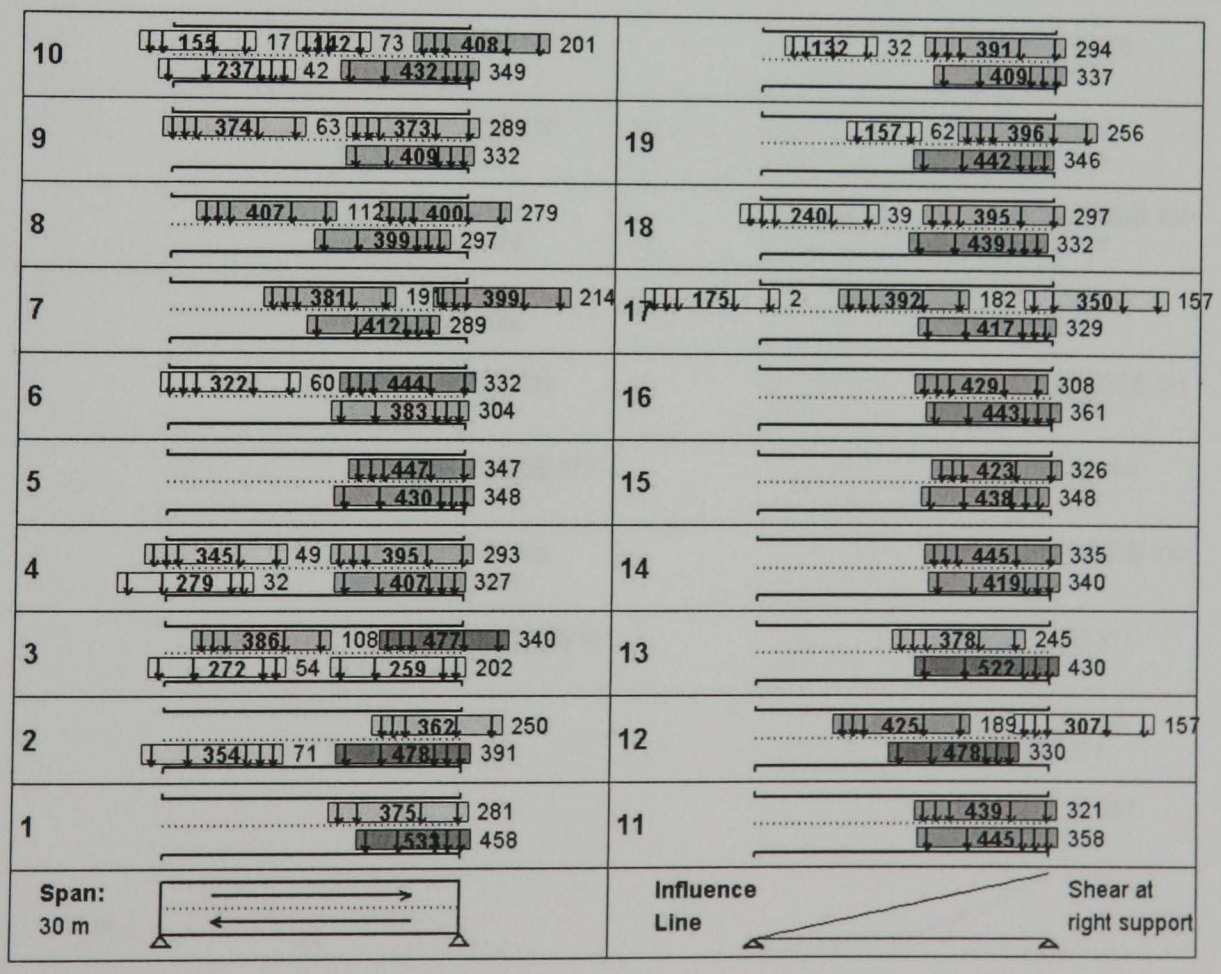
10
155 17 142 73 408 201
237 42 432 349
9
374 63 373 289
409 332
8
407 112 400 279
399 297
7
381 19 399 214
412 289
6
322 60 444 332
383 304
5
447 347
430 348
4
345 49 395 293
279 32 407 327
3
386 108 477 340
272 54 259 202
2
362 250
354 71 478 391
1
375 281
531 458
Span:
30 m
19
132 32 391 294
409 337
19
157 62 396 256
442 346
18
240 39 395 297
439 332
17
175 2 392 182 350 157
417 329
16
429 308
443 361
15
423 326
438 348
14
445 335
419 340
13
378 245
522 430
12
425 189 307 157
478 330
11
439 321
445 358
Influence
Line
Shear at
right support

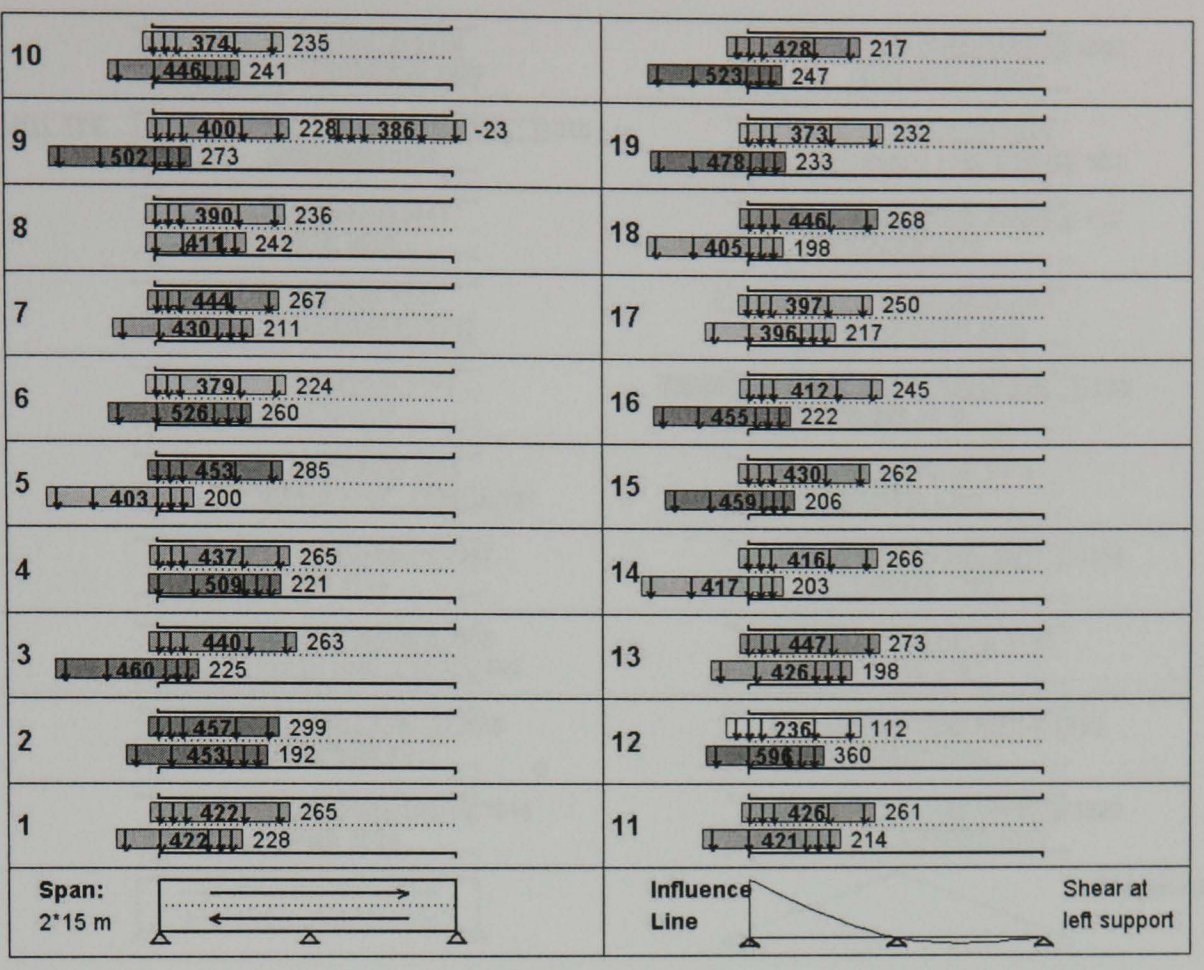
10
374 235
446 241
9
400 228 386 -23
502 273
8
390 236
411 242
7
444 267
430 211
6
379 224
526 260
5
453 285
403 200
4
437 265
509 221
3
440 263
460 225
2
457 299
453 192
1
422 265
422 228
Span:
2*15 m
19
428 217
523 247
19
373 232
478 233
18
446 268
405 198
17
397 250
396 217
16
412 245
455 222
15
430 262
459 206
14
416 266
417 203
13
447 273
426 198
12
236 112
596 360
11
426 261
421 214
Influence
Line
Shear at
left support

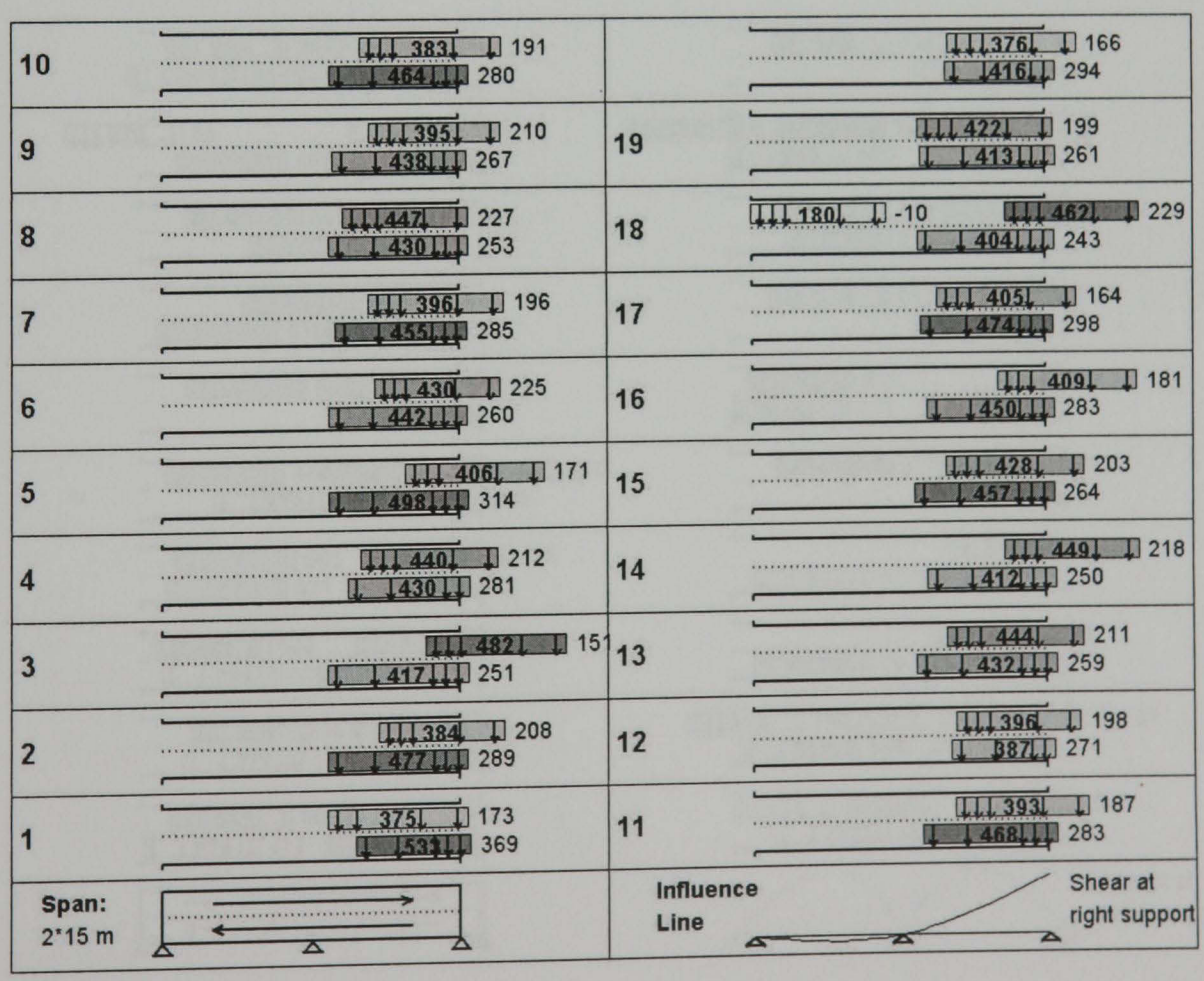
10
383 191
464 280
9
395 210
438 267
8
447 227
430 253
7
396 196
455 285
6
430 225
442 260
5
406 171
498 314
4
440 212
430 281
3
482 151
417 251
2
384 208
477 289
1
375 173
531 369
Span:
2*15 m
19
376 166
416 294
19
422 199
413 261
18
180 -10
462 229
404 243
17
405 164
474 298
16
409 181
450 283
15
428 203
457 264
14
449 218
412 250
13
444 211
432 259
12
396 198
387 271
11
393 187
468 283
Influence
Line
Shear at
right support

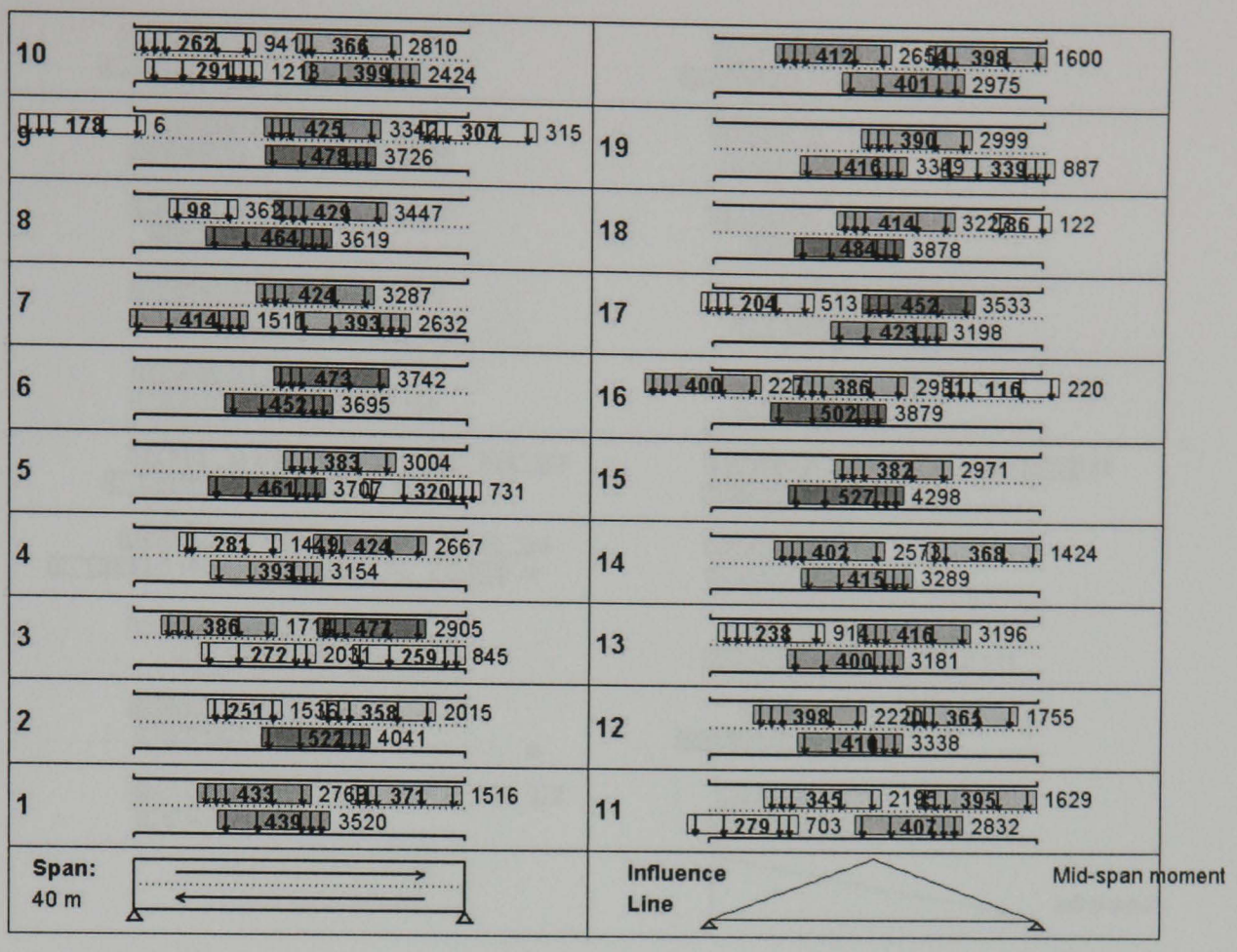
10
262 941 366 2810
291 1218 399 2424
9
178 6 425 3342 307 315
478 3726
8
98 362 429 3447
464 3619
7
424 3287
414 1510 393 2632
6
473 3742
452 3695
5
383 3004
461 3707 320 731
4
281 1449 424 2667
393 3154
3
386 1710 477 2905
272 2031 259 845
2
251 1536 358 2015
522 4041
1
433 2768 371 1516
439 3520
Span:
40 m
19
390 2999
416 3349 339 887
18
414 3228 122
484 3878
17
204 513 452 3533
423 3198
16
400 227 386 2951 116 220
502 3879
15
382 2971
527 4298
14
402 2573 368 1424
415 3289
13
238 914 416 3196
400 3181
12
398 2220 361 1755
410 3338
11
345 2195 395 1629
279 703 407 2832
Influence
Line
Mid-span moment

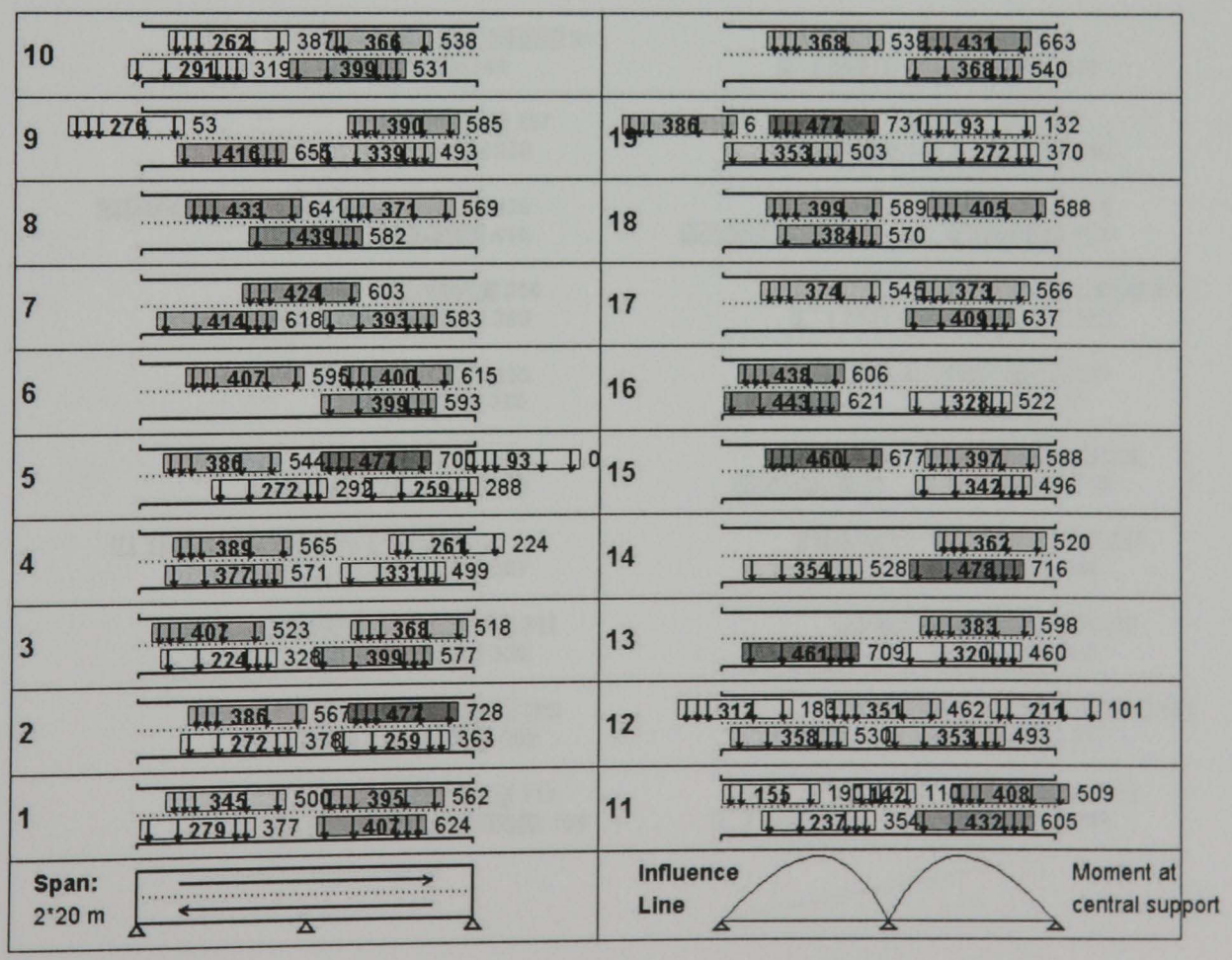
10
262 387 366 538
291 319 399 531
9
276 53 390 585
416 655 339 493
8
433 64 371 569
439 582
7
424 603
414 618 393 583
6
407 595 400 615
399 593
5
386 544 477 70 93 0
272 298 259 288
4
389 565 261 224
377 571 331 499
3
407 523 368 518
224 328 399 577
2
386 567 477 728
272 378 259 363
1
345 500 395 562
279 377 407 624
Span:
2*20 m
19
386 6 477 731 93 132
353 503 272 370
18
399 589 405 588
384 570
17
374 545 373 566
409 637
16
438 606
443 621 328 522
15
460 677 397 588
342 496
14
362 520
354 528 478 716
13
383 598
461 709 320 460
12
312 188 351 462 211 101
358 530 353 493
11
155 190 142 110 408 509
237 354 432 605
Influence
Line
Moment at
central support

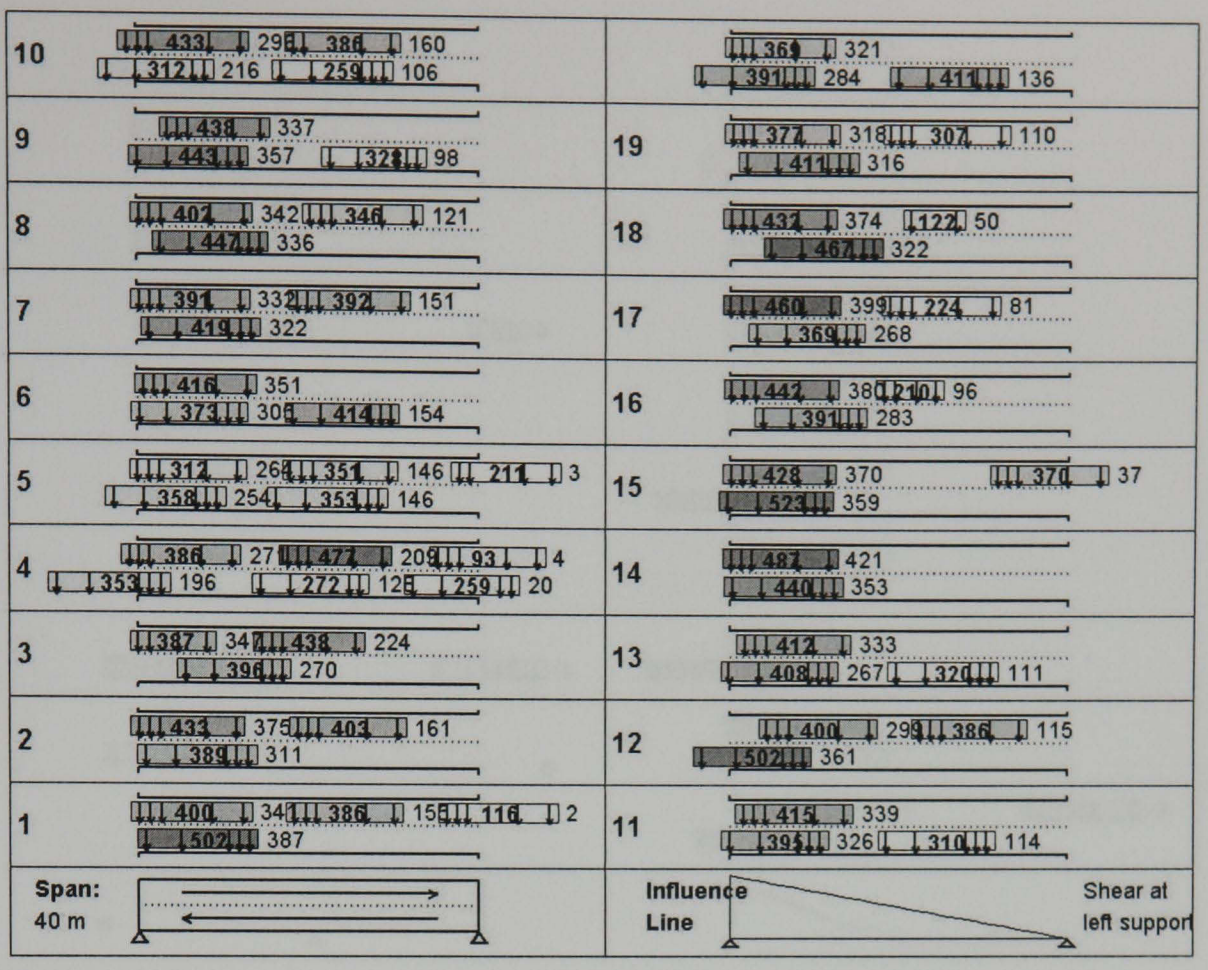
10
433 298 386 160
312 216 259 106
9
438 337
443 357 328 98
8
401 342 346 121
447 336
7
391 332 392 151
419 322
6
416 351
373 305 414 154
5
312 264 351 146 211 3
358 254 353 146
4
386 27 477 209 93 4
353 196 272 125 259 20
3
387 347 438 224
396 270
2
433 375 403 161
389 311
1
400 341 386 155 116 2
502 387
Span:
40 m
19
369 321
391 284 411 136
19
377 318 307 110
411 316
18
431 374 122 50
467 322
17
460 399 224 81
369 268
16
441 380 210 96
391 283
15
428 370 370 37
523 359
14
487 421
440 353
13
412 333
408 267 320 111
12
400 298 386 115
502 361
11
415 339
395 326 310 114
Influence
Line
Shear at
left support

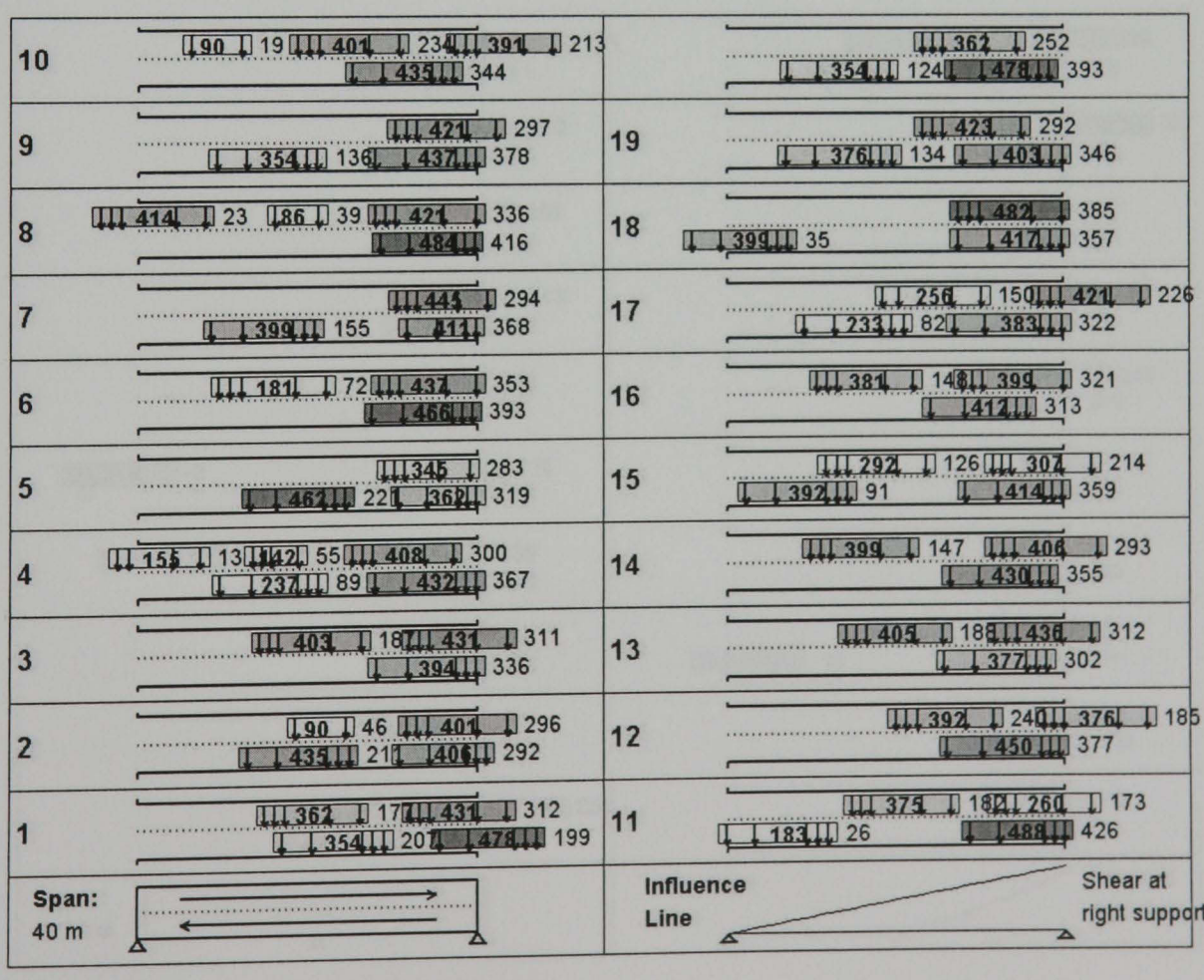
10
90 19 401 234 391 213
435 344
9
421 297
354 136 437 378
8
414 23 86 39 421 336
484 416
7
445 294
399 155 411 368
6
181 72 437 353
466 393
5
345 283
462 22 362 319
4
155 13 142 55 408 300
237 89 432 367
3
403 187 431 311
394 336
2
90 46 401 296
435 21 406 292
1
362 17 431 312
354 207 478 199
Span:
40 m
19
362 252
354 124 478 393
19
423 292
376 134 403 346
18
482 385
399 35 417 357
17
256 150 421 226
233 82 383 322
16
381 148 399 321
412 313
15
292 126 307 214
392 91 414 359
14
399 147 406 293
430 355
13
405 188 436 312
377 302
12
392 240 376 185
450 377
11
375 182 260 173
183 26 488 426
Influence
Line
Shear at
right support

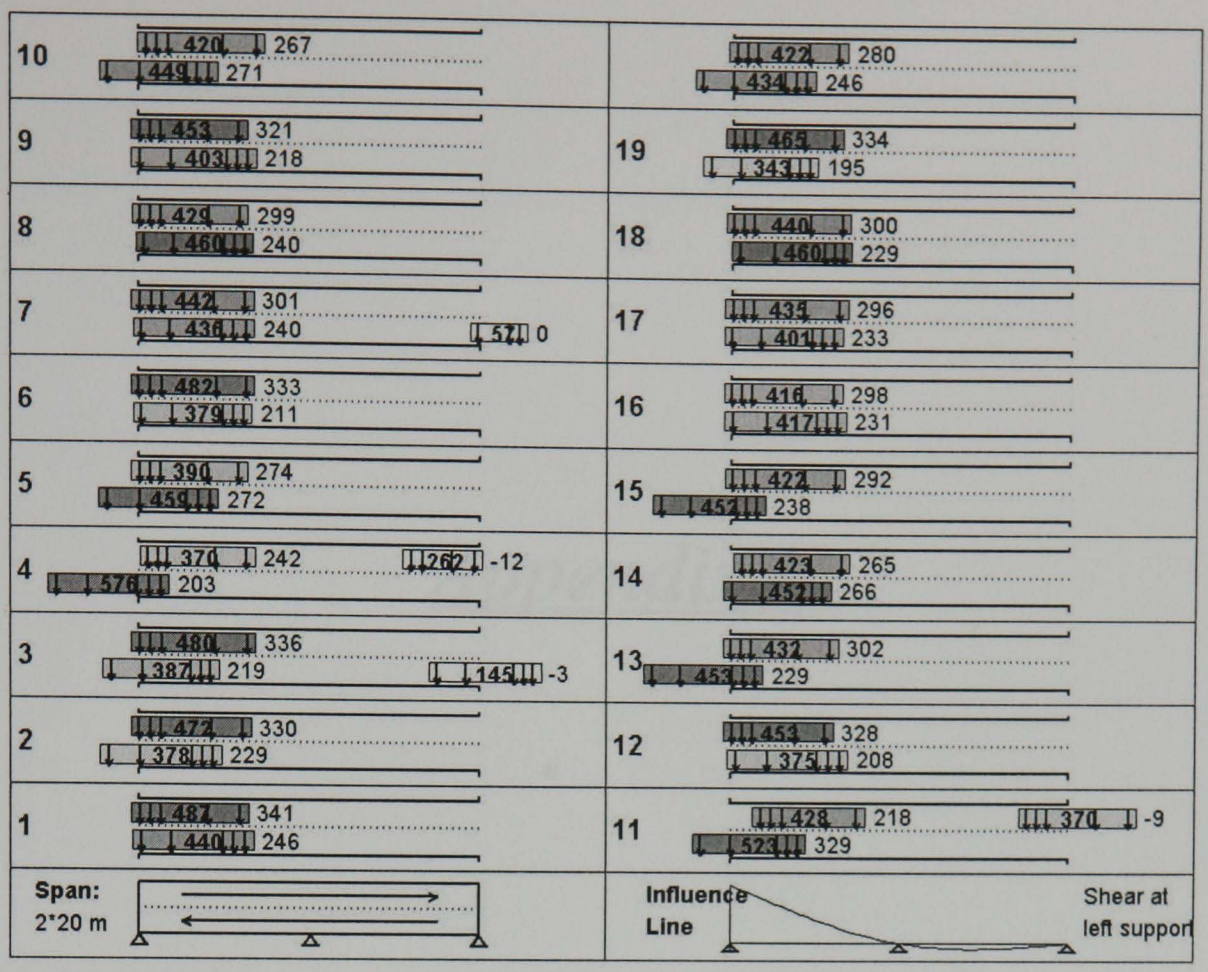
10
420 267
449 271
9
453 321
403 218
8
429 299
460 240
7
442 301
436 240
57 0
6
482 333
379 211
5
390 274
459 272
4
370 242
262 -12
576 203
3
480 336
387 219
145 -3
2
472 330
378 229
1
487 341
440 246
Span:
2*20 m
19
422 280
434 246
19
465 334
343 195
18
440 300
460 229
17
435 296
401 233
16
416 298
417 231
15
422 292
452 238
14
423 265
452 266
13
432 302
453 229
12
453 328
375 208
11
428 218
370 -9
523 329
Influence
Line
Shear at
left support

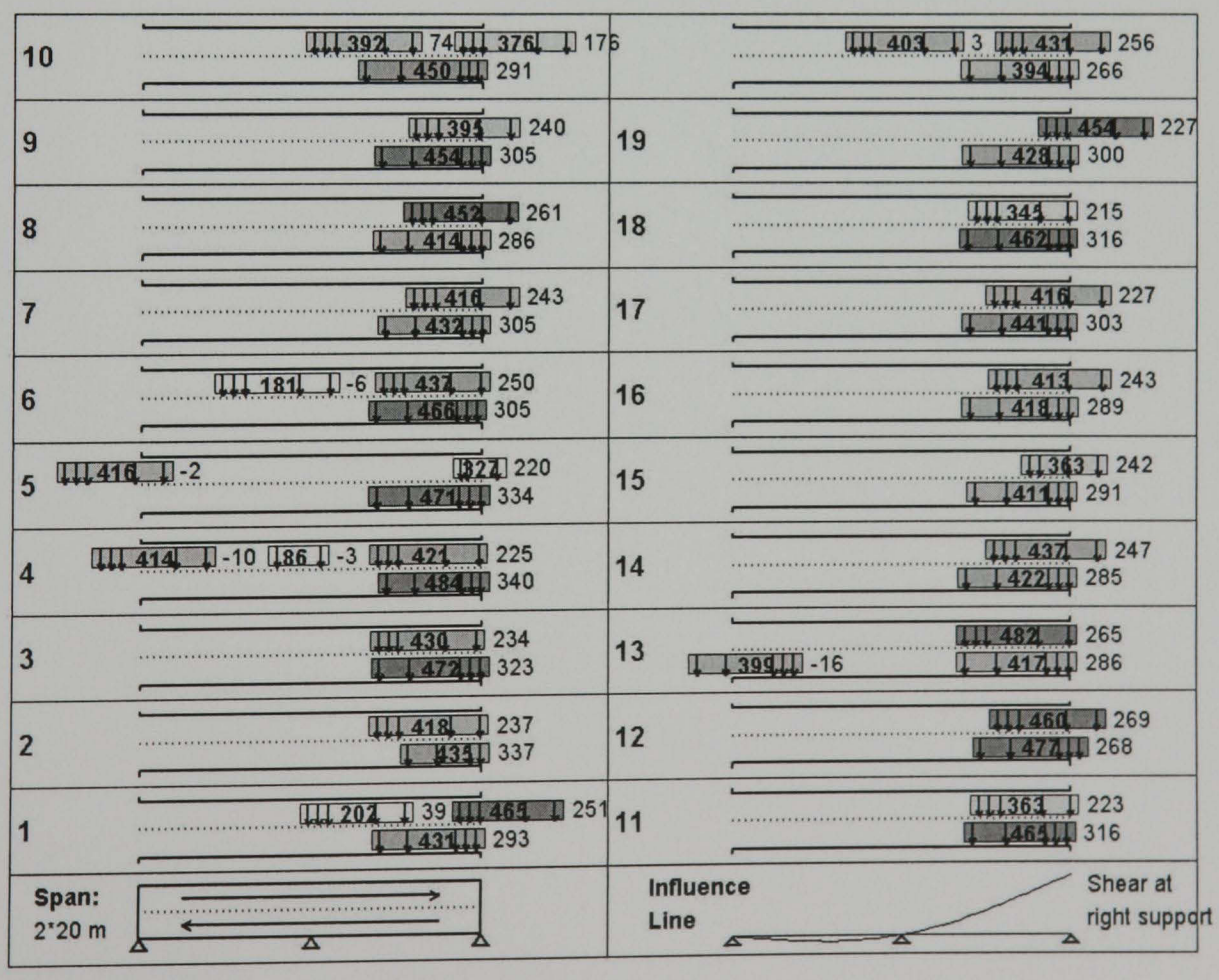
10
392 74
376 176
450 291
9
395 240
454 305
8
452 261
414 286
7
416 243
432 305
6
181 -6
437 250
466 305
5
416 -2
327 220
471 334
4
414 -10
186 -3
421 225
484 340
3
430 234
472 323
2
418 237
435 337
1
202 39
465 251
431 293
Span:
2*20 m
19
403 3
431 256
394 266
19
454 227
428 300
18
345 215
462 316
17
416 227
441 303
16
413 243
418 289
15
363 242
411 291
14
437 247
422 285
13
482 265
399 -16
417 286
12
460 269
477 268
11
363 223
465 316
Influence
Line
Shear at
right support

Appendix K

PLOTS OF THE MODELLED EFFECTS FOR BI-DIRECTIONAL TRAFFIC

Appendix K Plots Of Modelled Effects For Unidirectional Traffic

20M BRIDGES ____ 328
30M BRIDGES ____ 333
40M BRIDGES ____ 338

20M BRIDGES

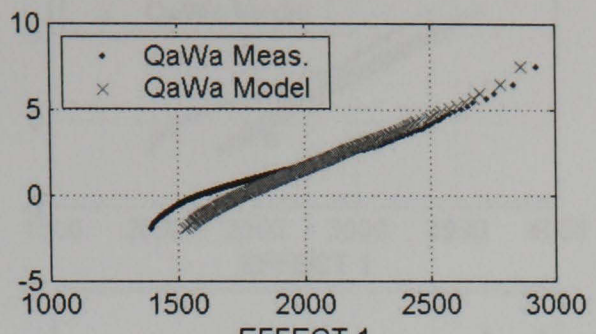

EFFECT 1

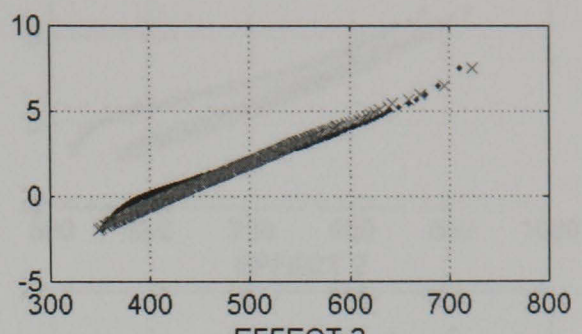

EFFECT 2

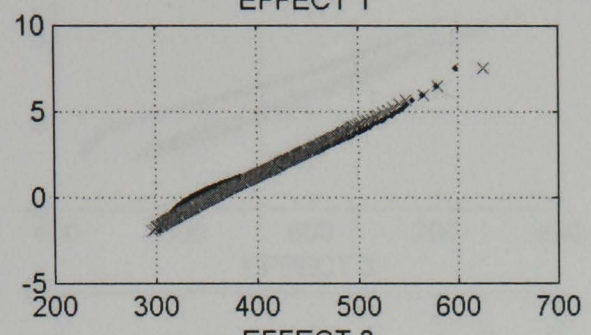

EFFECT 3

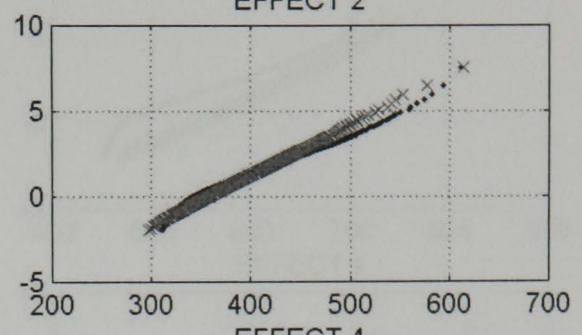

EFFECT 4

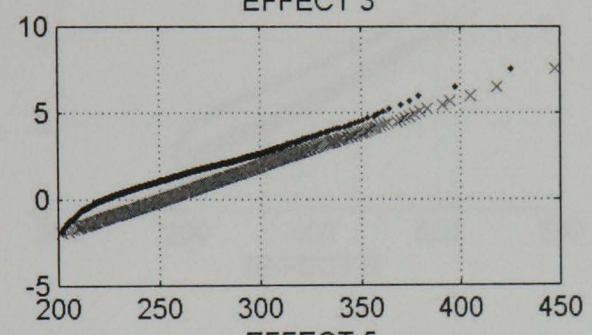

EFFECT 5

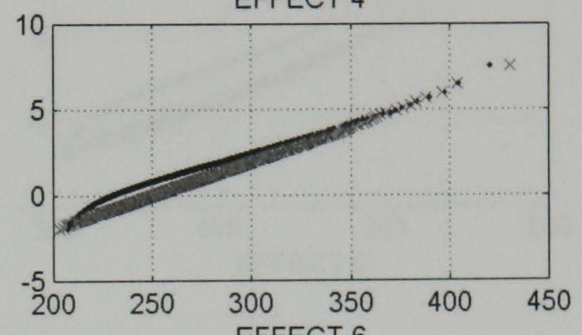

EFFECT 6

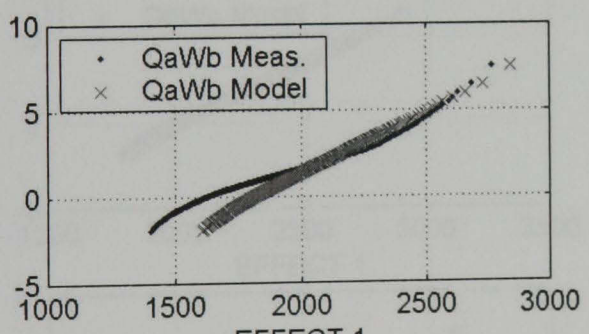

EFFECT 1

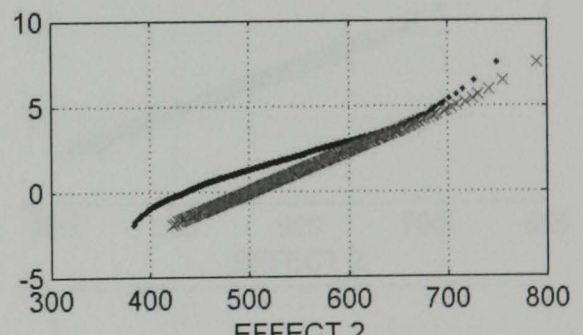

EFFECT 2

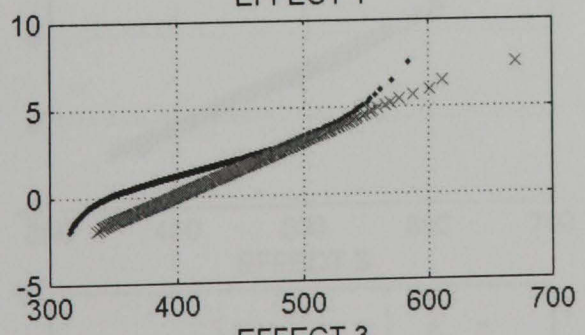

EFFECT 3

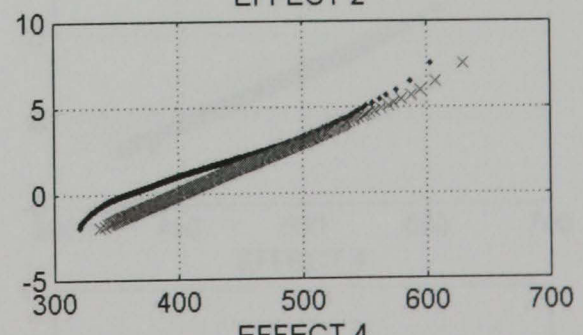

EFFECT 4

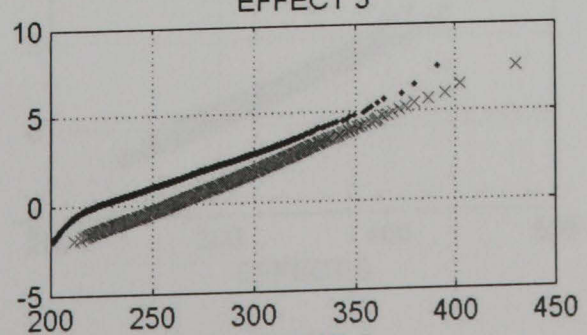

EFFECT 5

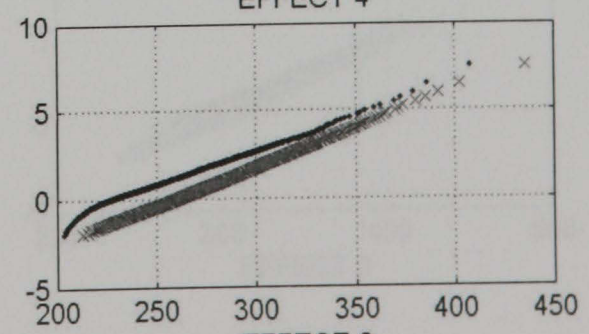

EFFECT 6

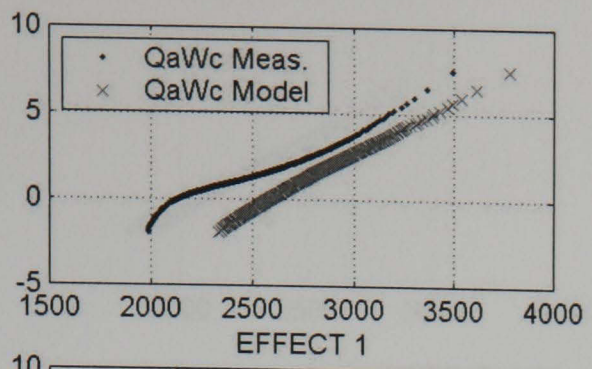
QaWc Meas.
QaWc Model
10
5
0
-5
1500
2000
2500
3000
3500
4000
EFFECT 1

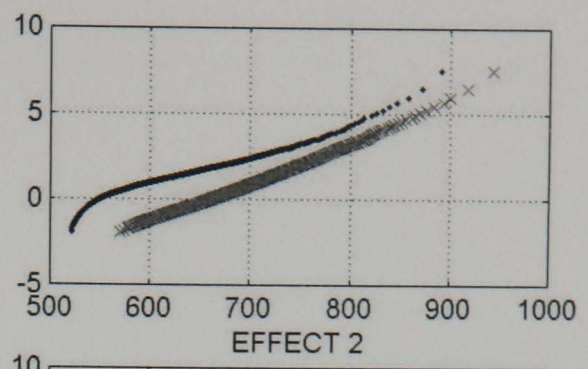
10
5
0
-5
500
600
700
800
900
1000
EFFECT 2

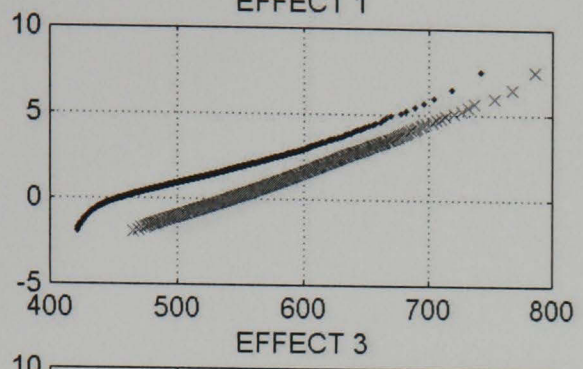
10
5
0
-5
400
500
600
700
800
EFFECT 3

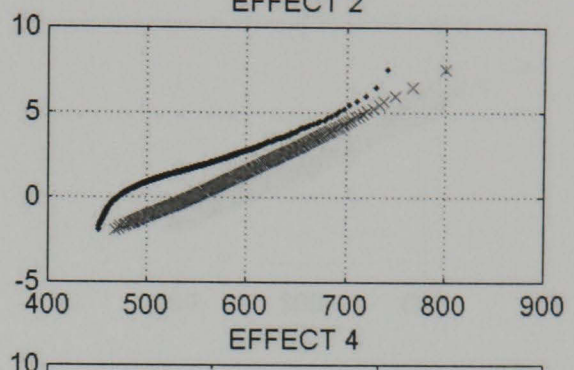
10
5
0
-5
400
500
600
700
800
900
EFFECT 4

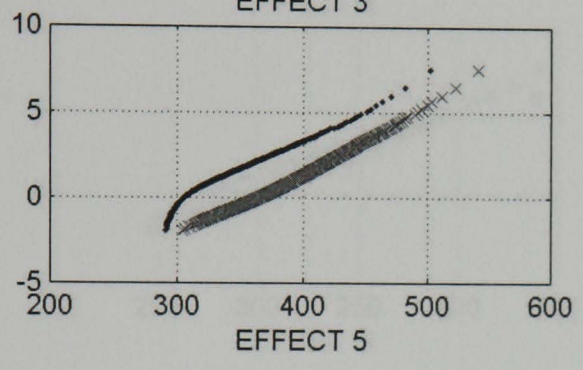
10
5
0
-5
200
300
400
500
600
EFFECT 5

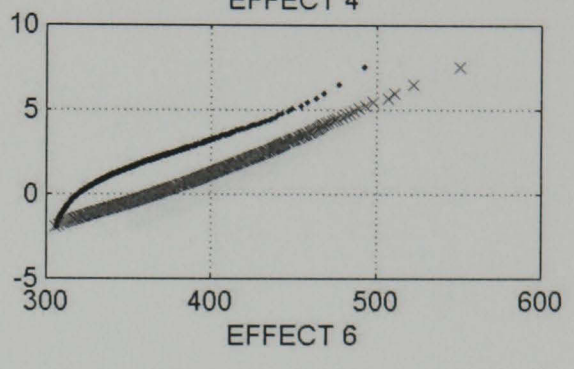
10
5
0
-5
300
400
500
600
EFFECT 6

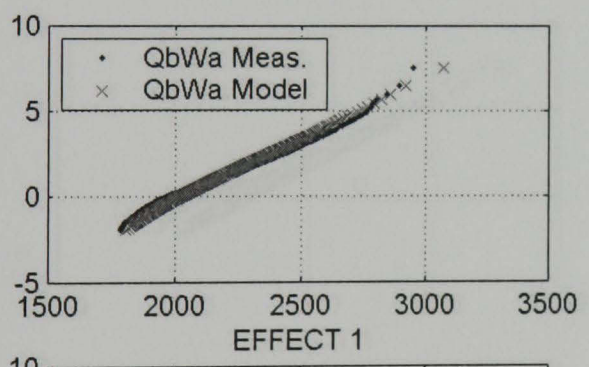
QbWa Meas.
QbWa Model
10
5
0
-5
1500
2000
2500
3000
3500
EFFECT 1

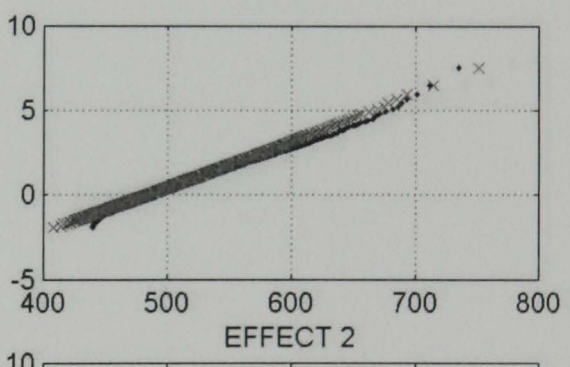
10
5
0
-5
400
500
600
700
800
EFFECT 2

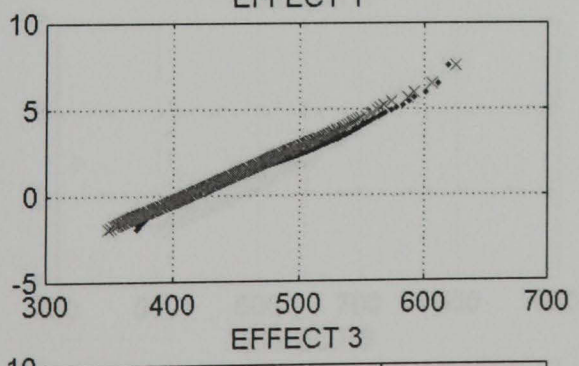
10
5
0
-5
300
400
500
600
700
EFFECT 3

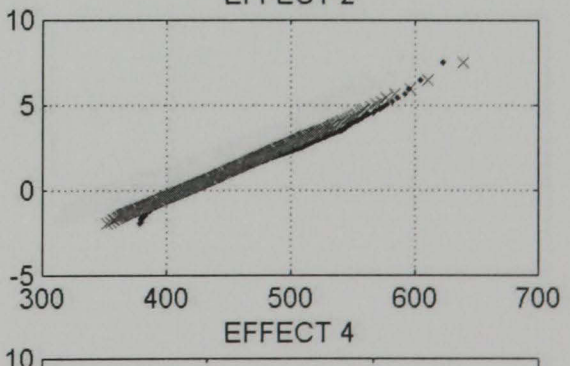
10
5
0
-5
300
400
500
600
700
EFFECT 4

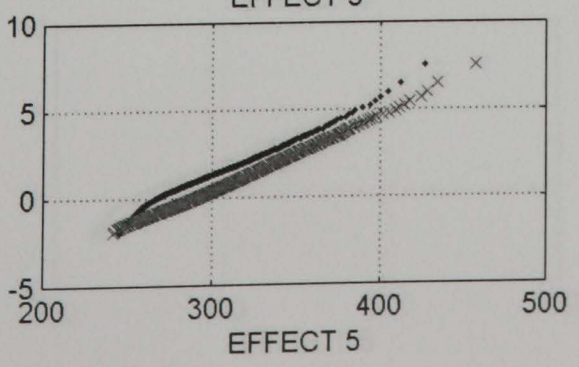
10
5
0
-5
200
300
400
500
EFFECT 5

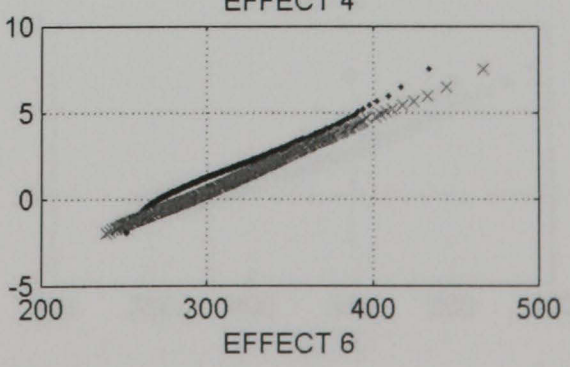
10
5
0
-5
200
300
400
500
EFFECT 6

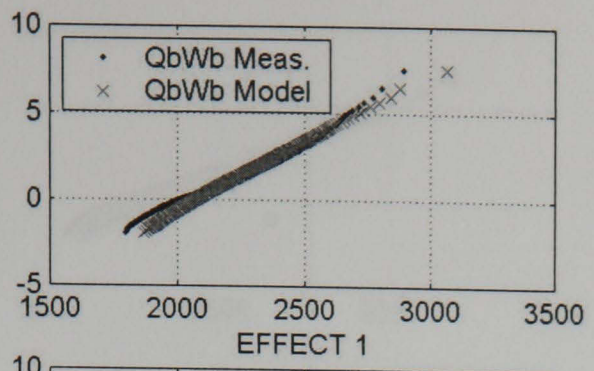
QbWb Meas.
QbWb Model
10
5
0
-5
1500
2000
2500
3000
3500
EFFECT 1

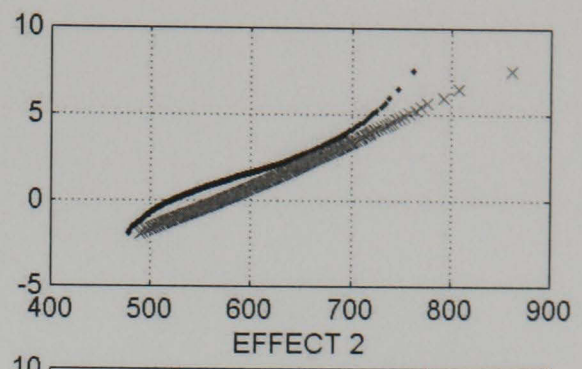
10
5
0
-5
400
500
600
700
800
900
EFFECT 2

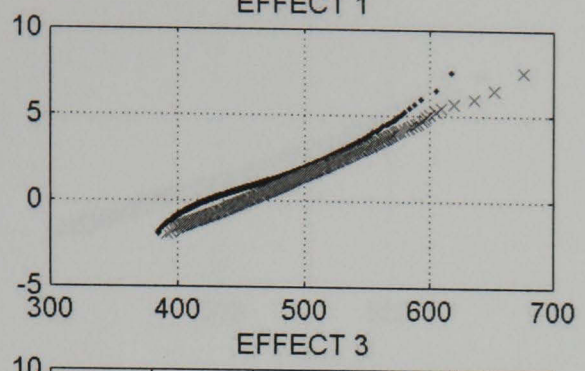
10
5
0
-5
300
400
500
600
700
EFFECT 3

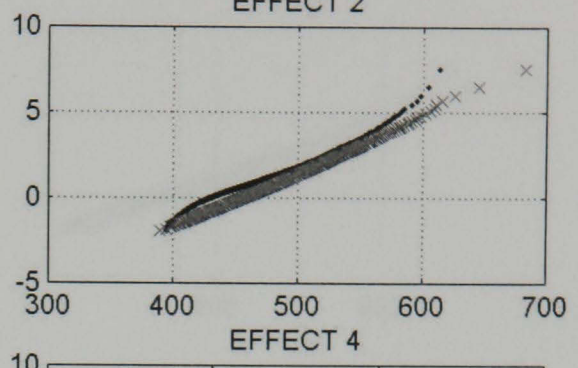
10
5
0
-5
300
400
500
600
700
EFFECT 4

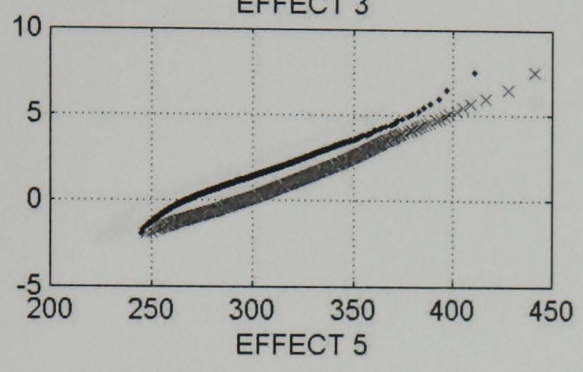
10
5
0
-5
200
250
300
350
400
450
EFFECT 5

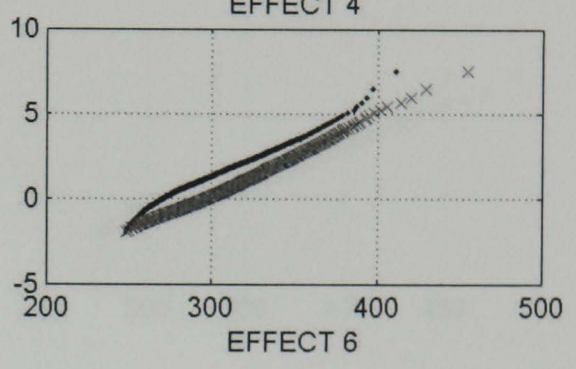
10
5
0
-5
200
300
400
500
EFFECT 6

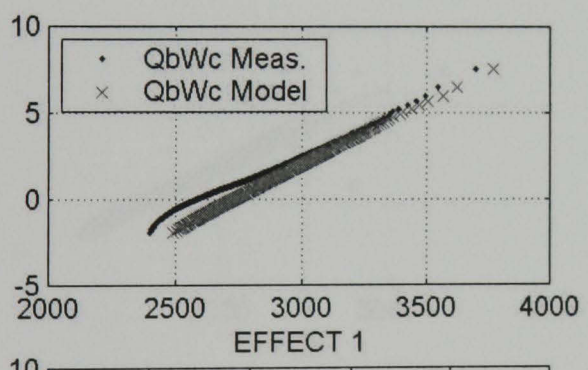
QbWc Meas.
QbWc Model
10
5
0
-5
2000
2500
3000
3500
4000
EFFECT 1

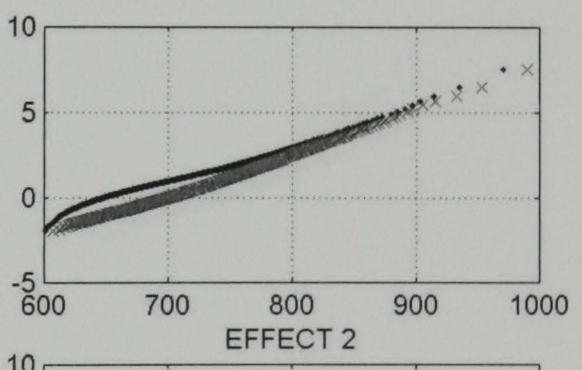
10
5
0
-5
600
700
800
900
1000
EFFECT 2

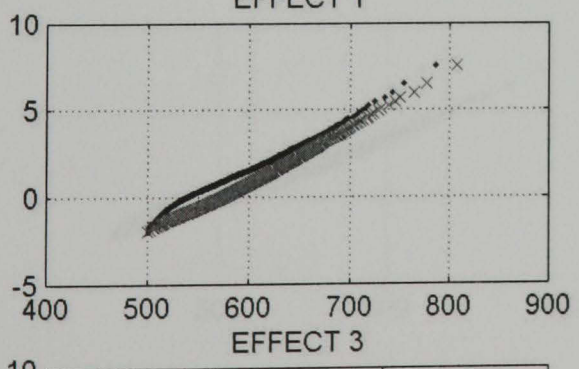
10
5
0
-5
400
500
600
700
800
900
EFFECT 3

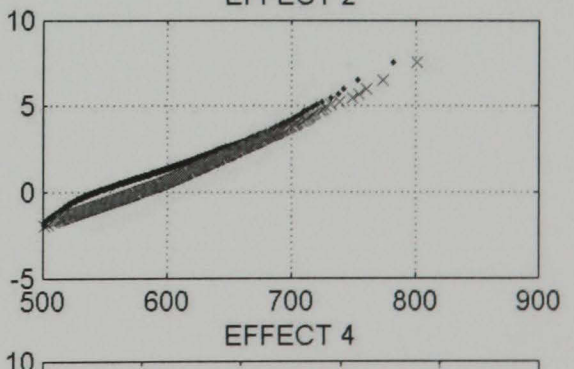
10
5
0
-5
500
600
700
800
900
EFFECT 4

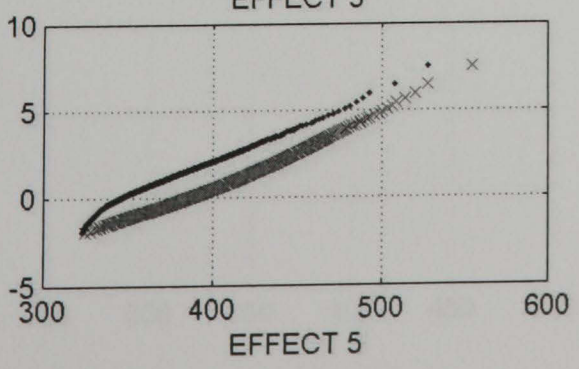
10
5
0
-5
300
400
500
600
EFFECT 5

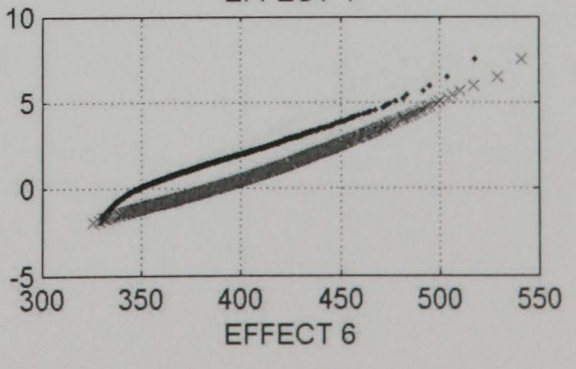
10
5
0
-5
300
350
400
450
500
550
EFFECT 6

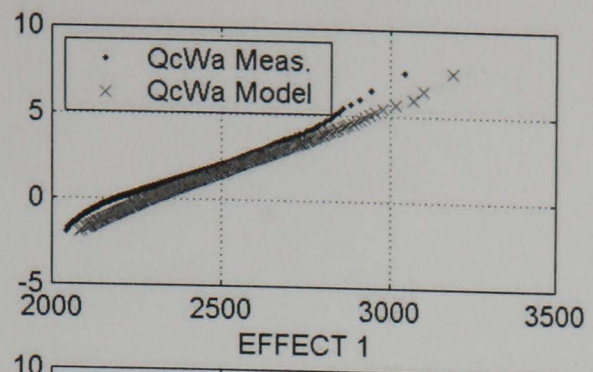
QcWa Meas.
QcWa Model
EFFECT 1

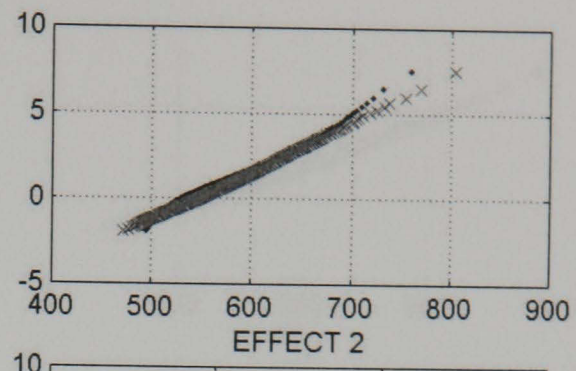
EFFECT 2

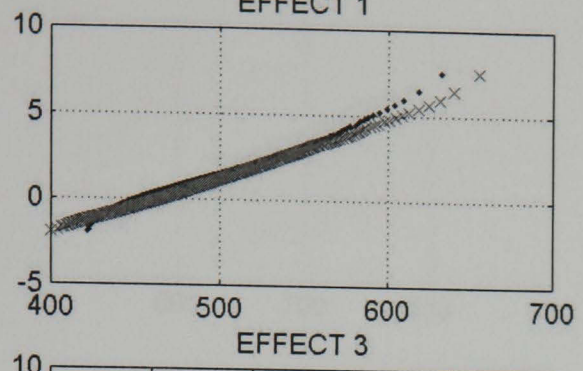
EFFECT 3

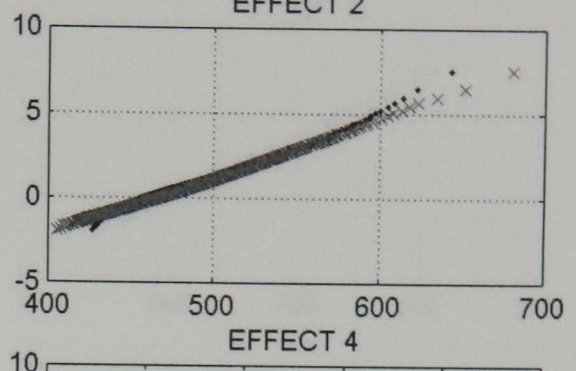
EFFECT 4

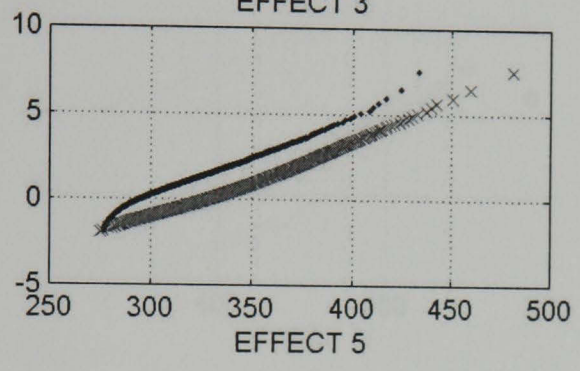
EFFECT 5

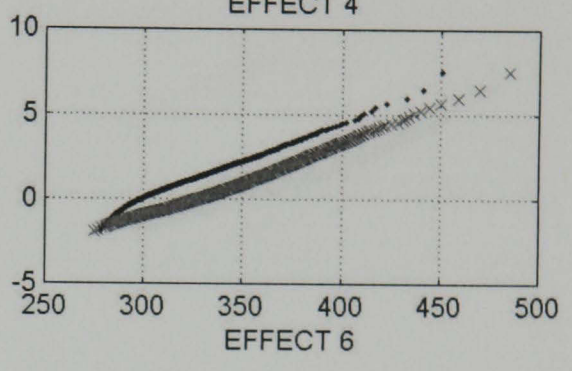
EFFECT 6

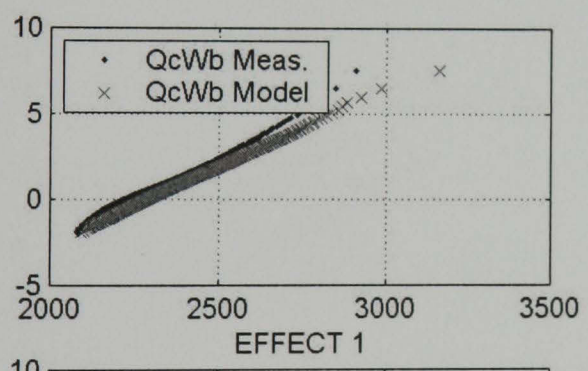
QcWb Meas.
QcWb Model
EFFECT 1

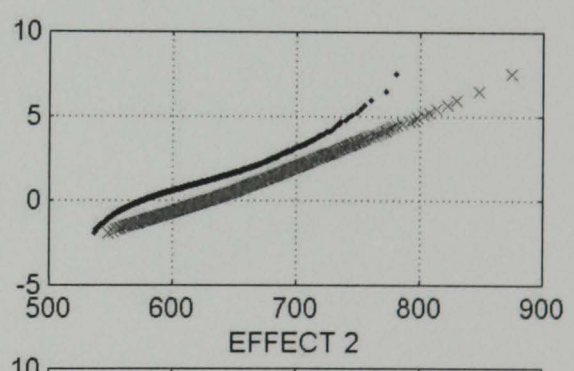
EFFECT 2

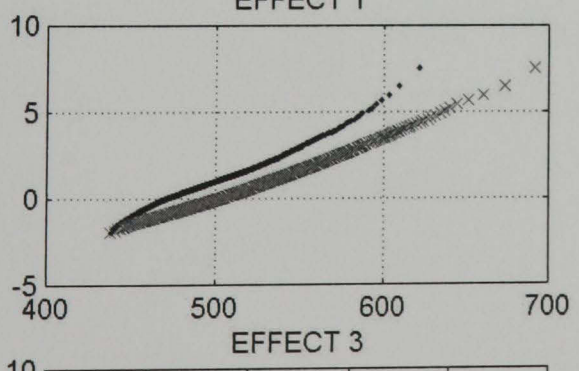
EFFECT 3

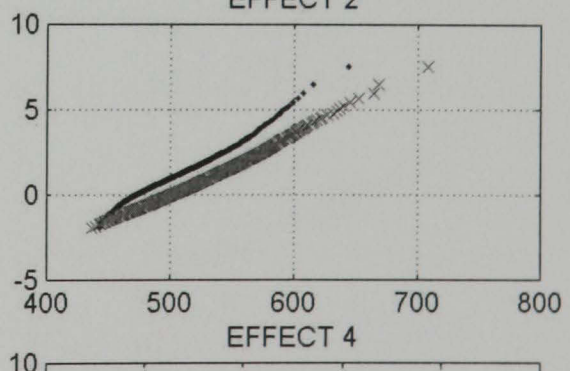
EFFECT 4

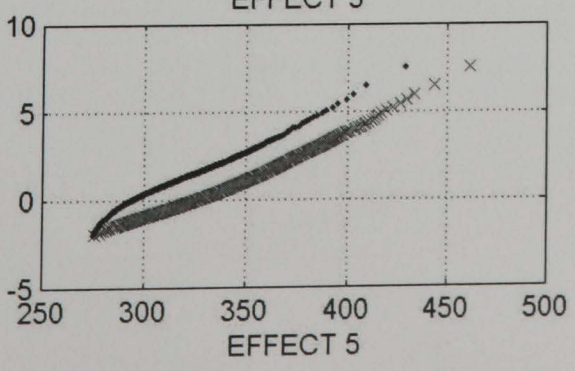
EFFECT 5

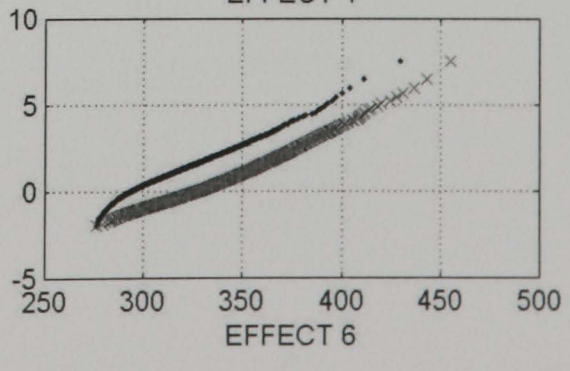
EFFECT 6

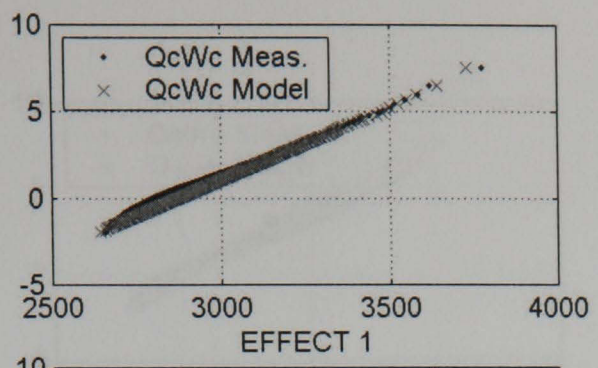
QcWc Meas.
QcWc Model
10
5
0
-5
2500
3000
3500
4000
EFFECT 1

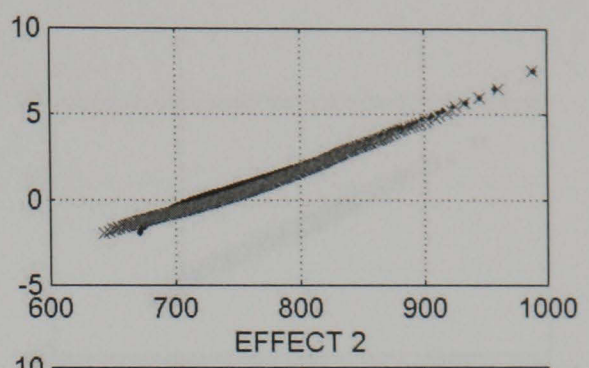
10
5
0
-5
600
700
800
900
1000
EFFECT 2

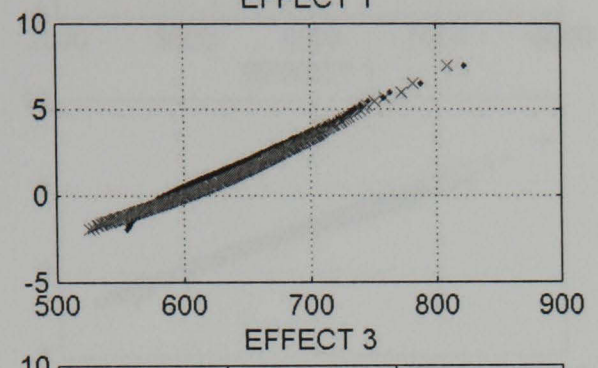
10
5
0
-5
500
600
700
800
900
EFFECT 3

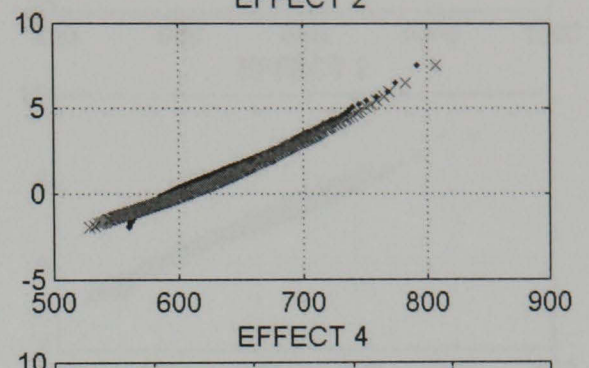
10
5
0
-5
500
600
700
800
900
EFFECT 4

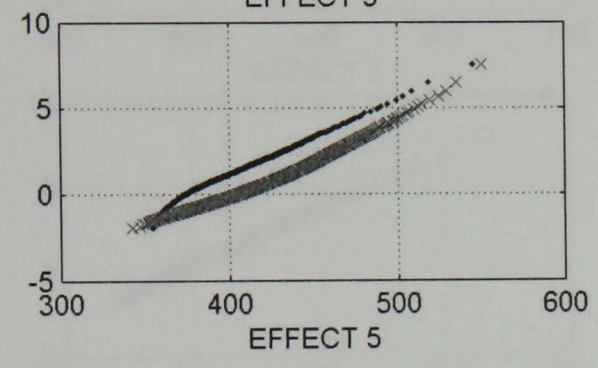
10
5
0
-5
300
400
500
600
EFFECT 5

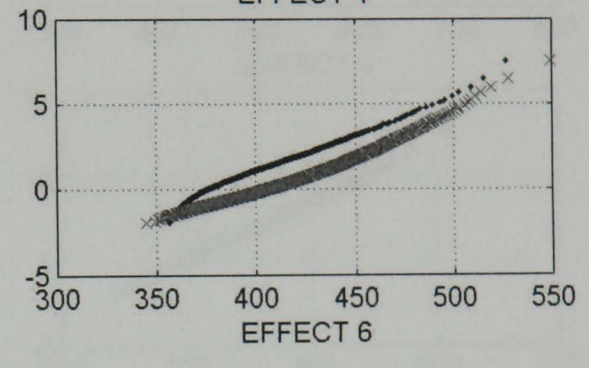
10
5
0
-5
300
350
400
450
500
550
EFFECT 6

30M BRIDGES

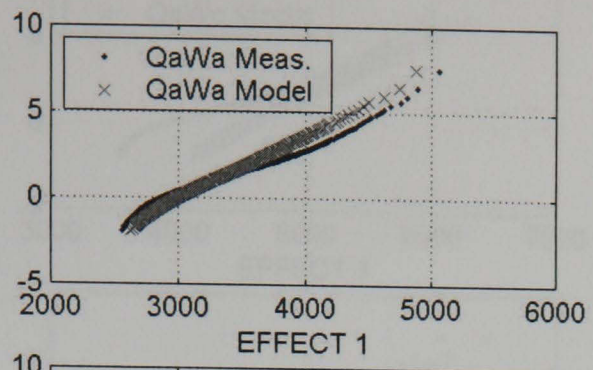
QaWa Meas.
QaWa Model
EFFECT 1

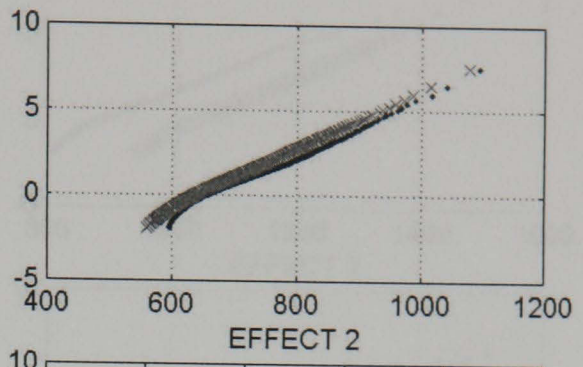
EFFECT 2

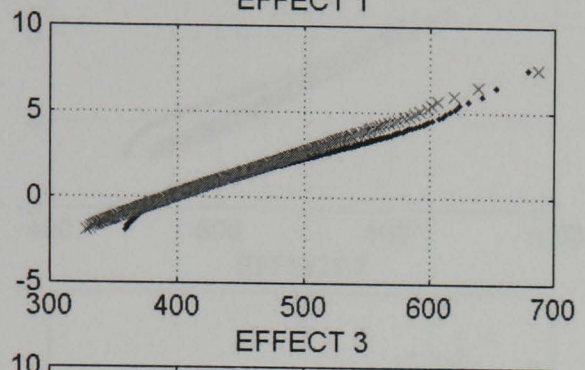
EFFECT 3

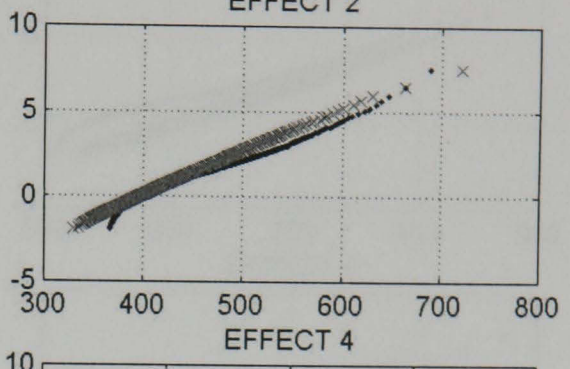
EFFECT 4

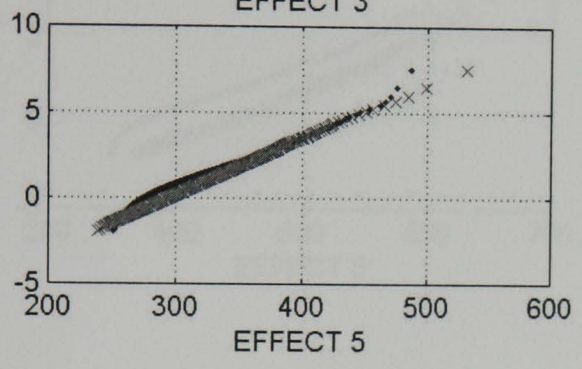
EFFECT 5

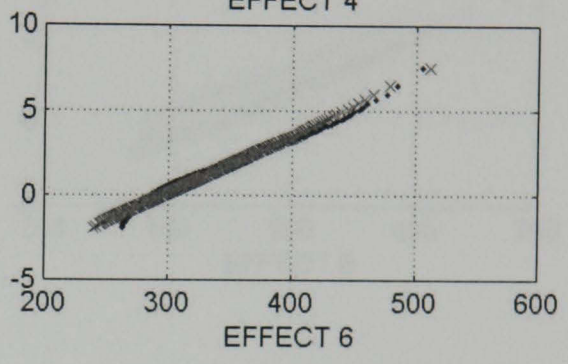
EFFECT 6

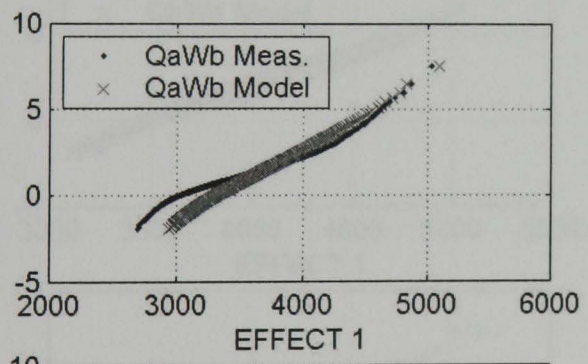
QaWb Meas.
QaWb Model
EFFECT 1

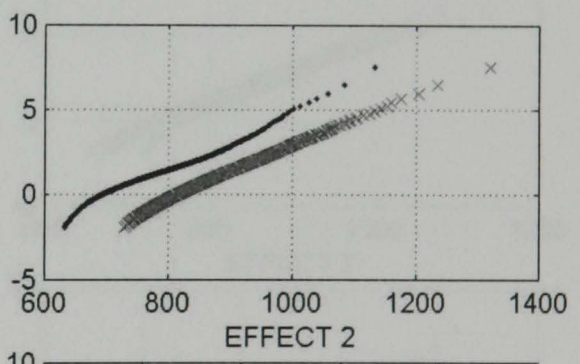
EFFECT 2

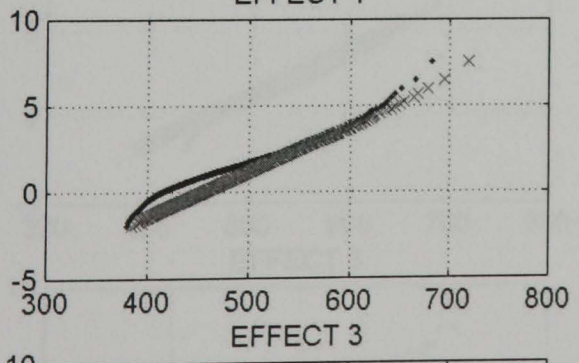
EFFECT 3

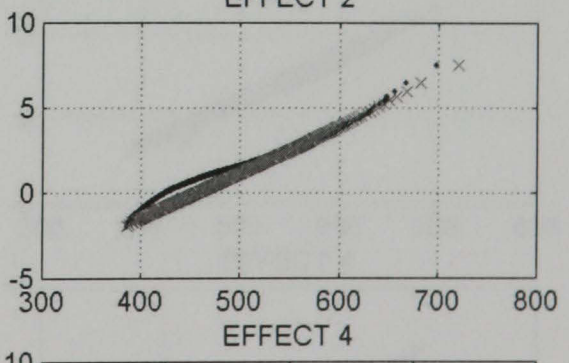
EFFECT 4

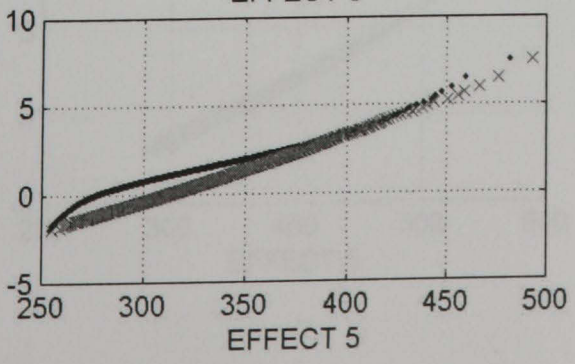
EFFECT 5

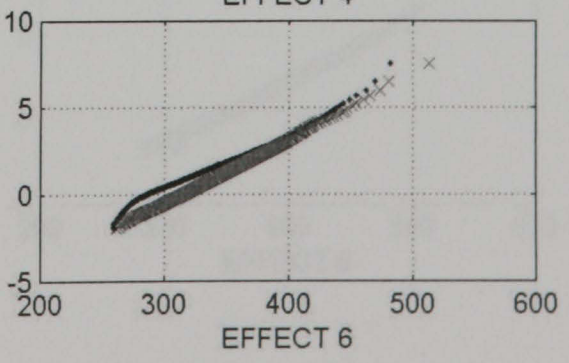
EFFECT 6

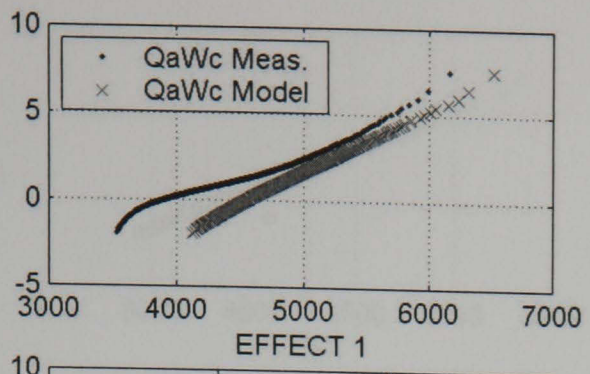
QaWc Meas.
QaWc Model
10
5
0
-5
3000
4000
5000
6000
7000
EFFECT 1

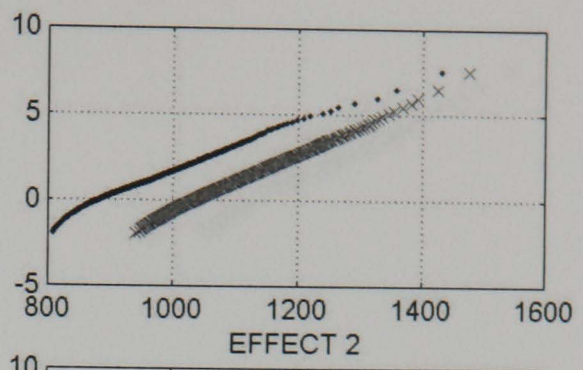
10
5
0
-5
800
1000
1200
1400
1600
EFFECT 2

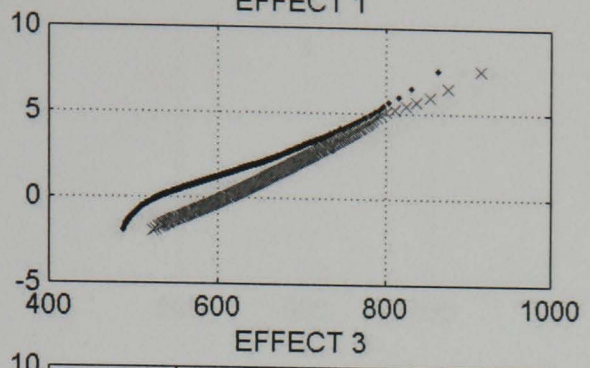
10
5
0
-5
400
600
800
1000
EFFECT 3

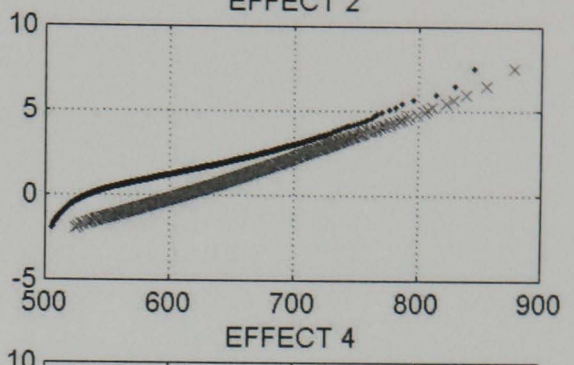
10
5
0
-5
500
600
700
800
900
EFFECT 4

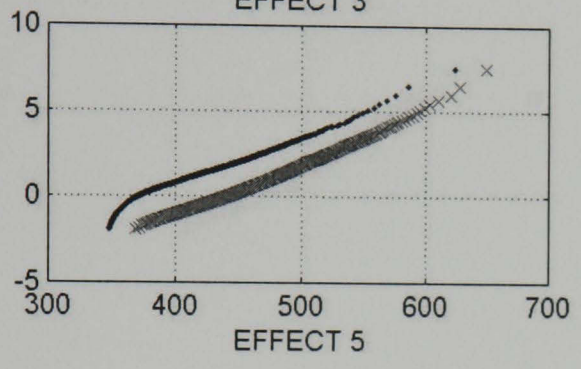
10
5
0
-5
300
400
500
600
700
EFFECT 5

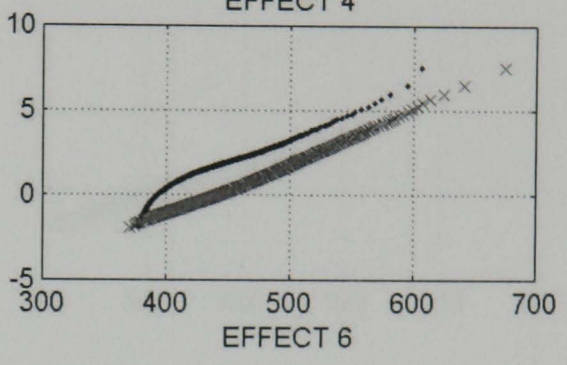
10
5
0
-5
300
400
500
600
700
EFFECT 6

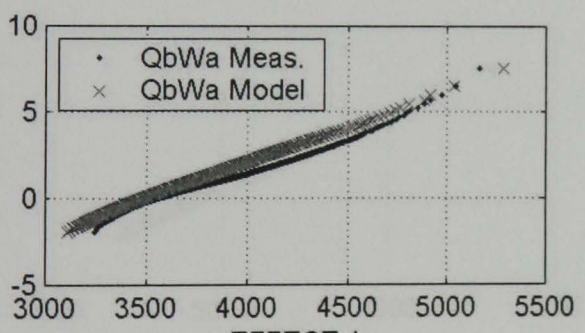
QbWa Meas.
QbWa Model
10
5
0
-5
3000
3500
4000
4500
5000
5500
EFFECT 1

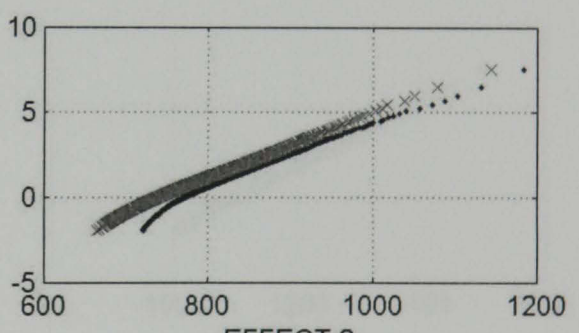
10
5
0
-5
600
800
1000
1200
EFFECT 2

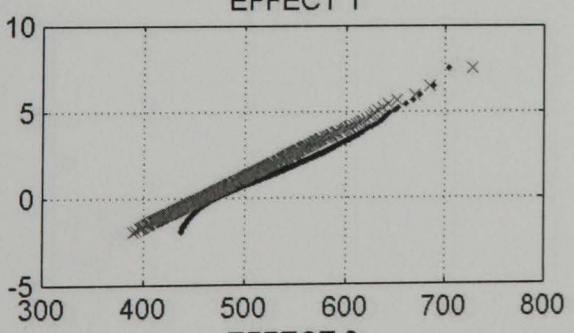
10
5
0
-5
300
400
500
600
700
800
EFFECT 3

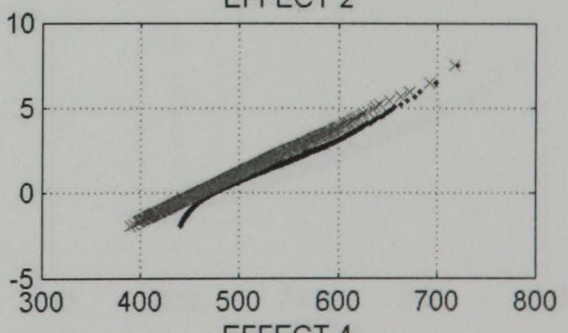
10
5
0
-5
300
400
500
600
700
800
EFFECT 4

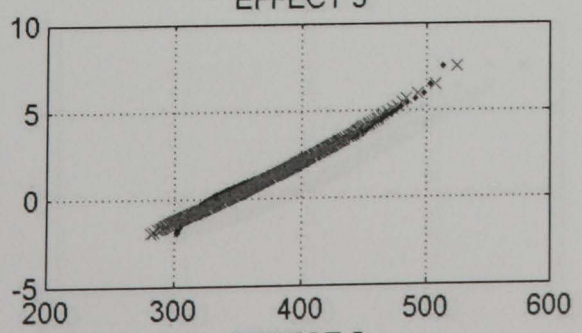
10
5
0
-5
200
300
400
500
600
EFFECT 5

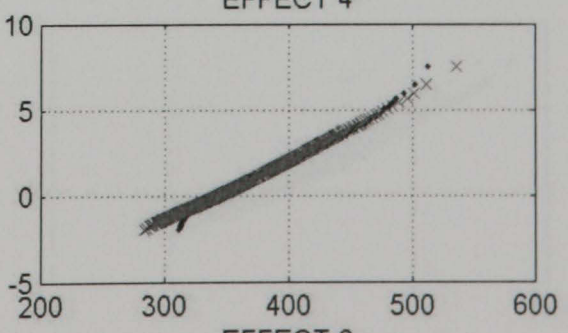
10
5
0
-5
200
300
400
500
600
EFFECT 6

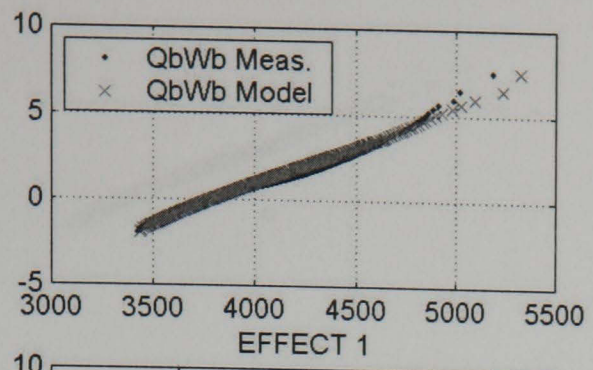
QbWb Meas.
QbWb Model
EFFECT 1

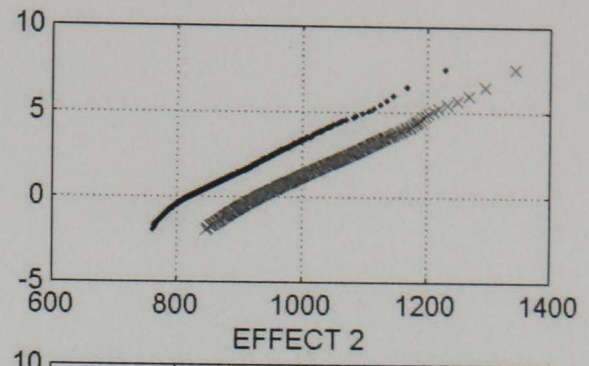
EFFECT 2

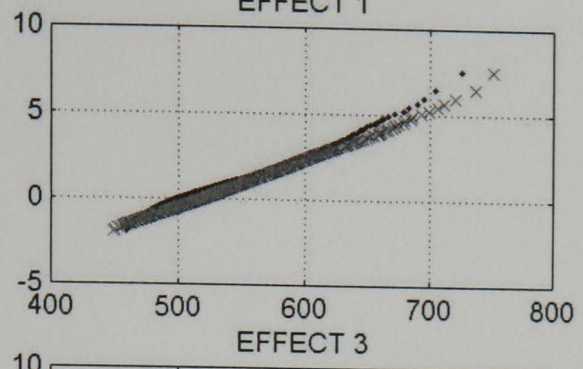
EFFECT 3

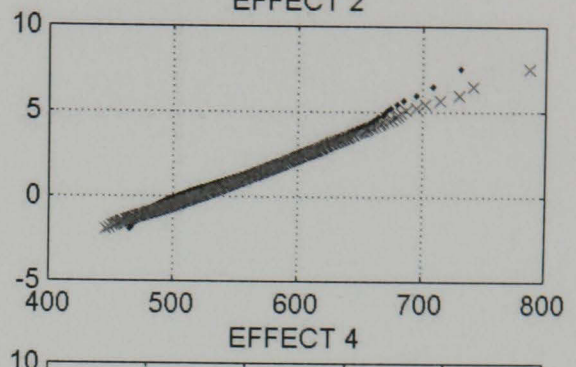
EFFECT 4

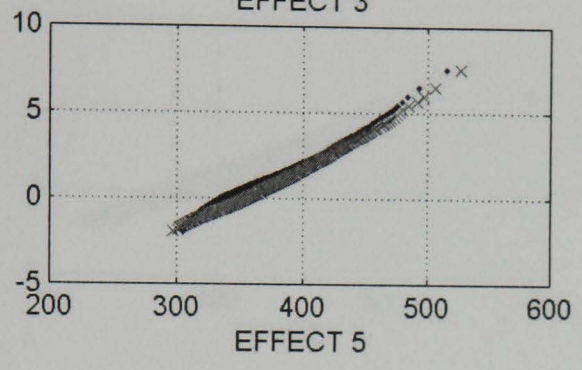
EFFECT 5

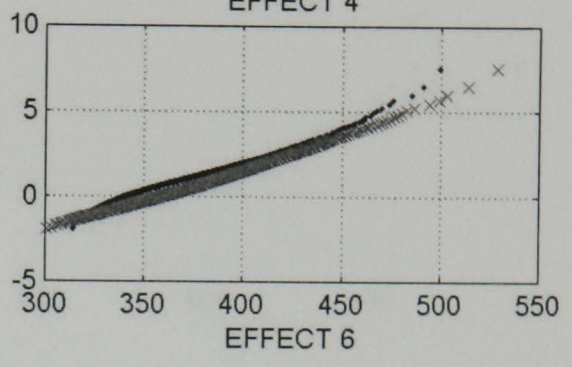
EFFECT 6

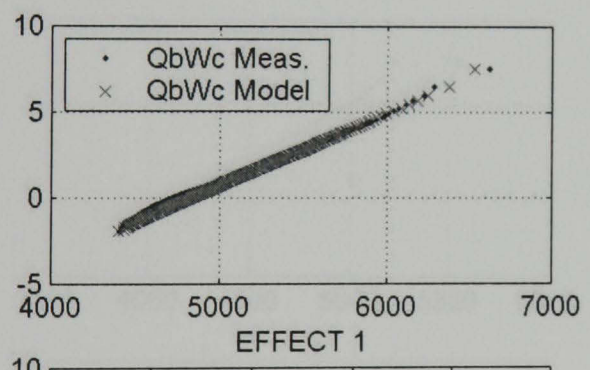
QbWc Meas.
QbWc Model
EFFECT 1

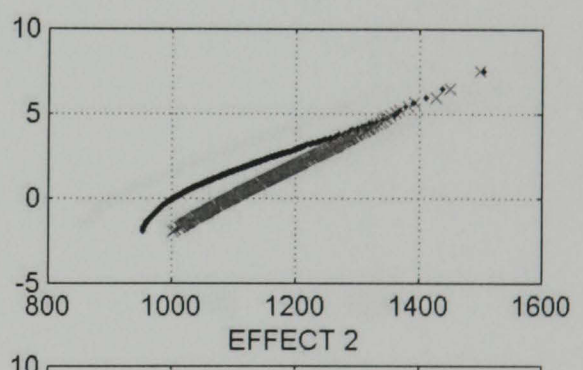
EFFECT 2

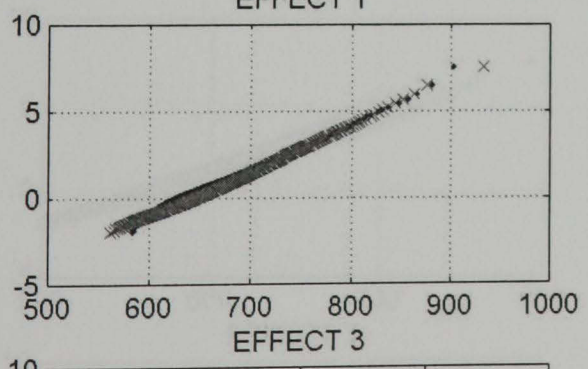
EFFECT 3

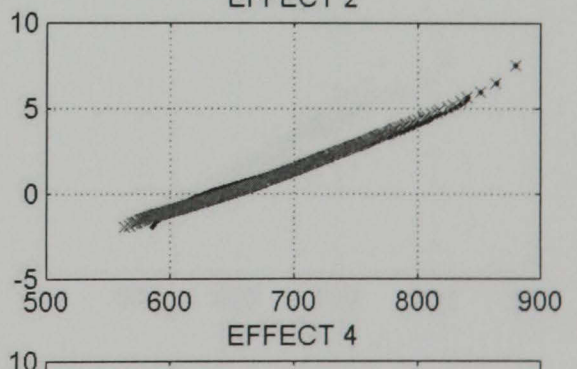
EFFECT 4

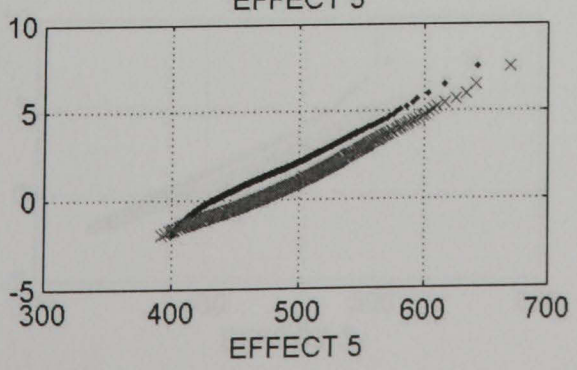
EFFECT 5

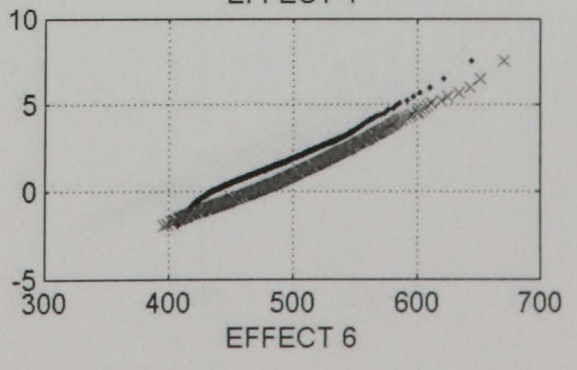
EFFECT 6

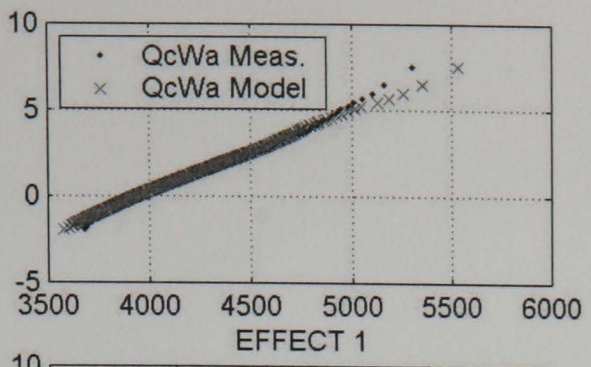
QcWa Meas.
QcWa Model
10
5
0
-5
3500
4000
4500
5000
5500
6000
EFFECT 1

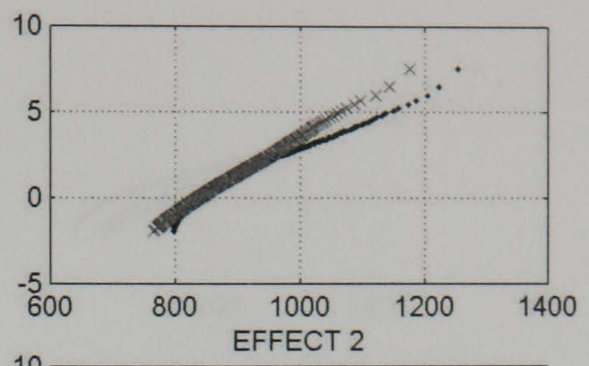
10
5
0
-5
600
800
1000
1200
1400
EFFECT 2

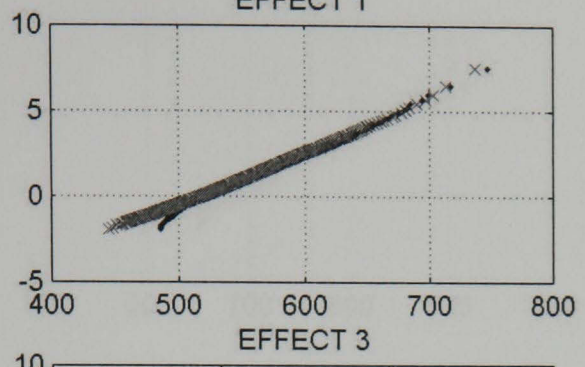
10
5
0
-5
400
500
600
700
800
EFFECT 3

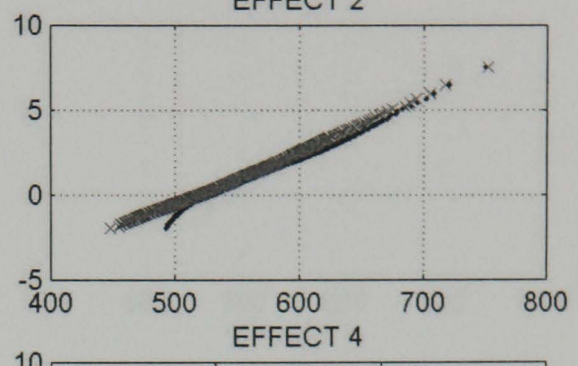
10
5
0
-5
400
500
600
700
800
EFFECT 4

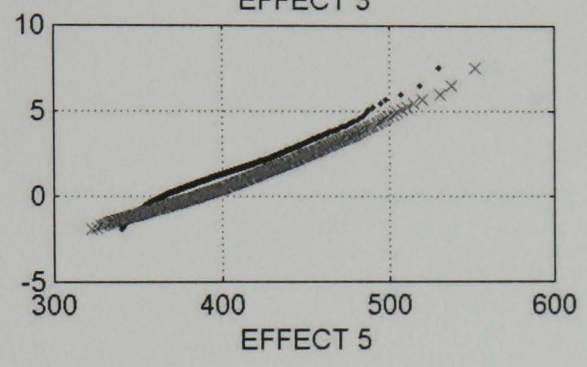
10
5
0
-5
300
400
500
600
EFFECT 5

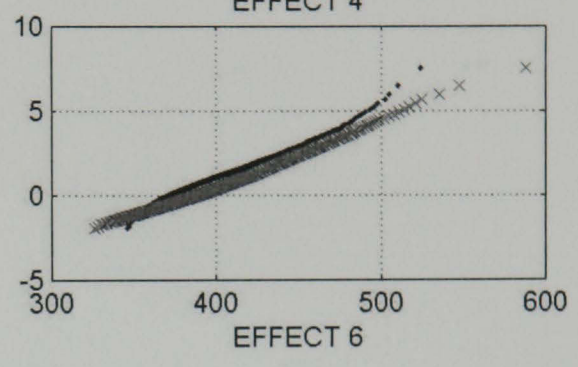
10
5
0
-5
300
400
500
600
EFFECT 6

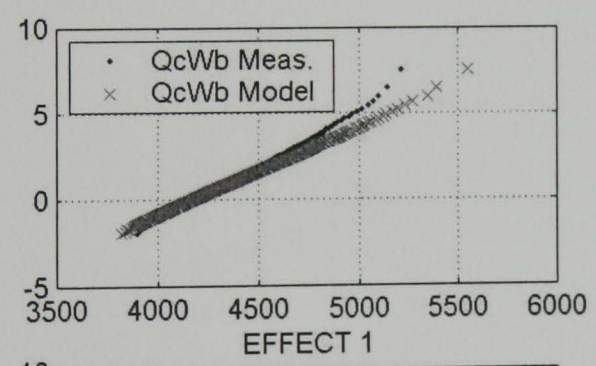
QcWb Meas.
QcWb Model
10
5
0
-5
3500
4000
4500
5000
5500
6000
EFFECT 1

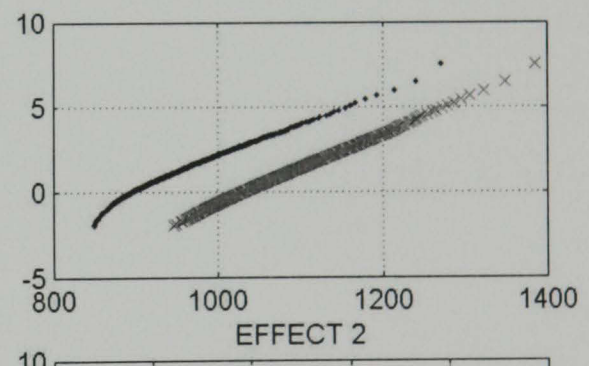
10
5
0
-5
800
1000
1200
1400
EFFECT 2

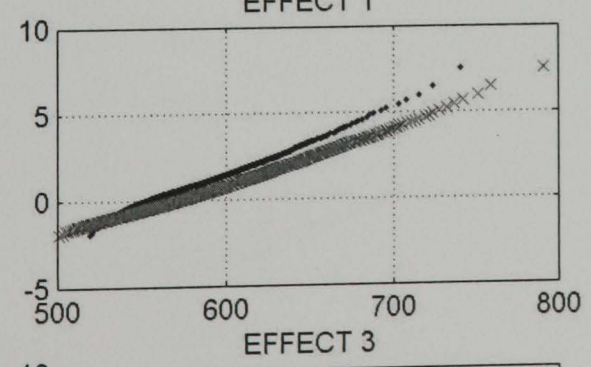
10
5
0
-5
500
600
700
800
EFFECT 3

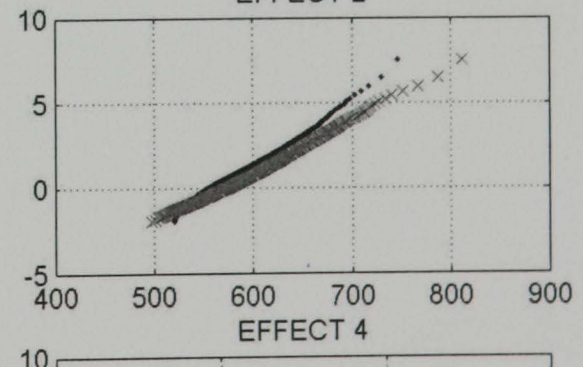
10
5
0
-5
400
500
600
700
800
900
EFFECT 4

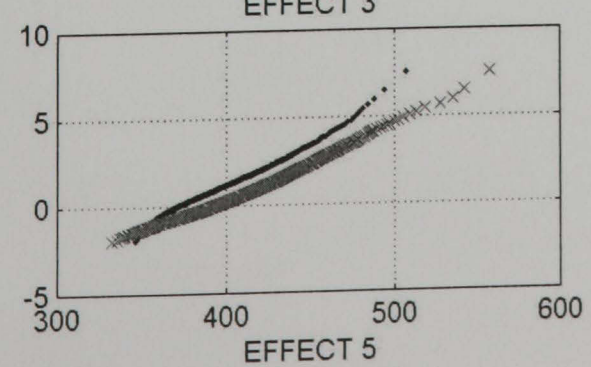
10
5
0
-5
300
400
500
600
EFFECT 5

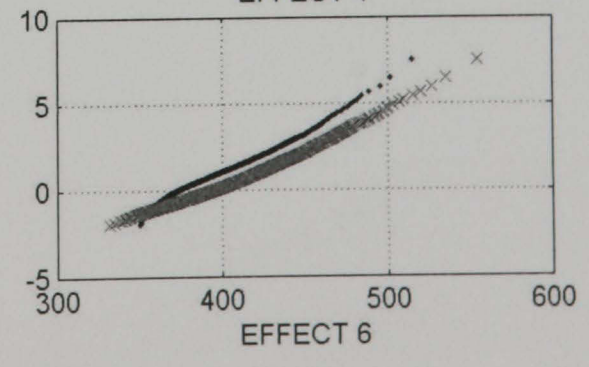
10
5
0
-5
300
400
500
600
EFFECT 6

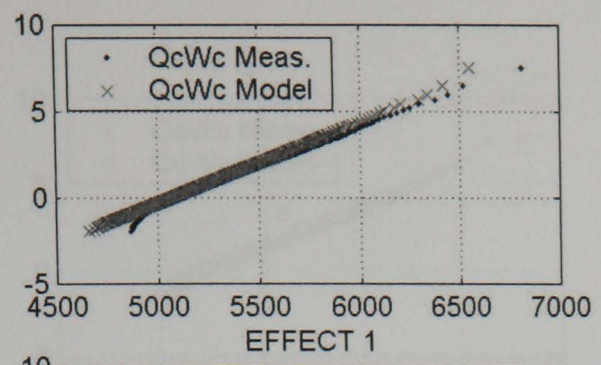
QcWc Meas.
QcWc Model
10
5
0
-5
4500
5000
5500
6000
6500
7000
EFFECT 1

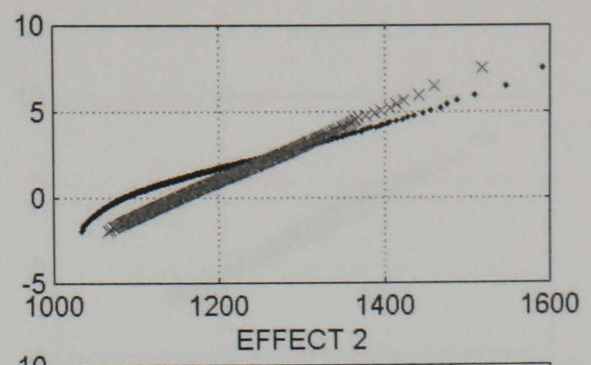
10
5
0
-5
1000
1200
1400
1600
EFFECT 2

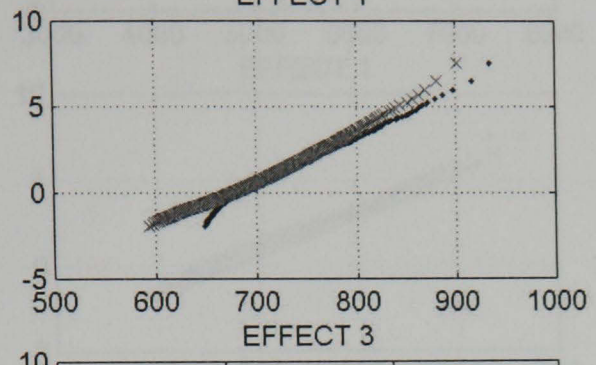
10
5
0
-5
500
600
700
800
900
1000
EFFECT 3

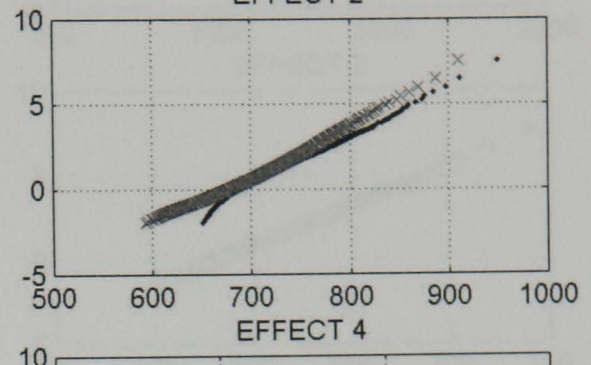
10
5
0
-5
500
600
700
800
900
1000
EFFECT 4

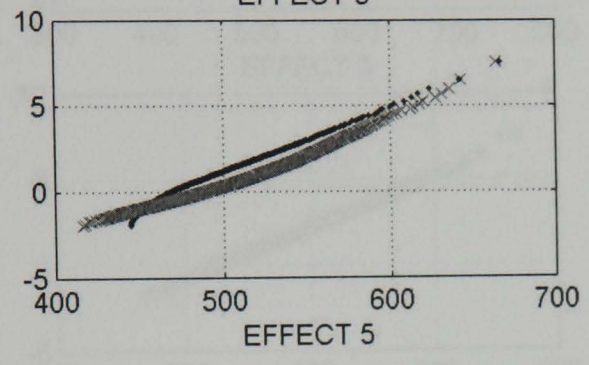
10
5
0
-5
400
500
600
700
EFFECT 5

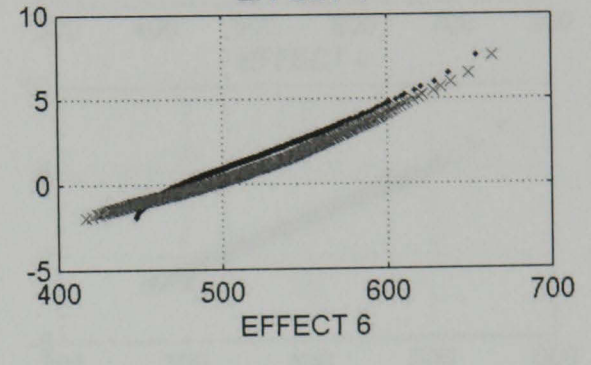
10
5
0
-5
400
500
600
700
EFFECT 6

40M BRIDGES

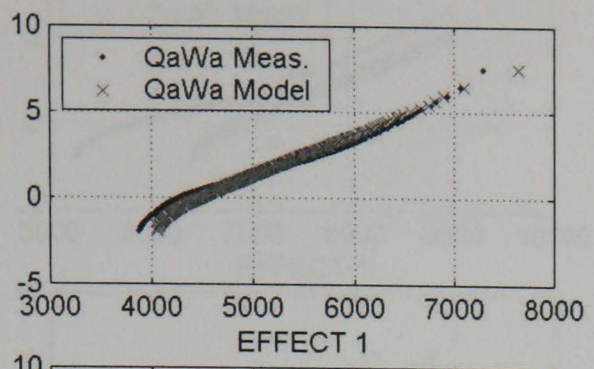
QaWa Meas.
QaWa Model
EFFECT 1

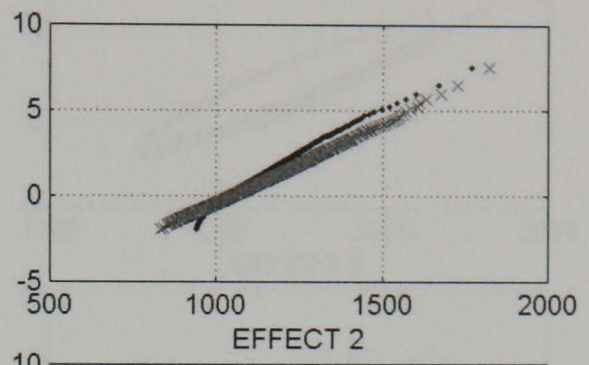
EFFECT 2

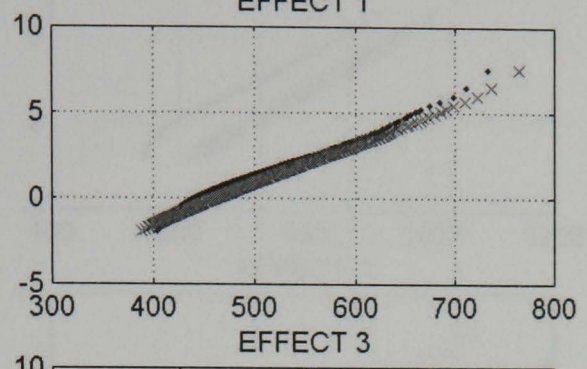
EFFECT 3

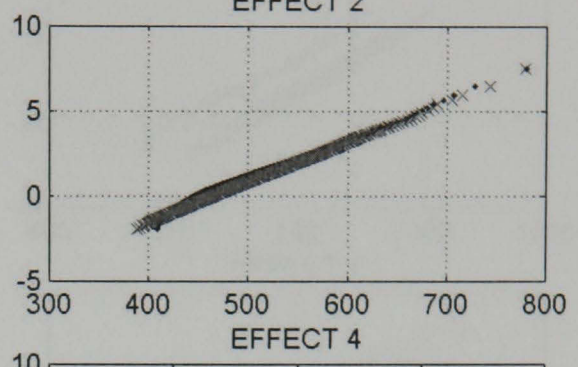
EFFECT 4

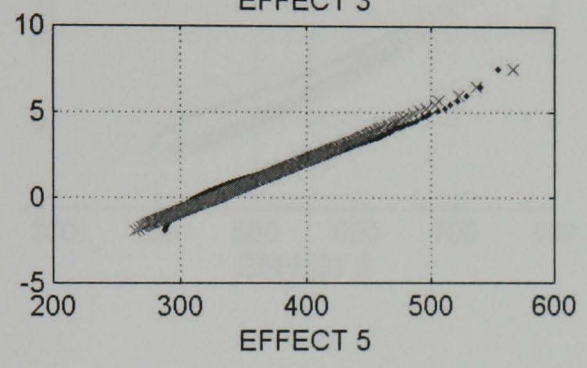
EFFECT 5

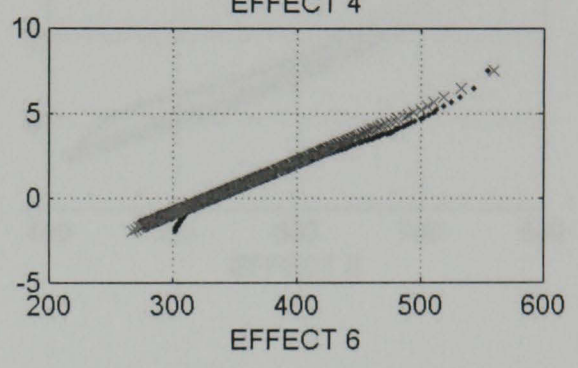
EFFECT 6

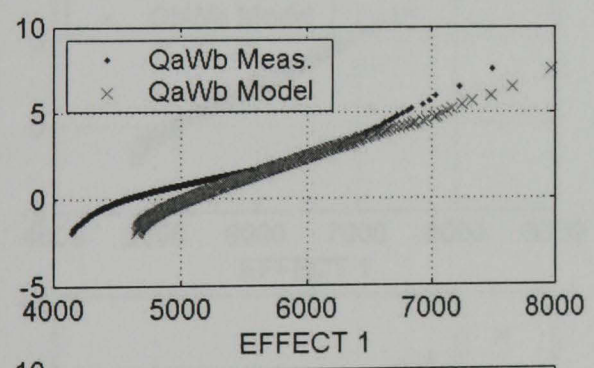
QaWb Meas.
QaWb Model
EFFECT 1

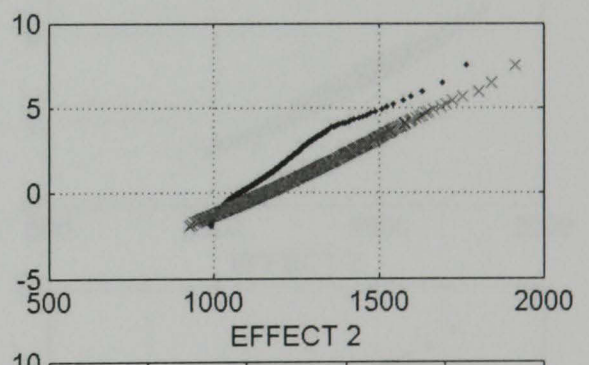
EFFECT 2

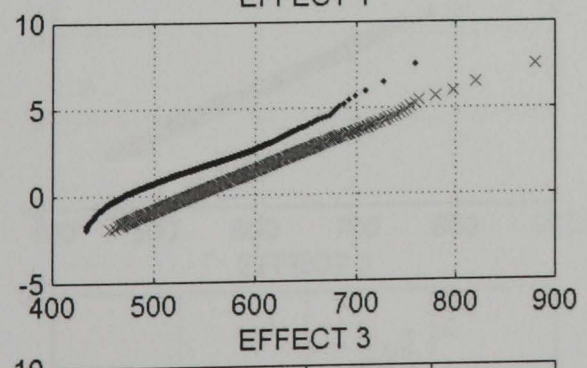
EFFECT 3

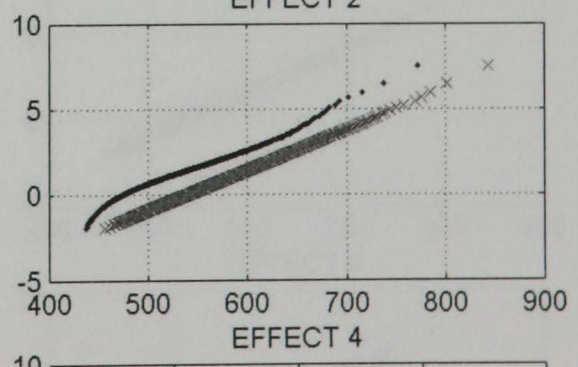
EFFECT 4

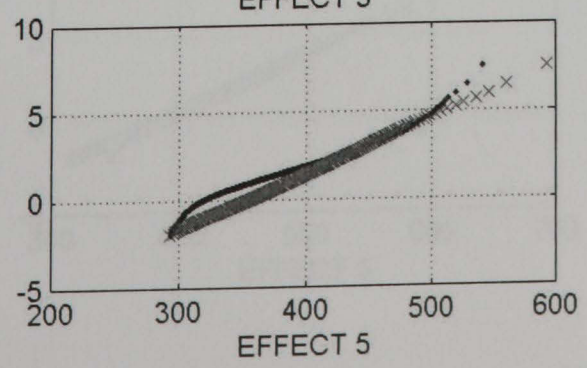
EFFECT 5

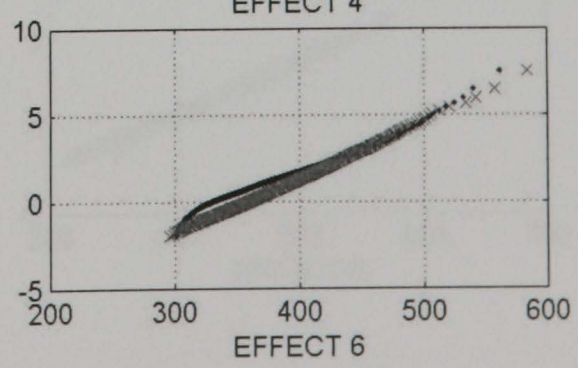
EFFECT 6

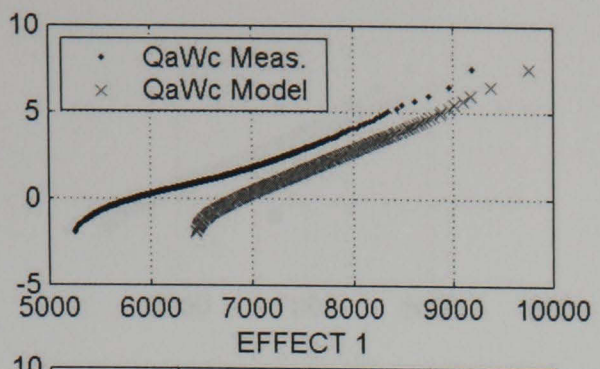
QaWc Meas.
QaWc Model
10
5
0
-5
5000
6000
7000
8000
9000
10000
EFFECT 1

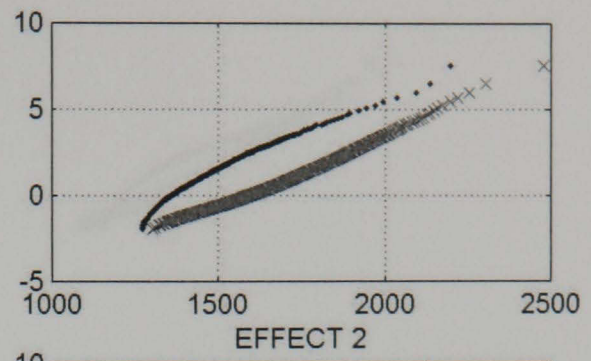
10
5
0
-5
1000
1500
2000
2500
EFFECT 2

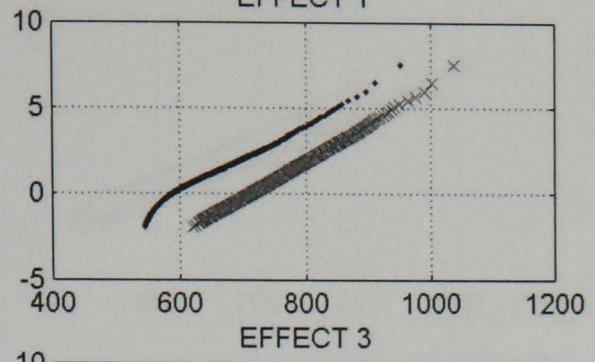
10
5
0
-5
400
600
800
1000
1200
EFFECT 3

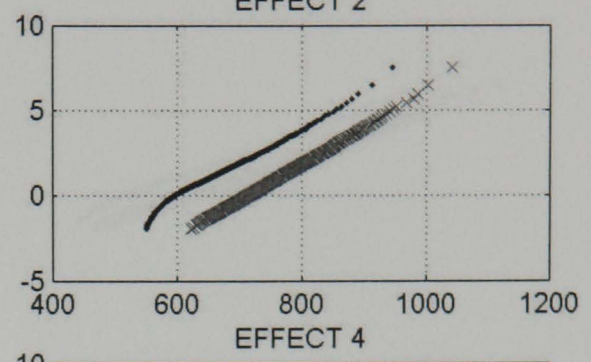
10
5
0
-5
400
600
800
1000
1200
EFFECT 4

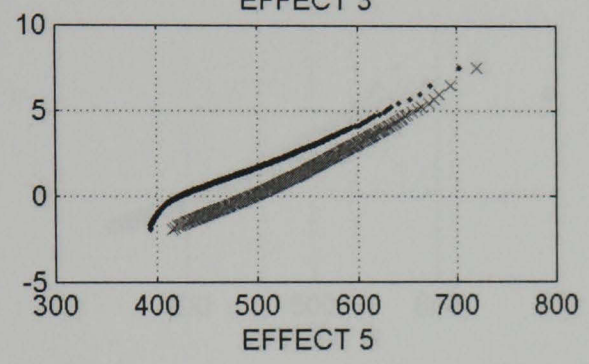
10
5
0
-5
300
400
500
600
700
800
EFFECT 5

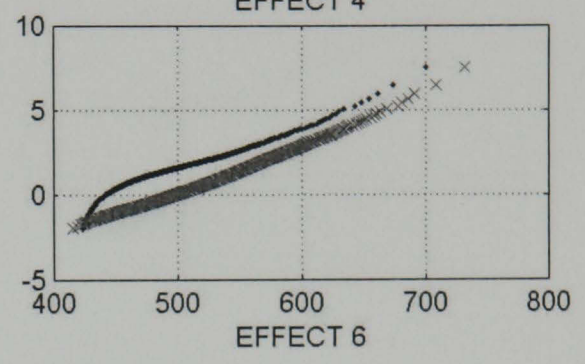
10
5
0
-5
400
500
600
700
800
EFFECT 6

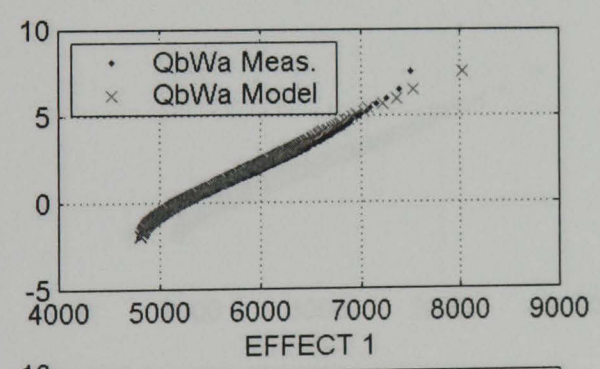
QbWa Meas.
QbWa Model
10
5
0
-5
4000
5000
6000
7000
8000
9000
EFFECT 1

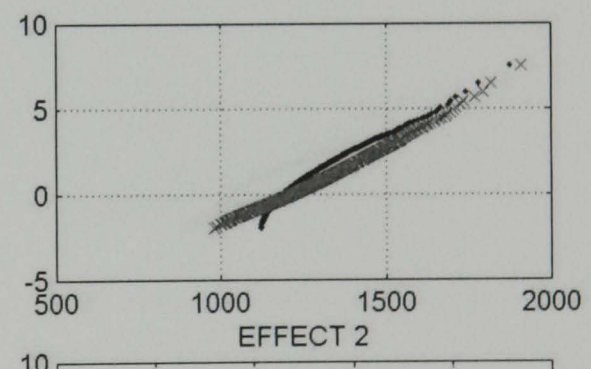
10
5
0
-5
500
1000
1500
2000
EFFECT 2

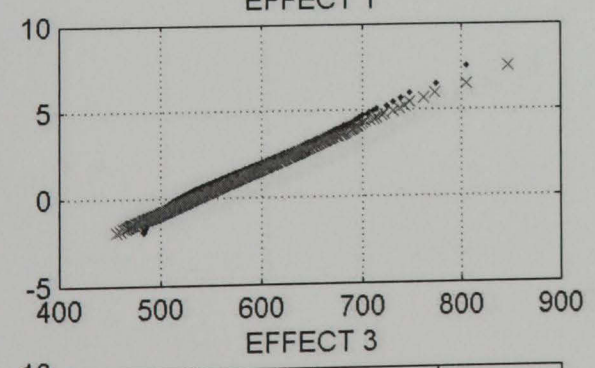
10
5
0
-5
400
500
600
700
800
900
EFFECT 3

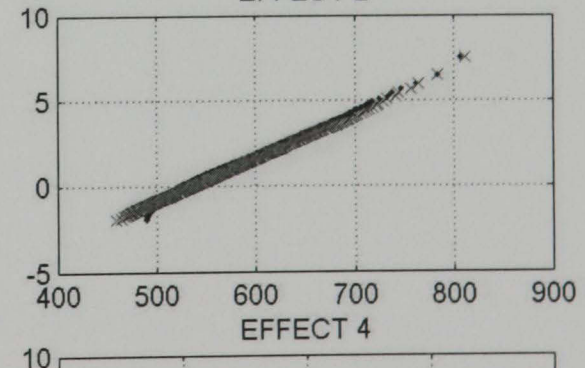
10
5
0
-5
400
500
600
700
800
900
EFFECT 4

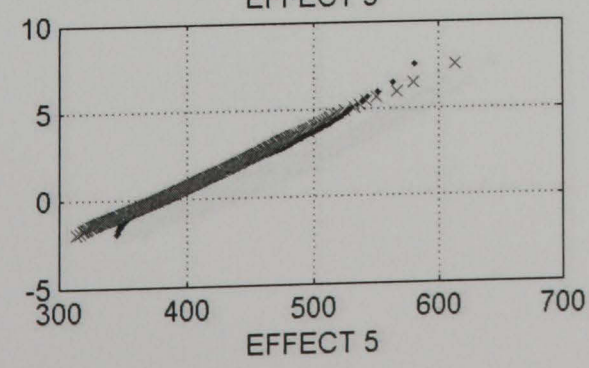
10
5
0
-5
300
400
500
600
700
EFFECT 5

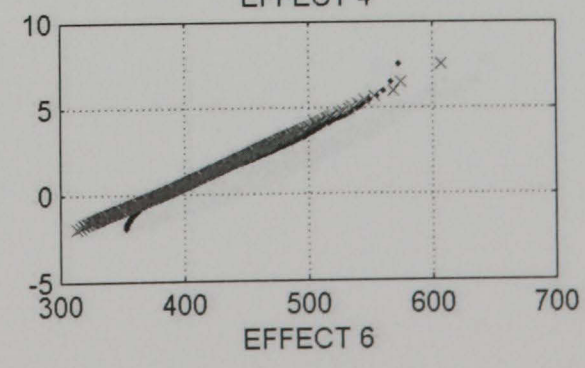
10
5
0
-5
300
400
500
600
700
EFFECT 6

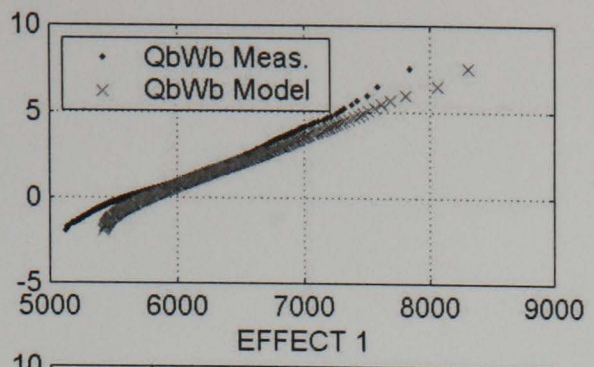
QbWb Meas.
QbWb Model
10
5
0
-5
5000
6000
7000
8000
9000
EFFECT 1

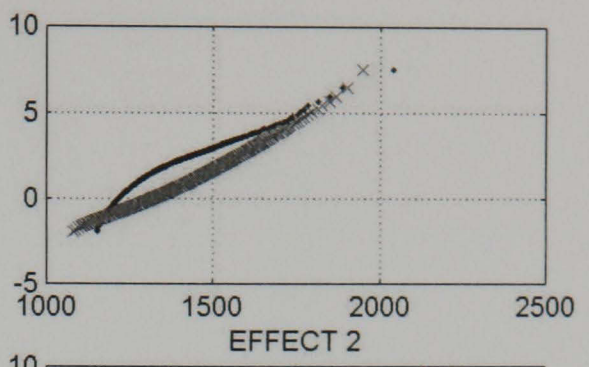
10
5
0
-5
1000
1500
2000
2500
EFFECT 2

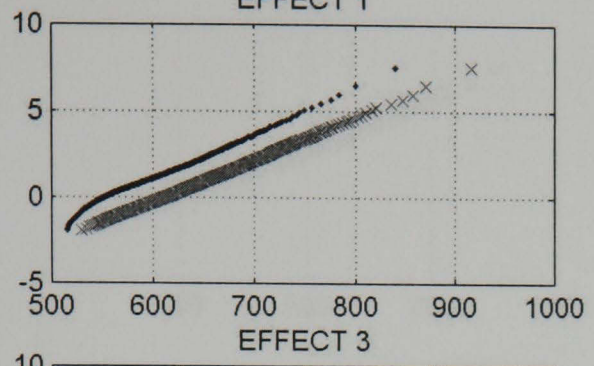
10
5
0
-5
500
600
700
800
900
1000
EFFECT 3

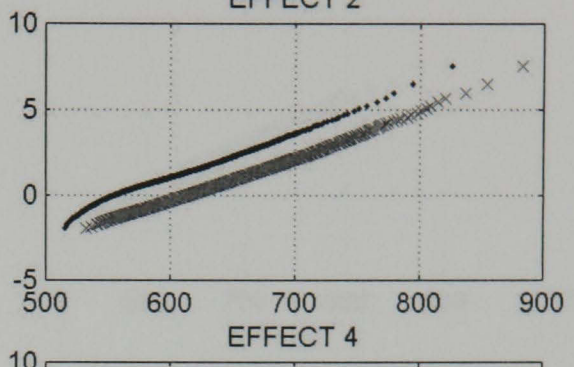
10
5
0
-5
500
600
700
800
900
EFFECT 4

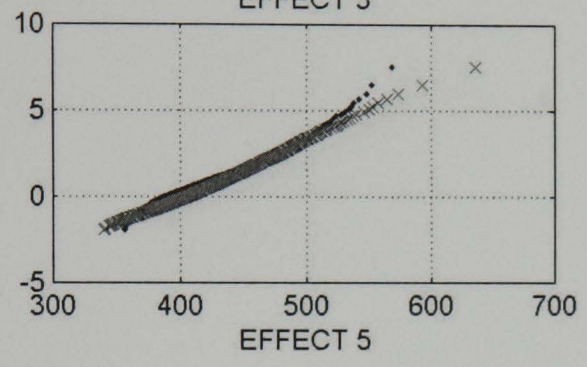
10
5
0
-5
300
400
500
600
700
EFFECT 5

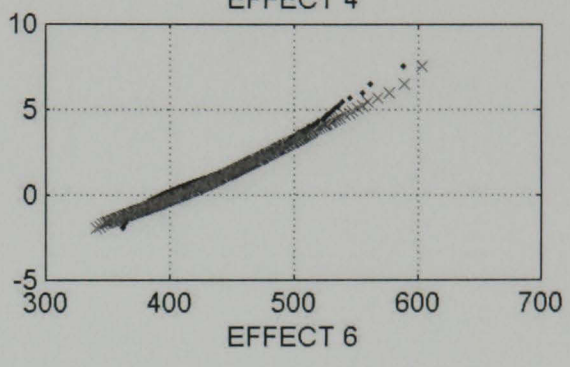
10
5
0
-5
300
400
500
600
700
EFFECT 6

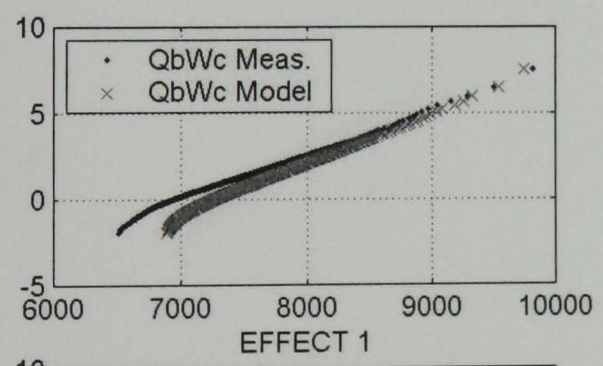
QbWc Meas.
QbWc Model
10
5
0
-5
6000
7000
8000
9000
10000
EFFECT 1

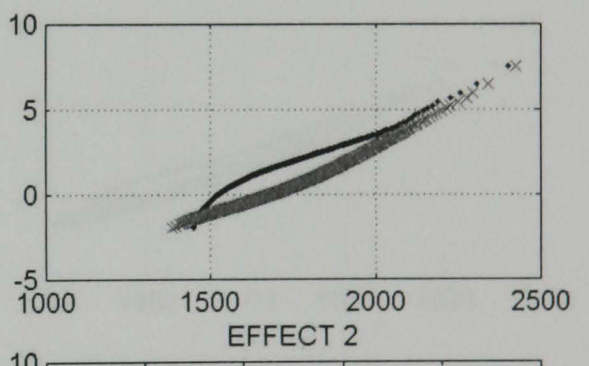
10
5
0
-5
1000
1500
2000
2500
EFFECT 2

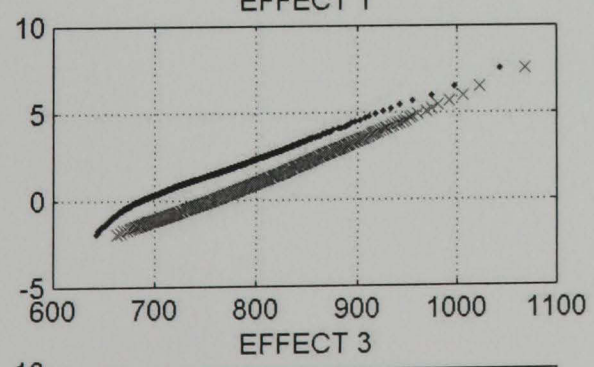
10
5
0
-5
600
700
800
900
1000
1100
EFFECT 3

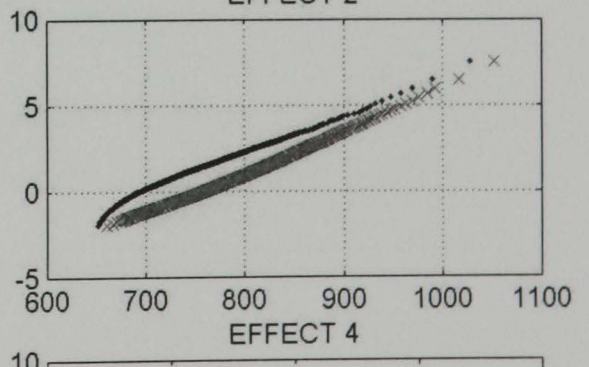
10
5
0
-5
600
700
800
900
1000
1100
EFFECT 4

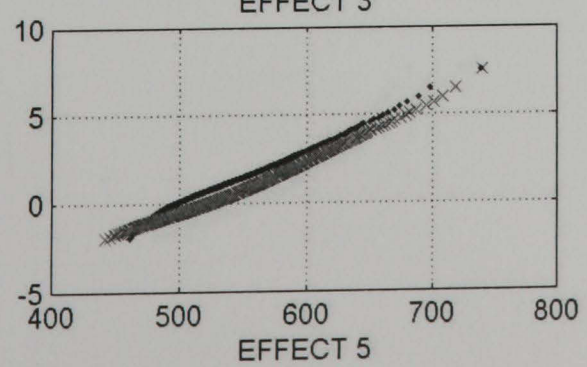
10
5
0
-5
400
500
600
700
800
EFFECT 5

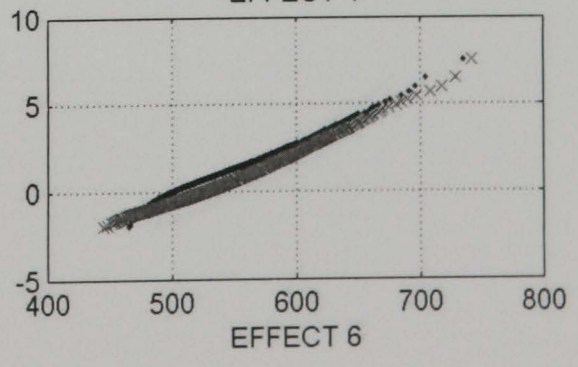
10
5
0
-5
400
500
600
700
800
EFFECT 6

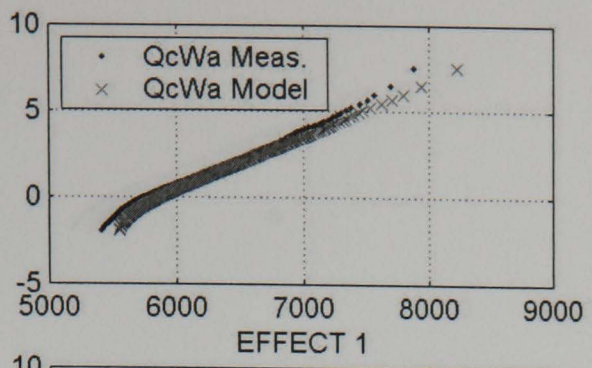

EFFECT 1

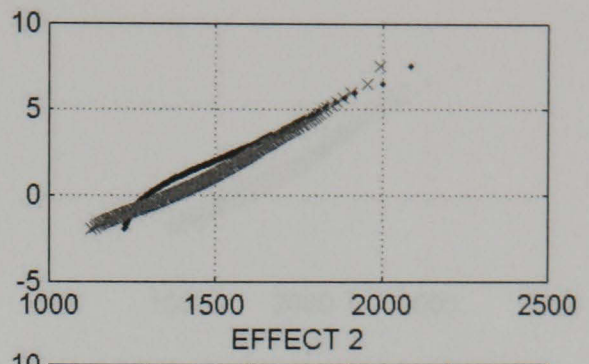

EFFECT 2

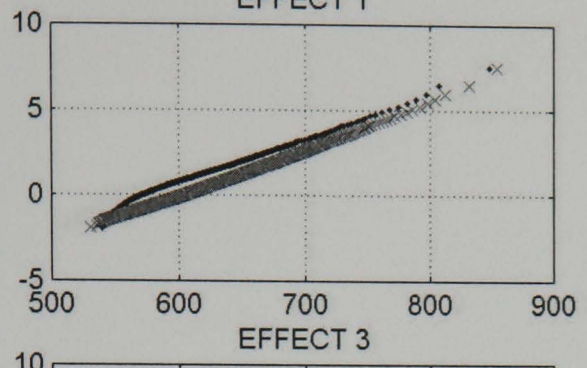

EFFECT 3

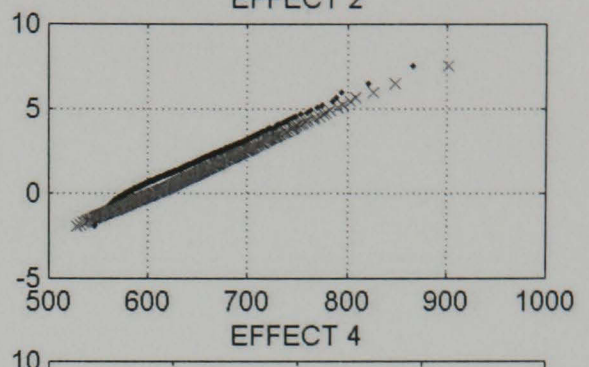

EFFECT 4

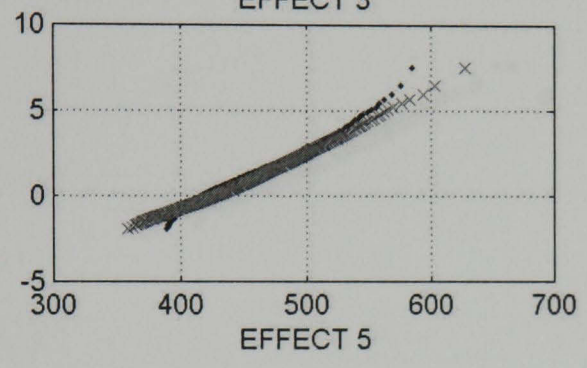

EFFECT 5

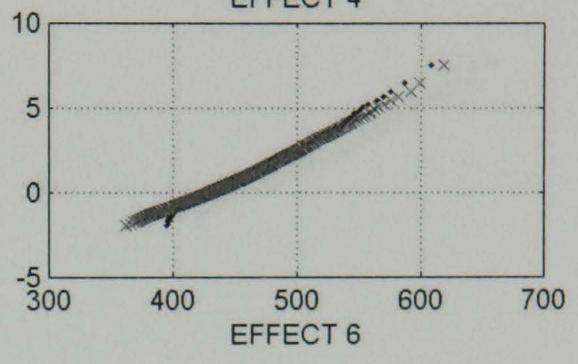

EFFECT 6

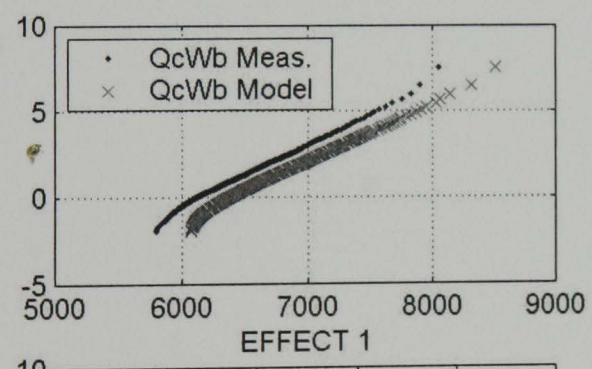

EFFECT 1

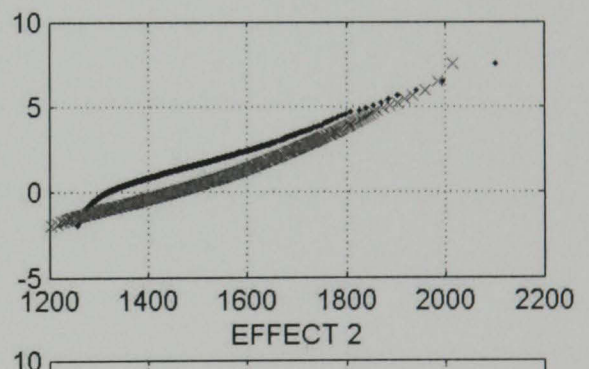

EFFECT 2

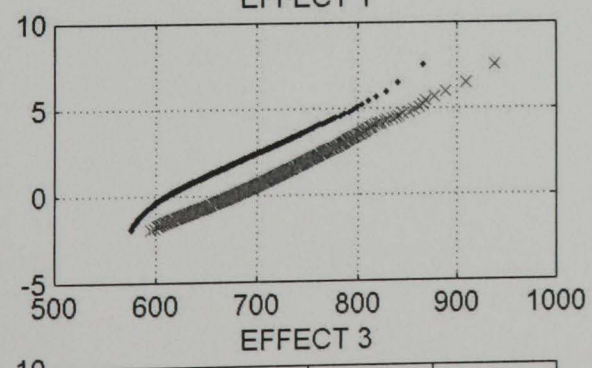

EFFECT 3

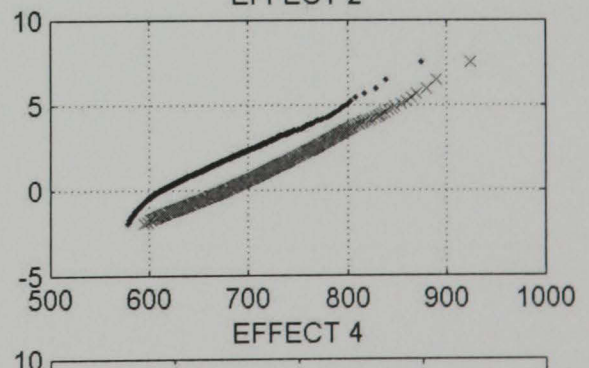

EFFECT 4

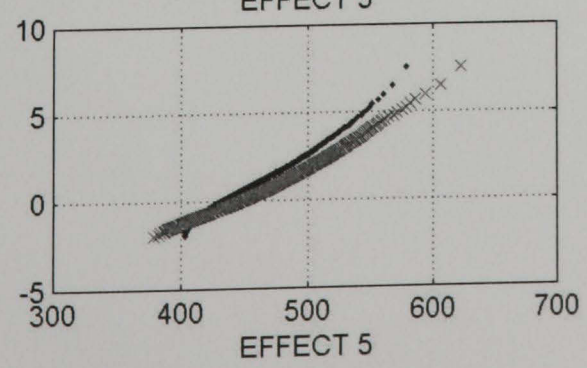

EFFECT 5

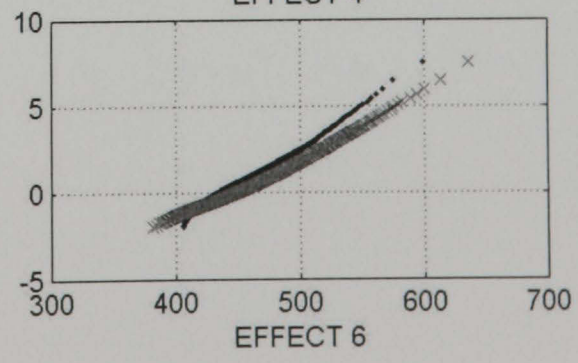

EFFECT 6

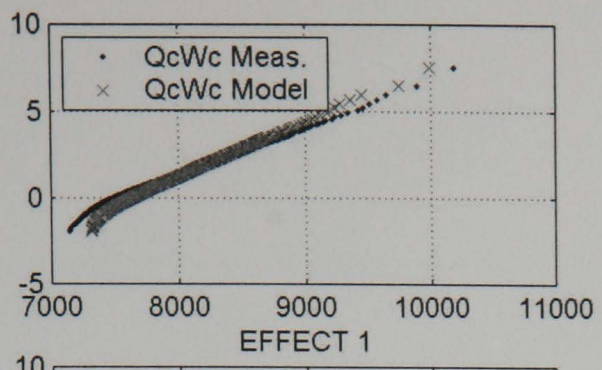
QcWc Meas.
QcWc Model
10
5
0
-5
7000
8000
9000
10000
11000
EFFECT 1

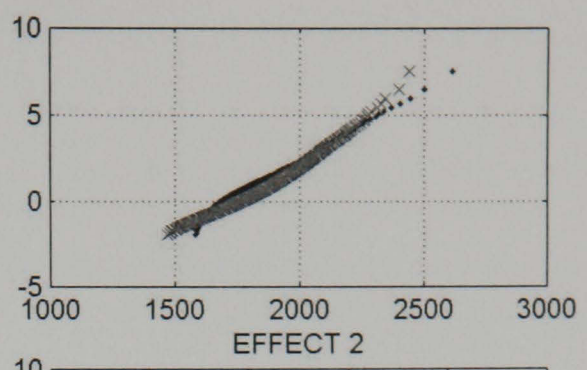
10
5
0
-5
1000
1500
2000
2500
3000
EFFECT 2

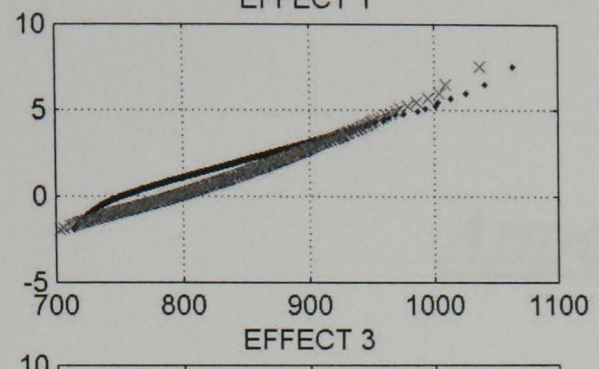
10
5
0
-5
700
800
900
1000
1100
EFFECT 3

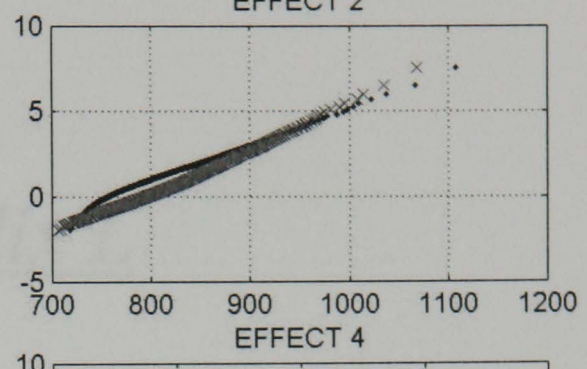
10
5
0
-5
700
800
900
1000
1100
1200
EFFECT 4

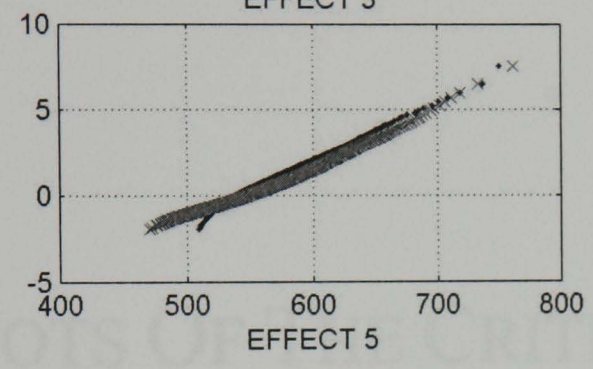
10
5
0
-5
400
500
600
700
800
EFFECT 5

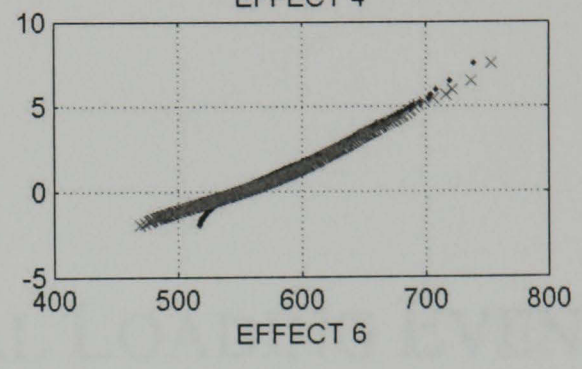
10
5
0
-5
400
500
600
700
800
EFFECT 6

Appendix L

Plots Of The Critical Loading Events For Unidirectional Traffic

Appendix L PLOTS OF THE CRITICAL LOADING EVENTS FOR UNIDIRECTIONAL TRAFFIC

Traffic type 'A196' - Direction 1 – Set 0

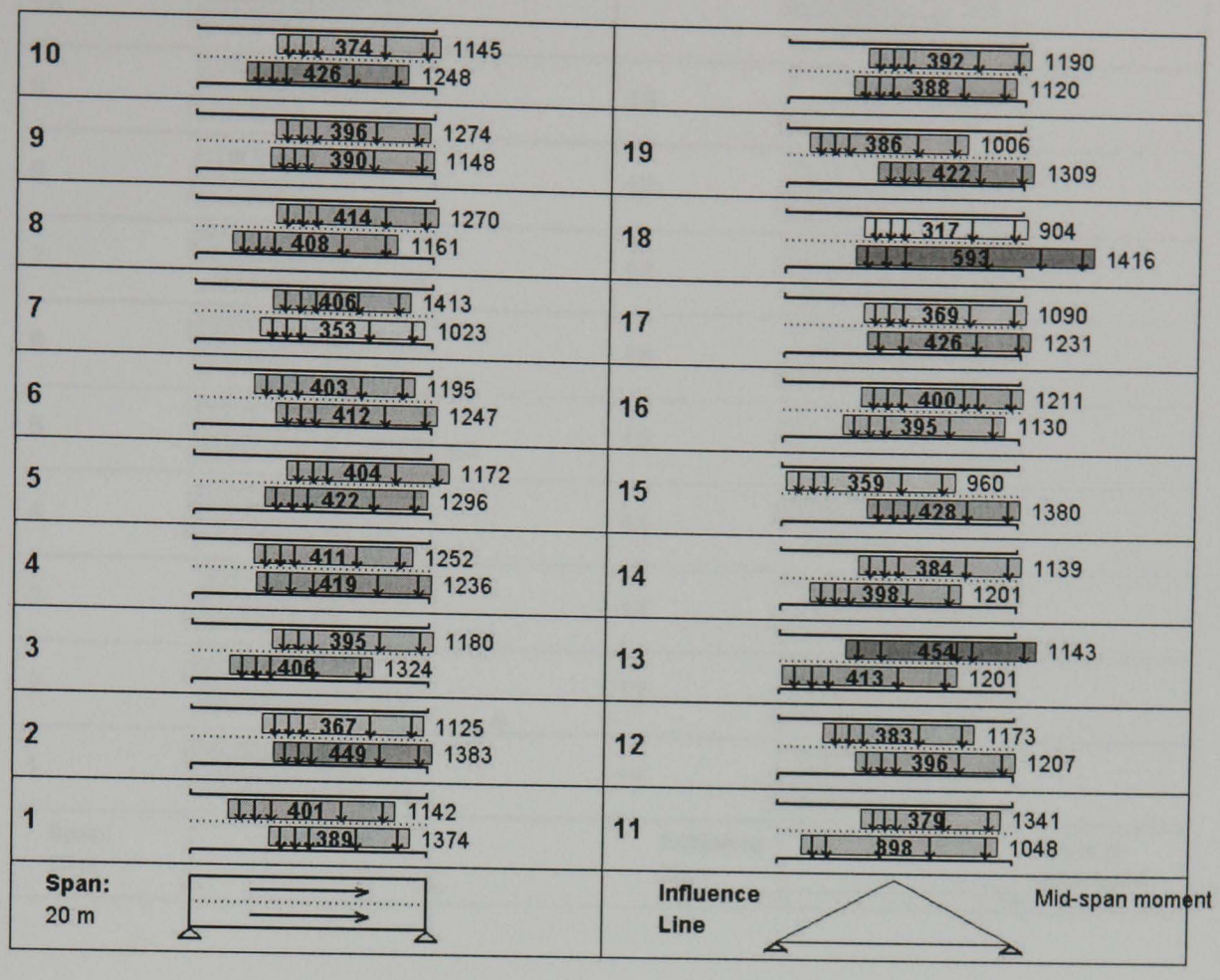

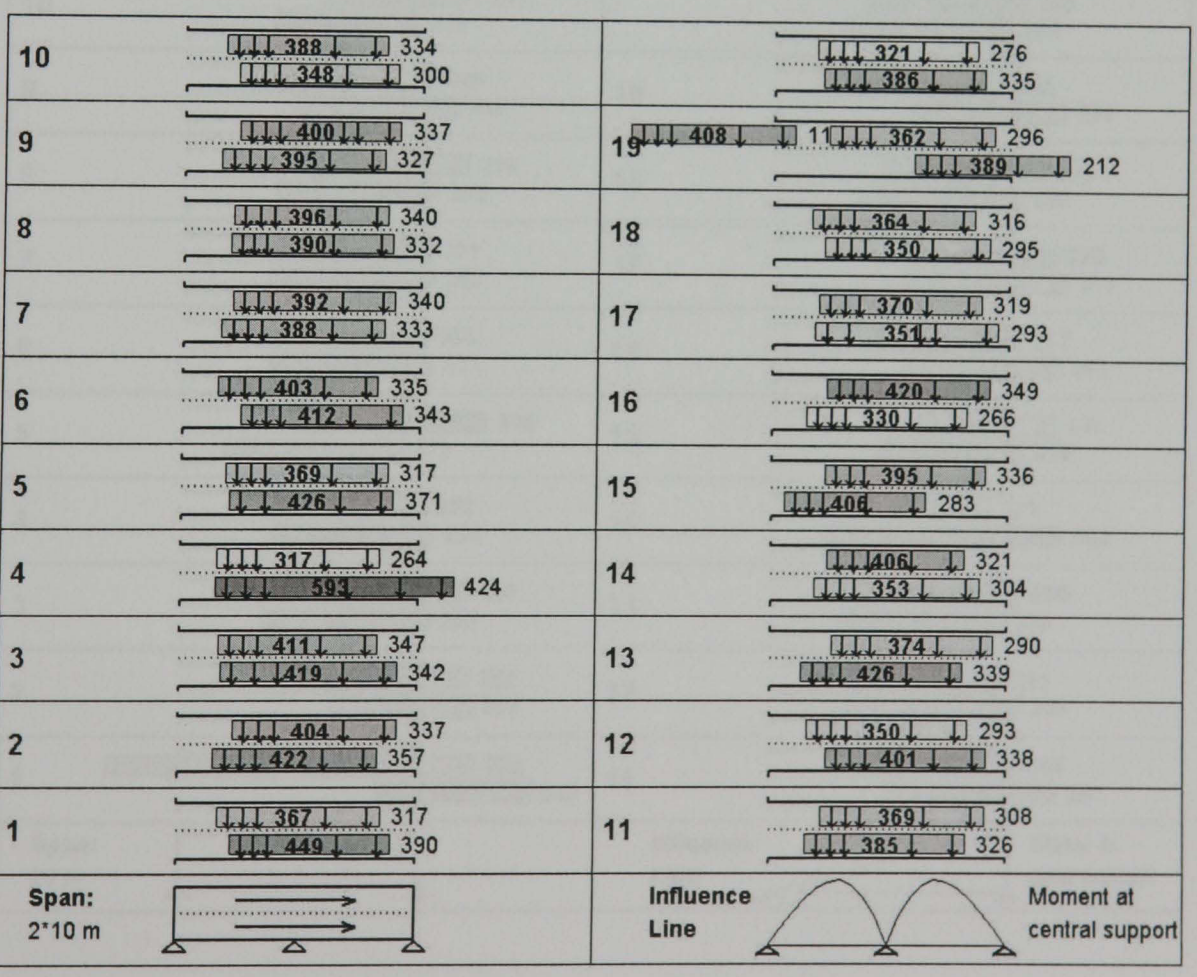

10	400 267 395 278		401 285 389 226
9	406 300 353 256	19	384 207 398 304
8	392 278 388 279	18	346 210 402 308
7	403 301 412 258	17	350 262 401 258
6	369 267 426 300	16	414 233 408 295
5	317 226 593 350	15	388 288 348 241
4	396 299 390 284	14	383 295 396 235
3	404 271 422 314	13	395 221 406 319
2	367 276 449 310	12	369 259 385 283
1	411 310 419 283	11	374 233 426 310
Span: 20 m	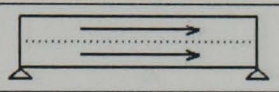	Influence Line	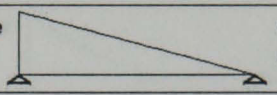 Shear at left support

10	395 259 406 239		392 250 388 230
9	403 255 412 243	19	386 210 422 274
8	374 218 426 282	18	404 217 422 267
7	396 251 390 252	17	406 270 353 219
6	369 230 426 271	16	383 247 396 243
5	454 296 413 212	15	346 216 402 274
4	367 222 449 290	14	317 171 593 320
3	414 258 408 260	13	400 260 395 236
2	401 252 389 267	12	411 231 419 264
1	408 41 362 222 389 215	11	398 256 384 240
Span: 20 m	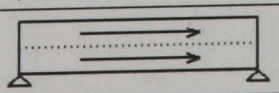	Influence Line	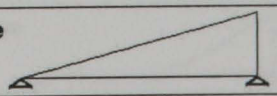 Shear at right support

10	317 137 593 198		417 207 298 102
9	369 154 385 183	19	414 166 396 149
8	392 167 388 172	18	400 185 395 126
7	406 183 353 162	17	403 201 412 116
6	369 167 426 179	16	382 176 402 142
5	413 200 274 151	15	359 109 428 217
4	404 191 422 165	14	388 188 348 139
3	411 209 419 156	13	415 172 388 155
2	367 148 449 220	12	379 214 398 114
1	396 198 390 179	11	411 176 385 153
Span: 2*10 m		Influence Line	Shear at left support

10	396 188 390 146		393 165 368 140
9	359 126 428 207	19	314 125 386 180
8	384 160 398 178	18	338 144 368 162
7	411 164 419 177	17	415 197 388 117
6	369 161 426 181	16	366 139 408 178
5	401 155 389 189	15	408 -14 362 134 389 192
4	403 162 412 183	14	406 183 353 138
3	454 172 413 182	13	419 196 302 124
2	395 167 406 192	12	404 184 422 139
1	367 170 449 206	11	388 166 348 159
Span: 2*10 m		Influence Line	Shear at right support

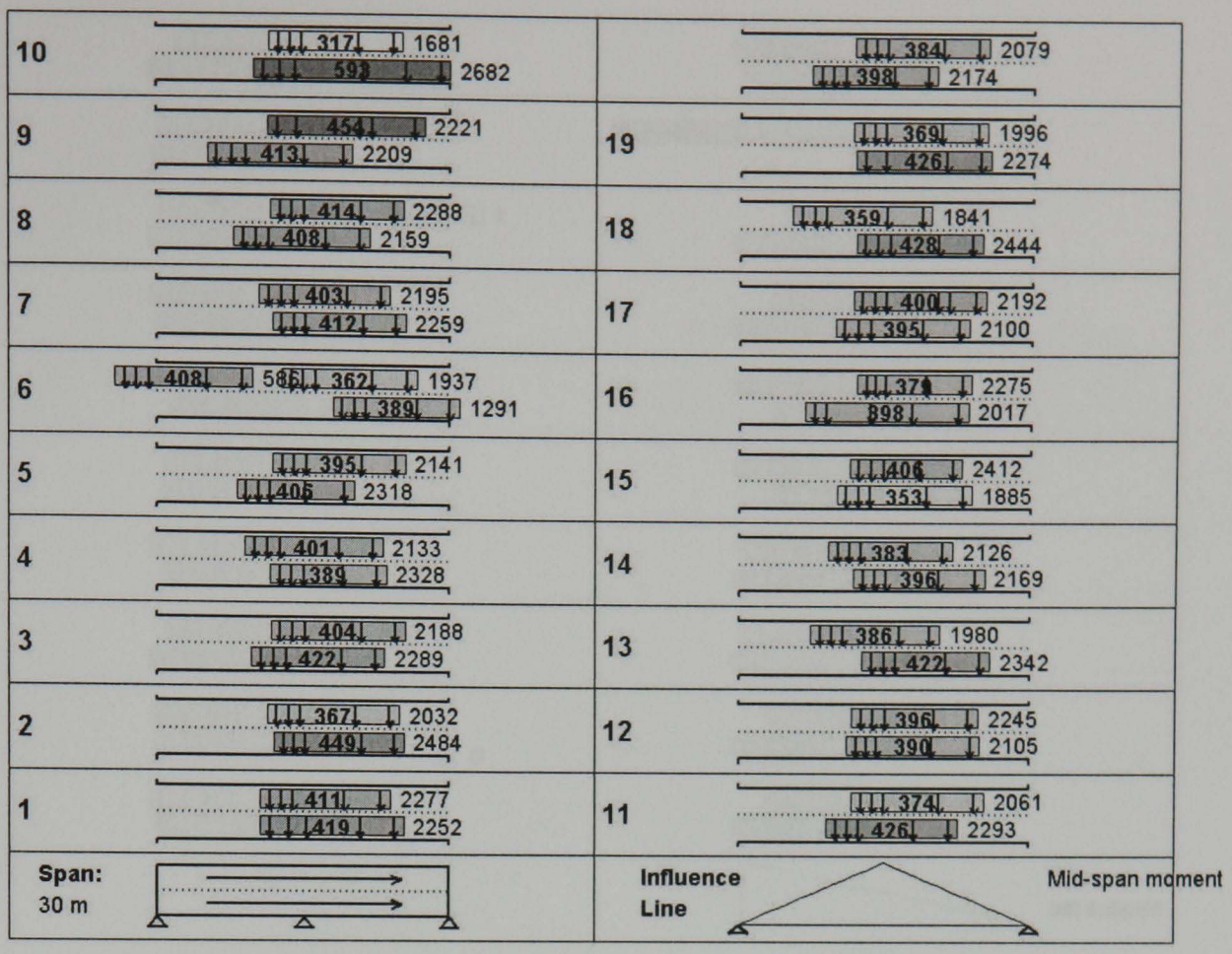
10
317 1681
593 2682
9
454 2221
413 2209
8
414 2288
408 2159
7
403 2195
412 2259
6
408 586 362 1937
389 1291
5
395 2141
405 2318
4
401 2133
389 2328
3
404 2188
422 2289
2
367 2032
449 2484
1
411 2277
419 2252
Span:
30 m
384 2079
398 2174
19
369 1996
426 2274
18
359 1841
428 2444
17
400 2192
395 2100
16
374 2275
398 2017
15
406 2412
353 1885
14
383 2126
396 2169
13
386 1980
422 2342
12
396 2245
390 2105
11
374 2061
426 2293
Influence
Line
Mid-span moment

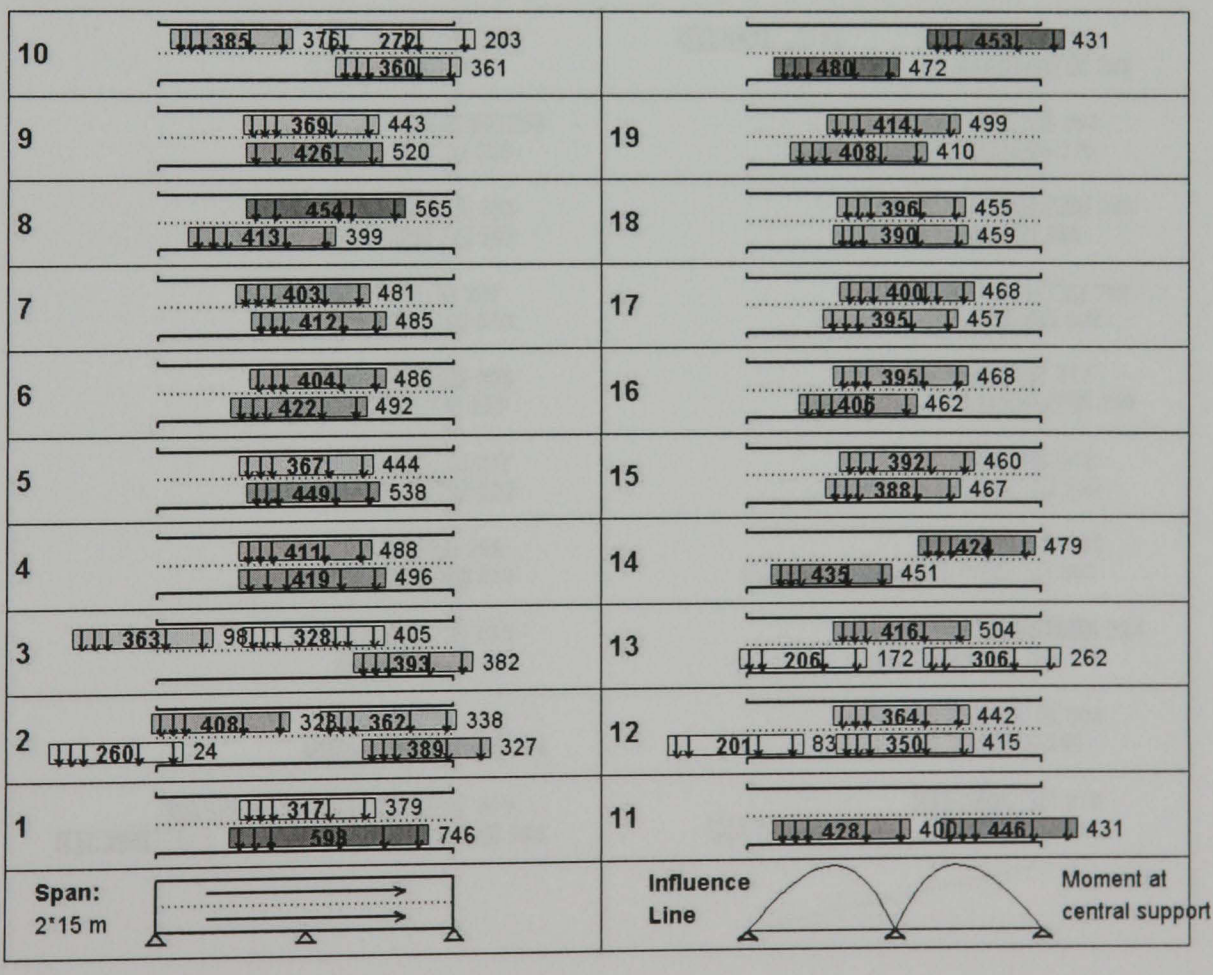
10
385 376 272 203
360 361
9
369 443
426 520
8
454 565
413 399
7
403 481
412 485
6
404 486
422 492
5
367 444
449 538
4
411 488
419 496
3
363 98 328 405
393 382
2
408 328 362 338
260 24 389 327
1
317 379
593 746
Span:
2*15 m
453 431
480 472
19
414 499
408 410
18
396 455
390 459
17
400 468
395 457
16
395 468
406 462
15
392 460
388 467
14
424 479
435 451
13
416 504
206 172 306 262
12
364 442
201 83 350 415
11
428 400 446 431
Influence
Line
Moment at
central support

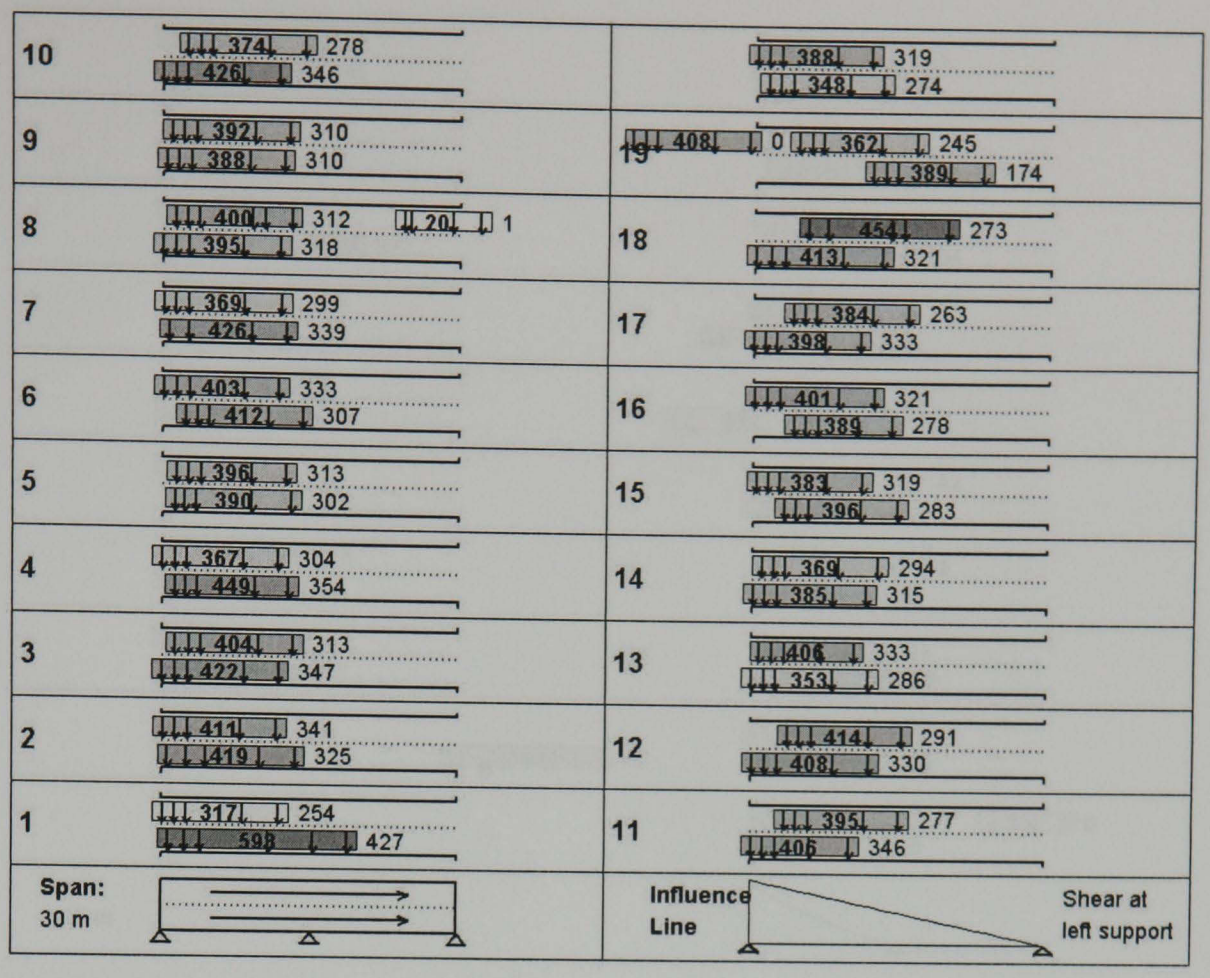
10
374 278
426 346
9
392 310
388 310
8
400 312
20 1
395 318
7
369 299
426 339
6
403 333
412 307
5
396 313
390 302
4
367 304
449 354
3
404 313
422 347
2
411 341
419 325
1
317 254
593 427
Span:
30 m
388 319
348 274
19
408 0
362 245
389 174
18
454 273
413 321
17
384 263
398 333
16
401 321
389 278
15
383 319
396 283
14
369 294
385 315
13
406 333
353 286
12
414 291
408 330
11
395 277
406 346
Influence
Line
Shear at
left support

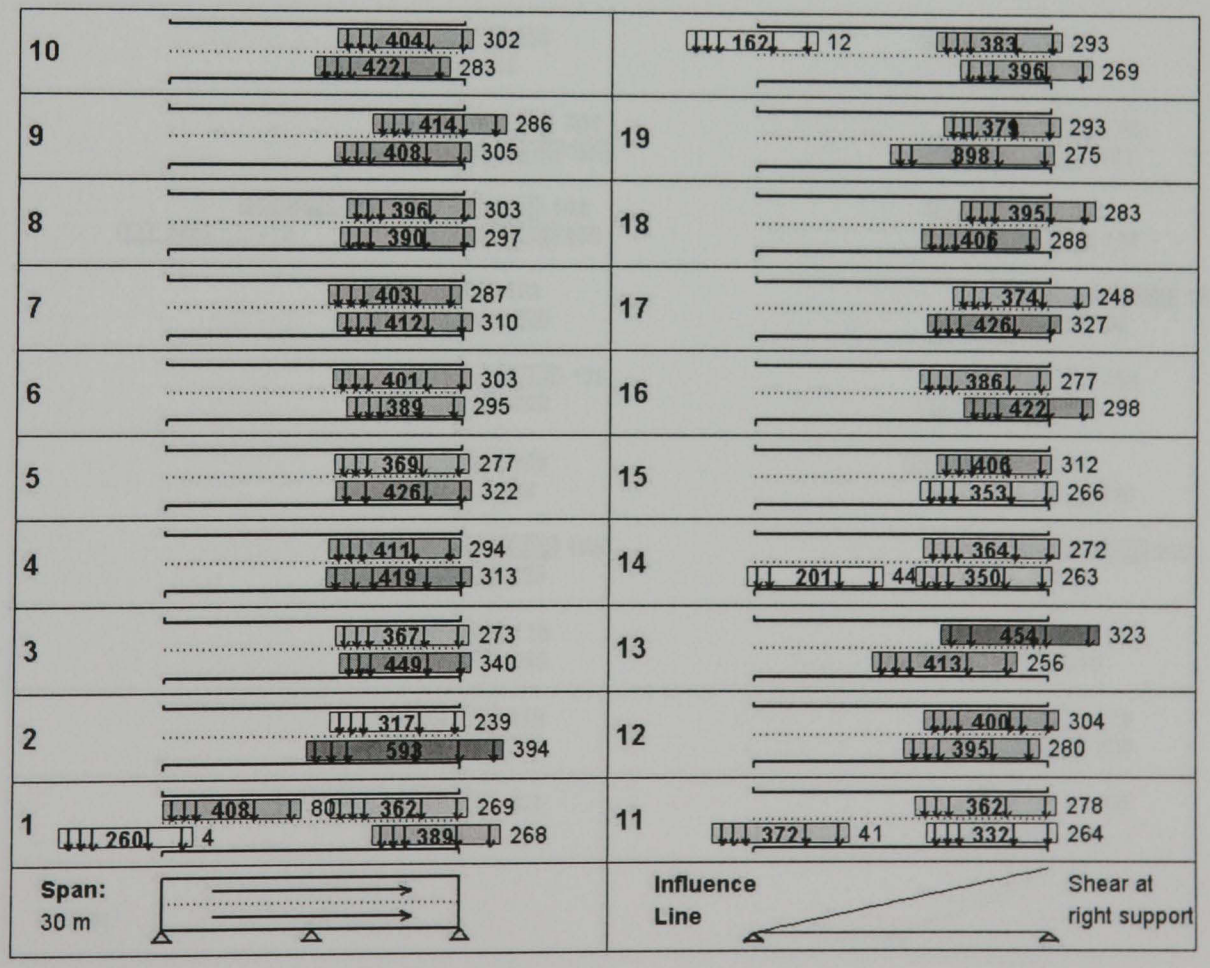
10
404 302
422 283
9
414 286
408 305
8
396 303
390 297
7
403 287
412 310
6
401 303
389 295
5
369 277
426 322
4
411 294
419 313
3
367 273
449 340
2
317 239
593 394
1
408 80 362 269
260 4 389 268
Span:
30 m
162 12 383 293
396 269
19
379 293
398 275
18
395 283
406 288
17
374 248
426 327
16
386 277
422 298
15
406 312
353 266
14
364 272
201 44 350 263
13
454 323
413 256
12
400 304
395 280
11
362 278
372 41 332 264
Influence
Line
Shear at
right support

10	403 251 412 184		346 144 402 258
9	369 206 385 233	19	350 217 401 188
8	317 181 598 260	18	383 244 396 154
7	392 215 388 218	17	379 260 398 153
6	406 244 353 208	16	413 252 274 163
5	369 216 426 238	15	395 142 405 273
4	404 208 422 260	14	374 166 426 252
3	367 230 449 241	13	396 214 390 199
2	396 249 390 231 380 -1	12	388 238 348 188
1	411 260 419 217	11	400 209 20 0 395 226
Span: 2*15 m	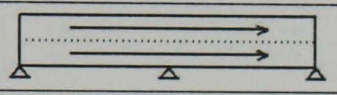	Influence Line	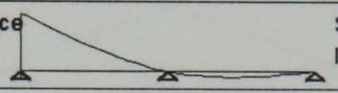 Shear at left support

10	414 208 408 184		386 149 422 224
9	411 201 419 200	19	379 223 398 151
8	408 4 362 142 260 -12 389 206	18	382 180 376 194
7	403 173 412 225	17	454 181 413 195
6	384 179 398 222	16	406 204 356 178
5	401 208 389 196	15	359 148 428 230
4	395 178 406 229	14	415 210 388 168
3	396 113 390 199	13	374 171 426 210
2	367 179 449 239	12	369 173 426 220
1	406 241 353 180	11	346 185 402 208
Span: 2*15 m	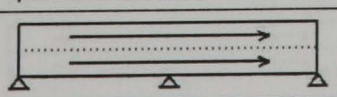	Influence Line	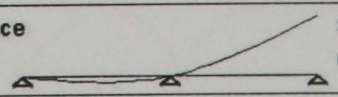 Shear at right support

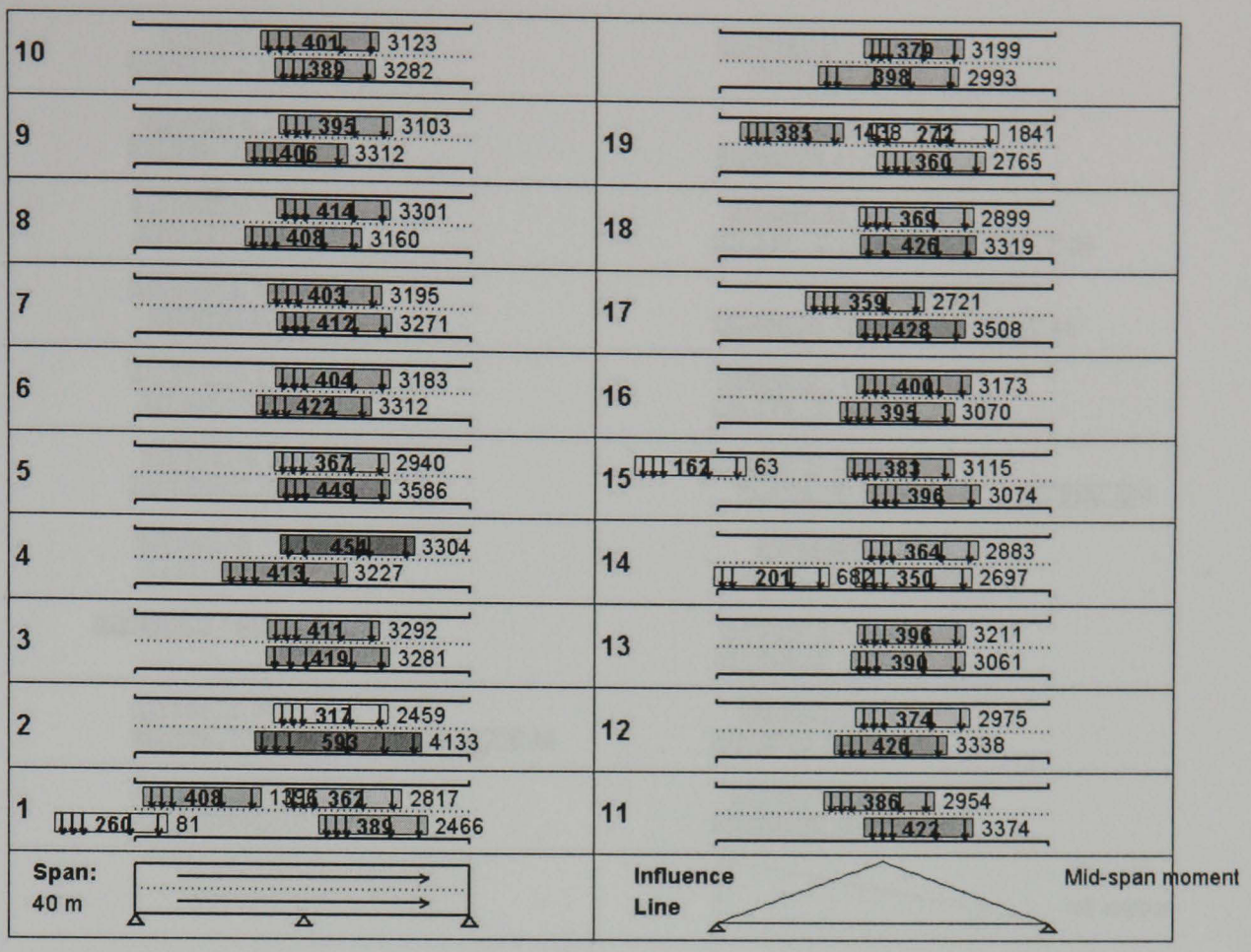
10
401 3123
389 3282
9
395 3103
406 3312
8
414 3301
408 3160
7
403 3195
412 3271
6
404 3183
422 3312
5
367 2940
449 3586
4
450 3304
413 3227
3
411 3292
419 3281
2
317 2459
593 4133
1
408 1296 361 2817
260 81 389 2466
Span:
40 m
Influence
Line
Mid-span moment
379 3199
398 2993
19
385 1438 272 1841
360 2765
18
369 2899
426 3319
17
359 2721
428 3508
16
400 3173
395 3070
15
162 63 383 3115
396 3074
14
364 2883
201 682 350 2697
13
396 3211
390 3061
12
374 2975
426 3338
11
386 2954
422 3374

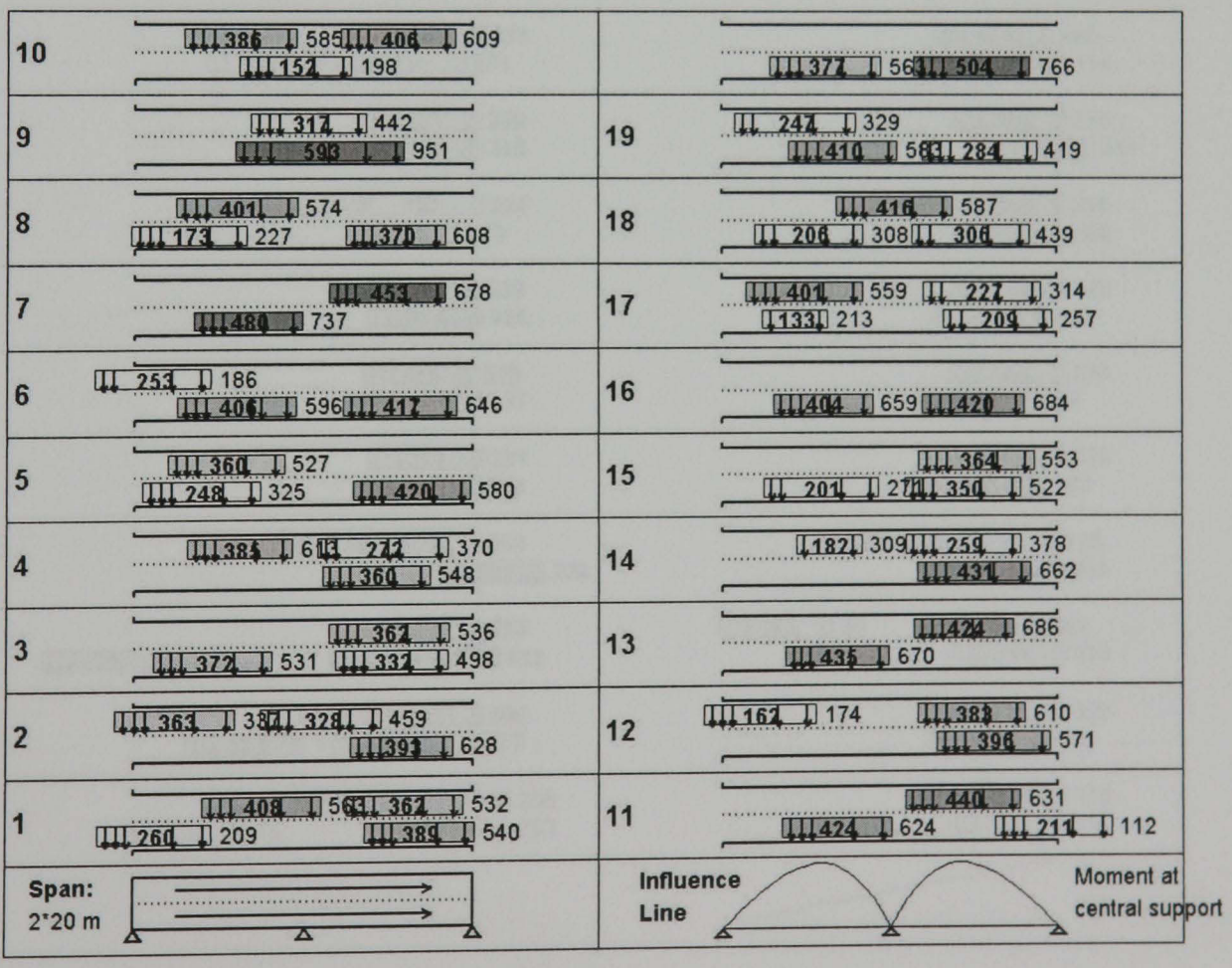
10
386 585 406 609
152 198
9
317 442
593 951
8
401 574
173 227 370 608
7
453 678
480 737
6
253 186
406 596 417 646
5
360 527
248 325 420 580
4
385 613 272 370
360 548
3
362 536
372 531 332 498
2
363 387 328 459
393 628
1
408 563 362 532
260 209 389 540
Span:
2*20 m
19
247 329
410 583 284 419
18
416 587
206 308 306 439
17
401 559 227 314
133 213 209 257
16
404 659 420 684
15
364 553
201 270 350 522
14
182 309 259 378
431 662
13
424 686
435 670
12
162 174 383 610
396 571
11
440 631
424 624 211 112
Influence
Line
Moment at
central support

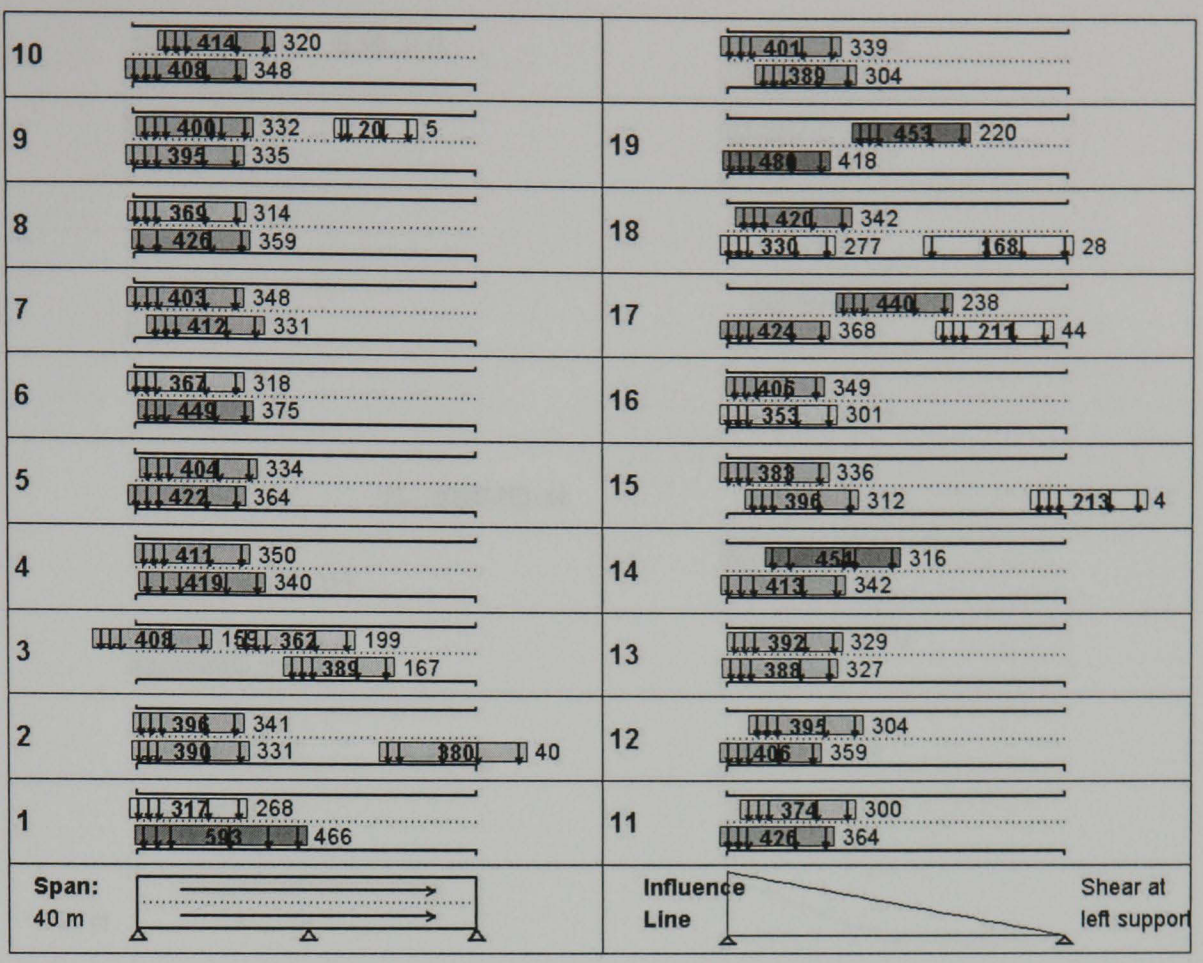
10
414 320
408 348
401 339
389 304
9
400 332
20 5
395 335
453 220
480 418
8
369 314
426 359
420 342
330 277
168 28
7
403 348
412 331
440 238
424 368
211 44
6
367 318
449 375
406 349
353 301
5
404 334
422 364
383 336
396 312
213 4
4
411 350
419 340
458 316
413 342
3
408 199
362 167
392 329
388 327
2
396 341
390 331
380 40
395 304
406 359
1
317 268
593 466
374 300
426 364
Span:
40 m
Influence
Line
Shear at
left support

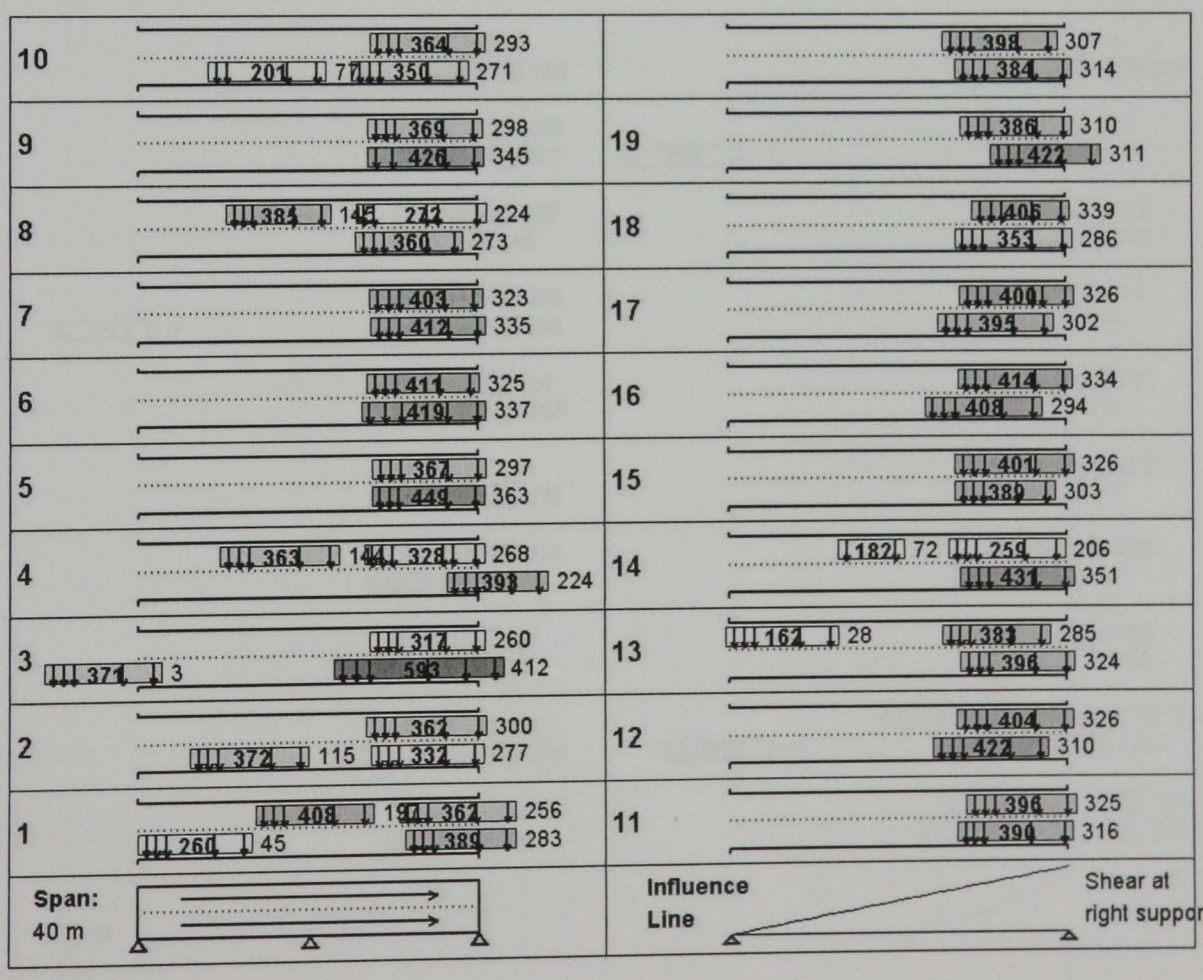
10
364 293
201 77
350 271
398 307
384 314
9
369 298
426 345
386 310
422 311
8
384 145
272 224
360 273
406 339
353 286
7
403 323
412 335
400 326
395 302
6
411 325
419 337
414 334
408 294
5
367 297
449 363
401 326
389 303
4
363 144
328 268
393 224
182 72
259 206
431 351
3
317 260
371 3
593 412
162 28
383 285
396 324
2
362 300
372 115
331 277
404 326
422 310
1
408 194
362 256
260 45
389 283
398 325
390 316
Span:
40 m
Influence
Line
Shear at
right support

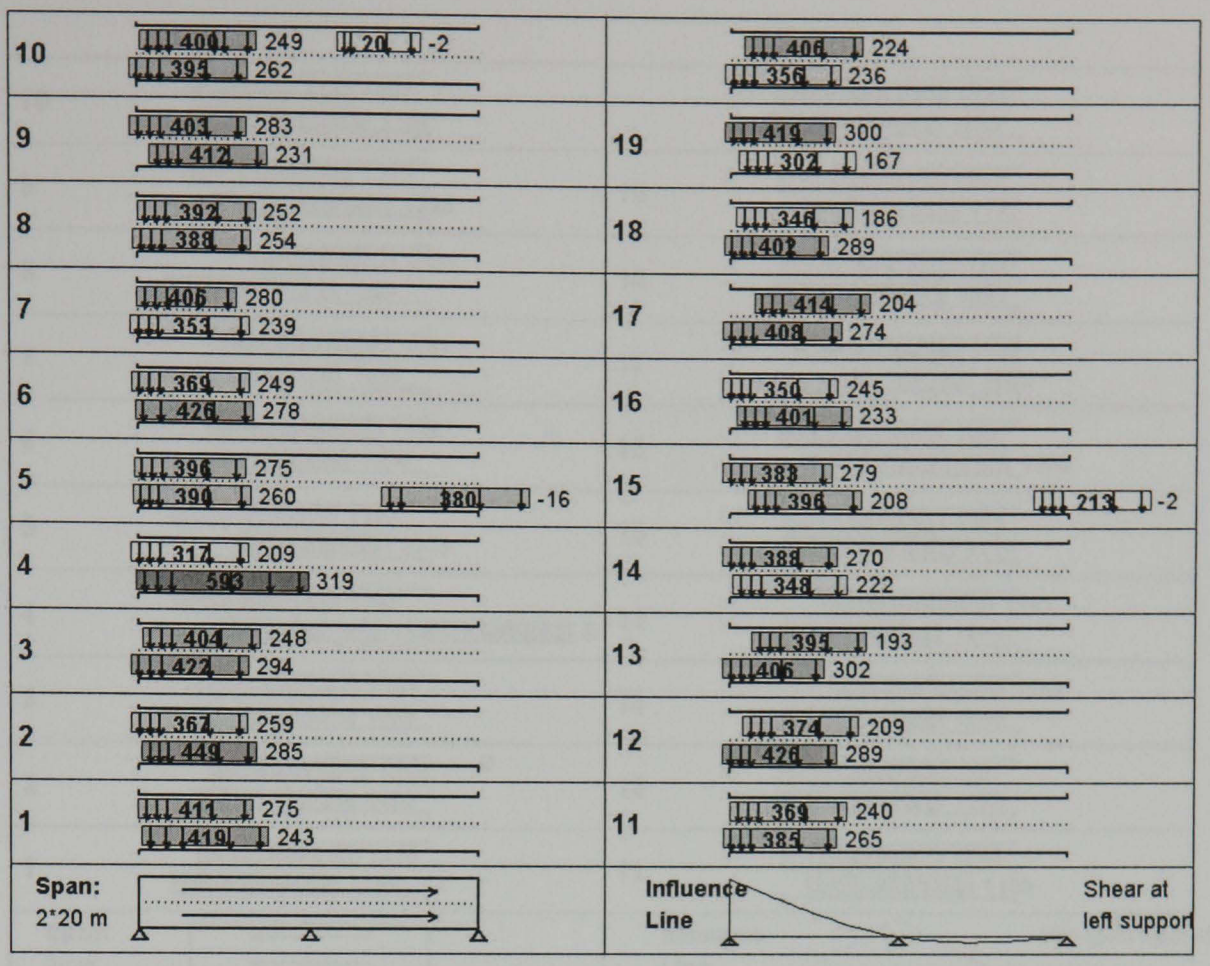
10
400 249
20 -2
395 262
406 224
356 236
9
403 283
412 231
419 300
302 167
8
392 252
388 254
346 186
402 289
7
405 280
353 239
414 204
408 274
6
369 249
426 278
350 245
401 233
5
396 275
390 260
380 -16
383 279
396 208
213 -2
4
317 209
593 319
388 270
348 222
3
404 248
422 294
395 193
406 302
2
367 259
449 285
374 209
426 289
1
411 275
419 243
369 240
385 265
Span:
2*20 m
Influence
Line
Shear at
left support

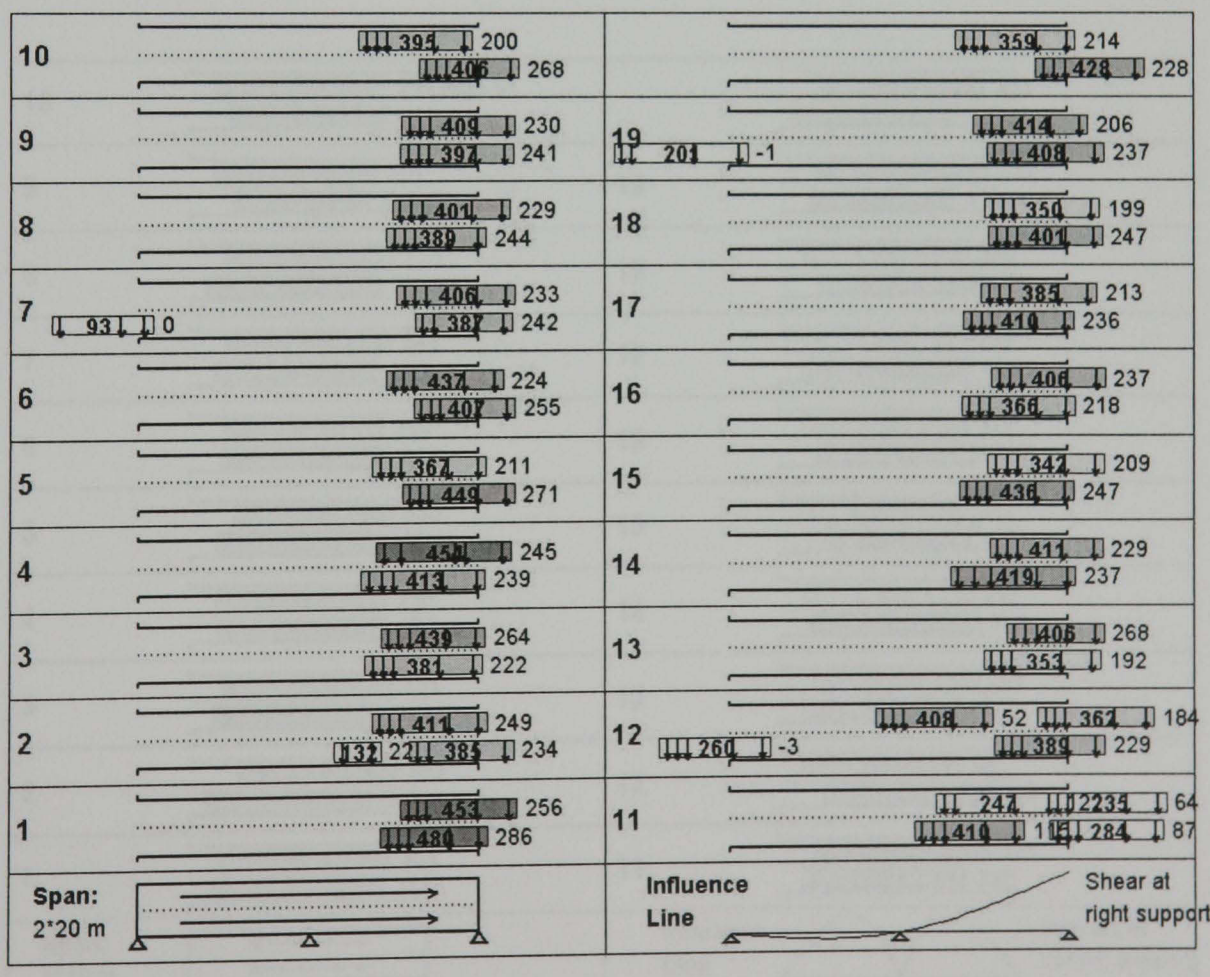
10
395 200
406 268
359 214
428 228
9
409 230
397 241
19
414 206
201 -1
408 237
8
401 229
389 244
350 199
401 247
7
406 233
93 0
387 242
385 213
410 236
6
437 224
407 255
406 237
366 218
5
367 211
449 271
342 209
436 247
4
450 245
413 239
411 229
419 237
3
439 264
381 222
406 268
353 192
2
411 249
132 22
385 234
408 52
362 184
260 -3
389 229
1
453 256
480 286
247
2235 64
410
284 87
Span:
2*20 m
Influence
Line
Shear at
right support

Traffic type 'A196' - Direction 2 – Set 0

10	396 1297 403 1192		382 1121 426 1288
9	409 1262 439 1223	19	414 1247 383 1177
8	409 1301 396 1204	18	384 1100 435 1327
7	508 1487 424 1034	17	477 1399 291 1032
6	411 1155 400 1374	16	459 1446 391 1000
5	408 1229 418 1313	15	413 1333 396 1119
4	442 1293 409 1210 391 3	14	436 1167 402 1293
3	429 1258 414 1309	13	413 1205 397 1266
2	403 1262 434 1400	12	407 1307 413 1170
1	451 1418 432 1289	11	421 1344 396 1135
Span: 20 m	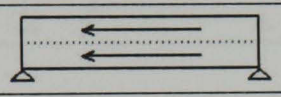	Influence Line	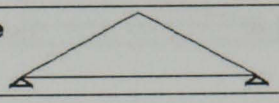 Mid-span moment

10	366 312 36 0 406 346		430 353 375 289
9	414 351 383 321	19	411 332 400 314
8	382 328 426 363	18	357 300 414 351
7	407 341 413 352	17	291 253 481 400
6	413 350 396 343	16	396 327 403 327
5	403 330 434 368	15	378 318 402 337
4	387 330 433 372	14	334 287 439 369
3	384 331 435 372	13	360 307 404 350
2	451 363 432 342	12	421 341 396 323
1	429 361 414 357	11	405 339 394 328
Span: 2*10 m	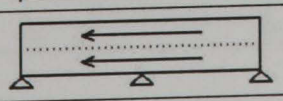	Influence Line	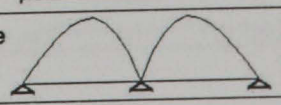 Moment at central support

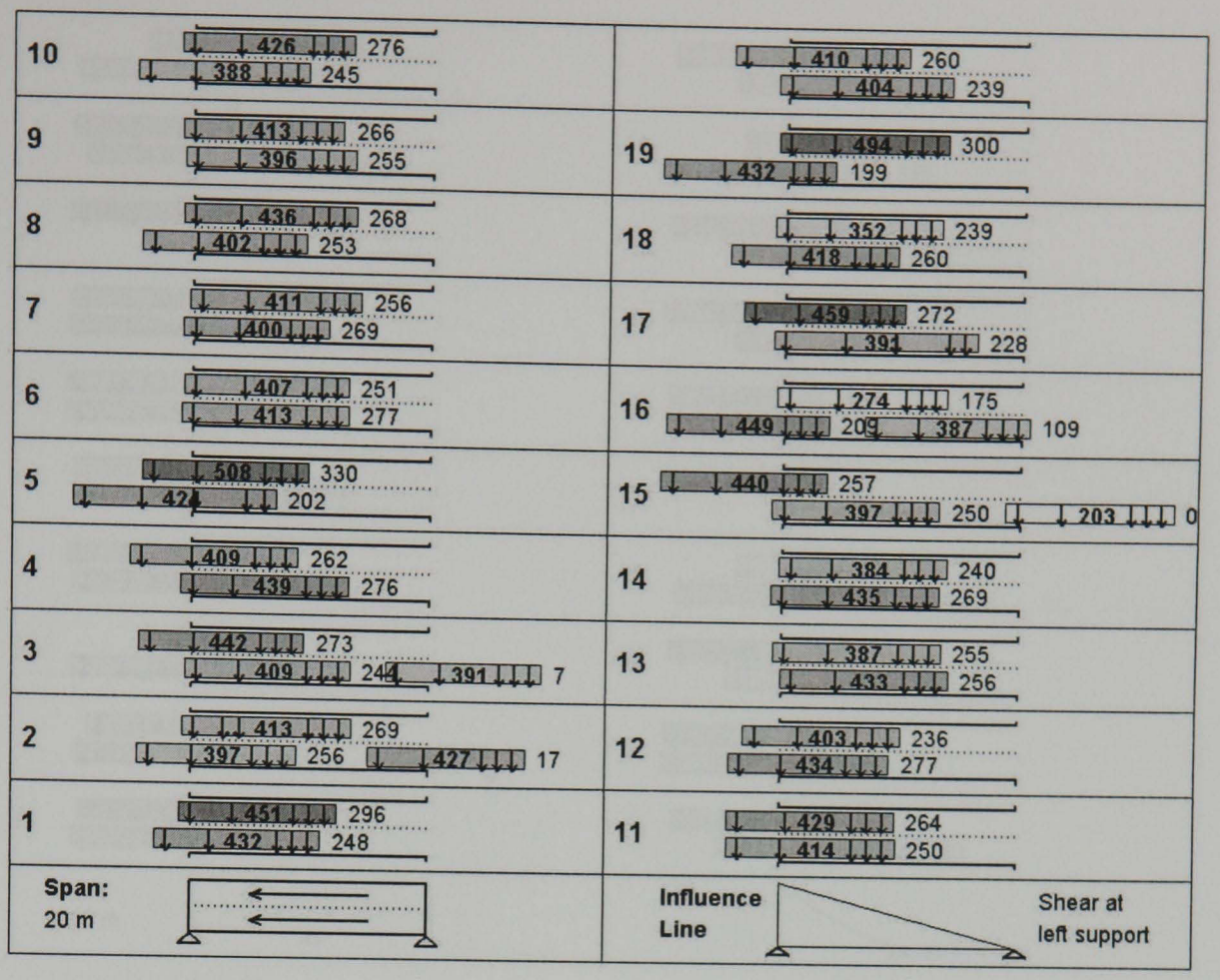
10
426 276
388 245
9
413 266
396 255
8
436 268
402 253
7
411 256
400 269
6
407 251
413 277
5
508 330
424 202
4
409 262
439 276
3
442 273
409 244
391 7
2
413 269
397 256
427 17
1
451 296
432 248
Span:
20 m
410 260
404 239
19
494 300
432 199
18
352 239
418 260
17
459 272
391 228
16
274 175
449 209
387 109
15
440 257
397 250
203 0
14
384 240
435 269
13
387 255
433 256
12
403 236
434 277
11
429 264
414 250
Influence
Line
Shear at
left support

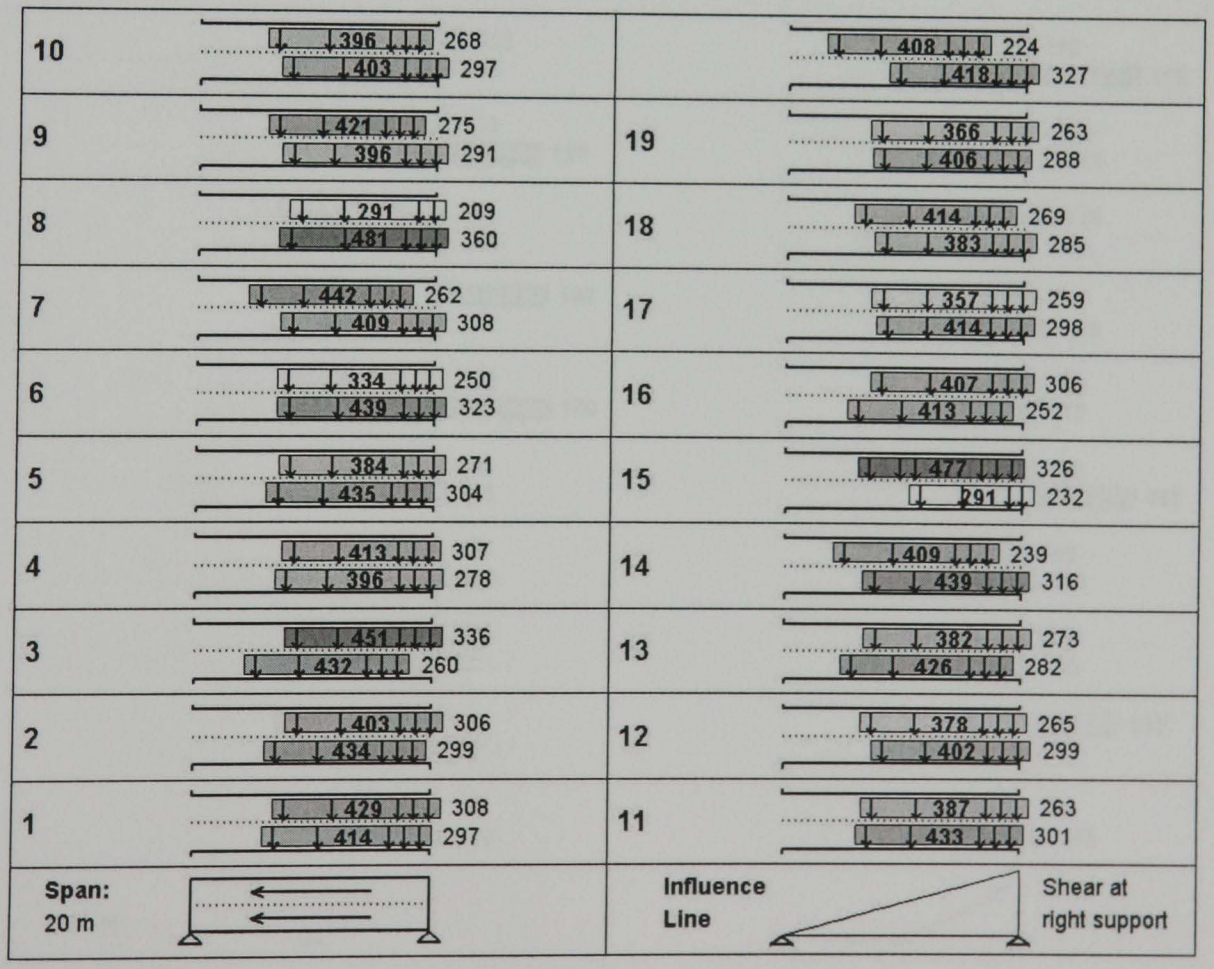
10
396 268
403 297
9
421 275
396 291
8
291 209
481 360
7
442 262
409 308
6
334 250
439 323
5
384 271
435 304
4
413 307
396 278
3
451 336
432 260
2
403 306
434 299
1
429 308
414 297
Span:
20 m
408 224
418 327
19
366 263
406 288
18
414 269
383 285
17
357 259
414 298
16
407 306
413 252
15
477 326
291 232
14
409 239
439 316
13
382 273
426 282
12
378 265
402 299
11
387 263
433 301
Influence
Line
Shear at
right support

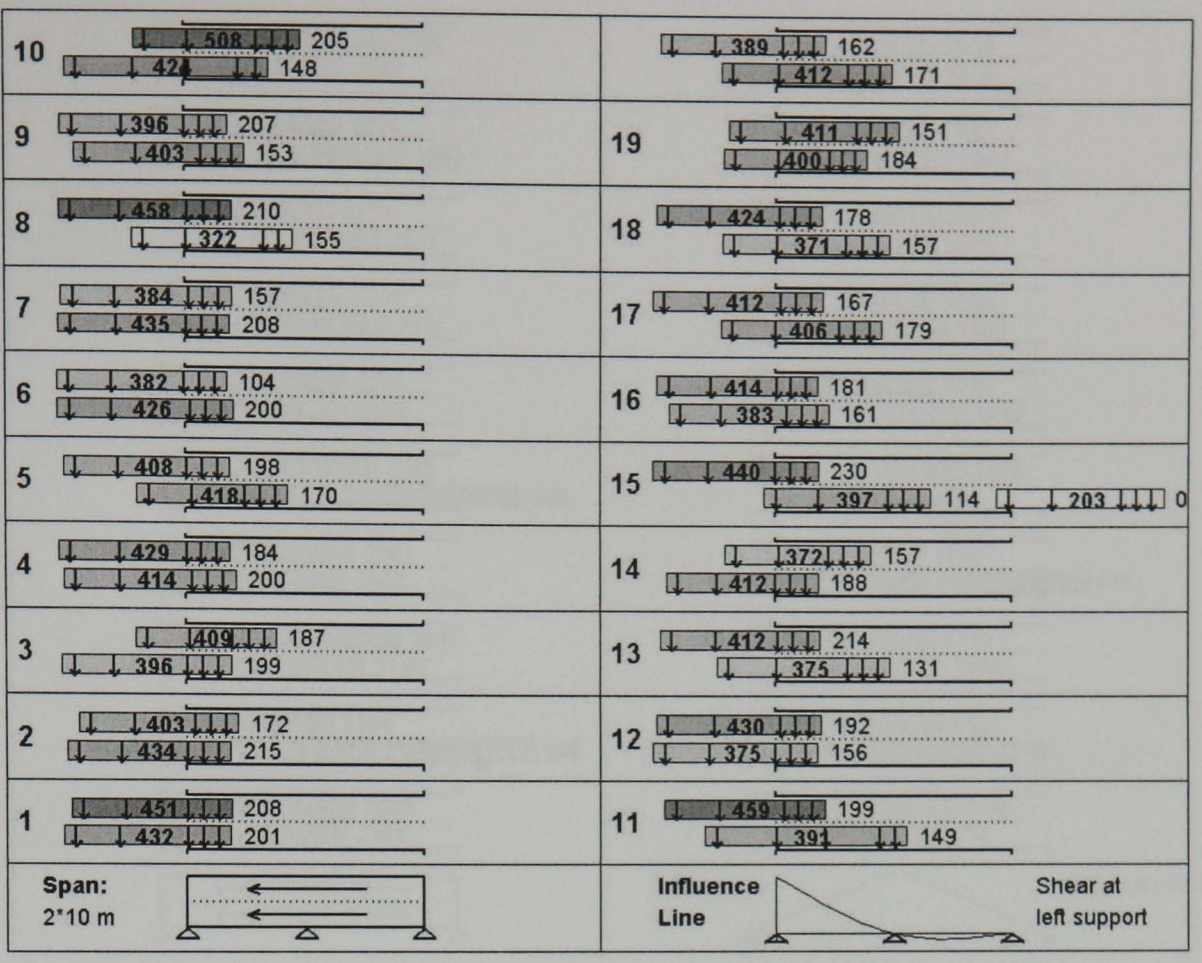
10
508 205
424 148
9
396 207
403 153
8
458 210
322 155
7
384 157
435 208
6
382 104
426 200
5
408 198
418 170
4
429 184
414 200
3
409 187
396 199
2
403 172
434 215
1
451 208
432 201
Span:
2*10 m
19
389 162
412 171
19
411 151
400 184
18
424 178
371 157
17
412 167
406 179
16
414 181
383 161
15
440 230
397 114
203
0
14
372 157
412 188
13
412 214
375 131
12
430 192
375 156
11
459 199
391 149
Influence
Line
Shear at
left support

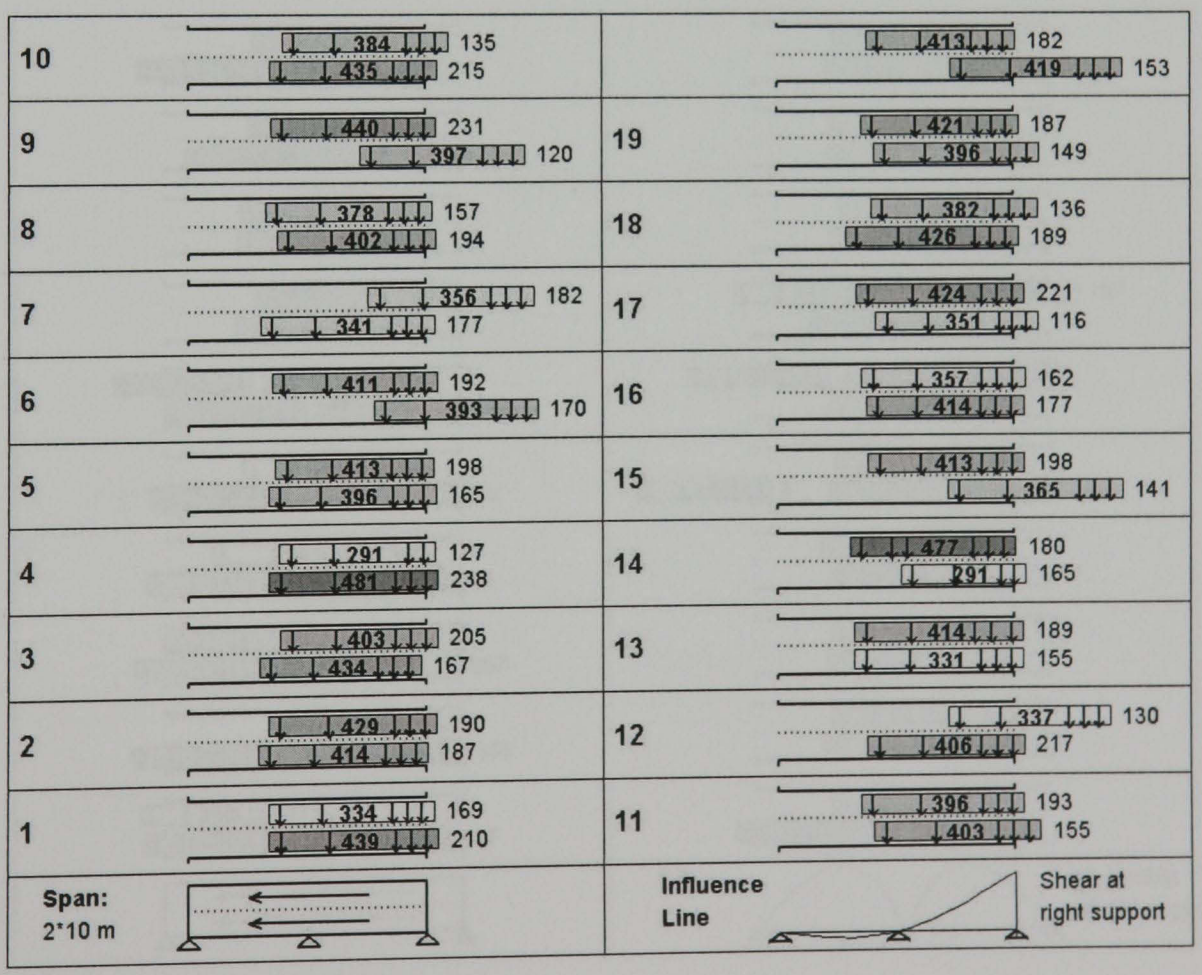
10
384 135
435 215
9
440 231
397 120
8
378 157
402 194
7
356 182
341 177
6
411 192
393 170
5
413 198
396 165
4
291 127
481 238
3
403 205
434 167
2
429 190
414 187
1
334 169
439 210
Span:
2*10 m
19
413 182
419 153
19
421 187
396 149
18
382 136
426 189
17
424 221
351 116
16
357 162
414 177
15
413 198
365 141
14
477 180
291 165
13
414 189
331 155
12
337 130
406 217
11
396 193
403 155
Influence
Line
Shear at
right support

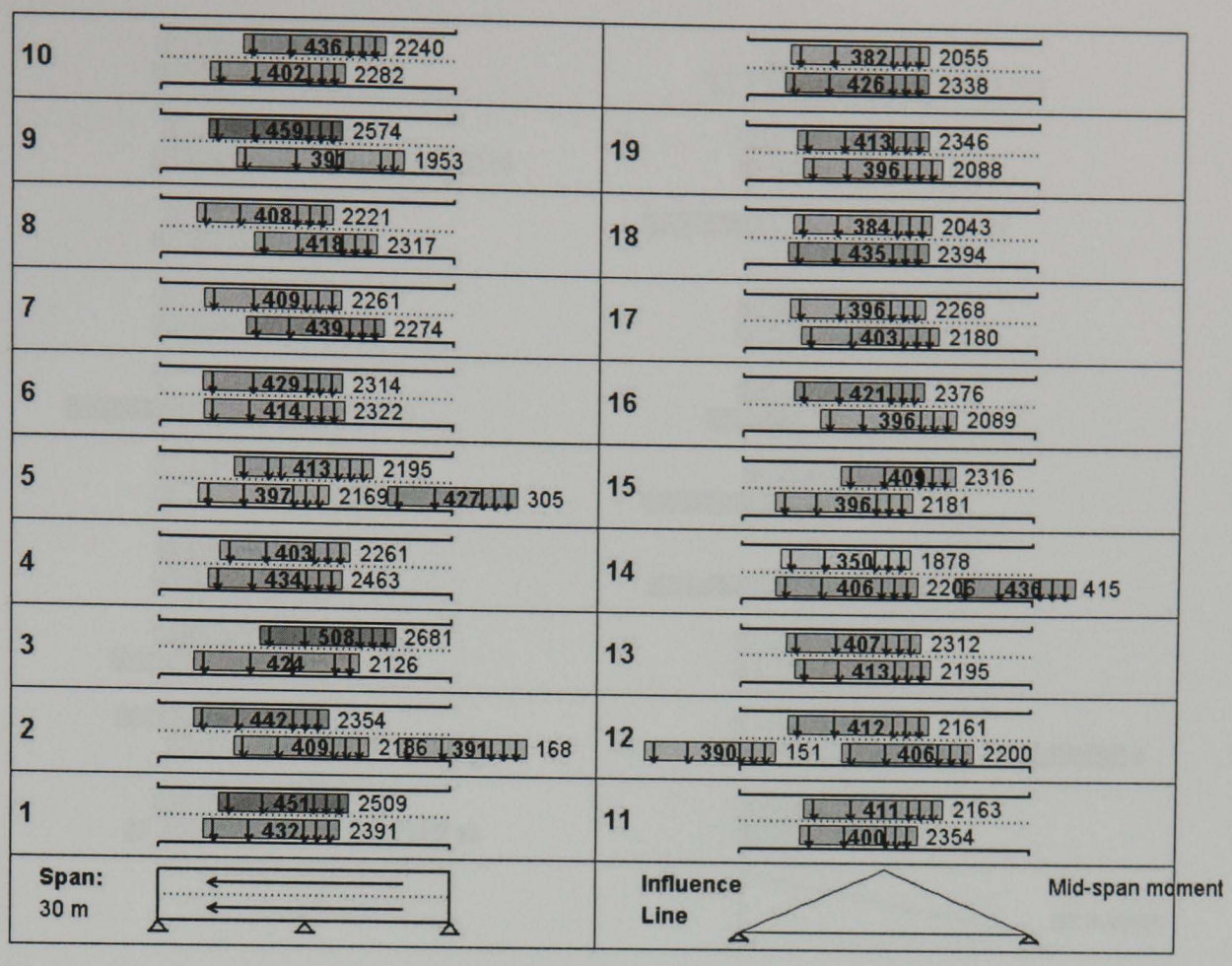
10
436 2240
402 2282
9
459 2574
391 1953
8
408 2221
418 2317
7
409 2261
439 2274
6
429 2314
414 2322
5
413 2195
397 2169
427 305
4
403 2261
434 2463
3
508 2681
424 2126
2
442 2354
409 2186
391 168
1
451 2509
432 2391
Span:
30 m
382 2055
426 2338
19
413 2346
396 2088
18
384 2043
435 2394
17
396 2268
403 2180
16
421 2376
396 2089
15
409 2316
396 2181
14
350 1878
406 2206
436 415
13
407 2312
413 2195
12
412 2161
390 151
406 2200
11
411 2163
400 2354
Influence
Line
Mid-span moment

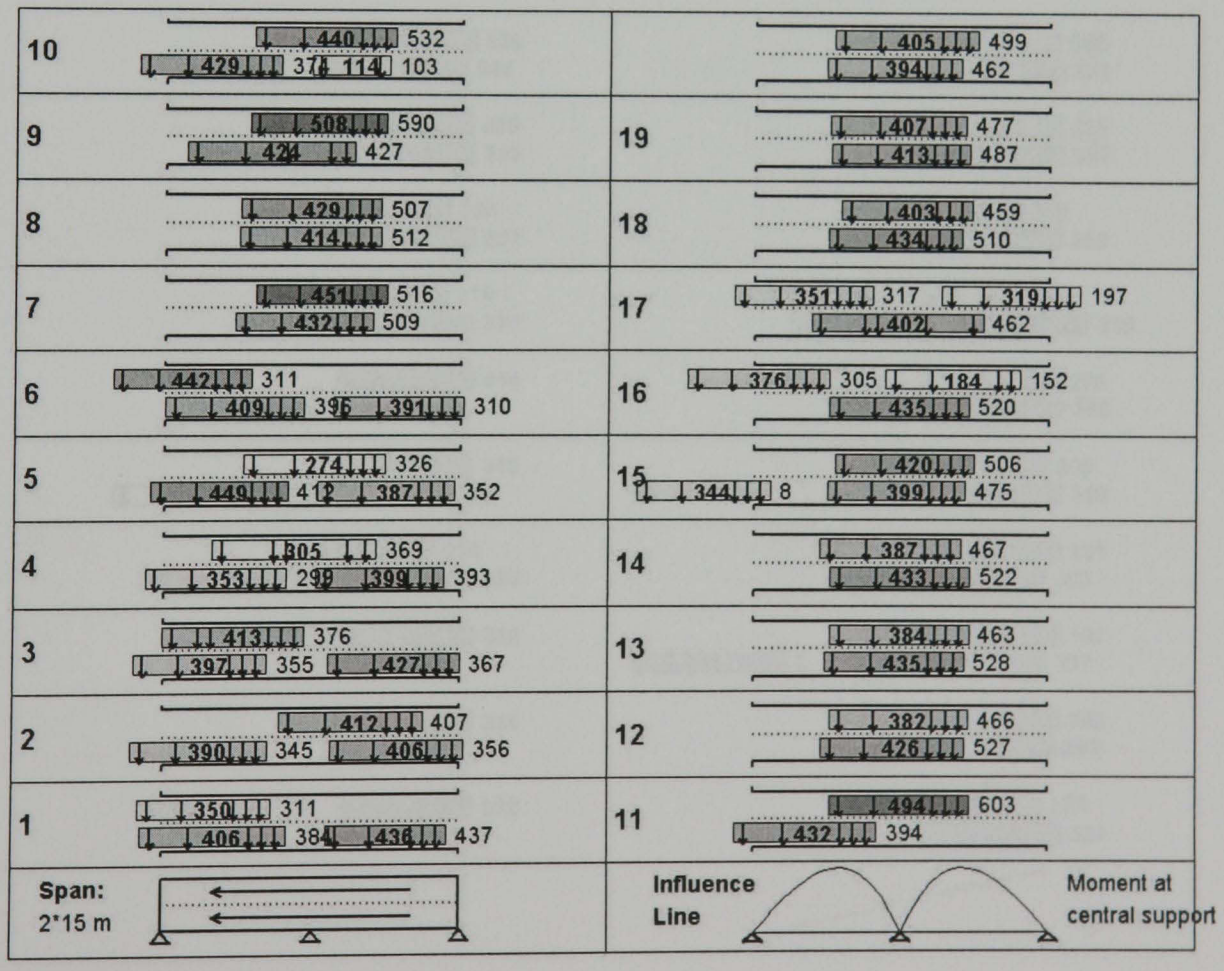
10
440 532
429 378
114 103
9
508 590
424 427
8
429 507
414 512
7
451 516
432 509
6
442 311
409 396
391 310
5
274 326
449 412
387 352
4
305 369
353 299
399 393
3
413 376
397 355
427 367
2
412 407
390 345
406 356
1
350 311
406 384
436 437
Span:
2*15 m
405 499
394 462
19
407 477
413 487
18
403 459
434 510
17
351 317
319 197
402 462
16
376 305
184 152
435 520
15
420 506
344 8
399 475
14
387 467
433 522
13
384 463
435 528
12
382 466
426 527
11
494 603
432 394
Influence
Line
Moment at
central support

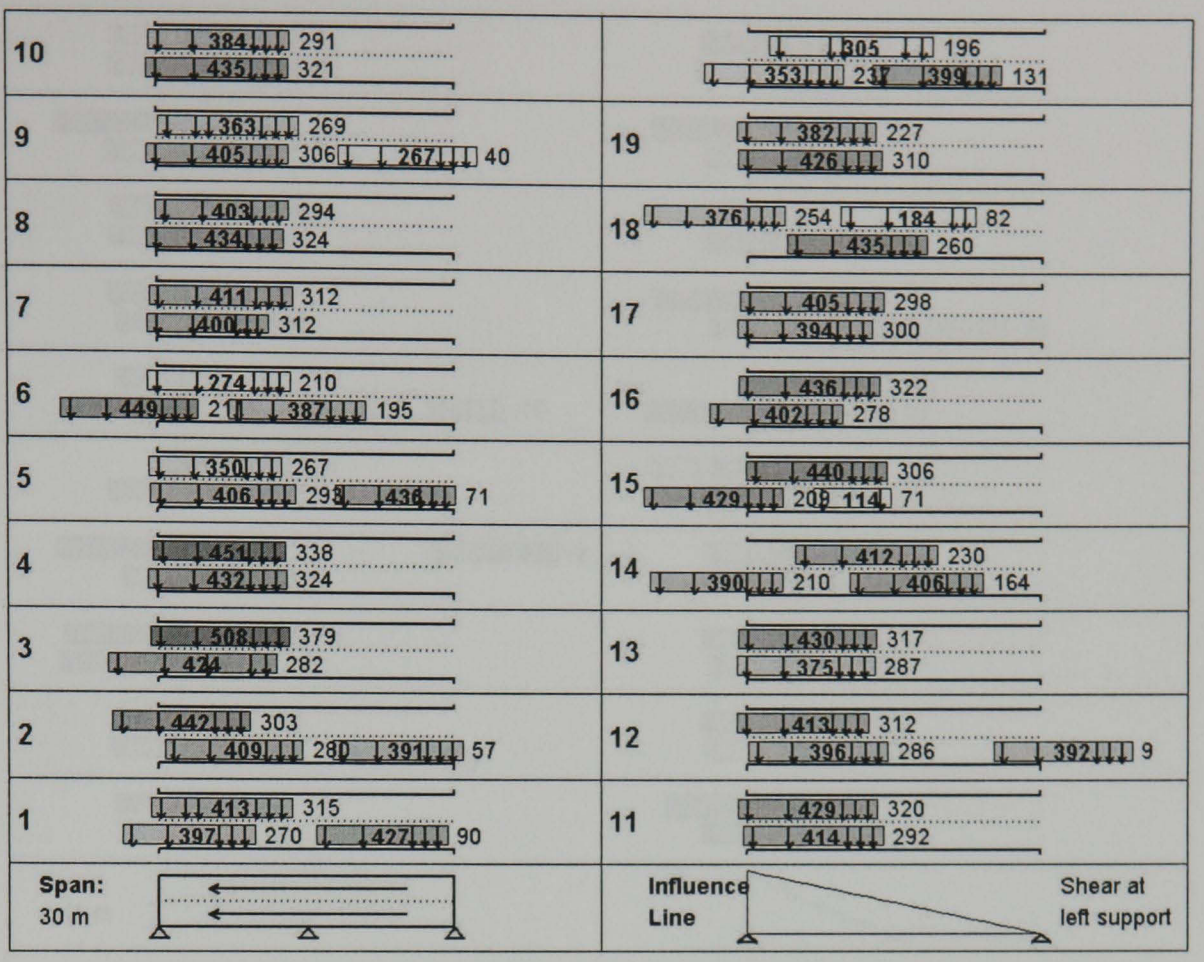
10
384 291
435 321
9
363 269
405 306 267 40
8
403 294
434 324
7
411 312
400 312
6
274 210
449 21 387 195
5
350 267
406 298 436 71
4
451 338
432 324
3
508 379
424 282
2
442 303
409 280 391 57
1
413 315
397 270 427 90
Span:
30 m
19
305 196
353 237 399 131
19
382 227
426 310
18
376 254 184 82
435 260
17
405 298
394 300
16
436 322
402 278
15
440 306
429 209 114 71
14
412 230
390 210 406 164
13
430 317
375 287
12
413 312
396 286 392 9
11
429 320
414 292
Influence
Line
Shear at
left support

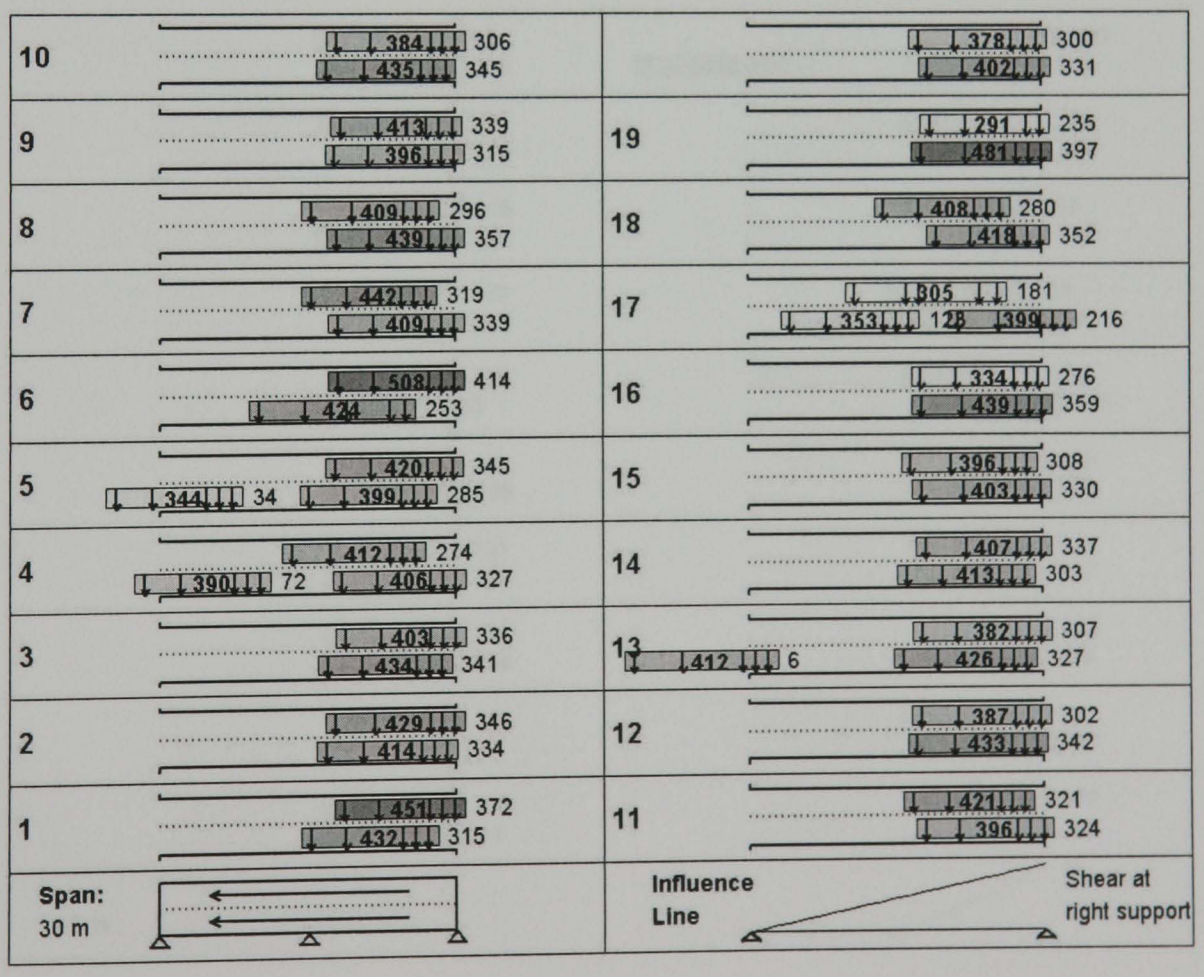
10
384 306
435 345
9
413 339
396 315
8
409 296
439 357
7
442 319
409 339
6
508 414
424 253
5
420 345
344 34 399 285
4
412 274
390 72 406 327
3
403 336
434 341
2
429 346
414 334
1
451 372
432 315
Span:
30 m
19
378 300
402 331
19
291 235
481 397
18
408 280
418 352
17
305 181
353 128 399 216
16
334 276
439 359
15
396 308
403 330
14
407 337
413 303
13
382 307
412 6 426 327
12
387 302
433 342
11
421 321
396 324
Influence
Line
Shear at
right support

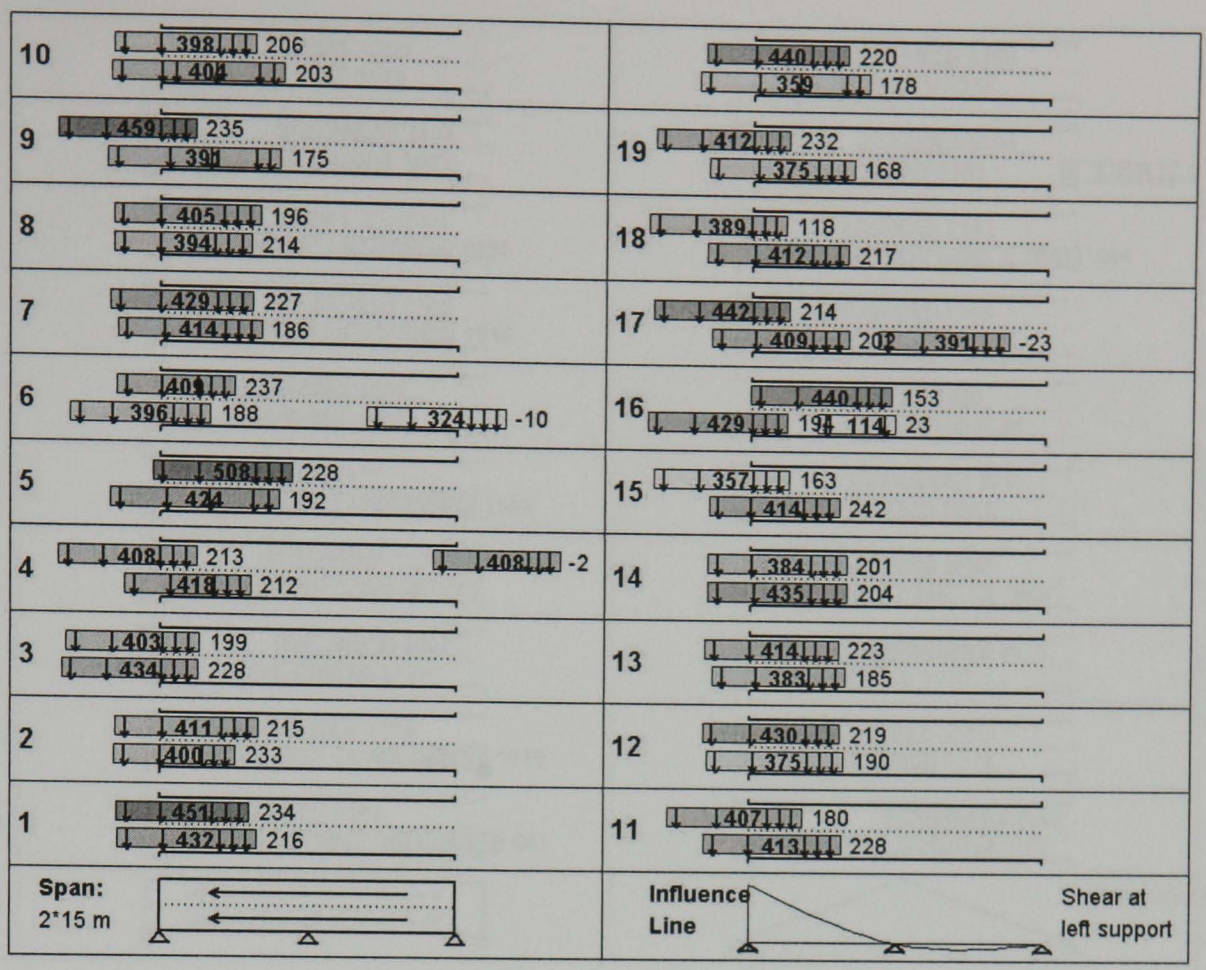
10
398 206
404 203
440 220
359 178
9
459 235
395 175
412 232
375 168
8
405 196
394 214
389 118
412 217
7
429 227
414 186
442 214
409 202 391 -23
6
401 237
396 188
324 -10
440 153
429 194 114 23
5
508 228
424 192
357 163
414 242
4
408 213
418 212
408 -2
384 201
435 204
3
403 199
434 228
414 223
383 185
2
411 215
400 233
430 219
375 190
1
451 234
432 216
407 180
413 228
Span:
2*15 m
Influence
Line
Shear at
left support

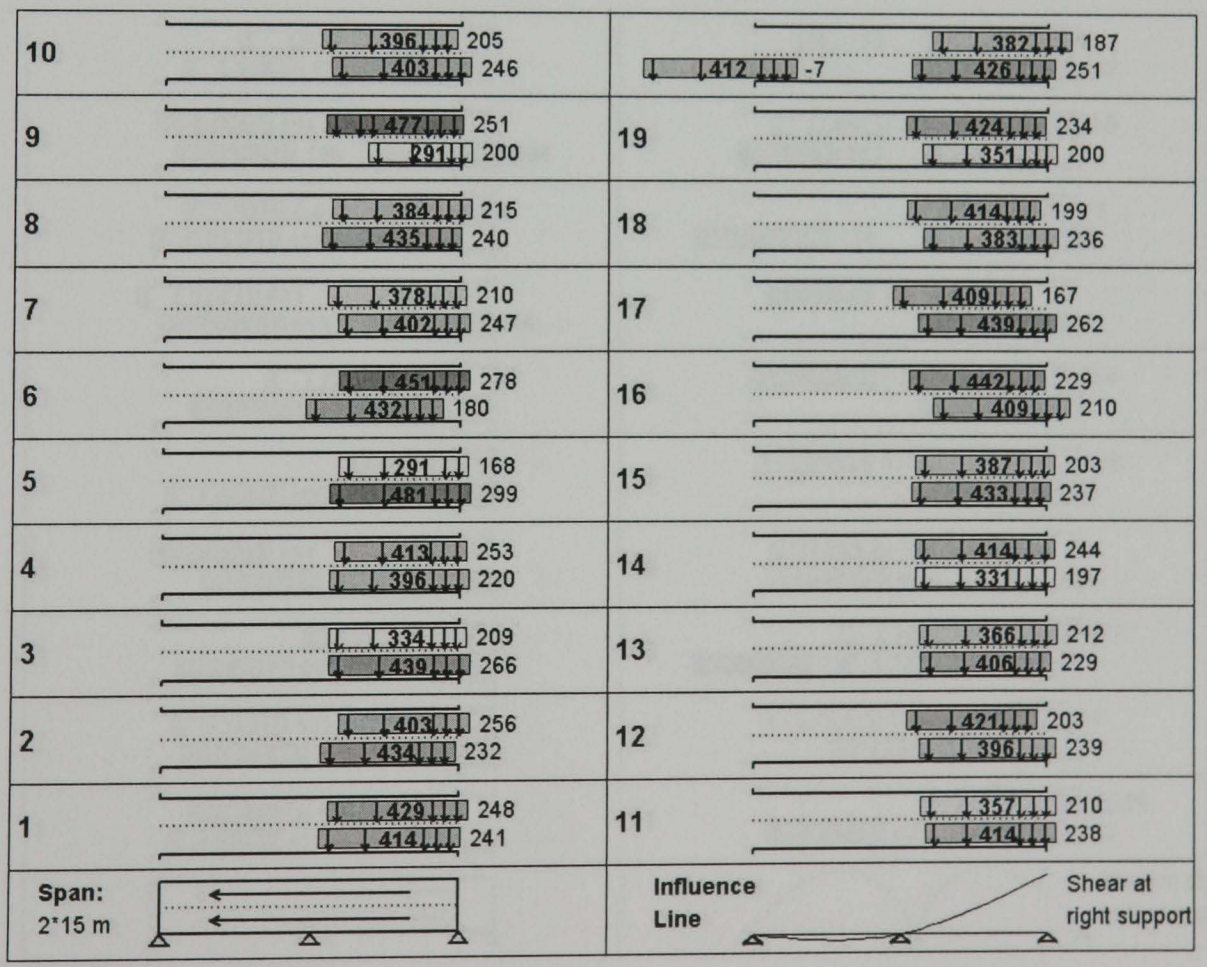
10
396 205
403 246
382 187
412 -7 426 251
9
477 251
291 200
424 234
351 200
8
384 215
435 240
414 199
383 236
7
378 210
402 247
409 167
439 262
6
451 278
432 180
442 229
409 210
5
291 168
481 299
387 203
433 237
4
413 253
396 220
414 244
331 197
3
334 209
439 266
366 212
406 229
2
403 256
434 232
421 203
396 239
1
429 248
414 241
357 210
414 238
Span:
2*15 m
Influence
Line
Shear at
right support

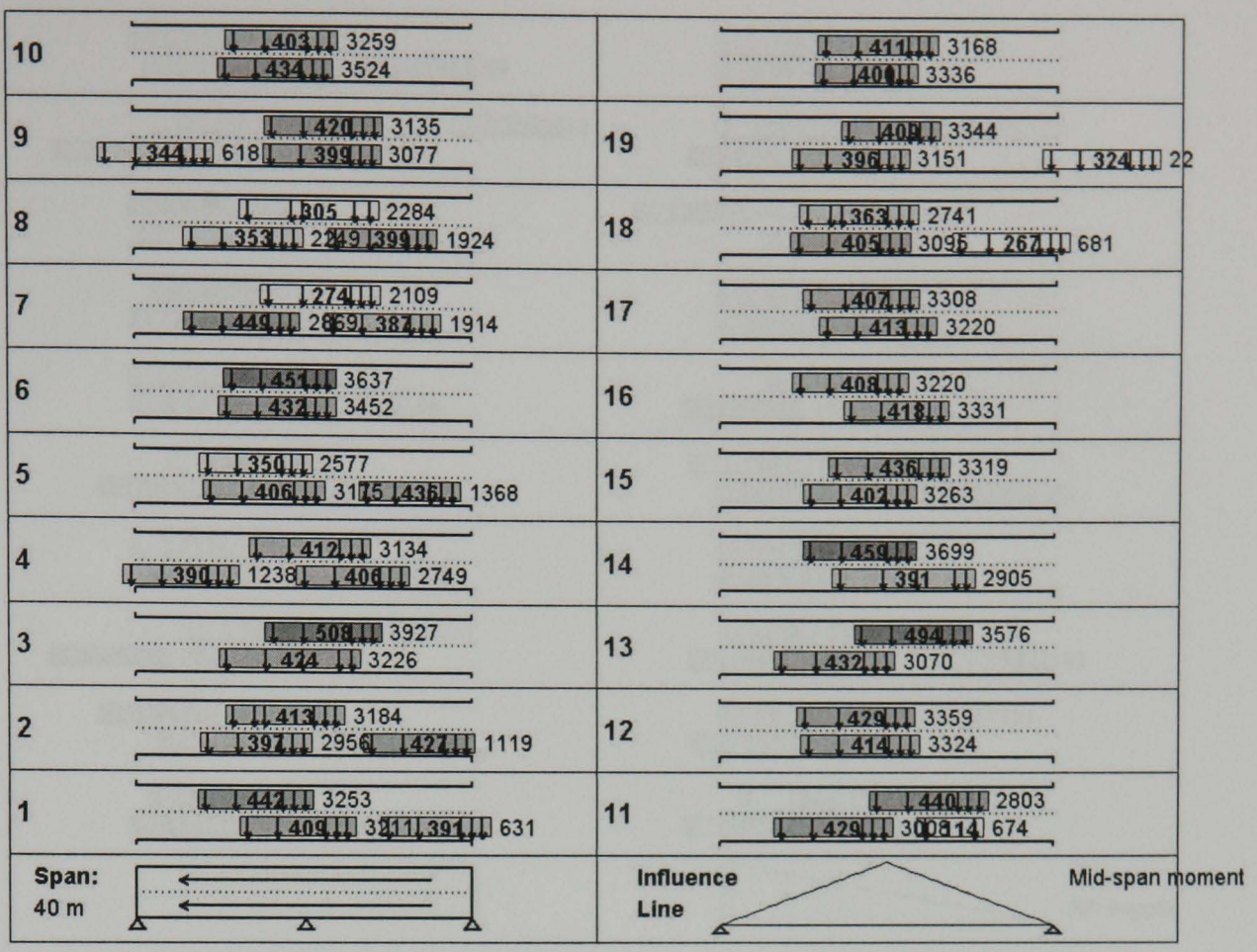
10
403 3259
434 3524
411 3168
406 3336
9
420 3135
344 618 399 3077
408 3344
396 3151 324 22
8
305 2284
353 2849 399 1924
363 2741
405 3095 267 681
7
274 2109
449 2859 387 1914
407 3308
413 3220
6
451 3637
432 3452
408 3220
418 3331
5
350 2577
406 3175 436 1368
436 3319
402 3263
4
412 3134
390 1238 406 2749
459 3699
391 2905
3
508 3927
424 3226
494 3576
432 3070
2
413 3184
397 2956 427 1119
429 3359
414 3324
1
442 3253
409 3211 391 631
440 2803
429 3005 314 674
Span:
40 m
Influence
Line
Mid-span moment

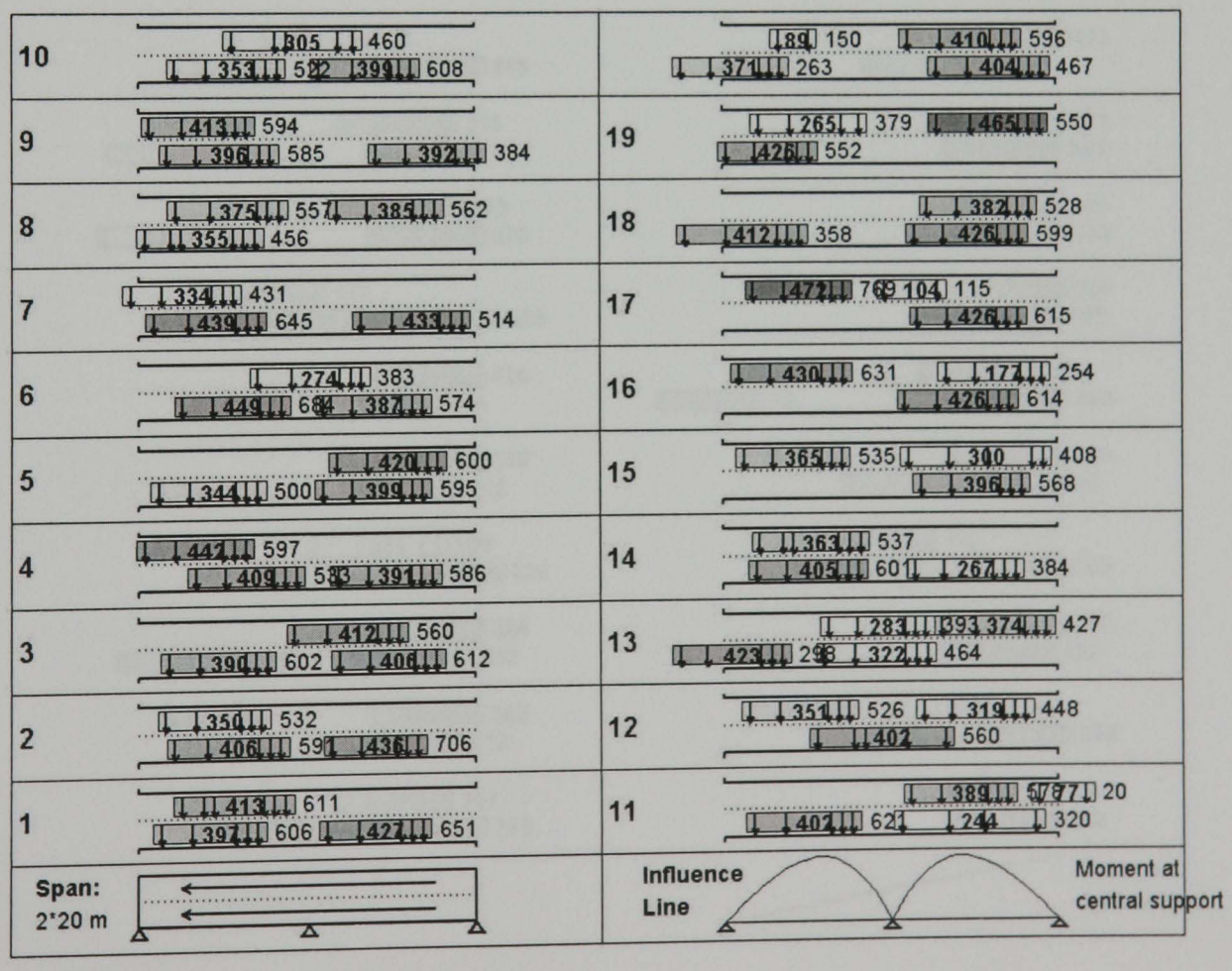
10
305 460
353 522 399 608
89 150 410 596
371 263 404 467
9
413 594
396 585 392 384
265 379 465 550
426 552
8
375 557 385 562
355 456
382 528
412 358 426 599
7
334 431
439 645 433 514
472 769 104 115
426 615
6
274 383
449 684 387 574
430 631 177 254
426 614
5
420 600
344 500 399 595
365 535 300 408
396 568
4
442 597
409 583 391 586
363 537
405 601 267 384
3
412 560
390 602 406 612
283 393 374 427
423 298 322 464
2
350 532
406 591 436 706
351 526 319 448
402 560
1
413 611
397 606 427 651
389 577 20
402 621 244 320
Span:
2*20 m
Influence
Line
Moment at
central support

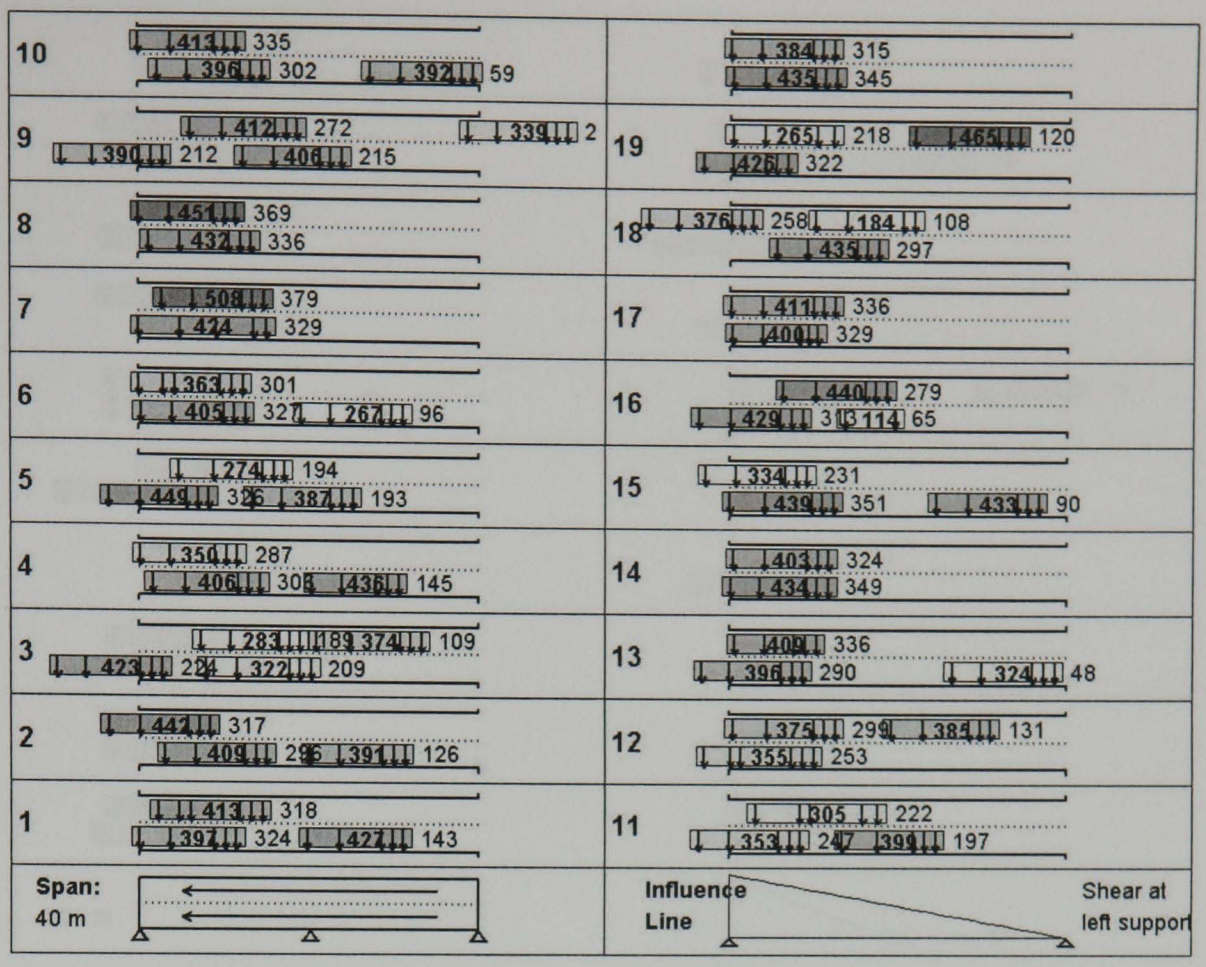
10
413 335
396 302
392 59
9
412 272
339 2
390 212
406 215
8
451 369
432 336
7
508 379
424 329
6
363 301
405 327
267 96
5
274 194
449 326
387 193
4
350 287
406 305
436 145
3
283 189
374 109
423 284
322 209
2
442 317
409 295
391 126
1
413 318
397 324
427 143
Span:
40 m
19
384 315
435 345
19
265 218
465 120
426 322
18
376 258
184 108
435 297
17
411 336
400 329
16
440 279
429 313
114 65
15
334 231
439 351
433 90
14
403 324
434 349
13
409 336
396 290
324 48
12
375 299
385 131
355 253
11
305 222
353 247
399 197
Influence
Line
Shear at
left support

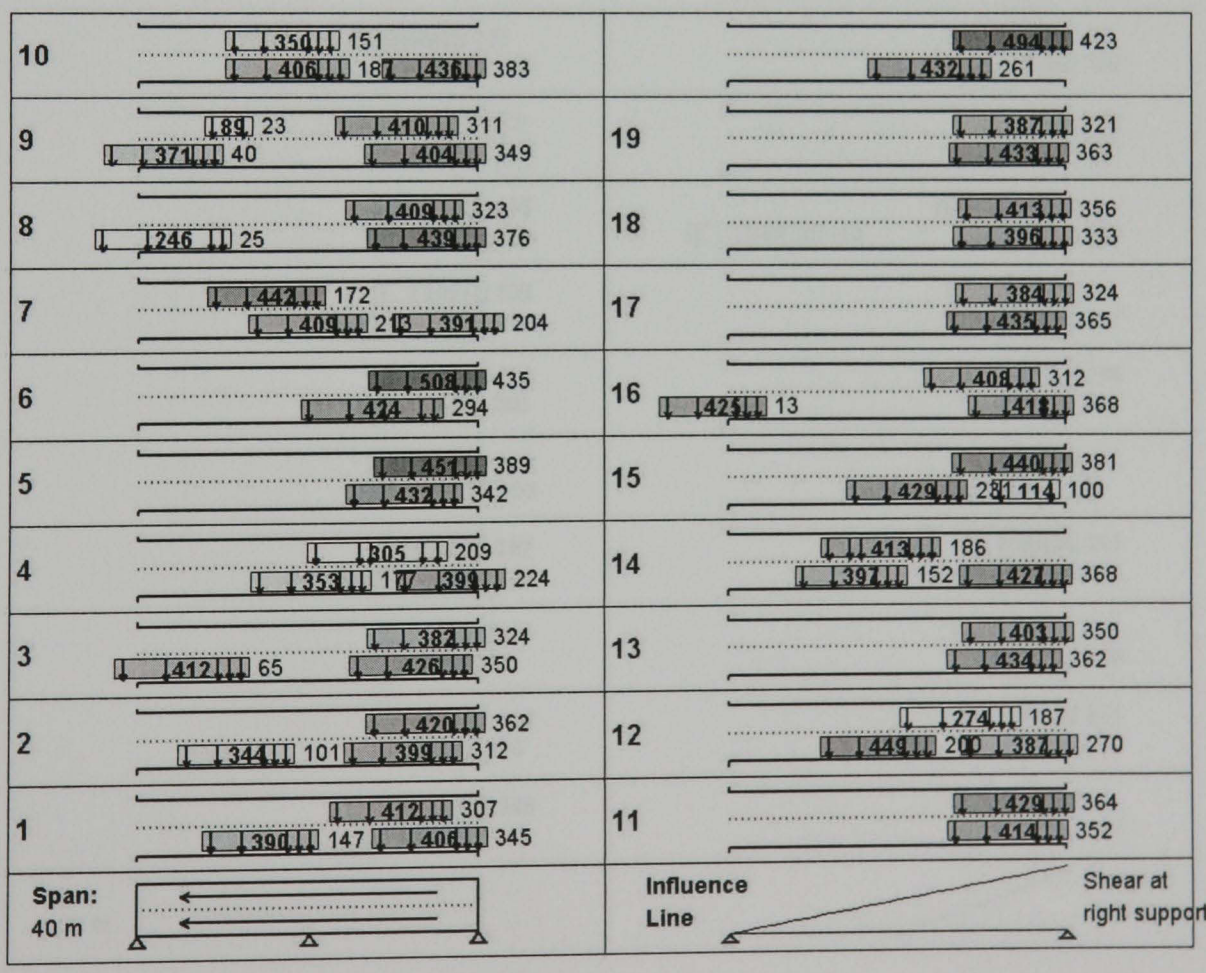
10
350 151
406 187
436 383
9
89 23
410 311
371 40
404 349
8
409 323
246 25
439 376
7
442 172
409 213
391 204
6
508 435
424 294
5
451 389
432 342
4
305 209
353 177
399 224
3
382 324
412 65
426 350
2
420 362
344 101
399 312
1
412 307
390 147
406 345
Span:
40 m
19
494 423
432 261
19
387 321
433 363
18
413 356
396 333
17
384 324
435 365
16
408 312
425 13
413 368
15
440 381
429 281
114 100
14
413 186
397 152
427 368
13
403 350
434 362
12
274 187
449 200
387 270
11
429 364
414 352
Influence
Line
Shear at
right support

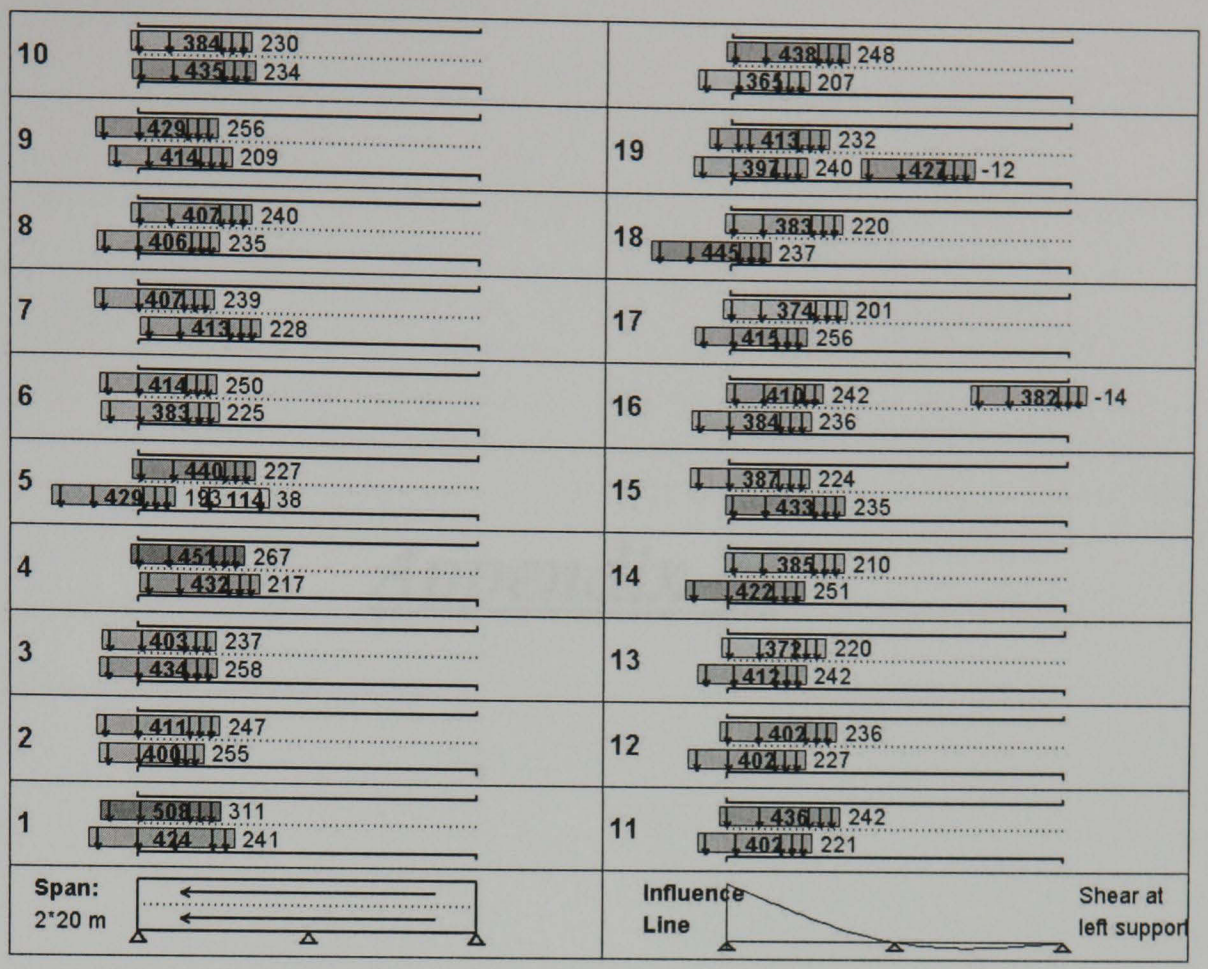
10
384 230
435 234
438 248
365 207
9
429 256
414 209
19
413 232
397 240
427 -12
8
407 240
406 235
18
383 220
445 237
7
407 239
413 228
17
374 201
415 256
6
414 250
383 225
16
410 242
382 -14
384 236
5
440 227
429 193 114 38
15
387 224
433 235
4
451 267
432 217
14
385 210
422 251
3
403 237
434 258
13
372 220
412 242
2
411 247
400 255
12
402 236
402 227
1
508 311
474 241
11
436 242
402 221
Span:
2*20 m
Influence
Line
Shear at
left support

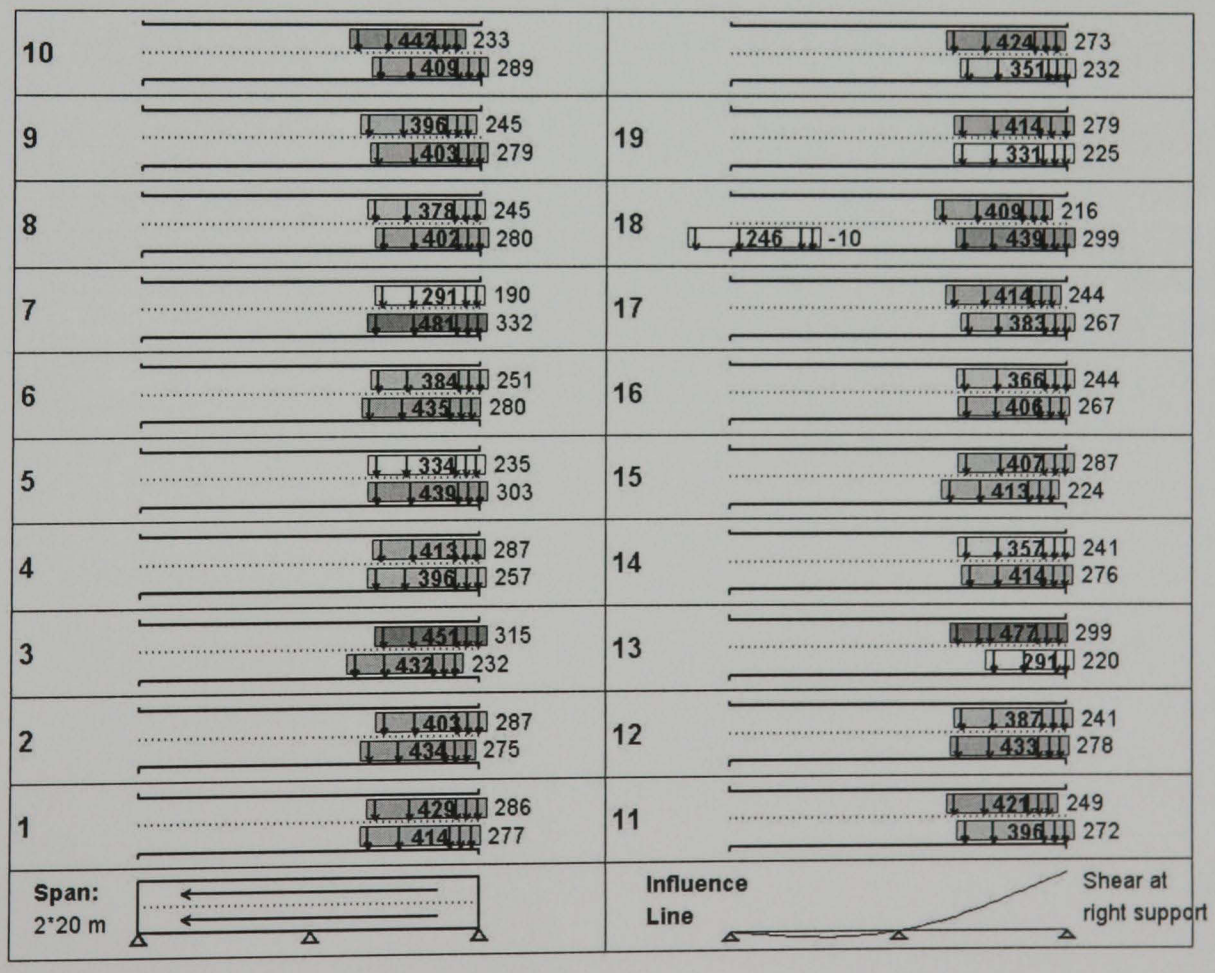
10
442 233
409 289
424 273
351 232
9
396 245
403 279
19
414 279
331 225
8
378 245
402 280
18
409 216
246 -10
439 299
7
291 190
481 332
17
414 244
383 267
6
384 251
435 280
16
366 244
406 267
5
334 235
439 303
15
407 287
413 224
4
413 287
396 257
14
357 241
414 276
3
451 315
432 232
13
477 299
291 220
2
403 287
434 275
12
387 241
433 278
1
429 286
414 277
11
421 249
396 272
Span:
2*20 m
Influence
Line
Shear at
right support

Appendix M

TYPICAL CRITICAL LOADING EVENTS FOR UNIDIRECTIONAL TRAFFIC

Appendix M Typical Critical Loading Events For Unidirectional Traffic

Table M-1: Location of trucks for the typical critical loading events for 20m bridges

Load Effect	Influence Line	Number of trucks	Location of trucks
1	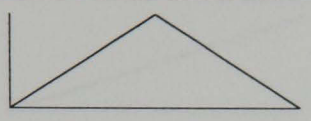	2	Both trucks have 5 axles and have their 2nd axle or 3rd axle (1st axle of the tridem) at mid-span
2	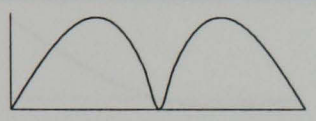	2	Both trucks have 5 axles and have the front 2 axles on one span and the tridem on the other span
3	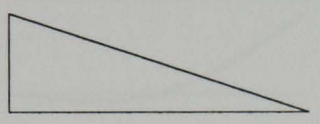	2	Both trucks have 5 axles and have their last axle exactly on the left support or very near
4	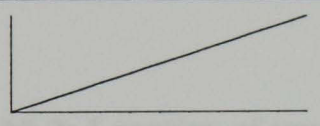	2	Both trucks have 5 axles and have their 1st or 2nd axle exactly on the right support or very near
5	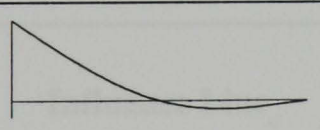	2	Both trucks have 5 axles and have their last axle exactly on the left support or very near
6	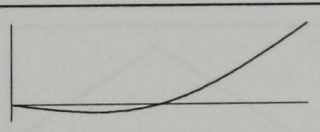	2	Both trucks have 5 axles and have their 3rd axle (1st axle of the tridem) exactly on the left support or very near

Table M-2: Location of trucks for the typical critical loading events for 30m bridges

Load Effect	Influence Line	Number of trucks	Location of trucks
1	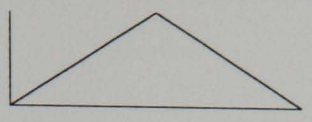	2	Both trucks have 4/5 axles and have their 2nd axle or 3rd axle (1st axle of the tridem) at mid-span
2	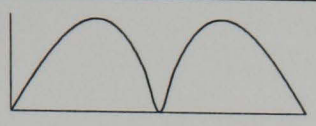	2(/3)	Both trucks have 4/5 axles and have the front 2 axles on one span and the tridem on the other span
3	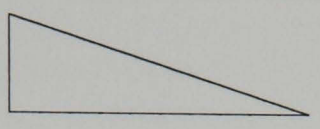	2	Both trucks have 4/5 axles and have their last axle exactly on the left support or very near
4	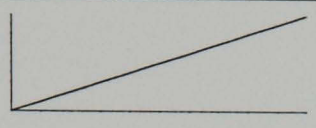	2	Both trucks have 4/5 axles and have their 1st or 2nd axle exactly on the right support or very near
5	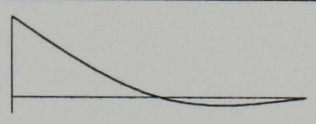	2	Both trucks have 4/5 axles and have their last axle exactly on the left support or very near
6	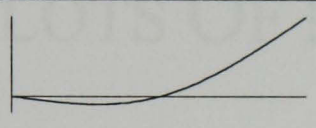	2	Both trucks have 4/5 axles and have their 2nd axle exactly on the left support or very near

Table M-3: Location of trucks for the typical critical loading events for 40m bridges

Load Effect	Influence Line	Number of trucks	Location of trucks
1	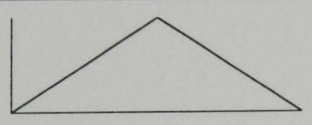	2(/3)	Both trucks have 5 axles and have their 2nd axle or 3rd axle (1st axle of the tridem) at mid-span
2	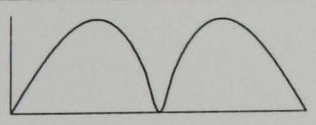	3(/2)	The 3 trucks are fully located on a single span (2 in one lane behind each other and 1 in the other lane)
3	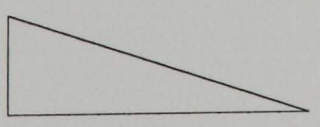	2(/3)	Both trucks have 5 axles and have their last axle exactly on the left support or very near
4	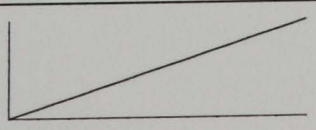	2(/3)	Both trucks have 5 axles and have their 1st axle exactly on the right support or very near
5	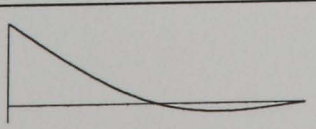	2	Both trucks have 5 axles and have their last axle exactly on the left support or very near
6	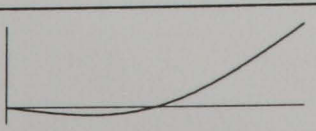	2	Both trucks have 5 axles and have their 1st or 2nd exactly on the left support or very near

Appendix N

Plots Of Modelled Effects For Unidirectional Traffic

Appendix N PLOTS OF MODELLED EFFECTS FOR UNIDIRECTIONAL TRAFFIC

Figure D-1:Simplified Model 1 – 20m bridges – Direction 1 368
Figure N-2: Simplified Model 1 – 30m bridges – Direction 1 368
Figure N-3: Simplified Model 1 – 40m bridges – Direction 1 369
Figure N-4: Simplified Model 1 – 20m bridges – Direction 2 369
Figure N-5: Simplified Model 1 – 30m bridges – Direction 2 370
Figure N-6: Simplified Model 1 – 40m bridges – Direction 2 370
Figure N-7: Simplified Model 2 – 20m bridges – Direction 1 371
Figure N-8: Simplified Model 2 – 30m bridges – Direction 1 371
Figure N-9: Simplified Model 2 – 40m bridges – Direction 1 372
Figure N-10: Simplified Model 2 – 20m bridges – Direction 2 372
Figure N-11: Simplified Model 2 – 30m bridges – Direction 2 373
Figure N-12: Simplified Model 2 – 10m bridges – Direction 2 373
Figure N-13: Simplified Model 3 – 20m bridges – Direction 1 374
Figure N-14: Simplified Model 3 – 30m bridges – Direction 1 374
Figure N-15: Simplified Model 3 – 40m bridges – Direction 1 375
Figure N-16: Simplified Model 3 – 20m bridges – Direction 2 375
Figure N-17: Simplified Model 3 – 30m bridges – Direction 2 376
Figure N-18: Simplified Model 3 – 40m bridges – Direction 2 376

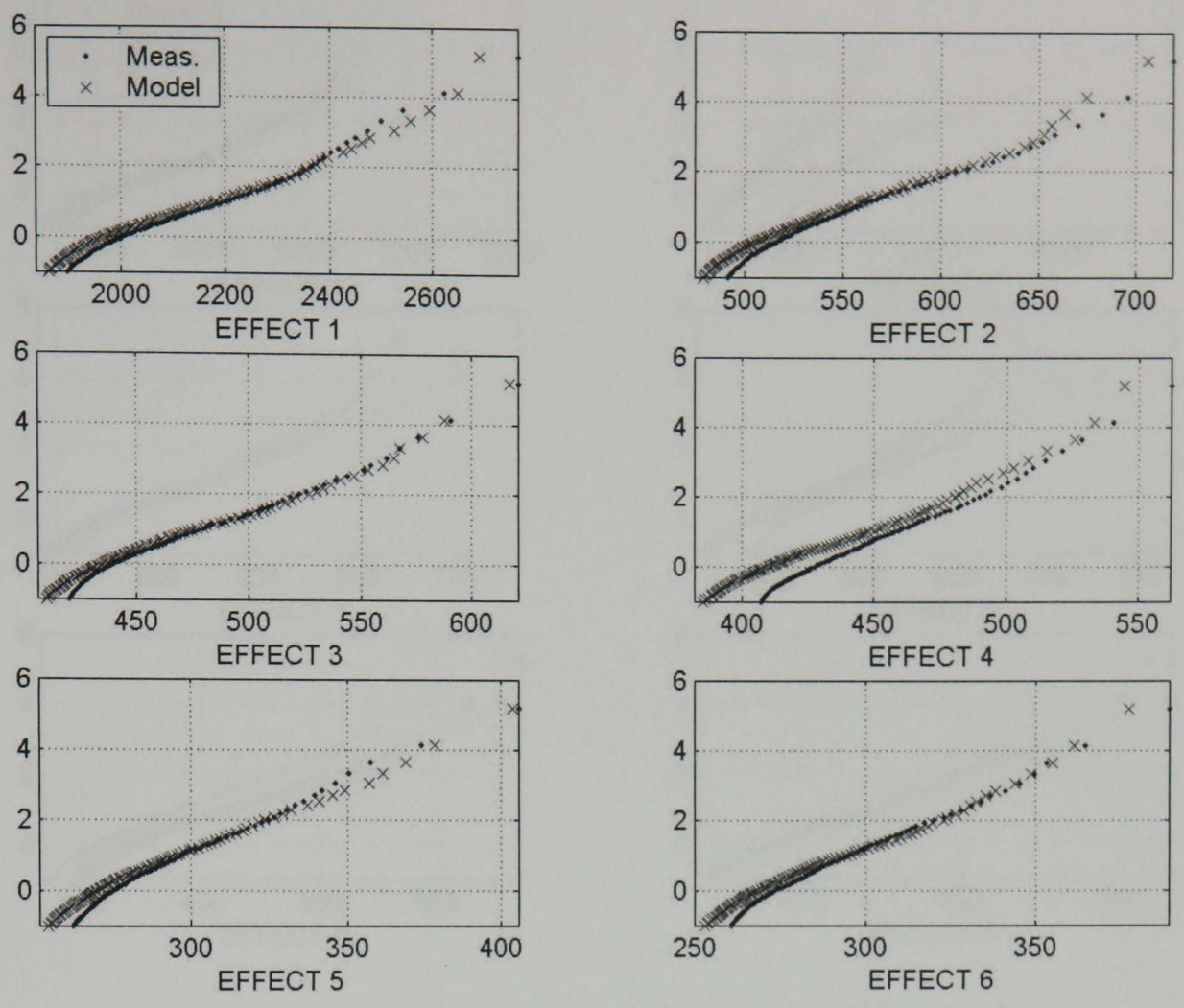

Figure D-1:Simplified Model 1 – 20m bridges – Direction 1

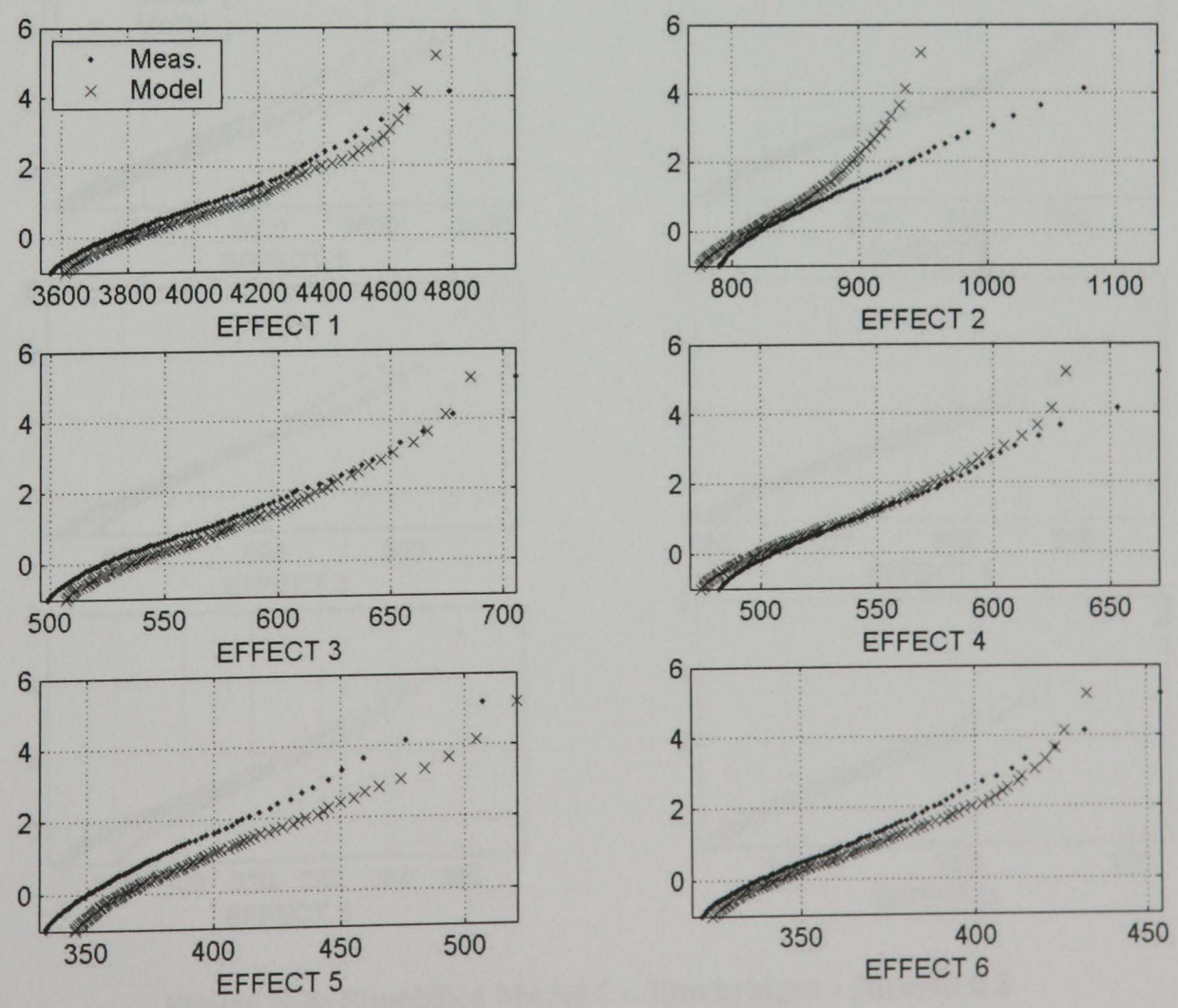

Figure N-2: Simplified Model 1 – 30m bridges – Direction 1

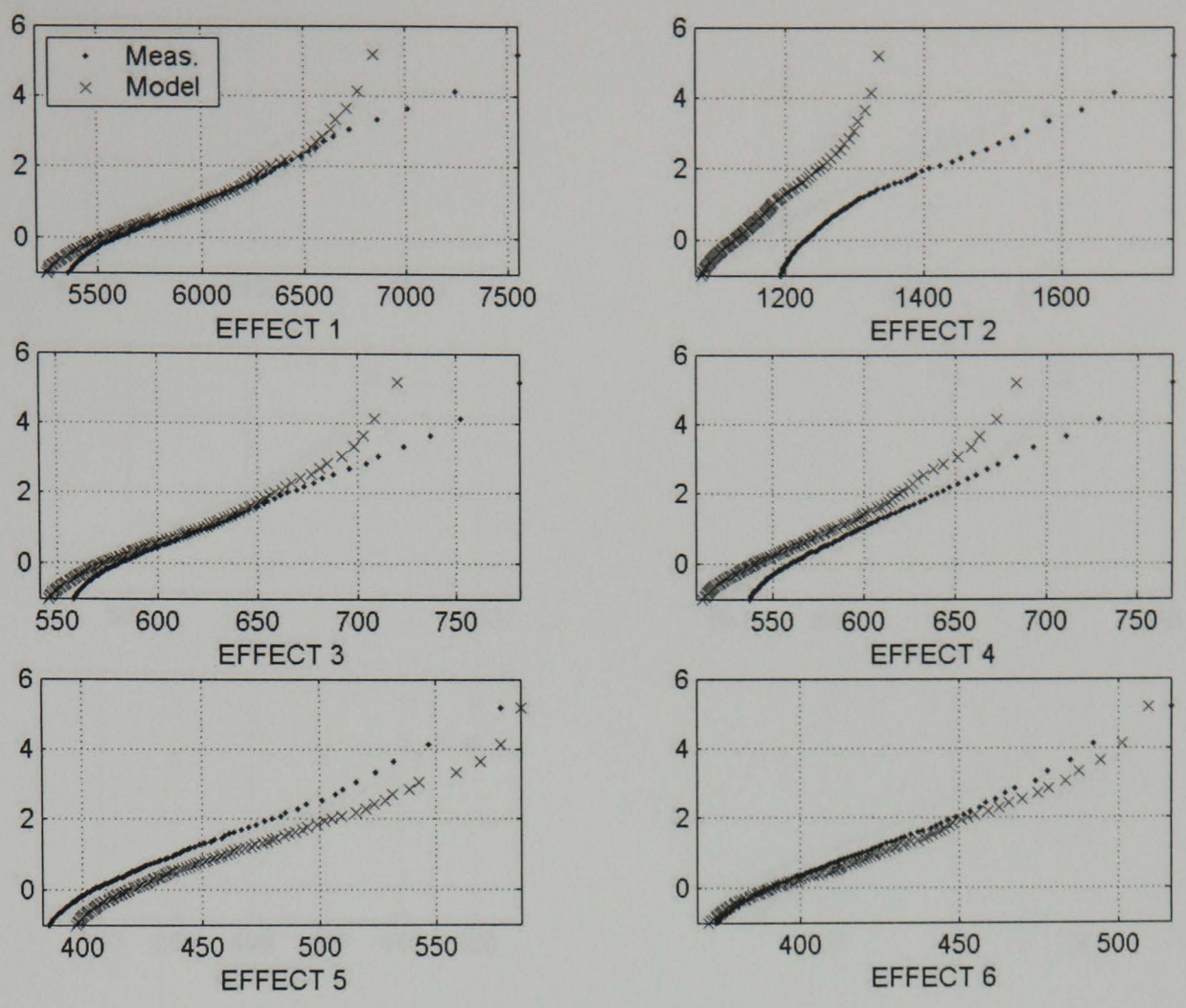

Figure N-3: Simplified Model 1 – 40m bridges – Direction 1

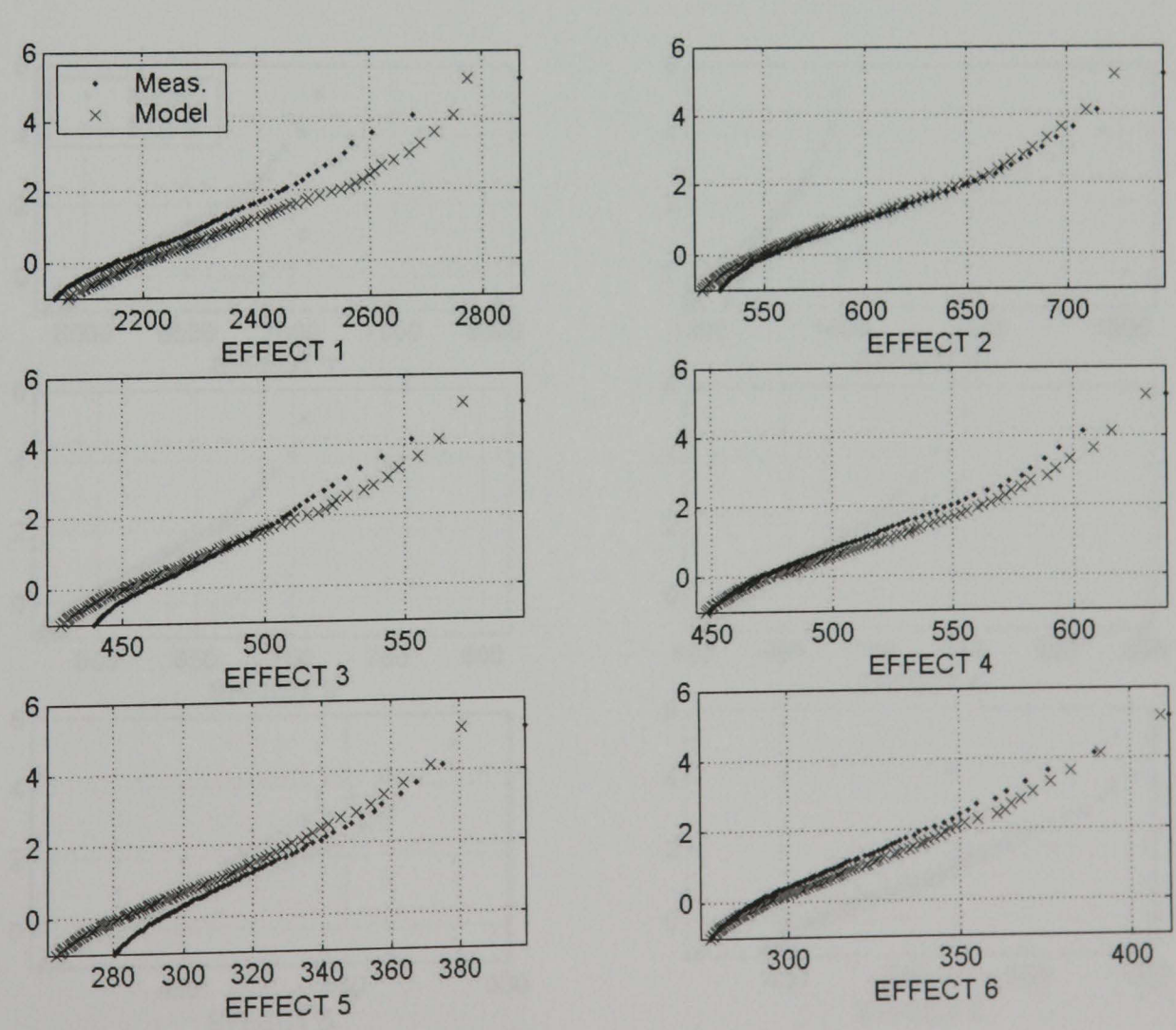

Figure N-4: Simplified Model 1 – 20m bridges – Direction 2

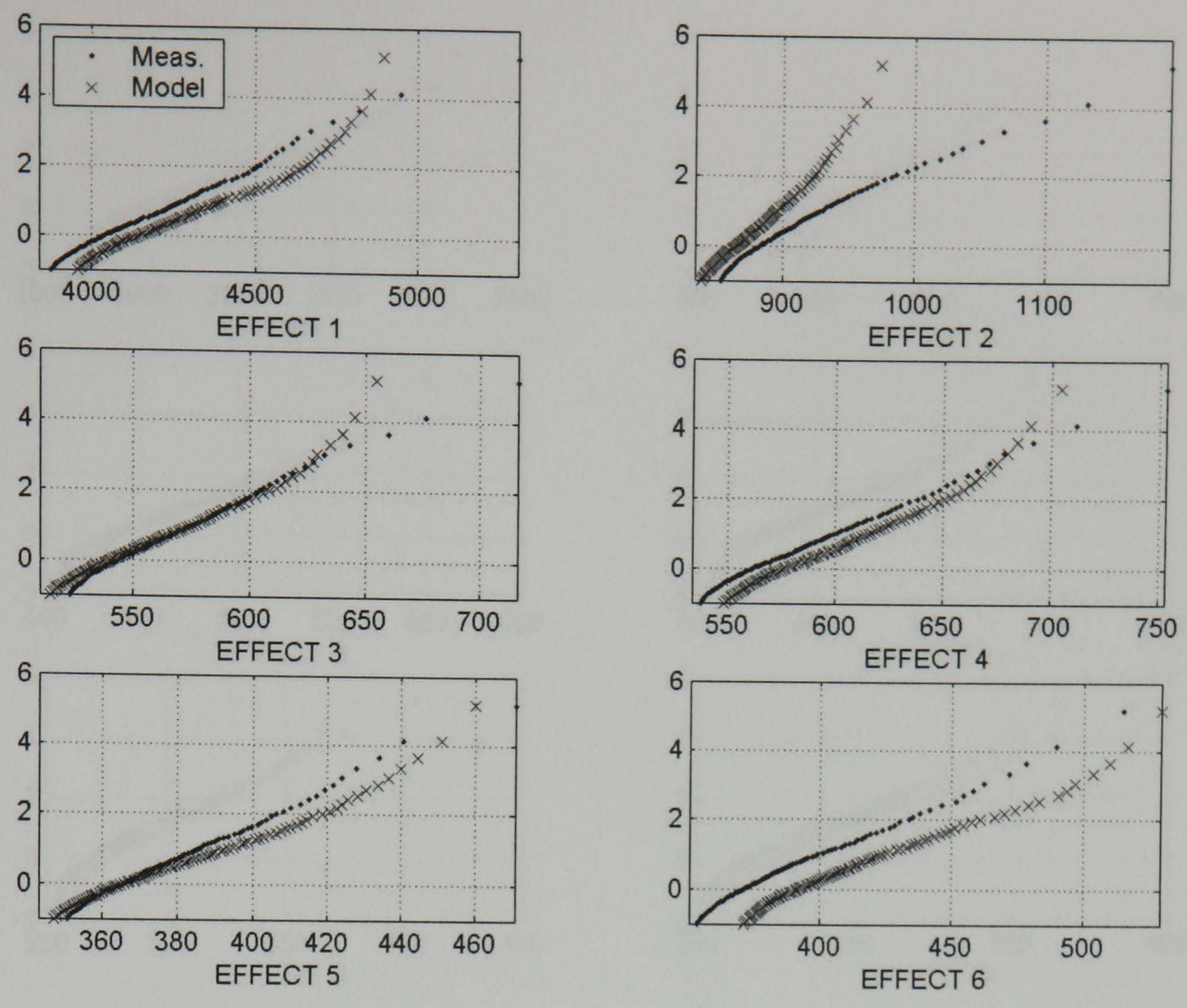

Figure N-5: Simplified Model 1 – 30m bridges – Direction 2

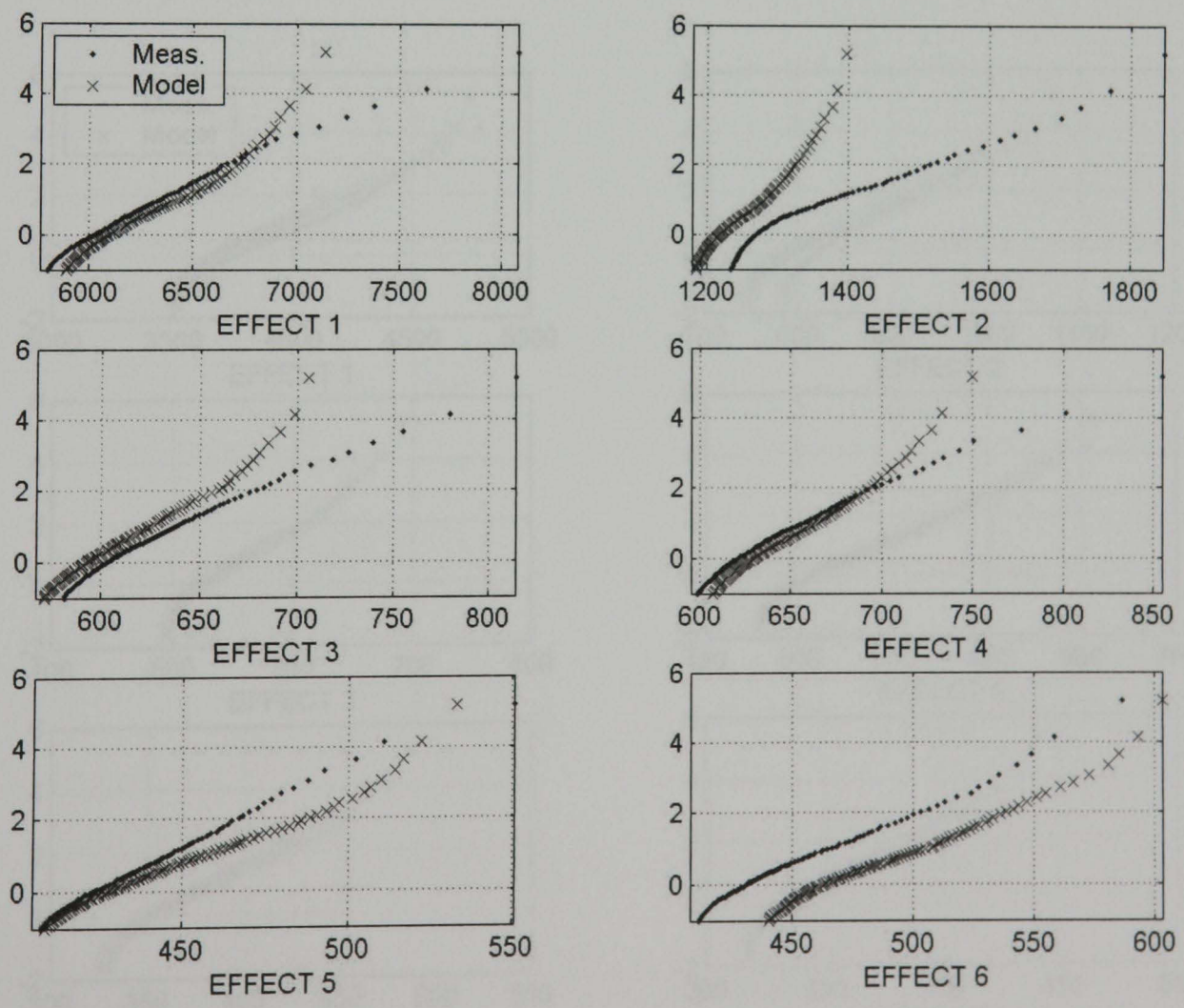

Figure N-6: Simplified Model 1 – 40m bridges – Direction 2

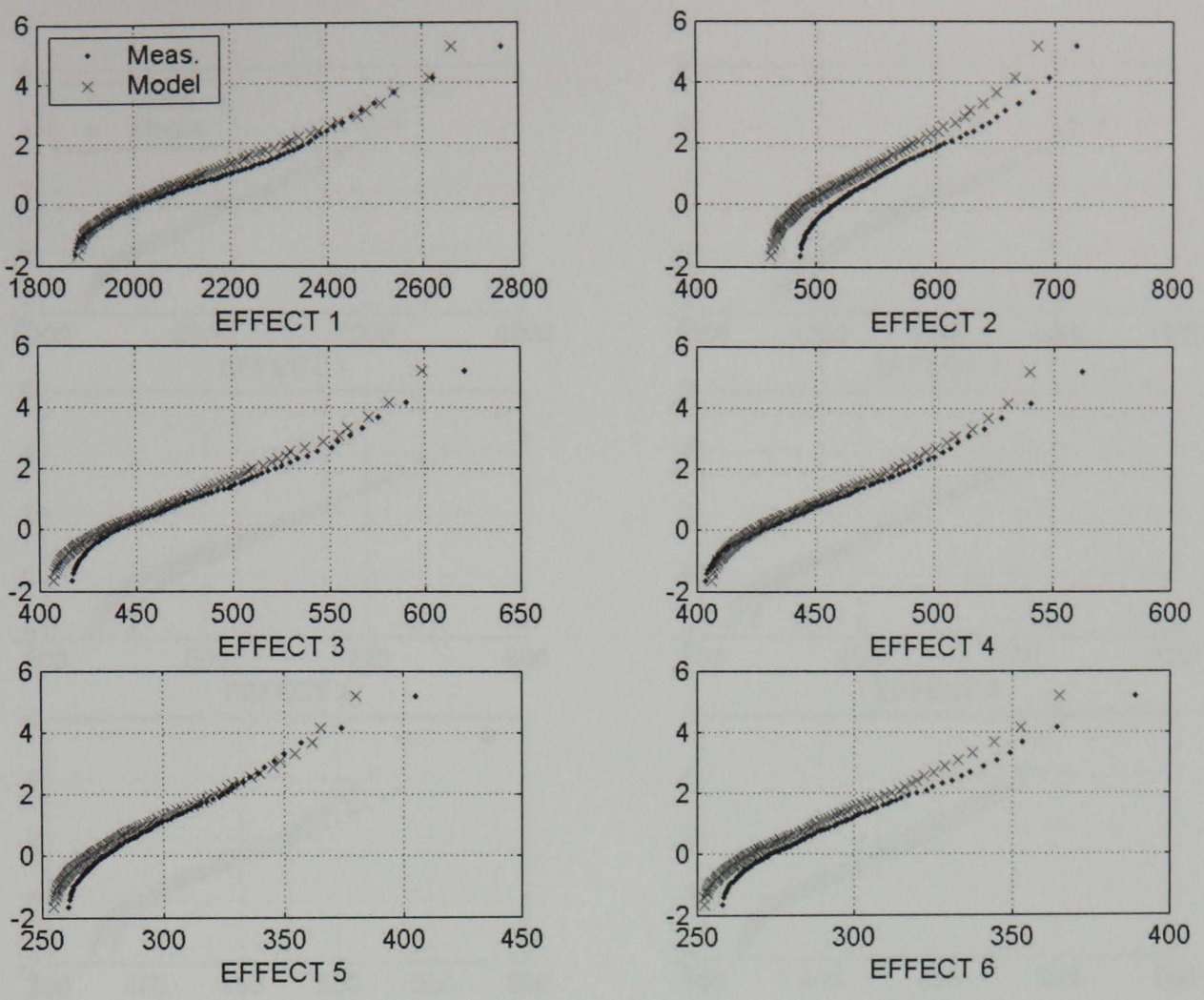

Figure N-7: Simplified Model 2 – 20m bridges – Direction 1

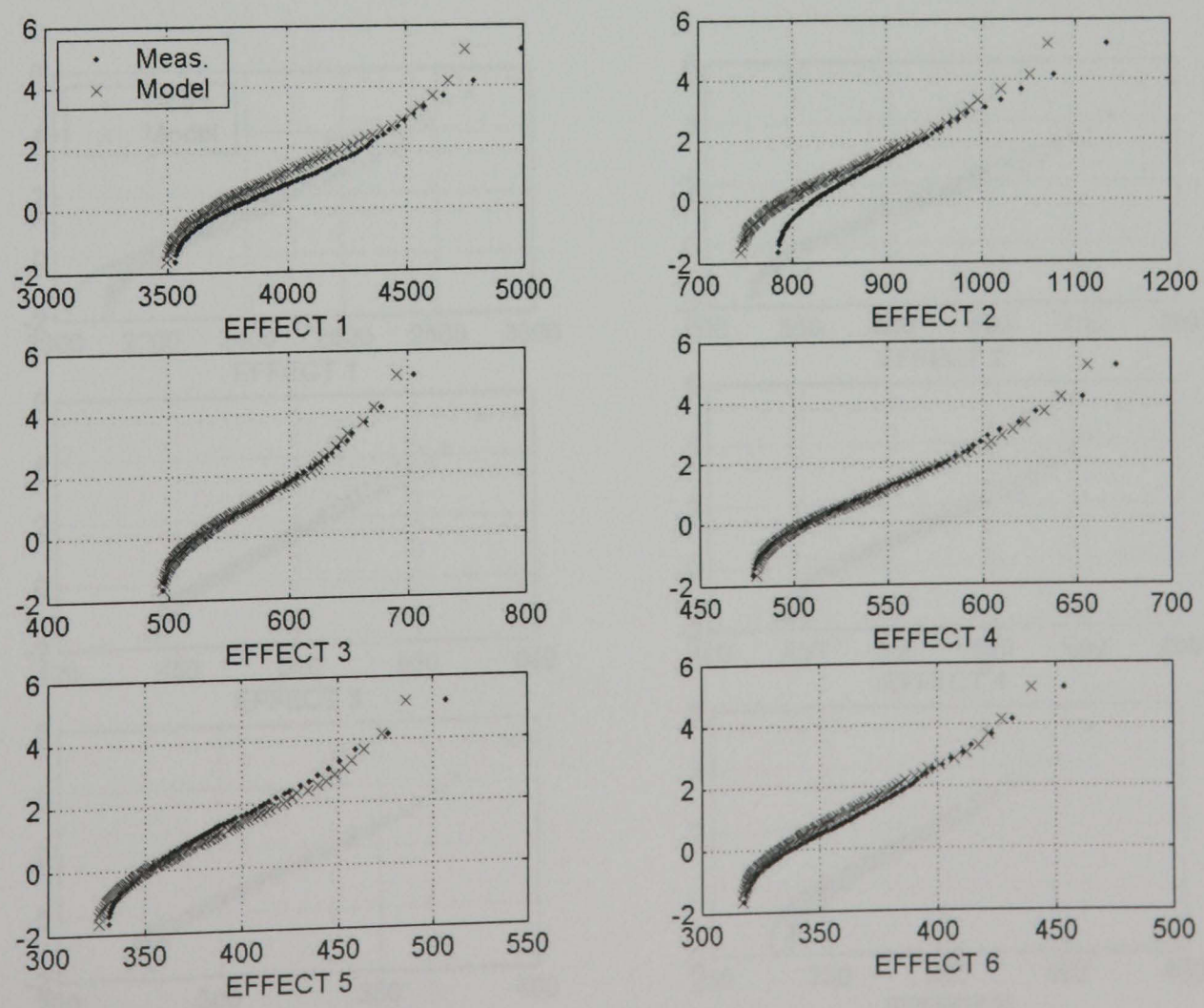

Figure N-8: Simplified Model 2 – 30m bridges – Direction 1

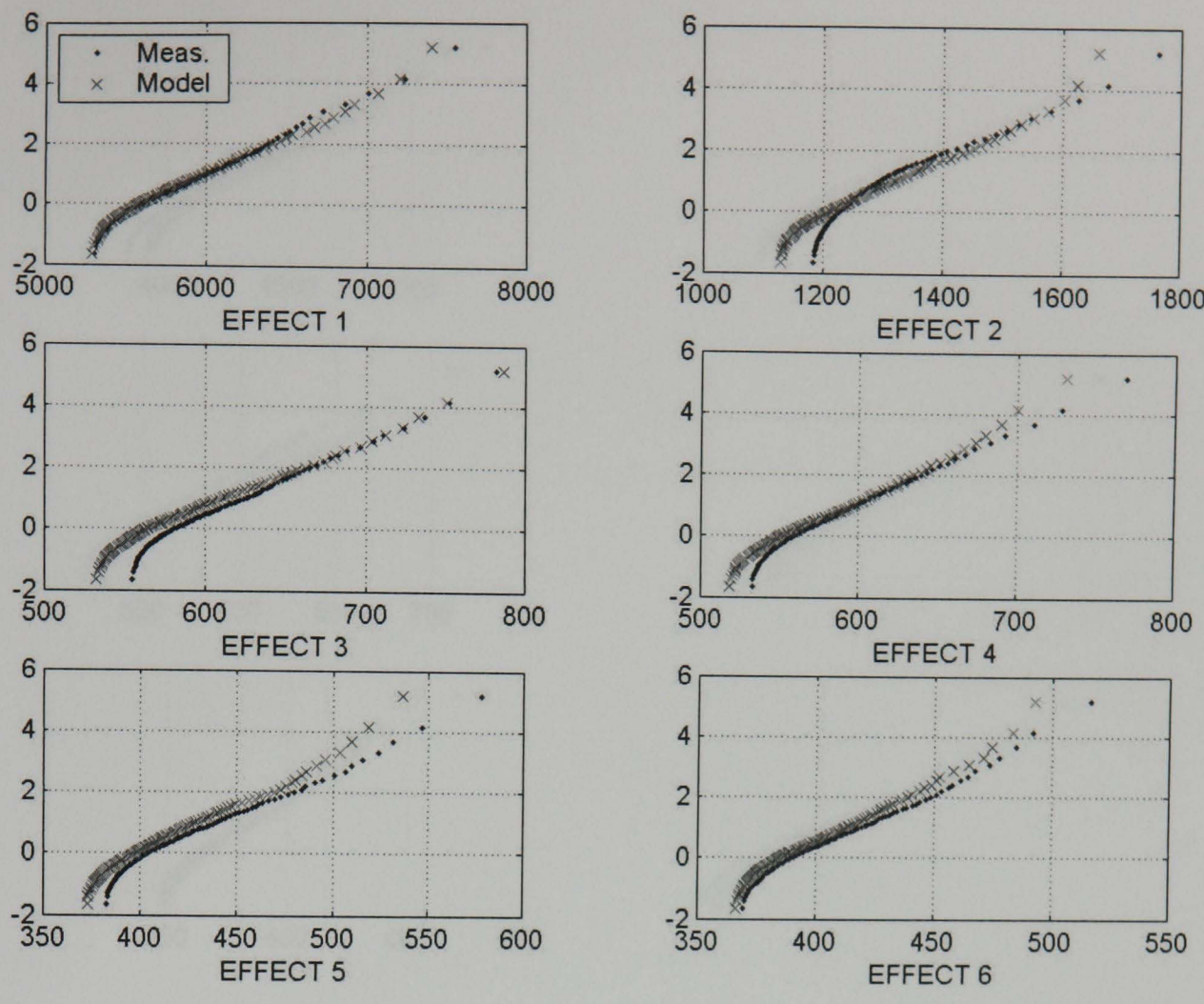

Figure N-9: Simplified Model 2 – 40m bridges – Direction 1

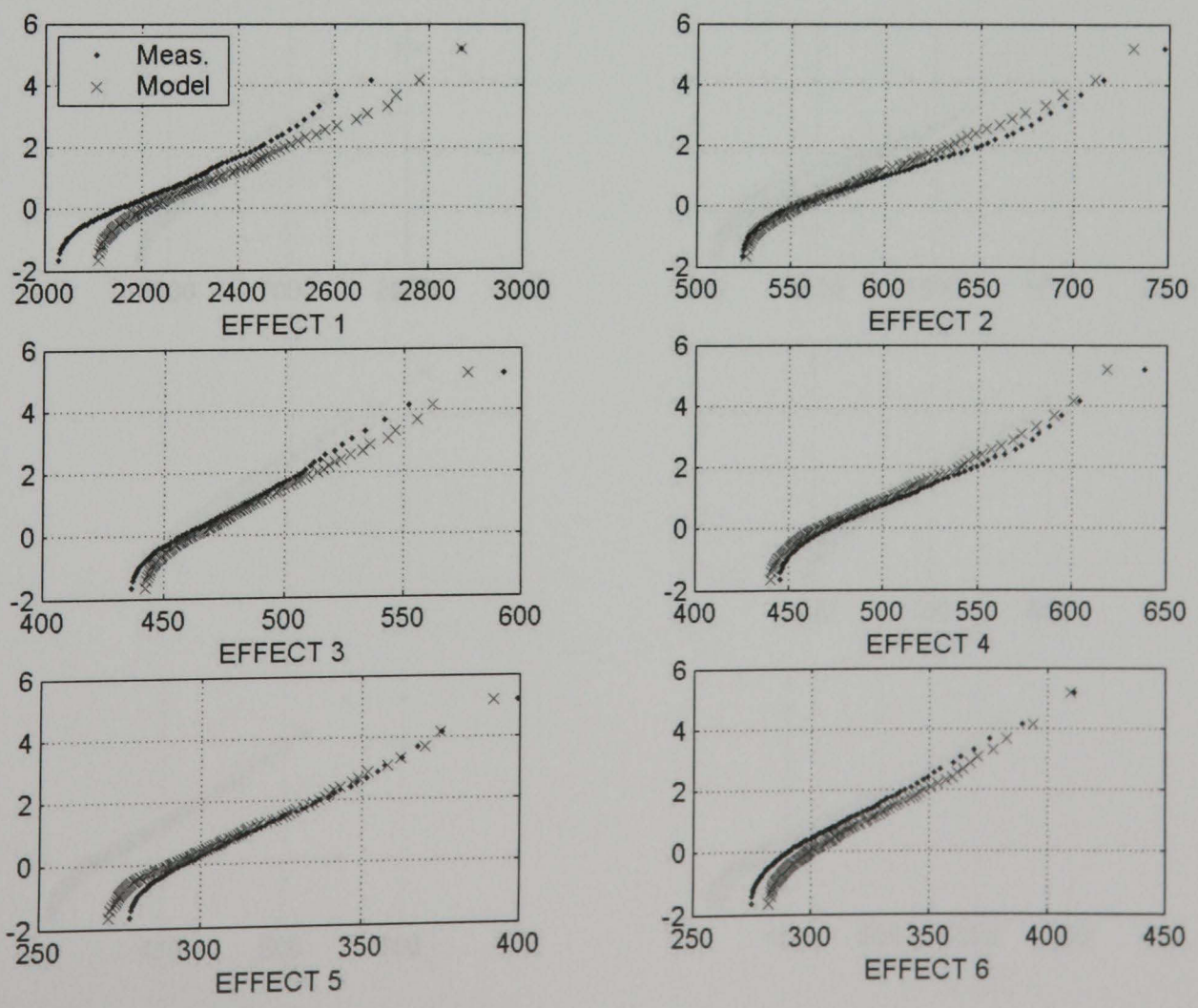

Figure N-10: Simplified Model 2 – 20m bridges – Direction 2

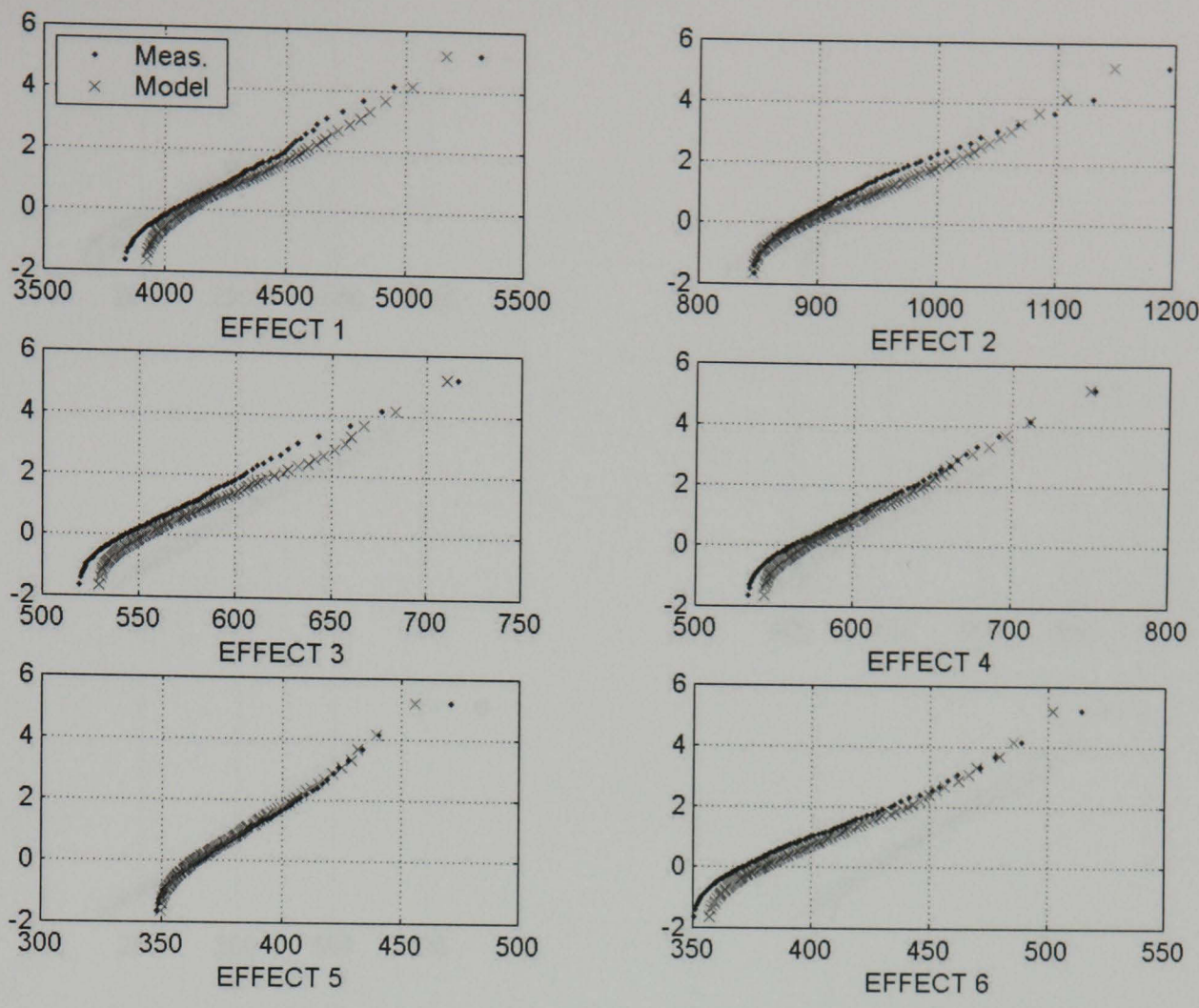

Figure N-11: Simplified Model 2 – 30m bridges – Direction 2

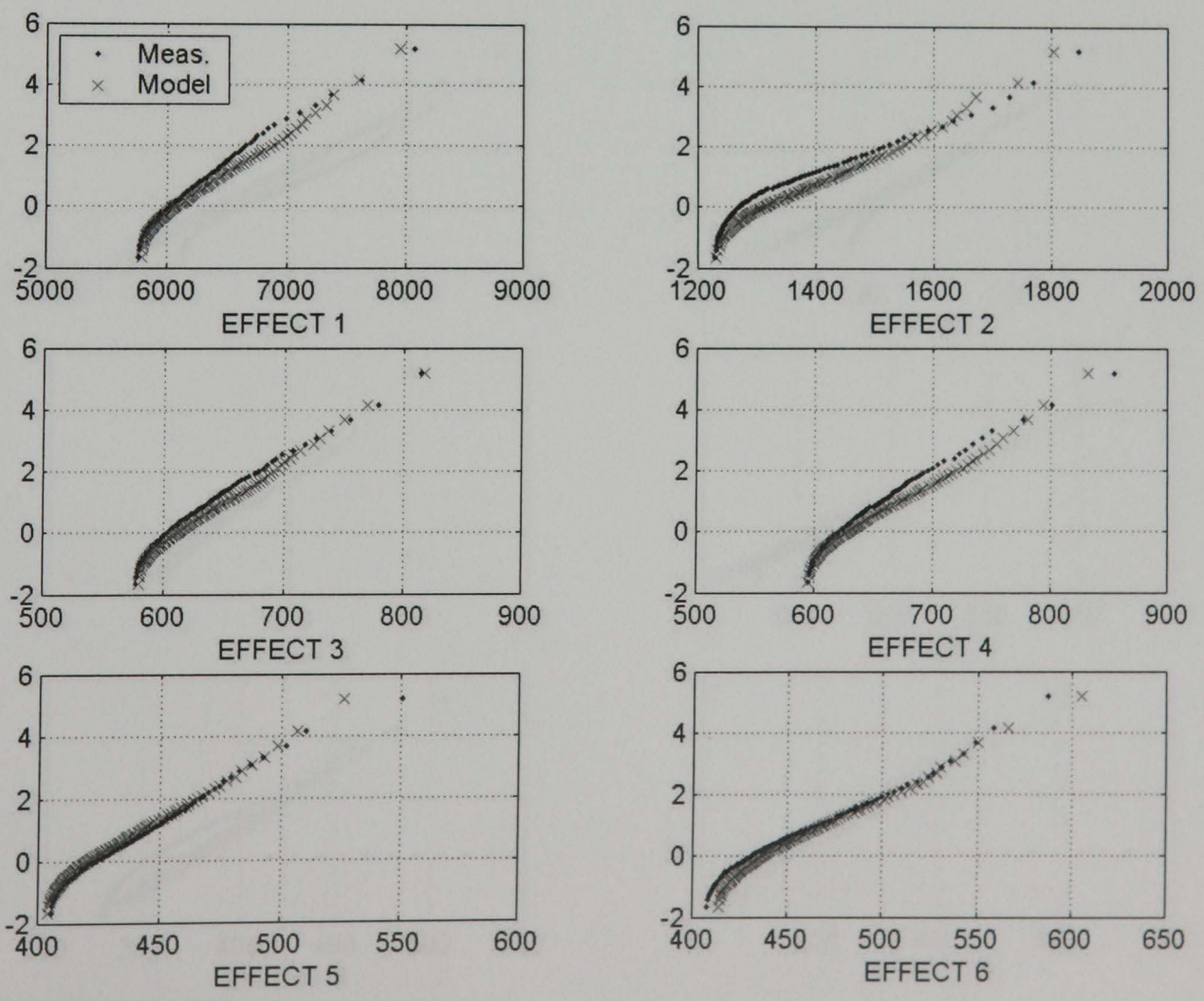

Figure N-12: Simplified Model 2 – 10m bridges – Direction 2

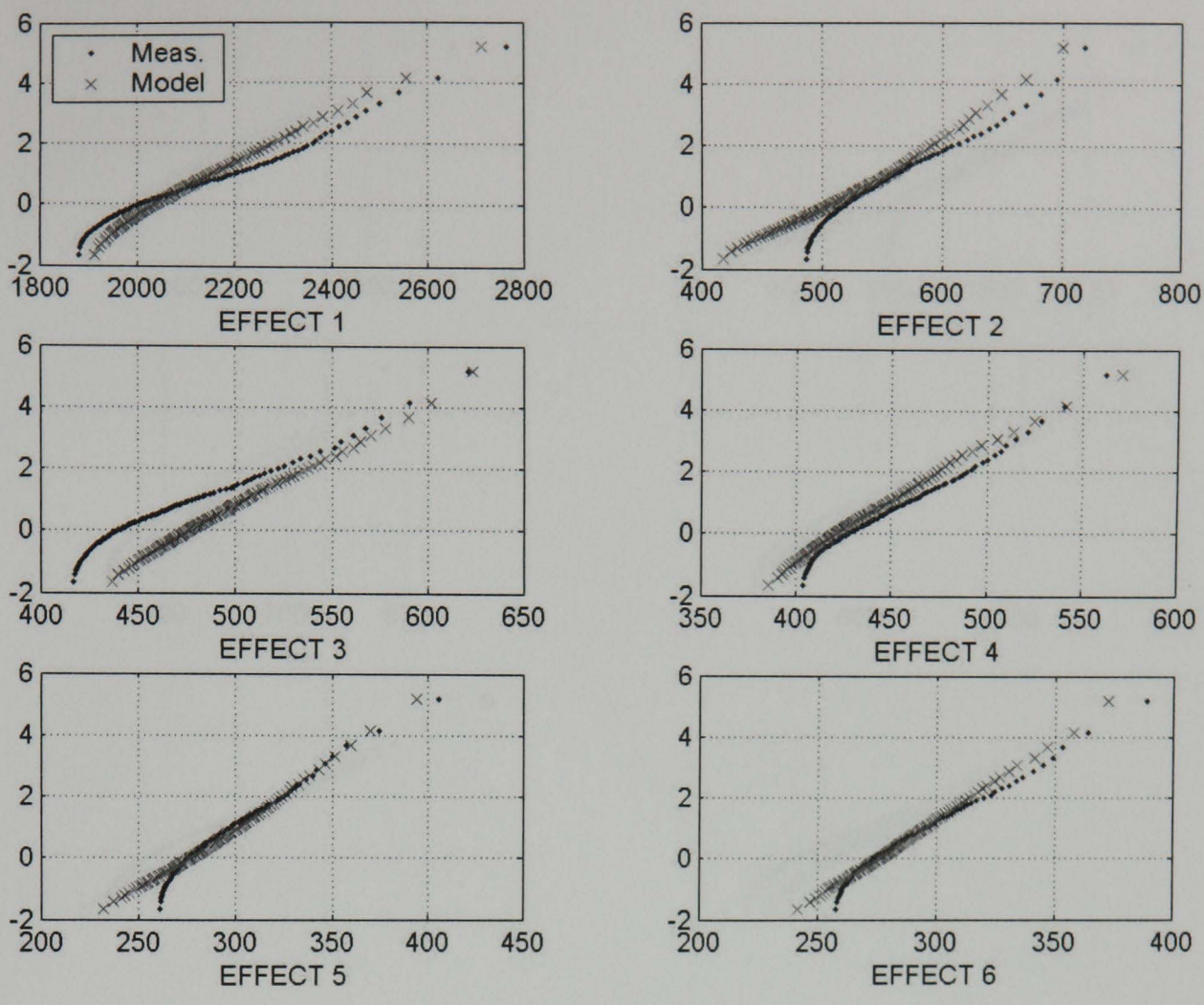

Figure N-13: Simplified Model 3 – 20m bridges – Direction 1

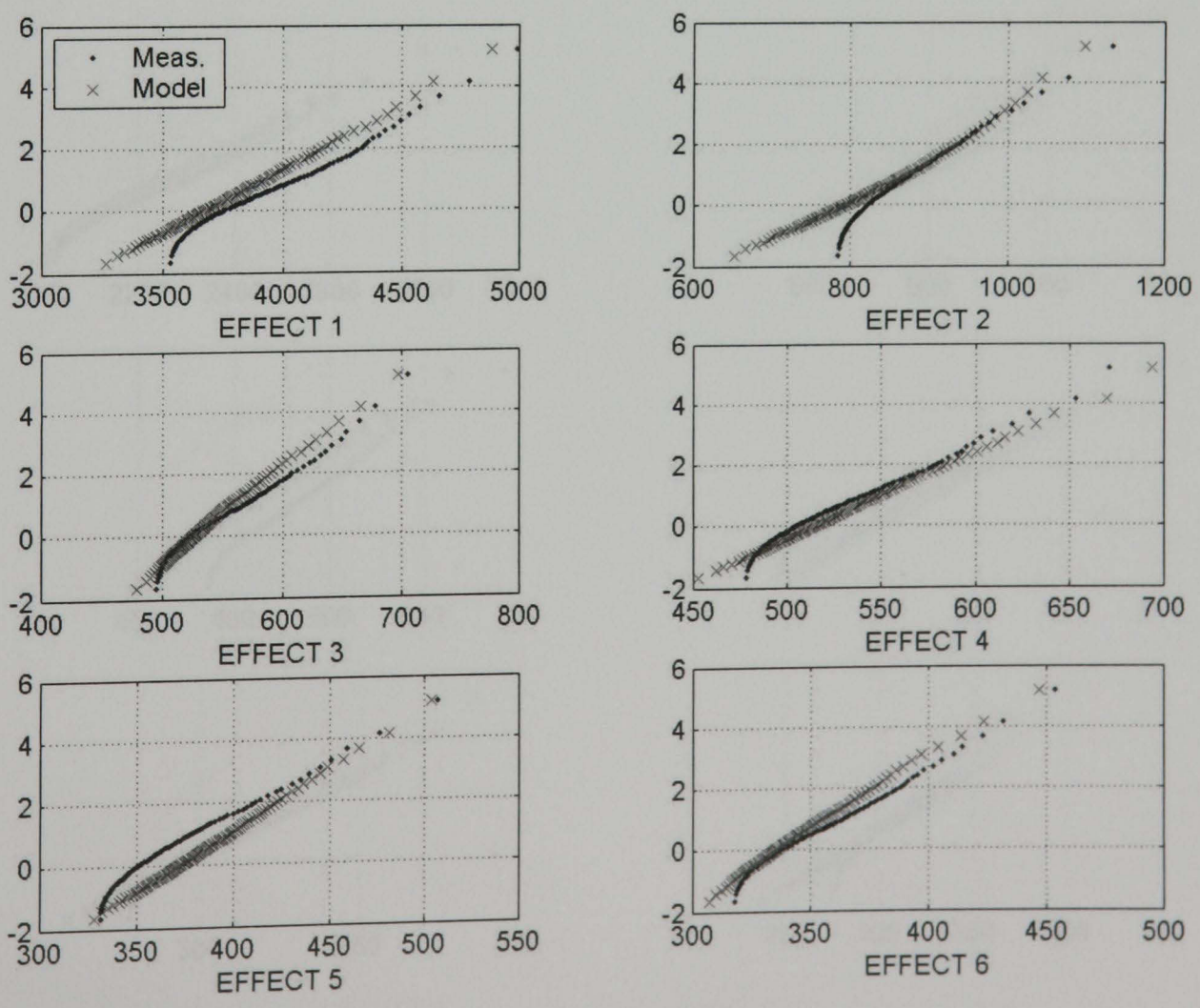

Figure N-14: Simplified Model 3 – 30m bridges – Direction 1

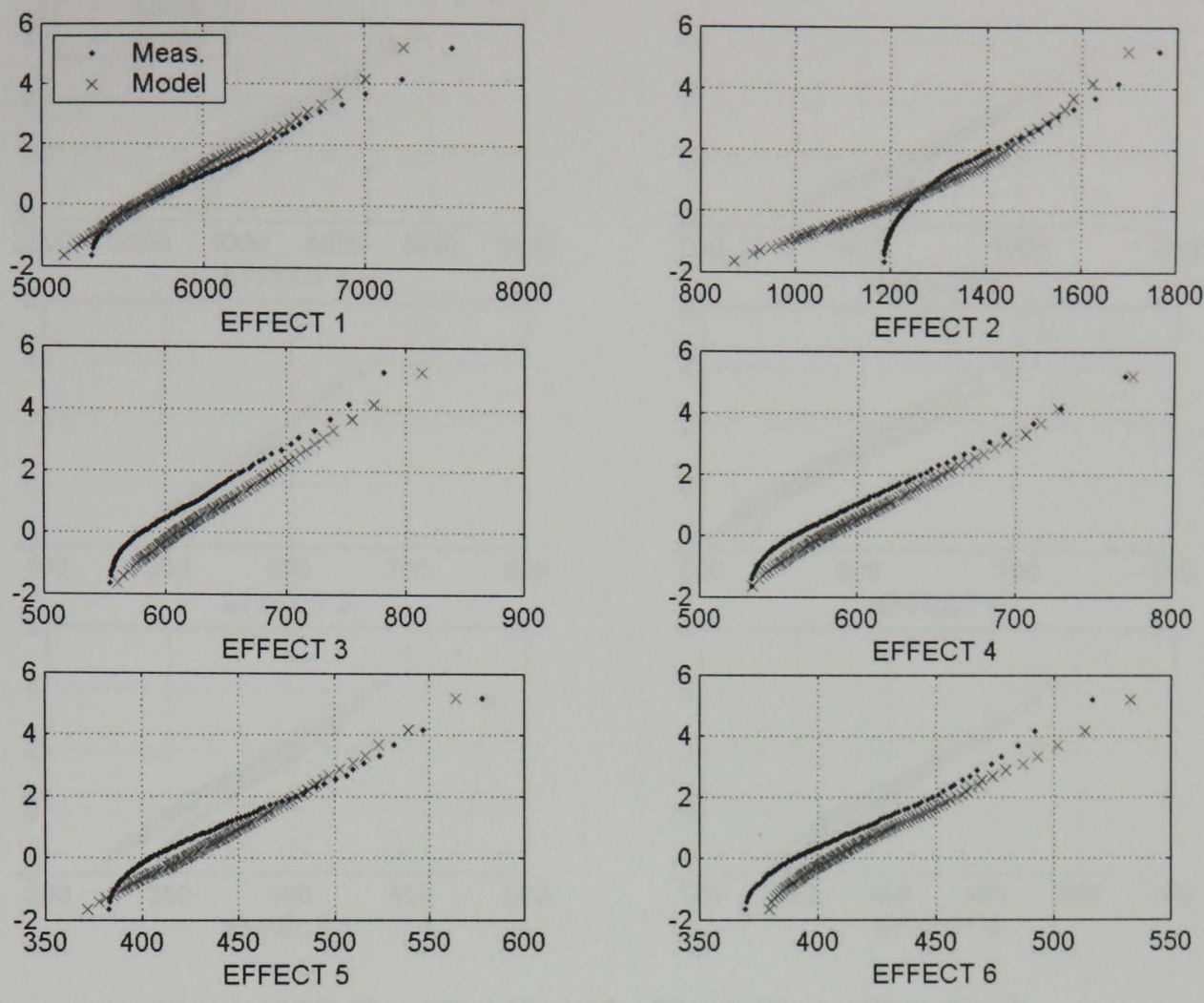

Figure N-15: Simplified Model 3 – 40m bridges – Direction 1

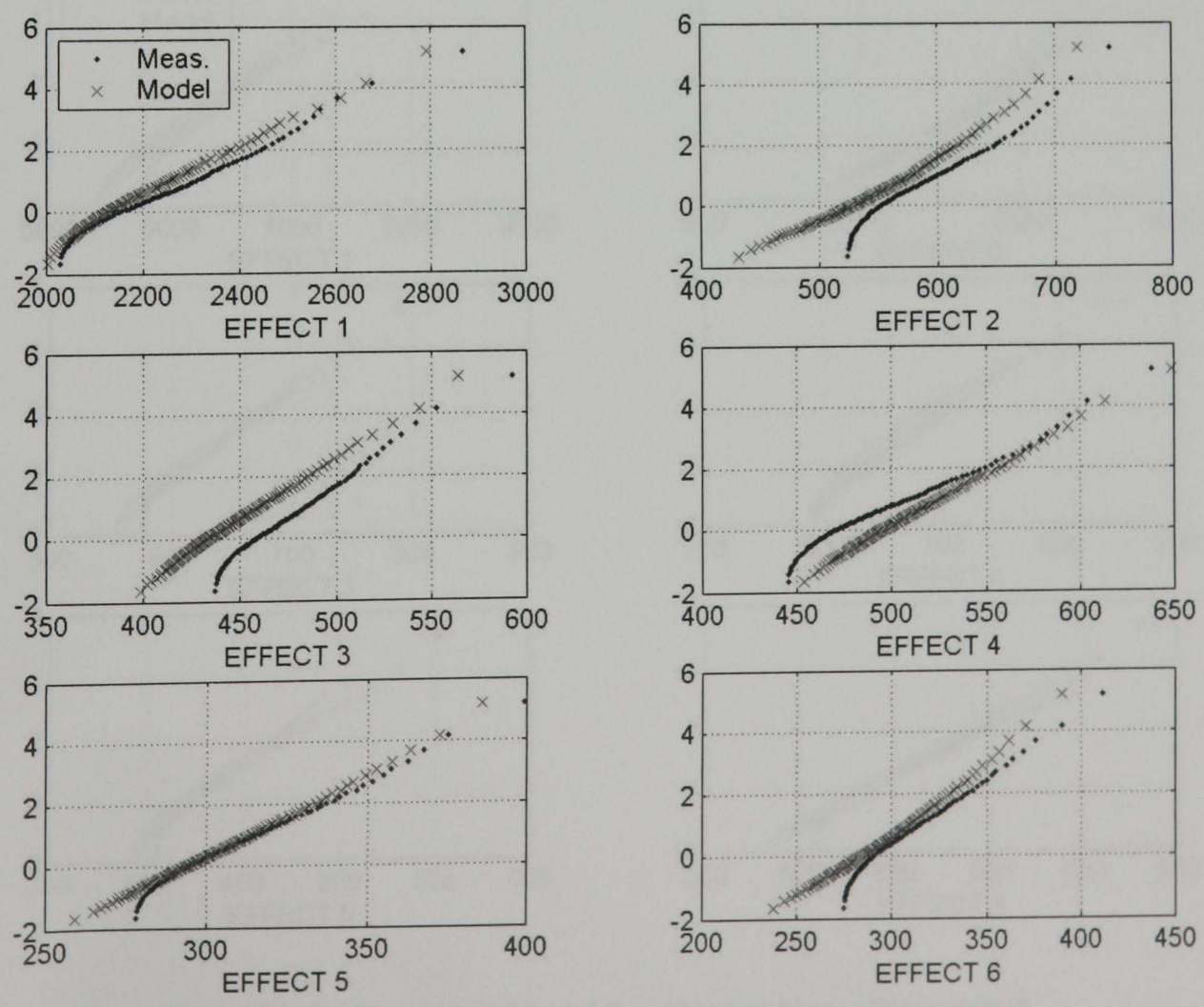

Figure N-16: Simplified Model 3 – 20m bridges – Direction 2

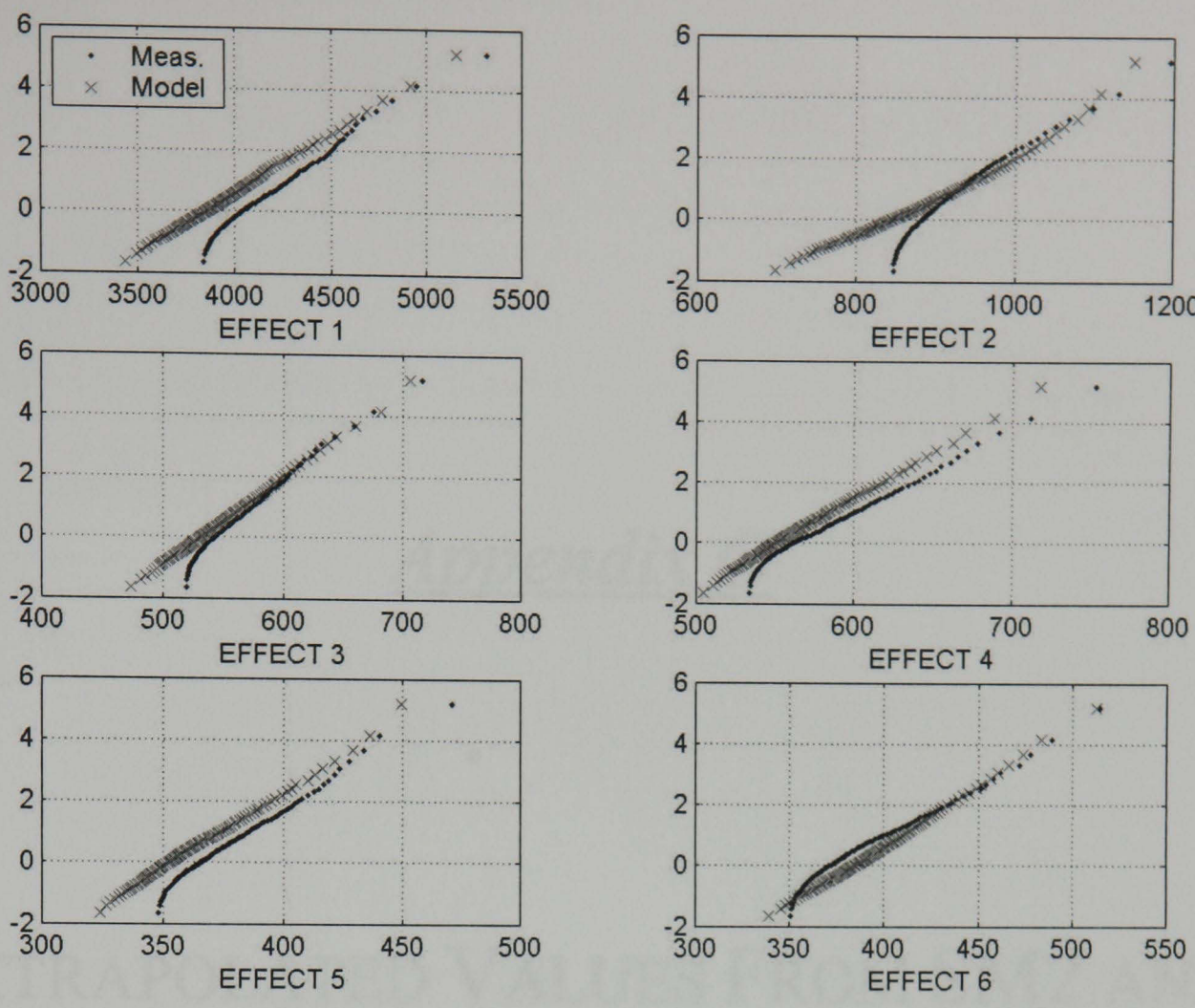

Figure N-17: Simplified Model 3 – 30m bridges – Direction 2

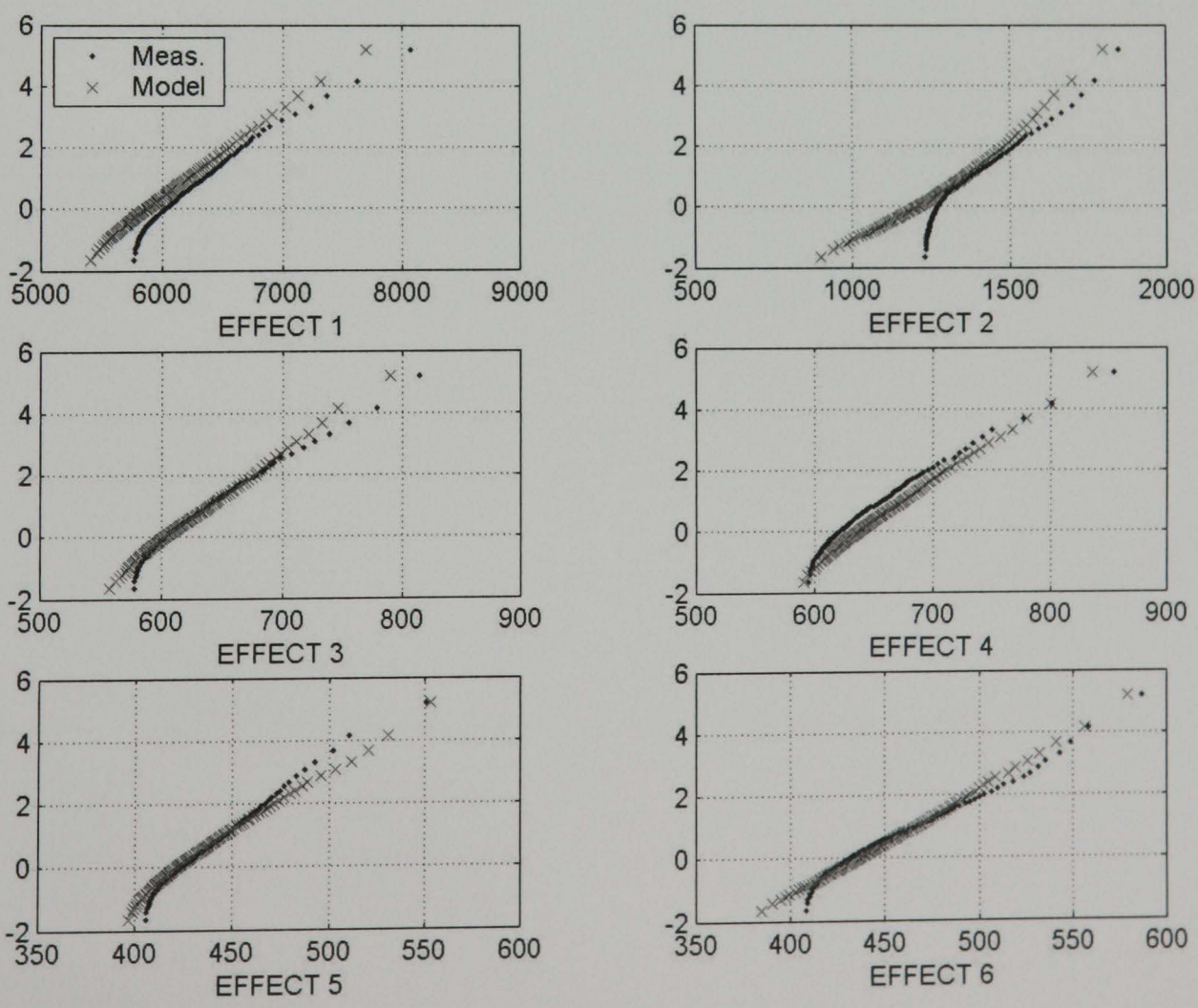

Figure N-18: Simplified Model 3 – 40m bridges – Direction 2

Appendix O

EXTRAPOLATED VALUES FROM SM2 AND SM3 FOR UNIDIRECTIONAL TRAFFIC

Appendix O Extrapolated Values From SM2 and SM3 For Unidirectional Traffic

Table O-1: Extrapolated values from full simulations and simplified model 2 (SM2)

Bridge Length	Load Effect	Direction 1			Direction 2		
		Full Sim.	SM2	Diff. (%)	Full Sim.	SM2	Diff. (%)
20 m	1	3814	3749	*-1.7*	3677	3972	*8.0*
	2	1054	1001	*-5.0*	1072	1021	*-4.7*
	3	898	858	*-4.5*	725	770	*6.1*
	4	765	749	*-2.1*	890	880	*-1.1*
	5	580	583	*0.5*	539	545	*1.2*
	6	562	524	*-6.8*	552	588	*6.5*
30 m	1	6971	6850	*-1.7*	6481	6951	*7.3*
	2	1559	1566	*0.4*	1507	1572	*4.3*
	3	1023	1001	*-2.2*	885	957	*8.2*
	4	945	920	*-2.6*	972	1003	*3.2*
	5	742	737	*-0.7*	587	599	*2.0*
	6	628	630	*0.3*	699	717	*2.6*
40 m	1	10290	10502	*2.1*	9731	10826	*11.3*
	2	2567	2505	*-2.4*	2724	2593	*-4.8*
	3	1092	1147	*5.0*	1028	1100	*7.0*
	4	1062	1015	*-4.4*	1055	1161	*10.0*
	5	862	789	*-8.5*	664	690	*4.0*
	6	726	677	*-6.7*	820	851	*3.8*
	Max			*-8.5*			*-4.8*
	Min			*5.0*			*11.3*

Table O-2: Extrapolated values from full simulations and simplified model 3 (SM3)

Bridge Length	Load Effect	Direction 1			Direction 2		
		Full Sim.	SM3	Diff. (%)	Full Sim.	SM3	Diff. (%)
20 m	1	3814	3795	*-0.5*	3677	3969	*7.9*
	2	1054	963	*-8.6*	1072	997	*-7.0*
	3	898	839	*-6.6*	725	769	*6.0*
	4	765	771	*0.8*	890	861	*-3.2*
	5	580	537	*-7.4*	539	543	*0.8*
	6	562	518	*-7.8*	552	562	*1.8*
30 m	1	6971	6996	*0.4*	6481	6984	*7.8*
	2	1559	1579	*1.3*	1507	1615	*7.2*
	3	1023	948	*-7.3*	885	901	*1.9*
	4	945	908	*-3.9*	972	966	*-0.7*
	5	742	683	*-8.0*	587	631	*7.4*
	6	628	604	*-3.8*	699	693	*-0.9*
40 m	1	10290	10281	*-0.1*	9731	10448	*7.4*
	2	2567	2600	*1.3*	2724	2748	*0.9*
	3	1092	1103	*1.0*	1028	1082	*5.2*
	4	1062	1051	*-1.0*	1055	1098	*4.0*
	5	862	783	*-9.2*	664	696	*4.9*
	6	726	684	*-5.8*	820	806	*-1.7*
	Max			*-9.2*			*-7.0*
	Min			*1.3*			*7.9*